

Protein Phosphatase Protocols

Edited by
Greg Moorhead

Protein Phosphatase Protocols

386. **Peptide Characterization and Application Protocols**, edited by Gregg B. Fields, 2007
385. **Microchip-Based Assay Systems: Methods and Applications**, edited by Pierre N. Floriano, 2007
384. **Capillary Electrophoresis: Methods and Protocols**, edited by Philippe Schmitt-Kopplin, 2007
383. **Cancer Genomics and Proteomics: Methods and Protocols**, edited by Paul B. Fisher, 2007
382. **Microarrays, Second Edition: Volume 2, Applications and Data Analysis**, edited by Jang B. Rampal, 2007
381. **Microarrays, Second Edition: Volume 1, Synthesis Methods**, edited by Jang B. Rampal, 2007
380. **Immunological Tolerance: Methods and Protocols**, edited by Paul J. Fairchild, 2007
379. **Glycoviropology Protocols**, edited by Richard J. Sugrue, 2007
378. **Monoclonal Antibodies: Methods and Protocols**, edited by Maher Albitar, 2007
377. **Microarray Data Analysis: Methods and Applications**, edited by Michael J. Korenberg, 2007
376. **Linkage Disequilibrium and Association Mapping: Analysis and Application**, edited by Andrew R. Collins, 2007
375. **In Vitro Transcription and Translation Protocols: Second Edition**, edited by Guido Grandi, 2007
374. **Biological Applications of Quantum Dots**, edited by Marcel Bruchez and Charles Z. Hotz, 2007
373. **Pyrosequencing® Protocols**, edited by Sharon Marsh, 2007
372. **Mitochondrial Genomics and Proteomics Protocols**, edited by Dario Leister and Johannes Herrmann, 2007
371. **Biological Aging: Methods and Protocols**, edited by Trygve O. Tollefsbol, 2007
370. **Adhesion Protein Protocols, Second Edition**, edited by Amanda S. Coutts, 2007
369. **Electron Microscopy: Methods and Protocols, Second Edition**, edited by John Kuo, 2007
368. **Cryopreservation and Freeze-Drying Protocols, Second Edition**, edited by John G. Day and Glyn Stacey, 2007
367. **Mass Spectrometry Data Analysis in Proteomics**, edited by Rune Matthiesen, 2007
366. **Cardiac Gene Expression: Methods and Protocols**, edited by Jun Zhang and Gregg Rokosh, 2007
365. **Protein Phosphatase Protocols**, edited by Greg Moorhead, 2007
364. **Macromolecular Crystallography Protocols: Volume 2, Structure Determination**, edited by Sylvie Doublié, 2007
363. **Macromolecular Crystallography Protocols: Volume 1, Preparation and Crystallization of Macromolecules**, edited by Sylvie Doublié, 2007
362. **Circadian Rhythms: Methods and Protocols**, edited by Ezio Rosato, 2007
361. **Target Discovery and Validation Reviews and Protocols: Emerging Molecular Targets and Treatment Options, Volume 2**, edited by Mouldy Sioud, 2007
360. **Target Discovery and Validation Reviews and Protocols: Emerging Strategies for Targets and Biomarker Discovery, Volume 1**, edited by Mouldy Sioud, 2007
359. **Quantitative Proteomics by Mass Spectrometry**, edited by Salvatore Sechi, 2007
358. **Metabolomics: Methods and Protocols**, edited by Wolfram Weckwerth, 2007
357. **Cardiovascular Proteomics: Methods and Protocols**, edited by Fernando Vivanco, 2006
356. **High-Content Screening: A Powerful Approach to Systems Cell Biology and Drug Discovery**, edited by D. Lansing Taylor, Jeffrey Haskins, and Ken Guiliano, and 2007
355. **Plant Proteomics: Methods and Protocols**, edited by Hervé Thiellement, Michel Zivy, Catherine Damerval, and Valerie Mechin, 2006
354. **Plant-Pathogen Interactions: Methods and Protocols**, edited by Pamela C. Ronald, 2006
353. **Protocols for Nucleic Acid Analysis by Nonradioactive Probes, Second Edition**, edited by Elena Hilario and John Mackay, 2006
352. **Protein Engineering Protocols**, edited by Kristian Müller and Katja Arndt, 2006
351. **C. elegans: Methods and Applications**, edited by Kevin Strange, 2006
350. **Protein Folding Protocols**, edited by Yawen Bai and Ruth Nussinov, 2007
349. **YAC Protocols, Second Edition**, edited by Alasdair MacKenzie, 2006
348. **Nuclear Transfer Protocols: Cell Reprogramming and Transgenesis**, edited by Paul J. Verma and Alan Trounson, 2006
347. **Glycobiology Protocols**, edited by Inka Brockhausen, 2006
346. **Dictyostelium discoideum Protocols**, edited by Ludwig Eichinger and Francisco Rivero, 2006
345. **Diagnostic Bacteriology Protocols, Second Edition**, edited by Louise O'Connor, 2006
344. **Agrobacterium Protocols, Second Edition: Volume 2**, edited by Kan Wang, 2006
343. **Agrobacterium Protocols, Second Edition: Volume 1**, edited by Kan Wang, 2006
342. **MicroRNA Protocols**, edited by Shao-Yao Ying, 2006
341. **Cell-Cell Interactions: Methods and Protocols**, edited by Sean P. Colgan, 2006
340. **Protein Design: Methods and Applications**, edited by Raphael Guerois and Manuela López de la Paz, 2006
339. **Microchip Capillary Electrophoresis: Methods and Protocols**, edited by Charles S. Henry, 2006

METHODS IN MOLECULAR BIOLOGY™

Protein Phosphatase Protocols

Edited by

Greg Moorhead

*Department of Biological Sciences, University of Calgary,
Calgary, AB, Canada*


HUMANA PRESS  TOTOWA, NEW JERSEY

© 2007 Humana Press Inc.
999 Riverview Drive, Suite 208
Totowa, New Jersey 07512

www.humanapress.com

All rights reserved. No part of this book may be reproduced, stored in a retrieval system, or transmitted in any form or by any means, electronic, mechanical, photocopying, microfilming, recording, or otherwise without written permission from the Publisher. Methods in Molecular Biology™ is a trademark of The Humana Press Inc.

All papers, comments, opinions, conclusions, or recommendations are those of the author(s), and do not necessarily reflect the views of the publisher.

This publication is printed on acid-free paper. 
ANSI Z39.48-1984 (American Standards Institute)

Permanence of Paper for Printed Library Materials.

Cover illustration: Figure 1 from Chapter 12, "Visualization of Intracellular PP1 Targeting Through Transiently and Stably Expressed Fluorescent Protein Fusions," by Laura Trinkle-Mulcahy, Janet Chusainow, Yun Wah Lam, Sam Swift, and Angus Lamond

Cover design by Patricia F. Cleary.

For additional copies, pricing for bulk purchases, and/or information about other Humana titles, contact Humana at the above address or at any of the following numbers: Tel.: 973-256-1699; Fax: 973-256-8341; E-mail: orders@humanapress.com; or visit our Website: www.humanapress.com

Photocopy Authorization Policy:

Authorization to photocopy items for internal or personal use, or the internal or personal use of specific clients, is granted by Humana Press Inc., provided that the base fee of US \$30.00 per copy is paid directly to the Copyright Clearance Center at 222 Rosewood Drive, Danvers, MA 01923. For those organizations that have been granted a photocopy license from the CCC, a separate system of payment has been arranged and is acceptable to Humana Press Inc. The fee code for users of the Transactional Reporting Service is: [978-1-58829-711-2 • 1-58829-711-X/07 \$30.00].

Printed in the United States of America. 10 9 8 7 6 5 4 3 2 1

eISBN: 1-59745-267-X

Library of Congress Cataloging in Publication Data
Protein phosphatase protocols / edited by Greg Moorhead.

p. ; cm. — (Methods in molecular biology ; 365)

Includes bibliographical references and index.

ISBN-13: 978-1-58829-711-2

ISBN-10: 1-58829-711-X (alk. paper)

1. Phosphoprotein phosphatases—Laboratory manuals.

[DNLN: 1. Phosphoprotein Phosphatase—analysis. 2. Phosphoprotein Phosphatase—isolation & purification. QU 136 P9671655 2006] I. Moorhead, Greg. II. Series: Methods in molecular biology (Clifton, N.J.) ; v. 365.

QP609.P56P762 2006

572'.68—dc22

2006007128

Preface

Phosphorylation is recognized as one of the most prevalent and versatile means to regulate protein function. Alteration in the normal target protein phosphorylation state is also established as a major contributor to disease and, as a consequence the enzymes that add a phosphate group to proteins, the protein kinases, are considered the second largest drug target of the pharmaceutical industry. Given the role of protein kinases, it is natural to think then that the enzymes that remove phosphate from proteins are equally important and thus are likely contributors to disease when functioning aberrantly. The acceptance of the protein phosphatases as equal in importance to protein kinases and as potential drug targets has been slow in coming. Nevertheless, a number of important research articles over the last few years have dramatically shifted this paradigm [for instance see, MacKeigan et al. *Nat. Cell Biol.* 7(6):591–600]. With a growing interest in protein phosphatase function, *Protein Phosphatase Protocols* represents a timely revisit to phosphatase methodologies.

I have tried to assemble a series of articles covering a broad range of protein phosphatase methodologies (proteomics, genomics, biochemistry, RNAi and genetics) with examples from several model organisms, including yeast, *Drosophila*, plant and human cells. By including a variety of approaches across many organisms, I was able to get contributions from many of the leading and emerging protein phosphatase researchers from around the world, but at the same time this meant that many were unable to contribute to this volume. Undoubtedly, research by other phosphatase laboratories is referenced within many of these chapters. I hope that the techniques explained here generate ideas on new approaches to protein phosphatase research in your laboratory.

Greg Moorhead

Contents

Preface	v
Contributors	xi
1 Analysis of Protein Phosphatases: <i>Toolbox For Unraveling Cell Signaling Networks</i> Shirish Shenolikar	1
2 A Brief Introduction to the Protein Phosphatase Families Tomas Mustelin	9
3 Small-Molecule Inhibitors of Ser/Thr Protein Phosphatases: <i>Specificity, Use, and Common Forms of Abuse</i> Mark Swingle, Li Ni, and Richard E. Honkanen	23
4 Synthesis and Use of the Protein Phosphatase Affinity Matrices Microcystin–Sepharose and Microcystin–Biotin–Sepharose Greg B. G. Moorhead, Timothy A. J. Haystead and Carol MacKintosh	39
5 Utilizing Protein Phosphatase Inhibitors to Define PP2A as a Regulator of Ataxia-Telangiectasia Mutated (ATM) Aaron A. Goodarzi, Pauline Douglas, Greg B. G. Moorhead, and Susan P. Lees-Miller	47
6 An Automated Fluorescence-Based Method for Continuous Assay of PP2A Activity Adam M. Wegner, Jamie L. McConnell, Randy D. Blakely, and Brian E. Wadzinski	61
7 An In Vivo Assay to Quantify Stable Protein Phosphatase 2A (PP2A) Heterotrimeric Species Matthew S. Gentry, Richard L. Hallberg, and David C. Pallas	71
8 Mutagenesis and Expression of the Scaffolding A α and A β Subunits of PP2A: Assays for Measuring Defects in Binding of Cancer-Related A α and A β Mutants to the Regulatory B and Catalytic C Subunits Ralf Ruediger, Jin Zhou, and Gernot Walter	85
9 Isolation and Characterization of PP2A Holoenzymes Containing FLAG-Tagged B Subunits Deanna G. Adams and Brian E. Wadzinski	101
10 Purification of PP2A Holoenzymes by Sequential Immunoprecipitation with Anti-Peptide Antibodies Gernot Walter, Jin Zhou, and Ralf Ruediger	113

11	Purification of PP2Ac from Bovine Heart Hue T. Tran, Tony S. Ferrar, Anne Ulke-Lemée, and Greg B. G. Moorhead	127
12	Visualization of Intracellular PP1 Targeting Through Transiently and Stably Expressed Fluorescent Protein Fusions Laura Trinkle-Mulcahy, Janet Chusainow, Yun Wah Lam, Sam Swift, and Angus Lamond	133
13	Yeast Two-Hybrid Screens To Identify <i>Drosophila</i> PP1-Binding Proteins Daimark Bennett and Luke Alphey	155
14	Identification of Cellular Protein Phosphatase-1 Regulators David W. Roadcap, Matthew H. Brush, and Shirish Shenolikar	181
15	Assay for Three-Way Interaction of Protein Phosphatase-1 (Glc7) with Regulatory Subunits Plus Phosphatase Inhibitor-2 Masumi Eto and David L. Brautigan	197
16	Phosphorylation of the Protein Phosphatase Type 1 Inhibitor Protein CPI-17 by Protein Kinase C Michael P. Walsh, Marija Susnjar, Jingti Deng, Cindy Sutherland, Enikó Kiss, and David P. Wilson	209
17	Purification of Smooth Muscle Myosin Phosphatase Using a Thiophosphorylated Myosin Light-Chain-Affinity Resin Meredith Borman and Justin MacDonald	225
18	Proteins Interacting with <i>Saccharomyces cerevisiae</i> Type 1 Protein Phosphatase Catalytic Subunit Identified by Single-Step Affinity Purification and Mass Spectrometry Edmund P. Walsh, Douglas J. Lamont, Kenneth A. Beattie, and Michael J. R. Stark	235
19	Expression of Protein Histidine Phosphatase in <i>Escherichia coli</i> , Purification, and Determination of Enzyme Activity Nicole Bäumer, Anette Mäurer, Josef Krieglstein, and Susanne Klumpp	247
20	The Use of RNA Interference to Analyze Protein Phosphatase Function In Mammalian Cells Iain Fraser, Wei Liu, Robert Rebres, Tamara Roach, Joelle Zavzavadjian, Leah Santat, Jamie Liu, Estelle Wall, and Marc Mumby	261
21	Recognition of a PP2C Interaction Motif in Several Plant Protein Kinases Niranjan Chakraborty, Masaru Ohta, and Jian-Kang Zhu	287

22	Use of Yeast Genetic Tools to Define Biological Roles of Novel Protein Phosphatases Joaquín Ariño, Antonio Casamayor, Amparo Ruiz, Ivan Muñoz, and Maribel Marquina	299
23	Targeting of PP2C in Budding Yeast Irene M. Ota and James Mapes	309
24	Phosphatase Targets in TOR Signaling Estela Jacinto	323
25	Functional Characterization of the Small CTD Phosphatases Michele Yeo and Patrick S. Lin	335
26	Genome-Scale Discovery and Characterization of Class-Specific Protein Sequences: <i>An Example Using the Protein Phosphatases of Arabidopsis thaliana</i> David Kerk	347
27	Yeast Substrate-Trapping System for Isolating Substrates of Protein Tyrosine Phosphatases Masahide Fukada and Masaharu Noda	371
	Index	383

Contributors

DEANNA G. ADAMS • *Department of Pharmacology, Vanderbilt University Medical Center, Nashville, Tennessee, USA*

LUKE ALPHEY • *Department of Zoology, University of Oxford, Oxford, United Kingdom*

JOAQUÍN ARIÑO • *Department of Biochemistry and Molecular Biology, Universitat Autònoma de Barcelona, Bellaterra, 08193, Barcelona, Spain*

NICOLE BÄUMER • *Institut für Pharmazeutische und Medizinische Chemie, Westfälische Wilhelms-Universität, Münster, Germany*

KENNETH A. BEATTIE • *School of Life Sciences, University of Dundee, United Kingdom*

DAIMARK BENNETT • *Department of Zoology, University of Oxford, Oxford, United Kingdom*

RANDY D. BLAKELY • *Department of Pharmacology, Vanderbilt University Medical Center, Nashville, Tennessee, USA*

MEREDITH BORMAN • *Department of Biochemistry and Molecular Biology, Smooth Muscle Research Group, University of Calgary, Calgary, AB, Canada*

DAVID L. BRAUTIGAN • *Center for Cell Signaling and Department of Microbiology, University of Virginia School of Medicine, Charlottesville, Virginia, USA*

MATTHEW H. BRUSH • *Department of Pharmacology and Cancer Biology, Duke University Medical Center, Durham, North Carolina, USA*

ANTONIO CASAMAYOR • *Department of Biochemistry and Molecular Biology, Universitat Autònoma de Barcelona, Bellaterra, 08193, Barcelona, Spain*

NIRANJAN CHAKRABORTY • *National Centre for Plant Genome Research Aruna Asaf Ali Marg JNU Campus, New Delhi, India*

JANET CHUSAINOW • *Division of Gene Regulation and Expression, School of Life Sciences, MSI/WTB Complex, University of Dundee, Dundee, United Kingdom*

JINGTI DENG • *Smooth Muscle Research Group, Department of Biochemistry & Molecular Biology, University of Calgary, Calgary, Alberta, Canada*

PAULINE DOUGLAS • *Southern Alberta Cancer Research Institute and Department of Biochemistry & Molecular Biology, University of Calgary, Calgary, AB, Canada*

MASUMI ETO • *Department of Physiology, Thomas Jefferson College of Medicine, Philadelphia, Pennsylvania, USA*

- TONY S. FERRAR • *Department of Biological Sciences, University of Calgary, Calgary, Alberta, Canada*
- IAIN FRASER • *AfCS Molecular Biology Laboratory, Division of Biology, California Institute of Technology, Pasadena, California, USA*
- MASAHIDE FUKADA • *Division of Molecular Neurobiology, National Institute for Basic Biology, 5-1 Higashiyama, Myodaiji-cho, Okazaki, Aichi 444-8787, Japan*
- MATTHEW S. GENTRY • *Department of Pharmacology, University of California, San Diego, California, USA*
- AARON A. GOODARZI • *Southern Alberta Cancer Research Institute and Department of Biochemistry & Molecular Biology, University of Calgary, Calgary, AB, Canada*
- RICHARD L. HALLBERG • *Department of Biology, Syracuse University, Syracuse, New York, USA*
- TIMOTHY A. J. HAYSTEAD • *Department of Pharmacology and Cancer Biology, Duke University Medical Center, Durham, North Carolina, USA*
- RICHARD E. HONKANEN • *Department of Biochemistry and Molecular Biology, University of South Alabama, Mobile, Alabama, USA*
- ESTELA JACINTO • *Department of Physiology and Biophysics UMDNJ, Robert Wood Johnson Medical School, Piscataway, New Jersey, USA*
- ENIKÓ KISS • *Smooth Muscle Research Group, Department of Biochemistry & Molecular Biology, University of Calgary, Calgary, Alberta, Canada*
- DAVID KERK • *Department of Biology, Point Loma Nazarene University, San Diego, California, USA*
- SUSANNE KLUMPP • *Institut für Pharmazeutische und Medizinische Chemie, Westfälische Wilhelms-Universität, Münster, Germany*
- JOSEF KRIEGLSTEIN • *Institut für Pharmakologie and Toxikologie, Philipps-Universität, Marburg, Germany*
- YUN WAH LAM • *Division of Gene Regulation and Expression, School of Life Sciences, MSI/WTB Complex, University of Dundee, Dundee, United Kingdom*
- ANGUS LAMOND • *Division of Gene Regulation and Expression, School of Life Sciences, MSI/WTB Complex, University of Dundee, Dundee, United Kingdom*
- DOUGLAS J. LAMONT • *School of Life Sciences, University of Dundee, United Kingdom*
- SUSAN P. LEES-MILLER • *Southern Alberta Cancer Research Institute and Department of Biochemistry & Molecular Biology, University of Calgary, Calgary, AB, Canada*
- PATRICK S. LIN • *Division of Oncology, Stanford University School of Medicine, Stanford, California, USA*

- JAMIE LIU • *AfCS Molecular Biology Laboratory, Division of Biology, California Institute of Technology, Pasadena, California, USA*
- WEI LIU • *Department of Pharmacology, University of Texas Southwestern Medical Center, Dallas, Texas, USA*
- JUSTIN MACDONALD • *Department of Biochemistry and Molecular Biology, Smooth Muscle Research Group, University of Calgary, Calgary, AB, Canada*
- CAROL MACKINTOSH • *MRC Protein Phosphorylation Unit, School of Life Sciences, University of Dundee, Dundee, Scotland*
- JAMES MAPES • *Department of Molecular, Cellular, and Developmental Biology, University of Colorado, Boulder, Colorado, USA*
- MARIBEL MARQUINA • *Department of Biochemistry and Molecular Biology, Universitat Autònoma de Barcelona, Bellaterra, 08193, Barcelona, Spain*
- ANETTE MÄURER • *Institut für Pharmazeutische und Medizinische Chemie, Westfälische Wilhelms-Universität, Münster, Germany*
- JAMIE L. MCCONNELL • *Department of Pharmacology, Vanderbilt University Medical Center, Nashville, Tennessee, USA*
- GREG B. G. MOORHEAD • *Department of Biological Sciences, University of Calgary, Calgary, Alberta, Canada*
- MARC MUMBY • *Department of Pharmacology, University of Texas Southwestern Medical Center, Dallas, Texas, USA*
- IVAN MUÑOZ • *Department of Biochemistry and Molecular Biology, Universitat Autònoma de Barcelona, Bellaterra, 08193, Barcelona, Spain*
- TOMAS MUSTELIN • *The Burnham Institute, La Jolla, California, USA*
- LI NI • *Department of Biochemistry and Molecular Biology, University of South Alabama, Mobile, Alabama, USA*
- MASAHARU NODA • *Division of Molecular Neurobiology, National Institute for Basic Biology, 5-1 Higashiyama, Myodaiji-cho, Okazaki, Aichi 444-8787, Japan*
- MASARU OHTA • *Graduate School of Life and Environmental Sciences, University of Tsukuba, Tsukuba, Ibaraki, Japan*
- IRENE M. OTA • *Huntsman Cancer Institute, University of Utah, Salt Lake City, Utah, USA*
- DAVID C. PALLAS • *Department of Biochemistry and Winship Cancer Institute, Emory University School of Medicine, Atlanta, Georgia, USA*
- ROBERT REBRES • *AfCS Macrophage Biology, Northern California Institute for Research and Education, San Francisco Veterans Administration Hospital, San Francisco, California, USA*
- TAMARA ROACH • *AfCS Macrophage Biology, Northern California Institute for Research and Education, San Francisco Veterans Administration Hospital, San Francisco, California, USA*

- DAVID W. ROADCAP • *Department of Pharmacology and Cancer Biology, Duke University Medical Center, Durham, North Carolina, USA*
- RALF RUEDIGER • *Department of Pathology, University of California at San Diego, La Jolla, California, USA*
- AMPARO RUIZ • *Department of Biochemistry and Molecular Biology, Universitat Autònoma de Barcelona, Bellaterra, 08193, Barcelona, Spain*
- LEAH SANTAT • *AfCS Molecular Biology Laboratory, Division of Biology, California Institute of Technology, Pasadena, California, USA*
- SHIRISH SHENOLIKAR • *Department of Pharmacology and Cancer Biology, Duke University Medical Center, Durham, North Carolina, USA*
- MICHAEL J. R. STARK • *School of Life Sciences, University of Dundee, United Kingdom*
- MARIJA SUSNJAR • *Smooth Muscle Research Group, Department of Biochemistry & Molecular Biology, University of Calgary, Calgary, Alberta, Canada*
- CINDY SUTHERLAND • *Smooth Muscle Research Group, Department of Biochemistry & Molecular Biology, University of Calgary, Calgary, Alberta, Canada*
- SAM SWIFT • *Division of Gene Regulation and Expression, School of Life Sciences, MSI/WTB Complex, University of Dundee, Dundee, United Kingdom*
- MARK SWINGLE • *Department of Biochemistry and Molecular Biology, University of South Alabama, Mobile, Alabama, USA*
- HUE T. TRAN • *Department of Biological Sciences, University of Calgary, Calgary, Alberta, Canada*
- LAURA TRINKLE-MULCAHY • *Division of Gene Regulation and Expression, School of Life Sciences, MSI/WTB Complex, University of Dundee, Dundee, United Kingdom*
- ANNE ULKE-LEMÉE • *Department of Biological Sciences, University of Calgary, Calgary, Alberta, Canada*
- BRIAN E. WADZINSKI • *Department of Pharmacology, Vanderbilt University Medical Center, Nashville, Tennessee, USA*
- ESTELLE WALL • *AfCS Molecular Biology Laboratory, Division of Biology, California Institute of Technology, Pasadena, California, USA*
- EDMUND P. WALSH • *University of Newcastle, United Kingdom*
- MICHAEL P. WALSH • *Smooth Muscle Research Group, Department of Biochemistry & Molecular Biology, University of Calgary, Calgary, Alberta, Canada*
- GERNOT WALTER • *Department of Pathology, University of California at San Diego, La Jolla, California, USA*

ADAM M. WEGNER • *Department of Pharmacology, Vanderbilt University Medical Center, Nashville, Tennessee, USA*

DAVID P. WILSON • *Smooth Muscle Research Group, Department of Biochemistry & Molecular Biology, University of Calgary, Calgary, Alberta, Canada*

MICHELE YEO • *Division of Neurology, Duke University Medical Center, Durham, North Carolina, USA*

JOELLE ZAVZAVADJIAN • *AfCS Molecular Biology Laboratory, Division of Biology, California Institute of Technology, Pasadena, California, USA*

JIN ZHOU • *AmCyte, Santa Monica, California, USA*

JIAN-KANG ZHU • *Department of Botany and Plant Sciences, Institute for Integrative Genome Biology, University of California Riverside, California, USA*

Analysis of Protein Phosphatases

Toolbox for Unraveling Cell Signaling Networks

Shirish Shenolikar

Summary

Protein phosphatases reverse the covalent modifications of numerous cellular proteins imposed by the activation of protein kinases. Although protein phosphatases generally demonstrate broader substrate specificity than protein kinases, at least in vitro, these enzymes have evolved complex mechanisms to target specific physiological substrates and respond to physiological stimuli to control numerous physiological events. This chapter provides a brief overview of the challenges that faced researchers in protein phosphatases in years past and highlights numerous state-of-the-art techniques (described in greater detail in other chapters in this volume) available to today's scientists. These methods should equip investigators with a rich toolbox of reagents and techniques and promise a brighter future for the study of eukaryotic protein phosphatases. These experimental approaches should also facilitate future investigations directed at unraveling the role of phosphatases in signaling networks in human health and disease.

Key Words: Phosphorylation; phosphoproteins; phosphatases; signaling; networks

1. Introduction

Nearly a century after the discovery of the first protein containing a covalently bound phosphate, it has become apparent that more than a third of all eukaryotic cellular proteins undergo reversible phosphorylation. Almost all of these phosphoproteins are subject to modifications on multiple serines, threonines, and tyrosines. The covalent modifications allow cells to translate a wide variety of environmental signals into functional changes in cellular proteins and, thus, orchestrate the physiological response that dictates cell growth and viability. A growing appreciation of the complex signaling networks present in all eukaryotic systems has also meant that even after decades of groundbreaking

research, we lack a full understanding of the protein phosphorylation–dephosphorylation events that control cell function and physiology. However, sequencing of multiple genomes over the last 5 yr has now provided us with a large complement of molecular tools and innovative approaches for analyzing cellular protein phosphorylation. This should accelerate future studies of cell signaling pathways that define human health and disease.

2. Genome Devoted to Protein Kinases and Phosphatases

Alterations in the phosphorylation state of a cellular protein induced in response to any environmental stimulus reflect changes in the activities of the protein kinases and phosphatases that act on this protein. In this regard, a total of 518 human genes encode protein kinases. Of these, 90 genes encode kinases that modify their substrates on tyrosine residues. Identification of viral genes (or oncogenes) that encoded protein tyrosine kinases and were the causative agents of human and rodent tumors first drew attention to this family of protein kinases. The remarkable observation was made that the viral genes encoding protein tyrosine kinases were highly homologous to mammalian genes, termed proto-oncogenes, that regulated normal cell physiology. Later studies showed that the viral genes encoding mutant or activated forms of the tyrosine kinases were “highjacked” from the host genome and, thus, enhanced growth of the host cells to promote viral expansion. It is worth noting that phosphotyrosines account for at most approx 3% of the total protein-bound phosphate in cells transformed by the oncogenic viruses. However, this small fraction represents a nearly 10-fold increase in the cellular phosphotyrosine content seen in normal or nontransformed cells and is sufficient to elicit dramatic changes in cell growth, metabolism, migration, and morphology. Nevertheless, it was still surprising to find that a significant portion of the human kinome, namely 90 genes, was devoted to the expression of protein tyrosine kinases. Similarly, 107 human genes encode the protein phosphatases that catalyze the dephosphorylation of phosphotyrosines (1,2). This represents a fairly balanced complement of protein tyrosine kinases and phosphatases and suggests an equal partnership of these enzymes in regulating protein tyrosine phosphorylation, and the large number of genes regulating tyrosine phosphorylation might simply highlight the importance of this covalent modification in human health and disease.

The majority of protein phosphorylation (>99%) in normal healthy tissues occurs on serines and threonines and is catalyzed by the remaining 428 protein serine/threonine kinases. The serine/threonine kinases are structurally related to tyrosine kinases and suggest a divergent evolution of the kinome. By comparison, a small number of human genes, approx 15, encode the catalytic subunits of protein serine/threonine phosphatases (3). These enzymes are both structurally and mechanistically distinct from the tyrosine phosphatases and

provide evidence of convergent evolution. The fewer protein serine/threonine phosphatases imply that these enzymes must display much broader substrate specificity than the complementary kinases. Indeed, *in vitro* biochemical studies confirm that the catalytic subunits of all known protein serine/threonine phosphatases dephosphorylate multiple phosphoproteins and phosphorylation sites. These findings labeled protein serine/threonine phosphatases as “pleotropic.” However, physiological studies have shown that hormones, growth factors, and other physiological stimuli modulate a subset of phosphorylation events to regulate selected aspects of mammalian cell physiology. Moreover, studies over the last 20 yr show that these physiological stimuli modulate the activities of both protein kinases and phosphatases. Although this suggested that coordinate regulation of protein kinases and phosphatases is essential for controlling physiological events, it raised a significant challenge for experimental biologists in understanding how functional alterations in “pleotropic” enzymes, such as the protein serine/threonine phosphatases, could lead to selective regulation of mammalian physiology.

Whereas the above discussion refers to a vast majority of known protein phosphatases, recent work has highlighted members of the haloacid dehydrogenase (HAD) superfamily (found in prokaryotes and eukaryotes) as novel protein phosphatases. Prior work had shown that some HAD family members could dephosphorylate phosphoamino acids, specifically phosphoserines, *in vitro*. However, their potential to dephosphorylate phosphoproteins had not been fully investigated. Recent studies in flies and mammals (4–7) have identified a protein component of a transcriptional complex termed Eyes Absent or Eya, that contains a HAD domain and represents a novel class of protein tyrosine phosphatases. Eya represents the first transcription factor with associated protein phosphatase activity and plays a key role in eye development in the fruit fly. Functional disruption of the human EYA1 gene has been linked with the branchio-oto-renal syndrome (8). More recent studies (9,10) identified chronophin as a highly selective cofilin phosphatase containing a HAD domain. In this case, however, the HAD domain specifically dephosphorylated a phosphoserine. These data hint at the future discovery of additional functionally selective or dedicated protein phosphatases, which will not be discussed in this volume.

3. Structure and Regulation of Protein Phosphatases

Most protein tyrosine phosphatases share a common catalytic mechanism involving the formation of a phospho-intermediate at a conserved catalytic cysteine (1) and can be broadly divided into transmembrane receptor protein tyrosine phosphatases or soluble protein tyrosine phosphatases. Expression of protein tyrosine phosphatases in cultured cells suggested a significant

functional redundancy in these enzymes, as multiple phosphatases were shown to dephosphorylate specific phosphoproteins. The generation of substrate-trapping mutants of a number of different tyrosine phosphatases that bound but failed to dephosphorylate cellular substrates also highlighted their ability to trap similar phosphoproteins. However, more recent genetic studies that have functionally inactivated tyrosine phosphatase genes have begun to suggest that the apparent redundancy displayed by these enzymes could be the result of their overexpression in mammalian cells and that in mammalian tissues, they also served unique functions ([11](#)).

Protein (serine/threonine) phosphatase catalytic subunits are cation-dependent enzymes that can be further differentiated by their subunit composition, in vitro substrate specificity, divalent cation requirement, and sensitivity to various protein inhibitors ([12](#)). These criteria classified the eukaryotic serine/threonine phosphatase into two broad categories, namely type-1 or PP1 ([13](#)) and several Type-2 phosphatases, including PP2A ([14](#)), PP2B, and PP2C. Molecular cloning subsequently identified additional PP2A-like enzymes, termed PP4 ([15](#)), PP5 ([16](#)), PP6, and PP7. Moreover, multiple genes encoding the individual phosphatases have been identified in different species, hinting at a level of functional complexity that is not apparent in prior biochemical studies. For example, 3 human genes (alternate splicing of the human PP1 γ gene yields two distinct isoforms, PP1 γ 1 and PP1 γ 2), 4 *Drosophila* genes, and 7–11 genes in plants ([17](#)) encode PP1 catalytic subunits and 38 PP1 genes have been predicted in the *Caenorhabditis elegans* genome (see www.wormbase.org). The most dramatic example of gene duplication of phosphatases is the finding that in the complete *Arabidopsis* genome, 70 genes encode PP2C. Although the phosphatase isoforms share a conserved catalytic core, they demonstrate significant variability in their amino- and carboxyl-terminal sequences, which might contribute their unique function and regulation.

Although extensive in vitro studies have shown indistinguishable biochemical characteristics of different recombinant PP1 isoforms, genetic manipulations of individual PP1 genes have been undertaken in genetically tractable organisms, such as fruit fly, yeast, and, to a lesser degree, mouse ([18](#)). These studies have highlighted the distinct phenotypes associated with the loss-of-function of individual PP1 isoforms and strongly suggested that the PP1 isoforms controlled distinct physiological events in these eukaryotic organisms. Indeed, extensive mutational analysis of the single gene, GLC7, encoding the PP1 catalytic subunit in *Saccharomyces cerevisiae* also highlighted multiple alleles, indicating that the mutations compromised a subset of PP1 functions in the budding yeast. Together, these data hinted at additional regulatory components recognized by the individual PP1 isoforms that expanded the diversity of PP1 functions in all eukaryotic cells.

Thus, we now know that the modest structural differences among the individual phosphatase isoforms direct their selective association with regulatory subunits and represent a simple and widely utilized paradigm for increasing the functional diversity of most protein serine/threonine phosphatases. In this regard, the number of multiprotein complexes that account for PP1 activity in mammalian cells may exceed well over 50 enzymes (13) and more than 100 different complexes may represent mammalian PP2A activity (14). The regulatory subunits direct the localization of the endogenous phosphatase (19) or can relocalize ectopically expressed phosphatase (20–22), highlighting a critical role of these regulators in defining the subcellular distribution of the phosphatase catalytic subunits. In addition, the regulators severely restrict the substrate specificity of the phosphatase (13), promoting the dephosphorylation of phosphoproteins that often colocalize with the phosphatase in cells.

Interestingly, emerging studies suggest direct association of some protein phosphatases with protein kinases to create a potential autoregulatory module. In some of these complexes, the kinase phosphorylates the phosphatase to transiently suppress its function. Conversely, the phosphatase can counteract the kinase activity by dephosphorylating phosphoamino acids in the “activation loop,” thereby functioning as a timer for transient downstream phosphorylation events. Yet other kinase–phosphatase complexes utilize intermediate protein scaffolds (23). This allows the signaling complex to recruit additional proteins, specifically those that might act as common substrates for the kinase and the phosphatase. Such kinase–phosphatase complexes function as integrated nanomachines that allow for a rapid signaling response and regulation of cellular functions.

Many phosphatase catalytic subunits and most regulators or scaffolds are themselves phosphoproteins. These covalent modifications provide for changes in the affinity and function of the assembled phosphatase complex (24), the assembly and disassembly of these signaling complexes, and/or dynamic localization of the phosphatase complex in specific subcellular compartments (25). The reversal of covalent modifications of such phosphatase complexes could occur via autocatalysis by the integrated phosphatase or via other phosphatases not incorporated in these complexes or not sensitive to these regulators. This generates phosphatase signaling cascades whereby activation of one phosphatase can amplify the function of another downstream phosphatase. Finally, altered expression of phosphatase regulators and their regulated assembly into functional phosphatase complexes might represent additional mechanisms for tight physiological control of protein phosphatases. Together, these mechanisms allow for highly sophisticated regulation of protein phosphatases in complex signaling networks that integrates the cellular response to any changing environment.

4. Small-Molecule Phosphatase Inhibitors

Because protein phosphatases play key roles in regulating diverse physiological events as cell division, metabolism, migration, transcription, and translation, it comes as no surprise that they have been targeted by toxins produced by a variety of micro-organisms that compete for survival in a shared environment. The known environmental toxins or xenobiotics possess diverse chemical structures but potently inhibit protein phosphatases to elicit deleterious effects in mammalian cell physiology. This also provides us with a wide array of cell-permeable small-molecule inhibitors as tools for investigating the role of phosphatases in cell signaling (26). Some microbial products, such as cyclosporin A and FK506, that inhibit PP2B activity have become very effective medicines and are currently the most effective immunosuppressive agents available. This suggests that phosphatase inhibition should enhance signaling by protein kinases and provide treatments for many endocrine disorders. This has prompted major efforts by pharmaceutical companies to identify small-molecule modifiers of protein phosphatases as potential therapeutic agents (27,28). Whether all of these compounds will become useful medicines remains unclear. However, the availability of a plethora of pharmacological and genetic tools to manipulate cellular phosphatases should further accelerate future studies on the biology of these enzymes.

5. Concluding Remarks

This volume outlines many of the key techniques required to analyze protein phosphatases. The following chapters will describe methods for the purification of protein phosphatases, assays for their catalytic function, identification and analysis of regulatory components, and the genetic and functional modulation of phosphatases in eukaryotic cells. Together with the ability to image the dynamic movement of phosphatases in living cells, these methods should equip future experimentalists with better tools to investigate the physiological mechanisms that control the function of protein phosphatases, direct their substrate recognition and subcellular localization, and define their role in cell signaling in human health and disease.

References

1. Alonso, A., Sasin, J., Bottini, et al. (2004) Protein tyrosine phosphatases in the human genome. *Cell* **117**, 699–711.
2. Anderson, J. N., Del Vecchio, R. L., Kannan, N., Gergel, J., Neuwald, A. F., and Tonks, N. K. (2004) Computational analysis of protein tyrosine phosphatases: practical guide to bioinformatics and data resources. *Methods* **35**, 90–114.
3. Cohen, P. and Cohen, P. T. (1989) Protein phosphatases come of age. *J. Biol. Chem.* **264**, 21,435–21,438.

4. Epstein, J. A. and Neel, B. G. (2003) Studies in flies and mice have revealed a surprising way in which cells regulate gene activity, with consequences for our understanding of organ formation during development. *Nature* **236**, 238–239.
5. Li, X., Oghi, K. A., Zhang, J., et al. (2003) Eya protein phosphatase activity regulates Six1-Dach-Eya transcriptional effects in mammalian organogenesis. *Nature* **426**, 247–254.
6. Rayapureddi, J. P., Kattamuri, C., Steinmetz, B. D., et al. (2003) Eyes absent represents a class of protein tyrosine phosphatases. *Nature* **426**, 295–298.
7. Tootle, T. L., Silver, S. J., Davies, E. L., et al. (2003) The transcription factor Eyes absent is a protein tyrosine phosphatase. *Nature* **426**, 299–302.
8. Kim, S. H., Shin, J. H., Yeo, C. K., et al. (2005) Identification of a novel mutation in the EYA1 gene in a Korean family with branchio-oto-renal (BOR) syndrome. *Int. J. Pediatr. Otorhinolaryngol.* **69**, 1123–1128.
9. Wiggan, O., Bernstein, B. W., and Bamburg, J. R. (2005) A phosphatase for cofilin to be HAD. *Nature Cell. Biol.* **7**, 8–9.
10. Gohal, A., Birkenfeld, J., and Bokoch, G.M. (2005) Chronophin, a novel HAD-type serine protein phosphatase, regulates cofilin-dependent actin dynamics. *Nature Cell. Biol.* **7**, 21–29.
11. Stoker, A. W. (2005) Protein tyrosine phosphatases and signaling. *J. Endocrinol.* **185**, 19–33.
12. Shenolikar, S. and Nairn, A. C. (1991) Protein phosphatases : recent progress. *Adv. Second Messenger Phosphoprotein Res.* **23**, 1–121.
13. Ceulemans, H. and Bollen, M. (2003) Functional diversity of protein phosphatase-1, a cellular economizer and reset button. *Physiol. Rev.* **84**, 1–39.
14. Janssens, V. and Goris, J. (2001) Protein phosphatase 2A: a highly regulated family of serine/threonine phosphatases implicated in cell growth and signaling. *Biochem. J.* **353**, 417–439.
15. Cohen, P. T. W., Philp, A., and Vasquez-Martin, C. (2005) Protein phosphatase 4—from obscurity to vital functions. *FEBS Lett.* **579**, 3278–3286.
16. Bakkenist, C. J. and Kastan, M. B. (2004) Phosphatases join kinases in DNA-damage response pathways. *Trends Cell. Biol.* **14**, 339–341.
17. Luan, S. (2003) Protein phosphatases in plants. *Annu. Rev. Plant Biol.* **54**, 63–92.
18. Shenolikar, S. (1994) Protein phosphatases—new avenues for cell regulation. *Annu. Rev. Cell Biol.* **10**, 55–86.
19. Brush, M. H., Weiser, D. C., and Shenolikar, S. (2003) The growth arrest and DNA-damage-inducible gene product, GADD34, targets protein phosphatase-1 to endoplasmic reticulum and promotes the dephosphorylation of α -subunit of the eukaryotic translation initiation factor 2. *Mol. Cell. Biol.* **23**, 1292–1303.
20. Trinkle-Mulcahy, L., Sleeman, J. E., and Lamond, A. I. (2001) Dynamic targeting of protein phosphatase 1 within the nuclei of living mammalian cells. *J. Cell Sci.* **114**, 4219–4228.
21. Trinkle-Mulcahy, L., Andrews, P. D., Wickramasinghe, S., et al. (2003) Time-lapse imaging reveals dynamic relocation of PP1 γ throughout the mammalian cell cycle. *Mol. Biol. Cell* **14**, 107–117.

22. Lesage, B., Beullens, M., Nuytten, M., et al. (2004) Interactor-mediated nuclear translocation and retention of protein phosphatase-1. *J. Biol. Chem.* **279**, 55,978–55,984.
23. Bauman, A. L. and Scott, J. D. (2002) Kinase- and phosphatase-anchoring proteins: harnessing the dynamic duo. *Nature Cell Biol.* **4**, 203–206.
24. Oliver, C. J. and Shenolikar, S. (1998) Physiological importance of protein phosphatase inhibitors. *Front. Biosci.* **3**, 961–972.
25. Cohen, P. T. W. (2002) Protein phosphatase 1—targeted in many directions. *J. Cell Sci.* **115**, 241–256.
26. Fernandez, J. J., Cadenas, M. I., Souto, M. I., Trujillo, M. M., and Norte, M. (2002) Okadaic acid, useful tool for studying cellular processes. *Curr. Med. Chem.* **9**, 229–262.
27. Schmid, A. C. and Woscholski, R. (2004) Phosphatases as small molecule targets: inhibiting the endogenous inhibitors of kinases. *Biochem. Soc. Trans.* **32**, 348–349.
28. Honkanen, R. E. and Golden, T. (2002) Regulators of serine/threonine protein phosphatases at the dawn of a clinical era? *Curr. Med. Chem.* **9**, 2055–2075.

A Brief Introduction to the Protein Phosphatase Families

Tomas Mustelin

Summary

This chapter introduces the main families of protein phosphatases encoded by the human genome and discusses their classification, overall structure, regulation, and physiological functions in human health and diseases. The topics of redundancy, diversity, and dynamic expression in individual cell types are briefly introduced, and the importance of technological approaches to phosphatase research is emphasized.

Key Words: Protein phosphatases; PTPs, DSPs; HAD family; drug targets

1. Introduction

Protein phosphorylation is a fundamental mechanism for numerous important aspects of eukaryote physiology, as well as human health and disease (*1–4*). It has been estimated that at least one-third of cellular proteins contain covalently bound phosphate. Among the many phospho-acceptor amino acids, serine phosphorylation is the most prevalent, whereas tyrosine phosphorylation (*5*) stands out as a feature of higher eukaryotes, where it is used as a regulatory mechanism in cell-to-cell communication and functions that coordinate the behavior of cell populations within these multicellular organisms (*1*). However, tyrosine phosphorylation has recently also been found in bacteria and *Archaea* (*6–8*), the sequenced genomes of which usually contain several genes for PTPs. Thus, tyrosine phosphorylation might have flourished in more recent evolution, but its roots lay very far back. Bacterial genomes also contain Ser/Thr phosphatases, but usually lack eukaryote-type protein kinases. Instead, there are protein kinases of a different kind, which are not found in mammals. Nevertheless, it seems that protein phosphorylation is not nearly as central a regulatory mechanism in prokaryotes as it is in eukaryotes.

With some very rare possible exceptions, protein phosphorylation is a reversible posttranslational modification catalyzed by protein kinases and reversed by protein phosphatases. Thus, the state of phosphorylation of a protein, at a given moment in time, is the net result of the opposing activities of the relevant kinase(s) and phosphatase(s). A change in phosphorylation state can be the result of a change in the activity (or access) of either enzyme. Particularly in the realm of tyrosine phosphorylation, a general rule is that the balance is skewed very far toward the dephosphorylated state: Most tyrosine phosphorylated proteins are phosphorylated to a stoichiometry of only a few percent even under the most extreme inducing conditions and are often not phosphorylated at all under “resting” conditions. Thus, one could argue that phosphatases are more important than kinases in setting the levels of protein phosphorylation and that they should be much better drug targets. Indeed, phosphatases often play very specific, nonredundant, highly regulated, and very active roles in many cellular processes (9–17). Phosphatases are also often “positive” components of signaling events (18–20) and many phosphatase knockout mice have unique and complex phenotypes (21–30). Finally, the completion of the human genome has demonstrated that (1) there are more tyrosine phosphatases than tyrosine kinases (3,31), (2) the possible number of Ser/Thr phosphatase holoenzymes, generated by a combinatorial mechanism, far exceeds the number of all protein kinases (32), and (3) there are additional large families of protein phosphatases, such as the haloacid dehalogenase (HAD) family, and possibly others.

2. The Many Families of Protein Phosphatases

Based on structure, rather than function, the protein phosphatases can be classified into several completely separate families (*see Table 1*) that do not share any structural similarities and apparently evolved independently from different ancestral folds. Naturally, we cannot exclude the possibility that some of these folds may have evolved from one another at an ancient time beyond the abilities of bioinformatics tools to resolve. It is important to note that this newer structural classification overlaps, but does not coincide, with the older classification of protein phosphatases by substrate specificity into Ser/Thr-specific, Tyr-specific, and dual-specific phosphatases. Particularly, the so called dual-specific phosphatases (DSPs) (3) include many enzymes that are highly specific for Tyr, Ser, phosphoinositides, or mRNA. There are also examples of “Ser/Thr phosphatases” that dephosphorylate Tyr and enzymes that can dephosphorylate more than one type of substrate. Clearly, evolution cares little for our desires for simplicity and classification. In fact, the many solved crystal structures of protein phosphatases demonstrate that subtle alterations in structure can drastically alter substrate specificity (e.g., from

Table 1
Phosphatase Families

Phosphatase families	Examples of members
1. PPM family	PP2C
2. FCP family	FCP
3. PPP family	PP1, PP2A, calcineurin, PP5
4. HAD family (Asp-based)	Eya, CTD, cronophin
5. Class I Cys-based PTPs	
5.1. Classical PTPs	
5.1.1. Transmembrane PTPs	PTP α , CD45, CD148, IA-2, GLEPP1
5.1.2. NRPTPs	PTP1B, TCPTP, SHP1, LYP, MEG2
5.2. DSPs or VH1-like PTPs	
5.2.1. MKPs	MKP1–5, MKP7, PAC1
5.2.2. Atypical DSPs	VHR, PIR, Laforin, VHZ, STYX
5.2.3. Slingshots	SSH1, SSH2, SSH3
5.2.4. PRLs	PRL-1, PRL-2, PRL-3
5.2.5. CDC14s	CDC14A, KAP, PTP9Q22
5.2.6. PTENs	PTEN, TPIP, tensin, C1ten
5.2.7. Myotubularins	MTM1, MTMR1–15
6. Class II Cys-based PTPs	CDC25A, CDC25B, CDC25C
7. Class III Cys-based PTPs	LMPTP

phosphoamino acid to phospholipid; *see* **refs. 33** and **34**) and that the same substrate specificity can be achieved in many different ways.

The Ser/Thr phosphatases have been classified into three structurally distinct families: (1) the PPM family of Mg²⁺-dependent phosphatases, including PP2C, (2) the Mg²⁺-dependent FCP family, and (3) the PPP family, which is the largest and contains the well-known enzymes PP1, PP2A, PP2B (calcineurin), PP5, and many others (**32**). Altogether there are 25–30 genes for catalytic subunits of these enzymes in the human genome. In addition, there are numerous regulatory subunits, which participate in the formation of heterodimeric or trimeric phosphatase holoenzymes with unique substrate specificities, regulatory mechanisms, subcellular locations, and physiological functions (**32**).

We defined PTPs as the proteins with structural homology to the catalytic domains of any of the known enzymes with PTP activity, regardless of their specificity (**3**). There are four evolutionary distinct families of such genes: the class I, II, and III Cys-based PTPs, and the Asp-based phosphatases, exemplified by the Eya (eyes absent) tyrosine phosphatases (**14**). These Asp-based PTPs are part of the HAD family, which is now emerging as a very large protein family with representatives in plants (**35**), prokaryotes (**36**), and mammals

and includes numerous enzymes with other than Tyr-specificity — indeed, with a broader substrate spectrum than hydroxyl-containing amino acid residues in proteins, such as phospholipids (37), sugars (38), nucleotides (39), and epoxides (40). The protein phosphatases of the HAD family can be specific for tyrosine (14) or serine, as in the case of the cofilin phosphatase chronophin (41) and RNA polymerase C-terminal phosphatase (42). Several crystal structures of HAD family phosphatases have already been reported (43–46) and a more definitive picture of this family is now emerging.

Class I Cys-based PTPs are structurally related to the first PTP PTP1B, whose amino acid sequence was determined (47). There are at least 99 members of this family in the human genome (3) and they can be further subclassified into the classical PTPs (receptorlike and nonreceptor), and the VH1-like phosphatases, which contain the mitogen-activated protein (MAP) kinase phosphatase (MKPs), the atypical DSPs, the slingshots, the PRLs, the CDC14s, the PTEN group, and the myotubularins. The two latter dephosphorylate inositol phospholipids (48,49). Within all of these homologous phosphatases, it appears that the atypical DSPs represent the evolutionary most ancient members of the family. Genes with a high degree of similarity can be found across all kingdoms of life, including *Archaea* and plants (50). In contrast, the classical PTPs, particularly the receptorlike group, seem to be more recent groups that have flourished and diversified in multicellular organisms.

The class II Cys-based protein phosphatases comprise a small group of cell-cycle regulators known as the CDC25 phosphatases. Although their catalytic machinery is very similar to the class I enzymes, they are structurally unrelated and, instead, bear considerable resemblance to bacterial rhodanese enzymes (51), and are thought to have evolved relatively late in eukaryote evolution. Interestingly, the MAP kinase phosphatases, which belong to the class I family, have incorporated a catalytically inactive rhodaneselike domain, which functions as a MAP kinase docking module (52). This creates a region of homology between the CDC25s and the MAP kinases, which, however, is not indicative of a common ancestry of their catalytic domains.

The class III Cys-based protein phosphatases are widely distributed in all kingdoms of life and most bacteria have the genes for one or two such enzymes in their genomes. In *Escherichia coli*, one such phosphatase regulates the tyrosine phosphorylation of a transmembrane tyrosine autokinase, which regulates synthesis of polysaccharides of the bacterial capsule (53). In the Gram-negative *Bacillus subtilis*, the two class III phosphatases YfkJ and YwIE have clearly distinct properties and bacterial knockout strains have distinct phenotypes (54). The human genome contains a single gene for a class III PTP, the low-*Mr* PTP (LMPTP), which undergoes alternative splicing to yield two active and one inactive isoforms. Although a polymorphism in this gene correlates with

numerous common human diseases (4), the function of LMPTP has remained obscure.

3. Single-Chain Multidomain Versus Single-Domain Multi-Subunit Organization

As mentioned above, many PTPs are larger proteins with multiple modular domains, whereas Ser/Thr phosphatases consist of catalytic polypeptides that can associate with several different regulatory or targeting subunits, resulting in numerous different holoenzymes. Thus, the end result is similar, but one cannot help wondering why the strategies are so different. What are the advantages of each strategy? Are single-chain multidomain enzymes more strictly regulated? Does a combinatorial mechanism allow for more flexibility in cellular responses? The completion of many genomic sequencing projects has revealed that the number of PTP genes has increased during evolution, whereas the number of Ser/Thr phosphatases has remained nearly constant. Instead, the number of regulator/targeting subunits has increased sharply in eukaryote evolution (17). Perhaps the large increase in protein phosphorylation during early evolution outpaced the diversification of Ser/Thr phosphatase domains and, instead paradoxically, led to a situation in which a few phosphatase catalytic domains with broad substrate specificity fulfill the need better, as long as their regulation and targeting is taken into account.

4. Regulation of Phosphatases

Both Ser/Thr phosphatases and PTPs seem to be regulated to a large extent by similar mechanisms, which are also shared by protein kinases, namely by protein–protein and protein–phospholipid interactions. Both targeting to substrate-containing locations or complexes and direct allosteric modulation of the catalytic domain/subunit seem to play important roles. Catalytic activation is often accomplished by the removal of pseudosubstrate motifs or blocking regulatory subunits/domains from the active site of the phosphatase as a result of interaction of the holoenzyme with ligands or phospholipids. Another interesting aspect of regulation is the abundance of catalytically inactive PTP domains (approx 10% of all PTPs), which often partner with active PTPs and perform crucial regulatory or targeting functions. Good examples of this is provided by many receptorlike PTPs, which have two tandem catalytic domains in their intracellular C-terminus. In most cases, the second domain has less than 1% as much activity as the first (membrane-proximal) domain; in some PTPs, the second domain does not even have the catalytic cysteine. Nevertheless, in many cases, the second domain is still crucial for the physiological function of the phosphatase (55). Another striking example can be found within the myotubularins: whereas many patients with the inherited nerve myelina-

tion disease Charcot–Marie–Tooth syndrome type 4B have a debilitating mutation in the class I Cys-based phosphatase myotubularin-related protein 2 (*MTMR2*) (56), a subset of patients were found to have a mutation in the catalytically inactive phosphatase *MTMR13* (57). In both cases, the disease is the same, raising the question of how the loss of an inactive phosphatase can lead to the same disease as the loss of an active phosphatase. The answer to this puzzle was provided by the discovery that the two proteins form a heterodimer, in which the catalytically inactive *MTMR13* provides critical aid to the function of the active *MTMR2*.

Phosphatases are often phosphorylated themselves, suggesting that they are also substrates for protein kinases and phosphatases and can be part of kinase cascades, phosphatase cascades, or mixed cascades. Dephosphorylation of phosphatases can occur by autocatalysis, but in some cases (e.g., VHR), the phosphorylated residue is not accessible to the catalytic pocket of the same molecule and therefore dephosphorylation must occur either *in trans* or by another PTP. As with many other signaling molecules, tyrosine phosphorylation of phosphatases is typically of very low stoichiometry and difficult to study. Nevertheless, there are a few examples where tyrosine phosphorylation of a PTP is of regulatory importance, such as the cases of RPTP α (58), LMPTP (59), VHR (60). Phosphotyrosine can also be found in dozens of other phosphatases, but is still in most cases of unknown physiological relevance.

5. How Many Phosphatase Are There in a Cell?

Although it has become increasingly apparent that phosphatases often have a high degree of specificity and that there are so many phosphatase genes in the human genome, the question of functional redundancy is still largely unresolved. It is probably prudent to assume that closely related phosphatases have at least partly overlapping sets of substrates. There is some evidence for this, for example, from mouse knockouts where the phenotype has been milder than expected [e.g., MKP1 (61) or PEP (62)]. A more systematic analysis of redundancy is complicated by issues of tissue expression profile, relative expression levels, and differential regulation of expression during embryogenesis and development. An alternative approach to study the question of redundancy is to take a given cell and first ask how many of the existing phosphatase genes are expressed in it and then study this set (e.g., by RNA interference). From preliminary analysis carried out in our laboratory, it seems that each cell type expresses a surprisingly large portion of the 107 PTP genes (the “PTPome”); for example, monocytes and T-lymphocytes express at least 68 PTPs each, whereas B-cells contain over 70. The set expressed in each cell type is unique (albeit overlapping) both in terms of which PTPs are expressed and in their relative expression levels. The entire set responds with both qualitative and

quantitative changes to many external stimuli, cell activation, differentiation, and so forth. Interestingly, each stimulus elicits a unique response and identical stimuli elicit somewhat different responses in different cells, even when they are closely related. Finally, the PTP expression profile is somewhat different in identical cell types from different individuals. All of these levels of complexity will need to be considered when studying the extent of possible redundancy of phosphatases.

6. Protein Phosphatases and Human Disease

Whether phosphatases exhibit some overlaps in function or not, it is clear that even subtle alterations in many of them can cause human disease (2,3). As might be expected, loss of phosphatases has been reported in cancer: The list contains over 30 different PTPs and loss can occur by genetic (e.g., chromosomal abnormalities, frame-shift mutations, or point mutations) or epigenetic (e.g., promoter methylation or changes in transcription) mechanisms. More interestingly, several phosphatases have been found to be overexpressed in human malignancies, such as PRL3 in metastatic colon cancer (63).

Phosphatases are also implicated in inherited genetic diseases, including Noonan syndrome (SHP2; 64), Lafora's epilepsy (laforin; 65), muscle dystrophies (myotubularin; 66), and immunodeficiencies (CD45; 67,68), as well as in autoimmune diabetes (LYP; 69–71, and PTPRN; 72) and other major autoimmune diseases (LYP; 73–75), and myelodysplastic syndrome and acute myeloblastic leukemia (SHP1; 76, and HePTP; 77,78). Also, PP2A has been implicated in a monogenic disorder, Opitz BBB/G syndrome (79), which is characterized by malformations of the ventral midline, as well as in tumorigenesis (80,81). Given the broad significance of protein phosphorylation and the very limited studies performed so far, I predict that a very large number of human health concerns will be found to involve a central role for protein phosphatases. I also predict that the pharmaceutical industry will become increasingly interested in phosphatases as drug targets. In fact, this trend is already evident (82–91).

7. Concluding Remarks

The mission of my laboratory is to make the scientific community more familiar with the PTPs and their importance in human health and disease. We strive to elucidate the molecular mechanisms of PTP function in normal as well as pathological cellular processes and to explore the value of individual PTPs as drug targets. Over the years, I have come to value the inclusion of multiple phosphatases in each experiment and a more unbiased comparison of enzymes, rather than a strict focus on a single one at a time. We often ask “Which phosphatase does this?” rather than “What does this phosphatase do?”

This approach not only gives a better insight into questions of specificity vs redundancy, but often reveals unexpected or novel functions. I believe that the time has come to consider and analyze entire families of phosphatases.

This volume of *Methods in Molecular Biology* addresses a perceived obstacle in phosphatase research: the notion that phosphatases are technically difficult to study. Not so, there are numerous well-established techniques and protocols, as well as an increasingly complete coverage of antibodies and plasmids, plus many new avenues, such as small-molecule inhibitors, activity-based probes (92), and technologies for RNA interference and “substrate-trapping” mutants. I hope that this volume of *Methods in Molecular Biology* will entice more researchers to enter the field of protein phosphatases and will stimulate work with the numerous enzymes that so far have received little attention.

Acknowledgments

I thank the members of my laboratory, as well as Nunzio Bottini, Michael David, Jack Dixon, Rob Edwards, Gen-Sheng Feng, Adam Godzik, Andrei Osterman, Maurizio Pellecchia, Robert Rickert, Zhong-Yin Zhang, and many other colleagues and friends for many stimulating discussions about phosphatases and I apologize to all colleagues whose excellent papers I could not cite here due to space limitations. This work was supported by grants AI35603, AI48032, AI53114, AI53585, AI55741, AI55789, and CA96949 from the National Institutes of Health.

References

1. Hunter, T. (1998) The role of tyrosine phosphorylation in cell growth and disease. *Harvey Lect.* **94**, 81–119.
2. Andersen, J. N., Jansen, P. G., Echwald, S. M., et al. (2004) A genomic perspective on PTPs: gene structure, pseudogenes, and genetic disease linkage. *FASEB J.* **18**, 8–13.
3. Alonso, A., Sasin, J., Osterman, A., et al. (2004) The PTPs in the human genome. *Cell* **117**, 699–711.
4. Bottini, N., Bottini, E., Gloria-Bottini, F., and Mustelin, T. (2002) LMPTP and human disease: in search of biochemical mechanisms. *Arch. Immunol. Ther. Exp. (AITE)* **50**, 95–104.
5. Hunter, T. and Sefton, B. M. (1980) Transforming gene product of Rous sarcoma virus phosphorylates tyrosine. *Proc. Natl. Acad. Sci. USA* **77**, 1311–1315.
6. Chow, K., Ng, D., Stokes, R., and Johnson, P. (1994) Protein tyrosine phosphorylation in *Mycobacterium tuberculosis*. *FEMS Microbiol. Lett.* **124**, 203–207.
7. Kennelly, P. J. (2003) Archaeal protein kinases and protein phosphatases: Insights from genomics and biochemistry. *Biochem. J.* **370**, 373–389.
8. Cozzone, A. J., Grangeasse, C., Doublet, P., and Duclos, B. (2004) Protein phosphorylation on tyrosine in bacteria. *Arch. Microbiol.* **181**, 171–181.

9. Walton, K. M. and Dixon, J. E. (1993) Protein tyrosine phosphatases. *Annu. Rev. Biochem.* **62**, 101–120.
10. Tonks, N. K. and Neel, B. G. (1996) From form to function: signaling by PTPs. *Cell* **87**, 365–368.
11. Mustelin, T., Vang, T., and Bottini, N. (2005) Protein tyrosine phosphatases and the immune response. *Nat. Rev. Immunol.* **5**, 43–57.
12. Stoker, A. W. (2005) Protein tyrosine phosphatases and signaling. *J. Endocrinol.* **185**, 19–33.
13. Kappert, K., Peters, K. G., Bohmer, F. D., and Ostman, A. (2005) Tyrosine phosphatases in vessel wall signaling. *Cardiovasc. Res.* **65**, 587–598.
14. Rebay, I., Silver, S. J., and Tootle, T. L. (2005) New vision from Eyes absent: transcription factors as enzymes. *Trends Genet.* **21**, 163–171.
15. Wong, W. and Scott, J. D. (2004) AKAP signalling complexes: focal points in space and time. *Nat. Rev. Mol. Cell. Biol.* **5**, 959–970.
16. Cohen, P. T. (2002) Protein phosphatase 1: targeted in many directions. *J. Cell. Sci.* **115**, 241–256.
17. Ceulemans, H. and Bollen, M. (2004) Functional diversity of protein phosphatase-1, a cellular economizer and reset button. *Physiol. Rev.* **84**, 1–39.
18. Feng, G. S. (1999) Shp-2 tyrosine phosphatase: Signaling one cell or many. *Exp. Cell Res.* **253**, 47–54.
19. Mustelin, T., Coggeshall, K. M., and Altman, A. (1989) Rapid activation of the T cell tyrosine protein kinase pp56lck by the CD45 phosphotyrosine phosphatase. *Proc. Natl. Acad. Sci. USA.* **86**, 6302–6306.
20. Bottini, N., Stefanini, L., Williams, S., et al. (2002) Activation of ZAP-70 through specific dephosphorylation at the inhibitory Tyr-292 by the low molecular weight phosphotyrosine phosphatase (LMPTP). *J. Biol. Chem.* **277**, 24,220–24,224.
21. Cote, J. F., Charest, A., Wagner, J., and Tremblay, M. L. (1998) Combination of gene targeting and substrate trapping to identify substrates of PTPs using PTP-PEST as a model. *Biochemistry* **37**, 13,128–13,137.
22. Saxton, T. M., Henkemeyer, M., Gasca, S., et al. (1997) Abnormal mesoderm patterning in mouse embryos mutant for the SH2 tyrosine phosphatase Shp-2. *EMBO J.* **16**, 2352–2364.
23. Gronda, M., Arab, S., Iafrate, B., Suzuki, H., and Zanke, B. (2001) Hematopoietic PTP suppresses extracellular stimulus-regulated kinase activation. *Mol. Cell. Biol.* **21**, 6851–6858.
24. Elchebly, M., Payette, P., Michaliszyn, E., et al. (1999) Increased insulin sensitivity and obesity resistance in mice lacking the PTP-1B gene. *Science* **283**, 1544–1548.
25. You-Ten, K. E., Muise, E. S., Itie, A., et al. (1997) Impaired bone marrow microenvironment and immune function in T cell PTP-deficient mice. *J. Exp. Med.* **186**, 683–693.
26. Byth, K. F., Conroy, L. A., Howlett, S., et al. (1996) CD45-null transgenic mice reveal a positive regulatory role for CD45 in early thymocyte development in the selection of CD4⁺CD8⁺ thymocytes and B-cell maturation. *J. Exp. Med.* **183**, 1707–1718.

27. Wharram, B. L., Goyal, M., Gillespie, P. J., et al. (2000) Altered podocyte structure in GLEPP1 (Ptpro)-deficient mice associated with hypertension and low glomerular filtration rate. *Clin. Invest.* **106**, 1281–1290.
28. Uetani, N., Kato, K., Ogura, H., et al. (2000) Impaired learning with enhanced hippocampal long-term potentiation in PTPdelta-deficient mice. *EMBO J.* **19**, 2775–2785.
29. Di Cristofano, A., Pesce, B., Cordon-Cardo, C., and Pandolfi, P. P. (1998) Pten is essential for embryonic development and tumour suppression. *Nat. Genet.* **19**, 348–355.
30. Koop, E. A., Gebbink, M. F. B. G., Sweeney, T. E., et al. (2005) Impaired flow-induced dilation in mesenteric resistance arteries from receptor protein tyrosine phosphatase- μ -deficient mice. *Am. J. Physiol. (Heart Circ. Physiol.)* **288**, H1218–H1223.
31. Manning, G., Whyte, D. B., Martinez, R., Hunter, T. and Sudarsanam, S. (2002) The protein kinase complement of the human genome. *Science* **298**, 1912–1934.
32. Schonthal, A. H. (1998) Role of PP2A in intracellular signal transduction pathways. *Front. Biosci.* **3**, D1262–1273.
33. Lee, J. O. Yang, H., Georgescu, M. M., et al. (1999) Crystal structure of the PTEN tumor suppressor: implications for its phosphoinositide phosphatase activity and membrane association. *Cell* **99**, 323–334.
34. Begley, M. J. Taylor, G. S., Kim, S. A., Veine, D. M., Dixon, J. E., and Stuckey, J. A. (2003) Crystal structure of a phosphoinositide phosphatase, MTMR2: insights into myotubular myopathy and Charcot-Marie-Tooth Syndrome. *Mol. Cell* **12**, 1391–1402.
35. Rayapureddi, J. P., Kattamuri, C., Chan, F. H., and Hegde, R. S. (2005) Characterization of a plant, tyrosine-specific phosphatase of the aspartyl class. *Biochemistry* **44**, 751–8.
36. Roberts, A., Lee, S. Y., McCullagh, E., Silversmith, R. E., and Wemmer, D. E. (2005) Ybiv from *Escherichia coli* K12 is a HAD phosphatase. *Proteins* **58**, 790–801.
37. Roberts, S. J., Stewart, A. J., Sadler, P. J., and Farquharson, C. (2004) Human PHOSPHO1 exhibits high specific phosphoethanolamine and phosphocholine phosphatase activities. *Biochem. J.* **382**, 59–65.
38. Allegrini, S., Scaloni, A., Careddu, M. G., et al. (2004) Mechanistic studies on bovine cytosolic 5'-nucleotidase II, an enzyme belonging to the HAD superfamily. *Eur. J. Biochem.* **271**, 4881–4891.
39. Lunn, J. E., Ashton, A. R., Hatch, M. D., and Heldt, H. W. (2000) Purification, molecular cloning, and sequence analysis of sucrose-6F-phosphate phosphohydrolase from plants. *Proc. Natl. Acad. Sci. USA* **97**, 12,914–12,919.
40. Cronin, A., Mowbray, S., Durk, H., et al. (2003) The N-terminal domain of mammalian soluble epoxide hydrolase is a phosphatase. *Proc. Natl. Acad. Sci. USA* **100**, 1552–1557.
41. Gohla, A., Birkenfeld, J., and Bokoch, G. M. (2005) Chronophin, a novel HAD-type serine protein phosphatase, regulates cofilin-dependent actin dynamics. *Nat. Cell Biol.* **7**, 21–29.

42. Yeo, M., Lin, P. S., Dahmus, M. E., and Gill, G. N. (2003) A novel RNA polymerase II C-terminal domain phosphatase that preferentially dephosphorylates serine 5. *J. Biol. Chem.* **278**, 26,078–26,085.
43. Peisach, E., Selengut, J. D., Dunaway-Mariano, D., and Allen, K. N. (2004) X-ray crystal structure of the hypothetical phosphotyrosine phosphatase MDP-1 of the haloacid dehalogenase superfamily. *Biochemistry* **43**, 12,770–12,779.
44. Stewart, A. J., Schmid, R., Blindauer, C. A., Paisey, S. J., and Farquharson, C. (2003) Comparative modelling of human PHOSPHO1 reveals a new group of phosphatases within the haloacid dehalogenase superfamily. *Protein Eng.* **16**, 889–895.
45. Allen, K. N. and Dunaway-Mariano, D. (2004) Phosphoryl group transfer: evolution of a catalytic scaffold. *Trends Biochem. Sci.* **29**, 495–503.
46. Lahiri, S. D., Zhang, G., Dai, J., Dunaway-Mariano, D., and Allen, K. N. (2004) Analysis of the substrate specificity loop of the HAD superfamily cap domain. *Biochemistry* **43**, 2812–2820.
47. Charbonneau, H., Tonks, N. K., Kumar, S., et al. (1989) Human placenta protein-tyrosine phosphatase: amino-acid sequence and relationship to a family of receptor-like proteins. *Proc. Natl. Acad. Sci. USA* **86**, 5252–5256.
48. Maehama, T. and Dixon, J. E. (1998) The tumor suppressor, PTEN/MMAC1, dephosphorylates the lipid second messenger, phosphatidylinositol 3,4,5-trisphosphate. *J. Biol. Chem.* **273**, 13,375–13,378.
49. Wishart, M. J. and Dixon, J. E. (2002) PTEN and myotubularins phosphatases: from 3-phosphoinositide dephosphorylation to disease. *Trends Cell Biol.* **12**, 579–585.
50. Alonso, A., Sasin, J., Burkhalter, S., et al. (2004) The minimal essential core of a cysteine-based PTP revealed by a novel 16-kDa VH1-like phosphatase, VHZ. *J. Biol. Chem.* **279**, 35,768–35,774.
51. Bordo, D. and Bork, P. (2002) The rhodanese/Cdc25 phosphatase superfamily. Sequence–structure–function relations. *EMBO Rep.* **3**, 741–746.
52. Alonso, A., Rojas, A., Godzik, A., and Mustelin, T. (2003) The dual-specific PTP family. *Top. Curr. Genet.* **5**, 333–358.
53. Vincent, C., Duclos, B., Grangeasse, C., et al. (2000) Relationship between exopolysaccharide production and protein-tyrosine phosphorylation in Gram-negative bacteria. *J. Mol. Biol.* **304**, 311–321.
54. Musumeci, L., Tautz, L., Perego, M., Mustelin, T., and Bottini, N. (2005) Characterization of the YfkJ protein tyrosine phosphatase of *Bacillus subtilis* and *Bacillus anthracis*. *J. Bacteriol.*, in press.
55. Kashio, N., Matsumoto, W., Parker, S., and Rothstein, D.M. (1998). The second domain of the CD45 protein tyrosine phosphatase is critical for interleukin-2 secretion and substrate recruitment of TCR ζ in vivo. *J. Biol. Chem.* **273**, 33856–33863.
56. Bolino, A., Muglia, M., Conforti, F. L., et al. (2000) Charcot-Marie-Tooth type 4B is caused by mutations in the gene encoding myotubularin-related protein-2. *Nat. Genet.* **25**, 17–19.

57. Azzedine, H., Bolino, A., Taieb, T., et al. (2003) Mutations in MTMR13, a new pseudophosphatase homologue of MTMR2 and Sbf1, in two families with an autosomal recessive demyelinating form of Charcot-Marie-Tooth disease associated with early-onset glaucoma. *Am. J. Hum. Genet.* **72**, 1141–1153.
58. Mustelin, T. and Hunter, T. (2002) Meeting at mitosis: cell cycle-specific regulation of c-Src by RPTP α . *Science's STKE*. http://stke.sciencemag.org/cgi/content/full/OC_sigtrans;2002/115/pe3.
59. Tailor, P., Williams, S., Gilman, J., Couture, C., and Mustelin, T. (1997) Regulation of the low molecular weight phosphotyrosine phosphatase (LMPTP) by phosphorylation at tyrosines 131 and 132. *J. Biol. Chem.* **272**, 5371–5376.
60. Alonso, A., Rahmouni, S., Williams, S., et al. (2003) Tyrosine phosphorylation of VHR phosphatase by ZAP-70. *Nat. Immunol.* **4**, 44–48.
61. Dorfman, K., Carrasco, D., Gruda, M., Ryan, C., Lira, S. A., and Bravo, R. (1996) Disruption of the *erp/mkp-1* gene does not affect mouse development: normal MAP kinase activity in ERP/MKP-1-deficient fibroblasts. *Oncogene* **13**, 925–931.
62. Hasegawa, K., Martin, F., Huang, G., Tumas, D., Diehl, L., and Chan, A. C. (2004) PEST domain-enriched tyrosine phosphatase (PEP) regulation of effector/memory T cells. *Science* **303**, 685–689.
63. Saha, S., Bardelli, A., Buckhaults, P., et al. (2001) A phosphatase associated with metastasis of colorectal cancer. *Science* **294**, 1343–1346.
64. Tartaglia, M., Mehler, E. L., Goldberg, R., et al. (2001) Mutations in *PTPN11*, encoding the PTP SHP-2, cause Noonan syndrome. *Nat. Genet.* **29**, 465–468.
65. Minassian, B. A., Lee, J. R., Herbrick, J. A., et al. (1998) Mutations in a gene encoding a novel PTP cause progressive myoclonus epilepsy. *Nat. Genet.* **20**, 171–174.
66. Laporte, J., Hu, L. J., Kretz, C., et al. (1996) A gene mutated in X-linked myotubular myopathy defines a new putative tyrosine phosphatase family conserved in yeast. *Nat. Genet.* **13**, 175–182.
67. Tchilian, E. Z., Wallace, D. L., Wells, R. S., Flower, D. R., Morgan, G., and Beverley, P. C. L. (2001) A deletion in the gene encoding the CD45 antigen in a patient with SCID. *J. Immunol.* **166**, 1308–1313.
68. Kung, C., Pingel, J. T., Heikinheimo, M., et al. (2000) Mutations in the tyrosine phosphatase CD45 gene in a child with severe combined immunodeficiency disease. *Nat. Med.* **6**, 343–345.
69. Bottini, N., Musumeci, L., Alonso, A., et al. (2004) A functional variant of lymphoid tyrosine phosphatase is associated with type 1 diabetes. *Nat. Genet.* **36**, 337–338.
70. Smyth, D., Cooper, J. D., Collins, J. E., et al. (2004) Replication of an association between the lymphoid tyrosine phosphatase locus (LYP/*PTPN22*) with type 1 diabetes, and evidence for its role as a general autoimmunity locus. *Diabetes* **53**, 3020–3023.
71. Ladner, M. B., Bottini, N., Valdes, A. M., and Noble, J. A. (2005) Association of the single-nucleotide polymorphism C1858T of the *PTPN22* gene with type 1 diabetes. *Hum. Immunol.* **66**, 60–64.

72. Kawasaki, E., Hutton, J. C., and Eisenbarth, G. S (1996) Molecular cloning and characterization of the human transmembrane PTP homologue, phogrin, an autoantigen of type I diabetes. *Biochem. Biophys. Res. Commun.* **227**, 440–447.
73. Begovich, A. B., Carlton, V. E., Honigberg, L. A., et al. (2004) A missense single-nucleotide polymorphism in a gene encoding a PTP (*PTPN22*) is associated with rheumatoid arthritis. *Am. J. Hum. Genet.* **75**, 330–337.
74. Kyogoku, C., Langefeld, C. D., Ortmann, W. A., et al. (2004) Genetic association of the R620W polymorphism of PTP *PTPN22* with human SLE. *Am. J. Hum. Genet.* **75**, 504–507.
75. Velaga, M. R., Wilson, V., Jennings, C. E., et al. (2004) The codon 620 tryptophan allele of the lymphoid tyrosine phosphatase (LYP) gene is a major determinant of Graves' disease. *J. Clin. Endocrinol. Metab.* **89**, 5862–5865.
76. Mena-Duran, A. V., Togo, S. H., Bazhenova, L., et al. (2005) SHP1 expression in bone marrow biopsies of myelodysplastic syndrome patients: a new prognostic marker. *Br. J. Haematol.*, **129**, 791–794.
77. Fonatsch, C., Haase, D., Freund, M., Bartels, H., and Tesch, H. (1991) Partial trisomy 1q. A nonrandom primary chromosomal abnormality in myelodysplastic syndromes? *Cancer Genet. Cytogenet.* **56**, 243–253.
78. Zanke, B., Squire, J. Griesser, H. et al. (1994) A hematopoietic PTP (HePTP) gene that is amplified and overexpressed in myeloid malignancies maps to chromosome 1q32.1. *Leukemia* **8**, 236–244.
79. Schweiger, S. and Schneider, R. (2003) The MID1/PP2A complex: a key to the pathogenesis of Opitz BBB/G syndrome. *Bioessays* **25**, 356–366.
80. Ito, A., Koma, Y.-I., and Watabe, K. (2003) A mutation in protein phosphatase type 2A as a cause of melanoma progression. *Histol. Histopathol.* **18**, 1313–1319.
81. Chen, W., Possemato, R., Campbell, K. T., Plattner, C. A., Pallas, D. C., and Hahn, W. C. (2004) Identification of specific PP2A complexes involved in human cell transformation. *Cancer Cell* **5**, 127–136.
82. Tautz, L., Bruckner, S., Sareth, S., et al. (2005) Inhibition of *Yersinia* tyrosine phosphatase by furanyl salicylate compounds. *J. Biol. Chem.* **280**, 9400–9408.
83. Liang, F., Huang, Z., Lee, S.-Y., et al. (2003) Aurintricarboxylic acid blocks both *in vitro* and *in vivo* activity of YopH, an essential virulent factor from *Yersinia* that cause the plague. *J. Biol. Chem.* **278**, 41,734–41,741.
84. Lazo, J. S. and Wipf, P. (2003) Small molecule regulation of phosphatase-dependent cell signaling pathways. *Oncol. Res.* **13**, 347–352.
85. Ducruet, A. P., Vogt, A., Wipf, P., and Lazo, J. (2005) Dual specificity protein phosphatases: therapeutic targets for cancer and Alzheimer's disease. *Annu. Rev. Pharmacol. Toxicol.* **45**, 725–750.
86. Pellecchia, M., Becattini, B., Crowell, K. J., Fattorusso, R., Forino, M., Fragai, M., Jung, D., Mustelin, T., and Tautz, L. (2004) NMR-based techniques in the hit identification and optimization process. *Expert Opin. Ther. Targets* **8**, 597–611.
87. Umezawa, K., Kawakami, M., and Watanabe, T. (2003) Molecular design and biological activities of protein-tyrosine phosphatase inhibitors. *Pharmacol. Ther.* **99**, 15–24.

88. Li, X., Bhandari, A., Holmes, C. P., and Szardenings, A. K. (2004) Alpha, alpha-difluoro-beta-ketophosphonates as potent inhibitors of protein tyrosine phosphatase 1B. *Bioorg. Med. Chem. Lett.* **14**, 4301–4306.
89. Bialy, L. and Waldmann, H. (2005) Inhibitors of protein tyrosine phosphatases: next-generation drugs? *Angew. Chem. Int. Ed. Engl.*, **44**, 3814–3839.
90. Pei, Z., Liu, G., Lubben, T. H., and Szczepankiewicz, B. G. (2004) Inhibition of protein tyrosine phosphatase 1B as a potential treatment of diabetes and obesity. *Curr. Pharm. Des.* **10**, 3481–3504.
91. Black, E., Breed, J., Breeze, A.L., et al. (2005) Structure-based design of protein tyrosine phosphatase-1B inhibitors. *Bioorg. Med. Chem. Lett.* **15**, 2503–2507.
92. Kumar, S., Zhou, B., Liang, F., Wang, W. Q., Huang, Z., and Zhang, Z.-Y. (2004) Activity-based probes for protein tyrosine phosphatases. *Proc. Natl. Acad. Sci. USA* **101**, 7943–7948.

Small-Molecule Inhibitors of Ser/Thr Protein Phosphatases

Specificity, Use and Common Forms of Abuse

Mark Swingle, Li Ni, and Richard E. Honkanen

Summary

Natural product extracts have proven to be a rich source of small molecules that potentially inhibit the catalytic activity of certain PPP-family ser/thr protein phosphatases. To date, the list of inhibitors includes okadaic acid (produced by marine dinoflagellates, *Prorocentrum* sp. and *Dinophysis* sp.), calyculin A, dragmacidins (isolated from marine sponges), microcystins, nodularins (cyanobacteria, *Microcystis* sp. and *Nodularia* sp.), tautomycin, tautomycetin, cytostatin, phospholine, leustroducsins, phoslactomycins, fostriecin (soil bacteria, *Streptomyces* sp.), and cantharidin (blister beetles, approx 1500 species). Many of these compounds share structural similarities, and several have become readily available for research purposes. Here we will review the specificity of available inhibitors and present methods for their use in studying sensitive phosphatases. Common mistakes in the employment of these compounds will also be addressed briefly, notably the widespread misconception that they only inhibit the activity of PP1 and PP2A. Inhibitors of PP2B (calcineurin) will only be mentioned in passing, except to state that, in our hands, cypermethrin, deltamethrin, and fenvalerate, which are sold as potent inhibitors of PP2B, do not inhibit the catalytic activity of PP2B.

Key Words: Okadaic acid; fostriecin; calyculin A; microcystin; cantharidin; protein phosphatase inhibitors; natural products

1. Introduction

In a landmark study, Bialojan and Takai revealed that okadaic acid, a complex polyether identified as the causative agent of diarrhetic shellfish poisoning, acts as a potent inhibitor of protein phosphatases PP1 and PP2A (*1*). This opened the door for the use of small-molecule inhibitors to study the roles of sensitive protein phosphatases. Indeed to date, although a more selective inhibitor has been identified (fostriecin), okadaic acid is still the most widely used

inhibitor in studies designed to provide insight into the biological actions of PP1 and PP2A. However, okadaic acid also potently inhibits the activity of PP4, PP5 and likely PP6 (*see Note 1*), a fact that is often missed or ignored by investigators using this compound. In actuality, it appears that most, if not all, of the above-mentioned inhibitors act against PP1, PP2A, PP4, PP5, and PP6 (2). It should also be mentioned that in humans there are four isoforms of the catalytic subunit of PP1 (α , β/δ , $\gamma 1$, and $\gamma 2$) and two isoforms of PP2Ac (α and β). Therefore, to construct valid arguments for a role of a particular phosphatase based on studies using these inhibitors, it is important to understand their specificity and the limitations of their use.

For the sake of brevity, the focus of this chapter will be on inhibitors that are commercially available (i.e., okadaic acid, calyculin A, microcystin-LR, tautomycin, fostriecin, and cantharidin). Based on published studies conducted using purified catalytic subunits of the indicated phosphatases and phosphoproteins as substrates, the relative sensitivity of PP1–PP7 to commonly used inhibitors is summarized in **Table 1**. Comparison of the relative IC_{50} values reveals that the most toxic inhibitors (microcystin-LR, calyculin A, and nodularin) are all very potent inhibitors of PP1, PP2A, PP4 and PP5, markedly inhibiting the activity of each enzyme at nanomolar concentrations. They have very limited activity against PP2B or PP7 and virtually no effect on PPM-family ser/thr phosphatases or phosphotyrosine phosphatases. To date more than 50 variants of microcystin and approx 10 variants of nodularin have been identified. The microcystins/nodularins are cyclic peptides, and many (i.e., microcystin-LR) demonstrate substantial solubility in aqueous solutions. Still, they are not readily taken up by most cell types, with the notable exception of hepatocytes and intestinal epithelial cells from the distal ileum that are capable of actively transporting these molecules across their plasma membranes (likely via the bile acid transporter). Accordingly, microcystins/nodularins are most useful as inhibitors when added to cell homogenates or extracts, where they rapidly diffuse in an aqueous environment and potently inhibit the activity of PP1, -2A, -4, -5 and, likely, -6. Because of its very limited membrane permeability, microcystin-LR is also useful for patch-clamp studies when it is desirable to restrict an inhibitor to a particular side of a lipid membrane (6).

In contrast to the microcystins, calyculin A readily partitions into cell membranes. However, calyculin A is essentially insoluble in aqueous solutions. Therefore, when added to a living cell culture, most of the calyculin A ends up in an “oil slick” on the surface of the culture media, separated from the cells by an “ocean” of media in which it has very limited solubility. The same thing, to a slightly lesser extent, occurs with the other hydrophobic inhibitors (i.e., okadaic acid, tautomycin, and, to a much lesser extent, cantharidin). As a result the uptake of a hydrophobic inhibitor by cells is influenced by (1) the partition-

ing of the inhibitor from the “oil slick” into the aqueous media (i.e., water solubility), (2) the passive diffusion through the aqueous media, (3) the partitioning into the cell membrane, and (4) the partitioning from the membrane into the cytoplasm of the cells, where it binds with high affinity to sensitive phosphatases. This makes it very difficult to determine how much inhibitor actually enters a cell. Nonetheless, although limited by very low water solubility, as a result of its high affinity for PPases and ability to cross cell membranes, calyculin A will enter living cells and can be used in a limited fashion as an inhibitor of PP1, -2A, -4, and -5. For such studies, calyculin A is most useful for distinguishing the actions of calyculin A-sensitive PPases from the actions of PP2B/calcineurin, PP2C, and PTPases. When employed alone, calyculin A cannot be used to distinguish the actions of the sensitive PPase from each other. It should also be noted that the concentration commonly employed (50–100 nM) will kill most, if not all, human cells when free-inhibitor concentrations inside a cell approach 10 nM (*see Note 2*).

The most selective inhibitors disclosed to date are fostriecin, okadaic acid, and tautomycetin, with fostriecin by far demonstrating the most selectivity (PP2A/PP4 vs PP1/PP5 selectivity $\leq 10^4$). In comparison, the PP2A/PP4 vs PP1/PP5 selectivity of okadaic acid is $<10^2$, and the PP1 vs PP2A/PP4 selectivity of tautomycin is approx 5 (tautomycetin approx 40). All three compounds readily enter living cells. Both okadaic acid and tautomycin/tautomycetin are fairly hydrophobic compounds that readily partition into cell membranes but have low (picomolars to low nanomolars) water solubility. Fostriecin, which demonstrates substantial water solubility (μM to low mM), appears to be capable of entering cells via a carrier-mediated transporter, likely the reduced folate carrier system (7). This makes fostriecin especially attractive for studies conducted with living cells. Like microcystin and calyculin A, fostriecin, okadaic acid, and tautomycin demonstrate little inhibitory activity against PP2B or PP7 and have virtually no effect on PP2C or PTPases. Cantharidin also demonstrates some selectivity (PP2A/PP4 > PP5 > PP1). However, the selectivity of cantharidin is less than that of okadaic acid or fostriecin. It should also be noted that okadaic acid is a fairly stable compound. In contrast, the lactone ring of fostriecin, which is necessary for selectivity (4) is sensitive to oxidation, light, and changes in pH. Fostriecin is not stable above pH 8.0 and very labile in dilute acid. Therefore, fostriecin should be kept in solutions buffered with ascorbate to protect from oxidation and with buffers adjusted to maintain a pH range of 5.5–7.5.

Given the above, the known inhibitors are very powerful tools for studying the actions of PP1, PP2A, PP4, PP5, and PP6. They can be most effectively employed in studies conducted using appropriately diluted cell extracts, (including immunoprecipitations) to gain insight into the involvement of a

sensitive PPase and in vivo studies to distinguish the actions of broad classes of phosphatases (PP1/2A/4/5/6 vs PP2B/7/PP2Cs/PTPases). With care, fostriecin can be employed in vivo to distinguish between PP2A/4/6 and PP1/PP5. However, for proper interpretation of the data, it is necessary to first determine the total amount of sensitive PPase(s) contained in a given preparation. This can be accomplished using a microcystin-LR titration assay, described below. Methods to produce phosphoprotein substrates with very high specific activity, and a very sensitive phosphatase assay are also provided, which when used in combination with fostriecin and okadaic acid can be employed to obtain insight into the involvement of PP2A/PP4 in a given event.

2. Materials

2.1. Inhibitors (Numbers Refer to the Structures in Fig. 1)

1. Okadaic acid [$C_{44}H_{68}O_{13}$; molecular weight (MW) 804.5]. Principal source: marine dinoflagellates *Prorocentrum lima*, *Prorocentrum elegans*, and *Prorocentrum concavum*; also produced by several species of *Dinophysis*. Okadaic acid [1] is a complex hydrophobic polyether that comes as a white crystalline solid. It is readily soluble in many organic solvents and degrades in acid or base. Although soluble in dimethyl sulfoxide (DMSO) and a number of organic solvents, the recommended solvent is *N,N*-dimethylformamide (DMF). When stored in DMF at -20°C okadaic acid is stable for years (>5).
2. Microcystin-LR ($C_{49}H_{74}N_{10}O_{12}$; MW 995). Principal source: cyanobacteria (blue-green algae) *Microcystis aeruginosa*. Microcystins [2] are cyclic heptapeptides that come as a dry white powder. Microcystin-LR is soluble in most aqueous solutions; DMSO, and DMF (recommended). It is unstable at $\text{pH} > 7.7$ and can be stored at -20°C in DMF for approx 1 yr.
3. Nodularin ($C_{41}H_{60}N_8O_{10}$; MW 824) Principal source: cyanobacteria *Nodularia spumigena*. Nodularin [3] is a cyclic pentapeptide with similar properties to microcystin-LR. It is readily soluble in most aqueous solutions, DMSO, and DMF. Nodularin is unstable at $\text{pH} > 7.7$ and can be stored at -20°C in DMF for approx 1 yr.
4. Calyculin A ($C_{50}H_{81}N_4O_{15}P$; MW 1009). Principle source: unknown; purified from a marine sponge *Discodermia calyx*. Calyculin A [4] is a novel spiro ketal-bearing phosphate, oxazole, nitrile and amide functionalities. It comes as a white solid and is soluble in DMSO, ethanol, and DMF. Calyculin A is virtually insoluble in water. During storage it should be protected from light and moisture. As a concentrated solution in DMF calyculin A is fairly stable and can be stored for >6 mo at -20°C .
5. Fostriecin ($C_{19}H_{26}O_9PNa$; MW 452.4). Principal source: *Streptomyces pulveraceus* (subspecies *fostreus*). Fostriecin [5] is a structurally novel phosphate ester that comes as a colorless or yellow solid. It is soluble in water, methanol, ethanol, and DMF and should be protected from light both as a powder and in solution. It is recommended to store the dry powder at -80°C . Concentrated stock solutions can be made by dissolving fostriecin in DMF. In solution fostriecin should be

stored in a tightly sealed vial under argon. DMF stocks can be stored under argon for ~2 mo at -20°C with minimal loss of potency. When diluted in aqueous solution, fostriecin should be used fresh. It is sensitive to oxidation and **MUST** be maintain at a pH range between 5.5 and 7.5. Even brief exposure to weak acids or bases will result in the loss of inhibitory activity. Buffered or pH adjusted freshly prepared ascorbic acid (1 mM) can be added to aqueous solutions to help protect against oxidation (*see Note 3*). Although concentrated stocks solutions in DMF can be stored at -20°C for 2–3 mo, even highly concentrated aqueous stocks cannot be stored at 4°C for more than a few days.

6. Tautomycin ($\text{C}_{41}\text{H}_{66}\text{O}_{13}$; MW 767.0). Principal source: *Streptomyces* sp. (i.e., *S. spiroverticillatus*). Tautomycin [6] exists as a tautomeric mixture in solution (hence the name) and comes as a lyophilized solid. It is soluble in ethanol, ethyl acetate, DMSO, and DMF. Tautomycin is fairly stable and can be stored for approx 1 yr at -20°C as a lyophilized solid or in a concentrated DMF solution. Dilute solutions in DMF can be stored at -20°C for approx 3–6 mo.
7. Cantharidin ($\text{C}_{10}\text{H}_{12}\text{O}_4$; M. W. 196.2). Principal source; blister beetles (i.e., *Cantharis vesicatoria*). Cantharidin [7; left] comes a solid white powder that can be stored at room temperature (20°C). It should be protected from light and moisture. Cantharidin is soluble in DMSO and DMF ($>25\text{ mg/mL}$) and in ethanol (1.0 mg/mL). As a dry powder, it is quite stable and can be stored for up to 5 yr. Concentrated stock solutions should be stored at -20°C and are stable for approx 3–6 mo. Cantharidic acid [7; right] might be the active form of the inhibitor in a cell, for structure–activity relationship (SAR) studies indicate that derivatives that prevent ring opening have markedly lower inhibitory activity (3). It should also be noted that Mn^{2+} , which is commonly employed in assays using recombinant PPases expressed in bacteria, blocks the inhibitory activity of cantharidin, likely by inhibiting is binding to the catalytic site (Swingle, Li, and Honkanen, unpublished observation).

2.2. Buffers

1. 4X Assay buffer 1: 200 mM Tris-HCl, pH 8.3, at 37°C , 200 mM MgCl_2 , 200 mM *p*-nitrophenyl phosphate (pNPP), and 0.4% 2-mercaptoethanol.
2. 4X Assay buffer 2: 200 mM Tris-HCl, pH 7.4, 2 mM dithiothreitol (DTT), 0.4 mM EDTA, phosphoprotein (8 μM incorporated PO_4).
3. Buffer A: 10 mM cAMP, 40 mM PIPES, pH 6.8 (at 37°C), 7 mM MgCl_2 , 0.1 mM EDTA, and 5 mM DTT.

2.3. Reagents and Solutions

1. 50 mM pNPP.
2. Ethanol/ethyl ether (1 : 4, v : v).
3. Acidified ethanol/ethyl ether (1 : 4, v : v; 0.1 N HCl).
4. Assay stop solution: 1 N H_2SO_4 containing 1 mM K_2HPO_4 (H_3PO_4 at pH 1).
5. Ammonium molybdate: 7.5% (w/v) in 1.4 N H_2SO_4 .
6. Isobutanol : benzene (1 : 1, v/v).

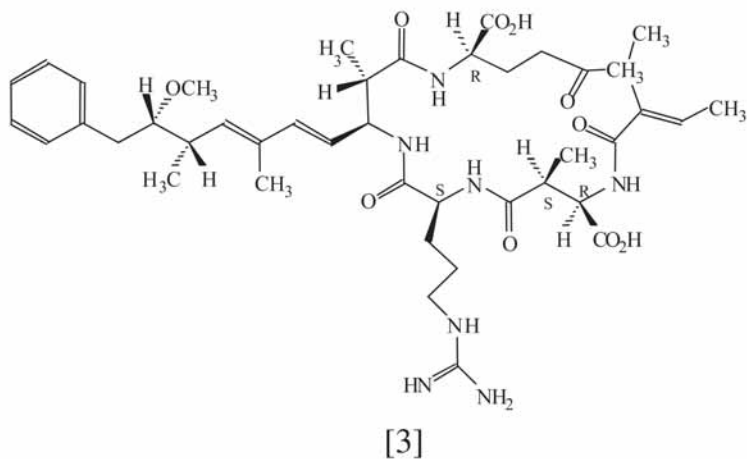
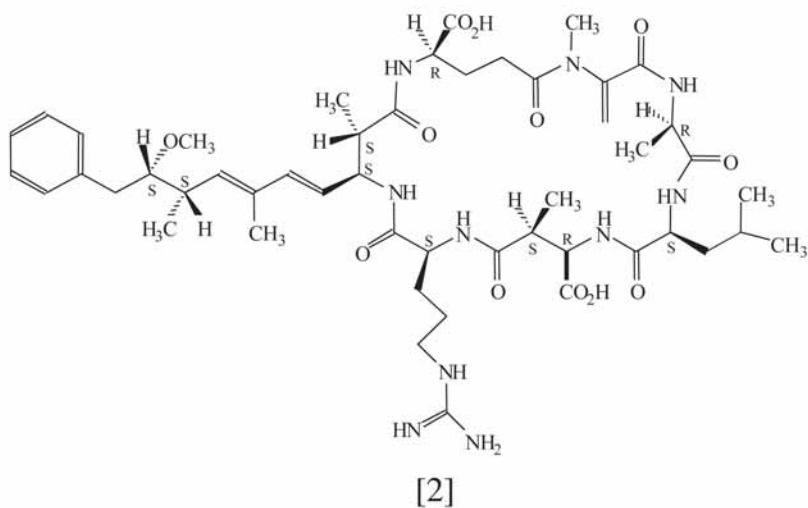
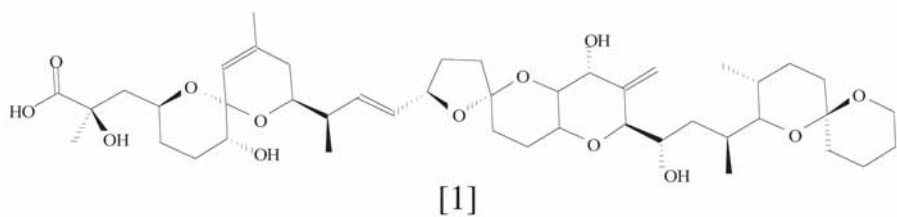


Fig. 1. Structures of commercially available protein phosphatase inhibitors.

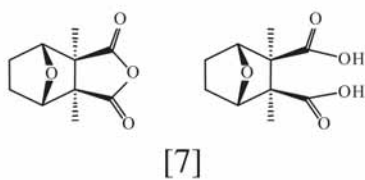
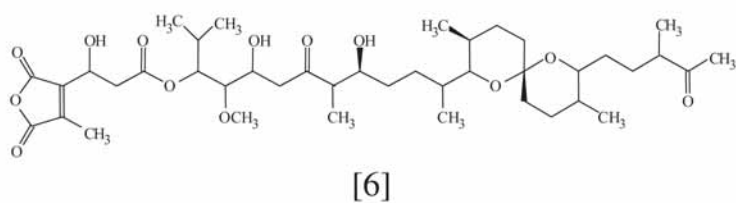
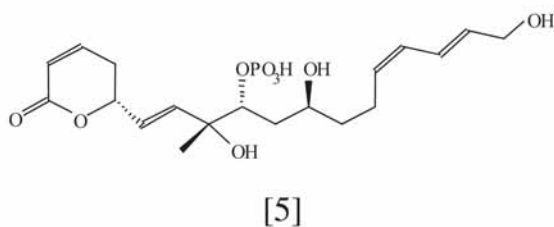
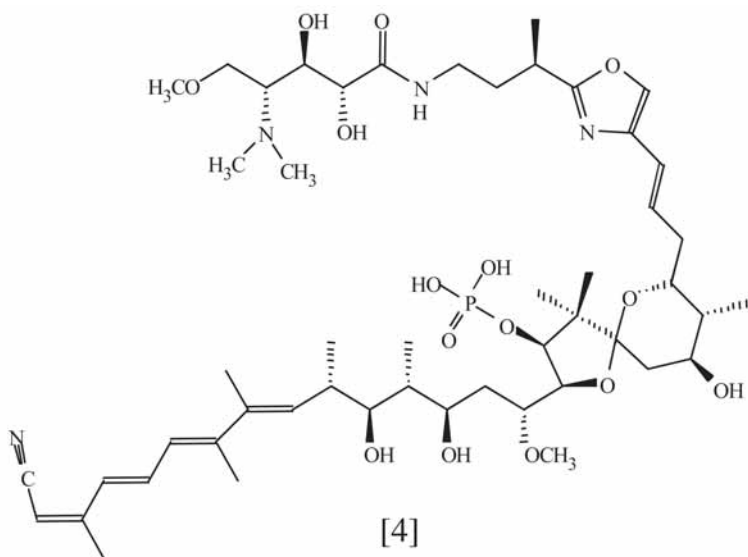


Fig. 1.(continued)

3. Methods

Of the above-mentioned, inhibitors fostriecin, okadaic acid, tautomycin and calyculin A are most useful for distinguishing the activity of the “toxin-sensitive” PPP-family phosphatases (PP1, PP2A, PP4, PP5, and, likely, PP6) from the toxin-insensitive PPP phosphatases (PP2B/calcineurin, PP7), PPM-family phosphatases, phosphotyrosine phosphatases (PTPases), and “dual-specific” phosphatases. For this purpose, any of these compounds can be added to an assay (or to cells in culture) at an appropriate concentration to test the hypothesis that a “toxin-sensitive” phosphatase participates in a given event. The identification of a toxin-sensitive PPase in a particular event can most easily be accomplished by conducting dose–response studies using assays conducted with appropriately diluted (see below) cell extracts, immunoprecipitates, or reconstituted systems, and the ability of any of these inhibitors to affect a given response in a crude cell homogenate at a concentration close to the IC_{50} values listed in [Table 1](#) is a reasonable indication that PP1, PP2A, PP4, PP5, or PP6 is involved. Similarly, when applied at a sublethal concentration to cells, the ability of any of these inhibitors to affect a given response in living cells is also a good indication that at least one of the toxin-sensitive PPases is involved. However, demonstrating the involvement of a particular “toxin-sensitive” PPase is more difficult, and in living cells, it might not be possible with a high degree of certainty.

Calyculin A and okadaic acid are commonly used both *in vitro* and *in vivo* to study the actions of PP1 and PP2A, and the conclusions drawn from such studies are often inaccurate. Most notably, in the literature, it is often incorrectly reported that the ability of calyculin A to affect a given response that is not influenced by 5–10 nM okadaic acid indicates the involvement of PP1. This argument is flawed in several ways. First and foremost, the argument ignores the possible involvement of PP4, PP5, or PP6. Second, such studies usually assume “instant equilibrium” of the inhibitors. The problem is that different cell-permeant compounds do not necessarily diffuse into cells at the same rate (see [Note 2](#)), especially if the compounds are added at different concentrations ([8](#)). Third, organic anion efflux pumps (i.e., the multidrug resistance pump) may use these compounds as substrates. Finally, okadaic acid, like all of the above-mentioned inhibitors, binds to PP2A, PP4, PP5, and PP1 with high affinity at a molar ratio of 1 : 1, and most of the okadaic acid-sensitive PPase are expressed at fairly high levels in eukaryotic cells. Therefore, unless the assays using okadaic acid are conducted with dilute samples, 5–10 nM okadaic acid might not be sufficient to fully inhibit the most OA-sensitive PPases (PP2A α /beta, PP4, PP5, and probably PP6) present in the assays, because undiluted samples might contain concentrations of these PPases near to, or in excess of 10 nM (greater than or equal to their respective inhibitor

Table 1
Natural Compounds That Inhibit PPP-Family Ser/Thr Protein Phosphatases
 (See Note 11)

Compound	IC ₅₀ ^a					
	PP1	PP2A	PP2B (calcineurin)	PP4	PP5	PP7
Okadaic acid	15–50	0.1–0.3	~4000	0.1	3.5	> 1000
Microcystin-LR	0.3–1	< 0.1–1	~1000	0.15	1.0	> 1000
Nodularin	2.4	0.3	> 1000	ND	~4	> 1000
Calyculin A	0.4	0.25	> 1,000	0.4	3	>1,000
Tautomycin	0.23–22	0.94–32	> 1000	0.2	10	ND
Cantharidin	1,100	194	> 10,000	50	600	ND
Fostriecin	45,000– 58,000	1.5–5.5	> 100,000	3.0	50,000– 70,000	ND

^a The IC₅₀ values provided are nanomolars and represent the amount of inhibitor needed to inhibit 50% of the activity in an assay. Because IC₅₀ values are influenced by the concentration of inhibitor, the mode of inhibition, and the amount of both enzyme and substrate employed in an assay, the different values shown likely reflect variations in the assay conditions used by the labs reporting these values. Details of the structure–activity relationship for okadaic acid, calyculin A, microcystin-LR, cantharidin, and tautomycin can be found in a recent review by Sakoff and McClusky (3). Details of the structure–activity relationship for fostriecin has been published recently (4), and more information about the “fostriecinlike” compounds produced by *Streptomyces* can be found in a review by Lewy et al. (5)

^b ND: not determined.

^b Source: Adapted from ref. 2.

dissociation constants). In such a regime, IC₅₀ values deviate substantially from the *K_i* values because the free-inhibitor concentrations are reduced significantly through binding and sequestration of inhibitors by the PPases (i.e., “titration”). Indeed, when $[E] \gg K_i$, essentially all inhibitor is bound and the IC₅₀ is simply $[E]/2$. This phenomenon forms the basis for the microcystin-LR titration assay described below. Accordingly, to appropriately interpret data obtained with okadaic acid, calyculin A, or tautomycin, it is necessary to first determine the amount of toxin-sensitive PPase contained in a given preparation and then dilute the extracts so that such titration effects are minimized.

To date, the most selective inhibitor that has been disclosed is fostriecin, and although its use is somewhat hampered by the above-mentioned storage stability issues, when handled properly fostriecin can be employed in combination with parallel studies using calyculin A, cantharidin, or okadaic acid to distinguish the actions of PP2A/PP4/PP6 from those of PP1/PP5 in assays that are conducted in vitro and possibly in vivo as well. The major advantages of

fostricetin are its high selectivity for PP2A/PP4, its water solubility, and its ability to enter cells via the reduced folate transporter.

At present, inhibitors capable of distinguishing the actions of PP2A from PP4/PP6 have not been reported. Therefore, currently it is not possible to use small-molecule inhibitors alone to distinguish the actions of PP2A from that of PP4/PP6 or the actions of PP1 from the actions of PP5. Nonetheless, fostricetin can be used for in vitro characterization of the toxin-sensitive PPases that contribute to a given response and to indicate the involvement of PP2A/PP4/PP6 in vivo. However, because the inhibition of PP1/PP2A/PP4 and PP5 is lethal to most, if not all, human cells, despite numerous claims in the literature it is actually very difficult to use either okadaic acid or fostricetin to attribute any given observation to the suppression of PP1 or PP5. To do so, numerous additional experiments are needed using a combination of small-molecule inhibitors and protein inhibitors (i.e., inhibitors 1 and 2), time-course studies, and phosphatase assays using different substrates. An excellent example of such studies using MCF-7 cells can be found in an article by Favre et al. (8). Fortunately, recent advances using antisense oligonucleotides and siRNA indicate that virtually any protein that is expressed in a cell can be suppressed. Thus, the development of siRNA for each PPase should greatly aid in the assignment of roles to a given PPase. Indeed, methods for suppressing the expression of human PP5 have already been reported (9). Still, small-molecule inhibitors are very useful in “culling experiments,” which are designed to eliminate PPases that are not involved in a given response. In addition, the actions of the small molecules are more rapid and reversible.

3.1. Microcystin-LR Titration Assay

Because microcystin-LR binds sensitive phosphatases with high affinity and with a molar ratio of 1:1, it can be employed to determine the concentrations of sensitive PPases in partially purified protein preparations and crude cell extracts by conducting detailed dose–response inhibition studies (see Fig. 2). Because enzyme concentrations are often high in these assays, it is important to ensure that substrate depletion is negligible when compared to total substrate concentration. For the example given below, the assay is conducted using partially purified PP5 and pNPP (50 mM) as the substrate. For use in crude cell homogenates, phosphoproteins substrates, such as phosphohistone (methods for production given below) can be employed. For all substrates, with the microcystin-LR titration assay lower temperature and shorter reaction times help reduce substrate depletion and product inhibition.

1. Aliquots of extracts (approx 20 μ L) are diluted to 27.5 μ L with water whereupon 2.5 μ L of microcystin-LR or vehicle (DMF) is added and mixed by pipetting. For

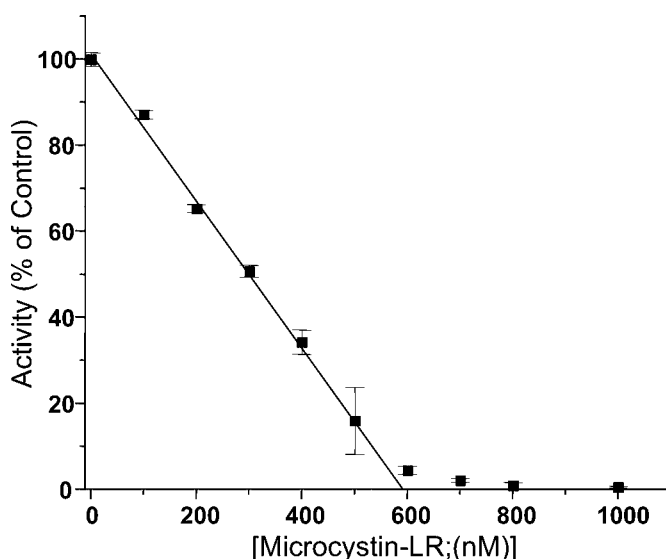


Fig. 2. Inhibition of PP5 activity by microcystin-LR. For this reaction it is necessary that the concentration of enzymes $[E]$ is greater than the K_i , $[E] \gg K_i$. Thus, for a mixture of PPases the K_i s and differences in K_i s become irrelevant.

such studies, concentrated microcystin-LR stocks are diluted in DMF using serial dilutions to produce stock solutions that will produce the concentrations indicated when 2.5 μL of the stocks are added to the assays (*see* Fig. 2).

2. The enzyme/extract is preincubated with microcystin-LR for 10 min at room temperature and reactions are started by the addition of 10 μL of 4X assay buffer 1 followed by incubation at 37°C for 10 min.
3. Reactions are stopped by the addition of 100 μL of 1 M EDTA, pH 10, and absorbance is measured at 400 nm using a spectrophotometer. The data are plotted as shown and the intercept of the linear portion of the curve with the x -axis provides a fairly accurate indication of the amount of toxin-sensitive PPase present. In the example provided, there are nearly 600 nM microcystin-LR sensitive PPase in the assay.

3.2. Preparation of Phosphohistone Substrate

For microcystin-titration assays conducted in crude cell homogenates, pNPP is not the substrate of choice because microcystin-LR-insensitive phosphatases that can use pNPP as a substrate are often present (i.e., PP2B, PP2C, and PTPase), which will result in a high background. Therefore, a phosphoprotein substrate might be more useful. In addition, substrates with very high specificity, when combined with a sensitive phosphatase assay, can be employed along

with fostriecin and okadaic acid to detect changes in the activity of PP2A/PP4 in dilute crude cell homogenates and immunoprecipitations. Histone phosphorylated with cAMP-dependent protein kinase (PKA) is a good substrate for PP1, PP2A, PP4, and PP5 (*see Note 4*) and phosphohistone with specific activity $> 5 \times 10^6$ dpm/nmol incorporated phosphate can be produced as follows:

1. Histone (type-2AS) is phosphorylated with cAMP-dependent PKA in a reaction containing buffer A plus 10 mg/mL histone, 2 mg/mL PKA, and 6 mCi/mL [γ - 32 P]ATP (200 mM ATP). The reaction volume is 1.5-mL, and the reaction is conducted in a 15 mL conical polypropylene test tube (*see Note 5*). Aliquots (usually $2 \times 5 \mu\text{L}$) are removed for use in the calculation of specific activity, and the reaction is carried out overnight at 37°C .
2. The reaction is terminated by the addition of ice-cold trichloroacetic acid (TCA) to 25%. The tube is placed on ice for at least 10 min, and the precipitated phosphohistone is collected by centrifugation (approx $3000 \times g$ for 7 min). The supernatant is discarded and the pellet resuspended in 1 M Tris-HCl, pH 8.5; the phosphohistone is precipitated again by the addition of ice-cold TCA to 25%.
3. The precipitation–resuspension cycle is repeated five times, which is the minimum number of washes that are required to wash free [32 P], ATP, and free phosphate from the preparation (*see Note 6*).
4. To remove the TCA, the pellet produced upon the sixth TCA precipitation is washed four times with ethanol/ethyl ether (1 : 4, v : v), then twice with acidified ethanol/ethyl ether (1 : 4, v : v; 0.1 N HCl). Between each wash, the pellet is mixed using a small glass rod to break up any clumps that are observed. Each time prior to removal of the wash, the pellet is stabilized by centrifugation as above.
5. The washed histone pellet is then air-dried and dissolved in 5 mM Tris-HCl, pH 7.4 (*see Note 7*). After the histone is dissolved, aliquots can be stored at -20°C . If performed correctly, the above procedure generates sufficient substrate for approx 3000 assays with approx 500,000 CPM of phosphohistone and a background (free ^{32}P) of approx 300.
6. Calculations:
 1. ATP incorporation ratio (R):

$$R = \frac{\text{CPM in incubation mixture (incubation volume / volume of aliquot counted)}}{\text{CPM in redissolved pellet (final volume / volume of aliquot counted)}}$$

2. Concentration of incorporated phosphate (C_p):

$$C_p = \frac{\text{Initial concentration of ATP} = 200 \mu\text{M}}{200 \mu\text{M} \times R \times (\text{incubation volume/final volume})}$$

3.3. Measurement of Phosphatase Activity

To take advantage of substrates with very high specific activity, a very sensitive assay is often needed. The following phosphatase assay can be employed.

1. With this method, phosphatase activity against phosphoproteins is determined by the quantification of [^{32}P] liberated from phosphohistone, prepared as described above. The assay (80 μL final volume) is performed in assay buffer 2. The assay is conducted in a 1.5-mL microcentrifuge tube at 30°C for 10 min, and is initiated by adding 30 μL of phosphohistone substrate (dissolved in 5 mM Tris-HCl, pH 7.4) to diluted crude cell extracts containing 4X assay buffer 2 and water. Typically, a reaction contains 20 μL of 4X assay buffer 2, 5–10 μL dilute cell extract, water to bring the volume to 50 μL , and 30 μL substrate).
2. The dephosphorylation reaction is stopped by the addition of 100 μL of acid (1 N H_2SO_4) containing 1 mM $\text{K}_2\text{H PO}_4$ (H_3PO_4 at pH 1) (assay stop solution).
3. [^{32}P] liberated by the enzymes is then extracted as a phosphomolybdate complex and measured based on the methods of Killilea et al. (10). Free phosphate is extracted by adding 20 μL of ammonium molybdate (7.5%, w/v, in 1.4 N H_2SO_4) and 250 μL of isobutanol:benzine (1 : 1, v/v) to each tube. The tubes are mixed vigorously for approx 10 s (vortex set at maximum speed), followed by centrifugation at 14,000g for 2 min. This results in a biphasic solution. The radioactivity (phosphate liberated from the phosphohistone) is contained in the upper phase and is quantified by counting 100 μL aliquots in a scintillation counter (see **Note 8**).
4. For inhibition studies, inhibitors are generally dissolved and diluted in DMF (see **Note 9**) and added to the enzyme mixture 10 min before the initiation of the reaction with the addition of substrate. Controls receive solvent alone, and in all experiments, the amount of enzyme is diluted to ensure that the samples are below the titration end point. The titration end point is defined as the concentration of enzyme after which further dilution no longer affects the IC_{50} of the inhibitor and can be determined using the microcystin-titration assay described earlier. It represents a point where the concentration of enzyme used in the assay is no longer large in comparison to its inhibitor dissociation constant. This ensures that the IC_{50} represents the potency of the inhibitor alone and is not representative of a combination of potency of the inhibitor and titration artifacts of the assay system. Preliminary assays must also be performed to ensure that the dephosphorylation reaction is linear with respect to enzyme concentration and time.

3.4. Identification of the Activity of PP2A/PP4 Using Fostriecin and Okadaic Acid

Typical dose–response inhibition curves that can be obtained using purified PP2A (similar results are expected for PP4) or PP1/PP5 are shown in **Fig. 3A**. **Figure 3B** is a theoretical example illustrating the inhibition by fostriecin in appropriately dilute samples containing a mixture of PP1, PP2A, PP4, and PP5, such as that present in crude cell homogenate. As illustrated in **Fig. 3A** by a shaded bar and in **Fig. 2B** by the plateau in the inhibition curve, approx 1 μM fostriecin is sufficient to completely inhibit the activity of PP2A/PP4 while having little, if any, effect on PP1 or PP5. Thus, the addition of approx 1 μM

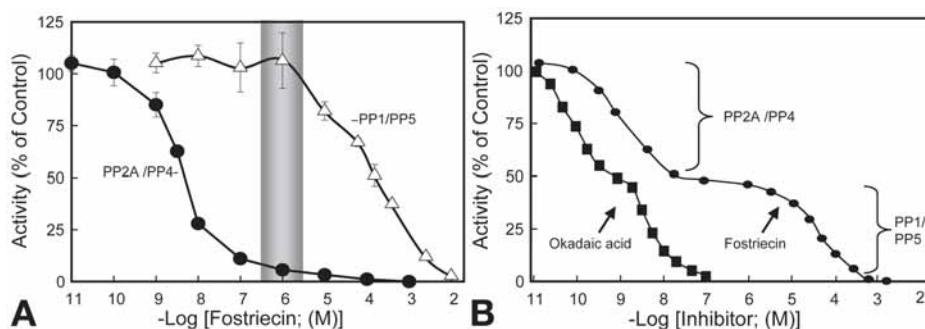


Fig. 3. Dose-response inhibition curves with fostriecin and okadaic acid.

fostriecin to a sufficiently dilute crude cell homogenate is sufficient to completely inhibit the activity of these enzymes and can be used to implicate the role of PP2A/PP4 in a given event. With great care, okadaic acid can be employed in a similar fashion, and 1–5 nM okadaic acid can be used to inactivate PP2A/PP4 in dilute crude cell homogenates following mixing. However, when compared to fostriecin, okadaic acid has higher affinity for PP2A/PP4 and is not nearly as selective. Thus, studies with okadaic acid are much more likely to be influenced by “titrations artifacts.” Still both of these inhibitors can be used in a wide variety of biological studies, and such dose–response studies can be employed with immunoprecipitation studies to characterize a phosphatase that coimmunoprecipitates with other proteins. Similarly, approx 1 μM fostriecin should be sufficient to inhibit the actions of PP2A and PP4 in living cells, assuming that the cells have a functioning reduced folate carrier system and sufficient volume is used during treatment. However, it should be noted that at this time, it is not clear if the reduced folate carrier system can concentrate fostriecin intracellularly, which might be accomplished with folate (*see Note 10*).

4. Notes

1. To date, the sensitivity of PP6 to the inhibitors listed has not been reported. However, because of the extreme conservation of the amino acids in the toxin-binding domain of PP6 with that of PP2A and PP4, it is predicted that PP2A, PP4, and PP6 will demonstrate comparable sensitivity to most, if not all, of the inhibitors discussed.
2. When added to cell cultures, for hydrophobic inhibitors such as calyculin A and okadaic acid, it might take 24–48 h before equilibrium conditions are archived inside a cell. This equilibrium process is dependent on the amount of inhibitor added, the water solubility of the inhibitor, and the ability of the inhibitor to cross

the membrane. As a result, adding higher amounts of inhibitor to cells in culture will help saturate the media, but, ultimately, the water solubility becomes limiting. Once the culture media becomes saturated, the inhibitors must still cross the membrane to have access to the PPases. Assuming that the process is passive, the inhibitor has to first partition into the lipid bilayer (a rapid process) and then partition back into an aqueous environment (a slower process). So again, water solubility becomes an issue. However, inside the cell, the PPases have very high-affinity binding sites, which is reflected by the K_i for a given compound. As a result, the free cytosolic inhibitor rapidly binds to sensitive PPases, and there is a net flux of inhibitor into the cell until all of the high-affinity binding sites are occupied. Because of the very low water solubility of the hydrophobic inhibitors, the entire process is relatively slow.

3. When diluted in solutions containing ascorbic acid, the solution should be clear (it might have a tinge of yellow, if the ascorbic acid is getting old). When the solution turns yellow it is very likely that the fostriecin has been oxidized and will no longer be useful.
4. Phosphohistone is a very poor substrate for PP2B. In addition, because they require divalent cations for activity, EDTA and EGTA can be added to assays using this substrate to inhibit the activity of PP2B and the PPM-family phosphatases (e.g., PP2C) that might be present.
5. The tube must be able to withstand both acid (trichloroacetic acid) and ether. Polystyrene tubes commonly used in tissue culture will dissolve and are thus not suitable.
6. For resuspension, it is not necessary that the solution become clear, but no visible "chunks" should be present. Failure to adequately resuspend or thoroughly remove the supernatant after centrifugation will result in increased background in the phosphatase assay. If this should occur, the substrate can be precipitated with TCA and the ethanol/ether washes can be repeated to salvage the preparation.
7. It takes time for the pellet to hydrate and go completely go back into solution. It usually takes approx 1 h with vortexing every 5–10 min.
8. The phosphohistone will be concentrated at the interface of the organic (top) and aqueous (bottom) solutions. When removing a sample of the organic phase to count, it is important not to allow the tip to hit the interface. If the tip breaks the interface, radioactive histone will stick to the outside of the tip. If this should happen, the tip should be discarded and the sample should be taken with a fresh tip after the sample is centrifuged again.
9. A common mistake is to conduct serial dilutions in assay buffer. This will not work for hydrophobic inhibitors.
10. Because of its uptake via the reduced folate carrier system it is possible that fostriecin accumulates inside a cell. However, for folate, intracellular accumulation might be the result of prevention of efflux following polyglutamylation.
11. Safety in handling. Although several studies have shown that fostriecin and cantharidin possess antitumor activity, both okadaic acid and microcystin-LR have been touted to act as tumor-promoting agents. For all of the inhibitors

discussed, the pharmacological and toxicological properties have not been fully investigated. Exercise caution in use and handling. They should be handled as if they were carcinogenic, and they are all toxic. Wear gloves when handling the product and wear a mask when dispensing large amounts. Avoid contact by all modes of exposure.

Acknowledgments

This work was supported, in part, by a research grant from the National Institutes of Health, (NCI grant CA 60750) and was conducted in a facility constructed with support from a Research Facilities Improvement Program Grant (CO6 RR11174) from the National Center for Research Resources.

References

1. Bialojan, C. and Takai, A. (1988) Inhibitory effect of a marine-sponge toxin, okadaic acid, on protein phosphatases. Specificity and kinetics. *Biochem. J.* **256**, 283–290.
2. Honkanen, R. E. and Golden, T. (2002) Regulators of serine/threonine protein phosphatases at the dawn of a clinical era? *Curr. Med. Chem.* **9**, 2055–2075.
3. Sakoff J. A. and McCluskey, A. (2004) Protein phosphatase inhibition: structure based design. Towards new therapeutic agents. *Curr. Pharm. Des.* **10**, 1139–1159.
4. Buck, S. B., Hardouin, C., Ichikawa, S., et al. (2003) Fundamental role of the fostriecin unsaturated lactone and implications for selective protein phosphatase inhibition. *J. Am. Chem. Soc.* **125**, 15,694–15,695.
5. Lewy, D. S., Gauss, C. M., Soenen D. R., and Boger, D. L. (2002) Fostriecin: chemistry and biology. *Curr. Med. Chem.* **9**, 2005–2032.
6. Ichinose, M., Endo, S., Critz, S. D., Shenolikar, S., and Byrne, J. H. (1990) Microcystin-LR, a potent protein phosphatase inhibitor, prolongs the serotonin- and cAMP-induced currents in sensory neurons of *Aplysia californica*. *Brain Res.* **533**, 137–140.
7. Fry, D. W., Besserer, J. A., and Boritzki, T. J. (1984) Transport of the antitumor antibiotic CI-920 into L1210 leukemia cells by the reduced folate carrier system. *Cancer Res.* **44**, 3366–3370.
8. Favre, B., Turowski P., and Hemmings, B. A. (1997) Differential inhibition and posttranslational modification of protein phosphatase 1 and 2A in MCF7 cells treated with calyculin-A, okadaic acid, and tautomycin. *J. Biol. Chem.* **272**, 13,856–13,863.
9. Golden, T. A. and Honkanen, R. E. (2003) Regulating the expression of protein phosphatase type 5. *Methods Enzymol.* **366**, 372–930.
10. Killilea, S. D., Mellgren, R. L., Aylward, J. H., and Lee, E. Y. (1978) Inhibition of phosphorylase phosphatase by polyamines. *Biochem. Biophys. Res. Commun.* **81**, 1040–1046.

Synthesis and Use of the Protein Phosphatase Affinity Matrices Microcystin–Sepharose and Microcystin–Biotin–Sepharose

Greg B. G. Moorhead, Timothy A. J. Haystead, and Carol MacKintosh

Summary

Microcystin-based affinity matrices have been utilized to demonstrate the association of signaling proteins with protein phosphatases and for the purification of low-abundance microcystin-sensitive protein phosphatases. Here, we describe the procedure for the synthesis and use of microcystin–Sepharose and microcystin–biotin–Sepharose.

Key Words: Microcystin, okadaic acid; protein phosphatase; biotin; affinity chromatography; cyclic-peptide; hepatotoxin; cyanobacteria

1. Introduction

Protein phosphatase catalytic subunits associate with a diverse array of proteins, which function to localize and alter the activity of the protein phosphatase (1–5). Many protein phosphatase-binding or regulatory subunits, particularly those associated with PP1, are low-abundance proteins that are very susceptible to proteolysis and often dissociate during classical purification procedures. These properties had hindered the identification of new protein phosphatase-binding proteins. Many protein phosphatases are the targets of a number of small-molecule toxins produced by a wide variety of organisms (6). Okadaic acid, the agent responsible for diarrhetic shellfish poisoning, was the first potent and selective protein phosphatase inhibitor to be characterized. To date, this toxin is known to target PP1, PP2A, PP4, and PP5—all members of the PPP family of protein phosphatases. Microcystins are cyclic heptapeptides produced by certain blue-green algae that have been demonstrated to inhibit the activity of several PPP family members with nanomolar affinity. Microcystins

covalently couple to their target proteins through a highly conserved cysteine found in each of these enzymes (equivalent to Cys-273 of human PP1 γ 1) (7). We exploited the reactive group of the *N*-methyldehydroalanine residue of microcystin that normally couples to the cysteine side chain of the protein phosphatase and attached the toxin to the linker molecule aminoethanethiol. The introduced amino group of microcystin–aminoethanethiol (MC–AET) can be directly coupled to a reactive Sepharose bead or reacted with iodoacetyl–LC–biotin to generate MC–biotin (8,9). MC–biotin–phosphatase complexes are then easily captured on avidin–Sepharose. MC–Sepharose and MC–biotin both retain their high affinity for the PPP family of protein phosphatases and these matrices have subsequently aided in the discovery and purification of many novel protein phosphatase complexes or demonstrated the association of a protein phosphatase with another protein or complex (8–16).

The procedures described for the synthesis of microcystin–Sepharose and MC–biotin–Sepharose yield products with high capacity and stability. For MC–Sepharose, 1 mg of microcystin coupled to 6 mL of matrix has a binding capacity of about 1 mg of protein phosphatase catalytic subunit per milliliter of matrix.

2. Materials

2.1. Reagents

1. Microcystin (Calbiochem, Sigma-Aldrich).
2. Trifluoroacetic acid ((TFA) Pierce).
3. pH indicator strip, NaHCO₃ (BDH).
4. C₁₈ Sep-pak cartridge (Waters).
5. Activated CH–Sepharose (Amersham-Pharmacia).
6. Iodoacetyl–LC–biotin; trifluoroacetic acid (TFA) (Pierce).
7. C₈ Reverse-phase high-performance liquid chromatography (HPLC) column (3.9 × 150 mm) (Phenomenex).
8. Biotin; aminoethanethiol hydrochloride; leupeptin; benzamidine; phenylmethylsulfonyl fluoride (PMSF); tosylphenylalanyl chloromethyl ketone; aprotinin; dimethyl sulfoxide (DMSO); NP-40; avidin–Sepharose; Tris-(2-carboxyethyl) phosphine hydrochloride (TCEP); and sodium isothiocyanate (Sigma-Aldrich).
9. Centriprep-10 and microcon-10 (Amicon).

2.2. Buffers and Solutions

1. Buffer A: 25 mM Tris-HCl, pH 7.5, 0.1 mM EGTA, 0.1% (v/v) β -mercaptoethanol.
2. Buffer B: 25 mM Tris-HCl, pH 7.5, 0.1 mM EGTA, 0.1% (v/v) β -mercaptoethanol, 3 M sodium isothiocyanate.
3. Buffer C: 25 mM HEPES, pH 7.0, 25 mM NaF, 0.15 mM sodium orthovanadate, 1 mM EDTA, 1 mM EGTA, 0.1% (v/v) β -mercaptoethanol plus the protease

inhibitors 4 $\mu\text{g/mL}$ leupeptin, 1 mM benzamidine, 0.1 mM PMSF, 0.5 mM tosylphenylalanyl chloromethyl ketone, 10 $\mu\text{g/mL}$ soya bean trypsin inhibitor, and 0.1 $\mu\text{g/mL}$ aprotinin.

4. Buffer D: buffer C containing 0.2% (v/v) NP-40 and 0.6 M KCl.
5. Make a 0.1% (v/v) TFA solution by diluting 0.020 mL TFA into 19.98 mL of distilled water.
6. Make a 0.1% (v/v) TFA solution in 10% (v/v) acetonitrile in water by diluting 0.020 mL TFA into 17.98 mL of distilled water and 2 mL of acetonitrile.
7. Make a 0.1% (v/v) TFA solution in acetonitrile by diluting 0.020 mL TFA into 19.98 mL of acetonitrile.
8. 100 mM NaHCO_3 , pH 8.2.
9. 100 mM Tris-HCl, pH 8.
10. 50 mM Tris-HCl, pH 8, 0.5 M NaCl.
11. 50 mM Acetate pH 4, 0.5 M NaCl.
12. Sodium azide, 0.05% (w/v).
13. 0.1% (v/v) TFA containing 1 mM Tris-(2-carboxyethyl) phosphine hydrochloride (TCEP).
14. Make a 0.1% (v/v) TFA solution in 25% (v/v) acetonitrile in water by diluting 0.20 mL TFA into 149.8 mL of distilled water and 50 mL of acetonitrile.
15. 50 mM Borate, pH 9.2, 1 mM TCEP.

3. Methods

3.1. Preparation of MC-Sepharose

1. Briefly purge water, DMSO, and 5 N NaOH separately with N_2 gas (*see Note 1*).
2. Dissolve aminoethanethiol hydrochloride in water just before use (0.75 g to every 0.25 mL water, which gives an approx 1 g/mL solution).
3. Dissolve 1 mg microcystin in 1000 μL 95% ethanol, and add 1.5 vol (1500 μL) water, 2 vol. DMSO (2000 μL), 0.67 vol (666 μL) 5 N NaOH, and 1 vol (1000 μL) aminoethanethiol hydrochloride (1 g/mL) to a 10-mL screw-cap reaction vial, in that order (*see Note 2*).
4. Briefly purge the container with N_2 gas, seal, and incubate at 50°C for 60 min on a heating block.
5. Let the solution cool for 15 min at room temperature, and in a fume hood, add 990 μL of acetic acid. Dilute with 19.8 mL 0.1% (v/v) TFA. Take the pH to 1.5 by dropwise addition of 100% (v/v) TFA (approx 200 μL), checking the pH by spotting onto a pH indicator strip.
6. Apply the sample to a C_{18} Sep-Pak cartridge (*see Note 3*) equilibrated in 0.1% (v/v) TFA (prewet with methanol). Collect the flow-through into a tube and seal for disposal. Wash the cartridge with 0.1% (v/v) TFA in 10% (v/v) acetonitrile in water. Elute the AET-MC with 0.1% (v/v) TFA in acetonitrile (collect 10–12 1-mL fractions), dry by rotary evaporation, and dissolve each in 20 μL of methanol (*see Note 4*).
7. Add about 600 μL of 100 mM NaHCO_3 , pH 8.2, to each tube and vortex again.

8. Swell 2 g of activated CH-Sepharose in water for 15 min (this should yield approx 6 mL of matrix) and then wash with ice-cold 1 mM HCl (41 μ L concentrated HCl in 500 mL water) in a 50-mL Falcon tube. Pellet the matrix by spinning gently (500 rpm for 30 s in a tabletop centrifuge), carefully remove the liquid portion, and wash with 5 vol of 100 mM NaHCO₃, pH 8.2. Resuspend matrix in 2 vol of 100 mM NaHCO₃, pH 8.2, and use immediately.
9. React the amino group of AET-MC (from the pooled fractions of **step 7**) with activated CH-Sepharose end over end for 1.5 h at 25°C.
10. After reaction, pellet matrix gently and dispose of liquid portion. Wash excess ligand away with 100 mM NaHCO₃ pH 8.2, block unreacted groups with 100 mM Tris-HCl, pH 8 for 1 h, and then alternate with 50 mM Tris-HCl, pH 8, 0.5 M NaCl and with 50 mM acetate, pH 4, 0.5 M NaCl by gently pelleting matrix, removing liquid, and resuspending in the next buffer.
11. Store the prepared and washed MC-Sepharose in 20 mM Tris-HCl, pH 7.5, containing a bactericide, such as 0.05% (w/v) sodium azide, and wash before use.

3.2. Synthesis of MC-Biotin

1. The *N*-methyldehydroalanine residue of MC is derivatized with ethanedithiol (EDT) to form the product EDT-MC using a modification of the reaction conditions described by Moorhead et al. (8). Dissolve approx 5.0 mg of MC in 90 ethanol and 200 μ L water, 65 μ L of 5 M NaOH, 6 μ L of 250 mM EDTA, 245 μ L DMSO, and 15 μ L EDT. To avoid excessive degradation of MC make sure that the NaOH is added last to the mixture (*see Note 2*). All components should be gassed thoroughly with nitrogen prior to mixing.
2. After 60 min at 55°C, add 1.0 mL of 17.4 M glacial acetic acid and then dilute the mixture 10-fold with 0.1% (v/v) TFA containing 1 mM TCEP. Check efficiency of the reaction by reverse-phase HPLC (use C₈ reverse-phase column (3.9 \times 150 mm) equilibrated in 25% (v/v) acetonitrile, 0.1% (v/v) TFA and develop with increasing gradient of acetonitrile in 0.1% (v/v) TFA over 50 min). Reaction of MC with EDT should result in a shift in an approx 6-min reduction in retention time of MC, consistent with the formation of the product EDT-MC. Reaction efficiency for the conversion of MC to EDT-MC should be >95%.
3. Apply the products of the reaction to a C18 Sep-Pak cartridge equilibrated in 0.1% (v/v) TFA, wash with 0.1% (v/v) TFA, 1 mM TCEP solution, and elute EDT-MC in a minimal volume of acetonitrile. Evaporate to dryness and dissolve EDT-MC in 1.0 mL of 50 mM borate, pH 9.2, 1 mM TCEP. Incubated in the dark with 6 mmol of iodoacetyl-LC-biotin/mmol of EDT-MC for 90 min at room temperature. Upon HPLC, reaction of EDT-MC with iodoacetyl-LC-biotin should result in a dramatic increase in retention time of EDT-MC by approx 16 min, consistent with the formation of MC-biotin. The efficiency of conversion of EDT-MC to MC-biotin should be >95%.
4. MC-biotin was purified by preparative reverse-phase HPLC, evaporated to dryness, and stored in ethanol at -20°C.

3.3. Use of MC-Sepharose to Purify Protein Phosphatases

Microcystin is a potent inhibitor of the activity of PP1, PP2A, PP4, and PP5, but not PP2B or PP7. PP1, PP2A, PP4, PP5, and PP6 (*see Note 5*) have been shown to bind to MC-Sepharose, and several novel protein phosphatase complexes have been purified on this matrix. When trying to purify complexes from crude fractions, we generally run a control or 'blank' matrix in parallel to account for nonspecific binding to the Sepharose bead. To synthesize a control matrix, we generally react the swollen matrix with the quenching agent Tris-HCl, pH 8, as described earlier.

1. Incubate sample end over end with 0.5–2 mL of matrix for 1 h at 4°C. Pour slurry into a chromatography column and wash with up to 300 mL of buffer A plus 150 mL to 1 M NaCl (*see Note 6*). Once washed, pass 1 vol of buffer B through the matrix and stop flow. Add an additional 2 mL of buffer B to the matrix and mix gently by sucking up with a pipet; then let sit for 30 min at 4°C. For a 1-mL column, collect 15-mL of eluant by adding buffer B to the column.
2. Dialyze the eluant versus appropriate buffer; concentrate with a centrprep 10 then centricon or microcon 10 to desired volume. If analysis on sodium dodecyl sulfate–polyacrylamide gel electrophoresis (SDS-PAGE) is required, we suggest concentration to <50 μ L before the addition of the SDS cocktail.

3.4. Purification of Protein Phosphatases by MC-Biotin Affinity Chromatography.

1. Homogenize tissue/cells in 2.5 vol (w/v) buffer C and centrifuge at 15,000g for 10 min at 4°C. The pellet (membrane fraction) and supernatant (cytosolic fraction) are sources of PP1, PP5, and PP2A_C binding proteins. Clarify the cytosolic fraction by centrifugation (100,000g) for 90 min at 4°C.
2. Preclear the supernatant of endogenous biotinylated proteins by passing over avidin-Sepharose (2 \times 5 cm) equilibrated in buffer C. Repeat steps with particulate fraction following resolubilization in buffer D and centrifugation.
3. Mix the precleared extracts with 10 mM MC-biotin and apply to fresh avidin-Sepharose (1–2 mL). Wash the avidin column extensively with buffer C containing 1 M salt and then buffer C. Elute the bound proteins with buffer C containing 1 mM biotin.

4. Notes

1. We add reagents to a 10-mL screw-cap vial and purge for 1 min by inserting a needle in the vial to supply a gently stream of gas and then seal with the lid after degassing.
2. Microcystins are degraded under alkali conditions, so it is necessary to modify the microcystin with a thiol reagent that reacts sufficiently quickly. The product of the reaction, AET-MC, is stable in alkali.

3. In the fume hood, attach the Sep-Pak cartridge to a retort stand and insert a 20-mL syringe into the top of the cartridge. This allows the sample, wash, and elution solutions to be added in large volumes.
4. After the addition of methanol to each tube in a fume hood, alternately pipet up and down and vortex each tube to aid in dissolving the product.
5. We have purified plant PP4 and PP6 on MC–Sepharese (Moorhead, unpublished data).
6. The salt concentration in the wash buffer will have to be determined for particular systems. Some complexes are sensitive to salt and will be dissociated at high (>500 mM) concentration. We generally start by using 150 mM NaCl in the wash buffer.

Acknowledgment

Research in the Moorhead laboratory is supported by the Natural Sciences and Engineering Research Council of Canada.

References

1. Cohen, P. T. (2002) Protein phosphatase 1: targeted in many directions. *J. Cell. Sci.* **115**, 241–256.
2. Bollen, M. (2001) Combinatorial control of protein phosphatase-1. *Trends Biochem. Sci.* **26**, 426–431.
3. Janssens, V. and Goris, J. (2001) Protein phosphatase 2A: a highly regulated family of serine/threonine phosphatases implicated in cell growth and signalling. *Biochem. J.* **353**, 417–439.
4. Cohen, P. T. (1997) Novel protein serine/threonine phosphatases: variety is the spice of life. *Trends Biochem. Sci.* **22**, 245–251.
5. Shenolikar, S. (1994) Protein serine/threonine phosphatases—new avenues for cell regulation. *Annu. Rev. Cell Biol.* **10**, 55–86.
6. MacKintosh, C. and MacKintosh, R. W. (1994) Inhibitors of protein kinases and phosphatases. *Trends Biochem. Sci.* **19**, 444–448.
7. MacKintosh, R. W., Dalby, K. N., Campbell, D. G., Cohen, P. T., Cohen, P., and MacKintosh, C. (1995) The cyanobacterial toxin microcystin binds covalently to cysteine-273 on protein phosphatase 1. *FEBS Lett.* **371**, 236–240.
8. Moorhead, G. B. G., MacKintosh, R. W., Morrice, N., Gallagher, T., and MacKintosh, C. (1994) Purification of type 1 protein (serine/threonine) phosphatases by microcystin–Sepharese affinity chromatography. *FEBS Lett.* **356**, 46–50.
9. Campos, M., Fadden, P., Alms, G., Qian, Z., and Haystead, T. A. (1996) Identification of protein phosphatase-1-binding proteins by microcystin-biotin affinity chromatography. *J Biol Chem.* **271**, 28,478–28,484.
10. Moorhead, G., Johnson, D., Morrice, N., and Cohen, P. (1998) The major myosin phosphatase in skeletal muscle is a complex between the β -isoform of protein phosphatase-1 and the MYPT2 gene product. *FEBS Lett.* **438**, 141–144.

11. Moorhead, G. B. G., MacKintosh, C., Morrice, N., and Cohen, P. (1995) Purification of the hepatic glycogen-associated form of protein phosphatase-1 by microcystin–Sephacryl affinity chromatography. *FEBS Lett.* **362**, 101–105.
12. Johnson, D. F., Moorhead, G. B. G., Caudwell, F. B., et al. (1996) Identification of protein phosphatase-1-binding domains on the glycogen and myofibrillar targeting subunits. *Eur J Biochem* **239**, 317–325.
13. Boudrez, A., Evens, K., Beullens, M., Waelkens, E., Stalmans, W., and Bollen, M. (1999) Identification of MYPT1 and NIPP1 as subunits of protein phosphatase 1 in rat liver cytosol. *FEBS Lett.* **455**, 175–178.
14. Meek, S., Morrice, N., and MacKintosh, C. (1999) Microcystin affinity purification of plant protein phosphatases: PP1C, PP5 and a regulatory A-subunit of PP2A. *FEBS Lett.* **457**, 494–498.
15. Stubbs, M. D., Tran, H., Atwell, A. J., Smith, C. S., Olson, D., and Moorhead, G. B. G. (2001) Purification and properties of *Arabidopsis thaliana* type one protein phosphatase (PP1). *Biochim. Biophys. Acta* **1550**, 52–63.
16. Tran, H. T., Ulke, A., Morrice, N., Johannes, C. J., and Moorhead, G. B. (2004) Proteomic characterization of protein phosphatase complexes of the mammalian nucleus. *Mol. Cell. Proteomics* **3**, 257–265.

Utilizing Protein Phosphatase Inhibitors to Define PP2A as a Regulator of Ataxia-Telangiectasia Mutated

Aaron A. Goodarzi, Pauline Douglas, Greg B.G. Moorhead, and Susan P. Lees-Miller

Summary

Ataxia-telangiectasia mutated (ATM) is a serine/threonine protein kinase that plays a central role in controlling the cellular response to DNA double-strand breaks caused by ionizing radiation. Ionizing radiation induces the autophosphorylation of ATM on serine 1981; however, the precise mechanisms that regulate ATM autophosphorylation are not fully understood. By treating cells with okadaic acid, a cell-permeable protein phosphatase inhibitor, together with assays to quantify the activity of particular protein phosphatases, we have demonstrated that the autophosphorylation of ATM on serine 1981 is regulated by a protein phosphatase 2A-like activity. Here, we describe the series of experiments that employed protein phosphatase inhibitors to establish that ATM was regulated by a type-2A protein phosphatase.

Key Words: Okadaic acid; ATM; autophosphorylation; protein phosphatase; PP2A; ionizing radiation

1. Introduction

The resourceful use of specific inhibitors of the phospho-protein phosphatase (PPP) family of protein phosphatases can be invaluable while examining the role of reversible protein phosphorylation in regulating cellular events. This type of approach has been aided by the discovery of protein phosphatase inhibitors that are both cell permeable and relatively specific for a given phosphatase activity ([1,2](#)). Recently, we utilized several such inhibitors to discern the role of protein phosphatases in the regulation of the ionizing radiation (IR)-induced DNA-damage signaling pathway where the ataxia-telangiectasia mutated (ATM) protein kinase is a key player. In response to IR, ATM is rapidly activated and this action is mediated, at least in part, by autophosphorylation

From: *Methods in Molecular Biology, Volume 365: Protein Phosphatase Protocols*
Edited by: G. Moorhead © Humana Press Inc., Totowa, NJ

on serine 1981 (3). The autophosphorylation of ATM has been shown to occur on nearly every ATM molecule within the nucleus, is maximal within a few minutes of IR exposure, and persists for more than 48 h after irradiation. The unusually rapid kinetics and the “on/off” nature of ATM autophosphorylation at serine 1981 suggested the possibility that a protein phosphatase could play a part in regulating ATM by dephosphorylation of this residue in resting cells, similar to the interplay between cdc25 phosphatases and cyclin-dependent kinases that controls entry into mitosis (discussed in ref. 4). A series of in vivo experiments with the protein phosphatase inhibitor okadaic acid, followed by in vitro assays for an activity that would dephosphorylate ATM phosphoserine 1981 demonstrated that a PP2A-like activity was responsible for this event. Subsequent studies confirmed that PP2A associates with ATM, maintaining serine 1981 of ATM in a dephosphorylated state in resting cells, and dissociates from ATM in response to IR, allowing activation of the ATM pathway (5). Here, we describe the series of experiments that contributed to these conclusions.

2. Materials

2.1. Tissue Culture, Irradiation and Cell Lysis

1. C35ABR and L3 cells cultured in RPMI 1640 medium containing 10% fetal bovine serum (FBS) (FetalClone III; Hyclone, Logan, UT), 100 units/mL streptomycin (Invitrogen, Carlsbad, CA) and 100 units/mL penicillin (Invitrogen).
2. A source of contained radioactivity for safe delivery of gamma-radiation to cells, such as the Gammacell™ 1000 ¹³⁷Cs source (MDS Nordion).
3. 1X Phosphate-buffered saline (PBS): 137 mM NaCl, 1.47 mM KH₂PO₄, 10 mM Na₂HPO₄, 2.7 mM KCl, pH is 7.4, prepared from an autoclaved 10X stock in ice-cold water (see Note 1).
4. Protease inhibitors: 200 mM phenylmethylsulfonylfluoride (PMSF) (see Note 2), 10 mg/mL pepstatin, 10 mg/mL leupeptin, and 10 mg/mL aprotinin, all individually prepared in 100% methanol and stored at −20°C.
5. NETN (NaCl, EDTA, Tris-HCl, NP-40) buffer for cell lysis, containing 150 mM NaCl, 0.2 mM ethylenediamine tetraacetic acid (EDTA) pH 8.0, 50 mM Tris-HCl, pH 7.5, and 1% (v/v) NP-40 detergent. NETN buffer should be stored at 4°C. Before addition to cells, NETN buffer should be supplemented freshly with 0.2 mM PMSF, 0.1 µg/mL pepstatin, 0.1 µg/mL aprotinin and 0.1 µg/mL leupeptin to inhibit proteases in cell lysates.
6. A Bio-Rad detergent-compatible protein concentration assay kit.
7. A 10 mg/mL solution of bovine serum albumin (BSA) prepared in NETN buffer for use as a protein concentration standard.
8. A 6X solution of sodium dodecyl sulfate (SDS) protein sample buffer: 15 mL glycerol, 12 mL of 1 M Tris-HCl, pH 6.8, 6 g SDS, 1.4 mL of β-mercaptoethanol, and a “pinch” of bromophenol blue.

2.2. Antibodies, Immunoblotting, and Immunoprecipitation

1. Solutions of 30% (w/v) acrylamide and 2% (w/v) bis-acrylamide, prepared in filtered water. Both solutions should be stored at 4°C in the dark.
2. A 20% (w/v) SDS solution, prepared in filtered water. This concentration of SDS might require heating to approx 50°C to dissolve initially.
3. Solutions of 1 M Tris-HCl at both pH 8.8 and pH 6.8 (at 21°C), prepared in water and autoclaved.
4. A 10% (w/v) ammonium persulfate (APS) solution, prepared in water, within the past 7 d, and N,N,N,N'-Tetramethyl-ethylenediamine (TEMED) from Bio-Rad.
5. Electrophoresis SDS running buffer: 60 g Tris, 288 g glycine, and 10 g SDS per litre of water.
6. High-molecular-weight (HMW) electrophoresis transfer buffer containing 48 mM Tris-HCl, 39 mM glycine, 20% (v/v) methanol and 0.036% (w/v) SDS. This solution is stored at 4°C and can be reused up to five times.
7. Tris-buffered saline (TBS): 20 mM Tris-HCl pH 7.5, 150 mM NaCl, containing Tween-20 (T-TBS: TBS with 0.1% (v/v) Tween-20 detergent), prepared freshly from a 10X stock of autoclaved TBS and a solution of 20% [v/v] Tween-20 (prepared in water and stored at 4°C).
8. Immunoblot blocking buffer (*see Note 3*): 25% (w/v) skim milk powder (*see Note 4*) in 1X T-TBS.
9. Anti-ATM phosphoserine 1981 polyclonal rabbit antibody (Rockland), stored at -20°C. Working solutions are prepared at a 1 : 500 dilution in a solution of 1X T-TBS supplemented with 0.1% (w/v) gelatin (from a 10% stock, prepared in water and heated to approx 50°C to liquefy) and 0.05% (w/v) sodium azide (from a 10% stock prepared in water).
10. Anti-ATM polyclonal rabbit antibody 4BA (a kind gift from Dr. M. Lavin, Queensland Institute Medical Institute).
11. Anti-ATM polyclonal rabbit antibody Ab-3 PC116 (Oncogene Research Products, La Jolla, CA).
12. Anti-rabbit IgG horseradish peroxidase (HRP)-conjugated goat antibodies (Bio-Rad) are stored at 4°C. Working solutions for secondary antibody incubations are prepared at a 1 : 2000 dilution in 1X T-TBS buffer containing 5% (w/v) skim milk powder. This solution should be made the same day as it is to be used and should not be reused.
13. Enhanced chemiluminescent (ECLTM) Western blotting detection reagents from GE Healthcare.
14. Antibody stripping buffer: 2% (w/v) SDS, 60 mM Tris-HCl, pH 6.8, and 0.7% (v/v) β -mercaptoethanol.
15. Protein A-Sepharose beads (GE Healthcare), prepared as a 1 : 1 slurry in NETN buffer.
16. Fuji-Film super HR-S30 film (Fuji Photofilm Co., Tokyo)

2.3. Protein Phosphatase Inhibitors

1. Okadaic acid (OA) (*see Note 5*) is from Sigma and is dissolved in dimethyl sulfoxide (DMSO) to a stock concentration of 1 mM.
2. Microcystin-LR (MC-LR) (*see Note 6*) is from Sigma and is dissolved in 100% methanol to a stock concentration of 1 mM.
3. Fostriecin is supplied dry, combined in a 1 : 1.5 ratio with ascorbic acid to prevent oxidation and inactivation. It should be freshly dissolved in water to a 2 mM stock and used immediately.
4. Inhibitor-2 is prepared as described in **ref. 6**, and is stored in 20 mM Tris-HCl, pH 7.5, 0.1 mM EGTA, 0.1 mM EDTA, 0.1% (v/v) β -mercaptoethanol, and 50% glycerol at -20°C .

2.4. Protein Phosphatase Assays

1. A 75-mM solution of caffeine (*see Note 7*) (pH 7.0), prepared in water.
2. ^{32}P -Labeled phosphorylase- α (prepared as described in **ref. 1**).
3. Phosphatase assay buffer A: 50 mM Tris-HCl, pH 7.5, 0.1 mM EGTA, 0.1% (v/v) β -mercaptoethanol, and 1 mg/mL BSA.
4. Phosphatase assay buffer B: 50 mM Tris-HCl, pH 7.5, 0.1 mM EGTA, and 0.03% (v/v) Brij-35.
5. Phosphatase assay buffer C: 50 mM Tris-HCl, pH 7.5, 0.1 mM EGTA, and 0.1% (v/v) β -mercaptoethanol.
6. A 20% (w/v) solution of ice-cold trichloroacetic acid (TCA).

3. Methods

For carrying out the experiments described here, the laboratory should be equipped for standard biochemical techniques and the use of radioactive reagents. Work with ^{32}P should be carried out with the appropriate shielding, in an area equipped with a 30°C water bath and a microcentrifuge. Access to a scintillation counter, refrigerated centrifuge (for preparing cell extracts), and cell culture facilities is also required.

The methodologies described in the following subsections refer to the specific example of the regulation of ATM autophosphorylation by PP2A. However, it is important to note that these techniques should be applicable to the study of other systems of protein phosphorylation and dephosphorylation and could be used as a model for examining the phosphatase-mediated regulation of any phospho-protein.

3.1. Treating Cells and Preparing Cell Extracts

3.1.1. Treating Cells with Okadaic Acid

1. Cells (*see Note 8*) should be cultured such that they are undergoing logarithmic growth at $>95\%$ viability at the time of treatment. For C35ABR (ATM $^{+/+}$) and L3

- (ATM^{-/-}) cells, cultures should be no more than 5×10^5 cells/mL at the time of treatment.
2. Generally, a 100X working stock of OA is prepared in DMSO for each desired condition (e.g., 50 μ M working stock for a desired final treatment concentration of 0.5 μ M). OA loses potency if kept in a dilute manner (< 100 μ M) at room temperature in the light for too long; therefore, it is best to prepare dilutions freshly and immediately before treatment.
 3. Add OA (*see Note 9*) to cell culture media and return cells to incubator for the desired amount of time, being sure to add an equal volume of DMSO to the “no treatment” control. While being treated with OA, cultures should not be exposed to light more than absolutely necessary.
 4. After treatment, cells should be gently pelleted (no more than 2500g) for 2–5 min, placed on ice, and washed at least twice with between 1 and 10 mL of ice-cold 1X PBS. Adherent cell lines can be either scraped into media or removed using a solution of trypsin–EDTA (*see Note 10*).

3.1.2 Treating Cells with Ionizing Radiation

1. Irradiation, using a MDS Nordion Gammacell 1000 ¹³⁷Cs source, is delivered at a dose rate of 250 cGy/min. Maximal, rapid ATM autophosphorylation at serine 1981 is achieved at any dose greater than 2 Gy.
2. Irradiation of cells should be carried out in conditioned medium (i.e., the culture medium that cells were grown in should be irradiated along with cells). Following irradiation, both cells and media can be returned to the tissue culture for a desired amount of time (*see Note 11*).
3. After irradiation, cells should be processed as in **Subheading 3.1.1.4., step 4**.

3.1.3. Preparing and Quantitating NETN Whole-Cell Extracts

1. Washed cell pellets can be successfully lysed by resuspending cells in a volume of ice-cold NETN buffer (*see Note 12*) equal to twice the packed-cell volume. Generally, 30–60 min on ice is sufficient time for near total lysis of cells and extraction of proteins.
2. After cell lysis, NETN extracts should be centrifuged for 10 min at 10,000g to remove cell debris.
3. Because the presence of NP-40 detergent interferes with standard Bradford protein concentration assays, a Lowry-based assay must be used. The detergent-compatible Bio-Rad protein assay provides accurate measurements of NETN whole-cell extract (WCE) concentrations and should be carried out as per the manufacturer’s instructions using BSA dissolved in NETN buffer as a standard.

3.2. Immunoblotting ATM

3.2.1. SDS–Polyacrylamide Gel Electrophoresis

1. Prepare a 75-mm-thick separating PAGE gel containing 8.4% (w/v) acrylamide, 0.075% (w/v) bis-acrylamide, 375 mM Tris–HCl, pH 8.8, and 0.1% (w/v) SDS.

2. Generally, 40–60 μg (*see Note 13*) of total protein in a NETN WCE is sufficient for an immunoblot of ATM. Before SDS-PAGE, 6X SDS sample buffer should be added to a 1X final concentration to prepared aliquots of NETN extracts and heated to approx 90°C for at least 1 min.

3.2.2. Electrophoretic Transfer of ATM

1. To successfully immunoblot ATM (approx 370 kDa), the PAGE gels (described in **Subheading 3.2.1.1., step 1**) must be electrophoretically transferred to nitrocellulose in HMW electrophoresis transfer buffer at 100 V for 1 h.
2. Immunoblots should be incubated in blocking buffer for a minimum of 30 min, before being rinsed twice in T-TBS buffer (to remove all traces of residual milk from blocking buffer) and placed in primary antibody.

3.2.3. ATM Antibodies

1. The ATM phosphoserine 1981 antibody working solution should be incubated with the immunoblot at 4°C, with gentle agitation, for a minimum of 3 h and not longer than overnight (approx 16 h).
2. Following removal of primary antibody (which can be reused a minimum of five times if stored at –20°C), the immunoblot is washed at least twice with T-TBS buffer (10 min per wash), with rocking.
3. The goat anti-rabbit secondary antibody working solution should be incubated with the immunoblot at room temperature, for between 30 and 60 min, with gentle agitation.
4. Following the removal of secondary antibody, the immunoblot is washed at least twice with T-TBS buffer as earlier. Before each wash is removed, vigorously shake the container to generate bubbles. This serves to dramatically reduce the problem of nonspecific background signal(s).
5. The ECL reagent should be employed as per the manufacturer's instructions. With GE Healthcare ECL reagent, the ATM phosphoserine 1981 signal (induced by either a ≥ 2 Gy dose of IR or a 2-h, 0.5- μM treatment with OA) is generally detectable with an exposure time of approx 2 min (*see Fig. 1A*).
6. After a suitable exposure is obtained from the ATM phosphoserine 1981 specific antibody, the blot should be stripped by incubation in 50 mL of stripping buffer for 30 min at approx 60°C (in a fume hood).
7. After stripping, the immunoblot should be rinsed with several successive water washes (*see Note 14*) until all traces of SDS are removed and then washed with two 10-min T-TBS washes, followed by reblocking as described in **Subheading 3.2.2.**
8. To detect total ATM protein levels (which should not change with either IR or OA treatment), the immunoblot should then be incubated with a working solution of anti-ATM (4BA) antibody for a minimum of 3 h and not longer than overnight (approx 16 h). This is then followed by a repeat of **steps 2–5**.

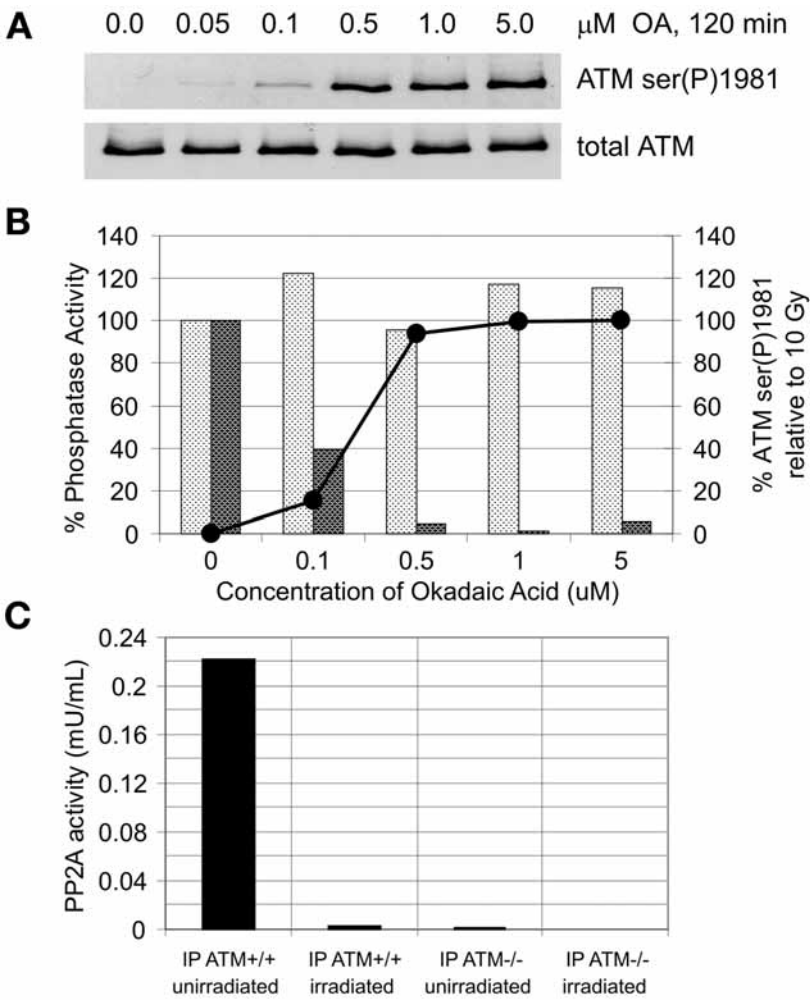


Fig. 1. A PP2A-like protein phosphatase activity regulates phosphorylation of ATM at serine 1981. (A) C35ABR cells were treated for 2 h with increasing concentrations of OA as indicated and processed as described in **Subheading 3.1**. (B) The extracts shown were assayed for the percent of PP1 (light bars) or PP2A-like (dark bars) activity remaining. The solid line with black circles indicates the quantitated ATM ser(P)1981 signals induced by the indicated concentrations of OA relative to those produced by 10 Gy IR. (C) C35ABR (ATM+/+) and L3 (ATM-/-) cells were either left untreated or irradiated with 10 Gy and harvested immediately. Whole-cell extracts were prepared in the absence of phosphatase inhibitors and ATM was immunoprecipitated and assayed for PP2A-like protein phosphatase activity.

3.3. Assaying for protein phosphatase activity

3.3.1. Measuring Total Protein Phosphatase Activity of Cell Extracts

(The following was adapted from **ref. 1**).

1. NETN WCE, prepared (as in **Subheading 3.1.3.**) without protein phosphatase inhibitors from C35ABR cells treated (as in **Subheading 3.1.1.**) for 2 h with 0, 0.1, 0.5, 1, or 5 μM OA must be made the same day as they are to be used in protein phosphatase assays (see **Note 15**) and should be diluted to 10–15 mg/mL with phosphatase assay (PA) buffer A.
2. Add 0.1 mL of 75 mM caffeine and 0.4 mL of PA buffer C to 1.5 mL of preprepared ^{32}P -labeled phosphorylase- α (phos- α) to make a 3-mg/mL (30 μM) solution and store on ice. If the diluted phos- α is cloudy, warm to 30°C for 2 min and centrifuge at 12,000g for 2 min, discarding any pellet.
3. Thirteen micrograms (see **Note 16**) of NETN WCE is diluted to a final volume of 10 μL with PA buffer A, followed by the addition of 10 μL of PA buffer B. All assays should be done in triplicate. Be sure to include two or more blanks, containing only PA buffer A with no extract.
4. Phosphatase assays are initiated by the addition of 10 μL ^{32}P -labeled phos- α , which are carried out at 30°C for 20 min.
5. Terminate reaction by adding 100 μL of 20% (w/v) trichloroacetic acid (TCA), followed by centrifugation at 12,000g for 10 min.
6. Remove 100 μL of supernatant (containing released ^{32}P) for quantitative analysis by Cerenkov counting.
7. To calculate phosphatase activity, use the following formula:

$$\text{Activity (mU/mL)} = \left(\frac{\text{cpm (released)} - \text{cpm (blank)}}{\text{cpm (total)}} \right) \left(\frac{0.3 \text{ (nmol phos-}\alpha\text{)}}{\text{minutes (assay time)}} \right) \times 130$$

The dilution factor is 130 [(130 μL total assay volume/100 μL counted volume) \times 100]; the factor of 100 is used to convert units into activity per 1 mL versus activity per 10 μL of assayed protein.

3.3.2. Measuring Relative PP1 and PP2A-Like Protein Phosphatase Activity

(The following was adapted from **ref. 1**).

1. To assay for a certain protein phosphatase activity using the technique described in **Subheading 3.3.1.**, inhibitors are included in PA buffer B to specifically target a given class of phosphatase. In all cases, preincubate samples with inhibitor for at least 10 min before assaying.
2. To determine PP1 activity, 15 nM OA is added to PA buffer B such that the final concentration of OA in the assay is 5 nM, sufficient to completely inhibit PP2A-like enzymes (including PP2A, PP4, and PP5), but not PP1.

3. To determine PP2A-like activity, 600 nM Inhibitor-2 is added to PA buffer B such that the final concentration of Inhibitor-2 in the assay is 200 nM, sufficient to inhibit 100% of PP1, but no PP2A-like enzymes.
4. It is also important to calculate the background phosphatase activity once both PP1 and PP2A-like activities have been eliminated. Assays containing both 5 nM OA and 200 nM Inhibitor-2 must also be carried out, and this activity must be subtracted from the values obtained for PP1 and PP2A-like activity.
5. In the case of NETN WCE prepared from C35ABR cells, PP2A-like activity accounts for approx 60–70% of total protein phosphatase activity, whereas PP1 activity accounts for approx 20–30% of total, with an approx 5–10% residual background activity.
6. By carrying out assays under each of the above-described conditions, using extracts prepared from cells treated with a range of OA concentrations, the relative inhibition of each protein phosphatase activity may be determined and correlated with the incidence of phospho-specific events immunoblotted from the same cell source (see **Fig. 1B**).

3.3.3. Assaying Protein Phosphatase Activity on ATM Immunoprecipitates

1. The NETN WCEs are prepared and quantitated as described in **Subheading 3.1.3.** from both ATM positive (C35ABR) and negative (L3) cells.
2. For each immunoprecipitate (IP), between 1 and 2 mg (see **Note 17**) of WCE should be incubated for a minimum of 3 h at 4°C with 4 μ L of anti-ATM Ab-3 PC116 (see **Note 18**), with rotation.
3. Thirty microliters of 1:1 protein A–Sepharose slurry is then added to each IP for 30 min at 4°C, with rotation.
4. After incubation with protein A–Sepharose, the beads are pelleted at 3000g for 3 min, and the supernatant is replaced with 1 mL of ice-cold NETN containing no phosphatase inhibitors.
5. The beads should be gently inverted (do not vortex) several times and pelleted as earlier. This is repeated so that beads receive four sequential 1-mL NETN washes.
6. After the last wash, remove as much liquid as possible from the beads and resuspend them in 10 μ L of PA buffer A.
7. The beads can then be assayed exactly as described in **Subheadings 3.3.2.** and **3.3.3.** We have found that only PP2A-like activity is associated with an ATM IP, and that this is not present in ATM IPs from irradiated cells (see **Fig. 1C**).

3.3.4. Examining Protein Phosphatase Activity by Phospho-Specific Immunoblot

1. Both an irradiated (10 Gy, immediate harvest) and unirradiated culture of C35ABR cells should be prepared as described in **Subheading 3.1.** Four times as many irradiated cells should be prepared versus unirradiated cells.
2. Four separate solutions of NETN buffer (all with protease inhibitors) should be prepared containing either of the following:

- a. 1 μM MC-LR (inhibits PP1 and PP2A-like activities);
 - b. no phosphatase inhibitor;
 - c. 1 μM fostreicin (inhibits PP2A-like activity but not PP1 or PP5);
 - d. 200 nM inhibitor-2 (inhibits PP1 activity).
3. The washed cell pellet from the unirradiated culture of cells should be resuspended in the NETN buffer containing 1 μM MC-LR and lysed as described in **Subheading 3.1.3.**
 4. The washed cell pellet from the irradiated culture of cells should be split equally into four equal portions, and then each portion should be resuspended in one of the four different NETN buffers prepared in **Subheading 3.4.2.**
 5. The NETN WCE should then be prepared as described in **Subheading 3.1.3.**, and (after centrifugation) incubated at 30°C for 30 min to allow “native” protein phosphatases to dephosphorylate available substrates in vitro.
 6. The cell extracts are then immunoblotted for ATM phosphoserine 1981 and total ATM as described in **Subheading 3.2.** (see **Fig. 2**). In the absence of an inhibitor of PP2A-like enzymes, the PP2A active in the extract almost completely removes the IR-induced phosphate from serine 1981 of ATM, indicating a PP2A-like activity targets ATM in vitro. Conditions in which PP1 or PP5 are fully active show no loss of phosphoserine 1981 signal, indicating that these phosphatases cannot target ATM in vitro.

4. Notes

1. In all cases, buffers should be prepared in water that has been filtered through a 0.2- μm filter (i.e., a Milli-Q system).
2. Please note that PMSF is particularly toxic, and especially so if inhaled in its dry form. Solutions of PMSF should be prepared in the fume hood.
3. This solution should be prepared freshly before each use; it will sour and curdle if left at room temperature in excess of 36 h.
4. Purchase from any supermarket.
5. Okadaic acid should be stored in small aliquots at -20°C . Once dissolved, OA should be stable for at least 3–6 mo. Notably, OA is the principle component responsible for diarrhetic shellfish poisoning and is toxic if consumed/inhaled.
6. The MC-LR should be stored in small aliquots at -20°C . MC-LR is generally very stable and should not expire if properly stored. MC-LR is the principle component responsible for the toxicity associated with certain blue-green algae blooms and is extremely toxic if consumed/inhaled.
7. Dissolved caffeine should be stored in the dark, as it will slowly degrade if left exposed to light.
8. We have successfully observed OA-induced ATM autophosphorylation at serine 1981 in the following cell lines: HeLa, HL60, MCF7, A549, M059K, C35ABR, L3, AT1ABR, C3ABR, and normal human fibroblast Hs68 cells. We have used C35ABR, L3, and HeLa cells for phosphatase assays on whole-cell NETN extracts and have used C35ABR (ATM^{+/+}) and L3 (ATM^{-/-}) cells for phosphatase assays on ATM immunoprecipitates. The methods described here might be appli-

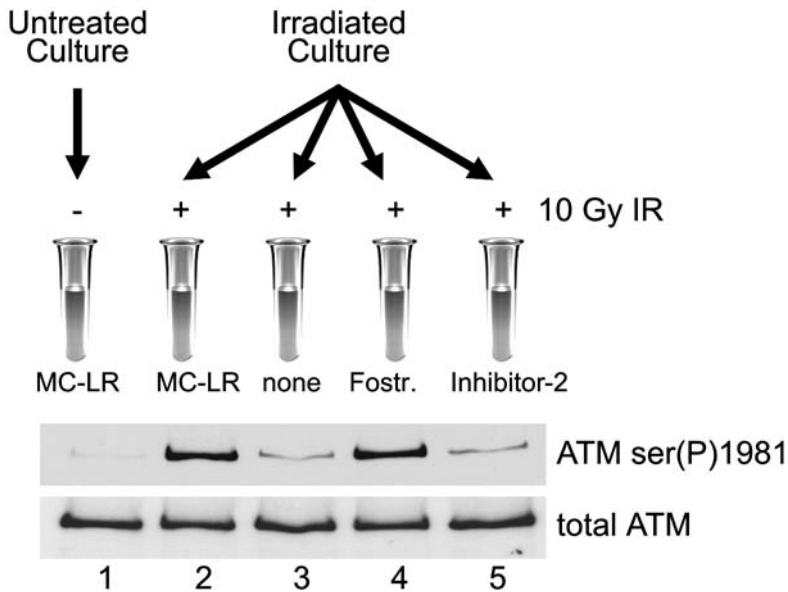


Fig. 2. PP2A-like but not PP1 or PP5 protein phosphatase activity can dephosphorylate ATM phosphoserine 1981 in cell free extracts. C35ABR cells were either left unirradiated or irradiated with 10 Gy IR and harvested immediately. Irradiated cell cultures were divided and lysed in NETN buffer with or without protein phosphatase inhibitors as indicated. Whole-cell extracts were incubated at 30°C for 30 min before being resolved by SDS-PAGE and immunoblotted for ATM ser(P)1981 and total ATM.

cable to other human cell lines, which should be cultured according to their specific needs and growth rates.

9. Using C35ABR cells, a 2-h treatment with 0.5 μM OA is sufficient to inhibit more than 90–95% of subsequently assayed PP2A-like protein phosphatase activity and induce maximal ATM autophosphorylation at serine 1981 (see Fig. 1B). Treatments in excess of 10 μM OA (for 2 h) are required to achieve inhibition of PP1 activity.
10. Notably, treatments with OA (>100 nM) for more than 1 h will usually cause adherent cells to partially or completely lift from the plate; therefore, care should be taken not to lose cells by discarding the media prematurely.
11. Ataxia–telangiectasia mutated autophosphorylation at serine 1981 is readily detectable within 1 min following irradiation, will reach maximal levels within 5 min of IR exposure, and will persist (at maximal levels) for at least 3–4 h before slowly declining over the next 48 h.
12. Phosphatase inhibitors should be added to the NETN buffer (before addition to cells) as needed. For example, the addition of 1 μM MC-LR to the NETN lysis

buffer will completely and irreversibly inhibit PP1 and PP2A-like protein phosphatases. This is used if cell extracts are intended for immunoblotting. If the extracts are to be used for protein phosphatase assays, then *no inhibitor* should be added to the NETN lysis buffer.

13. The same amount of each cell extract should be used for a given immunoblot.
14. In this case, tap water is perfectly suitable, and it is convenient to simply hold the blot (in a container) under a lukewarm flow of tap water until all of the bubbles are removed.
15. Extracts that are over of 36 h old, or that have been previously frozen either do not work or produce ambiguous results because of progressively declining activity.
16. To ensure linearity of protein phosphatase activity, conditions are designed to keep the percent release of ^{32}P between 10% and 30% of total. In the case of C35ABR NETN WCE, 13 μg of extract assayed for 20 min produced a linear release of phosphate. These conditions must be determined for each cell line and type of extract being used.
17. This refers to variation between experiments, as a slightly different amount of cell extract will be generated each time. Within an experiment, however, the same quantity of cell extract must be used for each condition (in the IP).
18. We have observed that this antibody is very sensitive to improper storage, and if frozen or allowed to warm up for extended periods of time, it will lose IP efficacy. If working properly, the total ATM immunoblot signal for the ATM IP should greatly exceed the signal derived from approx 30 μg of total protein (run side-by-side on the same gel). A “bad” aliquot of antibody will not only poorly immunoprecipitate ATM but will also not be useful for examining coimmunoprecipitating proteins such as the components of PP2A.

Acknowledgments

We thank Dr. M. F. Lavin, Dr. M. Roberge, and Dr. Y. Shiloh for kindly providing various reagents. AAG was supported by graduate studentship scholarships from the Alberta Heritage Foundation for Medical Research and the Natural Science and Engineering Research Council of Canada. SPLM is a Scientist of the Alberta Heritage Foundation for Medical Research, an Investigator of the Canadian Institutes for Health Research and holds the Engineered Air Chair in Cancer Research. This work was funded by grant no. 11053 from the National Cancer Institute of Canada with funds from the Canadian Cancer Society.

References

1. MacKintosh, C. and Moorhead, G. B. G. (1999) Assay and purification of protein serine/threonine phosphatases, in *Protein Phosphorylation: A Practical Approach*. (Hardie, D.G., ed.), Oxford University Press, Oxford, pp. 153–181.
2. Honkanen, R. E. and Golden, T. (2002) Regulators of serine/threonine protein phosphatases at the dawn of a clinical era? *Curr. Med. Chem.* **9**, 2055–2075.

3. Bakkenist, C. J. and Kastan, M. B. (2003) DNA damage activates ATM through intermolecular autophosphorylation and dimer dissociation. *Nature* **421**, 499–506.
4. Goodarzi, A. A. and Lees-Miller, S. P. (2005) Regulation of ATM by protein phosphatase 2A. *Cell Cycle*, in press.
5. Goodarzi, A. A., Jonnalagadda, J. C., Douglas, P., et al. (2004) Autophosphorylation of ataxia–telangiectasia mutated is regulated by protein phosphatase 2A. *EMBO J.* **23**, 4451–4461.
6. Cohen, P., Foulkes, J. G., Holmes, C. F. B., Nimmo, G. A., and Tonks, N. A. (1988) Protein phosphatase inhibitor-1 and inhibitor-2 from rabbit skeletal muscle, in *Methods in Enzymology* (Corbin, J. D. and Johnson, R. A., eds.), Academic, London, Vol. 159, pp. 427–437.

An Automated Fluorescence-Based Method for Continuous Assay of PP2A Activity

Adam M. Wegner, Jamie L. McConnell, Randy D. Blakely,
and Brian E. Wadzinski

Summary

Protein serine/threonine phosphatase (PP2A) is a major cellular enzyme implicated in the control of numerous signaling processes. The accurate measurement of PP2A activity in crude cell lysates, immune complexes, and purified preparations provides insight into the function and regulation of this essential enzyme, which, in turn, can lead to a better understanding of the signaling pathways that it modulates. The method presented here utilizes 6,8-difluoro-4-methylumbelliferyl phosphate (DiFMUP) and a FLEXstation for the continuous measure of PP2A activity associated with many different protein preparations. This automated fluorescence-based assay offers several distinct advantages over colorimetric and radioactive assays of phosphatase activity including (1) decreased substrate preparation time, (2) real-time kinetic data, (3) high sensitivity, and (4) the capability to analyze a wide variety of phosphatases.

Key Words: Phosphatase; PP2A; DiFMUP; phosphatase assay; immune complex

1. Introduction

Reversible protein phosphorylation, catalyzed by the opposing actions of protein kinases and phosphatases, is a major mechanism for the relay of information through numerous cellular signal transduction pathways. Although often underappreciated, protein phosphatases play an equally important role as protein kinases in maintaining the phosphorylation equilibrium, and both must be extensively characterized to understand control of a certain protein's phosphorylation state. A common approach to study the role of protein phosphatases in a specific signal transduction pathway is the application of phosphatase inhibitors to whole cells followed by evaluation of changes in the phosphorylation state of target proteins within the pathway. Although these

From: *Methods in Molecular Biology*, Volume 365: *Protein Phosphatase Protocols*
Edited by: G. Moorhead © Humana Press Inc., Totowa, NJ

experiments might identify potential phosphatase targets, they do not provide unequivocal evidence that the target protein is a direct substrate for the phosphatase of interest. To complement these cellular experiments, *in vitro* phosphatase assays are often utilized to examine direct dephosphorylation of various signaling proteins by purified phosphatases. The oldest and most commonly used phosphatase assays employ radiolabeled substrates. Although very sensitive, these procedures are time-consuming (e.g., synthesis and purification of a radiolabeled substrate) and not well suited for the large number of samples necessary for kinetic analysis. Colorimetric phosphatase assays, in which the level of liberated inorganic phosphate is monitored spectrophotometrically as a complex of malachite green and acidified phosphomolybdate ([1](#)), provide newer alternatives to radioactive assays. These procedures are generally easy to perform and eliminate handling of radioactivity, but their limited sensitivity necessitates the use of relatively large amounts of enzyme and substrate.

Fluorescence-based methods for measuring protein phosphatase activity have recently been developed. These assays offer several advantages over standard radioactive and colorimetric procedures, including lower limits of detection of phosphatase activity and continuous monitoring of product levels. One compound that has been used as a fluorogenic substrate for protein phosphatases is 6,8-difluoro-4-methylumbelliferyl phosphate (DiFMUP) (*see* **Note 1**). Phosphatase-mediated hydrolysis of DiFMUP, a compound with low fluorescence, converts it to 6,8-difluoro-4-methylumbelliferone (DiFMU), a highly fluorescent compound ([2](#)). DiFMUP is a versatile substrate, as it can be dephosphorylated by a wide variety of phosphatases, including protein tyrosine phosphatases ([3](#)), protein serine/threonine phosphatases ([4](#)), human T-cell phosphatase ([5](#)), mitogen-activated protein (MAP) kinase phosphatase 3 ([6](#)), acid phosphatase ([7](#)), and alkaline phosphatase ([7](#)). In this chapter we show how DiFMUP can be utilized in an automated procedure to monitor phosphatase activities of isolated immune complexes and purified enzyme preparations. As an application of this technique, we assayed the phosphatase activity associated with immune complexes of the human norepinephrine transporter (hNET), which has previously been shown to interact with protein serine/threonine phosphatase 2A (PP2A) ([8](#)). In addition, we demonstrate the utility of this method for assaying phosphatase activity of purified PP2A preparations, such as those described in Chapter 9. Together with previous reports ([3–7](#)), our studies indicate that DiFMUP is an excellent phosphatase substrate that can be used to monitor real-time phosphatase activities in a variety of different samples, including crude cell extracts, immune complexes, and purified enzyme preparations.

2. Materials

2.1. Isolation of HA-hNET/PP2A Immune Complexes

2.1.1. Cell Culture and Transfection

1. COS-7 cells (ATCC, Manassas, VA).
2. Dulbecco's modified Eagle's medium (DMEM) (Vanderbilt Media Core) supplemented with 10% fetal bovine serum (FBS) (Gibco, Grand Island, NY), 100 U/mL penicillin (Gibco), 100 mg/mL streptomycin (Gibco), and 2 mM L-glutamine (Sigma, St. Louis, MO).
3. HA-tagged human norepinephrine transporter (HA-hNET) cloned into the pcDNA3 mammalian expression vector (Invitrogen, Carlsbad, CA) (*see Note 2*).
4. Phosphate-buffered saline (PBS): 10 mM Na₂PO₄, 0.17 mM KH₂PO₄, pH 7.4, 137 mM NaCl, and 0.27 mM KCl. Store at 4°C.
5. Trypsin–EDTA: Filter 10X trypsin–ethylenediamine tetraacetic acid (EDTA) (Gibco) through a 2-μm SFCA filter (Nalge Nunc International, Rochester, NY), dilute with sterile PBS to a 1X working solution, and store at 4°C.
6. TransIT-LT1 Transfection Reagent (Mirus, Madison, WI) stored at 4°C.

2.1.2. Cell Lysis and Immunoprecipitation

1. Aprotinin (Sigma).
2. 1 mg/mL Pepstatin A (Sigma) in 100% ethanol.
3. 100 mM Phenylmethylsulfonylfluoride (PMSF) (Sigma) in 100% isopropanol.
4. 10 mg/mL Leupeptin (Sigma) in water.
5. Cell lysis and immunoprecipitation buffer: 50 mM Tris-HCl, pH 8.0, 100 mM NaCl, 2 mM EDTA, and 1% (v/v) Igepal CA-630. Add 5 μg/mL aprotinin, 1 μg/mL pepstatin A, 1 μg/mL leupeptin, and 1 mM PMSF to the buffer immediately before use.
6. Anti-HA Affinity Matrix (Roche, Indianapolis, IN).
7. BD Falcon Cell Scraper: Falcon 353085 (Becton Dickinson, Franklin Lake, NJ).

2.2. Purification of Specific PP2A Holoenzymes

FLAG-tagged Bα- and Bδ-containing PP2A holoenzymes prepared as described in Chapter 9.

2.3. DiFMUP Phosphatase Assay

1. 10 mM stock of DiFMUP (Molecular Probes, Eugene, OR) in dimethylsulfoxide (DMSO) (Sigma). Store in 50 μL single-use aliquots at –20°C.
2. 50 mM Tris-HCl, pH 7.0.
3. 40 mM NiCl₂ in water.
4. 5 mg/mL Bovine serum albumin (BSA) (Sigma) in 50 mM Tris-HCl, pH 7.0.
5. 1 M CaCl₂ in water.
6. Assay plate: Corning/Costar 3691 black 96 well with clear, flat bottom (Corning, Corning, NY).

7. Compound plate: Falcon Microtest U-Bottom 353077 (Becton Dickinson, Franklin Lakes, NJ).
8. 250 μ M Okadaic acid–sodium salt (Alexis USA, San Diego, CA) in DMSO. Store in 10- μ L aliquots at -20°C .
9. SoftMax Pro 4.3.1 software (Molecular Devices, Sunnyvale, CA).
10. FLEXstation (Molecular Devices).
11. GraphPad Prism 4 (GraphPad Software, San Diego, CA).

3. Methods

3.1 Isolation of HA-hNET/PP2A Immune Complexes (see Note 2)

3.1.1 Cell Culture and Transfection

1. Plate 300,000 COS-7 cells per 35-mm dish in DMEM 24 h before transfection. Grow cells at 37°C in a humidified atmosphere with 5% CO_2 .
2. Combine 100 μ L of serum-free DMEM and 3 μ L of TransIT (per transfection) in a 1.5-mL microfuge tube. Vortex and incubate at room temperature for 10 min. Add 1 μ g pcDNA3 or HA-hNET/pcDNA3 and incubate at room temperature for 15 min. Add the solution dropwise to the respective dishes.

3.1.2. Cell Lysis and Immunoprecipitation

1. Forty-eight hours post-transfection, place dishes of cells on ice and gently wash once with 1 mL of ice-cold PBS.
2. Add 200 μ L of lysis buffer and scrape cells off the dish with a cell scraper.
3. Combine cell lysates from two dishes into one 1.5-mL microfuge tube and incubate for 15 min on ice.
4. Centrifuge at 16,000g for 15 min at 4°C and transfer supernatant to a new 1.5-mL microfuge tube.
5. Wash Anti-HA Affinity Matrix (15 μ L of a 50% slurry per immunoprecipitation) three times with ice-cold lysis buffer by centrifuging at 2,000g, aspirating supernatant, and resuspending in 1 mL of lysis buffer for each wash.
6. After the final wash, remove supernatant and resuspend beads in half of the original volume to make a 50% slurry.
7. Add 15 μ L of the washed slurry of Anti-HA Affinity Matrix to each 1.5-mL microfuge tube containing cell extract (from two wells) and rotate end-over-end overnight at 4°C .
8. Wash beads three times with ice-cold lysis buffer as described in **step 5**.
9. Keep samples on ice and use immediately for phosphatase assay (see **Note 3**).

3.2. Purification of Specific PP2A Holoenzymes

Refer to Chapter 9 for details.

3.3. DiFMUP Phosphatase Assay (see Note 4 and Fig. 1)

1. Open SoftMax Pro on the computer connected to the FLEXstation and click the thermometer button on the toolbar to set the temperature in the reading chamber to 37°C .

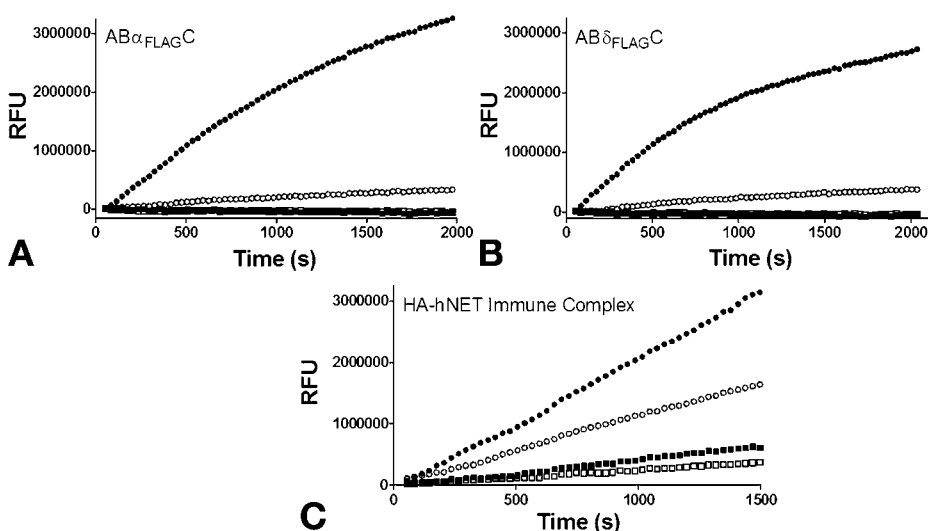


Fig. 1. DiFMUP assay of $AB_{\alpha_{FLAG}C}$ and $AB_{\delta_{FLAG}C}$ PP2A holoenzymes and HA-hNET immune complexes. Anti-FLAG immunoprecipitations were performed on lysates from cells transfected with FLAG- B α , FLAG-B δ , or empty vector and the resulting immune complexes were eluted with FLAG peptide (see Chapter 9 for details). Approximately 1 ng of PP2A holoenzyme containing the indicated FLAG-tagged B-subunits and an equal volume of FLAG eluted material from a control immunoprecipitation were assayed for 2000 s with 100 μ M DiFMUP. The y-axis represents relative fluorescence units (RFUs). HA immunoprecipitations were performed on lysates from COS-7 cells transiently transfected with HA-hNET/pcDNA3 or pcDNA3 vector. Immune complexes on beads were assayed for 1500 s with 100 μ M DiFMUP. The decrease in RFUs observed in the presence of 2 nM okadaic acid represents PP2A specific activity. (A) FLAG-B α (●), FLAG-B α + 2 nM okadaic acid (○), FLAG vector (■), and FLAG vector + 2 nM okadaic acid (□). (B) FLAG-B δ (●), FLAG-B δ + 2 nM okadaic acid (○), FLAG vector (■), and FLAG vector + 2 nM okadaic acid (□). (C) HA-hNET/pcDNA3 (●), HA-hNET/pcDNA3 + 2 nM okadaic acid (○), pcDNA3 vector (■), and pcDNA3 vector + 2 nM okadaic acid (□).

2. Prepare compound plate: Dilute DiFMUP in Tris-HCl, pH 7.0, to desired concentration (see Note 5). Determine which wells are to be used on the assay plate and add 150 μ L of diluted DiFMUP to the corresponding wells of the compound plate (see Note 6).
3. Prepare assay plate:
 - a. Make the desired volume of phosphatase assay buffer (PAB): 50 mM Tris-HCl pH 7.0, and 0.1 mM $CaCl_2$ (diluted from the 1 M $CaCl_2$ stock solution; see Note 7).
 - b. Dilute any phosphatase inhibitors (e.g., okadaic acid; see Note 8) in 50 mM Tris-HCl, pH 7.0, to a working concentration (see Note 9).

- c. Dilute holoenzyme preparation with PAB (*see Note 10*) or resuspend beads from one immunoprecipitation in 40 μL PAB.
- d. Combine 5 μL of 5 mg/mL BSA, 5 μL of 40 mM NiCl_2 , 35 μL of sample to be analyzed (phosphatase on beads or diluted holoenzyme preparation), and 35 μL of 50 mM Tris-HCl, pH 7.0, in the appropriate well of the assay plate. If any inhibitors are to be used, add them at this time and adjust the amount of 50 mM Tris-HCl, pH 7.0, so that the total volume is 80 μL .
4. Place compound plate into the compounds drawer, assay plate into the reading chamber drawer, and tip box into the tip rack drawer and allow them to equilibrate to 37°C for 10 min.
5. Click the “Setup” button on the toolbar of the active plate to adjust FlexStation settings as follows:

Reading mode:	“FLEX”
Wavelength:	Excitation: 358 nm Emission: 455 nm Auto Cutoff: 435 nm
Sensitivity:	Readings: 6
PMT sensitivity:	High
Timing:	Time: Varies (<i>see Note 5</i>) Interval: 30 s
Auto Mix:	Before: 5 s
Auto calibrate:	Once
Assay plate type:	96-well Costar blk/clrbtm (<i>see Note 11</i>)
Wells to read:	Varies (<i>see Note 12</i>)
Compound source:	Costar 96 Ubtm clear 0.3 mL
Compound transfer:	Initial volume: 80 μL Pipette height: 200 μL Volume: 120 μL Rate: 8 Time Point: 30 s
Triturate:	
Compound Source:	Volume: 75 μL Cycles: 3
Assay Plate:	Volume 50 μL Cycles: 3 Height: 100 μL
Compound & tip columns:	Entire tip rack
Auto read:	Off

6. Start reading by clicking the “Read” button on the top toolbar.
7. Once the experiment is complete, copy the data into Prism.
8. Subtract PAB control data from all other columns (*see Note 6*).
9. Click “statistical analysis” on the toolbar to perform a linear regression, the slope of which indicates phosphatase activity in relative fluorescence units per minute (RFU/min) (*see Notes 13 and 14*).

4. Notes

1. Other fluorogenic substrates utilized in fluorescent microplate assays include fluorescein diphosphate (FDP) and 4-methylumbelliferone (MUP). The substrate used in this assay is 6,8 difluoro-4-methylumbelliferyl phosphate (DiFMUP), a fluorinated derivative of MUP. In contrast to the hydrolysis product of MUP, which only fluoresces under alkaline conditions ($pK_a = 7.9$), has a low quantum yield (0.63), and has a high rate of photobleaching (22% in 33 min), the hydrolysis product of DiFMUP (DiFMU) fluoresces over a wide pH range ($pK_a = 4.9$), has a high quantum yield (0.89) and exhibits low photobleaching (5% in 33 min) without a change in excitation coefficient or excitation/emission maxima (2). DiFMUP is also superior to FDP as it eliminates biphasic kinetics resulting from sequential dephosphorylation of the two phosphate moieties on FDP (9).
2. Any immune complex containing PP2A (or another phosphatase) can be assayed for phosphatase activity using DiFMUP.
3. Storage at -20°C greatly diminishes phosphatase activity; however, some activity is usually observed after one freeze/thaw cycle.
4. Different forms of PP2A (e.g., AC core dimer or free catalytic subunit), as well as other phosphatases, can be assayed using this protocol. Phosphatase activity in crude cell lysates can also be analyzed, provided an appropriate set of phosphatase inhibitors is used to discriminate the activity of the phosphatase of interest from the activities of other phosphatases.
5. Typically, 100–500 μM DiFMUP is used in the phosphatase assays; however, concentrations as low as 12 μM (5) and as high as 1 mM (10) have been used. Assays can be run to saturation, but only the linear portion of the data should be considered for calculation of phosphatase activity. Substrate concentrations can be adjusted to increase the linear range, but it should be noted that higher substrate concentrations result in increased background activity. Enzyme concentrations can also be diluted to achieve the optimum linear range.
6. Include a control reaction containing only phosphatase assay buffer and DiFMUP to determine background DiFMUP hydrolysis. In addition, when using phosphatase inhibitors, include a control reaction containing only PAB, DiFMUP, and the corresponding volume of inhibitor vehicle (e.g., DMSO).
7. The PAB goes bad with time, causing an increase in background activity. To eliminate this problem, prepare fresh PAB for each experiment.
8. Okadaic acid should be kept frozen and thawed only once. Because okadaic acid is dissolved in DMSO, a control well containing the same volume of DMSO with PAB and DiFMUP should be run. DMSO alone should not have any significant effect on phosphatase activity. PP2A is inhibited by 2 nM okadaic acid, whereas PP1 is inhibited by 10–50 mM okadaic acid (11).
9. Because DiFMUP is a good substrate for a variety of phosphatases, control experiments with pharmacological inhibitors of PP2A (e.g., okadaic acid) must be performed to show that PP2A is responsible for the observed DiFMUP dephosphorylation. Inhibitor concentrations in the working stock solution should be adjusted so that addition of a small volume (2–10 μL) of the working stock solution to the assay plate gives the desired final concentration.

10. Typically, 0.5 μL of holoenzyme prep (approx 1 ng) should be sufficient to observe activity. To minimize pipetting error, dilute 2 μL of the holoenzyme preparation with 138 μL PAB and use 35 μL of the diluted sample for the assay.
11. Plates with clear sides can be substituted; however, these plates could result in higher background fluorescence.
12. In “FLEX” mode, the FLEXstation is only able to read one column of eight wells at a time. Therefore, experiments should be set up in columns and not rows. A high-throughput version of the assay can be performed with a 96-well microplate fluorescence reader that reads the whole plate at once.
13. A portion of the immune complex or a duplicate immunoprecipitation should be subjected to immunoblot analysis to confirm coimmunoprecipitation with PP2A and to compare activity levels with the amount of enzyme. Protein from individual wells can also be analyzed by immunoblot analysis after the readings are obtained.
14. Moles of phosphate released can be calculated by comparison of the measured RFUs with the fluorescence of DiFMU standards; these values can be used to calculate specific activity if the concentration of phosphatase is known. *Kcat*, *Vmax*, and *Km* can be determined using the initial velocities at several DiFMUP concentrations.

Acknowledgments

The authors would like to thank Dr. Deanna Adams for providing the purified PP2A holoenzyme preparations and for critical evaluation of the manuscript. We would also like to thank Dr. Uhna Sung for providing the HA-hNET/pcDNA3 construct. This research was supported by the National Institutes of Health grants GM51366 and DK070787 (to BEW) and MH58921 (to RDB). AMW was supported in part by National Institutes of Health training grant MH64913.

References

1. Geladopoulos, T. P., Sotiroidis, T. G., and Evangelopoulos, A. E. (1991) A malachite green colorimetric assay for protein phosphatase activity. *Anal. Biochem.* **192**, 112–116.
2. Sun, W. C., Gee, K. R., and Haugland, R. P. (1998) Synthesis of novel fluorinated coumarins: excellent UV-light excitable fluorescent dyes. *Bioorg. Med. Chem. Lett.* **8**, 3107–3110.
3. Montalibet, J., Skorey, K.I., and Kennedy, B. P. (2005) Protein tyrosine phosphatase: enzymatic assays. *Methods (Duluth)* **35**, 2–8.
4. Fontal, O. I., Vieytes, M. R., Baptista de Sousa, J. M., Louzao, M. C., and Botana, L. M. (1999) A fluorescent microplate assay for microcystin-LR. *Anal. Biochem.* **269**, 289–296.
5. Kerby, M., and Chien, R.L. (2001) A fluorogenic assay using pressure-driven flow on a microchip. *Electrophoresis.* **22**, 3916–3923.

6. Fjeld, C. C., Rice, A. E., Kim, Y., Gee, K. R., and Denu, J. M. (2000) Mechanistic basis for catalytic activation of mitogen-activated protein kinase phosphatase 3 by extracellular signal-regulated kinase. *J. Biol. Chem.* **275**, 6749–6757.
7. Gee, K. R., Sun, W. C., Bhalgat, M. K., et al. (1999) Fluorogenic substrates based on fluorinated umbelliferones for continuous assays of phosphatases and beta-galactosidases. *Anal. Biochem.* **273**, 41–48.
8. Bauman, A. L., Apparsundaram, S., Ramamoorthy, S., Wadzinski, B. E., Vaughan, R. A., and Blakely, R. D. (2000) Cocaine and antidepressant-sensitive biogenic amine transporters exist in regulated complexes with protein phosphatase 2A. *J. Neurosci.* **20**, 7571–7578.
9. Huang, Z., Wang, Q., Ly, H. D., et al. (1999) 3,6-Fluorescein diphosphate: a sensitive fluorogenic and chromogenic substrate for protein tyrosine phosphatases. *J. Biomol. Screen.* **4**, 327–334.
10. Welte, S., Baringhaus, K.-H., Schmider, W., Muller, G., Petry, S., and Tennagels, N. (2005) 6,8-Difluoro-4-methylumbiliferyl phosphate: a fluorogenic substrate for protein tyrosine phosphatases. *Anal. Biochem.* **338**, 32–38.
11. Favre, B., Zolnierowicz, S., Turowski, P., and Hemmings, B. A. (1994) The catalytic subunit of protein phosphatase 2A is carboxyl-methylated in vivo. *J. Biol. Chem.* **269**, 16,311–16,317.

An In Vivo Assay to Quantify Stable Protein Phosphatase 2A (PP2A) Heterotrimeric Species

Matthew S. Gentry, Richard L. Hallberg, and David C. Pallas

Summary

Protein phosphatase 2A (PP2A) regulates a broad spectrum of cellular processes. The enzyme is, in fact, largely a collection of varied heterotrimeric species composed of a catalytic (C) subunit and regulatory (B-type) subunit bound together by a structural (A) subunit. One important feature of the C subunit is that its carboxy-terminus can be modified by phosphorylation and methylation. The mechanisms that trigger such posttranslational modifications, as well as their consequences, are still under investigation. However, data collected thus far indicate that these modifications alter the binding to B subunits for an AC dimer, thereby affecting the makeup of the PP2A species in the cell. In this chapter, we describe an in vivo assay for assessing stable PP2A heterotrimer formation that is based on specific subcellular localizations of PP2A heterotrimers. This assay can be used to study the impact of a wide variety of alterations (such as mutations and covalent modifications) on PP2A heterotrimer formation. We specifically describe the use of this assay to quantify the effects of methylation on the stable formation of PP2A_{Rts1p} and PP2A_{Cdc5p} heterotrimers.

Key Words: Protein phosphatase 2A; PP2A; GFP; methylation; phosphorylation

1. Introduction

Protein phosphatase 2A (PP2A), a major eukaryotic serine/threonine protein phosphatase, plays a critical role in a wide array of cellular processes, including DNA replication, RNA transcription, RNA splicing, and cell-cycle progression (*1–4*). PP2A is able to participate in such a variety of processes, dephosphorylating multiple substrates, because of the enzyme's inherent heterogeneity. PP2A's heterogeneity is largely supplied via the B-type subunits. In mammals, five different classes of B-type subunits have been reported (*5*). In addition, each class possesses several isoforms, generating the potential for more than 40 different PP2A heterotrimeric species to exist (*5*).

From: *Methods in Molecular Biology, Volume 365: Protein Phosphatase Protocols*
Edited by: G. Moorhead © Humana Press Inc., Totowa, NJ

In the yeast *Saccharomyces cerevisiae*, the PP2A community is far simpler, encompassing only five genes. The A subunit is encoded by *TPD3* (6,7). The C subunits are encoded by two highly similar genes, *PPH21* and *PPH22* (8). *S. cerevisiae* has only two classes of B-type subunits and only one member in each class: *CDC55* encodes the B-class subunit (9) and *RTS1* encodes the B'-class subunit (10,11). Mutations in each PP2A subunit gene elicit complex pleiotropic phenotypes.

The complexity of PP2A in *S. cerevisiae* can be traced to the enzyme's community dynamics. These dynamics encompass three general areas.

1. Post-translational modifications of PP2A subunits (see Fig. 1A). The C subunits are methylated at their C-terminal leucine by Ppm1p and, by analogy with mammalian C subunits, can be phosphorylated on three residues by an unknown kinase(s) (12–15). Methylation and one phosphorylation event differentially affect stable formation of PP2A_{Cdc55p} and PP2A_{Rts1p} species (16–21). Likewise, Rts1p is phosphorylated in its N-terminus, but the function is unknown (11).
2. The stoichiometry of PP2A subunits (see Fig. 1B). The C subunits are the most abundant of the PP2A subunits (22). Rts1p (B-type subunit) is approx 12-fold more abundant than Cdc55p (B-type subunit), and Tpd3p (A subunit) serves as the limiting subunit for trimer formation (22). Thus, there is competition between B-type subunits for binding to the A-subunit.
3. The subcellular localization of PP2A (see Fig. 1C). One role of the B-type subunits is to target the heterotrimer to different cell-cycle-specific subcellular localizations via two different methods: Rts1p must be incorporated into a heterotrimer to achieve and/or maintain subcellular localization, whereas Cdc55p can be targeted to and accumulate at subcellular sites independent of heterotrimer assembly to a certain degree (22).

Cumulatively, all of the above factors endow just five proteins the flexibility needed to participate in multiple cellular events and pathways.

The idea for a novel quantitative assay to monitor stable heterotrimer formation arose from our recent studies defining these community dynamics (18,22–24). The crux of this assay is that PP2A_{Rts1p} and PP2A_{Cdc55p} heterotrimers exhibit distinct cell-cycle-specific subcellular localization patterns that can be easily visualized by fluorescence microscopy (see Figs. 1C and 2) (22). PP2A_{Rts1p} heterotrimers localize to the kinetochore of small/medium budded cells and to the bud neck of large budded, posttelophase cells (see Figs. 1C and 2) (22). Conversely, PP2A_{Cdc55p} heterotrimers localize to the bud tip of small/medium budded cells and to the bud neck of large budded, post-telophase cells (see Figs. 1C and 2) (22). Moreover, GFP-Tpd3p and Rts1p-GFP subcellular localizations are entirely dependent on heterotrimer formation, whereas GFP-Cdc55p can maintain some subcellular localization independent of heterotrimer formation (22). Therefore, GFP-Tpd3p subcellular localization to the kineto-

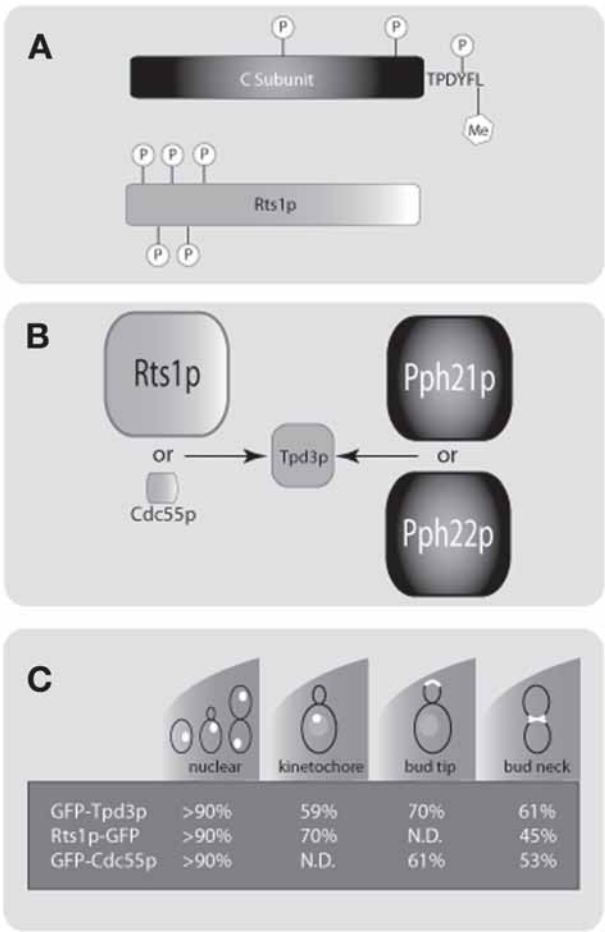


Fig. 1. The community dynamics of PP2A. **(A)** A schematic of PP2A subunit posttranslational modifications. The C-subunit of PP2A is modified with four post-translational modifications: methylation (Me) of the conserved C-terminal leucine, phosphorylation (P) of a conserved tyrosine two residues from the C-terminus, phosphorylation of an unidentified serine, and phosphorylation of an unidentified threonine. Rts1p is multiply phosphorylated in its first 216 amino acids. **(B)** A schematic of PP2A subunit stoichiometry. The size of the subunits reflect the relative abundances. In asynchronous *S. cerevisiae* cells, the ratio Rts1p : Cdc55p : Tpd3p : Pph21p : Pph22p is 4 : 0.25 : 1 : 4 : 4. **(C)** A summary of GFP-PP2A subunit localization patterns in asynchronous cells. Cells were divided into four classes: nonbudded, small/medium budded, large budded with one nucleus, and large budded with two nuclei. Cells in each class were scored as having or lacking the trademark localization in question. N.D. = not detected. (Part 1C was modified from [ref. 22](#), with permission from The American Society for Cell Biology.)

chore (via PP2A_{Rts1p}) and to the bud tip (via PP2A_{Cdc55p}) can be monitored and quantified as a measurement of stable PP2A_{Rts1p} and PP2A_{Cdc55p} heterotrimer formation, respectively. Quantification is done simply by visualizing cells expressing GFP-Tpd3p and scoring cells as having or lacking the trademark localization. Additionally, Rts1p-GFP and GFP-Cdc55p subcellular localizations can be used to verify the GFP-Tpd3p localization results.

Previously, quantitation of PP2A heterotrimeric species was monitored solely via immunoprecipitation and Western analysis. These techniques, although very powerful, have intrinsic flaws that are avoided by our *in vivo* assay. For instance, our assay circumvents instability issues with Rts1p that occur upon cell lysis, it avoids artifactual *in vitro* association of subunits that might have been compartmentalized *in vivo*, it allows the measurement of effects on PP2A_{Cdc55p} and PP2A_{Rts1p} stable heterotrimer formation in the same cells, and it measures the functional localization of PP2A heterotrimers. It must be noted that our assay does not specifically measure heterotrimer assembly or heterotrimer formation. The assay directly measures localization, which we use as an indirect measurement of the formation of localization competent heterotrimers, hence the wording “stable heterotrimer formation.”

2. Materials

1. *Saccharomyces cerevisiae* strain α W303 or other haploid or diploid strain with the appropriate genotype (e.g., appropriate mutant alleles of genes used as selectable markers for expression from plasmids) (*see Note 1*). The method described uses the strains and plasmid listed in **Note 2**.
2. Yeast extract, peptone, adenine, dextrose (YPAD; a variation of YPD/YEPD) medium to grow yeast under nonselection conditions (*see Note 3*). YPAD can be made via two methods:
 - a. Dissolve 50 g YPD medium (BD Biosciences) and 80 mg adenine hemisulfate salt (Sigma) in 1 L of water. Be sure to fully dissolve the YPD medium, as the dextrose can burn upon autoclaving. Autoclave for 30 min to sterilize.
 - b. Dissolve the following in order in 1 L of water: 20 g dextrose (Fisher Scientific), 80 mg adenine hemisulfate salt (Sigma), 10 g Bacto™ yeast extract (BD Biosciences), 20 g Bacto™ peptone (BD Biosciences). Be sure to fully dissolve the dextrose so that it does not burn upon autoclaving. Autoclave for 30 min to sterilize. Alternatively, dextrose can be made at a 20% (10X) solution that has been filter-sterilized to prevent darkening of the media and added to the solution after autoclaving.
3. Synthetic complete (SC or CM) medium to resuspend yeast for visualization of GFP-tagged proteins.
 - a. Dissolve 26.7 g minimal SD base (BD Biosciences), 80 mg adenine hemisulfate salt (Sigma), and the appropriate amount of the appropriate dropout (DO) supplement (BD Biosciences) in 1 L of water. Autoclave for 30 min to sterilize.

- b. Dissolve the following in order in 1 L of water: 20 g dextrose (Fisher Scientific), 1.7 g yeast nitrogen base without amino acids and without ammonium sulfate (US Biological), 5 g ammonium sulfate, 80 mg adenine hemisulfate salt (Sigma), and the appropriate amount of the appropriate DO supplement (BD Biosciences) (*see Note 4*).
4. 1000X 4',6-diamidino-2-phenylindole (DAPI) solution: Prepare a 1 mg/mL DAPI stock solution by dissolving 1 mg DAPI (Sigma) in 1 mL of water. Store the stock solution at -20°C .
5. A BX60 epifluorescence microscope (Olympus) using a 10X UPlanFl objective (numerical aperture [N.A.] 0.30) (Olympus), a 40X UPlanFl objective (N.A. 0.75) (Olympus), a 100X UPlan Apo objective (N.A. 1.35) (Olympus), and a manual shutter. The microscope is equipped with the Endow GFP (EGFP) bandpass emission filter set #41017 (Chroma) and DAPI/Hoechst/AMCA filter set #31000v2 (Chroma), a MagnaFire CCD camera (Olympus, Model S99806; with an array of 1300×1030 , 6.7- μm pixels) and a BH2-RFL-T3 100 W high-pressure mercury burner power supply unit (Olympus; 100–120 V, approx 2.8 A 50–60 Hz) or a comparable system (*see Note 5*).
6. Microscope slides, $3 \times 1 \times 1$ mm (Fisher) and glass cover slips, 22×22 mm, No. 1 thickness (Sigma)

3. Methods

3.1. Growth of Cells

1. Inoculate a single colony of *GFP-TPD3 ppm1 Δ* with YCp22 *PPM1*, *GFP-TPD3 PPM1* and *GFP-TPD3 ppm1 Δ* from a fresh plate into 3–5 mL of the appropriate media (SC minus tryptophan [–Trp] for the first strain and SC or YPAD for the second and third) and grow shaking at 30°C overnight (*see Notes 6 and 7*). The next afternoon, inoculate 10 mL of the same media with 5 μL , 10 μL , and 50 μL of the overnight culture. This will ensure that at least one of the dilutions will be at an OD_{600} of 0.4–0.8 the following morning (*see Note 8*).
2. The next morning, choose cultures that are still growing in log phase (preferably OD_{600} of 0.4–0.8), add 10 μL of a 1-mg/mL stock of DAPI to each culture and continue shaking at 30°C for 1 h (*see Note 9*).

3.2. Preparation of Cells

1. Spin down one OD_{600} unit of each culture at 1000g (approx 3000 rpm in a microcentrifuge) for 3 min at room temperature.
2. If the cells were grown in YPAD (instead of SC), then wash the cells once in SC (*see Note 10*).
3. Gently resuspend each culture in 30 μL of SC by pipeting up and down (do not vortex the cells). Place 3.3 μL of each culture onto a microscope slide and place a cover slip over each. Two to three separate cultures can be placed side by side on one microscope slide.

4. Place the slide and cover slips inside of a folded Kimwipe® (Thomas Scientific) with the cover slip side down on a flat surface. Press down on the microscope slide and excess liquid will be wicked up by the Kimwipe. Look at the cells using a non-oil-immersion objective and transmitted light microscopy to see if the cells are floating in the suspension or if they are still. If they are floating, repeat the Kimwipe pressing technique until enough liquid is removed so that the cells are still.

3.3. Microscopic Analysis and Quantification

1. View each cell culture under the necessary magnification to view subcellular localization (we almost exclusively use 100× to photograph and score cells). There should be 40–80 cells in the field-of-view. Be sure that the cells are not too dense (e.g., not touching) so that cell morphology can be used to determine cell-cycle stages.
2. Capture a picture of the field using the EGFP filter set; and DAPI filter set, move to a new field and capture another set of pictures. Exposure times to capture the GFP and DAPI signals vary for each microscope and camera, but our system requires the following exposure times: DAPI, 0.05 s; GFP-Tpd3p, 3 s; Rts1p-GFP, 5 s; GFP-Cdc55p, 9 s.
3. Repeat this sequence until approx 400 cells (approx 10–20 fields) have been captured for each culture. Capture these fields as quickly as possible, preferably having the cells on the microscope slide for less than 20 min. If needed, make one slide at a time so that the cells are not sitting under the cover slip at room temperature any longer than necessary (*see Note 11*).
4. Using a lab counter (Fisher), score small/medium budded cells as having or lacking GFP-Tpd3p kinetochore and bud tip localization (*see Note 12*). These cells will all have one undivided nucleus (because they are all premitotic cells), thus there is no need to examine the DAPI pictures when scoring for these subcellular localizations. An example of the cells is shown in [Fig. 2](#).
5. Score large budded, posttelophase cells as having or lacking GFP-Tpd3p bud neck localization. An example of GFP-Tpd3p localization is shown in [Fig. 2](#) and an example of DAPI-stained cells is shown in [Fig. 3](#). Nuclear division must be monitored to determine which cells are post-telophase. This can be done via two methods (we usually use the first):
 - a. Merge the DAPI and GFP captured files using Photoshop (Adobe) to assess nuclear positioning/cell-cycle phase and GFP-Tpd3p localization.
 - b. Open each file and view them side by side to assess nuclear positioning/cell-cycle phase and GFP-Tpd3p localization.
6. Calculate the percentage of cells that display each trademark localization pattern (*see Note 13*). [Figure 1C](#) shows the percentage of wild-type cells that display the trademark PP2A localizations (*see Note 14*).
7. Divide the percentage obtained for each subcellular location by the corresponding percentage obtained at the same location for *GFP-TPD3 PPM1* cells and

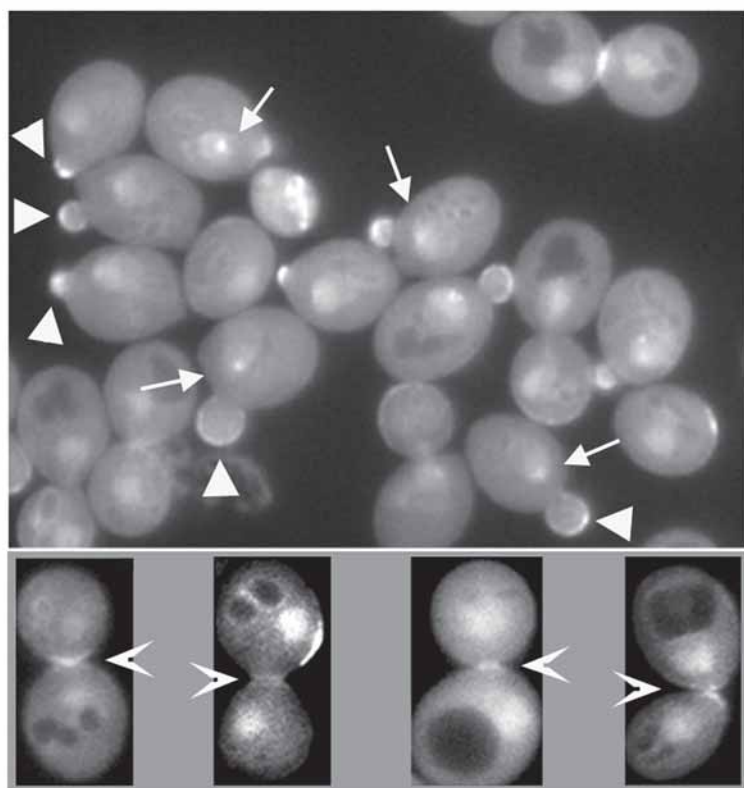


Fig. 2. GFP-Tpd3p localization. **(Top)** Asynchronous cells expressing GFP-Tpd3p were photographed using an EGFP filter set. Arrows denote kinetochore/spindle pole body localization; arrowheads denote bud tip localization. **(Bottom)** Single cells exhibit different phases of bud neck localization. Arrowheads denote bud neck localization. (Modified from [ref. 22](#), with permission from The American Society for Cell Biology.)

multiple by 100 to standardize all percentages to wild-type levels. An example of the results is shown in [Fig. 4](#).

4. Notes

1. Although we used haploid cells for our studies, diploid cells are often better for microscopy. Diploid cells are larger and often yield a brighter GFP signal (because of the increased protein products). Diploid a/α W303 cells with two integrated copies of the GFP genes expressing GFP-Tpd3p, Rts1p-GFP, or GFP-Cdc55p yield a brighter GFP signal than the respective haploid strain. However, the signal from haploid cells is more than sufficient for these experiments.

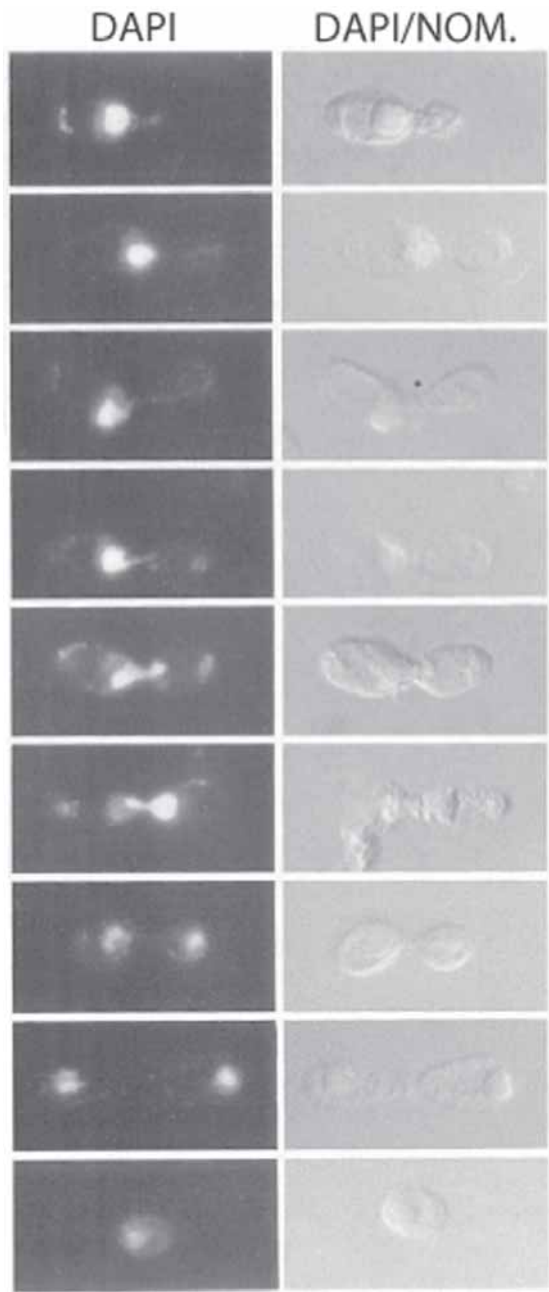


Fig. 3. DAPI-stained *S. cerevisiae* cells throughout the mitotic cell cycle. DAPI staining is shown in the left panels and DAPI with Nomarski is shown in the right panels. (Modified from **ref. 33**, with permission from Elsevier.)

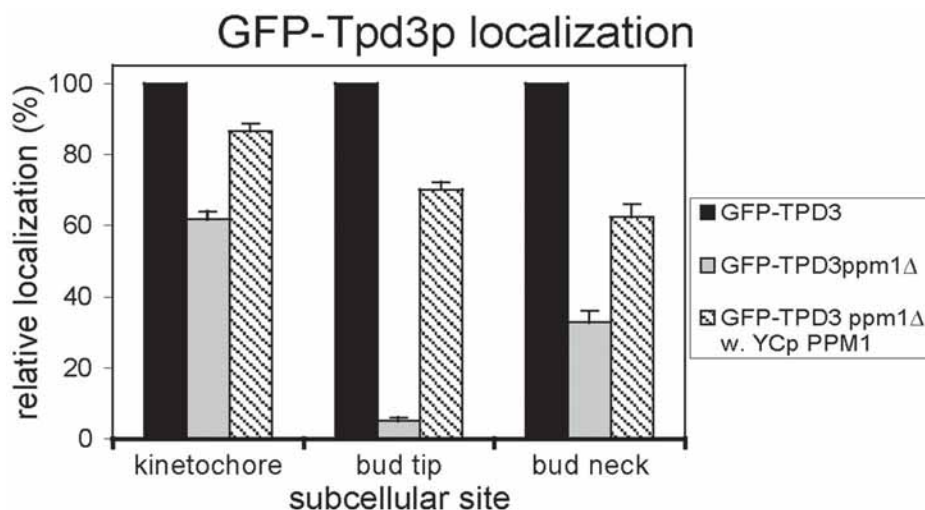


Fig. 4. Quantified GFP-Tpd3p kinetochore, bud tip and bud neck localization in *PPM1* and *ppm1Δ* cells. (Modified from [ref. 17](#), with permission from The American Society for Microbiology.)

2. We used two strains in this study: (MSG66) MAT α *ade2-1 ura3-1 his3-11 trp1-1 leu2-3,112 GFP-TPD3* and (MSG261) MAT α *ade2-1 ura3-1 his3-11 trp1-1 leu2-3,112 ppm1::KAN GFP-TPD3* ([17](#)). We used one plasmid in this study: (pMG528) YCp22 *PPM1*, *CEN* vector/*TRP1* ([17](#)).
3. Autofluorescence is a problem in *ade1* and *ade2* auxotrophic strains because of the accumulation of phosphoribosylaminoimidazole, a fluorescent metabolic precursor that accumulates in vacuoles ([25,26](#)). Thus, it is preferable to use adenine prototrophs. However, *ADE* prototrophic strains sometimes lightly autofluoresce. High concentrations of adenine (80 μ g/mL) will largely eliminate the autofluorescence of prototrophs and auxotrophs.
4. The DO supplement can be purchased as a premixed powder or can be made by adding the appropriate amino acids together ([27](#)).
5. An excellent review on using GFP in yeast cells, hardware (e.g., microscopes, CCD cameras, and objectives), and long-term live cell imaging protocols was written by Tatchell and Robinson ([28](#)).
6. We chose to write the methods using the *ppm1Δ* strain to show how lack of C-subunit methylation affects PP2A_{Rts1p} and PP2A_{Cdc55p} stable heterotrimer formation to different degrees. The assay can be used to test how other PP2A modifications (e.g., C-subunit phosphorylation) affect stable heterotrimer assembly as well ([17](#)). Additionally, we feel that this assay could easily be modified to test the stable assembly of other multimeric complexes, as long as at least one of the subunit's localization depends on complex formation.

7. In our experience, the localization of a GFP-tagged protein can vary immensely depending on whether the gene expressing the GFP is integrated or expressed from a YCp series vector (e.g., YCp22, YCp33, and YCp111) (29) versus expressed from a pRS series vector (e.g., pRS313, pRS314, pRS315, and pRS316) (30). The subcellular localizations of GFP-Tpd3p, GFP-Cdc55p, and Rts1p-GFP are nearly identical for integrated genes and those expressed from the YCp vector series. However, the localization changes dramatically when any of the three are expressed using the pRS vector series. This change in localization is likely the result of the copy number of the vectors. Although the YCp and pRS vector series both have a *CEN* sequence and are considered “single copy,” the pRS series often accumulates to multiple copies in each cell (31). Additionally, if we overexpress any of the PP2A subunits, the localization of the overexpressed subunit is disrupted and becomes ubiquitous throughout the cytoplasm. Furthermore, if we monitor the localization of a GFP-tagged subunit expressed from an integrated gene and overexpress a different subunit, the localization of the protein expressed from the integrated gene is disrupted. Thus, at least for PP2A, endogenous subunit stoichiometry is paramount for correct localization. For these reasons, we strongly recommend integrating the GFP-tagged gene and compare any protein levels from a vector-expressed gene to that of the integrated expression before doing any experiments from vector-expressed genes.
8. It is essential that the cultures all be at an OD₆₀₀ between 0.4 and 1.0 at the time of the experiment. The subcellular localization of Rts1p-GFP, GFP-Tpd3p, and GFP-Cdc55p changes at higher OD units. The subunits no longer localize to specific regions of the cell, but are ubiquitous throughout the cytoplasm. This is likely because PP2A_{Rts1p} and PP2A_{Cdc55p} heterotrimers carry out cell-cycle-specific functions and these functions are not needed because cell densities increase and cells slow down and stop their division cycles (eventually entering G₀).
9. The DAPI can be used as a vital stain, but the background staining of cell bodies (largely mitochondria) is higher in live cells than in fixed cells. However, cells cannot be fixed for this assay because the GFP signal for GFP-Tpd3p, GFP-Cdc55p, and Rts1p-GFP does not survive fixation. We made *rho0* strains via the protocol of Fox et al. (32) to decrease the background staining for publication-quality figures (22), but this is not necessary just to determine pre-telophase vs telophase cells.
10. Cells grown in YPAD need to be washed in SC because the yeast extract and peptone are highly fluorescent. GFP-PP2A subunit localization is essentially the same in cells grown in YPAD and SC.
11. Microscope slides made in this manner start to dry out after 15–20 min. Large bubbles start appearing under the cover slip and the cells start to be displaced. Additionally, cells start to look “unhealthy” after sitting on the microscope slide for more than 20–30 min.
12. To be able to quickly score cells, first learn the cellular morphologies. The best way to do this is to DAPI stain a population of cells and study the placement of the nucleus with respect to the bud size (see Fig. 3) (33). Once you can match the

bud size to the correct cell-cycle stage, use a lab counter to score “yes” or “no” for each subcellular localization.

13. To support the validity of our quantitation method, we used some of the same captured fields of cells and measured the area and intensity of the GFP signal at the bud tip and bud neck using NIH Image (National Institutes of Health, Bethesda, MD) and NIH ImageJ (National Institutes of Health, Bethesda, MD). The results with NIH Image and NIH ImageJ were very similar to our “yes”/“no” method, thus demonstrating the validity of our method. Using NIH Image to quantitate signal intensities was much more tedious and time-intensive and yielded no more information than our simple scoring method.
14. The percentage of cells displaying any PP2A trademark localization never reaches 100%. The two reasons for this are: (1) PP2A heterotrimer localization is a dynamic, cell-cycle-specific process and (2) we photographed cells to score for localizations; in each photograph a certain percentage of cells were not in focus. When we focused on each cell the percentage did increase, but it never reached 100%. (3) The amount of PP2A localization in a population of cells likely represents a Gaussian distribution with a portion of cells having a localization level not detectable above background. To compensate for these issues, we divide each experimental percentage localization value obtained by the percentage localization value obtained for wild-type cells in that same category.

Acknowledgments

The authors thank Farhana Syed, Yikun Li, Seema Mattoo, and Robert Downen for helpful comments and for critical reading of the manuscript. The work was supported by a National Institutes of Health Grant to DCP (CA57327) and a National Science Foundation grant to RLH (MCB-0113355).

References

1. Mumby, M. C. and Walter, G. (1993) Protein serine/threonine phosphatases: structure, regulation, and functions in cell growth. *Physiol. Rev.* **73**, 673–699.
2. Schonthal, A. H. (1998) Role of PP2A in intracellular signal transduction pathways. *Front. Biosci.* **3**, D1262–D1273.
3. Millward, T. A., Zolnierowicz, S., and Hemmings, B. A. (1999) Regulation of protein kinase cascades by protein phosphatase 2A. *Trends Biochem. Sci.* **24**, 186–191.
4. Virshup, D. M. (2000) Protein phosphatase 2A: a panoply of enzymes. *Curr. Opin. Cell. Biol.* **12**, 180–185.
5. Janssens, V. and Goris, J. (2001) Protein phosphatase 2A: a highly regulated family of serine/threonine phosphatases implicated in cell growth and signalling. *Biochem. J.* **353**, 417–439.
6. van Zyl, W., Huang, W., Sneddon, A. A., et al. (1992) Inactivation of the protein phosphatase 2A regulatory subunit A results in morphological and transcriptional defects in *Saccharomyces cerevisiae*. *Mol. Cell. Biol.* **12**, 4946–4959.

7. van Zyl, W. H., Wills, N., and Broach, J. R. (1989) A general screen for mutant of *Saccharomyces cerevisiae* deficient in tRNA biosynthesis. *Genetics* **123**, 55–68.
8. Ronne, H., Carlberg, M., Hu, G. Z., and Nehlin, J. O. (1991) Protein phosphatase 2A in *Saccharomyces cerevisiae*: effects on cell growth and bud morphogenesis. *Mol. Cell. Biol.* **11**, 4876–4884.
9. Healy, A. M., Zolnierowicz, S., Stapleton, A. E., Goebel, M., DePaoli-Roach, A. A., and Pringle, J. R. (1991) CDC55, a *Saccharomyces cerevisiae* gene involved in cellular morphogenesis: identification, characterization, and homology to the B subunit of mammalian type 2A protein phosphatase. *Mol. Cell. Biol.* **11**, 5767–5780.
10. Shu, Y. and Hallberg, R. L. (1995) SCS1, a multicopy suppressor of hsp60-ts mutant alleles, does not encode a mitochondrially targeted protein. *Mol. Cell. Biol.* **15**, 5618–5626.
11. Shu, Y., Yang, H., Hallberg, E., and Hallberg, R. (1997) Molecular genetic analysis of Rts1p, a B' regulatory subunit of *Saccharomyces cerevisiae* protein phosphatase 2A. *Mol. Cell. Biol.* **17**, 3242–3253.
12. Chen, J., Martin, B. L., and Brautigan, D. L. (1992) Regulation of protein serine–threonine phosphatase type-2A by tyrosine phosphorylation. *Science* **257**, 1261–1264.
13. Guo, H. and Damuni, Z. (1993) Autophosphorylation-activated protein kinase phosphorylates and inactivates protein phosphatase 2A. *Proc. Natl. Acad. Sci. USA* **90**, 2500–2504.
14. Turowski, P., Fernandez, A., Favre, B., Lamb, N. J., and Hemmings, B. A. (1995) Differential methylation and altered conformation of cytoplasmic and nuclear forms of protein phosphatase 2A during cell cycle progression. *J. Cell. Biol.* **129**, 397–410.
15. Kowluru, A., Seavey, S. E., Rabaglia, M. E., Nesher, R., and Metz, S. A. (1996) Carboxymethylation of the catalytic subunit of protein phosphatase 2A in insulin-secreting cells: evidence for functional consequences on enzyme activity and insulin secretion. *Endocrinology* **137**, 2315–2323.
16. Bryant, J. C., Westphal, R. S., and Wadzinski, B. E. (1999) Methylated C-terminal leucine residue of PP2A catalytic subunit is important for binding of regulatory B α subunit. *Biochem. J.* **339**(Pt. 2), 241–246.
17. Gentry, M. S., Li, Y., Wei, H., et al. (2005) A Novel Assay for Protein Phosphatase 2A (PP2A) Complexes In Vivo Reveals Differential Effects of Covalent Modifications on Different *Saccharomyces cerevisiae* PP2A Heterotrimers. *Eukaryot. Cell.* **4**, 1029–1040.
18. Wei, H., Ashby, D. G., Moreno, C. S., et al. (2001) Carboxymethylation of the PP2A catalytic subunit in *Saccharomyces cerevisiae* is required for efficient interaction with the B-type subunits Cdc55p and Rts1p. *J. Biol. Chem.* **276**, 1570–1577.
19. Wu, J., Tolstykh, T., Lee, J., Boyd, K., Stock, J. B., and Broach, J. R. (2000) Carboxyl methylation of the phosphoprotein phosphatase 2A catalytic subunit promotes its functional association with regulatory subunits in vivo. *EMBO J.* **19**, 5672–5681.

20. Tolstykh, T., Lee, J., Vafai, S., and Stock, J. B. (2000) Carboxyl methylation regulates phosphoprotein phosphatase 2A by controlling the association of regulatory B subunits. *EMBO J.* **19**, 5682–5691.
21. Yu, X. X., Du, X., Moreno, C. S., et al. (2001) Methylation of the protein phosphatase 2A catalytic subunit is essential for association of Balph α regulatory subunit but not SG2NA, striatin, or polyomavirus middle tumor antigen. *Mol. Biol. Cell.* **12**, 185–199.
22. Gentry, M. S. and Hallberg, R. L. (2002) Localization of *Saccharomyces cerevisiae* protein phosphatase 2A subunits throughout mitotic cell cycle. *Mol. Biol. Cell.* **13**, 3477–3492.
23. Ogris, E., Gibson, D. M., and Pallas, D. C. (1997) Protein phosphatase 2A subunit assembly: the catalytic subunit carboxy terminus is important for binding cellular B subunit but not polyomavirus middle tumor antigen. *Oncogene* **15**, 911–917.
24. Dobbelaere, J., Gentry, M. S., Hallberg, R. L., and Barral, Y. (2003) Phosphorylation-dependent regulation of septin dynamics during the cell cycle. *Dev. Cell* **4**, 345–357.
25. Rines, D. R., He, X., and Sorger, P. K. (2002) Quantitative microscopy of green fluorescent protein-labeled yeast. *Methods Enzymol.* **351**, 16–34.
26. Stotz, A. and Linder, P. (1990) The ADE2 gene from *Saccharomyces cerevisiae*: sequence and new vectors. *Gene* **95**, 91–98.
27. Sherman, F. (2002) Getting started with yeast. *Methods Enzymol.* **350**, 3–41.
28. Tatchell, K. and Robinson, L. C. (2002) Use of green fluorescent protein in living yeast cells. *Methods Enzymol.* **351**, 661–683.
29. Gietz, R. D. and Sugino, A. (1988) New yeast–*Escherichia coli* shuttle vectors constructed with in vitro mutagenized yeast genes lacking six-base pair restriction sites. *Gene* **74**, 527–534.
30. Sikorski, R. S. and Hieter, P. (1989) A system of shuttle vectors and yeast host strains designed for efficient manipulation of DNA in *Saccharomyces cerevisiae*. *Genetics* **122**, 19–27.
31. Cai, T., Reilly, T. R., Cerio, M., and Schmitt, M. E. (1999) Mutagenesis of SNM1, which encodes a protein component of the yeast RNase MRP, reveals a role for this ribonucleoprotein endoribonuclease in plasmid segregation. *Mol. Cell. Biol.* **19**, 7857–7869.
32. Fox, T. D., Folley, L. S., Mulero, J. J., et al. (1991) Analysis and manipulation of yeast mitochondrial genes. *Methods Enzymol.* **194**, 149–165.
33. Davis, L. I. and Fink, G. R. (1990) The NUP1 gene encodes an essential component of the yeast nuclear pore complex. *Cell* **61**, 965–978.

Mutagenesis and Expression of the Scaffolding A α and A β Subunits of PP2A

Assays for Measuring Defects in Binding of Cancer-Related A α and A β Mutants to the Regulatory B and Catalytic C Subunits

Ralf Ruediger, Jin Zhou, and Gernot Walter

Summary

Protein phosphatase 2A (PP2A) holoenzymes are composed of three subunits: one scaffolding A subunit, one regulatory B subunit, and one catalytic C subunit. The A subunit exists as two isoforms: A α and A β . The C subunit also exists as two isoforms (C α and C β) and B subunits fall into three families (B, B', and B'') comprising over 15 members. The A α and A β subunits consist of 15 nonidentical repeats, which are composed of two amphipathic α helices that are connected by a loop (intrarepeat loop). These loops are instrumental in binding regulatory B and catalytic C subunits. The genes encoding the A α and A β subunits are relatively frequent targets for mutation in human cancer. The mutations often affect the intrarepeat loops and cause defects in the binding of specific B subunits or of B and C subunits. Here, we describe in vitro and in vivo binding assays for measuring these defects. Knowing which B subunits are affected in binding to the mutant A subunits sheds light on which holoenzymes might be involved in growth control and cancer.

Key Words: Protein phosphatase 2A; in vitro and in vivo subunit interaction; A-subunit mutagenesis; mutations in human cancer; coimmunoprecipitation

1. Introduction

Protein phosphatase (PP2A) holoenzymes are composed of three subunits: one scaffolding A subunit, one regulatory B subunit, and one catalytic C subunit. The A subunit exists as two isoforms, A α and A β (also designated PR65 α and PR65 β), which share 86% sequence identity. The C subunit also exists as two isoforms, C α and C β , which are 97% identical. The B subunits fall into

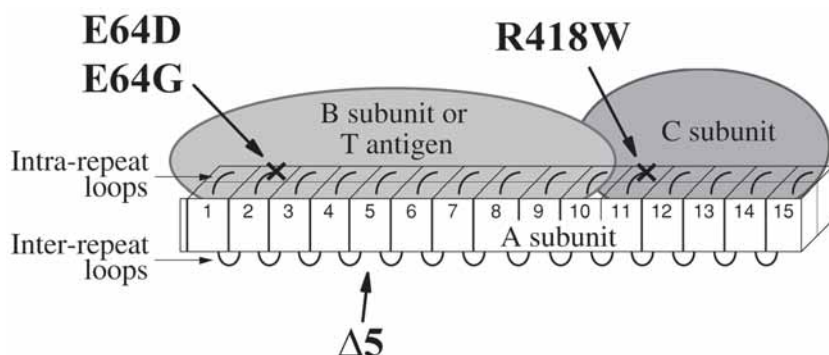


Fig. 1. Model of the PP2A holoenzyme. The location of three cancer-associated point mutations in the A α subunit is indicated.

three families, B, B', and B'', which are weakly related and together comprise over 15 members. B subunits determine substrate specificity and subcellular localization (*see* [ref. 1](#) for review and nomenclature of PP2A subunits).

The A α and A β subunits, which are composed of 15 nonidentical repeats (HEAT repeats) ([2–4](#)), mediate the interaction between B and C subunits ([5–8](#)). Each repeat is composed of two amphipathic α helices that are connected by a loop (intra-repeat loop). Adjacent repeats are connected by inter-repeat loops ([4,6](#)). The intra-repeat loops are involved in binding B and C subunits as well as viral tumor (T) antigens. The B subunits from all three families (B, B', B'') bind to repeats 1–10 and the C subunits bind to repeats 11–15 (*see* [ref. 6](#) and unpublished data) (*see* [Fig. 1](#)).

To find out which amino acids in repeats 1–10 are involved in binding the various B subunits, mutants were generated and their ability to bind B subunits was tested. Four categories of A α mutants could be distinguished: (1) no binding of any B subunits (**B-B'-B''**⁻); (2) no binding of B and B'', one-third reduction in B' binding (**B-B'+B''**⁻); (3) no binding of B' and B'', normal binding of B (**B+B'-B''**⁻); (4) no binding of B', normal binding of B and B'' (**B+B'-B''**⁺) ([9](#)). Importantly, A α and A β are mutated in a variety of human malignancies, including cancer of the lung, breast, colon, and skin ([10–12](#)) consistent with the idea that PP2A is a tumor suppressor whose function is destroyed by mutation of the A subunit. We investigated many of the cancer-associated A α and A β mutants described by Wang et al. ([10](#)) and Calin et al. ([12](#)) and found that all A α and most A β mutants are defective in binding B subunits, or both B and C subunits. Interestingly, two A α point mutants (E64G found in breast cancer and E64D found in lung cancer) were specifically defective in binding the B' α 1 (B56 γ 3) subunit, a member of the B' family, whereas binding of B α and B''/

PR72 was normal (category 4 mutants). These findings raise the possibility that a B'-containing holoenzyme functions as tumor suppressor ([13](#)).

In this chapter, we describe the methods used to study the binding properties of A α and A β mutants. They include site-directed mutagenesis, expression of mutant proteins in vitro and in vivo, and complex formation of mutant proteins with B and C subunits in vitro and in vivo. In vitro binding assays are of particular value when subunits are poorly expressed in vivo, which is the case for some A β mutants. The methods will be useful for the analysis of new A α and A β mutants that are likely to be discovered in human cancers and possibly other diseases in the future.

2. Materials

2.1. Tagging and Site-Directed Mutagenesis

1. PfuUltra Hotstart high-fidelity DNA polymerase (Stratagene cat. no. 600390).
2. QuickChange XL site-directed mutagenesis kit (Stratagene cat. no. 200517).

2.2. In Vitro Complex Formation

1. TNT T7 Quick coupled transcription/translation system (Promega cat. no. L1170) (*see Note 1*).
2. TNT T7 coupled transcription/translation system (Promega cat. no. L4610).
3. RNasin (Promega).
4. [³⁵S]methionine (Amersham cat. no. SJ-1515) (*see Note 2*).
5. Methionine (1 mM), unlabeled, is provided with the Quick system (Promega cat. no. L1170).
6. Plasmids encoding A α and A α mutants, B α , B' α 1, B''/PR72, C α , and C β . The vector backbone is pcDNA3 (*see Subheading 3.1.*). The plasmids were diluted to 0.1 g/L for in vitro synthesis.
7. Sodium dodecyl sulfate–polyacrylamide gel electrophoresis (SDS-PAGE) sample buffer, 1X concentration: 2% SDS, 10% glycerol, 100 mM dithiothreitol (DTT), 60 mM Tris-HCl, pH 6.8, and 0.001% bromophenol blue.
8. Anti-EE, mouse monoclonal antibody (Covance).
9. Anti-EE beads. The IgG fraction of anti-EE was covalently coupled to protein G Sepharose (GammaBind Plus, Amersham) using dimethylpimelimidate ([14](#)). The beads were suspended in 4 vol Triton-100 buffer. Therefore, when a recipe asks for 2.5- μ L beads, 10- μ L resuspended beads need to be pipetted. Because the beads settle quickly, they need to be resuspended repeatedly during pipetting (e.g., by low-speed vortexing).
10. Triton X-100 (TX-100) buffer: 0.5% Triton X-100 (Roche cat. no. 789 704), 150 mM NaCl, 50 mM Tris-HCl, pH 7.5. Add DTT from a 1 M stock stored at –20°C or below to 1 mM before use.
11. Leupeptin, 25 mM stock in water, store at –20°C (Sigma cat. no. L 2884).
12. Anti-KL, rabbit polyclonal antibody, generated in our lab ([5](#)).
13. KL peptide (KVTRTPDYFL) (Bachem).

14. KL buffer: 50 mM Tris-HCl, pH 7.5.
15. Protein A–Sepharose (PAS) beads, CL-4B (Amersham), suspended in 4 vols TX-100 buffer (*see Subheading 2.2., item 9*).

2.3. In Vivo Complex Formation

1. 293 Cells (American Type Culture Collection).
2. Dulbecco's modified Eagle's medium (DMEM) supplemented with 10% fetal bovine serum (FBS), glutamine to 2 mM, and pyruvate to 1 mM (all from Invitrogen).
3. Antibiotic-antimycotic (Invitrogen).
4. Opti-MEM (Invitrogen).
5. LipofectAMINE PLUS (Invitrogen cat. nos. 18324 and 11514).
6. Phosphate-buffered saline (PBS) (Invitrogen).
7. TX-100 buffer; *see Subheading 2.2., item 10*.
8. Leupeptin; *see Subheading 2.2., item 11*.
9. Anti-EE beads; *see Subheading 2.2., item 9*.
10. EE peptide (EEEEYMPME), Bachem.
11. BenchMark, prestained protein ladder (Invitrogen cat. no. 10748).
12. PVDF membrane (Immobilon P; Millipore cat. no. IPVH00010).
13. Transfer buffer: 57 g glycine, 12 g Tris (121 g/mol), and 800 mL methanol in 4 L (final volume).
14. Royal Genie blotter (Idea Scientific).
15. Tris-buffered saline with Tween-20 (TBST): 10 mM Tris-HCl, pH 7.5, 150 mM NaCl, 0.4% Tween-20 (Sigma cat. no. P-1379). A 20x stock can be prepared and is stable at room temperature.
16. Bovine serum albumin (BSA) (Roche cat. no. 100 018).
17. Sodium azide (Aldrich).
18. Anti-KT3, mouse monoclonal antibody (Covance).
19. Anti-mouse IgG labeled with horseradish peroxidase (HRP) (Jackson Immuno-Research cat. no. 115-035-146).
20. Western Lightning Plus, developing solution (PerkinElmer cat. no. 104).
21. Anti-HA, mouse monoclonal antibody (Roche).

3. Methods

3.1. Tagging

The binding assays described below involve the expression of exogenous PP2A subunits in assay systems that contain a variety of endogenous subunits. To identify the exogenous subunits, they were tagged: A α and A β at the C-terminus with the EE tag ([15,16](#)); B α , B' α 1, and B"/PR72 at the C-terminus with the KT3 tag ([17](#)); and C α and C β at the N-terminus with the HA tag ([14](#)). We determined that the tags do not interfere with the formation of core or holoenzymes. All tagged subunits are in pcDNA3, a vector suitable for in vitro and in vivo expression.

We employed two general strategies of tagging. If unique restriction enzyme sites exist upstream and downstream near the region to be tagged, that region can be replaced with a DNA fragment encoding the region and the tag. The DNA fragment is generated by synthesis of two complementary oligonucleotides. It can also be synthesized by polymerase chain reaction (PCR), in which case one of the unique restriction sites can be further away. We used these methods to tag the A α and A β subunits (9,13,18).

The other strategy does not rely on preexisting restriction sites. The complete coding region is amplified by high-fidelity PCR using primers that introduce cloning sites as well as the tag. The product should be sequenced. We used this method to tag the B α , B' α 1, B"/PR72, C α , and C β subunits (19).

All tagged subunits are available from this lab.

The EE tag corresponds to an internal region of polyomavirus middle T antigen:

gaa	gaa	gaa	gaa	tat	atg	cct	atg	gaa
E	E	E	E	Y	M	P	M	E

The KT3 tag corresponds to the C-terminus of the SV40 large T antigen:

aag	cct	cct	act	cct	cct	cct	gag	cct	gag	act
K	P	P	T	P	P	P	E	P	E	T

The HA tag corresponds to an internal region of influenza hemagglutinin:

tac	cca	tac	gac	gtt	cca	gat	tac	gct
Y	P	Y	D	V	P	D	Y	A

3.2. Site-Directed Mutagenesis

To generate mutations in the A α -subunit, we have been using the method by Kunkel and the GeneEditor system from Promega. Lately, we have used the QuickChange XL site-directed mutagenesis kit from Stratagene, which has a detailed protocol included and, therefore, will not be described here (*see Note 3*).

3.3. In Vitro Complex Formation Between A-Subunit Mutants and B-Subunits

To determine whether A subunit mutants bind B subunits, both are synthesized in separate reactions in reticulocyte lysate in the presence of [³⁵S]methionine. They are then mixed together and incubated to allow complex formation. The EE-tagged A subunit mutants and wild type are immunoprecipitated with anti-EE, and coimmunoprecipitated B subunits are visualized by SDS-PAGE and autoradiography or phosphorimaging. In addition to the B subunits, the A subunits are also visible on the image, which permits one to compare the synthesis and immunoprecipitation rates of the various A subunit mutants and wild type.

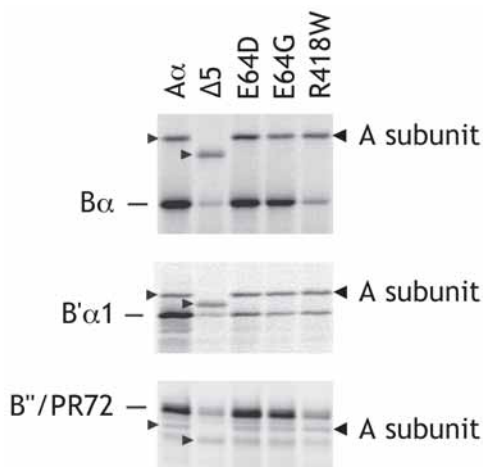


Fig. 2. In vitro complex formation of cancer-associated mutants of the A α subunit of PP2A with the regulatory B α , B' α 1, and B''/PR72 subunits. Translation mixtures of [35 S]methionine-labeled and EE-tagged A-subunit constructs, named at the top, were mixed with [35 S]methionine-labeled B α , B' α 1, or B''/PR72. After incubation at 30°C for 4 h in the presence of the unlabeled C-subunit present in the reticulocyte lysate, complexes were immunoprecipitated with anti-EE antibodies and analyzed by SDS-PAGE and phosphorimaging. C-Terminal mutant R418W binds none of the B subunits, whereas N-terminal mutants E64D and E64G are only defective in B' α 1 binding.

Because anti-EE precipitates 90–100% of the A subunits, but coprecipitates only approx 10% of the B subunits, B subunit bands are expected to be much weaker than A subunit bands. Therefore, the A subunits are synthesized with one-tenth the amount of [35 S]methionine. **Figure 2** shows the coimmunoprecipitation of B-subunits with A α point mutants that were found in human cancer (**13**).

1. Synthesis of A subunit mutants and B subunits using the TNT Quick system. Thaw the TNT T7 Quick Master-Mix by hand-warming and place it on ice. Thaw [35 S]methionine, unlabeled methionine, and plasmid DNAs at room temperature.

B Subunits. A 10- μ L reaction for B-subunit synthesis consists of 8 μ L Master-Mix, 0.4 μ L [35 S]methionine, and 1.6 μ L (160 ng) B-subunit DNA. Make a premix according to the number of A-subunit mutant and wild-type samples. Mix by low-speed vortexing, spin for a short time if droplets spilled to the tube walls, and incubate at 30°C for 90 min.

A subunits. A 10- μ L reaction to synthesize A subunit mutants consists of 8 μ L Master-Mix, 0.04 μ L [35 S]methionine, 0.36 μ L cold methionine, and 1.6 μ L

- (160 ng) DNA. Use wild-type A α as a positive control and A $\alpha\Delta$ 5, known not to bind any B subunit, as a negative control (A $\alpha\Delta$ 5 lacks repeat 5). Incubate as above.
2. Place the synthesis reactions at room temperature, mix by low-speed vortexing, take 1- μ L aliquots of the A subunit reactions into tubes preloaded with 20 μ L of 2X SDS-PAGE sample buffer, and boil for 5 min (*see Note 4*). These aliquots permit to compare the synthesis rates of the various A subunit mutants and wild type.
 3. For complex formation, combine 9 μ L of an A subunit mutant or wild-type reaction with 10 μ L of B subunit reaction, mix by low-speed vortexing, spin for a short time, and incubate at 30°C for 4 h (*see Note 5*).
 4. Optional: Mix 1- μ L aliquots with 20 μ L of 2X SDS-PAGE sample buffer and boil for 5 min. These aliquots should demonstrate identical amounts of B subunit per sample.
 5. To immunoprecipitate, add 5 μ L anti-EE beads to the remaining 18 or 19 μ L of lysate mixtures, mix by low-speed vortexing, spin at 2000 rpm for 10 s, and rotate the tubes along their axes at an angle of about 45° at room temperature for 1 h.
 6. Optional: Spin the tubes at 2000 rpm for 10 s, mix 10 μ L of supernatant with 10 μ L of 4X SDS-PAGE sample buffer, and boil for 5 min. Analyzing the supernatant above the beads permits one to determine whether the anti-EE beads worked well. The supernatants should barely contain the radioactive A subunit because the anti-EE beads are capable of depleting the samples. The bands for B subunits will be strong because approx 90% do not coimmunoprecipitate.
 7. To the remaining sample with the bead pellet, add 1 mL TX-100 buffer, rotate end over end 20–30 times (1–2 min) by hand, spin at 2000 rpm for 10 s, and suck off the supernatant (do not go too close to the pellet; it is OK to leave approx 50 μ L behind). Repeat this wash two more times. After the last wash, use a flat gel-loading tip to cautiously drain the pellet/beads (*see Note 6*).
 8. To the drained pellet, add 20 or 40 μ L of 2X SDS-PAGE sample buffer. Load 20 μ L on a 10% gel. Use 12% or 15% gels when analyzing short A subunit deletion mutants.
 9. To quantitate, fix and dry the gel, expose it to a phosphorimager plate for several hours to several days, and develop the plate on a phosphorimager (Molecular Dynamics). We use ImageQuant software to determine band intensities (*see Note 7*).

3.4. In Vitro Complex Formation Between A Subunit Mutants and C Subunit Endogenous to Reticulocyte Lysate

To determine whether A subunit mutants bind C subunits, the A subunit mutants are synthesized in reticulocyte lysate in the presence of [³⁵S]methionine or [³⁵S]cysteine. The reticulocyte lysate contains endogenous C subunits at a concentration of approximately 5 ng/ μ L, sufficient for complex formation. Because complex formation takes place during synthesis, no additional incubation is required. The C subunit is then immunoprecipitated with anti-KL

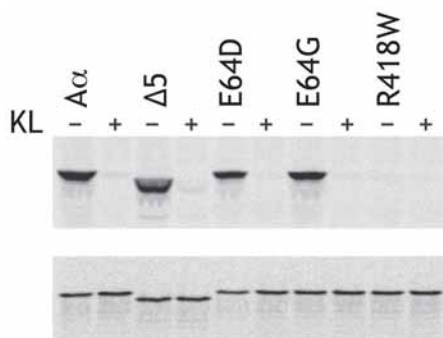


Fig. 3. In vitro complex formation of A α mutants with the catalytic C-subunit. Translation mixtures of [35 S]cysteine-labeled A α subunit constructs, named at the top, were incubated with anti-KL peptide antibodies for immunoprecipitation of unlabeled endogenous C-subunit and coimmunoprecipitation of radioactive A α -subunits (upper panel). Peptide KL was used as an inhibitor of immunoprecipitation. The lower panel shows the in vitro synthesized products, demonstrating that the synthesis rate was similar for all constructs. C-Terminal mutant R418W does not bind C subunit endogenous to reticulocyte lysate.

antibody, and coimmunoprecipitated A subunit mutants are visualized by SDS-PAGE and autoradiography or phosphorimaging. **Figure 3** shows the coimmunoprecipitation with the C-subunit of A α point mutants (**13**).

1. Synthesis of A subunit mutants using the TNT system (not the TNT Quick system; *see Note 8*). Thaw the TNT reticulocyte lysate by hand-warming and place it on ice. Thaw the TNT T7 RNA polymerase on ice. Thaw the other kit components as well as [35 S]cysteine, RNasin, and plasmid DNAs at room temperature. A 10- μ L reaction consists of 1.2 μ L water, 5 μ L TNT reticulocyte lysate, 0.4 μ L TNT reaction buffer, 0.2 μ L RNasin, 0.2 μ L amino acid mixture minus cysteine, 0.2 μ L TNT T7 RNA polymerase, 0.8 μ L [35 S]cysteine, and 2 μ L (200 ng) DNA. According to the number of plasmids to be transcribed/translated, make a premix without DNA. Pipet 8 μ L premix into microcentrifuge tubes placed on ice and add 2 μ L (200 ng) DNA. Mix by low-speed vortexing, spin for a short time, and incubate at 30°C for 90 min. Use wild-type A α as a positive control and A α Δ 11–15 as a negative control (A α Δ 11–15 lacks repeats 11–15 and does not bind the C subunits). As an additional control, the immunoprecipitation with anti-KL antibody can be inhibited by KL peptide (*see step 2*); if peptide competition is carried out, double the synthesis reaction to 20 μ L for each A subunit construct.
2. While the synthesis proceeds, mix 0.5 μ L anti-KL serum with 1 μ L (3 μ g) peptide KL as well as 0.5 μ L anti-KL serum with 1 μ L KL buffer (make premixes according to the number of A-subunit mutants tested) and incubate on ice for 30 min.

3. Place the synthesis reactions at room temperature, mix by low-speed vortexing, take 1- μ L aliquots into tubes preloaded with 100 μ L of 2X SDS-PAGE sample buffer, and boil for 5 min (*see Note 4*). These aliquots permit one to compare the synthesis rates of the various A subunit mutants and wild type.
4. To immunoprecipitate without peptide competition, add 0.5 μ L anti-KL serum to the remaining 9 μ L of lysate. If utilizing peptide competition, split the remaining 19 μ L into two 9- μ L aliquots and add 1.5 μ L anti-KL plus peptide KL or 1.5 μ L anti-KL minus peptide KL (from **step 2**). Incubate on ice for 1 h.
5. Wash protein A–Sepharose (PAS) beads four times with TX-100 buffer. Spin at room temperature at 2000 rpm for 1 min. Per sample, 10 μ L of settled beads are needed. After the last wash, adjust the total volume to four times the volume of the settled beads. Place the beads on ice.
6. To the 9.5 or 10.5 μ L from **step 4**, add 10 μ L PAS beads (40 μ L suspension), mix by low-speed vortexing, spin at 2000 rpm for 10 s, and rotate the tubes along their axes at an angle of about 45° at 4°C for 1 h. Alternatively, incubate the reactions on ice for 1 h and vortex at low speed every 5–10 min.
7. Continue with **steps 7, 8, and 9** of **Subheading 3.3**.

3.5. *In Vivo* Complex Formation between A-Subunit Mutants and B-Subunits

To determine whether A subunit mutants bind to B subunits *in vivo*, 293 cells are cotransfected with EE-tagged A subunit mutants and KT3-tagged B subunits. After 2 d, the cells are lysed, the A subunit mutants are immunoprecipitated with anti-EE, and coimmunoprecipitated B subunits are visualized by Western blotting with anti-KT3. The 293 cells provide the C subunits that are required for binding of B-subunits to A-subunits. **Figure 4** shows the coimmunoprecipitation of B-subunits with A α point mutants (**19**).

1. The day before transfection, plate 3.6×10^5 293 cells per 5-cm tissue culture plate in regular medium (DMEM with 10% FBS) without antibiotics. The next day, the cells should be approx 70% confluent.
2. Prepare transfection mixtures as described for LipofectAMINE PLUS. (1) Mix 250 μ L Opti-MEM with a total of 1.2 μ g of DNA (0.2 μ g A α DNA and 1 μ g B subunit DNA; *see Note 9*), add 8 μ L PLUS reagent, mix again, and incubate at room temperature for 15 min. (2) Mix 250 μ L Opti-MEM with 12 μ L Lipofectamine. (3) Mix the solutions from (1) and (2) and incubate at room temperature for 15 min.
3. Remove the medium from the cells, rinse the cells with 2 mL Opti-MEM, and cover the cells with 2 mL Opti-MEM. Treat 293 cells gently, as they tend to lift off the plate.
4. Add the mixture from **step 2(3)** to the cells for a total volume of 2.5 mL, swirl to mix, and incubate the cells at 37°C and 5% CO₂ for 3 h.
5. Replace the transfection medium with regular medium with antibiotics and incubate the cells at 37°C and 5% CO₂ for 2 d.

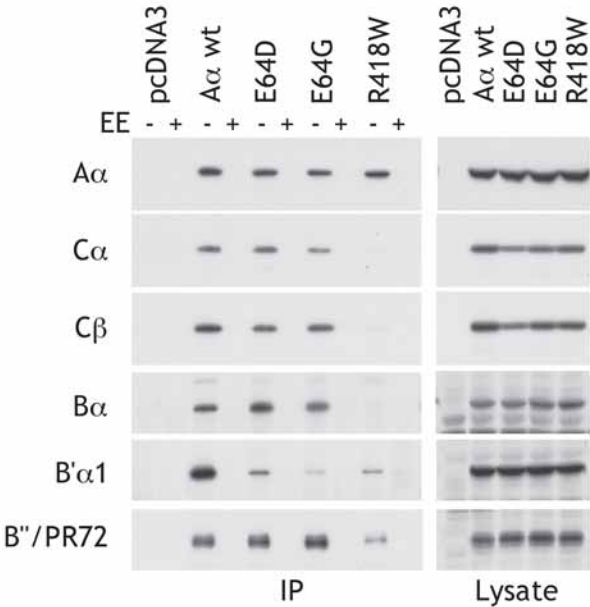


Fig. 4. In vivo complex formation of A α mutants with regulatory B and catalytic C subunits. 293 cells were cotransfected with constructs expressing EE-tagged wild type or mutant A α subunits, named at the top, and constructs expressing KT3-tagged B subunits or HA-tagged C subunits, named to the left. Complexes were immunoprecipitated with anti-EE antibody, and B or C subunits that bound to the A subunits were detected with anti-KT3 or anti-HA antibodies by Western blotting. Transfections with empty vector (pcDNA3) and inhibition of immunoprecipitation with EE peptide were used as negative controls. Western blotting of cell lysate aliquots shows that similar amounts of A, B, and C subunits were used for the immunoprecipitations (**right panel**). C-terminal mutant R418W is defective in binding all B and C subunits, whereas N-terminal mutants E64D and E64G are only defective in B' α 1 binding.

6. To harvest, wash the cells with 2 mL ice-cold PBS and then lyse with 160 μ L TX-100 buffer containing freshly added leupeptin to 50 μ M: float the plate on ice-cold water for 10–20 min, swirling it occasionally. Pour the lysate into a microcentrifuge tube and spin it at 15,000g and 4°C for 5 min. Pipet the supernatant into a fresh microcentrifuge tube and place it on ice.
7. To prepare for immunoprecipitation, wash anti-EE beads with TX-100 buffer and resuspend the beads in 4 vol TX-100 buffer. For peptide competition samples, mix 2.5 μ L anti-EE beads in 10 μ L TX-100 buffer with 5 μ L (50 μ g) peptide EE. Make a premix according to the number of samples. Incubate at room temperature for 30 min, mixing by rotation or by occasional low-speed vortexing.

8. Mix 20 μ L of each lysate with 5 μ L of 5X SDS-PAGE sample buffer and boil for 5 min (*see Note 4*). Load (at **step 10**) 10 μ L of these lysate aliquots twice to show the expression levels of A-subunit mutants and B-subunits in Westerns with anti-EE and anti-KT3.
9. To immunoprecipitate, mix 70 μ L lysate with 2.5 μ L anti-EE beads in 10 μ L TX-100 buffer, minus peptide (from **step 7**). Mix another 70 μ L of the same lysate with 2.5 μ L anti-EE beads plus peptide EE (from **step 7**). Spin at 300g for 10 s, and rotate the tubes along their axes at an angle of about 45° at room temperature for 1 h.
10. Spin the tubes at 300g for 10 s. (Optional: Mix 40 μ L supernatant with 10 μ L of 5X SDS-PAGE sample buffer and boil for 5 min; analyzing the supernatant above the beads by Western blotting with anti-EE permits one to determine how well the anti-EE beads worked.) Wash the samples three times with 1 mL TX-100 buffer as described before (*see Subheading 3.3., step 7*). To the drained pellet, add 20 or 40 μ L of 1X SDS-PAGE sample buffer and load 20 μ L on a 10% gel. Also load the lysate samples from **step 8**. Include a prestained protein ladder (e.g., BenchMark) on the left and right of the gel and between the IP and lysate samples (*see Note 10*).
11. For Western blotting, we transfer proteins from SDS-PAGE gels to PVDF membranes using a Royal Genie blotter. After the transfer, dry the membrane for better protein attachment. Rewet it in methanol and rinse it in TBST. Block the blot in TBST containing 3% BSA (do not use nonfat dry milk; *see Note 11*) on a shaker at room temperature for 10–60 min. Save the blocking solution (to be reused; see below) and replace it with antibody solution, which consists of TBST containing 3% BSA, 0.03% sodium azide, and the following antibodies:
 - (i) 3–12 μ g/mL mouse anti-KT3, to analyze the anti-EE immunoprecipitates for co-precipitated B subunits;
 - (ii) 3–12 μ g/mL mouse anti-KT3, to analyze the cell lysates for the expression level of transfected B subunits;
 - (iii) 2–6 μ g/mL mouse anti-EE, to analyze the cell lysates for the expression level of transfected A subunits.

Incubate the blots on a shaker at room temperature for 1 h.

12. *Save the antibody solutions! We store them at 4°C and reuse them many times.* Wash the blot three times with TBST for 5 min each. To the membrane, add the blocking solution saved at **step 11**. Per 10 mL of blocking solution, add 1 μ L secondary anti-mouse IgG antibody labeled with HRP (Jackson ImmunoResearch cat. no. 115–035–146). Incubate the blot on a shaker at room temperature for 45 min. Discard the secondary antibody solution. Wash the blot six to eight times with TBST for 5 min each (*see Note 12*).
13. Place about 5 mL water on a workbench and spread Saran Wrap over it. Place about 5 mL water onto the Saran Wrap and roll or pull a 25-ml pipet tip over it to flatten out the Saran Wrap, pushing out any air bubbles under it. Use paper towels or Kimwipes to remove excess water.

14. Mix equal volumes of the two components of the Western Lightning developing solution (luminol and oxidizing reagent) and wait 1 min. About 10 mL are needed per 100 cm² of the container holding the membrane. Add the developing solution to the washed blot from **step 12** (TBS removed), swirl, and place the blot face down onto the Saran Wrap from **step 13**. Avoid bubbles. Place a sheet of clear plastic as support onto the blot (*see Note 13*), wrap the Saran Wrap around the support film, turn the package over, dry its face off, push any bubbles to the side, and expose the membrane to film. Start with a 1-min and 3-min exposure; lengthen or shorten as needed. Work swiftly during this step, as the signal decreases exponentially.

3.6. *In vivo* complex formation between A-subunit mutants and C-subunits

To determine whether A subunit mutants bind C subunits *in vivo*, 293 cells are cotransfected with EE-tagged A subunit mutants and HA-tagged C subunits. After 2 d, the cells are lysed, the A subunit mutants are immunoprecipitated with anti-EE, and co-immunoprecipitated C subunits are visualized by Western blotting with anti-HA. Whereas the 293 cells provide endogenous B subunits, A-C dimer formation does not require B subunits. **Figure 4** shows the coimmunoprecipitation of C-subunits with A α point mutants (**19**).

Perform the experiments as described in **Subheading 3.5.** with the following exceptions:

1. Transfect the cells with 0.6 μ g A α DNA plus 0.6 μ g C α or C β DNA.
2. Run a 12% gel to better separate the C-subunit from a background band below it.
3. In Westerns, use a mixture of 3 μ g/mL mouse anti-EE and 0.2 μ g/mL rat anti-HA (*see Note 14*). Remember to add both anti-mouse and anti-rat secondary HRP-labeled antibody.

4. Notes

1. According to Promega's technical support, reticulocyte lysate contains about 5 μ M endogenous methionine. Because the reticulocyte lysate represents 50% of a translation reaction, the reactions contain 2.5 μ M methionine. All other amino acids are added to a final concentration of 20 μ M, plus their endogenous levels. [³⁵S]methionine is added to 0.6 or 1.2 μ M (*see Note 2*).
2. The [³⁵S]methionine, at 1000 Ci/mmol and 15 mCi/mL, is 15 μ M. It is used in translation reactions 25-fold or 12.5-fold diluted (i.e., at final concentrations of 0.6 μ M or 1.2 μ M) (*see Note 1*).
3. The use of NZY+ broth, rather than Luria–Bertani medium, recovers 10–100 times more colonies when transforming XL10 bacteria.
4. During the heating of samples in a boiling water bath, water can collect under the rim of a microcentrifuge tube. After boiling, when the tube cools down, the water can get sucked into the tube and dilute the sample. Avoid a vigorously bubbling water bath.

5. Complex formation between A and B subunits increases steadily over a 24-h period, but oxidation might occur, as evident by a brownish discoloration of the reaction mixtures. If an overnight incubation is desired, it should be carried out at room temperature. To further promote complex formation, it is also possible to mix 5 μ L of A-subunit reactions with 20 μ L of B-subunit reactions, instead of mixing 10 μ L with 10 μ L.
6. After the last wash of the beads, use a flat gel-loading tip attached to a pipettor to cautiously drain the pellet/beads. As more and more supernatant is removed, the flat tip approaches the beads and eventually touches them. When drained, the beads will appear more whitish. Only a few beads will be sucked up by the flat tip. The novice should try this on some old beads. This procedure can also be performed using slit tubes, which are described in Chapter 10 of this volume.
7. It is possible to determine the absolute activity of bands by comparing their intensity to known amounts of [35 S]methionine. For this purpose, spot onto a strip of Whatman paper 2 μ L of water containing 1, 3, 10, 30, 100, and 300 nCi of [35 S]methionine (same calibration date as used in the experiment). Expose this strip together with the gel to the phosphorimager plate. The gel can also be exposed to an X-ray film followed by scanning and analysis with appropriate software. For this purpose in particular, bands should be gray, not black. It is useful to load a dilution series of a wild-type coimmunoprecipitate to judge fold differences to mutant coimmunoprecipitates.
8. The TNT Quick system requires only a few pipetting steps but is limited to the use of [35 S]methionine. In contrast, the TNT system can be used with [35 S]methionine, [35 S]cysteine, [14 C]leucine, or [3 H]leucine. This flexibility can be advantageous; for example, a deletion mutant of A α , Δ 171–589, which lacks all amino acids from 171 to the end of the protein, contains only 1 methionine but 3 cysteines (wild-type A α contains 14 methionines and 14 cysteines). Therefore, using [35 S]cysteine achieves a stronger relative labeling.
9. Although transfected A α DNA expresses very well, B α DNA does not. Therefore, more B subunit DNA than A α DNA was used (*see Subheading 3.5., item 2*). Similarly, A β DNA expresses poorly. At least seven times more A β than A α DNA was used when comparing binding to B or C subunits. The expression level of A β mutants varies widely.
10. The A subunit migrates just above the pink marker of the BenchMark ladder, the B α subunit migrates below it, and the C subunits migrate two marker lanes below pink. The markers will show up on the Western membrane and make it possible to cut the membrane horizontally to incubate the upper part with anti-EE and the lower parts with anti-KT3 or anti-HA. This is not possible for B' and B"/PR72 because they migrate too close to the A subunit.
11. Although nonfat dry milk could be used for blocking, it should not be used in the primary antibody solution because nonfat dry milk goes bad upon storage. If using nonfat dry milk for blocking, the membrane needs to be washed several times with TBST before adding the primary antibody solution.
12. Extensive washing of the blot after incubation with the secondary, HRP-labeled antibody is essential. If the whole blot ends up black, you did not wash enough at

this step. Probably, a thin layer of HRP-labeled antibody remained on the surface. In this case, try to rewash the blot, apply the developing solution again, and reexpose.

13. Obtain the sheet of clear plastic by removing the coating of old exposed or unexposed film using full-strength bleach. Do that in a fume hood. Use gloves. Use paper towels to rub off the coating. Do not use film with coating.
14. We use a mixture of mouse anti-EE and rat anti-HA, because reblotting with one or the other antibody does not work, for unknown reasons.

Acknowledgments

This work was supported by the Tobacco-Related Disease Research Program, grant 8RT-0037, and by Public Health Service grant CA-36111.

References

1. Silverstein, A. M., Davis, A. J., Bielinski, V. A., Esplin, E. D., Mahmood, N. A., and Mumby, M. C. (2003) Protein phosphatase 2A, in: *Handbook of Cell Signaling* (Bradshaw, R. A. and Dennis, E. A., eds), Elsevier Academic Press, Chap. 189.
2. Walter, G., Ferre, F., Espiritu, O., and Carbone-Wiley, A. (1989) Molecular cloning and sequence of cDNA encoding polyoma medium tumor antigen-associated 61-kDa protein. *Proc. Natl. Acad. Sci. USA* **86**, 8669–8672.
3. Hemmings, B. A., Adams-Pearson, C., Maurer, F., et al. (1990) Alpha- and beta-forms of the 65-kDa subunit of protein phosphatase 2A have a similar 39 amino acid repeating structure. *Biochemistry* **29**, 3166–3173.
4. Groves M. R., Hanlon, N., Turowski, P., Hemmings, B. A., and Barford, D. (1999) The structure of the protein phosphatase 2A PR65/A subunit reveals the conformation of its 15 tandemly repeated HEAT motifs. *Cell* **96**, 99–110.
5. Ruediger, R., Roeckel, D., Fait, J., Bergqvist, A., Magnusson, G., and Walter, G. (1992) Identification of binding sites on the regulatory A subunit of protein phosphatase 2A for the catalytic C subunit and for tumor antigens of simian virus 40 and polyomavirus. *Mol. Cell. Biol.* **12**, 4872–4882.
6. Ruediger R., Hentz, M., Fait, J., Mumby, M., and Walter, G. (1994) Molecular model of the A subunit of protein phosphatase 2A: interaction with other subunits and tumor antigens. *J. Virol.* **68**, 123–129.
7. Kamibayashi, C., Lickteig, R. L., Estes, R., Walter, G., and Mumby, M. C. (1992) Expression of the A subunit of protein phosphatase 2A and characterization of its interactions with the catalytic and regulatory subunits. *J. Biol. Chem.* **267**, 21864–21872.
8. Kamibayashi, C., Estes, R., Lickteig, R. L., Yang, S., Craft, C., and Mumby, M. C. (1994) Comparison of heterotrimeric protein phosphatase 2A containing different B subunits. *J. Biol. Chem.* **269**, 20,139–20,148.
9. Ruediger R., Fields, K., and Walter, G. (1999) Binding specificity of protein phosphatase 2A core enzyme for regulatory B subunits and T antigens. *J. Virol.* **73**, 839–842.

10. Wang S. S., Esplin, E. D., Li, J. L., et al. (1998) Alterations of the PPP2R1B gene in human lung and colon cancer. *Science* **282**, 284–287.
11. Takagi Y., Futamura, M., Yamaguchi, K., Aoki, S., Takahashi, T., and Saji, S. (2000) Alterations of the PPP2R1B gene located at 11q23 in human colorectal cancers. *Gut* **47**, 268–271.
12. Calin G. A., di Iasio, M. G., Caprini, E., et al. (2000) Low frequency of alterations of the alpha (PPP2R1A) and beta (PPP2R1B) isoforms of the subunit A of the serine-threonine phosphatase 2A in human neoplasms. *Oncogene* **19**, 1191–1195.
13. Ruediger R., Pham, H. T., and Walter, G. (2001) Disruption of protein phosphatase 2A subunit interaction in human cancers with mutations in the A alpha subunit gene. *Oncogene* **20**, 10–15.
14. Harlow E. and Lane, D. (1999) Using Antibodies: A Laboratory Manual. Cold Spring Harbor Laboratory, Cold Spring Harbor, NY.
15. Grussenmeyer T., Scheidtmann, K. H., Hutchinson, M. A., Eckhart, W., and Walter, G. (1985) Complexes of polyoma virus medium T antigen and cellular proteins. *Proc. Natl. Acad. Sci. USA* **82**, 7952–7954.
16. Schaffhausen B., Benjamin, T. L., Pike, L., Casnellie, J., and Krebs, E. (1982) Antibody to the nonapeptide Glu-Glu-Glu-Glu-Tyr-Met-Pro-Met-Glu is specific for polyoma middle T antigen and inhibits in vitro kinase activity. *J. Biol. Chem.* **257**, 12467–12470.
17. MacArthur H., G. Walter (1984) Monoclonal antibodies specific for the carboxyl terminus of simian virus 40 large T antigen. *J. Virol.* **52**, 483–491.
18. Ruediger R., H. T. Pham, and G. Walter (2001) Alterations in protein phosphatase 2A subunit interaction in human carcinomas of the lung and colon with mutations in the A beta subunit gene. *Oncogene* **20**, 1892–1899.
19. Zhou J., Pham, H. T., Ruediger, R., and Walter, G. (2003) Characterization of the A alpha and A beta subunit isoforms of protein phosphatase 2A: differences in expression, subunit interaction, and evolution. *Biochem. J.* **369**, 387–398.

Isolation and Characterization of PP2A Holoenzymes Containing FLAG-Tagged B Subunits

Deanna G. Adams and Brian E. Wadzinski

Summary

Protein serine/threonine phosphatase 2A (PP2A) is a major cellular enzyme implicated in the control of a wide variety of biological processes. The predominant form of PP2A in cells is a heterotrimeric holoenzyme (ABC) consisting of a scaffolding (A) subunit, a regulatory (B) subunit, and a catalytic (C) subunit. Although numerous signal transduction pathways are known to be regulated by PP2A, the identity of the PP2A holoenzymes controlling each pathway remains unclear. Studies aimed at elucidating substrates for individual PP2A holoenzymes have been hindered by the limited availability of purified endogenous holoenzymes and the inability to differentiate cellular roles of closely related PP2A holoenzymes. In this chapter, we describe a strategy for the functional expression of select FLAG-tagged regulatory B subunits in human embryonic kidney-293 cells and subsequent purification of PP2A holoenzymes containing the FLAG-tagged B subunit and endogenous A and C subunits (AB_{FLAG}C). Biochemical analyses of the purified AB_{FLAG}C holoenzymes reveal that they exhibit virtually indistinguishable specific activities and sensitivities to inhibitors as compared to the corresponding endogenous PP2A holoenzymes. The strategy described herein provides a straightforward method to purify individual PP2A holoenzymes from target mammalian cells for subsequent *in vitro* studies, as well as a powerful approach to identify cellular substrates and roles for each holoenzyme.

Key Words: PP2A holoenzymes; regulatory subunits; epitope tag; phosphatase activity

1. Introduction

The protein phosphatase (PP2A) core dimer (AC), which consists of the scaffolding (A) subunit and catalytic (C) subunit, can functionally pair with a regulatory B subunit to form a heterotrimeric holoenzyme. Substrate selectivity and subcellular localization of PP2A is dictated by the regulatory subunit (*1-5*). Thus far, four distinct regulatory subunit families have been identified:

From: *Methods in Molecular Biology, Volume 365: Protein Phosphatase Protocols*
Edited by: G. Moorhead © Humana Press Inc., Totowa, NJ

B or PR55 (6–8), B' or PR61 (9,10), B'' or PR72 (11–13), and B''' or PR93/PR110 (14). Given the identification of 14 genes encoding for regulatory subunits, at least 70 different PP2A heterotrimers are predicted to exist in mammalian cells. The families of regulatory subunits share little amino acid sequence homology; however, isoforms within each family are highly homologous. The high degree of homology among family members makes it difficult to distinguish among PP2A holoenzymes containing related B subunits, as well as their cellular role in the control of PP2A activity and function.

PP2A has been shown to form stable complexes with several protein kinases (e.g., calcium/calmodulin-dependent protein kinase IV, p70 S6 kinase, casein kinase II, and p38 kinase) (15–18), and a large number of other cellular proteins (e.g., β_2 -adrenergic receptor, BAD, sodium/calcium exchanger, estrogen receptor- α , and the human norepinephrine transporter) (19–24). Although the PP2A catalytic subunit has been identified in a wide variety of macromolecular protein complexes, the precise oligomeric form of PP2A in most of these complexes remains largely unknown. The inability to overexpress the phosphatase catalytic subunit has hampered studies to elucidate the physiological role of PP2A in the control of its interacting proteins (25,26); however, we and others have recently developed a strategy to successfully overexpress regulatory B subunits in mammalian cells (9,27–31,34). Immunoblot analyses of extracts from cells overexpressing the targeted regulatory subunits (e.g., using phospho-specific antibodies) have led to the identification of signal transduction pathways that are under the control of specific PP2A holoenzymes (30,34). In this chapter, we describe the methodology for expression of FLAG epitope-tagged B α and B δ regulatory subunits in human embryonic kidney-293 cells and subsequent purification of PP2A holoenzymes containing these subunits. Because the ectopic B subunits form functional holoenzymes by stoichiometrically pairing with endogenous A and C subunits, the isolated complexes can be utilized for measuring phosphatase activities of individual PP2A holoenzymes toward multiple PP2A substrates. The overexpression of FLAG-tagged PP2A regulatory subunits in mammalian cells, followed by biochemical analyses of changes in the phosphorylation state of cellular proteins and *in vitro* phosphatase assays of isolated holoenzymes, provides a powerful approach to elucidate the functional role of specific PP2A holoenzymes in the control of various biological processes.

2. Materials

2.1. Expression of FLAG-Tagged B Subunits

1. Mammalian expression plasmids: B α -FLAG/pcDNA5/TO, B δ -FLAG/pcDNA5/TO, and pcDNA5/TO (Invitrogen; Carlsbad, CA) (see **Notes 1 and 2**).
2. Human embryonic kidney (HEK) T-Rex cells (Invitrogen).

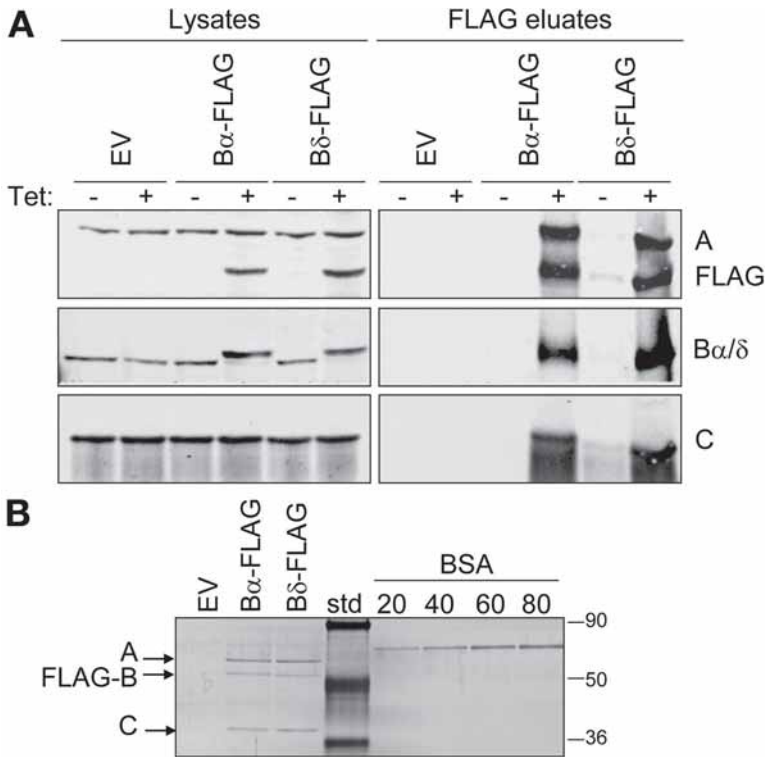


Fig. 1. Functional expression of FLAG-tagged B α and B δ regulatory subunits. HEK T-Rex cells stably transfected with pcDNA5/TO (empty vector, EV), B α -FLAG/pcDNA5/TO (B α -FLAG), or B δ -FLAG/pcDNA5/TO (B δ -FLAG) were treated with (+) or without (–) 1 μ g/mL tetracycline. Cell lysates were prepared 48 h post-tetracycline induction, and FLAG-B subunit complexes were isolated from the lysates using anti-FLAG agarose. Bound proteins were washed, eluted with FLAG peptide (FLAG eluates), resolved by SDS-PAGE, and subjected to immunoblot or silver stain analysis. **(A)** Cell lysates (approx 15 μ g of protein) and 10- μ L aliquots of the FLAG eluates were immunoblotted with specific antibodies recognizing the FLAG epitope and PP2A subunits (A, B α / δ , B δ , or C). **(B)** Silver stain analysis of FLAG eluates (10- μ L aliquots). The positions of A-, FLAG-B-, and C-subunits are denoted with arrows. Varying concentrations of BSA (20–100 ng) were used as standards to determine the amount of PP2A catalytic subunit (C) in the purified PP2A holoenzymes.

3. Monoclonal HEK T-Rex cells stably expressing pcDNA5/TO, B α -FLAG/pcDNA5/TO, or B δ -FLAG/pcDNA5/TO (see **Notes 3** and **4**).
4. Dulbecco's modified Eagle's medium (DMEM; Vanderbilt Media Core), supplemented with 10% fetal bovine serum (FBS; Vanderbilt Media Core), 2 mM L-glutamine (Sigma, St. Louis, MO), 100 U/mL penicillin (Invitrogen), 100 μ g/mL

streptomycin (Invitrogen), and 5 $\mu\text{g/mL}$ blasticidin (Invitrogen). If using the monoclonal cell lines, the medium should also be supplemented with 175 $\mu\text{g/mL}$ hygromycin (Invitrogen).

5. FuGENE-6 (Roche, Indianapolis, IN) for performing transient transfections.
6. Filter 10X trypsin–ethylenediamine tetraacetic acid (EDTA) (Gibco, Grand Island NY) through a 2 μM SFCA filter (Nalge Nunc International, Rochester, NY) and adjust to a 1X working solution (0.05% trypsin and 1 mM EDTA) with sterile phosphate-buffered saline (PBS; Vanderbilt Media Core).
7. 1 mg/mL solution of tetracycline (Invitrogen) in 100% ethanol. Store at -20°C .

2.2. Anti-FLAG Immunoprecipitation and Peptide Elution

Store all reagents at 4°C unless noted otherwise.

1. PBS: 10 mM Na_2HPO_4 , 0.17 mM KH_2PO_4 , pH 7.4, 137 mM NaCl, and 0.27 mM KCl.
2. Cell lysis buffer and immunoprecipitation buffer: 20 mM Tris-HCl, pH 7.6, 0.1% (v/v) Igepal CA-630, 150 mM NaCl, 3 mM EDTA, 3 mM EGTA, 1 mM phenylmethylsulfonylfluoride (PMSF), 17 $\mu\text{g/mL}$ aprotinin, and 5 $\mu\text{g/mL}$ leupeptin.
3. Bovine serum albumin Fraction V (Sigma, St. Louis, MO).
4. Phosphatase assay buffer: 25 mM Tris-HCl, pH 7.5, 1 mM EDTA, 1 mM EGTA, 1 mM dithiothreitol (DTT), and 0.25 mg/mL BSA.
5. Costar cell lifter (Fisher, Pittsburgh, PA).
6. 100 mM PMSF (Sigma) in isopropanol.
7. 10-mg/mL Stock solution of leupeptin (Sigma) in water. Store at -20°C .
8. Aprotinin (Sigma).
9. Anti-FLAG MZ-Agarose affinity gel (Sigma). Store at -20°C .
10. Tris-buffered saline (TBS): 25 mM Tris-HCl, pH 7.4, 137 mM NaCl, and 1.38 mM KCl.
11. 5-mg/mL solution of FLAG peptide (Sigma) in TBS. Store in 20- μL aliquots at -20°C .
12. Protein Assay Dye Reagent concentrate (Bio-Rad, Hercules, CA).
13. 2-mg/mL Bovine serum albumin Fraction V, in 0.9% (w/v) NaCl solution (Pierce, Rockford, IL); used to generate standard curve for protein assay.
14. Glycerol (Sigma).

2.3. Immunoblot Analysis

1. Optitran BA-S supported nitrocellulose membrane (VWR, Bristol, CT).
2. T-TBS: Tris-buffered saline containing 0.1% (v/v) Tween-20.
3. Blocking buffer: T-TBS containing 0.5% (w/v) BSA.
4. Anti-PP2A catalytic subunit mouse monoclonal antibody (BD Biosciences Pharmingen, San Diego, CA).
5. Anti-FLAG M2 rabbit and mouse antibodies (Sigma).
6. Anti-PP2A A and $\text{B}\alpha/\delta$ subunit rabbit antibodies (Calbiochem, San Diego, CA).

7. 5X Sodium dodecyl sulfate (SDS) sample buffer: 50% glycerol, 0.3 M Tris-HCl, pH 6.8, 11.5% SDS, 50 mM DTT, and 0.1% bromophenol blue. Adjust to 2X with Milli-Q water.
8. IRDye™ 800-labeled goat anti-rabbit secondary antibody (Rockland Immunochemicals, Gilbertsville, PA)
9. AlexaFluor® 680 goat anti-mouse IgG (Molecular Probes, Eugene, OR).
10. Odyssey™ Infrared Imaging System (Li-Cor, Lincoln, NE).

2.4. Silver Stain Analysis

1. 100% Ethanol (VWR).
2. Milli-Q water.
3. Fixing solution: 40% ethanol, 12% acetic acid (VWR), and 50 μ L of 37% formaldehyde (Sigma).
4. A 10% (w/v) solution of sodium thiosulfate (Sigma) in Milli-Q water.
5. Developing solution: 6 g sodium carbonate (Sigma), 50 μ L of 37% formaldehyde, and 4 μ L of 10% sodium thiosulfate.
6. Prepare a 0.2% (w/v) solution of silver nitrate (Fisher) in Milli-Q water.
7. Stop solution (40% ethanol and 12% acetic acid).

2.5. Phosphatase Assay

1. 32 P-labeled Histone H1 and phosphorylase *a* prepared as previously described (4,32).
2. Packard 1600 TR Liquid Scintillation Analyzer (Perkin-Elmer Life and Analytical Sciences, Shelton, CT).
3. Phosphatase assay buffer: 25 mM Tris-HCl, pH 7.5, 1 mM EDTA, 1 mM EGTA, 1 mM DTT, and 0.25 mg/mL BSA.
4. Wide-mouth copolymer plastic scintillation vials (Research Products International, Mt. Prospect, IL).
5. Ecoscint (National Diagnostics, Atlanta, GA).
6. Water bath set at 30°C.
7. 250 μ M Okadaic acid (Alexis USA Biochemicals, San Diego, CA) in dimethylsulfoxide (DMSO). Store in aliquots at -20°C.
8. 40% (w/v) Solution of trichloroacetic acid (TCA; Fisher) in water.

3. Methods

3.1. Expression of FLAG-tagged B Subunits

1. Plate HEK T-Rex cells (2×10^6 cells) stably expressing pcDNA5/TO (empty vector), B α -FLAG/pcDNA5/TO, or B δ -FLAG/pcDNA5/TO into one 10-cm tissue culture dish. Grow cells at 37°C in a humidified 5% CO₂ incubator. Alternatively, transiently transfect one 10-cm tissue culture dish of HEK T-Rex cells with pcDNA5/TO, B α -FLAG/pcDNA5/TO, or B δ -FLAG/pcDNA5/TO using FuGENE-6 (3 μ g of plasmid DNA and 9 μ L of FuGENE-6), (see Notes 3 and 4).

2. After overnight incubation, treat cells with 1 $\mu\text{g}/\text{mL}$ tetracycline for 48 h to induce protein expression (*see Note 5*).
3. Place each 10-cm dish of cells on ice and wash twice with 5 mL of ice-cold PBS.
4. Scrape cells off the dish with 500 μL of lysis buffer using a cell lifter.
5. Centrifuge for 15 min at 13,700g to pellet cell debris. Transfer supernatant into a new microfuge tube.
6. Perform Bradford assay on an aliquot of the supernatant to determine protein concentration.

3.2. Anti-FLAG Immunoprecipitation and Peptide Elution

1. Wash the appropriate amount of anti-FLAG MZ-Agarose affinity gel (20 μL of a 50% slurry for each immunoprecipitation) with 1 mL of lysis buffer. Centrifuge at 850g for 1 min, aspirate the supernatant, and resuspend resin in half of the original volume to make a 50% slurry.
2. Combine cell extract (approx 1 mg of protein) with 20 μL of washed anti-FLAG M2 slurry in a 1.5-mL microfuge tube and rotate end over end for 4–16 h at 4°C.
3. Centrifuge at 850g for 1 min and discard supernatant (*see Note 6*).
4. Wash bound proteins three times with 1 mL of immunoprecipitation buffer and once with 1 mL of phosphatase assay buffer. For each wash, centrifuge samples at 850g for 2 min and aspirate the supernatant using an ultrafine pipet tip.
5. After the last wash, elute bound proteins by adding 50 μL of phosphatase assay buffer containing 100 $\mu\text{g}/\text{mL}$ FLAG peptide and rotating end over end for 30 min at 4°C. Centrifuge for 1 min at 850g and collect the supernatant. Repeat the elution and combine the eluates.
6. Dilute the purified PP2A holoenzymes (FLAG peptide eluates) with an equal volume of 100% glycerol and store at –20°C (*see Note 7*).
7. Aliquots of the FLAG peptide eluates should then be subjected to silver stain and immunoblot analyses and also assayed for phosphatase activity (*see Subheading 3.5.*).

3.3. Immunoblot Analysis

1. Combine 10 μL of the FLAG eluates with 10 μL of 2X SDS sample buffer and place in a 95°C heating block for 5 min.
2. Fractionate samples on a 4% stacking/10% resolving SDS–polyacrylamide gel and electrophoretically transfer proteins to a nitrocellulose membrane.
3. Incubate membrane for 1 h in blocking buffer at room temperature on a rocking platform.
4. Discard blocking buffer and incubate membrane for 1 h at room temperature on rocking platform with the following primary antibodies diluted in 2 mL of blocking buffer: anti-FLAG rabbit antibody (1:1000), anti-PP2A A subunit antibody (1:1000), and anti-PP2A catalytic antibody (1:4000).
5. Remove solution containing primary antibodies and wash membrane three times with T-TBS (5 min for each wash).

6. Incubate membrane for 45 min at room temperature with the following secondary antibodies diluted in 2 mL of blocking buffer: IRDye 800-labeled goat anti-rabbit antibody (1:10,000) for detection of the A subunit and FLAG-tagged B subunit, and AlexaFluor 680-labeled goat anti-mouse antibody (1:10,000) for detection of the PP2A catalytic subunit (*see Note 8*). Protect the membrane from light until it is scanned (*see step 8*).
7. Discard secondary antibodies and wash membrane three times with T-TBS (5 min for each wash).
8. After the final wash, the immuno-labeled proteins can be visualized and quantified using the Odyssey Infrared Imaging System and Odyssey software, which measures integrated pixel intensity.

3.4. Silver Stain Analysis

1. After SDS-PAGE (polyacrylamide gel electrophoresis), place the gel in 100 mL of fixing solution for at least 30 min (*see Note 9*).
2. Discard fixing solution and wash gel twice in 50% ethanol (10 min each wash). For a 1-mm-thick gel, wash one more time with 50% ethanol. For a 0.75-mm-thick gel, perform final wash in 30% ethanol.
3. Remove the ethanol solution and treat the gel for 1 min with 0.02% sodium thio-sulfate (diluted from the 10% stock).
4. Rinse gel three times with Milli-Q water (20-s rinses).
5. Incubate gel for 20 min in 100 mL of solution containing 0.2% silver nitrate and 50 μ L of 37% formaldehyde.
6. Rinse gel twice with Milli-Q water (10-s rinses).
7. Visualize proteins with developing solution until protein standards and desired protein bands are seen (0.5–10 min).
8. Discard developing solution and add 100 mL of stop solution.
9. Gel can be scanned after development or preserved by drying.

3.5. Phosphatase Assay

1. Initiate the phosphatase assay by adding 2–10 μ L of 32 P-labeled substrate (diluted in phosphatase assay buffer) into a 0.7-mL microfuge tube containing FLAG-B α / δ PP2A holoenzymes (approx 2 ng) and the appropriate amount of phosphatase assay buffer to give a final reaction volume of 50 μ L (*see Notes 10 and 11*).
2. Allow the reactions to proceed for 15 min at 30°C. Stagger start times for each reaction by approx 10 s (*see Note 12*).
3. Terminate the reaction by adding 50 μ L of 40% TCA (20% final concentration).
4. Vortex the samples and store on ice for at least 30 min. Centrifuge for 10 min at 13,000g.
5. Carefully remove 80 μ L of the supernatant and transfer into 1.5-mL microfuge tube.
6. Add scintillation fluid (1.2 mL) and vortex at full speed for 10 s.
7. Place microfuge tubes into scintillation vials and quantify [32 P]_i using a scintillation counter (*see Notes 13 and 14*).

4. Notes

1. The experimental strategy detailed in this chapter can be utilized to isolate PP2A holoenzymes containing other FLAG-tagged regulatory subunits. Furthermore, as previously described (34), this approach can be used to monitor cellular signaling pathways targeted by individual PP2A holoenzymes.
2. Plasmids encoding B α and B δ with a FLAG tag on their C-terminus were used for these studies; however, we have successfully used this strategy for N-terminal FLAG-tagged regulatory subunits as well.
3. Transient expression of FLAG-tagged B subunits in target mammalian cells works equally well for subsequent isolation of the respective PP2A holoenzymes.
4. Monoclonal cell lines stably expressing tetracycline-inducible expression plasmids encoding B α -FLAG or B δ -FLAG were generated by transfecting HEK T-Rex cells with B α -FLAG/pcDNA5/TO or B δ -FLAG/pcDNA5/TO, followed by selection of individual clones in media containing 175 μ g/mL hygromycin.
5. Either tetracycline or doxycycline (1 μ g/mL) can be used for inducible-protein expression of B subunits in HEK T-Rex cells.
6. The supernatant from the first wash after anti-FLAG immunoprecipitation can be collected to monitor the efficiency of immunoprecipitation.
7. Purified PP2A holoenzymes are stable for several months at -20°C . The typical yield of PP2A catalytic subunit contained in each holoenzyme preparation is approx 0.4 μ g per each 10-cm tissue culture dish of cells.
8. The bound primary antibodies can also be visualized using alkaline phosphatase-conjugated or horseradish-peroxidase-conjugated secondary antibodies and the appropriate developing system.
9. Fresh solutions should be used for all steps of the silver stain analysis.
10. Less than 20% of total phosphorylated substrate should be dephosphorylated during assay to ensure that the substrate is not limiting.
11. Pretreatment of purified PP2A holoenzymes for 15 min with 2 nM okadaic acid (OA), a concentration of inhibitor that selectively inhibits PP2A (33) should completely abolish phosphatase activity.
12. Phosphatase reactions should be performed in triplicate.
13. Calculation of phosphatase activity:

$$\text{Phosphatase activity } [(\text{pmol}/\text{min}/\text{mg})/(\text{SRA})] = [\text{dpm observed in phosphatase reaction} - \text{background dpm}/(\text{time of assay})]/(\text{mg of PP2A}_c)]$$
 - a. Specific radioactivity (SRA) of $[\gamma\text{-}^{32}\text{P}]\text{ATP} = \text{dpm of } [\gamma\text{-}^{32}\text{P}]\text{ATP}/\text{cold ATP in substrate labeling reaction}.$
 - b. Background dpm equals the amount of radioactivity released in samples without holoenzyme.
14. AB α_{FLAG} C and AB δ_{FLAG} C holoenzymes exhibited specific activities of 0.24–0.64 μ mol/min/mg of catalytic subunit contained in the purified holoenzyme when radiolabeled histone H1 or phosphorylase-*a* were used as the substrate.

Acknowledgments

This work was supported by National Institutes of Health grants GM51366 and DK070787 (to BEW), DK20593 (to the Vanderbilt Diabetes Research & Training Center), CA68485 (to the Vanderbilt-Ingram Cancer Center), and MH19732 (to the Center for Molecular Neurosciences). DGA was supported in part by a National Institutes of Health Training grant 5T32DK07563.

References

1. Kamibayashi, C., Estes, R., Lickteig, R. L., Yang, S. I., Craft, C., and Mumby, M. C. (1994) Comparison of heterotrimeric protein phosphatase 2A containing different B subunits. *J. Biol. Chem.* **269**, 20139–20148.
2. McCright, B., Rivers, A. M., Audlin, S., and Virshup, D. M. (1996) The B56 family of protein phosphatase 2A (PP2A) regulatory subunits encodes differentiation-induced phosphoproteins that target PP2A to both nucleus and cytoplasm. *J. Biol. Chem.* **271**, 22081–22089.
3. Strack, S., Chang, D., Zaucha, J. A., Colbran, R. J., and Wadzinski, B. E. (1999) Cloning and characterization of B delta, a novel regulatory subunit of protein phosphatase 2A. *FEBS Lett.* **460**, 462–466.
4. Strack, S., Westphal, R. S., Colbran, R. J., Ebner, F. F., and Wadzinski, B. E. (1997) Protein serine/threonine phosphatase 1 and 2A associate with and dephosphorylate neurofilaments. *Mol. Brain Res.* **49**, 15–28.
5. Zhao, Y., Boguslawski, G., Zitomer, R. S., and DePaoli-Roach, A. A. (1997) *Saccharomyces cerevisiae* homologs of mammalian B and B' subunits of protein phosphatase 2A direct the enzyme to distinct cellular functions. *J. Biol. Chem.* **272**, 8256–8262.
6. Healy, A. M., Zolnierowicz, S., Stapleton, A. E., Goebl, M., DePaoli-Roach, A. A., and Pringle, J. R. (1991) CDC55, a *Saccharomyces cerevisiae* gene involved in cellular morphogenesis: identification, characterization, and homology to the B subunit of mammalian type 2A protein phosphatase. *Mol. Cell. Biol.* **11**, 5767–5780.
7. Zolnierowicz, S. (2000) Type 2A protein phosphatase, the complex regulator of numerous signaling pathways. *Biochem. Pharmacol.* **60**, 1225–1235.
8. Mayer, R. E., Hendrix, P., Cron, P., et al. (1991) Structure of the 55-kDa regulatory subunit of protein phosphatase 2A: evidence for a neuronal-specific isoform. *Biochemistry* **30**, 3589–3597.
9. McCright, B. and Virshup, D. M. (1995) Identification of a new family of protein phosphatase 2A regulatory subunits. *J. Biol. Chem.* **270**, 26123–26128.
10. Csontos, C., Zolnierowicz, S., Bako, E., Durbin, S. D., and DePaoli-Roach, A. A. (1996) High complexity in the expression of the B' subunit of protein phosphatase 2A0. Evidence for the existence of at least seven novel isoforms. *J. Biol. Chem.* **271**, 2578–2588.
11. Tanabe, O., Nagase, T., Murakami, T., et al. (1996) Molecular cloning of a 74-kDa regulatory subunit (B'' or delta) of human protein phosphatase 2A. *FEBS Lett.* **379**, 107–111.

12. Hendrix, P., Mayer-Jackel, R. E., Cron, P., et al. (1993) Structure and expression of a 72-kDa regulatory subunit of protein phosphatase 2A. Evidence for different size forms produced by alternative splicing. *J. Biol. Chem.* **268**, 15267–15276.
13. Voorhoeve, P. M., Hijmans, E. M., and Bernards, R. (1999) Functional interaction between a novel protein phosphatase 2A regulatory subunit, PR59, and the retinoblastoma-related p107 protein. *Oncogene* **18**, 515–524.
14. Moreno, C. S., Park, S., Nelson, K., et al. (2000) WD40 repeat proteins striatin and S/G(2) nuclear autoantigen are members of a novel family of calmodulin-binding proteins that associate with protein phosphatase 2A. *J. Biol. Chem.* **275**, 5257–5263.
15. Westphal, R. S., Anderson, K. A., Means, A. R., and Wadzinski, B. E. (1998) A signaling complex of Ca^{2+} -calmodulin-dependent protein kinase IV and protein phosphatase 2A. *Science*. **280**, 1258–1261.
16. Peterson, R. T., Desai, B. N., Hardwick, J. S., and Schreiber, S. L. (1999) Protein phosphatase 2A interacts with the 70-kDa S6 kinase and is activated by inhibition of FKBP12-rapamycin-associated protein. *Proc. Natl. Acad. Sci. USA* **96**, 4438–4442.
17. Heriche, J. K., Lebrin, F., Rabilloud, T., Leroy, D., Chambaz, E. M., and Goldberg, Y. (1997) Regulation of protein phosphatase 2A by direct interaction with casein kinase 2alpha. *Science*. **276**, 952–955.
18. Avdi, N. J., Malcolm, K. C., Nick, J. A., and Worthen, G. S. (2002) A role for protein phosphatase-2A in p38 mitogen-activated protein kinase-mediated regulation of the c-Jun NH(2)-terminal kinase pathway in human neutrophils. *J. Biol. Chem.* **277**, 40687–40696.
19. Davare, M. A., Avdonin, V., Hall, D. D., et al. (2001) A beta2 adrenergic receptor signaling complex assembled with the Ca^{2+} channel Cav1.2. [erratum: *Science* 2001 Aug 3;293(5531):804]. *Science* **293**, 98–101 [comment].
20. Chiang, C. W., Harris, G., Ellig, C., Masters, S. C., Subramanian, R., Shenolikar, S., Wadzinski, B. E., and Yang, E. (2001) Protein phosphatase 2A activates the proapoptotic function of BAD in interleukin-3-dependent lymphoid cells by a mechanism requiring 14–3–3 dissociation. *Blood* **97**, 1289–1297.
21. Shtrichman, R., Sharf, R., and Kleinberger, T. (2000) Adenovirus E4orf4 protein interacts with both Balpha and B' subunits of protein phosphatase 2A, but E4orf4-induced apoptosis is mediated only by the interaction with Balpha. *Oncogene* **19**, 3757–3765.
22. Schulze, D., Muqhal, M., Lederer, W., and Ruknudin, A. (2003) Sodium/calcium exchanger (NCX1) macromolecular complex. *J. Biol. Chem.* **278**, 28849–28855.
23. Lu, Q., Surks, H. K., Ebling, H., Baur, W. E., Brown, D., Pallas, D. C., and Karas, R. H. (2003) Regulation of estrogen receptor alpha-mediated transcription by a direct interaction with protein phosphatase 2A. *J. Biol. Chem.* **278**, 4639–4645.
24. Bauman, A. L., Apparsundaram, S., Ramamoorthy, S., Wadzinski, B. E., Vaughan, R. A., and Blakely, R. D. (2000) Cocaine and antidepressant-sensitive biogenic amine transporters exist in regulated complexes with protein phosphatase 2A. *J. Neurosci.* **20**, 7571–7578.

25. Wadzinski, B. E., Eisfelder, B. J., Peruski, L. F., Jr., Mumby, M. C., and Johnson, G. L. (1992) NH₂-terminal modification of the phosphatase 2A catalytic subunit allows functional expression in mammalian cells. *J. Biol. Chem.* **267**, 16883–16888.
26. Baharians, Z. and Schonthal, A. H. (1998) Autoregulation of protein phosphatase type 2A expression. *J. Biol. Chem.* **273**, 19019–19024.
27. Ruvolo, P. P., Clark, W., Mumby, M., Gao, F., and May, W. S. (2002) A functional role for the B56 alpha-subunit of protein phosphatase 2A in ceramide-mediated regulation of Bcl2 phosphorylation status and function. *J. Biol. Chem.* **277**, 22847–22852.
28. Chen, W., Possemato, R., Campbell, K. T., Plattner, C. A., Pallas, D. C., and Hahn, W. C. (2004) Identification of specific PP2A complexes involved in human cell transformation. *Cancer Cell* **5**, 127–136 [see comment].
29. Dagda, R. K., Zaucha, J. A., Wadzinski, B. E., and Strack, S. (2003) A developmentally regulated, neuron-specific splice variant of the variable subunit Bbeta targets protein phosphatase 2A to mitochondria and modulates apoptosis. *J. Biol. Chem.* **278**, 24976–24985.
30. Strack, S. (2002) Overexpression of the protein phosphatase 2A regulatory subunit Bgamma promotes neuronal differentiation by activating the MAP kinase (MAPK) cascade. *J. Biol. Chem.* **277**, 41525–41532.
31. Bennis, D. A., Don, A. S., Brake, T., et al. (2002) Cyclin G2 associates with protein phosphatase 2A catalytic and regulatory B' subunits in active complexes and induces nuclear aberrations and a G1/S phase cell cycle arrest. *J. Biol. Chem.* **277**, 27,449–27,467.
32. Jakes, S. and Schlender, K.K. (1988) Histone H1 phosphorylated by protein kinase C is a selective substrate for the assay of protein phosphatase 2A in the presence of phosphatase 1. *Biochim. Biophys. Acta* **967**, 11–16.
33. Favre, B., Turowski, P., and Hemmings, B. A. (1997) Differential inhibition and posttranslational modification of protein phosphatase 1 and 2A in MCF7 cells treated with calyculin-A, okadaic acid, and tautomycin. *J. Biol. Chem.* **272**, 13856–13863.
34. Adams, D. G., Coffee, R. L., Jr., Zhang, H., Pelech, S., Strack, S., and Wadzinski, B. E. (2005) Positive regulation of Raf1-MEK1/2-ERK1/2 signaling by protein serine/threonine phosphatase 2A holoenzymes. *J. Biol. Chem.* **280**, 42644–42654.

Purification of PP2A Holoenzymes by Sequential Immunoprecipitation with Anti-Peptide Antibodies

Gernot Walter, Jin Zhou, and Ralf Ruediger

Summary

Understanding the multiple functions of protein phosphatase 2A (PP2A) rests on elucidating the enzymatic properties of over 50 different possible forms of the PP2A holoenzyme. We describe a procedure for highly purifying each one of these forms. This procedure is based on coexpressing in 293 cells one scaffolding A subunit, one regulatory B subunit, and one catalytic C subunit, each tagged with a different sequence, and purifying the trimeric holoenzyme by three consecutive immunoprecipitations with antibodies against the tags. In a few hours and from a small number of cells, sufficient enzyme can be purified for enzymatic studies. Purification of six different holoenzymes in parallel can easily be accomplished.

Key Words: PP2A purification; anti-peptide antibodies; epitope tagging; phosphatase assay

1. Introduction

The great versatility of protein phosphatase 2A (PP2A) and its involvement in numerous cellular processes is based on the existence of a large number of subunits: two catalytic subunits ($C\alpha$ and $C\beta$), two scaffolding subunits ($A\alpha$ and $A\beta$), and three families of regulatory subunits (B, B', and B''), which are weakly related. The B family consists of four isoforms, the B' family consists of five isoforms and additional splice variants, and the B'' family has four members (*see* [ref. 1](#) for review and nomenclature of mammalian PP2A subunits). The combination of all subunits can give rise, in theory, to 64 different forms of the trimeric holoenzyme, each composed of one A, one B, and one C subunit. If one considers that $A\beta$ does not bind some or all members of the B family ([2](#)), this number would be reduced to 60 different forms. Furthermore, PP2A interacts with at least 40 cellular proteins, including protein kinases,

From: *Methods in Molecular Biology, Volume 365: Protein Phosphatase Protocols*
Edited by: G. Moorhead © Humana Press Inc., Totowa, NJ

tumor suppressors, and proteins involved in apoptosis and signal transduction (1,3). Until now, only a few holoenzymes have been purified and characterized. In order to study the multiple properties and functions of PP2A, it will be necessary to purify all holoenzymes—a daunting task if one relies on conventional methods of purification.

Antibodies against synthetic peptides are powerful tools for protein purification (see ref. 4 for review). As reported over 20 yr ago, antibodies against the C-terminal hexapeptide of polyomavirus middle T antigen (middle T) were used to purify middle T from extracts of infected cells 2500-fold (5). In this procedure, affinity-purified antipeptide antibodies, coupled to Sepharose, were first incubated with cell extract containing middle T. Then nonspecifically bound proteins were removed by extensive washing. In the final step, middle T was released with an excess of peptide at neutral pH. In a subsequent report, two different antipeptide antibodies were used in sequence to purify middle T even further (6). First, middle T from extracts was bound to antibodies against the C-terminal peptide and released with an excess of the peptide. In the second step, the released prepurified middle T was bound to antibodies against a different peptide, corresponding to an internal region of middle T (7), and released with an excess of this peptide. This procedure produced highly purified middle T. In addition, it led to the identification of cellular proteins, including the A α and C α subunits of PP2A (8,9), which are associated with middle T (10). Here, we describe a three-step procedure for the purification of PP2A holoenzymes, which is based on three consecutive immunoprecipitations with antibodies against epitope-tagged A, B, and C subunits. This procedure permits simultaneous purification of at least six different holoenzymes from a small number of cells (11). It enabled us to compare the enzymatic properties of holoenzymes containing either C α or C β , as well as holoenzymes differing only in their A-subunit isoforms, A α and A β .

2. Materials

2.1. Cell Culture

1. Dulbecco's modified Eagle's medium (DMEM) (Invitrogen, Carlsbad, CA) supplemented with 10% fetal bovine serum (FBS) (Invitrogen). Phosphate-buffered saline (PBS) (Invitrogen).
2. For transfection, we use Opti-MEM (Invitrogen).

2.2. Cell Transfection and Lysis

1. Plasmids: Vectors encoding A α and A β tagged at the C terminus with EE (EEEEYMPME), vectors encoding B α , B' α 1, and B"/PR72 tagged at the C terminus with KT3 (KPPTPPPEPET), and vectors encoding C α and C β tagged at the N terminus with HA (YPYDVPDYA) are described in Chapter 8.

2. Transfection reagents LipofectAMINE and the PLUS reagent are from Invitrogen.
3. Triton X-100 (TX-100) lysis buffer: 50 mM Tris-HCl, pH 7.5, 150 mM NaCl, 3 mM MgCl₂, 0.5% TX-100, 1 mM dithiothreitol (DTT) (Sigma), 50 μM leupeptin (Sigma). The latter two are added fresh before use.
4. Sodium dodecyl sulfate (SDS)–polyacrylamide gel electrophoresis (PAGE) sample buffer: 2% SDS, 100 mM DTT, 60 mM Tris-HCl, pH 6.8, 10% glycerol, 0.01% bromophenol blue.

2.3. Labeling Cells with [³⁵S]Methionine

1. Methionine-free DMEM (Invitrogen).
2. Labeling medium: 10% FBS, 15% regular DMEM, 75% methionine-free DMEM; supplemented with 20 mM HEPES (Gibco), 2 mM glutamine (Gibco), and 1 mM pyruvate (Gibco), final concentrations.
3. [³⁵S]Methionine, specific activity > 1000 Ci/mmol (Amersham).

2.4. Sequential Immunoprecipitation (IP)

1. Antibodies: mouse monoclonal anti-EE (6) (Covance), mouse monoclonal anti-KT3 (12) (Covance), mouse monoclonal anti-HA (Roche).
2. Release buffer: 2% TX-100, 10 mM Tris-HCl, pH 7.5, 150 mM NaCl. Add 1 mM DTT (final concentration) and EE or KT3 peptide before use.
3. TX-100 lysis buffer (*see Subheading 2.2., item 3*) for washing, and SDS-PAGE sample buffer (*see Subheading 2.2.4., item 4*).
4. Slit tubes are prepared from 500-μL microcentrifuge tubes by cutting 3–4 mm deep into the tube bottom with a utility knife. This generates a narrow slit that allows liquid to flow through during centrifugation but retains Sepharose beads. The liquid that passes through the slit is collected by placing the slit tube onto a 1.5-mL microcentrifuge tube.
5. EE and KT3 peptides (Bachem) are dissolved in 50 mM Tris-HCl, pH 7.5 at a concentration of 10–30 mg/mL and stored in aliquots at –20°C (*see Notes 1 and 2*).

2.5. Phosphatase Substrate Preparation and Protein Phosphatase Assay

1. Protein Serine/Threonine Phosphatase (PSP) Assay System from New England BioLabs.
2. Histone H1 (Roche); p34cdc2-cyclin B (New England BioLabs); [γ-³³P]ATP, specific activity >2500 Ci/mmol (Amersham).
3. Imidazole: To make 200 mL of a 1 M solution, dissolve 13.6 g imidazole (Sigma) in 100 mL water, adjust pH to 7.4 with 1 N HCl (approx 40 mL), and add water to 200 mL.
4. EGTA: To make a 0.5 M solution, dissolve 10 g EGTA (Sigma) in 20 mL water, adjust pH to above 7.6 with 10 N NaOH, and add water to 52 mL.
5. TCA: To make a 100% (w/v) trichloroacetic acid (TCA) (Sigma) solution, add 227 mL of water to 500 g of TCA.
6. Cdc2 reaction buffer: 50 mM Tris-HCl, pH 7.5, 10 mM MgCl₂, 1 mM EGTA, 2 mM DTT, 0.01% Brij35.

7. H1 solubilizing buffer: 50 mM imidazole-HCl, pH 7.4, 1 mM DTT, 5 mM EGTA, 0.01% Brij 35.
8. H1 dialysis buffer: 25 mM imidazole, pH 7.4, 1 mM DTT, 5 mM EGTA, 0.01% Brij 35.
9. MBP dialysis buffer: 25 mM Tris-HCl, pH 7.5, 0.1 mM EDTA, 2 mM DTT, 0.01% Brij 35.
10. Dialysis bag (Spectrum), molecular weight cutoff 6–8 kDa. Soak in distilled water at room temperature for 30 min, rinse thoroughly with distilled water, and store at 4°C in 0.03% sodium azide.
11. Scintillation fluid, CytoScint (ICN); scintillation counter LS6000SC from Beckman.
12. PP2A assay buffer: 50 mM Tris-HCl, pH 7.0, 0.1 mM EDTA, 5 mM DTT, 1 mM MnCl₂, 0.01% Brij 35 (*see Note 3*).

3. Methods

3.1. Purification Overview

Figure 1 illustrates schematically how the consecutive use of three antibodies yields a defined form of PP2A holoenzyme (e.g., $\text{A}\alpha\text{-B}''/\text{PR72-C}\alpha$). As a source for the enzyme, extract from HEK293 cells transfected with vectors encoding EE-tagged $\text{A}\alpha$ ($\text{A}\alpha^{\text{EE}}$), KT3-tagged $\text{B}''/\text{PR72}$ ($\text{B}''/\text{PR72}^{\text{KT3}}$), and HA-tagged $\text{C}\alpha$ ($^{\text{HA}}\text{C}\alpha$) is used. (Superscripts EE and KT3 to the right of $\text{A}\alpha$ and B'' indicate tagging on the C terminus; superscript HA to the left of $\text{C}\alpha$ indicates tagging at the N terminus.) The cell lysate contains a mixture of core enzymes and holoenzymes composed of endogenous (white) and exogenous (shaded) subunits. In the first IP with anti-EE peptide antibodies and the subsequent solubilization of the immune complexes with EE peptide, all forms of enzyme not containing $\text{A}\alpha^{\text{EE}}$ are eliminated, whereas excess free $\text{A}\alpha^{\text{EE}}$ as well as core enzymes and holoenzymes composed of $\text{A}\alpha^{\text{EE}}$ combined with untagged endogenous or tagged exogenous B or C are retained. In the second round, IP with anti-KT3 peptide antibodies and release with KT3 peptide, holoenzymes composed of $\text{A}\alpha^{\text{EE}}$, $\text{B}''/\text{PR72}^{\text{KT3}}$, and either $^{\text{HA}}\text{C}\alpha$ or the endogenous C subunits ($\text{C}\alpha$ or $\text{C}\beta$) are purified. In the last step, IP with anti-HA antibodies, holoenzymes containing endogenous C-subunits are eliminated, and only the desired form, $\text{A}\alpha^{\text{EE}}\text{-B}''/\text{PR72}^{\text{KT3}}\text{-}^{\text{HA}}\text{C}\alpha$, is bound to the beads (*see Note 4*).

To demonstrate the power of the method, we describe below the purification of $\text{A}\alpha^{\text{EE}}\text{-B}''/\text{PR72}^{\text{KT3}}\text{-}^{\text{HA}}\text{C}\alpha$ from [³⁵S]methionine-labeled 293 cell extracts according to Zhou et al. ([11](#)). For studies of enzyme activity, unlabeled extracts were used.

3.2. Covalent Binding of Anti-EE and Anti-KT3 Antibodies to Protein G-Sepharose

Anti-EE and anti-KT3 monoclonal antibodies are prepared from hybridoma supernatants and covalently coupled to protein G-Sepharose (GammaBind

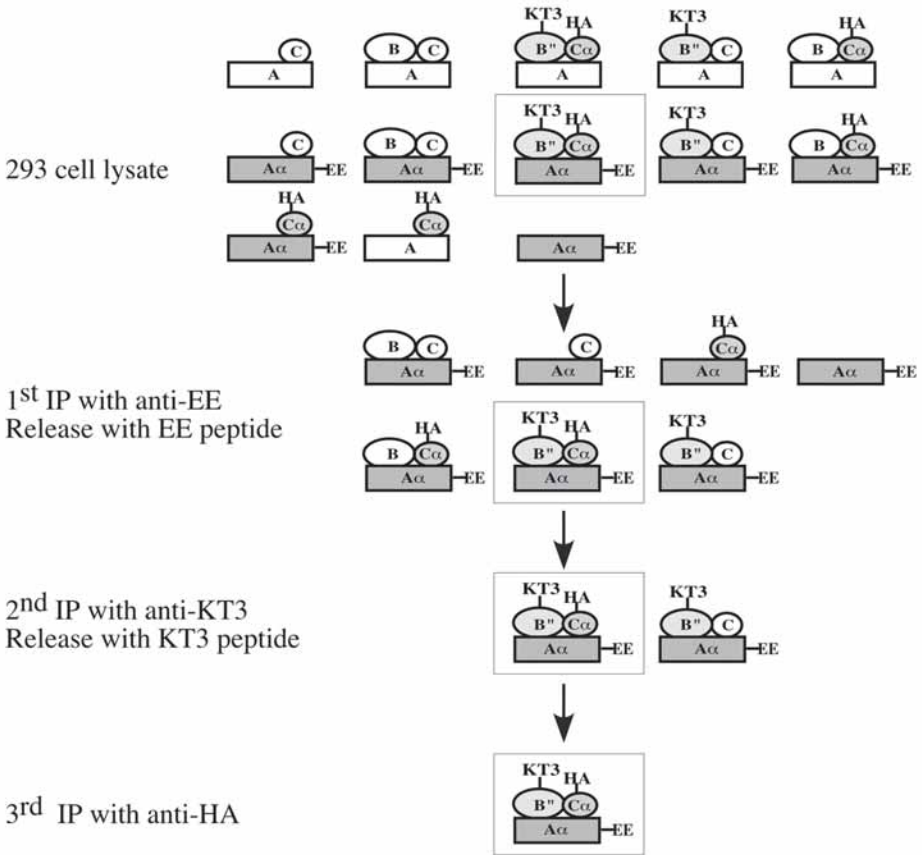


Fig. 1. Scheme of holoenzyme purification by sequential immunoprecipitations with anti-peptide antibodies. The endogenous subunits are in white; A could be A α or A β , C could be C α or C β , and B could be B, B', or B''. The exogenous subunits are shaded. The holoenzyme to be purified is framed by a rectangle. The lysate panel shows possible forms of core- and holoenzymes in 293 cells transfected with A α ^{EE}, B''/PR72^{KT3}, and ^{HA}C α . After the first immunoprecipitation (IP) with anti-EE and release with EE peptide, endogenous A subunit-containing core- and holoenzymes are eliminated. A second IP with anti-KT3 and release with KT3 peptide eliminates all enzymes that do not contain B''/PR72^{KT3}. The third IP with anti-HA eliminates holoenzymes with endogenous C α or C β . Only exogenously expressed holoenzyme remains: A α ^{EE}-B''/PR72^{KT3-HA}-C α .

Plus-Sepharose; Amersham) using dimethylpimelimidate as described (13). The hybridoma cells are grown in medium containing Ultra-Low IgG FBS (Gibco-BRL). This permits direct use of IgG prepared from hybridoma super-

natants without further purification of peptide-specific IgG fractions. For the PP2A purification described below, protein G–Sephadex was used that contained 17 μg anti-EE IgG/ μL beads and 15 μg anti-KT3 IgG/ μL beads.

3.3. Expression and [^{35}S]Methionine Labeling of Epitope-Tagged Holoenzyme in Transfected 293 Cells

As described by Zhou et al. (11), 293 cells are grown in DMEM supplemented with 10% FBS.

1. On a 10-cm culture dish, 1.5×10^6 cells are plated. The cells are 50–60% confluent after 24 h.
2. Before transfection, the cells are rinsed once with Opti-MEM. The cells are transfected with 3.9 μg of a mixture of three plasmid DNAs (0.6 μg A α^{EE} , 2.7 μg B"/PR72 $^{\text{KT3}}$, 0.6 μg $^{\text{HAC}\alpha}$) (see Note 5).
3. After 36 h, the cells are washed twice with 5 mL prewarmed (37°C) PBS, followed by one wash with 5 mL prewarmed methionine-free DMEM. The cells are then incubated for 12 h in 2 mL labeling medium containing 300 $\mu\text{Ci/mL}$ [^{35}S]methionine.
4. After labeling, the cells are washed with DMEM, harvested in 450 μL cold TX-100 lysis buffer, and spun at 15,000g for 5 min. The supernatant is used for IP.

3.4. Three-Step Purification of Holoenzyme

3.4.1. First IP

1. Save a 5- μL aliquot of the [^{35}S]methionine-labeled or unlabeled cell lysate (see Subheading 3.4., step 6).
2. The remaining lysate (approx 400 μL) is incubated in a 1.5-mL microcentrifuge tube for 1 h at room temperature (RT) with 30 μL settled anti-EE beads (17 μg IgG/ μL settled beads) to bind EE-tagged A α -subunit-containing core and holoenzymes, and an excess “free” A α -subunit. The tube is rotated at 8 rpm on an end-over-end rotator.
3. After incubation, the beads are washed three times with 1 mL TX-100 lysis buffer and centrifuged at 1300g for 1 min in a tabletop microfuge. The supernatant is carefully removed using a flat gel-loading tip to avoid loss of beads.

3.4.2. First Release

1. After the last wash, the beads are incubated with 100 μL release buffer containing 300 $\mu\text{g/mL}$ EE peptide (see Note 6). The tubes are rotated end over end at RT for 30 min.
2. The beads are spun down at 1300g for 1 min in a tabletop microfuge, and the supernatant is transferred to a 500- μL split tube sitting in a fresh 1.5-ml tube and spun at 300g for 10 s on a tabletop microfuge. This step eliminates carryover beads. The flow-through is used for the second IP.

3.4.3. Second IP

1. Save 5 μL of the first release (*see Subheading 3.4.6., step 1*). The remaining volume (approx 90 μL) is incubated with 10 μL anti-KT3 beads (15 μg IgG/ μL settled beads) for 1 h at RT while rotating to bind the KT3-tagged B"-subunit.
2. The beads are washed as described for the first IP.

3.4.4. Second Release

Bound PP2A is released from the anti-KT3 beads in 50 μL release buffer containing KT3 peptide (300 $\mu\text{g}/\text{mL}$) as described in **Subheading 3.4.2**.

3.4.5. Third IP

1. Save 5 μL of the second release. The remaining volume (approx 45 μL) is incubated with 5 μL anti-HA antibody at RT for 1 h. Then 7.5 μL settled protein G-Sepharose beads are added and the mixture is incubated for 30 min at RT while rotating.
2. After the incubation, the beads are washed three times as above. We do not release the protein with HA peptide, although this is an option.

3.4.6. Purity and Yield

1. To monitor the purity and yield, 5- μL aliquots from the lysate, the first and second release, and 1 μL settled beads of the last IP are analyzed on a 12.5% SDS-PAGE gel and quantitated by phosphorimaging (*see below*).
2. To estimate the amount of PP2A bound to beads, parallel purifications are carried out, in which aliquots from the beads of the first and second IP are analyzed by SDS-PAGE and phosphorimaging. The SDS-PAGE gels are also exposed to X-ray film and analyzed by autoradiography, which has the advantage of higher resolution.

The final yield after the third IP is determined by comparing the amount of A subunit in the purified holoenzyme to a serial dilution of pure A subunit using SDS-PAGE and silver staining or Western blotting with 6G3 monoclonal antibody that recognizes untagged and tagged A subunits ([14](#)).

3.5. Analysis of Purified Fractions by SDS-PAGE

That the above-described approach yields highly purified enzyme is shown in [Fig. 2](#). The 293 cell lysate contains numerous [^{35}S]methionine-labeled proteins including $\text{A}\alpha^{\text{EE}}$, which is detectable (lane 1) when compared with untransfected control lysate (lane 2). B"/PR72^{KT3} and $^{\text{HA}}\text{C}\alpha$ are undetectable. Precipitation with anti-EE and release with EE peptide achieves considerable purification so that B"/PR72^{KT3} and $^{\text{HA}}\text{C}\alpha$ can now be seen (lanes 3 and 4). Compared to B"/PR72^{KT3} and $^{\text{HA}}\text{C}\alpha$, $\text{A}\alpha^{\text{EE}}$ is in a large molar excess because of the presence of excess monomeric $\text{A}\alpha^{\text{EE}}$. That the holoenzyme in the released

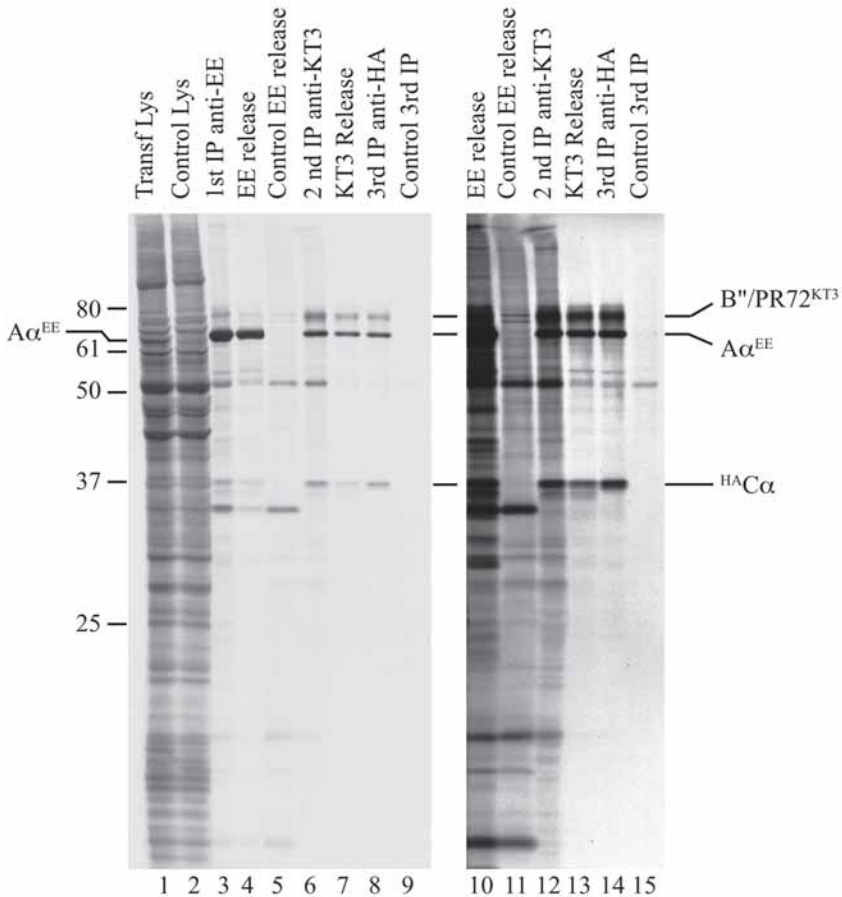


Figure 2. Purification of holoenzyme $A\alpha^{EE}$ -B''/PR72^{KT3}-HAC α from transfected 293 cells by sequential immunoprecipitation. 293 cells were transfected with plasmids encoding $A\alpha^{EE}$, B''/PR72^{KT3}, and HAC α , and labeled with [³⁵S]methionine. Equivalent amounts from each step of purification were analyzed. As a control, a mock purification was carried out in parallel using lysate from pcDNA3-transfected cells (lanes 2, 5, 9, 11, and 15). Numbers at the left, molecular mass in kDa. Lanes 1–9, 16-h exposure; lanes 10–15, 7-day exposure.

material still contains a large number of cellular proteins is apparent after a longer exposure time (compare lanes 10 and 4). The second precipitation with anti-KT3 (lanes 6 and 12) and the release with KT3 peptide (lanes 7 and 13) considerably improves the purity of the $A\alpha^{EE}$ -B''/PR72^{KT3}-HAC α holoenzyme. After IP with anti-HA antibodies, the product appears only slightly purer than

after the previous step (compare lanes 7 and 13 with lanes 8 and 14). One difference is the loss of two bands just below $^{\text{H}}\text{A}\alpha$ (compare lanes 13 and 14) that might represent untagged forms of endogenous C subunit expected to be removed at this step. B"/PR72 is heterogeneous, suggesting that it might be modified (*see Note 7*).

The radioactive bands for $\text{A}\alpha^{\text{EE}}$, B"/PR72 $^{\text{KT}3}$, and $^{\text{H}}\text{A}\alpha$ are quantitated using a Molecular Dynamics Storm Gel and Blot Imaging System and ImageQuant software. Adjustments are made for the number of methionine residues in each subunit, the amount of cell extract used, and the amount of protein loaded for each step of purification. The results of quantitation show that in the course of purification, the molar ratio of the A, B, and C subunits approaches 1 : 1 : 1. The large excess of $\text{A}\alpha^{\text{EE}}$ after the first purification step is the result of its high overexpression. The relatively higher intensity of $\text{A}\alpha$ in the final product (lane 8) results from its higher methionine content as compared to $\text{C}\alpha$ and B"/PR72. The yield of holoenzyme after the third IP is approx 3% in regard to the first IP (100%). Losses occur both during IP and release. Under the present condition, one 10-cm dish with 1.5×10^6 293 cells (approx 200 μg total protein containing 600 ng PP2A [0.3%]) yields approx 20–30 ng of purified enzyme after the third IP (*see Note 8*).

3.6. Phosphatase Substrates

After the last IP, the beads are washed twice with 500 μL PP2A assay buffer and the phosphatase assay is carried out without delay using myelin basic protein (MBP) or histone H1 as substrates (*see Note 9*).

3.6.1. Myelin Basic Protein

Phosphorylated MBP is prepared with the PSP assay system following the protocol provided by New England BioLabs.

1. Briefly, MBP is labeled by phosphorylation on serine and threonine residues with cAMP-dependent protein kinase (PKA) in the presence of $[\gamma\text{-}^{33}\text{P}]\text{ATP}$.
2. The reaction is terminated by adding TCA (final concentration, 10%) to precipitate the phosphorylated MBP, inactivate the protein kinase, and remove excess ATP. Labeled MBP is purified from residual ATP by washing with 20% TCA and by dialysis against MBP dialysis buffer.

3.6.2. Histone H1

1. Histone H1 is phosphorylated in the following reaction mixture (final volume, 1 mL): 1 mg histone H1 (Roche Molecular Biochemicals) dissolved in 0.5 mL cdc2 reaction buffer, 372 μL water, 50 μL of 10X cdc2 reaction buffer, 50 μL of 10 mM ATP, 12.5 μL $[\gamma\text{-}^{33}\text{P}]\text{ATP}$ (10 $\mu\text{Ci}/\mu\text{L}$, specific activity $>2500\text{ Ci}/\text{mmol}$), and 15 μL p34 $^{\text{cdc}2}$ (20 units/ μL) (New England BioLabs).

2. The mixture is incubated at 30°C overnight. Terminate the reaction by the addition of 350 μ L 100% cold TCA. Vortex and keep on ice for 30 min. Spin at 12,000g for 10 min at 4°C.
3. Wash three times with 1 mL of 20% cold TCA, dissolve the pellet in 200 μ L H1 solubilizing buffer, and transfer the solution to a dialysis bag. Wash the tube with 200 μ L of the same buffer and transfer the wash to the dialysis bag. Dialyze against 500 mL H1 dialysis buffer for 2 h at 4°C and against 1 L H1 dialysis buffer overnight at 4°C.
4. Transfer the sample to a microcentrifuge tube. Remove a 5- μ L aliquot to determine radioactivity. Calculate the incorporation of [33 P]ATP according to the PSP assay system protocol (New England BioLabs).
5. Dilute the sample with H1 solubilizing buffer to a concentration of 25 μ M with regard to the incorporated phosphate. Store at 4°C. The degree of phosphorylation is approx 1.4 mol of phosphate per mole of MBP and 0.6 mol of phosphate per mole of histone H1. The labeled substrates can be used for about two 33 P half-lives (50 d).

3.7. Phosphatase Assays

3.7.1. Myelin Basic Protein

The phosphatase assay with labeled MBP is carried out with 3 μ L of settled beads containing PP2A from the third IP using the PSP Assay System from New England BioLabs.

3.7.2. Histone H1

When using histone H1 as a substrate, the following procedure is recommended.

1. To 3 μ L settled beads containing PP2A from the third IP, add 35 μ L PP2A assay buffer. Start the phosphatase reaction by adding 5 μ L labeled histone H1 (final concentration, 2.5 μ M). Mix and incubate for 10 min at 30°C.
2. Terminate the reaction by adding 100 μ L water and 50 μ L of 100% TCA (final concentration, 25%). Keep on ice for 10 min and centrifuge 5 min at 12,000g at 4°C.
3. Carefully remove the TCA and add it to 5 mL CytoScint. Mix well and count in a scintillation counter to determine the amount of 33 P released.
4. Determine the total amount of radioactivity used for the assay by counting 5 μ L of the substrate. Calculate the units of phosphatase activity as described in the PSP Assay System (New England BioLabs).

Figure 3 shows the activities of six different holoenzymes consisting of A α and B α , B' α 1, or B''/PR72, and C α or C β . They were purified in parallel and assayed with MBP and histone H1 as substrates (**11**).

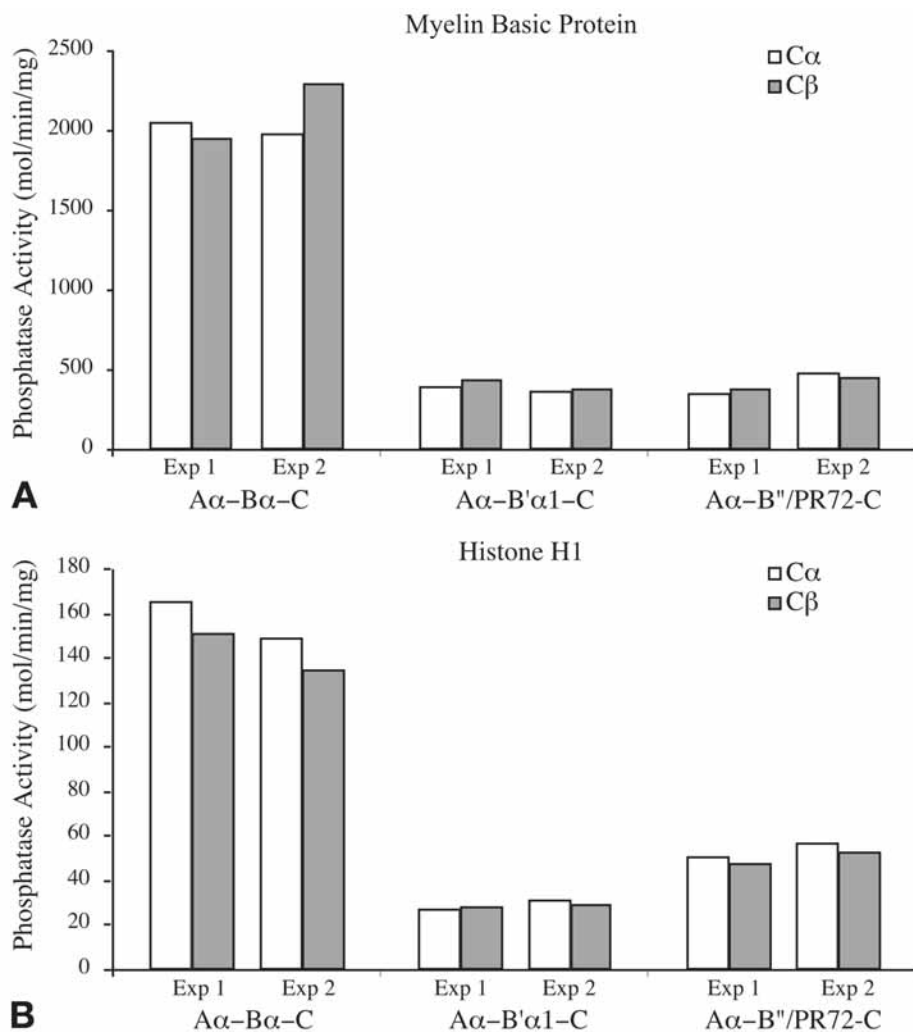


Figure 3. Specific phosphatase activity of six PP2A holoenzymes. Holoenzymes consisting of A α and B α , B' α 1, or B''/PR72, and C α or C β were purified as outlined in Figure 1. Phosphatase activity was determined using ^{33}P -labeled MBP (panel a) and ^{33}P -labeled histone H1 (panel b).

4. Notes

1. Check the pH of the peptide solution by placing a 0.05- μL aliquot on a pH indicator strip. If the peptide is very acidic or basic, the pH of the solution is adjusted with a small amount of 1 *N* NaOH or 1 *N* HCl, respectively.

2. Instead of the full-length EE and KT3 peptides one can also use the shorter peptides, EYMPME (15) and PPEPET (12), respectively.
3. The PP2A activity can be measured in a variety of buffers, including Tris-HCl, MES or MOPS. One millimolar of MnCl_2 activates the C-subunit, core enzymes, and holoenzymes and is recommended for all assay buffers (16). All forms of PP2A that have been tested are active between pH 5.6 and pH 8.5 (17). Note that holoenzyme activities vary strongly with the type of B subunit (17,18).
4. We have not attempted to release PP2A from the last IP with HA peptide, although this is an option as described (13).
5. Different amounts of plasmid DNA were used to express similar amounts of the three subunits. Because the B"/PR72 construct expressed weakly, a higher amount of DNA was used.
6. In comparison to the amount of bound antibodies, a 100-fold to 10,000-fold molar excess of peptide is needed for the release. The exact amount has to be optimized in each case. In some instances, efficient release is facilitated by the presence of detergent in the release buffer, such as Triton X-100, Nonidet P-40, or a mixture of 0.1% SDS, 1% deoxycholate, and 1% Nonidet P-40 (RIPA buffer). Raising the temperature of the elution buffer might also help, as in the case of elution with HA peptide (13). Another option is to moderately raise the pH of the elution buffer.
7. In spite of the high degree of purity of the final product, some proteins are still present at submolar quantities. Because they are not present in the untransfected control (lane 15), they might represent proteins specifically associated with the $\text{A}\alpha^{\text{EE-B}}/\text{PR72}^{\text{KT3-HA}}\text{C}\alpha$ holoenzyme. Of the over 40 such proteins that have been identified, it appears that each one binds only to a small fraction of the total PP2A.
8. Major losses occur both during immunoprecipitation and release. The yield could be improved considerably by optimizing each step with regard to the amount of beads, amount of peptide used for release, the choice and concentration of detergent, the temperature, and the pH.
9. Substrates phosphorylated by a variety of kinases are dephosphorylated by PP2A. These kinases include protein kinase A, protein kinase C, cyclin-dependent kinases, checkpoint kinase ATM, and casein kinases 1 and 2. The kinetic of dephosphorylation varies with different substrates and depends on the type of holoenzyme.

Acknowledgments

This work was supported by the Tobacco-Related Disease Research Program grant 8RT-0037 and by Public Health Service grant CA-36111.

References

1. Silverstein, A. M., Davis, A. J., Bielinski, V. A., Esplin, E. D., Mahmood, N. A., and Mumby, M. C. (2003) Protein phosphatase 2A, in *Handbook of Cell Signaling* (Bradshaw, R. A. and Dennis, E. A., eds.), Elsevier Academic Press, Chap. 189.

2. Zhou, J., Pham, H. T., Ruediger, R., and Walter, G. (2003) Characterization of the A alpha and A beta subunit isoforms of protein phosphatase 2A: differences in expression, subunit interaction, and evolution. *Biochem. J.* **369**, 387–398.
3. Janssens, V. and Goris, J. (2001) Protein phosphatase 2A: a highly regulated family of serine/threonine phosphatases implicated in cell growth and signalling. *Biochem. J.* **353**, 417–439.
4. Walter, G. (1986) Production and use of antibodies against synthetic peptides. *J. Immunol. Methods* **88**, 149–161.
5. Walter, G., Hutchinson, M. A., Hunter, T., and Eckhart, W. (1982) Purification of polyoma virus medium-size tumor antigen by immunoaffinity chromatography. *Proc. Natl. Acad. Sci. USA* **79**, 4025–4029.
6. Grussenmeyer T., K. H. Scheidtmann, M. A. Hutchinson, W. Eckhart, and G. Walter. (1985) Complexes of polyoma virus medium T antigen and cellular proteins. *Proc. Natl. Acad. Sci. USA* **82**, 7952–7954.
7. Schaffhausen, B., Benjamin, T. L., Pike, L., Casnellie, J., and Krebs, E. (1982) Antibody to the nonapeptide Glu-Glu-Glu-Glu-Tyr-Met-Pro-Met-Glu is specific for polyoma middle T antigen and inhibits in vitro kinase activity. *J. Biol. Chem.* **257**, 12467–12470.
8. Walter, G., Ruediger, R., Slaughter, C., and Mumby, M. (1990) Association of protein phosphatase 2A with polyoma virus medium tumor antigen. *Proc. Natl. Acad. Sci. USA* **87**, 2521–2525.
9. Walter, G., Ferre, F., Espiritu, O., and Carbone-Wiley, A. (1989) Molecular cloning and sequence of cDNA encoding polyoma medium tumor antigen-associated 61-kDa protein. *Proc. Natl. Acad. Sci. USA* **86**, 8669–8672.
10. Pallas, D. C., Shahrik, L. K., Martin, B. L., et al. (1990) Polyoma small and middle T antigens and SV40 small t antigen form stable complexes with protein phosphatase 2A. *Cell* **60**, 167–176.
11. Zhou, J., Pham, H. T., and Walter, G. (2003) The formation and activity of PP2A holoenzymes do not depend on the isoform of the catalytic subunit. *J. Biol. Chem.* **278**, 8617–8622.
12. MacArthur, H. and Walter, G. (1984) Monoclonal antibodies specific for the carboxyl terminus of simian virus 40 large T antigen. *J. Virol.* **52**, 483–491.
13. Harlow, E. and Lane, D. (1999) Using Antibodies: A Laboratory Manual. Cold Spring Harbor Laboratory, Cold Spring Harbor, NY.
14. Kremmer, E., Ohst, K., Kiefer, J., Brewis, N., and Walter, G. (1997) Separation of PP2A core enzyme and holoenzyme with monoclonal antibodies against the regulatory A subunit: abundant expression of both forms in cells. *Mol. Cell. Biol.* **17**, 1692–1701.
15. Stokoe, D. and McCormick F. (1997) Activation of c-Raf-1 by Ras and Src through different mechanisms: activation in vivo and in vitro. *EMBO J.* **16**, 2384–2396.
16. Scheidtmann, K. H., Mumby, M. C., Rundell, K., and Walter, G. (1991) Dephosphorylation of simian virus large T antigen and p53 protein by protein phosphatase 2A: inhibition by small T antigen. *Mol. Cell. Biol.* **11**, 1996–2003.

17. Price, N. E. and Mumby, M. C. (2000) Effects of regulatory subunits on the kinetics of protein phosphatase 2A. *Biochemistry* **39**, 11,312–11,318.
18. Cegielska, A., Shaffer, S., Derua, R., Goris, J., and Virshup, D. M. (1994) Different oligomeric forms of protein phosphatase 2A activate and inhibit simian virus 40 DNA replication. *Mol. Cell. Biol.* **14**, 4616–4623.

Purification of PP2Ac from Bovine Heart

Hue T. Tran, Tony S. Ferrar, Anne Ulke-Lemée,
and Greg B. G. Moorhead

Summary

The catalytic subunit of PP2A (PP2Ac) can be purified in milligram quantities from bovine heart using ethanol precipitation, ammonium sulfate precipitation, ion exchange and size exclusion chromatography. The detailed procedure is described to purify PP2Ac over 4 d.

Key Words: Protein phosphatase; PP2A; dephosphorylation; column chromatography; PP1; bovine heart; catalytic subunit

1. Introduction

Protein phosphatase 1 (PP1) and 2A (PP2A) catalytic subunits associate with various regulatory subunits in the cell and it is the targeting by these accessory subunits that play the key role in directing the dephosphorylation events catalyzed by PP1 and PP2A ([1–4](#)). Free of any regulatory subunits, PP1 and PP2Ac are regarded as promiscuous, dephosphorylating most serine or threonine phospho-proteins. This makes them a good tool in the research laboratory when it is necessary to dephosphorylate a protein in vitro. For instance, we have used PP2Ac to dephosphorylate proteins affinity-purified on a 14-3-3 matrix ([5,6](#)). Subsequent overlay with 14-3-3 then demonstrated that essentially every target purified on the 14-3-3 matrix associated with the 14-3-3 in a phosphorylation-dependent manner ([5,6](#)). The method described here is the one we use to routinely purify the free catalytic subunit of PP2A (PP2Ac) from bovine heart. This was adapted and modified from the method described to purify PP2Ac from rabbit skeletal muscle ([7](#)). This method is particularly useful because it has proven difficult to express and purify reasonable amounts of recombinant PP2Ac.

From: *Methods in Molecular Biology, Volume 365: Protein Phosphatase Protocols*
Edited by: G. Moorhead © Humana Press Inc., Totowa, NJ

2. Materials

2.1. Buffers

1. Buffer A: 20 mM Tris-HCl, pH 7.5 (4°C), 0.1 mM EGTA, 10% (v/v) glycerol, 0.1% 2-mercaptoethanol, 1 mM benzamidine, 0.1 mM phenylmethylsulfonyl fluoride.
2. Buffer B: 20 mM Tris-HCl, pH 7.0 (20°C), 0.1 mM EGTA, 10% (v/v) glycerol, 0.1% 2-mercaptoethanol, 1 mM benzamidine, 0.1 mM phenylmethylsulfonyl fluoride.
3. Buffer C: 50 mM Tris-HCl, pH 7.0 (20°C), 0.1 mM EGTA, 60% (v/v) glycerol, 0.1% 2-mercaptoethanol, 1 mM benzamidine, 0.1 mM phenylmethylsulfonyl fluoride.
4. Buffer D: 50 mM Tris-HCl, pH 7.5 (20°C), 0.1 mM EGTA, 0.1% (v/v) 2-mercaptoethanol, 1 mg/mL bovine serum albumin (BSA).
5. Buffer E: 50 mM Tris-HCl, pH 7.5 (20°C), 0.1 mM EGTA, 0.03% (v/v) Brij-35.

2.2. Other Materials

1. Ammonium hydroxide.
2. Ammonium sulfate.
3. Phenylmethylsulfonyl fluoride (dissolved in 95% ethanol).
4. DEAE-Sephacel column (Amersham Pharmacia).
5. Q-Sepharose (Amersham Pharmacia).
6. Centriprep-30 and Centricon-30 concentrators (Amicon).
7. HiLoad Superdex 200 column (120 mL; 1.6 × 60 cm) (Amersham Pharmacia).

2.3. PP2Ac Enzyme Assays

³²P-Labeled glycogen phosphorylase-*a* containing 1.0 mol phosphate per mole of subunit is prepared using phosphorylase-*b* (8) and phosphorylase kinase (9) purified from rabbit skeletal muscle by the methods described. Details of the assay can be found in **ref. 10**. Briefly, assays are performed at 30°C in a total volume of 30 µL that includes 10 µL of protein phosphatase diluted as required into buffer D plus 10 µL buffer E. The assays are initiated with 10 µL of 30 µM ³²P-labeled glycogen phosphorylase-*a*. In all cases, the dephosphorylation of substrate is kept less than 30% to ensure the linearity of the assay. All assays are done in duplicate.

3. Methods

3.1. Preparation of Extract and Ammonium Sulfate Fractionation

1. Two bovine hearts (approx 4 kg) are excised by slaughterhouse staff, placed in ice, and transported to the laboratory.
2. The tissue is then chopped, minced (using a commercially available meat mincer), and homogenized in a Waring blender in 1 vol (approx 4 L) of buffer A (except the EGTA concentration is 4 mM).

3. The homogenate is centrifuged at 4200g (4°C) for 30 min, the supernatant removed and filtered through glass wool in a large funnel, and the pH adjusted with constant stirring to 7.2 with ammonium hydroxide (*see Note 1*).
4. Ground ammonium sulfate (*see Note 2*) is added slowly to the supernatant with gentle stirring to bring the degree of saturation to 55% (351 g/L).
5. After standing for 30 min, the extract is centrifuged at 4200g (4°C) for 30 min and the supernatant is discarded.
6. The precipitate is resuspended in buffer A to give a final volume of one-tenth of the original extract (*see Notes 3 and 4*).

3.2. Dissociation of PP2Ac From Regulatory Subunits and Ammonium Sulfate Fractionation

1. Divide the resuspended fraction from **Subheading 3.1.** equally into large centrifuge bottles (1 L) such that approx 5 more volumes can be added to the bottle. Quickly add 5 vol of 95% ethanol containing 1 mM phenylmethylsulfonyl fluoride at ambient temperature.
2. Immediately centrifuge for 5 min at 4200g (4°C) (*see Note 1*).
3. The supernatant is discarded and the pellet extracted with 1600 mL of buffer A (without glycerol; *see Note 3*) and recentrifuged for 5 min at 4200g (4°C).
4. The supernatant is collected and the pellet re-extracted with 800 mL of buffer A (without glycerol) and recentrifuged for 5 min at 4200g (4°C).
5. The combined supernatants are adjusted to pH 7.2 with ammonium hydroxide and ammonium sulfate is added with gentle stirring to bring the degree of saturation to 65% (430 g/L; *see Note 2*).
6. After standing for 30 min, the suspension is centrifuged for 40 min at 13,000g (4°C) and the supernatant is discarded.
7. The precipitate is suspended in 100 mL of buffer A and dialyzed overnight against 20 vol of buffer A with three changes of dialysis buffer (two changes on this day, one change the next morning).

3.3. Ion-Exchange Chromatography on DEAE-Sepharose

1. The dialyzed protein fraction is loaded onto a 50-mL column of DEAE-Sepharose (5 × 2.6 cm) equilibrated in buffer A (*see Note 5*).
2. The column is washed with 50 mL of buffer A, followed by 250 mL of buffer A plus 80 mM NaCl (*see Note 6*).
3. PP2Ac is eluted in 10-mL fractions with 200 mL of buffer A plus 400 mM NaCl. (All load, wash, and elution steps are performed at approx 3 mL/min).
4. Fractions containing the protein peak are pooled and dialyzed against buffer B (3 × 2 L) overnight.

3.4. Ion-Exchange Chromatography on Q-Sepharose

1. The dialyzed pooled fractions (approx 50 mL) from the DEAE-Sepharose column are centrifuged to clarify (Beckman Ti45 rotor for 30 min at 35,000 rpm).

2. The supernatant is then chromatographed at ambient temperature on a Pharmacia FPLC Q-Sepharose ion-exchange column equilibrated in buffer B (20 mL; 1.6×10 cm).
3. The column is developed with a linear 300-mL gradient from 0 to 400 mM NaCl with a flow rate of 3 mL/min and 5-mL fractions are collected. PP2Ac should elute in fractions 33–36 and PP1 should elute in later fractions (*see Note 7*).

3.5. Gel-Filtration Chromatography on Hi-Load 16/60 Superdex 200

1. Fractions from the Q-Sepharose column containing enzymes are concentrated to 0.5 mL using a Centriprep-30 concentrator (Amicon), followed by a Centricon 30 (Amicon).
2. The sample is then gel-filtered on a Pharmacia HiLoad Superdex 200 column (120 mL; 1.6×60 cm) equilibrated in buffer B plus 200 mM NaCl.
3. Collect 1-mL fractions and start collection at the column void volume (the void should be determined for each individual column, but should be approx 46 mL for a HiLoad Superdex 200 column [1.6×60 cm]). PP2Ac elutes essentially pure as the last A_{280} peak at approx 35 kDa (*see Fig. 1A*).
4. Before pooling fractions, run a sample of each fraction on 12% sodium dodecyl sulfate-polyacrylamide gel (SDS-PAGE) and stain with Commassie blue (*see Fig. 1B*).
5. Peak PP2Ac fractions are pooled, concentrated in a Centricon 30 to about 1 mL and then dialyzed against buffer C and stored at -20°C . Pure PP2Ac should have specific activity of 3000 mU/mg (*see Note 8*). We find that if stored in 60% glycerol at -20°C , PP2Ac loses very little activity, even after 2 yr of storage at -20°C . A typical preparation yields approx 0.5 mg PP2Ac per kilogram of heart muscle.

4. Notes

1. We use 1-L bottles in either a Sorval fixed-angle rotor or a Beckman swing-out rotor.
2. Grind ammonium sulfate in a dry blender at room temperature (wear a mask).
3. Initially resuspend using a glass rod with a rubber end attached. We find that after this initial resuspension, a Dounce homogenizer works best from this point on, especially if you have one that is motorized.
4. If you had an original extract volume of 3.7 L, add approx 350 mL of buffer A to dissolve and this yields approx 1/10th the original volume.
5. The column size suggested here should be adequate for a preparation from 4 kg of tissue. Keep in mind that the capacity of the DEAE-Sepharose matrix is approx 50 mg/mL; the column size can be increased if necessary.
6. Before loading on the DEAE-Sepharose column, measure the conductivity of the sample and compare it to the conductivity of buffer A plus 80 mM NaCl. PP2Ac binds in buffer plus 80 mM NaCl; thus, if the conductivity of the sample is less than the wash buffer, it will bind. If the dialysis has not lowered the conductivity sufficiently, dilute sample with distilled water (dH_2O). We collect 10 mL fractions in 15-mL Falcon tubes.

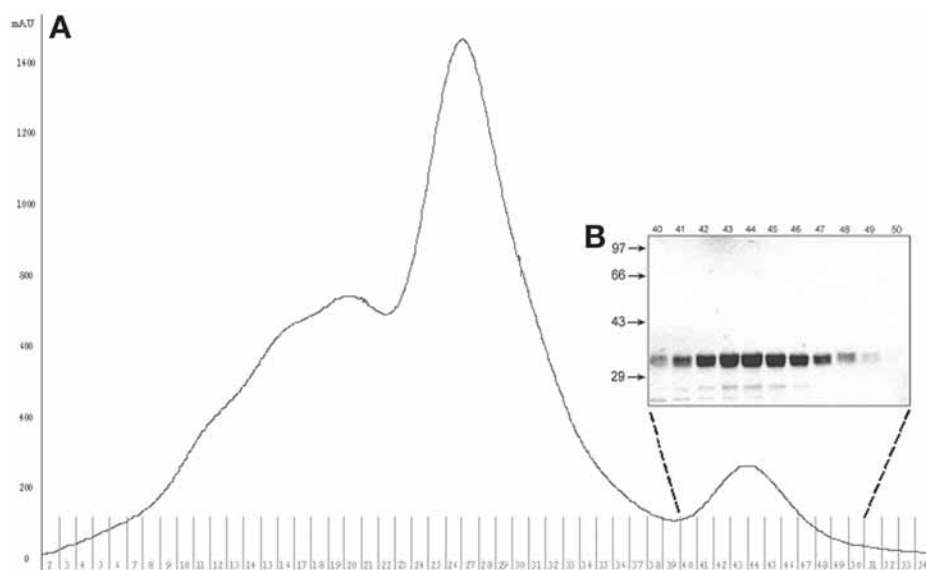


Fig. 1. Elution of PP2Ac during HiLoad Superdex 200 gel-filtration chromatography and SDS-PAGE. **(A)** PP2Ac from the Q-Sepharose pool was concentrated to 0.5 mL and further purified on HiLoad Superdex 200 gel filtration. Fractions of 1 mL were collected and the PP2Ac peak is indicated. The A_{280} was monitored and indicated with a solid line. The inset **(B)** shows SDS-PAGE of the HiLoad Superdex 200 gel filtration chromatography fractions containing PP2Ac. The fractions indicated from (A; 40–50) were heated in a SDS-PAGE cocktail and electrophoresed on a 12% gel and stained with Coomassie blue. The 36-kDa band is PP2Ac and molecular mass standards are shown on the left.

7. To assay for phosphorylase phosphatase activity at this stage, we suggest that you dilute the column fractions 3000- to 5000-fold. It turns out that the fractions with PP2Ac (fractions 33–36) also contain a “green” protein(s) (likely a Fe binding protein) that exactly copurifies on this step. We routinely pool these “green” fractions and do not bother with an assay, as this is very reproducible. We would suggest protein phosphatase assays when purifying the enzyme for the first time in your laboratory.
8. One unit (1 U) is defined as the amount of enzyme that catalyzes the release of 1 μ mol of phosphate in 1 min at 30°C.

Acknowledgments

Research in the Moorhead Laboratory is supported by the Natural Sciences and Engineering Research Council of Canada.

References

1. Hubbard, M. J. and Cohen, P. (1993) On target with a new mechanism for the regulation of protein phosphorylation. *Trends Biochem. Sci.* **18**, 172–177.
2. Johnson, D. F., Moorhead, G., Caudwell, F. B., et al. (1996) Identification of protein-phosphatase-1-binding domains on the glycogen and myofibrillar targeting subunits. *Eur. J. Biochem.* **239**, 317–325.
3. Moorhead, G., MacKintosh, R. W., Morrice, N., Gallagher, T., and MacKintosh, C. (1994) Purification of type 1 protein (serine/threonine) phosphatases by microcystin-Sepharose affinity chromatography. *FEBS Lett.* **356**, 46–50.
4. Janssens, V., and Goris, J. (2001) Protein phosphatase 2A: a highly regulated family of serine/threonine phosphatases implicated in cell growth and signalling. *Biochem. J.* **353**, 417–439.
5. Moorhead, G., Douglas, P., Cotelle, V., et al. (1999) Phosphorylation-dependent interactions between enzymes of plant metabolism and 14-3-3 proteins. *Plant J.* **18**, 1–12.
6. Rubio, M. P., Geraghty, K. M., Wong, B. H., et al. (2004) 14-3-3-Affinity purification of over 200 human phosphoproteins reveals new links to regulation of cellular metabolism, proliferation and trafficking. *Biochem. J.* **379**, 395–408.
7. Cohen, P., Alemany, S., Hemmings, B. A., Resink, T. J., Stralfors, P., and Tung, H. Y. (1988) Protein phosphatase-1 and protein phosphatase-2A from rabbit skeletal muscle. *Methods Enzymol.* **159**, 390–408.
8. Krebs, E. G., Kent, A. B., and Fischer, E. H. (1958) The muscle phosphorylase b kinase reaction. *J. Biol. Chem.* **231**, 73–83.
9. Cohen, P. (1983) Phosphorylase kinase from rabbit skeletal muscle. *Methods Enzymol.* **99**, 243–250.
10. MacKintosh, C. and Moorhead, G. (1999) Assay and purification of protein (serine/threonine) phosphatases, in *Protein Phosphorylation: A Practical Approach* (Hardie, D. G., ed.), Oxford University Press, New York, pp. 153–181.

Visualization of Intracellular PP1 Targeting Through Transiently and Stably Expressed Fluorescent Protein Fusions

Laura Trinkle-Mulcahy, Janet Chusainow, Yun Wah Lam, Sam Swift, and Angus Lamond

Summary

Protein phosphatase 1 (PP1) is a ubiquitous serine/threonine phosphatase that regulates many cellular processes, including cell division, signaling, differentiation, and metabolism. It is expressed in mammalian cells as three closely related isoforms: α , β/δ , and γ 1. These isoforms differ in their relative affinities for proteins, termed *targeting subunits*, that mediate their intracellular localization and substrate specificity. Because of the dynamic nature of these interactions, it is important to find experimental approaches that permit direct analyses of PP1 localization and PP1-targeting subunit interactions in live cells. When transiently or stably expressed as fluorescent protein (FP) fusions, the three isoforms are active phosphatases with distinct localization patterns and can interact with both endogenous and exogenous targeting subunits. Their changing spatio-temporal distributions can be monitored both throughout the cell cycle and following cellular perturbations by time-lapse fluorescence microscopy, and turnover rates of intracellular pools of the protein calculated by fluorescence recovery after photobleaching (FRAP). Interactions with targeting subunits can be visualized in vivo by fluorescence resonance energy transfer (FRET), using techniques such as sensitized emission, acceptor photobleaching, or fluorescence lifetime imaging.

Key Words: PP1; isoforms; targeting; GFP; fluorescence; microscopy; localization; FRAP; FRET; FLIM

1. Introduction

Reversible protein phosphorylation is the major general mechanism that regulates most physiological processes in eukaryotic cells. Protein phosphatase 1 (PP1) is involved in a wide range of cellular processes and is believed to

derive both its intracellular localization and its substrate specificity from proteins with which it associates, termed “targeting subunits” (for review, *see* **ref. 1**). Analysis of the subcellular targeting of PP1 is complicated by the fact that it is expressed in mammalian cells as three closely related isoforms (α , β/δ , and $\gamma 1$), which are encoded by separate genes (**2–4**). These isoforms are more than 89% identical in amino acid sequence, yet show distinct subcellular localization patterns (**5,6**) that most likely reflect their relative affinities for different targeting subunits. We have shown that overexpression of a targeting subunit can cause redistribution of all PP1 isoforms (**7**), which supports the targeting theory, yet indicates that overexpression assays cannot be used to assess differences in isoform specificity of the endogenous protein.

To study the properties of individual PP1 isoforms in living cells, including their localization and interaction with targeting subunits, we have taken advantage of the *in vivo* approach of fusing PP1 to fluorescent reporter molecules, in this case, chromatic variants of the green fluorescent protein (GFP) derived from the jellyfish *Aequorea victoria* (for review, *see* **ref. 8**). This method effectively “tags” the intracellular pool of the protein and allows analyses of dynamic properties in living cells. Fluorescence microscopy offers a unique approach to the study of living and fixed cells because of its sensitivity, specificity, and versatility. Fluorescence emitted from the biological sample can be simultaneously detected as both an image and as photometric data using the microscope, and it has great potential for qualitative and quantitative studies on the function and structure of cells. The fixed- and live-cell imaging of PP1 and/or targeting subunits described here can be performed on either a laser scanning microscope, such as a confocal, or a wide-field fluorescence microscope, provided a temperature-controlled chamber is available for the live-cell imaging.

More recently, increasingly elaborate techniques, including fluorescence recovery after photobleaching (FRAP), fluorescence lifetime imaging microscopy (FLIM), and fluorescence resonance energy transfer (FRET), have been developed that enable the visualization and analysis of ever more complex events in cells (for review, *see* **refs. 9 and 10**). For example, although time-lapse imaging can only show the steady-state distribution of a protein over time, FRAP analyses can reveal its kinetic properties, such as whether it is free to diffuse or is immobilized to a scaffold and if it is exchanging between particular compartments and at what rate. In short, bleaching a fluorescent pool of protein in one region of the cell using a high-intensity laser pulse renders that protein “invisible,” and recovery can then be monitored as the unbleached molecules from neighboring regions of the cell move into the bleached region.

Interactions between proteins, such as PP1 and a targeting subunit, can be shown *in vivo* using FRET measurement techniques such as those described

here. The basic principle of FRET is the transfer of energy from an excited donor fluorophore to an acceptor fluorophore in close proximity. FRET is strongly dependent on the distance between donor and acceptor, falling off with the sixth power of the distance between the two. Because of this, FRET can only occur when the proteins are within 1–10 nm of each other and in the proper orientation. A simplified diagram is presented in Fig. 3A, which demonstrates how excitation of the donor sensitizes emission from the acceptor that ordinarily would not occur. Therefore, FRET can be detected as sensitized emission of the acceptor.

Energy transfer from donor to acceptor depletes or “quenches” the excited-state population of the donor, and FRET will, therefore, reduce the fluorescence intensity of the donor. Photobleaching the acceptor to relieve this quenching of the donor (termed “acceptor photobleaching”) offers another option for detecting FRET *in vivo*.

FRET-induced donor quenching is also observed as a decrease in the donor’s fluorescence lifetime, which is the average time that a molecule spends in the excited state before emitting a photon and returning to the ground state. Comparison of donor lifetime in the presence and absence of acceptor is the last FRET method presented here, termed the FLIM/FRET technique. Key advantages of this approach are the independence of measurement on probe concentration and the use of infrared excitation wavelengths, which are less damaging to cells (for review, *see* refs. 11 and 12). For all three of these FRET techniques, the efficiency of energy transfer can be used as a molecular ruler to determine the scale of a particular interaction (13).

2. Materials

2.1. Cell Culture and Transfection

1. Enhanced GFP-C1 (EGFP-C1), EYFP-C1, and ECFP-C1 were purchased from Clontech (California, USA). These vectors contain an SV40 origin for replication and a neomycin-resistance gene for selection (using G418) in eukaryotic cells. A bacterial promoter upstream of the neomycin gene expresses kanamycin resistance in *Escherichia coli*.
2. Nonfluorescent tags can be used for fixed-cell analyses. An example is pSG8M, which allows expression of protein with an N-terminal 9E10 *c-myc* epitope tag (7).
3. HeLa cells (and other cell lines) are available from Promochem/ATCC (Teddington, UK).
4. Dulbecco’s modified Eagle’s medium (DMEM) (Invitrogen Life Technologies, California, USA) supplemented with 10% fetal bovine serum (FBS; Invitrogen) and 100 U/mL penicillin–streptomycin (Invitrogen). All growth media are stored at 4°C.
5. 1X Trypsin-EDTA solution (0.05% trypsin/0.53 mM EDTA; Invitrogen).

6. Dulbecco's-PBS (D-PBS; Invitrogen).
7. Cellstar 6-well and 24-well tissue culture plates (Greiner).
8. Nunclon 90-mm-diameter tissue culture dishes (VWR).
9. 25- and 75-cm² flasks with filter caps (Greiner).
10. Dimethyl sulfoxide (DMSO; Sigma-Aldrich).
11. Effectene transfection reagent (QIAGEN).
12. Geneticin (G418; Roche, Mannheim, Germany). Prepared as a 200-mg/mL stock in serum-free DMEM, filter-sterilized, and stored in 0.5 mL aliquots at -20°C. Add 0.5-mL to a 500-mL bottle of DMEM for a 200-μg/mL stock, or 1 mL to a 500-mL bottle of DMEM for a 400-μg/mL stock.

2.2. Live- and Fixed-Cell Imaging

1. Phenol red-free DMEM (Invitrogen).
2. CO₂-independent media (Invitrogen).
3. WillCo-dish 35-mm glass-bottom dishes (Intracel, Royston, UK).
4. Lab-Tek chambered cover glass (Sigma-Aldrich).
5. 40 mm diameter glass cover slips (Bioprotech Inc., Pennsylvania, USA).
6. Microscope cover slips (13 and 19 mm in diameter; Thickness No. 1; VWR).
7. Paraformaldehyde (Sigma-Aldrich) prepared fresh as a 3.7% (w/v) solution in phosphate-buffered saline (PBS). Heat to dissolve using a stirring hot plate in a fume hood and then cool to room temperature for use.
8. Permeabilization solution: 1% (v/v) Triton X-100 (Sigma-Aldrich) in PBS. Prepare this stock fresh, from a 20% Triton X-100 stock solution that can be stored at room temperature.
9. Blocking buffer and antibody dilution buffer: 1% donkey serum (Sigma-Aldrich) and 0.1% Tween[®]-20 (VWR) in PBS. Prepare fresh.
10. Primary antibody for staining *c-myc* fusion proteins: anti-*c-myc* epitope, clone 9E10 (Novus Biologicals) used at a 1 : 100 dilution.
11. Secondary antibody: antimouse IgG conjugated to Texas red (Jackson Immuno-research Laboratories, Inc.).
12. DNA stain for fixed cells: 4,6-diamidino-2-phenylindole (DAPI; Sigma-Aldrich). A 5-mg/mL stock solution in distilled water (dH₂O) was prepared and stored at 4°C. The working stock was a 1 : 15,000 dilution in dH₂O.
13. DNA stain for live cells: Hoechst No. 33342 (bisbenzimidazole; Sigma-Aldrich). A 25-mg/mL stock solution in dH₂O was prepared and stored at 4°C. The working solution, prepared fresh as needed, was a 1 : 1000 dilution in dH₂O (25 μg/mL final concentration), of which 20 μL was added to cells in 2 mL of DMEM in a 35-mm glass-bottom dish (adapted from [ref. 14](#)).
14. VECTASHIELD[®] mounting media (Vector Laboratories, California, USA).
15. FluorSave[™] mounting media (Calbiochem).
16. Immersion oils (Applied Precision) used with the wide-field fluorescence restoration microscopes had refractive indices of 1.514 (for fixed-cell imaging) and 1.520 (for live-cells imaging). Immersion oil 518 N (Carl Zeiss Inc., New York, USA) was used with the laser scanning confocal microscopes.

Table 1
Filter Sets Used With the DeltaVision Wide-Field Fluorescence Microscopes

Filter set/beam splitter	Excitation (P/BW)	Emission (P/BW)	Fluorophores
DAPI/PC	360/40 nm	457/50 nm	DAPI, Hoechst No. 33342
FITC/PC	490/20 nm	528/38 nm	Fluorescein; EGFP
RD-TR-PE/PC	555/28 nm	617/73 nm	Rhodamine; Texas red
CFP/JP4	436/10 nm	470/30 nm	ECFP
YFP/JP4	500/20 nm	535/30 nm	EYFP

2.3. Microscopes Used in This Study

1. Live-cell imaging and FRAP experiments were performed on a DeltaVision® Spectris wide-field deconvolution microscope (Applied Precision) equipped with a three-dimensional motorized-stage, temperature- and gas-controlled environmental chamber (Solent Scientific, Segensworth, UK) and 488-nm diode laser (for photobleaching EGFP; *see* **Note 1**). Images were collected using a 60x NA 1.4 Plan-Apochromat objective (Olympus, New York, USA) and recorded with a CoolSNAP coupled-charge device (CCD) camera (Roper Scientific, Ottobrun, Germany). The microscope is controlled by SoftWorx imaging and deconvolution software (Applied Precision). Specific excitation/emission filter sets and stationary beam splitters (Chroma Technology, Vermont, USA; *see* **Table 1**) were used to resolve the different fluorophore signals and minimize spectral bleed-through.
2. A similar system, the DeltaVision® DV3 wide-field fluorescence microscope mounted on a Zeiss inverted microscope with a slow readout CCD camera was used for the sensitized emission FRET studies. For temperature control, cells were grown on 40-mm-diameter glass cover slips and maintained in a closed, heated FCS2 POC (perfusion open/closed) chamber (Bioprotech). An objective heater (Bioprotech) was also used with this system to minimize temperature gradients between the objective and the cover slip, which can cause a drift in focus as the cover slip flexes. This is not necessary when using an environmental chamber that fully encloses the microscope and stage.
3. Acceptor photobleaching FRET experiments were performed on a Zeiss Confocal LSM 510 high-resolution confocal laser scanning microscope. Laser modules, scanning module, and the correct filter combinations for scanning (*see* **Table 2**) were controlled by the LSM 510 control module using the LSM 510 software. The microscope was fitted with a remote control to switch filter cubes for viewing, control focus, and switch objectives. Images were collected using a 63x NA 1.4 Plan-Apochromat objective and recorded with an AxioCam digital microscope camera using a scanning resolution of 256 × 256 pixels and employing bidirectional scanning mode to achieve a high scan speed (maximum 1.6 μs/pixel, resulting in a scan time of 123 ms) without losing quality.

Table 2
Filter Sets Used With the Zeiss Confocal LSM 510

Filter/dichroic	Characteristics
BP 440-505	Band-pass emission filter for ECFP; passes wavelengths 440–505 nm to the detector
LP 525	Long-pass emission filter for EYFP; passes wavelengths higher than 525 nm to the detector
HFT 413/514	Main dichroic beam splitter; deflects the indicated laser lines (413 nm and 514 nm) onto the specimen and allows the emitted fluorescent light to pass
NFT 505	Secondary dichroic beam splitter; is used to split the emitted light that will be guided into separate channels; light with wavelengths shorter than 505 nm is deflected, and light with a longer wavelength passes the NFT

4. FLIM/FRET experiments were performed on a Bio-Rad Radiance 2100MP confocal, multiphoton, and fluorescence lifetime imaging system (now Zeiss). Multiphoton excitation is provided by a Coherent Chameleon automatically tunable titanium sapphire laser (Coherent Inc.) controlled through Bio-Rad's LaserSharp 2000 software. The microscope (Nikon TE2000 inverted with an array of water- and oil-immersion high-NA objectives) is housed in a blacked-out environmental chamber (Solent Scientific) that controls CO₂ and temperature. This system is also equipped with two external detectors (for multiphoton laser scanning microscopy) and two FLIM detectors, which are used with an SPC830 board for time-correlated single-photon counting FLIM (Becker & Hickl, Berlin, Germany).

3. Methods

3.1 Transient Expression of FP-PP1 and Targeting Subunits

1. Subclone PP1 and/or any targeting subunits of interest into the required fluorescent protein vectors. EGFP is recommended for live-cell imaging and for FRAP experiments, and EYFP and ECFP are recommended for dual-wavelength live-cell imaging (i.e., imaging two proteins in the same cell) and for FRET measurement (*see Note 2*).
2. Targeting subunits can also be cloned into expression vectors with nonfluorescent tags. This permits analysis of the retargeting of FP-PP1 without the requirement for special filter sets to distinguish the green fluorescence protein (GFP) variants. An example is the 9E10 *c-myc* epitope (*see Fig. 1G–I*), which can be detected by immunostaining fixed cells, and it is also useful for detection on Western blots and for immunoprecipitation assays (*see Note 3*).
3. To increase the likelihood of DNA uptake, passage cells the day before transfection and allow them to reach 70–90% confluency.

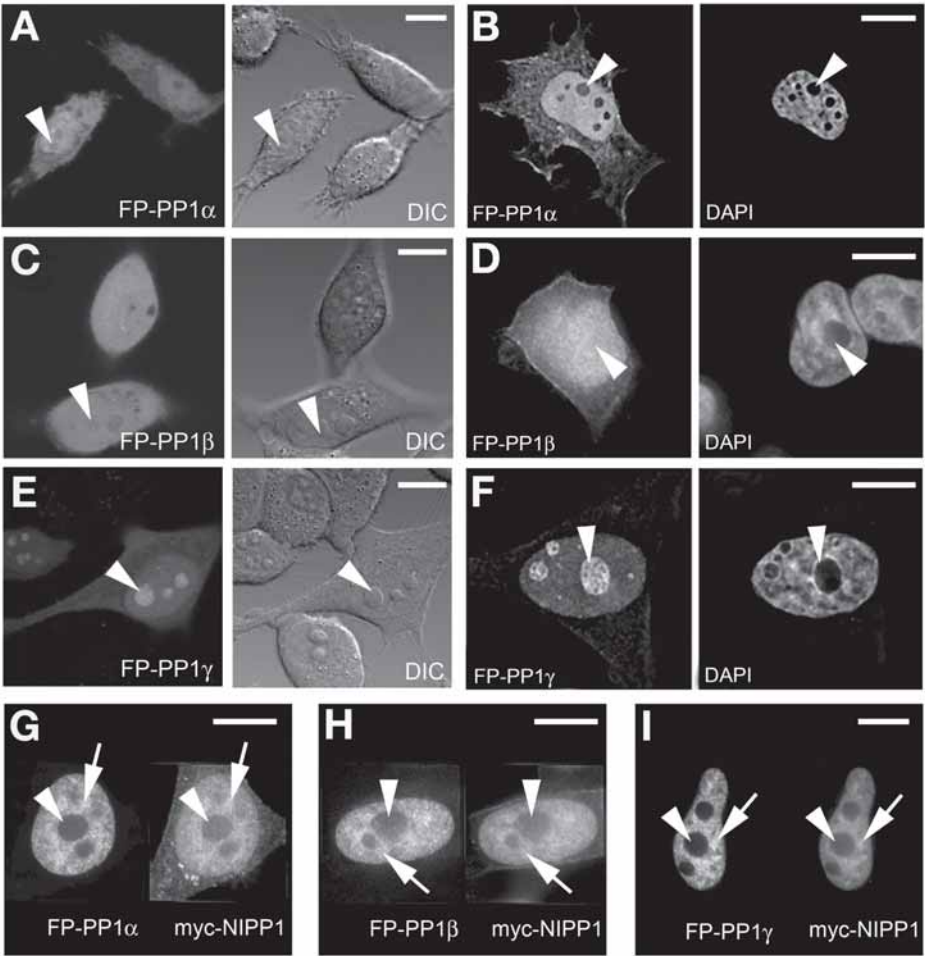


Fig. 1. Transient expression of FP-PP1 isoforms in mammalian cells. Localization of transiently expressed PP1 isoforms was visualized in both live (**A**, **C**, and **E**) and fixed (**B**, **D**, and **F**) HeLa cells. Differential interference contrast (DIC) imaging shows the cell structure in the live cells (**A**, **C**, **E**) and staining DNA with DAPI in fixed cells delineates the nucleus (**B**, **D**, **F**). All three isoforms have both cytoplasmic and nuclear pools, although FP-PP1 α (**A**, **B**) shows a greater accumulation within the nucleus, where it is largely excluded from nucleoli (arrowheads). FP-PP1 β is found in equal amounts in the nucleus and cytoplasm and within nucleoli (**C**, **D**). FP-PP1 γ shows a greater accumulation within the nucleus and a dramatic accumulation within nucleoli (**E**, **F**). These intrinsic localization patterns can be overridden by exogenous expression of a targeting subunit, such as FP-NIPP1, as shown in (**G**–**I**). In this case, all three isoforms adopt the nuclear speckle (interchromatin granule) localization pattern of NIPP1 (arrows). Scale bars are 5 μ M.

4. For transfection of a 90-mm-diameter dish of adherent cells, combine 2 μ g DNA with 16 μ L enhancer solution and 300 μ L DNA-condensation buffer and vortex to mix. Add 60 μ L of the nonliposomal lipid Effectene and vortex again.
5. Allow complexes to form for 15 min and then add the solution dropwise to the cells.
6. Incubate transfected cells at 37°C for 12–18 h, change the media, and then either prepare the cells for live-cell imaging (*see Note 4*) or fix for immunostaining (*see Subheading 3.3.*).

3.2. Establishing Stable Cell Lines Expressing FP-Tagged PP1

1. Grow HeLa cells (or desired cell line) in 90-mm dishes and transfect as described in **Subheading 3.1.**
2. Approximately 24 h after transfection, put cells under selective pressure by replacing the standard medium with medium containing 400 μ g/mL G418 (*see Note 5*).
3. Change the medium daily, taking care not to pipet directly onto the cells. Because of selective pressure, most of the cells will die and wash off the bottom of the dish after approx 10–14 d, leaving colonies of stable, G418-resistant cells behind.
4. To pick and screen resistant colonies for expression of fluorescently tagged protein, first rinse the cells with D-PBS and overlay them with warm D-PBS containing 5% trypsin-EDTA (a 1 : 20 dilution of the 1X solution in **Subheading 2.1., item 5**). Colonies can either be picked on an inverted fluorescent microscope, which offers a better chance of success because only fluorescent colonies are picked, or they can be picked “blind” on a standard light microscope. Using a P200 Gilson pipet and sterile tips, locate a colony of interest, touch the pipet tip to it, and then gently scrape across it while sucking it up into the pipet. Transfer to a 24-well plate with 1 mL of media in each well.
5. Allow picked colonies to grow to 80–90% confluency before splitting.
6. To split cells, rinse with D-PBS and then add 100 μ L of 1X trypsin-EDTA solution to each well. After approx 5 min, when the cells have detached from the well, resuspend in 2 mL media and transfer 1.5 mL to a 6-well plate as a stock and 0.5 mL to a 24-well plate containing 13-mm-diameter glass cover slips for screening.
7. One to two days after splitting, fix the cover slips for 5 min with 3.7% paraformaldehyde in PBS, wash well with PBS, and mount in FluorSave mounting media to screen the colonies by fluorescence microscopy (*see Note 6*).
8. Any colonies showing expression of the FP-tagged protein at appropriate levels (i.e., bright enough to image but not too highly overexpressed, which might affect localization and even cell viability) in more than 95% of the cells can be expanded from the six-well plates as stable cell lines. If necessary, an additional round of subcloning can be carried out before choosing colonies to be expanded as cell lines.
9. For subcloning, seed cells at clonal density. This is done by trypsinizing cells in the six-well plate with 0.5 mL of 1X trypsin-EDTA and resuspending in 4.5 mL

growth media. Add 1 mL of this cell suspension to 9 mL growth media in a 90-mm dish. Take 10 μ L of this 1 : 10 split and add to 10 mL of media containing G418 in another 90-mm dish. Mix well and allow cells to settle (*see Note 7*).

10. Grow the subclones under selection for a further 2 wk, and then pick and screen resistant colonies as described earlier.
11. To expand stable colonies from six-well plates, trypsinize with 0.5 mL of 1X trypsin-EDTA solution and resuspend in 5 mL media in a 75-cm² filter flask. Maintain newly established stable cell lines in standard growth medium containing 200 μ g/mL G418.
12. Stocks of newly established stable cell lines should be frozen down at early passage numbers in case they need to be recovered at a later date. To do this, set up an extra 75-cm² flask when passaging the cell line and allow the cells to grow to confluency. Trypsinize as described previously and resuspend in 10 mL of media. Pellet cells by centrifuging at 167g for 4 min, and resuspend in 1 mL of DMEM containing 10% sterile DMSO. Aliquot 0.5 mL each into two cryovials and allow to freeze slowly by placing the cryovials in a box in a -80°C freezer. Working stocks can be stored in this way for several months, but it is recommended that they be transferred to a liquid-nitrogen system for long-term storage (*see Note 8*).

3.3. Fixing and Immunostaining Cells

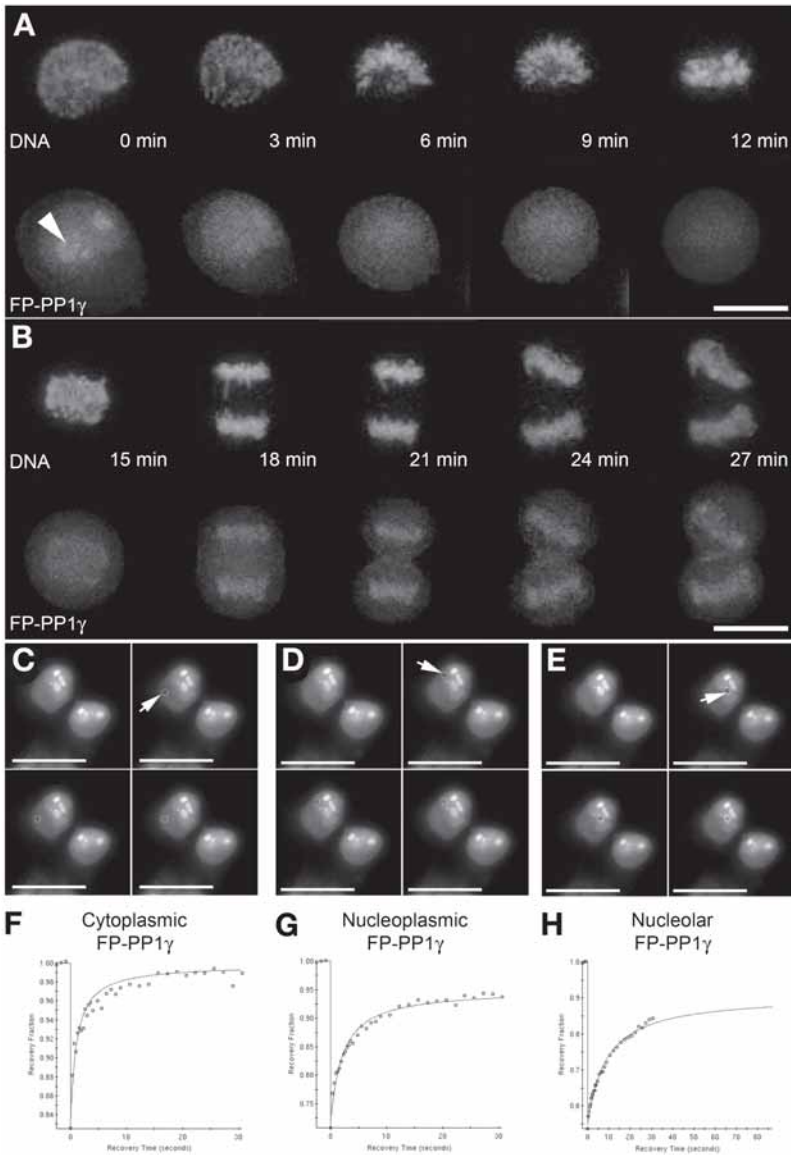
1. Fix transfected cells grown on glass cover slips for 5 min at room temperature with freshly prepared 3.7% (w/v) paraformaldehyde in PBS, followed by three 5-min washes with PBS (*see Note 9*).
2. Permeabilize cells with 1% Triton X-100 in PBS for 10 min at room temperature, followed by three 5-min washes with PBS (*see Note 10*).
3. For immunostaining, first block cells for 10 min with blocking buffer (**Subheading 2.2., item 9**) and then incubate with primary antibody prepared in this same blocking buffer. All blocking and antibody-staining steps can be done by removing the cover slip from the 90-mm dish with forceps, blotting off excess PBS with a tissue, and placing the cover slip, cell side up, on a piece of parafilm in a humidified chamber. This chamber is simply a box with a lid and a damp piece of paper or sponge in the corner to minimize evaporation. Pipet solutions gently onto the cells. For a 19-mm cover slip, 40–50 μ L of solution is adequate to cover the cells (*see Note 11*).
4. After incubating cells in primary antibody for 1 h, wash the cover slips three times in PBS by transferring them to wells in a six-well plate. Add the PBS directly to the wells (avoid squirting or pouring directly on top of the cells) and then pour it off into a waste beaker (the cover slips will stick to the bottom of the well).
5. Transfer the cover slips back to the humidified chamber as described above, blotting excess liquid onto a tissue, and incubate with secondary antibody for 1 h. Transfer back to the six-well plate and wash three times with PBS.

6. If desired, cells can be stained with DAPI (diluted 1:15,000 in water) to visualize DNA. Treat cells with DAPI for 1 min in the six-well plate and then wash three times with PBS (*see* **Note 12**). DAPI should not be used with ECFP since the two cannot be spectrally resolved.
7. Mount cells for imaging by blotting excess liquid off the cover slip and placing it cell side down on top of a small drop of VECTASHIELD mounting medium on a glass slide. Press down gently to displace bubbles and wipe away excess liquid with a tissue. Seal by brushing a small amount of nail varnish along the sides of the cover slip. When dry, clean slides with dH₂O first and then 70% ethanol and store at 4°C in the dark until analyzed (*see* **Note 13**).

3.4. Time-Lapse Imaging

1. For imaging live cells in glass-bottom dishes or POC chambers, replace the standard growth medium with phenol red-free medium supplemented with FBS and penicillin–streptomycin. If using an environmental chamber supplied with 5% CO₂, pH will be maintained. If not, add 20 mM HEPES to the medium as a buffer. Alternatively, a custom-made CO₂-independent phenol red-free medium (Invitrogen) can be used, supplemented with FBS and penicillin–streptomycin. This medium does not require additional buffering.
2. DNA can be stained in live cells, with the cells remaining viable and progressing through the cell cycle. To do this, treat cells for 30 min at 37°C with Hoechst No. 33342 dye diluted as previously described (**Subheading 2.2., item 13**) in normal growth medium. Replace the medium with phenol red-free DMEM or phenol red-free CO₂-independent medium for imaging. It is important to note that this dye cannot be used with ECFP-tagged proteins because the two cannot be spectrally resolved.
3. When imaging cells through the cell cycle, prophase cells can be found by their characteristic condensed DNA pattern (*see* **Fig. 2A**). Minimize the

Fig. 2. Time-lapse imaging of FP-PP1. A HeLa cell stably expressing FP-PP1 γ and stained with the cell-permeable DNA dye Hoechst No. 33372 was imaged as it progressed through mitosis (**A,B**). Images were taken every 3 min using low light levels and short exposure times to minimize photodamage. This cell starts in the prophase, with the DNA condensing and FP-PP1 γ still visible within nucleoli (arrowhead). Within 12 min, it has progressed to metaphase, at which point, FP-PP1 γ is primarily diffuse but also shows an accumulation at kinetochores. As the cell progresses through anaphase (at 15–18 min), FP-PP1 γ shows a relocalization to chromatin, where it remains, and starts to reaccumulate in nucleoli at late telophase (just visible at 27 min; for details, *see* **ref. 17**). The dynamic nature of different pools of FP-PP1 γ in interphase cells can be demonstrated by FRAP (**C–H**). A small circular region (hashed circle indicated by arrow) was photobleached in a region of the cell and recovery of fluorescent signal within that region monitored over time. For the same cell, a region was bleached in either the cytoplasm (**C**), nucleoplasm (**D**), or nucleolus (**E**). By plot-



ting recovery of fluorescence intensity vs time after photobleaching (**F–H**), half-times of recovery can be calculated for each pool of FP-PP1 γ PP129. Cytoplasmic FP-PP1 γ shows the fastest recovery, with a $t_{1/2}$ of approx 1 s (comparable to that for free GFP). Nucleoplasmic FP-PP1 γ shows a slower recovery rate ($t_{1/2}$ = 2 s), as does nucleolar FP-PP1 γ ($t_{1/2}$ = 9 s), but these rates still indicate a rapid flux of PP1 through these intracellular pools.

amount of light to which the cells are subjected during imaging by keeping exposure times as low as possible while maintaining adequate resolution. Hoechst No. 33342 can be imaged using a DAPI filter set, whereas EGFP can be imaged using a FITC filter set. EYFP and ECFP require special filter sets (see [Table 1](#)).

3.5. FRAP

1. The FRAP experiments are generally performed on cells expressing GFP- or EGFP-tagged proteins (see [Note 14](#)), and can be done using either laser scanning microscopes or wide-field fluorescence microscopes equipped with an external laser for photobleaching. When analyzing proteins with very fast turnover rates, such as those shown in [Fig. 2F–G](#), the microscope system used must offer the appropriate temporal resolution (i.e., image rapidly enough to capture early events). The experiments shown in [Fig. 2](#) were performed on the DeltaVision Spectris system described in [Subheading 2.3., item 1](#).
2. To perform a FRAP experiment, take two to three images of the cell prior to photobleaching and then bleach a region of interest to approx 50% of its original intensity, acquiring images over time after the photobleach period to monitor recovery of fluorescence signal within the bleached region (see [Fig. 2C–E](#)). If recovery is observed, it indicates that the fluorescently tagged proteins are mobile, and the rate of recovery is therefore an indication of the speed at which they are moving. For comparison, the same photobleaching experiment can be conducted on fixed cells, in which no recovery is observed (see [Note 15](#)).
3. For qualitative FRAP, it might be enough to simply plot fluorescence intensity over time (known as the recovery curve), as a fraction of the initial fluorescence prior to photobleaching (see [Fig. 2F–H](#)). Different pools of the same protein can be compared for relative mobility, or the same pool of protein can be assessed before and after a particular perturbation.
4. For quantitative FRAP, the most commonly published results are the mobile fraction (fraction of fluorescent molecules that are free to move within the bleached region) and the half-time for recovery of fluorescence ($t_{1/2}$), which is the time required for half of the mobile fraction to recover. The $t_{1/2}$ can then be used to calculate the diffusion coefficient (see [ref. 15](#), for a review of FRAP analysis).

3.6. Measuring FRET Between PP1 and a Targeting Subunit by Sensitized Emission

1. This approach requires independent control of emission and excitation filters, and for the study shown in [Fig. 3A,B](#), we used the DeltaVision DV3 system detailed in [Subheading 2.3., item 2](#). A laser scanning microscope fitted with a 436-nm laser, or one with a tunable laser, can also be used. Measurements are taken using a combination of three filter sets (ECFP [excite, 436 nm; emit, 470 nm], EYFP [excite, 514 nm; emit, 528 nm], and what we refer to as the FRET

channel [excite, 436 nm; emit, 528 nm]). The principle of FRET is detailed in [Fig. 3A](#).

2. Grow cells on the appropriate cover slips (e.g., 40-mm diameter for mounting in a POC chamber or 35-mm-diameter glass-bottom dishes for use in an environmental chamber; *see* **Note 16**).
3. Cotransfect cells with 1 μ g each of EYFP-PP1 and ECFP-targeting subunit (or the inverse, ECFP-PP1 and EYFP-targeting subunit. For control measurements, transfect some cells with the EYFP construct alone and some with the ECFP construct alone. As a negative control, cotransfect cells with PP1 and a mutant version of the targeting subunit that cannot bind PP1 (e.g., mutation of one or both hydrophobic residues in the RVXF motif, as described in [ref. 5](#)). An alternate control is the ECFP-tagged protein coexpressed with an EYFP-tagged protein that shows the same localization but does not interact with it.
4. Approximately 12–18 h after transfection, mount cells in the appropriate medium for live-cell imaging.
5. To correct for spectral bleed-through, first examine cells expressing either donor alone or acceptor alone with each of the three filter sets. For example, using our system, ECFP-NIPPI alone gives a strong signal in the ECFP channel and no signal in the EYFP channel, but it does show significant spectral bleed-through into the FRET channel (approx 70% of the signal measured in the ECFP channel). EYFP-PP1 γ alone gives a strong signal in the EYFP channel and no signal in the ECFP channel, but also shows spectral bleed-through into the FRET channel (approx 20% of the signal measured in the EYFP channel).
6. Measure FRET in cells expressing both PP1 and targeting subunit by exciting at the ECFP wavelength (436 nm) and detecting at the EYFP emission wavelength (528 nm).
7. The following equation is used for the correction of spectral bleed-through, in which FRET_N is Net Energy Transfer:

$$\text{FRET}_N = \text{FRET signal} - \alpha(\text{donor signal}) - \beta(\text{acceptor signal})$$

For this equation, α and β are determined by imaging the cells expressing each fusion protein on its own (0.7 for ECFP-NIPPI and 0.2 for EYFP-PP1 γ).

8. Certain software programs, such as the SoftWorx analysis software used with the DeltaVision system, allow image subtraction, to obtain a final FRET image showing the signal remaining in the FRET channel following this correction (*see* [Fig. 3A](#)).
9. The same analysis should then be applied to data collected from cells expressing PP1 and a mutant targeting subunit that cannot interact with it or, alternatively, two proteins that show the same localization but do not interact.

As shown in [Fig. 3B](#), after the data have been corrected for spectral bleed-through, there is no signal remaining in the FRET channel.

3.7. Measuring FRET Between PP1 and a Targeting Subunit by Acceptor Photobleaching

1. This approach, which is based on the increase in donor (ECFP) signal when FRET is disrupted by photobleaching the acceptor (EYFP) molecule, requires a laser

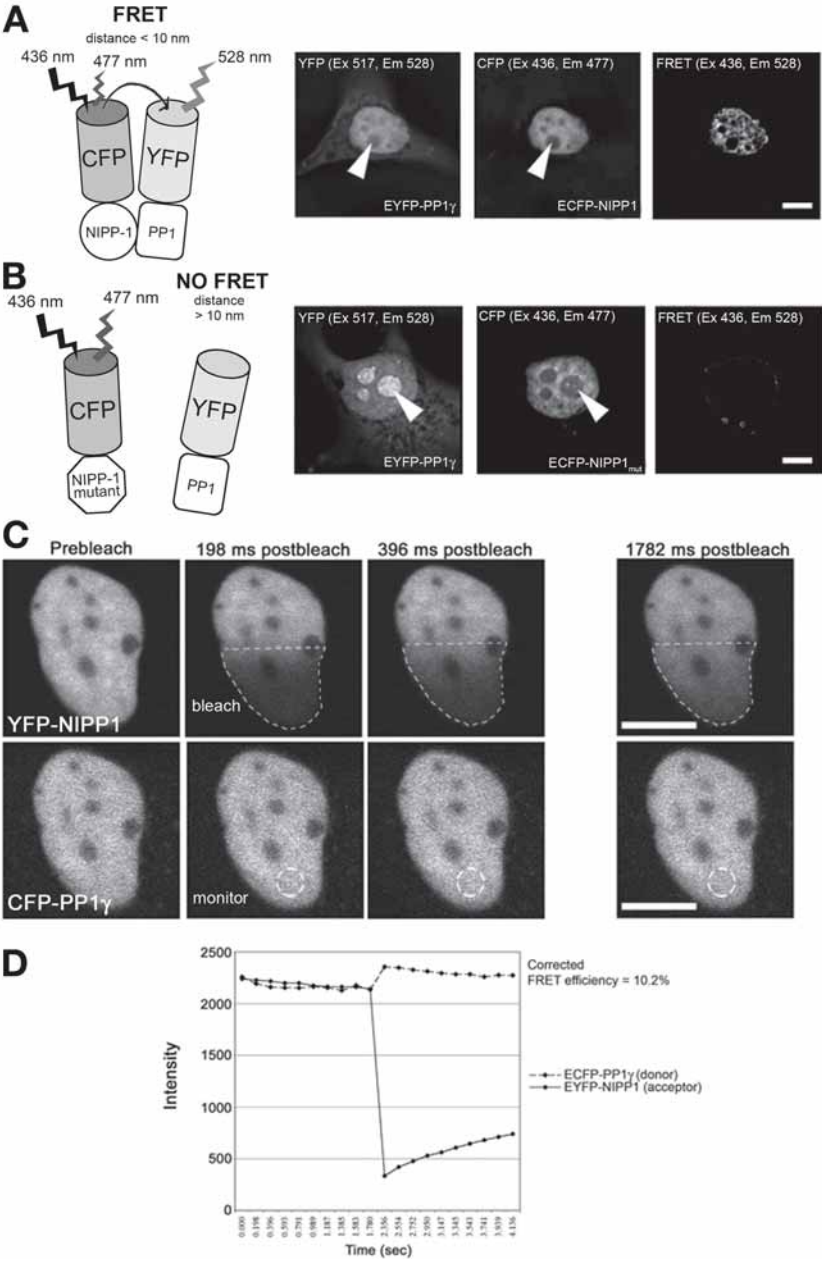


Fig. 3. Measurement of the direct interaction between PP1 and a targeting subunit by FRET. The FRET pair CFP (donor) and YFP (acceptor) were used to label PP1 and NIPP1 in transiently transfected HeLa cells. FRET depends on the close proximity of the donor and acceptor (1–10 nm), as shown in the diagram in (A) If the proteins are

line at approx 532 nm to photobleach EYFP (without bleaching ECFP) and appropriate excitation and emission filter sets to monitor ECFP fluorescence before and after this bleaching. It can be done using either a laser scanning microscope such as the Zeiss LSM 51 510 described in **Subheading 2.3., item 3**, or a wide-field fluorescence microscope equipped with an external laser, such as the DeltaVision Spectris system described in **Subheading 2.3., item 1**. The DeltaVision system offers slightly greater flexibility because of its improved temporal resolution, as the increased donor signal is only apparent until the photobleached pool of acceptor recovers and once again quenches the signal (*see Fig. 3D*). If the protein happens to turn over rapidly, as does PP1, then the unquenched donor signal will only be observed at very early time-points. This can be compensated for when using a system with slower postbleach imaging resolution by photobleaching a larger area of the cell, to ensure that acceptor recovery does not mask the unquenched donor signal in the region of interest (*see Fig. 3C*).

2. Grow cells on the appropriate cover slips (e.g., 40-mm diameter for mounting in a POC chamber or 35-mm-diameter glass-bottom dishes for use in an environmental chamber) and cotransfect with EYFP-PP1- and ECFP-targeting subunit or, alternatively, ECFP-PP1- and EYFP-targeting subunit (as shown in **Fig. 3C,D**).
3. Approximately 12–18 h after transfection, mount cells in the appropriate medium for live-cell imaging.
4. After obtaining several prebleach images of both the donor and the acceptor proteins, photobleach the acceptor in a region of the cell using the appropriate settings for the system used (e.g., 100% laser power and several iterations).

close enough and in the proper orientation, excitation of the donor (CFP-NIPP1) leads to a transfer of energy to the acceptor (YFP-PP1), thereby exciting it and causing it to fluoresce. This sensitized emission can be detected in the FRET channel, which excites CFP and detects emission of YFP. **(B)** demonstrates the absence of FRET between two proteins that do not interact, in which case the donor and acceptor are not close enough for energy transfer to occur. The donor shown here (CFP-NIPP1 with a mutated PP1-binding motif that disrupts interaction with PP1) cannot retarget YFP-PP1 γ from nucleoli (arrowheads) to nuclear speckles, and there is no signal in the FRET channel. **(C,D)** show a different approach to the measurement of FRET. In this case, the acceptor (YFP-NIPP1) is photobleached in half of the nucleus (indicated by the hashed polygon) and the fluorescence intensity of the donor (CFP-PP1 γ) monitored over time **(D)** in a region within this half of the nucleus (hashed circle). Photobleaching the acceptor “dequenches” the donor because the acceptor is no longer available for the transfer of energy from the donor. The intensity of the donor therefore shows a transient increase **(D)**, which can be used to calculate the efficiency of the FRET interaction. This increased intensity is transient, decreasing over time as new acceptor molecules replace the photobleached molecules in that region of the cell and quench the donor.

4. After bleaching, collect images at the desired time intervals, using the same settings used to obtain the prebleach images (see Fig. 3C).
5. Analyze the data utilizing the image analysis tools included in the imaging system's software. Most systems now include FRAP analysis tools in their software packages. Spreadsheet and biostatistics programs such as Microsoft Excel (Microsoft Corp.) and GraphPad Prism (GraphPad Software Inc.) are also useful tools for the analysis of photobleaching data.
6. In addition to the bleached region, include a region in the nonbleached portion of the same cell or in a neighboring cell in the data analysis as a control for bleaching resulting from imaging. A region of background fluorescence should also be defined outside of the cell and subtracted from both the bleached and control regions.
7. The FRET efficiency (see Fig. 3D) can be calculated using the following formula:

$$\text{FRET efficiency } E = (ID_{(\text{post})} - ID_{(\text{pre})})/ID_{(\text{post})}$$

$ID_{(\text{pre})}$ and $ID_{(\text{post})}$ are donor intensity before and after photobleaching, respectively;

$$\text{Bleach efficiency } B = (IA_{(\text{pre})} - IA_{(\text{post})})/IA_{(\text{pre})}$$

$$\text{Corrected FRET efficiency: } (E/B) \times 100\%$$

The subscript A denotes acceptor.

7. Using these equations, the ECFP-PP1 γ /EYFP-NIPP1 interaction shown in Fig. 3C has a FRET efficiency of 10.2%.

3.8. Measuring FRET Between PP1 and a Targeting Subunit by FLIM/FRET

1. To briefly summarize the principle of lifetime imaging, the fluorescence of organic molecules is not only characterized by their excitation and emission spectra but also by their lifetimes. When a fluorophore absorbs a photon, it goes into the excited state and returns to the ground state by emitting a fluorescence photon, converting the energy internally, or by transferring the energy to the environment. Although fluorescence lifetime imaging systems can seem overly complex at first, in reality the basics are fairly easy to grasp (see Fig. 4). We use the Bio-Rad Radiance Multiphoton Imaging System described in Subheading 2.3., item 4, which allows us to obtain both intensity and lifetime images for the fluorescent proteins of interest in live cells.
2. Grow cells in 35-mm glass-bottom dishes and co-transfect with either ECFP-targeting subunit and EYFP-PP1, or ECFP-PP1- and EYFP-targeting subunit. For control measurements, transfect cells with the ECFP construct alone (to measure the lifetime of unquenched ECFP), or with the ECFP construct and an EYFP-tagged protein that shows the same localization but does not interact with it (see Fig. 5F–J). Excite ECFP at a wavelength of 840 nm, allowing the external detectors to collect the fluorescence emission and calculate lifetimes.
3. In Fig. 5, lifetime maps have been plotted (i.e., each pixel is color-coded with a lifetime value to build up an image of differences in lifetime throughout the

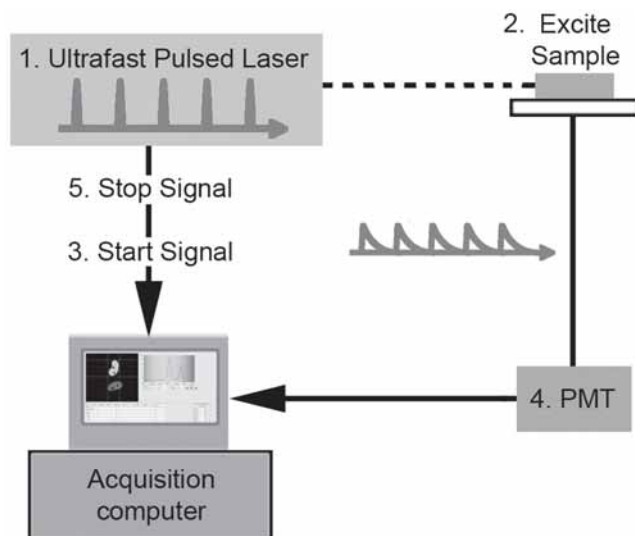


Fig. 4. Principle of FLIM. Illumination is provided by a pulsed laser (1); the pulsed laser excites the sample (2) and simultaneously sends a start signal to the computer (3). Fluorescence is emitted by the sample and recorded on the photomultiplier tubes (PMT; 4) while the next pulse of light leaves the laser and sends a stop signal to the computer (5). The process is repeated many times so that an average lifetime can be calculated for the population of excited fluorophores. If a large number of similar molecules with similar local environments are excited by a short laser pulse, the time taken for fluorescence to decay can be plotted as a single exponential curve. Therefore, FLIM is a measurement of the probability of fluorescence emission of a certain lifetime.

sample) for ECFP-NIPP1 in the presence of either EYFP-PP1 γ (see Fig. 5B) or EYFP-U1A (see Fig. 5G). They are shown next to corresponding intensity images for ECFP-NIPP1 (see Fig. 5A,F). Quenching of the donor (ECFP-NIPP1) causes a shift to a shorter lifetime, and FRET is observed as the appearance of a second, “quenched” lifetime (approx 1.6 ns, compared to the unquenched lifetime of approx 1.9 ns, as shown in Fig. 5D). In the presence of EYFP-U1A, which shows the same localization pattern but does not interact with ECFP-NIPP1, only a single, unquenched lifetime of approx 1.9 ns is observed (Fig. 5I). The quenched and unquenched lifetimes can also be color-coded to demonstrate more clearly where FRET is occurring within the cell (Fig. 5C,E). In this example, although NIPP1 is found throughout the cell nucleus, the predominant FRET signal is observed at nuclear speckles, where mRNA splicing factors are known to accumulate, suggesting a role for the complex in the regulation of pre-mRNA splicing (7).

4. The FRET efficiency can be calculated using the following formula:

FRET efficiency $E = 1 - (\tau_{DA}/\tau_D)$

τ_{DA} and τ_D are donor lifetime in the presence and absence of acceptor, respectively.

- Using this FRET efficiency, the distance between the donor and acceptor can also be calculated:

$$R_{\text{donor/acceptor}} = R_0((1/E) - 1)^{1/6}$$

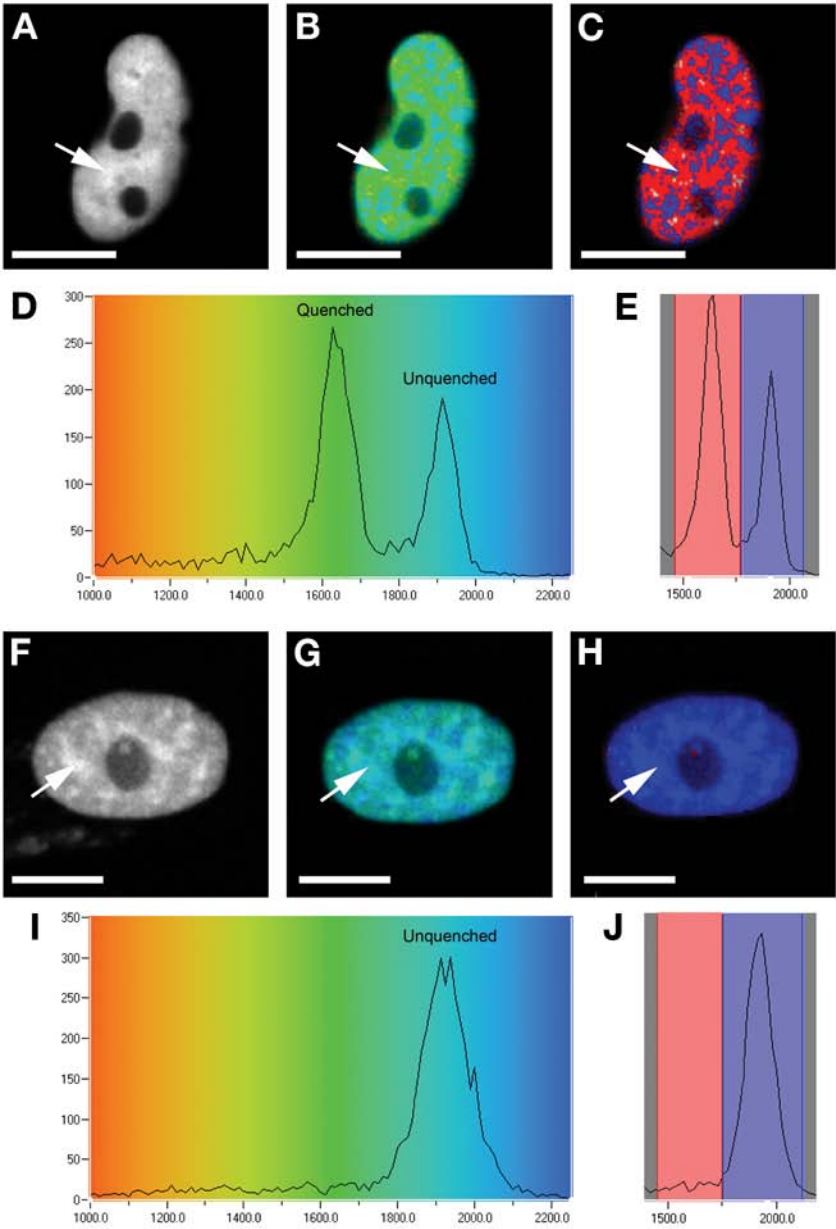
R_0 = Forster distance, which is 50 Å for the CFP/YFP pair

- For the example shown in Fig. 5 (ECFP-NIPP1 and EYFP-PP1 γ), a FRET efficiency of 15.8% is calculated, which translates into a donor/acceptor distance of approximately 66 Å.

4. Notes

- Lasers are also available on this system for photoactivatable GFP (PA-GFP; 405 nm) and for photobleaching EYFP (532 nm). PA-GFP (BD Biosciences/Clontech) offers an alternative approach to FRAP experiments. This GFP variant shows a 10- to 30-fold increase in fluorescence when activated with 405-nm light. The exchange of the activated pool with the non-activated pool can therefore be measured to monitor protein turnover, without any of the deleterious effects of photobleaching.
- Filter sets are available for dual imaging of either EGFP and EYFP or EYFP and ECFP coexpressed in the same cell. EGFP and ECFP cannot be resolved in the same cell because of their overlapping spectral curves.
- The GFP-tagged proteins can also be detected on Western blots and immunoprecipitated using a monoclonal antibody (Roche).
- If you do not have access to a live-cell imaging system, it is still possible to image FP-tagged proteins in live cells. Grow and transfect cells on cover slips and then mount in either growth medium or PBS on a glass slide, sealing the edges by melting a 2% agarose solution and pipetting it gently around the edges of the cover slip. Once the agarose hardens, clean the cover slip carefully with dH₂O and image on a fluorescence microscope. The cells will remain viable for a short time period (approx 10–20 min, depending on cell type).

Fig. 5. Measurement of the direct interaction between PP1 and a targeting subunit by FLIM/FRET. Coexpression of NIPP1 with PP1 γ in cells causes both the relocalization of PP1 to the nuclear speckles at which NIPP1 is found (A; speckles indicated by arrows), and the transfer of energy between the donor (CFP-NIPP1) and the acceptor (YFP-PP1 γ). This energy transfer leads to a decreased fluorescence lifetime for the donor, and two lifetimes (quenched, approx 1.6 ns; unquenched, approx 1.9 ns) are thus detected within the cell (D). When plotted as a lifetime map (B), it can be seen that although both proteins are located throughout the nucleus, the FRET interaction is mainly occurring at speckles. This is shown more clearly in (C), in which the two lifetimes have been assigned specific colors [red for quenched and blue for unquenched CFP, as assigned in the graph in (E)]. As a negative control, similar measurements were taken for CFP-NIPP1 coexpressed with YFP-U1A. Although both proteins local-



ize to nuclear speckles, they do not interact directly. This is evident from the lifetime maps (G–H), which show a single, unquenched lifetime of approx 1.9 ns throughout the cell (I–J).

5. The concentration of G418 must be calculated for each cell type, using serial dilutions and assaying cell viability. The appropriate dilution is that which kills all cells within 10–14 d.
6. This medium dries completely and does not require sealing with nail varnish; therefore, it is useful for mounting small cover slips (which are difficult to seal with nail varnish) and for screening large numbers of cover slips.
7. An optional technique for subcloning cells is to trypsinize the cells and dilute to 5 cells/mL. Place 0.1 mL in each well of a 96-well plate. There is a 50% chance of having a cell in that well, which will then expand to a clonal cell line.
8. If stable cell lines become contaminated with yeast, they should be discarded and a previously frozen aliquot recovered. However, if the contamination occurs before stocks have been frozen down, cells can be treated with a solution of the antimycotic agent amphotericin B (e.g., Fungizone from Sigma-Aldrich; available as a 100X stock, which is used at 1X in growth media to treat cells).
9. There are many different permeabilization methods, and it is best to test several to determine which works best for your particular protein of interest. Some antibody epitopes are destroyed by particular fixation methods, and some FP-tagged proteins show different localization patterns in fixed cells compared to live cells, depending on the fixation method. For example, the bulk of FP-PP1 is washed out of cells when they are fixed with methanol, presumably as a result of its rapid turnover rates throughout the cell (methanol destroys all cell membranes, allowing rapidly diffusing molecules to “escape” before they are fixed). Paraformaldehyde fixation is therefore recommended for all FP-PP1 experiments.
10. Fixed cells can be stored for up to 2 wk at 4°C in the dark prior to permeabilization and staining. Once cells are permeabilized, they must be used that same day.
11. Smaller volumes of liquid (20–40 μ L) can be used if you pipet the solution directly onto the parafilm and then flip the cover slip cell side down and place it on top of the solution.
12. For cells expressing the ECFP fusion protein, DNA should not be stained with DAPI because the two cannot be spectrally resolved. As an alternative, DNA can be stained with propidium iodide. This cannot be used in live cells, however, and because it fluoresces in the red channel, it cannot be used with rhodamine-labeled secondary antibodies or with red fluorescent proteins.
13. Slides can also be stored at –20°C, which allows them to be imaged for up to 3 mo. Various slide boxes are available for storage (we use cloth-covered cardboard boxes with card trays from VWR), although wrapping them in foil is also an option.
14. We do not recommend the use of EYFP-tagged constructs for FRAP experiments because we and others (16) have observed a small but significant amount of spontaneous recovery of the molecule from photobleaching, which complicates the interpretation of FRAP results
15. If you are unable to bleach your protein to 50% of the original intensity, that already indicates a rapid turnover, because the protein is recovering while it is still being bleached. To demonstrate this, photobleach the protein using the same parameters in fixed cells, in which recovery will not occur.

16. Fluorescence resonance energy transfer can also be measured in fixed cells, but in our experience it is not as reliable as live-cell FRET measurements (i.e., using our positive controls, we do not always see a FRET signal in fixed cells but can always measure it in live cells). Whether you set out to measure FRET in fixed or live cells, it is helpful to have a reliable set of positive and negative controls. A fusion of ECFP and EYFP works well as a positive control and can be generated by subcloning EYFP in frame into the multiple cloning site of ECFP (or vice versa). The choice of restriction sites will determine the number of amino acids separating the two proteins and, hence, their distance. We have made fusions that are either 7 or 15 amino acids apart, with the former showing a higher FRET efficiency. The latter is useful for FLIM/FRET experiments, however, because its lower FRET efficiency permits measurement of both a quenched and an unquenched donor pool. As a negative control, the EYFP and ECFP vectors can be cotransfected into cells. Both show a diffuse localization throughout the cell but do not interact.

Acknowledgments

The authors thank Dr. Judith Sleeman, and Dr. David Lleres at the University of Dundee (Dundee, UK) for advice and assistance, and Dr. Jan Ellenberg at EMBL (Heidelberg, Germany) for advice and the use of the Zeiss 510 LSM system. This work was supported by the Wellcome Trust.

References

1. Cohen, P. T. (2002) Protein phosphatase 1-targeted in many directions. *J. Cell Sci.* **115**, 241–256.
2. Sasaki, K., Shima, H., Kitagawa, Y., Irino, S., Sugimura, T., and Nagao, M. (1990) Identification of members of the protein phosphatase 1 gene family in the rat and enhanced expression of protein phosphatase 1 alpha gene in rat hepatocellular carcinomas. *Jpn. J. Cancer Res.* **81**, 1272–1280.
3. Barker, H. M., Craig, S. P., Spurr, N. K., and Cohen, P. T. (1993) Sequence of human protein serine/threonine phosphatase 1 gamma and localization of the gene (PPP1CC) encoding it to chromosome bands 12q24.1-q24.2. *Biochim Biophys Acta.* **1178**, 228–233.
4. Barker, H. M., Brewis, N. D., Street, A. J., Spurr, N. K., and Cohen, P. T. (1994) Three genes for protein phosphatase 1 map to different human chromosomes: sequence, expression and gene localisation of protein serine/threonine phosphatase 1 beta (PPP1CB). *Biochim Biophys Acta.* **1220**, 212–218.
5. Trinkle-Mulcahy, L., Sleeman, J. E., and Lamond, A.I. (2001) Dynamic targeting of protein phosphatase 1 within the nuclei of living mammalian cells. *J Cell Sci.* **114**, 4219–4228.
6. Andreassen, P. R., Lacroix, F. B., Villa-Moruzzi, E., and Margolis, R. L. (1998) Differential subcellular localization of protein phosphatase-1 alpha, gamma1, and delta isoforms during both interphase and mitosis in mammalian cells. *J. Cell Biol.* **141**, 1207–1215.

7. Trinkle-Mulcahy, L., Ajuh, P., Prescott, A., et al. (1999) Nuclear organisation of NIPPI1, a regulatory subunit of protein phosphatase 1 that associates with pre-mRNA splicing factors. *J. Cell Sci.* **112**, 157–168.
8. Ellenberg, J., Lippincott-Schwartz, J., and Presley, J. F. (1999) Dual-colour imaging with GFP variants. *Trends Cell Biol.* **9**, 52–56.
9. Lippincott-Schwartz, J. and Patterson, G. H. (2003) Development and use of fluorescent protein markers in living cells. *Science* **300**, 87–91.
10. Swift, S. R. and Trinkle-Mulcahy, L. (2004) Basic principles of FRAP, FLIM and FRET. *Proc. R. Microsc. Soc.* **39**, 3–10.
11. Peter, M. and Ameer-Beg, S. M. (2004) Imaging molecular interactions by multiphoton FLIM. *Biol. Cell* **96**, 231–236.
12. Periasamy, A., Elangovan, M., Elliot, E., and Brautigan, D. L. (2002) Fluorescence lifetime imaging (FLIM) of green fluorescent fusion proteins in living cells. *Methods Mol. Biol.* **183**, 89–100.
13. Stryer, L. (1978) Fluorescence energy transfer as a spectroscopic ruler. *Annu. Rev. Biochem.* **47**, 819–846.
14. Haraguchi, T., Kaneda, T., and Hiraoka, Y. (1997) Dynamics of chromosomes and microtubules visualized by multiple-wavelength fluorescence imaging in living mammalian cells: effects of mitotic inhibitors on cell cycle progression. *Genes Cells* **2**, 369–380.
15. Carrero G., McDonald D., Crawford E., de Vries G., and Hendzel, M. J. (2003) Using FRAP and mathematical modeling to determine the in vivo kinetics of nuclear proteins. *Methods* **29**, 14–28.
16. Jayaraman, S., Haggie, P., Wachter, R. M., Remington, S. J., and Verkman, A. S. (2000) Mechanism and cellular applications of a green fluorescent protein-based halide sensor. *J. Biol. Chem.* **275**, 6047–6050.
17. Trinkle-Mulcahy, L., Andrews, P. D., Wickramasinghe, S., et al. (2003) Time-lapse imaging reveals dynamic relocation of PP1 γ throughout the mammalian cell cycle. *Mol. Biol. Cell* **14**, 107–117.

Yeast Two-Hybrid Screens to Identify *Drosophila* PP1-Binding Proteins

Daimark Bennett and Luke Alphey

Summary

Protein phosphatase type 1 (PP1) is one of the major classes of serine/threonine protein phosphatases and has been found in all eukaryotic cells examined to date. Metazoans from *Drosophila* to humans have multiple genes encoding catalytic subunits of PP1 (PP1c), which are involved in a wide range of biological processes. Studies in the fruit fly *Drosophila melanogaster* have revealed some of the essential functions of the PP1c genes. However, the PP1c isoforms have pleiotropic and overlapping functions, making it difficult to characterize their many biological roles and identify their specific in vivo substrates. Regulatory subunits of PP1 provide the key to understanding the role of PP1, as they are responsible for directing PP1c to different intracellular locations and/or affecting their activity or substrate specificity. The existence of isoform-specific PP1 regulatory subunits might also help to explain the unique roles of different PP1 catalytic subunits. *Drosophila* is an excellent model organism in which to characterize the role of PP1 catalytic and regulatory subunits, because it combines molecular and biochemical approaches with powerful genetics, in a well-characterized animal model. In this chapter, we will describe how the two-hybrid system can be used to identify *Drosophila* PP1c-interacting proteins and study their interactions with different PP1c isoforms and variants. With the appropriate bait and library constructs, this method should also be equally applicable to identifying binding subunits of related phosphatases or PP1c from other organisms.

Key Words: Protein phosphatase type 1; PP1; catalytic subunit; regulatory subunit; *Drosophila melanogaster*; yeast two-hybrid; GAL4

1. Introduction

1.1. PP1 Catalytic Subunits in *Drosophila*

Protein phosphatase type 1 (PP1) is one of the major classes of protein serine/threonine phosphatases and has been found in all eukaryotic cells exam-

ined to date. A review of the classification of PP1 and related protein phosphatases can be found elsewhere in this volume. In this section, we will review what is known about *Drosophila* PP1 and hope to convince the reader that *Drosophila* is an excellent system in which to study the biological roles of this important family of phosphatases.

Protein phosphatase 1 is involved in regulating a large number of diverse cellular and developmental processes, including glycogen metabolism, the cell cycle, muscle formation and contraction, mRNA splicing, transcription, and intracellular signalling (1,2). Mammals and *Drosophila* have three and four PP1 catalytic subunit (PP1c) genes, respectively, that perform these various functions (3–5). The four PP1c genes in *Drosophila* are named according to their chromosome location and subtype: *PP1β9C*, *PP1α87B*, *PP1α96A*, and *PP1α13C* (3,4). Phylogenetic analysis reveals that *PP1α87B*, *PP1α96A*, and *PP1α13C* are equally related to mammalian *PP1α* and *PP1γ*, and *PP1β9C* corresponds to mammalian *PP1δ* (also known as *PP1β*) (see Fig. 1A). However, the degree of conservation between different PP1c isoforms is remarkably high, even when taking into account less conserved N-terminal and C-terminal regions (see Fig. 1B). Not surprisingly, therefore, the different isoforms have been shown to be indistinguishable biochemically, both in terms of in vitro substrate specificity and sensitivity to inhibitors (6). Therefore, the question of whether the different PP1c isoforms have separate or redundant roles in vivo has been largely intractable to biochemical analysis. However, specific differences between *PP1α/PP1γ* and *PP1β* isotypes are conserved between flies and humans indicating that *PP1α/PP1γ* and *PP1β* isoforms are likely to have one or more unique roles in these organisms (7). Genetic analysis offers a powerful way to examine this question because each of the PP1c genes can be analyzed independently to assess its essential and nonredundant functions. Of the mammalian genes, functional analysis by knockout in mice has only been performed so far for *PP1γ*, which reveals that *PP1γ* is essential for male fertility but is redundant with *PP1α* and/or *PP1δ* in somatic and female germline tissues (8). Genetic analysis in *Drosophila* has progressed more rapidly and, to date, three of the four *Drosophila* PP1c genes have been examined by mutational analysis.

PP1α87B contributes 80% of the total PP1 activity (9,10), indicating that it is the major PP1c isoform in *Drosophila*. Mutant alleles of *PP1α87B* show lethality, aberrant mitosis, suppression of position effect variegation, and reduced levels of protein phosphatase activity, with different alleles showing these phenotypes to different degrees (10,11). The principal mitotic phenotypes are chromosome hypercondensation and abnormal spindle structure, which are reminiscent of PP1c loss-of-function phenotypes in other organisms (12–14). Other phenotypes associated with *PP1α87B* mutants might be masked by the presence of the other three genes. *PP1β9C* contributes about 10% of the

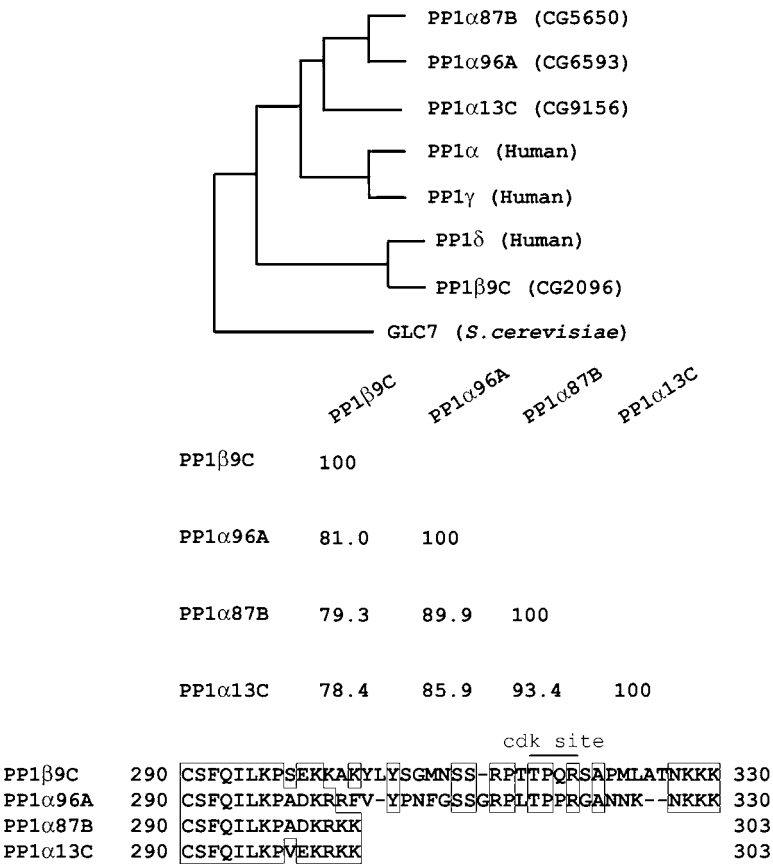


Fig. 1. Sequence comparison of *Drosophila* PP1 catalytic subunit isoforms. **(A)** Phylogenetic tree showing relationship among human, *D. melanogaster*, and *S. cerevisiae* PP1c isoforms. The tree was derived from distance matrices after multiple alignment of protein sequences. Only the core phosphatase domains (starting 60 amino acids before the invariant GDxHG motif and terminating 50 amino acids following the conserved SAPNY motif) were used to prevent spurious alignment. **(B)** Percentage identity among different full-length *Drosophila* PP1c isoforms. **(C)** Sequence alignment of C-termini of the four *Drosophila* PP1c isoforms. The position of the putative cdk phosphorylation site in PP1β9C and PP1α96A is indicated with a line.

total PP1 activity and corresponds to *flapwing* (*flw*), weak alleles of which are viable but flightless (7). Stronger alleles are semilethal and show defects in larval body wall muscle development (7). The *flw* loss-of-function phenotype is probably not the result of a loss of overall PP1c activity, but rather the result of a specific function unique to the PP1β9C protein mediated through interaction

with one or more distinctive regulatory proteins (15). A likely candidate for this regulatory protein is MYPT-75D, which binds specifically to PP1 β 9C and stimulates its nonmuscle myosin phosphatase activity (15). Of the remaining isoforms, PP1 α 96A probably contributes 10% of the total PP1 activity. Sequence comparison of PP1 α 96A and the other PP1 α isoforms reveals obvious differences at the C-terminus (see Fig. 1C). Conservation between PP1 α 96A and PP1 β 9C in this region implies that these isoforms might share some redundant roles not performed by the other two isoforms. However, mutant alleles of PP1 α 96A are not yet available to assess its unique and redundant functions. The remaining PP1c isoform, PP1 α 13C, is either expressed at low levels or only in a few cells (4) and is not required for viability (16).

1.2. PP1 Regulatory Subunits in *Drosophila*

In vitro, the purified catalytic subunits will dephosphorylate a wide variety of substrates, but in vivo, they are found complexed to a number of regulatory proteins that are thought to be much more specific for PP1's different functions and to be responsible for the regulation of PP1 activity by extracellular signals. The regulatory subunits of PP1c can act as activity-modulating proteins, such as inhibitors that block PP1c activity, or targeting subunits that localize PP1c to specific locations and/or modify its substrate specificity (1,2). Many of these regulatory proteins are themselves substrates of PP1c. Although the PP1c-binding proteins are largely structurally distinct from one another, a feature common to many of these proteins is a binding site that comprises a motif with the consensus sequence K/R/H/N/S-(x)-V/I/L-x-F/W/Y, where x is any amino acid (1,2). X-ray crystallographic analysis has revealed that the binding motif interacts with a hydrophobic channel in PP1c, which is located on the side opposite that of the active site (17). Although many regulatory subunits have other sites that also contribute to binding to PP1c, this motif could act as an anchor for PP1c, enabling it to make additional, weaker contacts in an ordered or cooperative manner (1). Therefore, binding of different regulatory proteins to PP1c is likely to be largely mutually exclusive, resulting in the formation of different holoenzymes consisting of a catalytic subunit and one of many different regulatory subunits.

A full understanding of the biological role of PP1 therefore requires the identification and characterization of the regulatory proteins. About 65 mammalian genes have been shown to encode proteins that interact with PP1c (1,2). In many cases however, the physiological role of these proteins is unknown. Sequence homology searches and two-hybrid screens have shown that many homologs of the key PP1 regulatory proteins exist in *Drosophila* (18) (Bennett and Alphey, unpublished data) and through two-hybrid screens we are starting to construct a picture of the complete PP1 interactome in *Drosophila* (Bennett

and Alphey, unpublished data). *Drosophila* is an excellent system in which to characterize these proteins and their interactions with PP1c not least because we know a great deal about the PP1 catalytic subunits in *Drosophila*. Armed with nearly 100 yr of accumulated tools and resources, information provided by the *Drosophila* genome project, and recent technological advances in genetic manipulation (19–23), it is now possible to rapidly determine the biological role of the *Drosophila* PP1 holoenzymes and dissect the biochemical pathways in which they act.

1.3. Identifying PP1-Interacting Proteins in the Yeast Two-Hybrid System

The ability of the targeting subunits to bind to PP1c is the only feature common to these otherwise disparate proteins. This property has been used as the basis for identifying the different regulatory subunits using a variety of biochemical and molecular biological approaches, each of which have their own merits (24–27). We have found the two-hybrid system to be a very successful technique for identifying *Drosophila* PP1c-binding proteins and to be a useful way of testing whether interactors show any specificity for particular PP1c isoforms (15,28–31). Our results have shown that two-hybrid screens can be used to identify interactions that might have been missed using other approaches and can thereby expand the repertoire of known regulatory proteins in *Drosophila* and mammals (28) (Bennett and Alphey, unpublished data). The principles of the two-hybrid system are described in detail elsewhere (32–35). In this chapter we will describe the particular methods we have used to identify *Drosophila* PP1c-interacting proteins and for counterscreening interactors against different PP1c isoforms and variants. An overview of our strategy for identifying putative PP1c-binding proteins and testing them in the two-hybrid system is shown in Fig. 2. This is cross-referenced to the Methods sections. In **Subheading 3.1.** we describe how to perform a large-scale two-hybrid screen for PP1-binding proteins and identify potential interactors. **Subheading 3.2.** describes the β -galactosidase assay, which is used as a measure of protein–protein interaction in this system. In **Subheading 3.3.** we explain a typical method for rescuing interacting plasmids from yeast for subsequent analysis. In **Subheading 3.4.** we outline how to verify the interacting plasmids and how to counterscreen positives against other baits.

Although we are particularly interested in proteins that bind *Drosophila* PP1c, the same methodologies that we describe, together with appropriate library and bait plasmids, could be used to identify proteins that bind to and potentially regulate other protein phosphatases. However, like other methods of identifying protein–protein interactions, the two-hybrid system is not infallible and, ultimately, it is necessary to verify binding using additional experimental approaches (36).

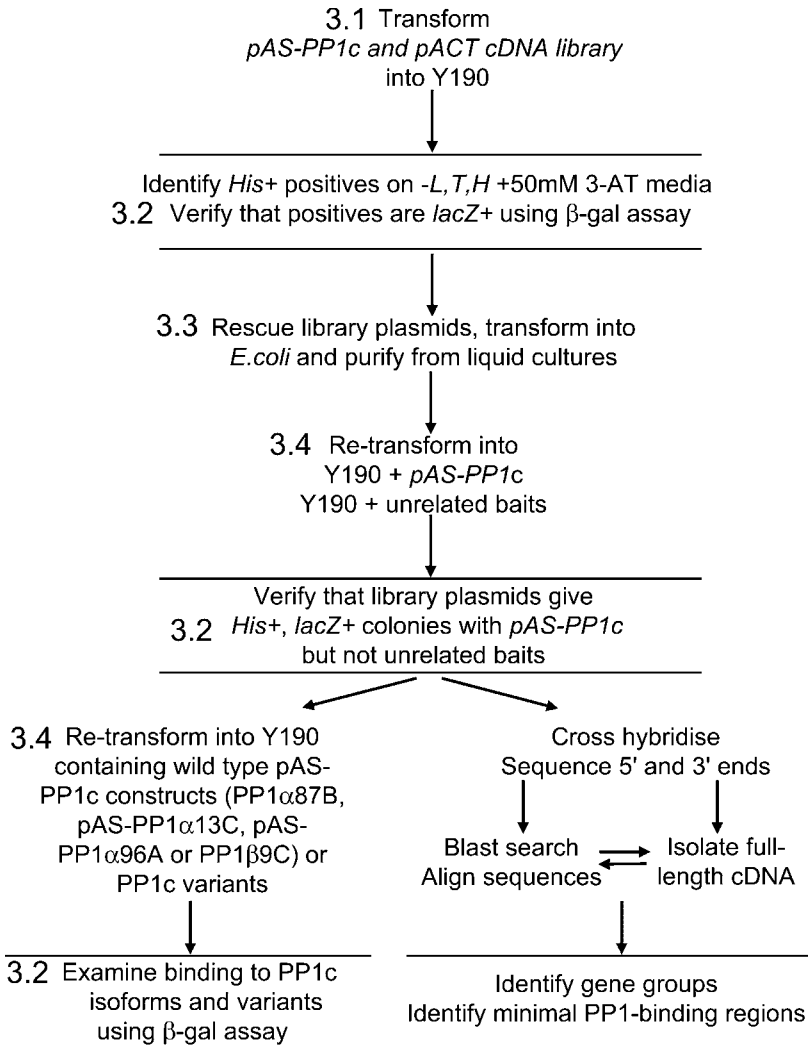


Fig. 2. Strategy for identifying putative PP1c-binding proteins and testing them in the two-hybrid system. Bait and library plasmids are cotransformed into the yeast strain Y190 (**Subheading 3.1.**). *His*⁺ and *lacZ*⁺ positives are selected by growth on synthetic defined media lacking histidine and by the ability to turn X-Gal blue in assays of β-galactosidase activity (**Subheading 3.2.**). The library plasmids are rescued from the positive yeast colonies and purified (**Subheading 3.3.**). Purified plasmids are tested for interaction with the original bait and for lack of interaction with unrelated baits by transformation into preprepared competent yeast cells containing the relevant bait constructs (**Subheading 3.4.**). Binding to different baits, including different PP1c isoforms and variants can be examined using a similar approach.

2. Materials

2.1. Large-Scale Two-Hybrid Screens in Yeast

2.1.1. Standard Yeast Transformation

1. Yeast strain Y190: *MATa*, *gal4Δ*, *gal80Δ*, *his3-Δ200*, *trp1-90I*, *ade2-101*, *ura3-52*, *leu2-3*, *leu2-112*, *URA3***GAL*>*lacZ*, *LYS2***GAL*>*HIS3*, *cyhr*. This strain can be obtained from the American Type Culture Collection (Rockville, MD) (ATCC no. 96400; *see Note 1*).
2. YAPD media: 20 g peptone, 10 g yeast extract, 20 g glucose, and 100 mg adenine hemisulfate per liter. For plates, add 15 g agar/L. Sterilize by autoclaving at 121°C for 20 min.
3. Dropout base (DOB) for synthetic defined dropout media: 1.7 g nitrogen base, 20 g dextrose, 5 g ammonium sulfate per liter, without amino acids (obtained as a mix; e.g., from Bio 101 Inc.). Sterilize by autoclaving at 121°C for 20 min.
4. Complete amino acid Supplement Mixture (CSM), dropout supplements, containing all essential amino acids except those used for the purposes of selection: CSM-tryptophan; CSM-leucine; CSM-leucine, -tryptophan; CSM-tryptophan and -histidine; CSM-leucine, -tryptophan, and -histidine (*see Note 2*).
5. Synthetic Defined (SD) dropout media: Add 0.63 g of relevant CSM dropout supplement to 1 L of DOB. For plates, add 15 g agar/L. Autoclave and store at 4°C in subdued light.
6. Standard 100-mm-diameter Petri dishes.
7. A GAL4 DNA-binding domain fusion (“bait”) construct. For this we subcloned the open reading frames of the *Drosophila* PP1c isoforms into pAS2 (pAS1-CYH2; ATCC no. 87008) as *NdeI/SalI* fragments into the *NdeI/SalI* sites of the vector; *see Note 3*. For the library transformation, the bait was purified using a plasmid purification kit (Qiagen).
8. Single-stranded carrier DNA: Dissolve 100 mg of herring testis DNA type XIV sodium salt (Sigma) in 25 mL TE (10 mM Tris-HCl, 1 mM EDTA, pH 8.0) and sonicate for 2 min at maximum power to reduce the average fragment size to approx 0.5 kb. Extract using phenol/chloroform and precipitate the DNA with 3 vol of 100% ethanol. Resuspend in sterile ddouble-distilled water (dH₂O) at 10 mg/mL and store at -20°C in 1-mL aliquots. Immediately prior to the transformation, boil for 10 min and cool quickly on ice to denature the DNA. *See Note 4*.
9. 50% polyethylene glycol (PEG) molecular weight (MW) 3350 (Sigma-Aldrich) in ddH₂O; *see Note 5*. Sterilize by autoclaving at 121°C for 20 min.
10. 1 M Lithium acetate in ddH₂O (should be a pH of between 8.4 and 8.9). Sterilize by autoclaving at 121°C for 20 min.
11. Sterile ddH₂O. Autoclave at 121°C for 20 min.

2.1.2. Preparation of the Library Plasmid

1. Luria-Bertani (LB) medium: 10 g/L bacto-tryptone, 5 g/L bacto-yeast extract, 10 g/L NaCl. For plates, add 15 g agar/L. Autoclave and store at room temperature.

2. Terrific Broth (TB) medium: Consists of solution 1 and solution 2, which are made up separately in distilled H₂O, autoclaved, and then mixed together in a ratio of 9 : 1 before use. To make solution 1, dissolve 12 g bacto-tryptone, 24 g bacto-yeast extract, 4 mL glycerol in 900 mL dH₂O and autoclave. For solution 2, dissolve 2.31 g KH₂PO₄ (0.17 M), 12.54 g K₂HPO₄ (0.72 M) in 100 mL dH₂O and autoclave. The separate solutions can be stored at room temperature.
3. Stock solutions of antibiotics: 100 mg/mL ampicillin (Amp) in ddH₂O; 34 mg/mL chloramphenicol (Chl) in 100% ethanol. Store at -20°C. Add to bacterial media just before use, to final concentrations of 100 µg/mL and 170 µg/mL for Amp and Chl, respectively.
4. Bacterial strain BNN132 (JM107/_KC): *endA1 gyr96 hsdR17 supE44 relA1 delta(lac-proAB) (F' traD36 proA+ proB+ lacIq delta(lacZ)M15) lambdaKC(kan-cre)*. This strain is a kan^r λ lysogen containing the *cre* site-specific recombinase gene (ATCC no. 47059).
5. λACT *Drosophila* third instar cDNA library (ATCC no. 87290) (see **Note 6**).
6. Sterile solutions (filter-sterilized or autoclaved): 10 mM MgSO₄; 20% glucose.
7. Plasmid purification kit (e.g., from Qiagen).

2.1.3. Library Transformation

Same as for standard transformation, but in addition:

1. 3-Amino-1,2,4-triazole (3-AT; Sigma-Aldrich) (see **Note 7**).
2. Sterile 245-mm × 245-mm dishes (Gibco-BRL) for transformation. For each plate, make 150 mL SD-Trp-Leu-His agar, microwave to dissolve agar, and then add 50 mM 3-AT and 50 µL of 5 M NaOH to pH before pouring. Before it sets, flame the surface with a Bunsen burner to remove any air bubbles.

2.2. β-Galactosidase Assay

1. 20 mg/mL 5-Bromo-4-chloro-3-indolyl β-D-galactoside (X-Gal; Sigma-Aldrich) solution in N,N-dimethylformamide. Store at -20°C, protect from exposure to light.
2. Z-buffer: Dissolve 16.1g Na₂HPO₄·7H₂O, 5.5 g NaH₂PO₄·H₂O, 0.75 g KCl, and 0.246 g MgSO₄·7H₂O in 1 L of distilled H₂O; adjust to pH 7.0. Autoclave and store at room temperature.
3. 75-mm and 90-mm diameter Whatman No.1 filter paper.
4. Standard approx 100-mm-diameter Petri dishes.
5. Staining solution, made fresh: 1.8 mL of Z-buffer, 4.9 µL β-mercaptoethanol, 30 µL X-Gal.
6. Liquid nitrogen.
7. Two pairs of flat-ended forceps (e.g., MF Filter Forceps; Millipore), to avoid damaging filters during handling.

2.3. Recovery of Library Plasmid DNA From Yeast

1. Lyticase solution: 40 U/mL Lyticase (Sigma-Aldrich), 1.2 M sorbitol, 0.1 M Na₂HPO₄, pH 7.5.

2. Alkaline lysis solution P2: 200 mM NaOH, 1% dodium dodecyl sulfate (SDS) (see **Note 8**).
3. Alkaline lysis solution P3 (prechilled to 4°C): 3.0 M KOAc, pH 5.5.
4. Phenol/chloroform (1: 1 mix, pH 7.5).
5. 100% Ethanol.
6. TE buffer: 10 mM Tris-HCl, 1 mM EDTA, pH 8.0.
7. Chemically competent or electrocompetent *Escherichia coli* cells, commercial or home-made (using your favorite method). Must be a recombination-deficient (*RecA*) strain (e.g., DH5 α) with a transformation efficiency of 10⁶ cells/ μ g DNA, or better.
8. QIAspin miniprep kit (Qiagen), or similar, for preparation of purified plasmid DNA.

2.4. Counterscreening Positives Against PP1 Isoforms and Variants

1. Solution 1: 1 M sorbitol, 10 mM bicine-NaOH, pH 8.0, 3% ethylene glycol, 5% DMSO.
2. Solution 2: 40% PEG 1000, 0.2 M bicine-NaOH, pH 8.0.
3. Solution 3: 0.15 M NaCl, 10 mM bicine-NaOH, pH 8.0.
4. GAL4 DNA-binding domain constructs: pAS2-TGT, pAS2-Lamin, pAS2-PP1c isoforms and variants.
5. Sterile 48-well micro-titer dishes.

3. Methods

3.1. Large-Scale Two-Hybrid Screens

We have used a GAL4-based version of the two-hybrid system in the yeast *Saccharomyces cerevisiae* (33), which, like other two-hybrid systems, has three critical components: (1) the yeast strain, (2) the GAL4 DNA-binding domain (“bait”) construct, and (3) the GAL4 activation-domain library construct. These components are discussed in turn below.

1. We used the yeast strain Y190, which contains two GAL4-dependent reporter genes, *HIS3* and *lacZ*, and is mutant for *his3*, *trp1*, *leu2*, *ade2*, and *ura3* (see **Note 1**). *HIS3*, which encodes imidazole glycerol phosphate (IGP) dehydratase, is a reporter for the interaction between bait and library fusion proteins and allows selection of interacting library plasmids on auxotrophic media lacking histidine. 3-AT, an inhibitor of IGP dehydratase, is used to adjust the stringency of selection on histidine-deficient media, because a low level of *HIS3* is required for prototrophy. In screens between the GAL4 DNA-binding domain (“bait”) and GAL4 activation-domain library plasmid in this system, positive interactors are initially identified as histidine autotrophs (see **Subheading 3.1.2**). Positives are then subsequently tested for β -galactosidase activity, to examine *lacZ* reporter gene expression (see **Subheading 3.2**). *trp1* and *leu2* are used to select for the bait and library plasmids (see components 3 and 4). *ade2* and *ura3* are used to

select for the yeast strain. *ade* mutants accumulate a red pigment, 5-aminoimidazole ribonucleotide, which is useful for distinguishing the strain from contaminating wild-type yeast colonies.

2. For the bait construct, we used the pAS2 vector (see **Note 3**). This contains the *TRP1* nutritional marker, which allows yeast auxotrophs to grow on tryptophan-deficient media, and the *bla* gene for ampicillin resistance in bacteria. The first step is to subclone your gene of interest into this vector, in frame with the GAL4 DNA-binding domain. Once you have made an appropriate construct, it is important to verify expression of the fusion protein (e.g., by immunoblotting) before proceeding. Fusion proteins produced from pAS2 constructs can be detected using anti-HA (hemagglutinin) antibodies (e.g., mouse monoclonal antibody 12CA5 from BABCO), which recognize the HA epitope tag encoded by the vector. It is also critical that you test that the construct fails to activate transcription of the yeast reporter genes in the absence of activation-domain plasmids. To do this, transform the construct into the yeast strain Y190 (see **Subheading 3.1.1.**) and plate on SD-Trp media (**Subheading 2.1.1.**). Then check the resulting strain for ability to activate the *HIS3* reporter by assessing growth on SD-Trp-His plates containing different concentrations of 3-AT (see **Note 7**) and on its ability to activate the *lacZ* reporter using the assay described in **Subheading 3.2**. Concentrations of 25–50 mM 3-AT are sufficient to select against pAS2 constructs that fail to activate transcription on their own. If the construct activates transcription alone, then it cannot be used in this assay.
3. For the library transformation, an excellent cDNA library from *Drosophila* third instar larval tissues is available, which has a complexity of between 1×10^7 and 1×10^8 independent clones (see **Subheading 2.1.2.**). This library first needs to be converted from phage (λ ACT) to plasmid. The method to do this is described in **Subheading 3.1.2**. The resulting plasmid, pACT, contains the *LEU2* nutritional gene that allows yeast auxotrophs to grow on leucine-deficient media and is ampicillin resistant for selection in bacteria. A number of other cDNA libraries are available commercially, including libraries from *Drosophila* adults and embryos in pACT2 (similar to pACT, derived from λ ACT2), which have 3.5×10^6 and 3×10^6 independent clones, respectively (BD Biosciences/Clontech). Commercially available kits (e.g., the Matchmaker Library Construction and Screening Kit [BD Biosciences Clontech]), are also available to make custom-made cDNA libraries, should you wish to screen for interacting proteins from other tissues (e.g., see **ref. 38**).

3.1.1. Standard Transformation Protocol

1. Grow 5 mL of Y190 overnight at 30°C in YAPD with shaking at 200 rpm, to an optical density (OD_{600}) of 0.7–1.0.
2. Pellet the cells by centrifugation at 3000g for 5 min and discard the supernatant.
3. Resuspend the cells in 50 μ L of ddH₂O.
4. Add components of the transformation mix (**39**), in the following order with gentle vortexing after the addition of each component: 240 μ L of 50% PEG 3500,

36 μL of 1.0 *M* LiAc, 10 μL of carrier DNA (10 mg/mL), and 1 μg (or less) of pAS2-PP1 in 24 μL ddH₂O.

5. Incubate at 30°C for 30 min and then heat shock for approx 30 min at 42°C.
6. Centrifuge the mixture at 3000g for 5 min, remove supernatant, and gently resuspend the cells (by gently pipetting up and down) in 1 mL sterile ddH₂O.
7. Plate 10- μL and 100- μL samples onto appropriate dropout media (i.e., SD-Trp for pAS2-PP1c).

3.1.2. Preparation of the Library Plasmid

1. Grow 10 mL of BNN132 overnight in TB to OD₆₀₀ = 2.0, which represents a cell density of approx 1.6×10^{10} cells/mL (see **Note 9**).
2. Harvest the cells and resuspend in 1/10th volume 10 mM MgSO₄. Inoculate this with 50 μL λACT (approx 1.1×10^8 PFU) for 30 min at 30°C. Infection with the library produces Amp^r cells.
3. Inoculate 100 mL TB with the absorbed phage and incubate for 60 min at 30°C with agitation. This allows the cells to express the *bla* gene, which confers ampicillin resistance, and excise pACT, the GAL4 activation domain fusion vector, via cre-lox-mediated recombination.
4. After 60 min, add Amp to 100 $\mu\text{g}/\text{mL}$ and glucose to 0.2%.
5. Grow to OD₆₀₀ 1.0. After recovery, plate a dilution series (1, 0.1, and 0.01 μL) on LB agar to estimate the number of independent clones.
6. Harvest cells in 50-mL tubes (Falcon) and resuspend in 4 L TB.
7. Regrow the culture in 1-L flasks to an OD 0.8 (15 generations, approx 21 h).
8. Add chloramphenicol to amplify the plasmid and prevent further replication of the host DNA (see **Note 10**).
9. After a further 4 h, harvest cells by centrifugation at 6000g for 30 min.
10. Purify the plasmid DNA. For convenience, we recommend a commercially available plasmid purification kit.

3.1.3. Library Transformation

The key to screening large numbers of clones in the two-hybrid interaction system is high transformation efficiency (at least 1×10^4 transformants/ μg DNA). The higher the efficiency, the more likely you are to detect rare and potentially novel interactions. Therefore, before starting a large-scale screen, it is worth spending a little time optimizing the conditions for transformation, such as period of heat shock and amount of carrier DNA, using a smaller scale (e.g., 1/10 size) transformations. Usually, sequential transformation of the bait followed by the library plasmids is more efficient than cotransformation of both simultaneously. However, we have found that *Drosophila* PP1c constructs have an adverse affect on growth of the yeast, consistent with previous studies showing that overexpression of wild-type *S. cerevisiae* PP1c (*DIS2S1/GLC7*) from a GAL promoter is highly detrimental, causing gross morphological abnormalities and lethality, dependent on the genetic background (41). Consequently,

pAS2-PP1c constructs are rapidly lost from the yeast if selection for the plasmid is withdrawn (*see* **Note 11**). Even with selection, there is likely to be pressure to introduce rearrangements or mutations in the plasmid or the host that result in loss of PP1c expression. Therefore, we strongly recommend cotransformation of pAS2-PP1c and library plasmids. This approach is probably also advisable if you are planning to use a related phosphatase instead of PP1c. The efficiency of taking up both the bait and library plasmids simultaneously (as determined by plating transformations on SD-Trp-Leu media) should be approx 5×10^4 transformants/ μg (assuming equal amounts of bait and library) using the method described below. This is only about half as efficient as transforming with a single plasmid (as assessed by numbers of colonies on SD-Trp or SD-Leu media). Therefore, a typical large-scale transformation using 100 μg of both bait and library should yield 5×10^6 transformants.

1. Use a saturated overnight culture of Y190 to inoculate 100 mL YAPD and grow overnight at 30°C with shaking at 200 rpm.
2. Dilute to an OD₆₀₀ of approx 0.19 in 500 mL YAPD and regrow for two generations until the OD₆₀₀ is 0.7–0.8, which typically takes approx 3–4 h.
3. Harvest the cells by centrifugation at 3000g for 5 min.
4. Wash the cell pellet by resuspending in 100 mL sterile ddH₂O and collection by centrifugation as in **step 3**.
5. Resuspend the pellet in 1.28 mL sterile ddH₂O (*see* **Note 12**).
6. Add components of the transformation mix in the following order with gentle vortexing after the addition of each component: 4.8 mL of 50% PEG 3350; 720 μL 1.0 M LiAc; 200 μL of 10 mg/mL carrier DNA; 100 μL of 1 $\mu\text{g}/\mu\text{L}$ library; 100 μL of 1 $\mu\text{g}/\mu\text{L}$ pAS2-PP1.
7. Incubate at 30°C for 30 min and then heat shock for approx 30 min at 42°C (*see* **Note 13**).
8. Centrifuge the mixture at 3000g for 5 min, remove supernatant, and gently resuspend (by gently pipetting up and down) in 10 mL sterile ddH₂O.
9. Take 0.2, 0.5, and 1 μL of resuspended cells and add to 100 μL of sterile ddH₂O. Plate on SD-Trp-Leu, SD-Trp, and SD-Leu media to determine the total number of transformants.
10. Plate equal amounts of the remaining cells on two 245-mm \times 245-mm dishes containing SD-Trp-Leu,-His, +50 mM 3-AT (*see* **Subheading 2**). Positives can then be identified after about a week at 30°C by the formation of large colonies (*see* **Note 14**).

3.2. Testing Positives Using the β -Galactosidase Assay

Having selected strong interactors on the basis of growth on media lacking histidine, pick the largest yeast colonies and patch them out on fresh -Trp, -Leu,-His media (\pm 50 mM 3-AT). To eliminate possible *his3* revertants and confirm interactions between the bait and library plasmids, take lifts from the

plates and test with X-Gal, a chromogenic substrate of β -galactosidase. Genuine positives, which are *lacZ*⁺, will turn blue in this assay (see **Note 15**).

1. Patch or streak the yeast colonies out on a fresh plate.
2. For each lift, pipet 1.8 mL of fresh staining solution into a clean Petri dish and soak a 90-mm filter placed into the solution.
3. Place a piece of 75-mm-diameter Whatman paper on top of the yeast colonies, allowing the paper to soak through (see **Note 16**).
4. Mark the orientation by making holes through both the filter and the agar plate using a needle in three or more asymmetric locations.
5. Using forceps, peel off the filters and put colony side up in a pool of liquid nitrogen for approx 5 s. Allow to thaw at room temperature.
6. Carefully place the colony lift, colony side up, onto the filter presoaked with staining solution avoiding the introduction of air bubbles.
7. Incubate the Petri dishes at 30°C until color develops (30 min to overnight). Colonies producing β -galactosidase can be identified by aligning the filter with the plate using the orientating marks.

3.3. Recovery of Interacting Plasmids From Yeast

A key advantage of the two-hybrid system is that the gene encoding the interacting protein can be readily identified from the interacting library plasmid. The purified interacting plasmid can also be used to test binding to other PP1c isoforms or variants (see **Subheading 3.4.**). To isolate the interacting plasmid, DNA is extracted from yeast cultures and is then transformed into *E. coli* to obtain sufficient a yield of plasmid DNA for further analysis. Although commercial kits for DNA isolation from yeast exist, we favor this rapid and relatively inexpensive method (see **Note 17**).

1. Inoculate 3 mL SD-Leu media with a colony pick and grow up overnight at 30°C or until cultures reach stationary phase (see **Note 18**).
2. Transfer cultures to microcentrifuge tubes and pellet cells by centrifugation at full speed for 30 s. Remove the supernatant and resuspend the pellet in 200 μ L of lyticase solution. Vortex the mixture briefly to resuspend the pellet and incubate at 37°C for 2 h to hydrolyze poly(β -1,3-glucose) in the yeast cell wall.
3. Add 200 μ L alkaline lysis solution P2 (see **Note 19**).
4. After 5 min, promptly add prechilled solution P3 and leave on ice for 5 min.
5. Centrifuge at full speed for 6 min.
6. Extract DNA using 600 μ L of phenol/chloroform.
7. Precipitate the aqueous phase with 3 vol of 100% ethanol.
8. Resuspend the pelleted cells in an appropriate volume of TE, pH 8.0.
9. Transform competent *E. coli* cells with extracted yeast DNA and plate on media containing Amp to select for pACT. In general, use one-fifth of the yeast DNA for transformation into subcloning efficiency DH5 α competent cells. We routinely use 2 μ L of DNA and 50 μ L of home-made chemically

competent cells (10^6 cells/ μ g DNA), essentially using the method described by Hanahan (44,45).

10. Pick one or more bacterial colonies into liquid LB + Amp media and grow overnight.
11. Miniprep the plasmid DNA using QiaSpin miniprep kit (Qiagen) or similar kits.

3.4. Counterscreening Positives Against Unrelated Baits, PP1 Isoforms, and Variants

Having isolated the plasmid DNA, there are a couple of important tests to perform before proceeding to investigate the gene that you have identified. First, it is important to reintroduce the plasmid back into yeast to confirm the interaction with the original bait (i.e., pAS2-PP1c). Yeast cells are capable of taking up more than one library plasmid, not all of which interact with the bait, so it is worth testing that the plasmid that you have isolated is the right one before investing any more time in it. If you find that the library plasmid fails to interact with the original bait, go back to the bacterial transformants for that two-hybrid positive (see **Subheading 3.3., step 10**) and test the library plasmids from a few other bacterial colonies. Second, the two-hybrid system is known to generate false positives, so it is important to test binding to one or more unrelated constructs. For this, we typically use the bait plasmids pAS2-TGT and pAS2-Lamin (obtained from Steven Elledge). Failure to interact with the TGT and Lamin controls is a good indication that the protein binds specifically to PP1, and these clones are then investigated further.

We have found that the easiest, and most unambiguous, way to reintroduce the plasmids back into yeast is by transformation (see **Note 20**). In contrast to the original library screen however, these secondary transformations do not have to be done with a very high transformation efficiency, so it is possible to do the transformation using preprepared competent cells already carrying the bait. To do this, transform the yeast with the pAS2 construct (e.g., pAS2-PP1, pAS2-TGT, or pAS2-Lamin) using the standard transformation method (**Subheading 3.1.2.**), and make the resulting strains competent for transformation by treatment with ethylene glycol and DMSO using the protocol described in **Subheading 3.4.1.**, which has been adapted from **ref. 46**. The competent cells can then be frozen in conveniently sized aliquots for transformation. Making large batches of frozen yeast competent cells in advance saves a great deal of time. Even with potentially toxic pAS2-PP1 constructs, these strains typically have a transformation efficiency of at least 5×10^2 transformants/ μ g DNA, which is perfectly adequate for this purpose. To perform the tests, transform the yeast strains carrying the bait plasmids with the isolated library plasmid (see **Subheading 3.4.2.**) and screen the resulting colonies for β -galactosidase activity (**Subheading 3.2.**). A fairly large number of bait and library plasmid combi-

nations can be tested at the same time. Because the transformation can be performed in a microtiter plate, this method has the potential for being automated.

This approach can also be used to counterscreen positives against different isoforms and variants of *Drosophila* PP1c to further characterize the binding properties of PP1c interactors and to identify specific residues that are required for protein–protein interaction. As PP1 β 9C has a unique role *in vivo*, one might expect to identify PP1 β 9C-specific binding subunits that mediate this role. These will be identified as binding only to PP1 β 9C, not to the other isoforms. Similarly, one might anticipate recovering clones that mediate redundant roles of PP1 α 96A and PP1 β 9C (e.g., through an interaction with the C-terminal regions of these isoforms). Expected outcomes of such counterscreening experiments are summarised in **Table 1**. To counterscreen putative PP1 β 9C-binding proteins against other *Drosophila* PP1c isoforms (see **Fig. 2**), we transformed the library plasmid into strains carrying pACT-PP1 β 9C, pACT-PP1 α 13C, pACT-PP1 α 87B, or pACT-PP1 α 96A (29). This analysis revealed that MYPT-75D specifically binds to PP1 β 9C (7). As with library screening, it is important to remember to test that the bait plasmids fail to activate *lacZ*⁺ or *HIS3*⁺ expression in the absence of GAL4 activation-domain fusions.

3.4.1. Preparation of Competent Yeast Cells Containing pAS2-PP1 Constructs

1. Transform Y190 with pAS2-PP1 constructs using the standard transformation method (**Subheading 3.1.1.**).
2. Inoculate 50 mL SD-Trp media with part of an overnight culture or a single colony carrying pAS2-PP1.
3. Grow cells overnight at 30°C to OD₆₀₀ 0.6–1.0, which represents a cell density of (0.6–1.0) $\times 10^7$ cells/mL.
4. Centrifuge the cells for 3 min at 3000g and wash in 0.5 vol of solution 1 and resuspend in a 1/50th volume (i.e., 1 mL for a 50-mL culture) of the same solution.
5. Dispense 50- μ L aliquots in sterile microcentrifuge tubes. Each aliquot is enough for 10 transformations. Freeze slowly at –80°C (see **Note 21**).

3.4.2. Transformation of Competent Cells With Interacting Library Plasmids

1. Aliquot 0.25 μ g library plasmid DNA into a 48-well microtiter dish in a volume of no more than 4 μ L. Place the microtiter dish on ice.
2. Thaw the competent cells quickly in your hands and then place on ice.
3. Add 50 μ g of carrier DNA in no more than 1/10 volume, and vortex the mixture briefly.
4. Add 350 μ L of solution 2 and vortex the mixture again briefly.
5. Add 40 μ L of this mixture to each of the ice-chilled DNA aliquots and incubate at 30°C for 1 hr. There is no need for agitation.

Table 1
Expected Outcomes From Binding Experiments Between
Two-Hybrid Positives and Different Isoforms and Variants of *Drosophila* PP1c

Binds to:	PP1 β 9C	PP1 β 9C with flightless point mutant	PP1 β 9C with C-terminal deletion	PP1 β 9C with T-V mutation at cdk site	PP1 β 9C with T-D mutation at cdk site	PP1 α 96A	PP1 α 96A with C-terminal deletion	PP1 α 87B	PP1 α 13C
β isoforms only	✓	?	?	?	?	×	×	×	×
C-terminus (<i>see</i> Fig. 1)	✓	✓	×	?	?	✓	×	×	×
cdk phosphorylated C-terminus only	✓	✓	×	×	✓	✓	×	×	×
Dephosphorylated C-terminus only	✓	✓	×	✓	×	✓	×	×	×
Wild-type but not mutant PP1c	✓	?	?	?	?	✓	?	✓	?

Note: Nine different PP1c baits are shown, including the four wild-type *Drosophila* PP1c isoforms, PP1 α 96A and PP1 β 9C mutants in which the C-terminal 30 amino acids are deleted, a PP1 β 9C mutant affecting flight, and PP1 β 9C point mutants mimicking phospho- (T-D) and dephospho- (T-V) forms of the PP1c cdk phosphorylation site (*see* Fig. 1). PP1c interactors can be classified according to which PP1c isoforms and variants they bind, as shown in the left-hand column. Question marks indicate where binding ability cannot be predicted.

6. Add 250 μ L of solution 3 to each well. Spread the contents of each well on a separate plate containing SD-Trp-Leu dropout media. Alternatively, centrifuge for 30 s at 6000g, remove most of the supernatant, resuspend the pellet in the residual liquid by vortexing, and plate the cells in rows and columns on a 24 \times 24 dish (see **Note 22**).
7. Test for interaction by patching or streaking out the yeast on fresh SD-Trp-Leu plates and performing the β -galactosidase assay (**Subheading 3.2.**) and by plating on SD-Trp-Leu-His, +30mM 3-AT plates to test for His3 autotrophy.

3.5. Concluding Remarks

Protein phosphatase 1c has many roles, each of which is thought to be mediated by a different regulatory or targeting subunit (**1,2**). The large number of potential PP1c-binding proteins is compounded by the fact that multiple, but independent, cDNAs representing the same gene are often isolated from the same screen (see **Fig. 3** and Bennett and Alphey, unpublished data). For organisms where the genome sequence is not yet available or is poorly annotated, an efficient, but fairly laborious, way of organizing a large number of clones into gene groups is to use cross-hybridization on dot blots (see **Fig. 3A,B**). Grouping and identifying two-hybrid positives in *Drosophila* is now relatively straightforward because of the *Drosophila* Genome Project. The complete *Drosophila melanogaster* genome sequence has been available since 2000 (**23**) and is one of the best annotated of all metazoan genomes sequenced to date. The identity of a clone (i.e., what gene it corresponds to) and identification of groups of clones can be rapidly established by obtaining limited sequences from the 5' and 3' ends of each clone (see **Fig. 3C,D**) and comparing them to sequences deposited in the databases. For fly sequences, this is done most quickly using BLAST at <http://flybase.net/blast/> (or UK mirror, <http://fbserver.gen.cam.ac.uk/blast/>). Hyperlinks from the search results then direct the investigator to individual entries in Flybase at <http://flybase.bio.indiana.edu/> (UK mirror <http://fbserver.gen.cam.ac.uk/>), which provides information about the complete cDNA and genomic sequence, chromosome location, nearest *P* element insertion, candidate mutants, transcription pattern, homologs in other organisms, and whatever functional information is known about the gene and gene product (**47**). Sequences from multiple clones representing the same gene can then be mapped onto the full-length sequences to delimit the minimal binding region (see **Fig. 3C**). BLAST searches can be done against sequences from other organisms at <http://www.ncbi.nlm.nih.gov/BLAST/>, which identifies potential homologs and allows the investigator to trace the evolutionary origins of the protein. Ultimately, the challenge for the phosphatase community is to understand the biological roles of the regulatory proteins and their functional interactions with PP1. *Drosophila* offers many tools and resources to per-

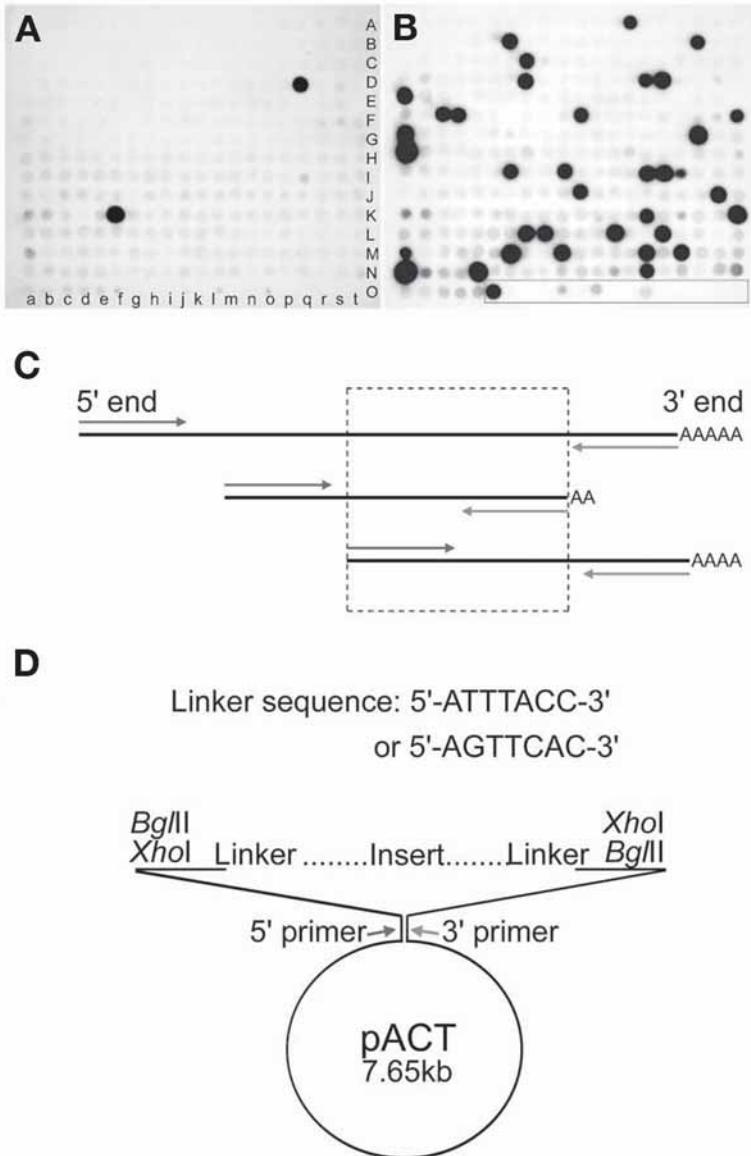


Fig. 3. Strategies for grouping and identifying positive yeast two-hybrid clones. For organisms where the genome sequence is not yet available or is poorly annotated, sequencing of cDNA ends is not the most efficient way of grouping a large number of clones together. This is because individual sequences might fail to overlap with each other or with the limited sequence data available in the databases. One solution to this problem, which has worked very well in our hands, is cross-hybridization (**A,B**). For

form this kind of analysis (19,20) and has great potential to guide experiments in more complex organisms, such as mammals.

4. Notes

1. A number of other yeast strains are available. We have also used the yeast strain HF7C (BD Biosciences Clontech and Teknova Inc.), which is *MATa*, *gal4-542*, *gal80-538*, *his3-200*, *lys2-801* *trp1-901*, *ade2-101*, *ura3-52*, *leu2-3-112*, *URA3*GAL>lacZ*, *LYS2*GAL>HIS3*, *cyhr*. Y190 and HF7C are essentially the same except the HF7C strain harbors an additional auxotrophic mutation (*lys2-801*) for selection of the host. The transformation efficiencies of HF7C and Y190 were approximately the same in our hands, although HF7C was more sensitive to the duration of heat shock and therefore might need more optimization to achieve the highest transformation efficiency. There was no difference between the growth of HF7C and Y190 on media lacking histidine.
2. We would strongly recommend that the reader buy premade dropout media (e.g., from Bio 101, Inc.). The individual amino acids can be bought individually to make dropout media, but this is possibly more expensive, weighing out all the

this method, each interacting library plasmid is spotted out in a gridded array on a set of identical filters and ultraviolet crosslinked. Radioactively labeled probes are made from gel-purified restriction fragments (e.g., *Xho*I or *Bgl*II fragments from pACT) corresponding to the cloned DNA. These are then used to probe the set of filters. Each hybridization experiment with a single probe identifies a unique gene group consisting of a number of clones with overlapping sequence. In the example shown here, equivalent filters have been hybridized with two different probes that identify distinct gene groups (compare hybridization pattern in **A** and **B**). Filters can be reused by washing off the labeled probe. Hybridization to the set of dot blots is repeated with different probes until, by a process of elimination, all of the clones are assigned to gene groups. Having multiple filters makes it possible to perform multiple hybridization experiments in parallel. Cloned DNA encoding predicted or previously identified *Drosophila* PP1c-binding proteins can be included on the filters (boxed region of the blot in **B**) speeding up the identification of isolated clones. Where the complete genome sequence is available, it is more efficient to sequence the ends of each clone and align the sequences with each other and the predicted cDNA sequence (C). Most cDNA clones in oligo-dT primed libraries will contain the 3' end of the gene. Occasionally, however, internal poly(A) sequences result in truncated cDNAs. The region of overlap between sequences identifies the shortest interaction region (indicated by dashed box). (**D**) Simplified pACT vector map showing position of *Bgl*II and *Xho*I restriction sites in the vector to cut out the insert for the generation of radiolabeled probes and the position of 5' and 3' primers for sequencing of the cDNA insert. pACT 5' sequencing primer: 5'-CGATGATGAAGATACCCAC-3'. pACT 3' sequencing primer: 5'-GCACAGTTGAAGTGAAGTTG-3'. Sequence of linkers used to subclone cDNAs into pACT during library construction are shown.

individual amino acids for each dropout media is time-consuming, and the mixtures tend to be difficult to dissolve.

3. A range of GAL4 DNA-binding domain vectors are available, including Kan^r bait plasmids such as pGBKT7 (BD Biosciences/Clontech). Having bait and library plasmids with different antibiotic resistance genes can be an advantage when it comes to isolating the library plasmid (*see Note 18*).
4. Carrier single-stranded DNA (ssDNA) can be freeze-thawed three to four times before having to be denatured again by boiling. The concentration of carrier ssDNA is critical to the transformation efficiency; *see Subheading 3.1*. When using crude plasmid preparations, it is necessary to reduce the carrier DNA concentration because RNA also acts as a carrier.
5. Care must be taken to ensure that the PEG solution is at the proper concentration. Store the PEG solution in a tightly capped container to prevent evaporation of water. Evaporation of the water from the PEG stock solution will result in an increase in the effective concentration of PEG in the transformation reaction and severely reduce the efficiency.
6. Upon receipt the phage should be titered and amplified to give a higher stock if necessary, and aliquots should be frozen with 9% dimethyl sulfoxide (DMSO) at -80°C . For library DNA preparation, the titer of the phage should be 1×10^9 PFU/mL with between 1×10^7 and 1×10^8 total recombinants. *Drosophila* cDNA inserts were selected to be >600 bp (*37*).
7. The concentration necessary to suppress basal growth should be determined in advance. We found that 50 mM 3-AT completely suppressed limited growth of Y190 alone or Y190 carrying pAS2-PP1 β 9C on SD-Trp-His media. Dissolve in sterile ddH₂O and add to media just before pouring into dishes. 3-AT is a possible carcinogen; use appropriate safety precautions when handling.
8. Check solution P2 for SDS precipitation resulting from low storage temperatures. If necessary, redissolve the SDS by warming the solution to 37°C .
9. Cell counts can be done using a hemocytometer and then subsequently estimated by measuring the optical density at 600 nm (OD₆₀₀) in a colorimeter.
10. Chloramphenicol inhibits protein synthesis and prevents replication of the bacterial chromosome while the plasmid DNA continues to replicate. This increases the yield of plasmid DNA and reduces the bulk of bacterial cells for the DNA preps. For further information, *see ref. 40*).
11. Growth in nonselective media immediately prior to transformation was essential for transformation efficiency. In our hands, methods excluding this procedure (e.g., *ref. 34*) yielded less than 10^3 transformants/ μg DNA. During this period of growth, plasmids expressing PP1 were lost from the yeast at a higher frequency than controls when assessed by plating on selective media. We would not recommend sequential transformation of pAS2-PP1 and pACT, as this was approx 10-fold less effective than cotransformation.
12. The volume of ddH₂O and plasmid DNA can be adjusted, but the total volume of the transformation mix must remain the same.
13. Optimize the duration of heat shock using smaller-scale transformations for the highest transformation efficiency. Optimum transformation rates were typically observed with a heat shock of between 25 and 35 min.

14. Often there is a lawn of very small colonies on the selection plates, but only the true positives continue to grow to form large colonies while the microcolonies appear to stop growing. The β -galactosidase assay eliminates any false positives that have been picked by mistake.
15. The volumes of solution suggested here normally provide good exposure to the substrate. Too little substrate leads to unequal exposure, whereas excess liquid typically yields diffuse spots. The assays can also be done by growing the yeast on X-Gal plates. Although these assays give a response that often corresponds well to increasing activator strength, they are far less sensitive than filter lifts. Assays of β -activity can also be done in solution with chlorophenolred- β -D-galactopyranoside (CPRG; Roche). When cleaved by β -galactosidase, CPRG yields a water-soluble red product measurable by spectrophotometry. In principle, this allows for quantitative measurements of activity, but measurements from the same yeast strain often show a very large standard deviation. For more information about β -galactosidase assays, refer to [ref. 42](#).
16. Nitrocellulose filters can be used, but they are more expensive and are prone to crack when frozen.
17. An alternative lysis method is as follows: Add 0.3 mL of lysis solution (2% Triton X-100, 1% SDS, 100 mM NaCl, 10 mM Tris-HCl, pH 8, 1.0 mM EDTA), 0.3 mL neutralized phenol/chloroform/isoamyl alcohol (25 : 24 : 1) and 0.3 g acid-washed glass beads (prewashed once with 1 M acetic acid and then ddH₂O) to the cell suspension. Vortex for 2 min and centrifuge at full speed immediately afterward for 5 min. Transfer the supernatant to a clean tube and precipitate with 3 vol of ethanol. This is very laborious for a large number of cultures because it involves more hands-on time, but quicker than the lyticase method if only processing a few samples.
18. The *CYH2* gene on pAS2 confers cycloheximide sensitivity to Y190, which is *cyh^r*, providing a way of selecting against the bait plasmid ([43](#)). However, pAS2-PP1c plasmids are invariably lost in the absence of positive selection (i.e., in SD-Leu media containing Trp) because of their toxicity. Consequently, selection with cycloheximide is typically unnecessary during purification of the interacting library plasmids. However, both pACT and pAS2 are *Amp^r*, so very occasionally the bait plasmid is recovered despite selection for just the library pACT plasmid. We have not found this to be an issue, but if you do face this problem, try using selection with cycloheximide or use a *Kan^r* bait plasmid such as pGBKT7 (BD Biosciences/Clontech) instead of pAS2.
19. This procedure is essentially identical to that of alkaline lysis for bacteria. Alkaline treatment for 5 min allows release of plasmid DNA without release of chromosomal DNA while minimizing the exposure of the plasmid to denaturing conditions. Long exposure to alkaline conditions might cause the plasmid to become irreversibly denatured. For convenience, P2 and P3 solutions can be obtained separately or part of a kit from Qiagen.
20. An alternative method is to introduce the two plasmids into the same cell by yeast mating using a MAT α strain (e.g., Y187: MAT α , *gal4 Δ* , *gal80 Δ* ,

his3, *trp1-901*, *ade2-101*, *ura3-52*, *leu2-3*, *leu2-112*, *URA3 GAL1*→*lacZ met*-([ATCC 96399]). See **ref. 43** for details.

21. Slow freezing has been observed to increase cell recovery. This can be done using a Nalgene Cryo 1°C freezing container, with isopropanol as indicated by the supplier. Alternatively, insulate the tubes in a polystyrene box before putting them at -80°C.
22. The decision to plate on standard Petri dishes or larger plates will depend on how many interactors and bait plasmids are to be counterscreened. If you are plating on a fraction of a large dish, you might need to adjust the amount of DNA used for the transformation so that there are an appropriate number of colonies per square millimeter.

Acknowledgments

Work in our laboratories is supported by the BBSRC, CRUK and MRC, with additional support from the Royal Society. DB is a Todd-Bird Research Fellow at New College, Oxford.

References

1. Bollen, M. (2001) Combinatorial control of protein phosphatase-1. *Trends Biochem. Sci.* **26**, 426–431.
2. Cohen, P. T. W. (2002) Protein phosphatase 1: targeted in many directions *J. Cell Sci.* **115**, 241–256.
3. Dombrádi, V., Axton, J. M., Brewis, N. D., da Cruz e Silva, E. F., Alphey, L., and Cohen, P. T. W. (1990) *Drosophila* contains three genes that encode distinct isoforms of protein phosphatase 1. *Eur. J. Biochem.* **194**, 739–745.
4. Dombrádi, V., Mann, D. J., Saunders, R. D. C., and Cohen, P. T. W. (1993) Cloning of the fourth functional gene for protein phosphatase 1 in *Drosophila melanogaster* from its chromosomal location. *Eur. J. Biochem.* **212**, 177–183.
5. Sasaki, K., Shima, H., Kitagawa, Y., Irino, S., Sugimura, T., and Nagao, M. (1990) Identification of members of the protein phosphatase 1 gene family in the rat and enhanced expression of protein phosphatase 1 alpha gene in rat hepatocellular carcinomas *Jpn. J. Cancer Res.* **81**, 1272–1280.
6. Zhang, Z., Bai, G., Shima, M., Zhao, S., Nagao, M., and Lee, E. Y. (1993) Expression and characterization of rat protein phosphatases-1 alpha, -1 gamma 1, -1 gamma 2, and -1 delta. *Arch. Biochem. Biophys.* **303**, 402–406.
7. Raghavan, S., Williams, I., Aslam, H., Thomas, D., et al. (2000) Protein phosphatase 1b is required for the maintenance of muscle attachments. *Curr. Biol.* **10**, 269–272.
8. Varmuza, S., Jurisicova, A., Okano, K., Hudson, J., Boekelheide, K., and Shipp, E. B. (1999) Spermiogenesis is impaired in mice bearing a targeted mutation in the protein phosphatase 1 gamma gene *Dev. Biol.* **205**, 98–110.
9. Dombrádi, V., Axton, J. M., Barker, H. M., and Cohen, P. T. W. (1990) Protein phosphatase activity in *Drosophila* mutants with abnormalities in mitosis and chromosome condensation. *FEBS Lett.* **275**, 39–43.

10. Baksa, K., Morawietz, H., Dombrádi, V., et al. (1993) Mutations in the protein phosphatase 1 gene at 87B can differentially affect suppression of position-effect variegation and mitosis in *Drosophila melanogaster*. *Genetics* **135**, 117–25.
11. Axton, J. M., Dombrádi, V., Cohen, P. T. W., and Glover, D. M. (1990) One of the protein phosphatase 1 isoenzymes in *Drosophila* is essential for mitosis. *Cell* **63**, 33–46.
12. Ohkura, H., Kinoshita, N., Miyatani, S., Toda, T., and Yanagida, M. (1989) The fission 11yeast *dis2+* gene required for chromosome disjoining encodes one of two putative type 1 protein phosphatases. *Cell* **57**, 997–1007.
13. Doonan, J. H., and Morris, N. R. (1989) The *bimG* Gene of *Aspergillus nidulans*, required for completion of anaphase encodes a homologue of mammalian phosphoprotein phosphatase 1. *Cell* **57**, 987–996.
14. Fernandez, A., Brautigan, D. L., and Lamb, N. J. C. (1992) Protein phosphatase type 1 in mammalian cell mitosis: chromosomal localisation and involvement in mitotic exit. *J. Cell Biol.* **116**, 1421–1430.
15. Vereshchagina, N., Bennett, D., Szoor, B., et al. (2004) The essential role of PP1beta in *Drosophila* is to regulate nonmuscle myosin *Mol. Biol. Cell* **15**, 4395–4405.
16. Clyne, P. J., Certel, S. J., de Bruyne, M., Zaslavsky, L., Johnson, W. A., and Carlson, J. R. (1999) The odor specificities of a subset of olfactory receptor neurons are governed by *Acj6*, a POU-domain transcription factor *Neuron* **22**, 339–347.
17. Egloff, M. P., Johnson, D. F., Moorhead, G., Cohen, P. T. W., Cohen, P., and Barford, D. (1997) Structural basis for the recognition of regulatory subunits by the catalytic subunit of protein phosphatase 1. *EMBO J.* **16**, 1876–1887.
18. Ceulemans, H., Stalmans, W., and Bollen, M. (2002) Regulator-driven functional diversification of protein phosphatase-1 in eukaryotic evolution. *Bioessays* **24**, 371–381.
19. Venken, K. J. and Bellen, H. J. (2005) Emerging technologies for gene manipulation in *Drosophila melanogaster*. *Nat. Rev. Genet.* **6**, 167–178.
20. Matthews, K. A., Kaufman, T. C., and Gelbart, W. M. (2005) Research resources for *Drosophila*: the expanding universe. *Nat. Rev. Genet.* **6**, 179–193.
21. Adams, M. D. and Sekelsky, J. J. (2002) From sequence to phenotype: reverse genetics in *Drosophila melanogaster*. *Nat. Rev. Genet.* **3**, 189–198.
22. St Johnston, D. (2002) The art and design of genetic screens: *Drosophila melanogaster*. *Nat. Rev. Genet.* **3**, 176–188.
23. Adams, M. D., Celniker, S. E., Holt, R. A., Evans, C. A., Gocayne, J. D., Amanatides, P. G., et al., (2000) The genome sequence of *Drosophila melanogaster*. *Science* **287**, 2185–2195.
24. Stralfors, P., Hiraga, A., and Cohen, P. (1985) The protein phosphatases involved in cellular regulation. Purification and characterisation of the glycogen-bound form of protein phosphatase-1 from rabbit skeletal muscle. *Eur. J. Biochem.* **149**, 295–303.
25. Helps, N., Street, A., Elledge, S., and Cohen, P. (1994) Cloning of the complete coding region for human protein phosphatase inhibitor 2 using the two hybrid system and expression of inhibitor 2 in *E. coli*. *FEBS Lett.* **340**, 93–98.

26. Campos, M., Fadden, P., Alms, G., Qian, Z., and Haystead, T. A. J. (1996) Identification of protein phosphatase-1-binding proteins by microcystin-biotin affinity chromatography. *J. Biol. Chem.* **271**, 28,478–28,484.
27. Walsh, E. P., Lamont, D. J., Beattie, K. A., and Stark, M. J. (2002) Novel interactions of *Saccharomyces cerevisiae* type 1 protein phosphatase identified by single-step affinity purification and mass spectrometry *Biochemistry* **41**, 2409–2420.
28. Bennett, D. and Alphey, L. (2002) PP1 binds Sara and negatively regulates Dpp signaling in *Drosophila melanogaster*. *Nature Genet.* **31**, 419–423.
29. Bennett, D., Szöör, B., and Alphey, L. (1999) The chaperone-like properties of mammalian Inhibitor-2 are conserved in a *Drosophila* homologue. *Biochemistry* **38**, 16,276–16,282.
30. Parker, L., Gross, S., Beullens, M., Bollen, M., Bennett, D., and Alphey, L. (2002) Functional interaction between NIPPI and PP1 in *Drosophila*: consequences of over-expression of NIPPI in flies and suppression by co-expression of PP1. *Biochem. J.* **368**, 789–797.
31. Rudenko, A., Bennett, D., and Alphey, L. (2003) Trithorax interacts with type 1 serine/threonine protein phosphatase in *Drosophila*. *EMBO Rep.* **4**, 59–63.
32. Miller, J. and Stagljar, I. (2004) Using the yeast two-hybrid system to identify interacting proteins *Methods Mol. Biol.* **261**, 247–262.
33. Fields, S. and Sternglanz, R. (1994) The two-hybrid system: an assay for protein–protein interactions *Trends Genet.* **10**, 286–291.
34. Finley, R. L. J. and Brent, R. (1995) Interaction trap cloning with yeast, in *DNA Cloning II: Expression systems*, Oxford University Press, Oxford.
35. Brent, R. and Finley, R. L. J. (1997) Understanding gene and allele function with two-hybrid methods. *Annu. Rev. Genet.* **31**, 663–704.
36. Van Eynde, A. and Bollen, M. (2003) Validation of interactions with protein phosphatase-1 *Methods Enzymol.* **366**, 144–156.
37. Durfee, T., Becherer, K., Chen, P.-L., et al. (1993) The retinoblastoma protein associates with the protein phosphatase type 1 catalytic subunit. *Genes Dev.* **7**, 555–569.
38. Perezgasga, L., Jiang, J., Bolival, B., Jr., et al. (2004) Regulation of transcription of meiotic cell cycle and terminal differentiation genes by the testis-specific Zn-finger protein matotopetli *Development* **131**, 1691–1702.
39. Gietz, R. D. and Woods, R. A. (2002) Transformation of yeast by lithium acetate/single-stranded carrier DNA/polyethylene glycol method *Methods Enzymol.* **350**, 87–96.
40. Sambrook, J., Fritsch, E. F., and Maniatis, T. (1989) *Molecular Cloning: A Laboratory Manual*, Cold Spring Harbor Press, Cold Spring Harbor, NY.
41. Stark, M. J., Black, S., Sneddon, A. A., and Andrews, P. D. (1994) Genetic analyses of yeast protein serine/threonine phosphatases. *FEMS Microbiol. Lett.* **117**, 121–130.
42. Serebriiskii, I. G. and Golemis, E. A. (2000) Uses of lacZ to study gene function: evaluation of beta-galactosidase assays employed in the yeast two-hybrid system *Anal. Biochem.* **285**, 1–15.

43. Harper, J. W., Adami, G. R., Wei, N., Keyomarsi, K., and Elledge, S. J. (1993) The p21 Cdk-interacting protein Cip1 is a potent inhibitor of G1 cyclin-dependent kinases. *Cell* **75**, 805–816.
44. Hanahan, D. (1985) Techniques for transformation of *Escherichia coli*, in *DNA Cloning: A Practical Approach* (Glover, D. M., ed.), IRL Press, Oxford, Vol. 1, pp. 109–135.
45. Hanahan, D. (1983) Studies on transformation of *Escherichia coli* with plasmids *J. Mol. Biol.* **166**, 557–580.
46. Schiestl, R. H., Manivaskam, P., Woods, R. A., and Gietz, R. D. (1993) Introducing DNA into yeast by transformation, in *Methods; A Companion to Methods in Enzymology* (Johnston, M. and Fields, S., eds.), Academic, San Diego, Vol. 5, pp. 79–85.
47. Gelbart, W. M., Crosby, M., Matthews, B., et al. (1997) FlyBase: a *Drosophila* database. The FlyBase consortium. *Nucleic Acids Res.* **25**, 63–66.

Identification of Cellular Protein Phosphatase-1 Regulators

David W. Roadcap, Matthew H. Brush, and Shirish Shenolikar

Summary

Protein phosphatase-1 (PP1) is a major phosphoserine/phosphothreonine phosphatase that regulates multiple physiological events in all eukaryotic cells. Action of PP1 in cells is dictated by the association of PP1 catalytic subunit with one or more regulatory subunits that define both its catalytic function and subcellular localization. This chapter describes key methods used to identify PP1-binding proteins and assess their ability to modulate PP1 functions in mammalian cells. These methods include affinity isolation of cellular PP1 complexes, analysis of direct PP1 binding, modulation of PP (protein phosphatase) activity, and testing for the presence of the newly identified PP1 complex in cells and cellular compartments. Together these techniques set the foundation for further studies that can establish the physiological significance of this PP1 complex.

Key Words: Protein phosphatase-1; regulatory subunits; overlays; affinity chromatography; enzyme assays; immunoprecipitation

1. Introduction

More than 97% of protein phosphorylation in eukaryotic cells occurs on serine and threonine residues. Remarkably, 40–70% of serine/threonine phosphatase activity in most mammalian tissues is represented by a single enzyme, termed protein phosphatase-1 (PP1). Whereas three human genes encode PP1 catalytic subunits, *in vitro* analyses of the isolated catalytic subunits PP1 α , PP1 β , and PP1 γ (alternate splicing in some human tissues generates two isoforms, PP1 γ 1 and PP1 γ 2) indicate that these enzymes were essentially indistinguishable in terms of exhibiting a broad substrate specificity and similar overall activity (*1*). However, cellular studies show that the PP1 isoforms are differentially distributed among organelles, where they act on phosphoprotein substrates that are colocalized in these subcellular compartments. Subsequent studies analyzed potential mechanisms of dictating the subcellular

From: *Methods in Molecular Biology*, Volume 365: *Protein Phosphatase Protocols*
Edited by: G. Moorhead © Humana Press Inc., Totowa, NJ

distribution and/or substrate specificity of PP1 isoforms in mammalian tissues, and to date, more than 65 PP1-binding proteins or putative regulatory subunits have been identified (2,3). Analysis of many PP1 regulators confirms that they associate with specific PP1 isoforms and target these enzymes to specific cellular compartments. Moreover, *in vitro* studies show that in the presence of these proteins, the activity of PP1 catalytic subunits is modified to promote dephosphorylation of some phosphoproteins while restricting or inhibiting dephosphorylation of other substrates. Thus, the emerging paradigm is that eukaryotic cells contain multiple PP1 complexes, each composed of a PP1 catalytic subunit bound to one or more regulators. However, it should be stressed that PP1-binding proteins might serve many different functions. In the simplest scenario, a PP1-associated protein might be a substrate of the bound phosphatase. Other proteins might associate with PP1 to regulate its phosphatase activity, either functioning as targeting subunits that direct its subcellular localization and substrate recognition or as inhibitors that modulate the overall phosphatase activity against multiple substrates.

Most if not all the known PP1-binding proteins are also phosphoproteins. Growing evidence suggests that the phosphorylation of PP1 regulators might be an important mechanism for decoding physiological signals that allow for the spatial and temporal regulation of phosphatase complexes. This, in turn, raises the possibility that PP1 functions in eukaryotic cells are regulated by other phosphatases that dephosphorylate the PP1 regulators to establish signaling pathways involving PP cascades. In any case, the dominant thinking among experimentalists is that to gain a full understanding of the function and regulation of PP1 in eukaryotic cells requires the identification of its binding proteins and regulators. In this regard, this chapter is focused on current methods of identifying PP1-interacting proteins and characterizing their association and function as PP1 regulators. Specifically, we will discuss the use of affinity approaches involving immobilized toxins that function as phosphatase inhibitors to purify cellular PP1 complexes. Yet other methods use overlays, far Westerns, and *in vitro* enzymatic assays to demonstrate direct association with PP1 and to examine the impact of recombinant or purified polypeptides on PP1 activity. Finally, we will describe a cell-based assay that can help to elucidate the physiological function and regulation of the newly identified PP1 complex.

2. Materials

1. Microcystin LR–Sepharose (see Chapter 4).
2. Phosphate-buffered saline (PBS): 4.3 mM sodium phosphate, dibasic (Na_2HPO_4), 137 mM sodium chloride (NaCl), 2.7 mM potassium chloride (KCl), 1.4 mM potassium phosphate, monobasic (KH_2PO_4).
3. Phenylmethylsulfonyl fluoride (PMSF): 100 mM stock.

4. Benzamidine: 100 mM aqueous stock.
5. NETN150: 10 mM Tris-HCl, pH 7.5, containing 1 mM EDTA, 150 mM NaCl and 0.5% Nonidet P-40 or NP-40.
6. 2X Sodium dodecyl sulfate (SDS) sample buffer: 100 mM Tris-HCl, pH 6.8, 3.5% SDS, 4% 2-mercaptoethanol, 10% glycerol, 0.12% bromophenol blue.
7. 50 mM Sodium bicarbonate, pH 8.0, containing 15 mM of 2-mercaptoethanol and 1 mM MgCl_2 .
8. Digoxigenin-3-*O*-methylcarbonyl- ϵ -aminocaproic acid-*N*-hydroxysuccinimide ester (Roche).
9. Dimethyl sulfoxide (DMSO).
10. 50 mM Tris-HCl, pH 7.5, containing 55% (v/v) glycerol, 15 mM of 2-mercaptoethanol, and 1 mM MnCl_2 .
11. SDS-PAGE (polyacrylamide gel electrophoresis) and Western transfer equipment.
12. Polyvinylidene fluoride (PVDF) membrane.
13. Tris-buffered saline (TBS): 50 mM Tris-HCl, pH 7.5, 150 mM NaCl.
14. TBS containing 4% (w/v) dried skim milk.
15. Bovine serum albumin (BSA) powder.
16. Overlay blocking reagent (proprietary Roche reagent).
17. 50 mM K_3PO_4 (aqueous).
18. Alkaline phosphatase-conjugated anti-digoxigenin antibody (Roche).
19. 200 mM Tris-HCl, pH 9.2, containing 10 mM MgCl_2 .
20. Aqueous nitroblue tetrazolium chloride (NBT, 50 mg/mL). This solution is light sensitive and should be kept in a dark container.
21. 5-Bromo-4-chloro-3-indolyl-phosphate (BCIP, 50 mg/mL) in dimethylformamide. This solution becomes discolored on storage and should be discarded if this occurs.
22. Cell transfection reagent. Our data suggests that Lipofectamine 2000 (Invitrogen) and FuGENE 6 (Roche) are equally effective for these experiments.
23. RIPA lysis buffer: 55 mM Tris-HCl, pH 8.0, containing 150 mM NaCl, 1% (w/v) NP-40, 0.5% (w/v) sodium deoxycholate, and 0.1% (w/v) SDS.
24. Protein-A conjugated to agarose or Sepharose.
25. Protein-G conjugated to agarose or Sepharose.
26. Anti-PP1 antibody (Upstate or Santa Cruz).

3. Methods

3.1. Isolation of Cellular PP1 Complexes (Affinity Chromatography on Microcystin-LR-Sepharose)

Microcystin-LR is an environmental toxin and a potent inhibitor of PP1 and PP2A-like phosphatases. Structural studies show that microcystin-LR binds within the PP1 catalytic center (4). This permits the use of immobilized microcystin-LR-Sepharose (MC-Sepharose) as an affinity matrix to rapidly purify cellular complexes containing PP1 [and PP2A, PP4, PP5, and PP6

(5–11)] from cell and tissue extracts. The protocol described below is designed to rapidly pull down or isolate cellular protein phosphatases, specifically PP1, and associated regulatory subunits. As MC–Sepharose targets the catalytic site of protein phosphatases, this approach is primarily directed at isolating active PP complexes, whereas inactive complexes containing inhibitors that occlude their catalytic site are not anticipated to bind this affinity matrix. Prior studies (9) suggest that for reasons that are still poorly understood, PP1 is preferentially isolated from tissue extracts using MC–Sepharose. Nevertheless, this affinity matrix can clearly associate with several different PP catalytic subunits. Thus, additional studies, such as PP1 overlays (described below) or Western immunoblotting with antibodies against known PP1 regulators, are used to establish the presence of PP1 regulators and/or define the composition of the cellular PP1 complexes (*see Figs. 1 and 2*).

1. Equilibrate MC–Sepharose in ice-cold PBS by repeatedly (three times) suspending the affinity matrix in the buffer, sedimenting the beads (centrifugation at 800g for 1 min), and removing the supernatant.
2. Aliquot the MC–Sepharose suspension into microfuge tubes (25- μ L bead bed volume per 1.5-mL tube).
3. Mix 250 μ L of ice-cold tissue extract or cell lysate (approx 10 mg/mL total protein) with MC–Sepharose (25 μ L bed volume). Note that the presence of detergents, reducing agents, and other critical constituents of the lysates preparation will not prevent or interfere with PP1 binding to MC–Sepharose; thus, this method can be used with a wide variety of cell lysates (*see Note 1*).
4. To avoid proteolysis of PP1 regulators, protease inhibitors such as PMSF (1 mM) and benzamidine (1 mM) should be included in the cell lysates/MC–Sepharose incubation mixture (*see Notes 2 and 3*).
5. Incubate the lysate/MC–Sepharose mixture using an end-over-end shaker at 4°C for approx 1 h. For quantitative extraction of less abundant PP1 regulators, the mixture should be incubated for periods up to 3 h (*see Note 4*).
6. Sediment the protein-bound MC–Sepharose using centrifugation at 800g for 1 min at 4°C and remove all excess supernatant. During this procedure and all subsequent washes, it is important to minimize disturbance of the beads as this could promote the removal of beads, and reduce the overall yield of bound proteins. (*see Note 5*)
7. Wash the protein-bound beads at least three times by resuspending the sedimented beads in 20 vol of ice-cold NETN150, gently shaking, sedimenting the beads by centrifugation at 800g for 1 min, and carefully removing all supernatant. (*see Notes 4 and 6*.)
8. To elute the PP1 complexes from the MC–Sepharose, add 25 μ L of 2X SDS sample buffer to the beads (*see Note 7*). After heating at 95°C for 5 min, solubilized proteins are subjected to SDS-PAGE and analyzed by direct protein staining or other techniques, including PP1 overlays (described in **Subheading 3.2.**) and Western immunoblotting with antibodies against known PP1 regulators.

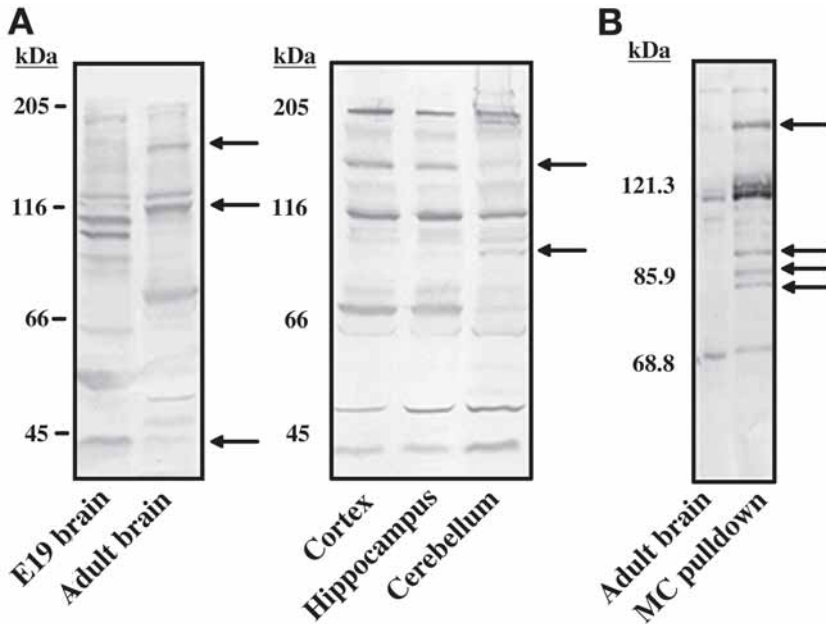


Fig. 1. Overlay detection of PP1-interacting proteins. **(A)** Whole brains were removed from adult and embryonic day 19 (E19) rats, and the isolated tissue was homogenized in a Dounce homogenizer in 3 vol of 50 mM Tris-HCl, pH 7.5, containing 5 mM EDTA, 5 mM EGTA, 10 mM NaCl, and a protease inhibitor cocktail. Following centrifugation to remove particulate matter, 60 μ g of adult and E19 lysates were subjected to SDS-PAGE and transferred to a PVDF membrane, where PP1-interacting proteins were detected by a PP1 overlay (left panel). Adult rat brain was also dissected, and cortex, hippocampus, and cerebellum were individually prepared, homogenized, and analyzed by PP1 overlay using the same protocol (right panel). Arrows highlight PP1-interacting proteins whose expression levels differed between E19 and adult rats or between brain regions. **(B)** MC-Sephacrose was utilized to isolate PP1-interacting proteins from whole adult rat brain lysates prepared as in **(A)**. The isolated PP1-interacting proteins and reserved lysate were analyzed by a PP1 overlay. Arrows highlight PP1-interacting proteins that were concentrated during MC-affinity isolation.

3.2. Detection of PP1 Regulators Using PP1 Overlays

Structural analyses of PP1 regulators has highlighted a tetrapeptide PP1-binding motif, K/R-I/V-X-F, that is highly conserved in most but not all PP1-binding proteins. Although most PP1 regulators also contain additional PP1-binding domains (3), single amino acid substitutions within the tetrapeptide sequence, particularly in place of the hydrophobic residues I/V or F,

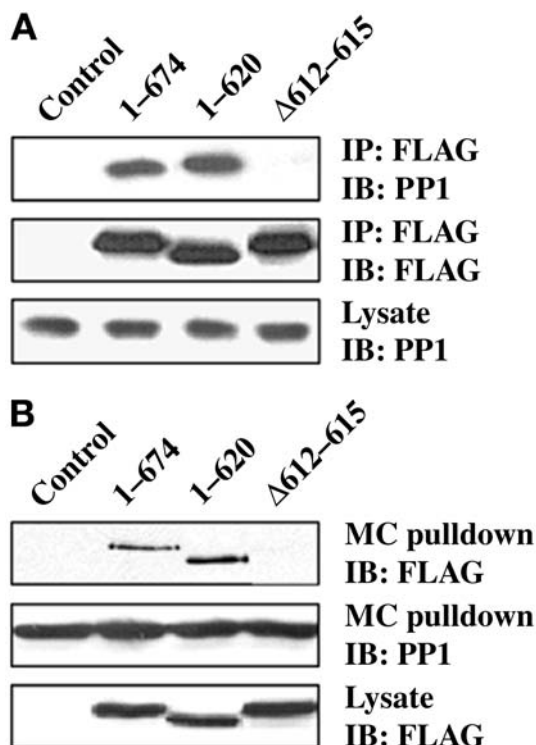


Fig 2. Coimmunoprecipitation and microcystin affinity isolation of cellular phosphatase complexes. **(A)** HEK293T cells overexpressing the indicated FLAG-tagged GADD34 proteins were lysed and subjected to immunoprecipitation (IP) with anti-FLAG M2 beads. The immunoprecipitates and lysates were then subjected to SDS-PAGE, transferred to a PVDF membrane, and immunoblotted (IB) with anti-PP1 and anti-FLAG antibodies. **(B)** Cellular PP1 complexes from HEK293T cells overexpressing the indicated FLAG-tagged GADD34 proteins were affinity isolated on MC-Sephrose. The cell lysates and microcystin-bound phosphatase complexes were then subjected to SDS-PAGE and immunoblotted (IB) with anti-FLAG and anti-PP1 antibodies. Note the absence of an interaction between the $\Delta 612-615$ GADD34 mutant and PP1, indicating a requirement for these residues for PP1 binding.

abrogated PP1 binding and established the pivotal role of this simple sequence in PP1 binding. X-ray crystallography suggested that the region encompassing the K/R-I/V-X-F motif in PP1 regulators is largely unstructured and docked as a linear peptide in a conserved hydrophobic groove found on the surface of all eukaryotic PP1 catalytic subunits. This simple mode of interaction, namely the lack of ordered structure of the PP1-binding domain in many cellular PP1 regulators, allowed the development of an overlay or far-Western assay that can

detect most but not all cellular PP1-binding proteins (*see Note 8*). This technique, which utilizes SDS-PAGE to separate cellular proteins, provides a convenient assay for evaluating a large number of tissue samples, yielding critical information on the number of PP1 interactors and their apparent molecular size (*see Fig. 1A*). When combined with prior affinity chromatography on MC-Sephrose, which concentrates PP1 complexes from cell lysates, the overlays can be used to detect even very low abundance PP1 complexes (*see Fig. 1B*). When combined with direct peptide sequencing, this approach has identified numerous novel PP1 regulators (*12*). However, the keys to these overlays is a source of highly purified PP1 catalytic subunits and a method for detecting the PP1 catalytic subunits when bound to the electrophoretically separated lysate proteins (*see Note 9*).

3.2.1. Preparation of Digoxigenin-Conjugated PP1 Catalytic Subunits

1. This protocol requires a source of highly purified PP1 catalytic subunits. This is most conveniently achieved by the expression of recombinant PP1 catalytic subunits in *Escherichia coli* (*13*), which are then extensively purified on either MC-Sephrose (*9*) or heparin-Sephrose (*14*). For this protocol, 2 mL of recombinant PP1 catalytic subunits (up to 0.5 mg/mL total protein) is used (*see Note 10*).
2. Dialyze the purified PP1 against 50 mM sodium bicarbonate, pH 8.0, containing 15 mM 2-mercaptoethanol and 1 mM of MnCl₂ (*see Note 11*).
3. Prepare a stock solution (1 mg/mL) of digoxigenin-3-O-methylcarbonyl- ϵ -aminocaproic acid-*N*-hydroxysuccinimide ester in dimethyl sulfoxide (DMSO).
4. Mix the dialyzed recombinant PP1 catalytic subunits with 200 μ L of digoxigenin *N*-hydroxysuccinimide ester, which modifies free amines (mostly lysines) on the surface of PP1, and incubate at room temperature for 1 h.
5. Dialyze the digoxigenin-conjugated PP1 against 50 mM Tris-HCl, pH 7.5, containing 55% (v/v) glycerol, 1 mM MnCl₂, and 15 mM of 2-mercaptoethanol at 4°C. The labeled phosphatase can be stored at -20°C for periods of up to 1 yr with no significant loss in overlay activity.
6. A critical test for the quality of the digoxigenin-PP1 probe and hence the reproducibility of the overlay assay is that there is no significant loss in the activity of digoxigenin-PP1, measured using phosphorylase *a* as substrate (*see below*), when compared with the unmodified purified recombinant PP1 catalytic subunit. Furthermore, the efficiency of the labeling can be confirmed by detection of a single 37-kDa band (with less than 1 ng total protein) by Western immunoblotting with an antidigoxigenin antibody.

3.2.2. Far-Westerns or Overlays with Digoxigenin-PP1

1. Tissue extracts or cell lysates should be subjected to SDS-PAGE to separate the polypeptides. A 10% (w/v) polyacrylamide gel provides for effective separation of a broad range of lysate proteins. Following SDS-PAGE, electrophoretic transfer of the polypeptides from the polyacrylamide gel to a PVDF membrane is

undertaken at 250 mA for 2 h. Following the transfer, block the PVDF membrane in TBS containing 4% (w/v) dried milk for 1 h at room temperature.

2. Dilute the stock digoxigenin–PP1 solution to a final concentration of 50 nM in TBS containing 1 mg/mL BSA (the presence of BSA promotes the stability of PP1 in these dilute solutions) and incubate with the blocked PVDF membrane for 3 h at room temperature to detect most PP1-binding proteins. However, incubation of the PVDF membrane with digoxigenin–PP1 can be prolonged to overnight at 4°C to enhance the detection of low-abundance PP1-binding polypeptides (see **Notes 12** and **13**).
3. Wash the membrane twice with TBS and incubate with the overlay blocking reagent (0.1 g/20 mL of 50 mM K₃PO₄, pH 8.5) for 30 min at room temperature (see **Note 14**).
4. Wash the blocked PVDF membrane three times with TBS, with a minimum of 5 min allowed for each wash.
5. Incubate the washed membrane with antidigoxigenin antibody conjugated to alkaline phosphatase (1 : 1000 dilution in TBS) for 1 h at room temperature. Further wash the PVDF membrane three times with TBS, allowing 5 min for each wash.
6. After the final wash, place the blot in 10 mL of 0.2 M Tris-HCl, pH 9.2, containing 10 mM MgCl₂, 66 µL NBT (stock solution of 50 mg/mL), and 33 µL BCIP (stock solution of 50 mg/mL) to develop the overlay. This volume of developing solution is sufficient for one overlay (see **Note 15**). Minimize exposure to light during the development process to enhance the activity of the development solution. Occasionally shake the dish containing the developing blot to ensure complete coverage of the PVDF membrane. Development of the color reaction detecting the bound PP1 might require between 5 and 45 min to achieve the desired contrast of stained protein bands over the membrane background.
7. To stop the development process, remove the development buffer and rinse the membrane repeatedly with deionized water. Allow the PVDF membrane to dry at room temperature and store enclosed in Saran Wrap or a sealed polythene bag prior to recording the results by photography or scanning.

3.3. Functional Effects of PP1-Binding: Protein Phosphatase Assays

Most PP1-binding proteins appear to modulate the activity of the bound PP1 catalytic subunit. This is most often seen as inhibition of the dephosphorylation of the commonly utilized substrate, phosphorylase *a* (**15**). This by itself does not constitute the functional or physiological designation of these PP1 interactors as endogenous PP1 inhibitors, because, when examined using a physiologically relevant substrate, the PP1 regulators might either show no inhibition or activate the dephosphorylation of these substrates. On the other hand, as stated above, the use of MC–Sepharose is anticipated to exclude the isolation of endogenous PP1 inhibitors, which also share the ability to inhibit PP1 activity against a wide range of phosphoprotein substrates. The phosphorylase *a* phosphatase assay not only provides evidence of the association of the

PP1 catalytic subunit with newly identified regulators but also might yield insights into the relative affinity of these proteins for specific PP1 isoforms (see **Note 16**). It should be noted that some PP1 regulators lack the conserved PP1-binding motif and utilize more complex multivalent modes of association with the PP1 catalytic subunits. Many of these regulatory subunits are not readily detected using overlays with digoxigenin-PP1. In this case, the protein phosphatase assay using purified or recombinant proteins provides good evidence for the direct association of these proteins with the PP1 catalytic subunit. Alternately, in vitro sedimentation of purified PP1 catalytic subunits using recombinant regulatory subunits expressed in *E. coli* as GST-fusion proteins (**16**) might provide further evidence for their direct association with the PP1 catalytic subunit. This protocol can be carried out as previously described by Beullens et al. (**15**) and can also be accomplished using commercially available kits (Gibco-BRL).

3.4. Immunoprecipitation of Cellular PP1 Complexes

As noted above, not all PP1 regulators, even those containing potential K/R-I/V-X-F motifs, are effectively identified using digoxigenin-PP1 overlays. With nearly 10% of proteins encoded in the human genome containing potential K/R-I/V-X-F motifs, this also raises the possibility that digoxigenin-PP1 overlays could identify polypeptides, which do not normally associate with PP1 in vivo. Thus, it is crucial for investigators to demonstrate the ability of these newly identified regulators to be present in cellular PP1 complexes, thereby excluding potential in vitro artifacts and building confidence in the ability of these proteins to regulate PP1 functions in eukaryotic cells. This can be achieved by evaluating the ability of proposed PP1 regulators to coimmunoprecipitate with various PP1 isoforms (see **Fig. 2**) (see **Note 17**). The coimmunoprecipitation of PP1 with putative regulators is best undertaken in cells that express both proteins. However, clearly this is more difficult to achieve if the PP1 regulators exists at very low abundance or where effective immunoprecipitating antibodies are unavailable. In these situations, the putative PP1 regulators might be overexpressed in cells prior to evaluating their ability to associate with PP1 by coimmunoprecipitation. The latter studies can be greatly enhanced by the introduction of convenient epitopes on the expressed proteins, which can be efficiently sedimented with commercially available antibodies. To exclude the possibility that the proteins of interest displayed non-specific association with PP1, this protocol can be combined with mutagenesis of the PP1-binding motif in the ectopically expressed PP1-binding proteins that might be predicted to attenuate or abrogate their association with the endogenous PP1 catalytic subunits. Furthermore, such mutagenesis studies can be used to define novel regions of PP1-binding proteins that are necessary for

PP1 interaction (*see* **Fig. 2**). Although the protocol described below can be used with lysates of tissues and cells, which contain both PP1 and the regulatory subunits, the method outlines experiments with epitope-tagged PP1 regulators that might be overexpressed in cultured cells by DNA transfection.

1. Many cultured cells, including COS-7, HeLa, and HEK293, can be transfected with expression plasmids in conjunction with commercially available transfection agents. We have noted that Lipofectamine 2000 and FuGENE 6 are effective transfection agents that facilitate robust expression of proteins in cultured cells. The following protocol is designed for the number of cells present in a single well of a standard six-well tissue culture dish.
2. After allowing adequate time for protein expression (24–48 h), place the transfected cells on ice and wash once with ice-cold PBS.
3. Remove PBS by aspiration and detach the cells from each well in 1 mL of ice-cold PBS using a rubber-tipped cell scraper.
4. Transfer cell suspension into a 1.5-mL microfuge tube and sediment the cells by centrifugation at 1000g for 5 min at 4°C.
5. After removal of PBS, add 500 μ L RIPA buffer containing a protease inhibitor cocktail (*see* **Note 18**) to each tube. Resuspend the cells by repeated pipetting and stand on ice for 10 min.
6. Spin down lysates in a microcentrifuge at approx 16,000g at 4°C for 10 min.
7. Transfer supernatant to a new microfuge tube and add 2 μ g of antibody against the epitope tag (*see* **Note 19**). Incubate the mixture using an end-over-end shaker at 4°C for 1.5 h (*see* **Note 4**).
8. Prepare a 50 : 50 mixture of protein-A–Sepharose and protein-G–Sepharose beads and equilibrate in ice-cold PBS by repeated (three times) resuspension and pelleting the beads at 800g for 1 min.
9. Add a 25- μ L bed volume of protein-A/G beads and continue incubation at 4°C for an additional 1.5 h.
10. Sediment the beads at 800g for 1 min and remove (and discard) the supernatants (*see* **Note 5**).
11. Wash the beads at least three times with ice-cold NETN150 (at least 20 volumes) and sediment at 800g for 1 min (*see* **Notes 4 and 6**).
12. Resuspend the beads in 25 μ L of 2X SDS sample buffer; heat at 95°C for 5 min. Detection of PP1-binding proteins is accomplished by SDS-PAGE coupled with immunoblotting for either PP1 and/or immunoprecipitated protein of interest (*see* **Notes 20 and 21**).

3.5. Summary

The above methods demonstrate the favored approach of our laboratory in the identification of novel PP1 regulators. Similar strategies developed by other laboratories have also been detailed previously (**16,17**). Our initial studies utilize affinity chromatography on MC–Sepharose to concentrate and purify endogenous PP1 complexes. The specific PP1-binding proteins are then iden-

tified using digoxigenin–PP1 overlays accompanied by either Western immunoblotting or direct peptide sequencing. As some PP1-binding proteins fail to overlay, exhibit low affinity, or display low abundance using digoxigenin–PP1 overlays, we also use enzyme assays with a recombinant or tissue-purified PP1 catalytic subunit to evaluate the ability of recombinant PP1 regulators to modulate PP1 activity, specifically to inhibit the *in vitro* dephosphorylation of phosphorylase *a*. Alternately, the recombinant regulators expressed as GST-fusion proteins are used to assess their ability to pull down specific PP1 isoforms. These latter assays allow for quantitative analysis of the mode of PP1 binding and analysis of critical PP1-binding domains, such as the R/K-I/V-X-F motif. Such studies are critical to generate appropriate non-PP1-binding polypeptides. Finally, the wild-type and non-PP1-binding (control) polypeptides are expressed in mammalian cells and assessed for their ability bind PP1, direct its subcellular redistribution (best visualized by immunocytochemistry with antibodies directed against appropriate PP1 isoform recognized by the PP1 regulator), and possibly identify the cellular substrate(s) and/or physiological effects of the newly formed PP1 complex.

4. Notes

1. When performing sedimentations with MC–Sepharose, ensure the presence of sufficient volume to allow effective mixing of the beads with cell lysates when shaken using the end-over-end shaker. For example, in a 1.5-mL microfuge tube, effective mixing requires a lysate volume of at least 250 μ L.
2. Early biochemical studies showed that in contrast to other protein serine/threonine phosphatases, the PP1 catalytic subunit is remarkably resistant to *in vitro* proteolysis by trypsin. However, many PP1 regulators are readily degraded by cellular proteases. To avoid extensive degradation of PP1 regulators during their affinity isolation on MC–Sepharose, additional protease inhibitors, specifically aprotinin (1 μ g/mL), leupeptin (1 μ g/mL), and pepstatin A (1 μ g/mL) can be added to the incubation mixture. These compounds have no effect on PP1 activity or the ability of PP1 complexes to bind MC–Sepharose.
3. Structural studies show that many phosphatase inhibitors, including microcystin LR, okadaic acid, tautomycin, and calyculin A bind at the same site on the PP1 catalytic subunit and thus compete for PP1 binding. These compounds prevent the association of cellular complexes to MC–Sepharose and the addition of excess PP1 inhibitors to cell lysates can be used a negative control to establish the specificity of the association of the putative PP1 regulators to the affinity matrix.
4. Potential nonspecific sedimentation of cellular proteins during the immunoprecipitation studies can be greatly decreased by the direct incubation of cell lysates with protein-A Sepharose for 30 min at 4°C prior to the addition of the anti-PP1 (or antiregulator) antibody. In addition, more stringent washes, increasing the salt concentration in the wash buffer, or increasing the number of washes could be considered.

5. The most convenient way of removing washes from MC–Sepharose chromatography is through aspiration using a small-bore (23-gauge) needle. This limits removal or loss of the affinity beads and hence maximizes the yield of PP1 complexes.
6. Interaction of some targeting subunits with the PP1 catalytic subunit might be of low affinity (perhaps like inhibitor-1 requiring covalent modification to enhance its affinity for PP1). PP1 association with these regulators might be particularly sensitive to higher salt or detergent concentrations. Thus, some experiments should be undertaken with reduced stringency of washes either by lowering salt concentration or eliminating detergents. Washing the beads with PBS or TBS might be a useful alternative but might also increase nonspecific protein binding.
7. The proteins bound on MC–Sepharose can also be eluted using chaotropic agents, such as 3 *M* sodium thiocyanate (18). Unlike SDS sample buffer, this will not denature the PP1 complexes, allowing their functional analysis following extensive dialysis.
8. A limitation of digoxigenin–PP1 overlays is the apparent requirement for a simple or unstructured PP1-binding domain, such as the R/K-I/V-X-F motif, which can be readily refolded following electrophoretic separation of the PP1 regulators using denaturing gels. Proteins that bind with PP1 via highly structured or multivalent domains might not be detected by overlays.
9. An alternate strategy to the use of digoxigenin-conjugated PP1 catalytic subunits as probes in the overlay assays is to express and purify epitope-tagged PP1 catalytic subunits. When utilized as probes in overlay assays, the epitope-tagged PP1 can be detected using a high-affinity antibody directed against the epitope. The use of an anti-PP1 antibody is not recommended as this antibody might detect the presence of endogenous PP1 catalytic subunits and thus compete with or attenuate the detection of the overlaid PP1 probe. Yet another approach is the use of ¹²⁵I-labeled PP1 catalytic subunit using Iodogen (Pierce) to detect PP1 binding by autoradiography. This approach, however, yields significant background radioactivity. In our experience, digoxigenin conjugation, possibly by enhancing its immunodetection by conjugating to multiple sites on the PP1 surface, provides for the most reliable and reproducible probes for PP1 overlays.
10. Three PP1 isoforms, PP1 α , PP1 β , and PP1 γ 1, are expressed in most mammalian cells. Some PP1 regulators [e.g., neurabin-I and neurabin-II (19)] demonstrate a high degree of specificity for selected PP1 isoforms and might be better detected by overlays that utilize the specific PP1 isoforms as probes (17).
11. Buffers containing primary amines, such as Tris-HCl or glycine, should not be used in the conjugation reactions containing PP1 and digoxigenin, as these amines will compete for conjugation with digoxigenin and thus impair the modification of the PP1 catalytic subunit.
12. The conjugation reactions sometimes yield somewhat lower-quality digoxigenin–PP1 overlay probes and thus should be evaluated using known PP1 regulators as positive controls. The variable quality often results from either inadequate or low conjugation of the PP1 catalytic subunit or excess modification that can result in

the inactivation or even denaturation of the PP1 catalytic subunit. In this regard, the analysis of PP1 activity before and after digoxigenin conjugation provides an excellent readout of excessive PP1 modification. An excellent control for extensive nonspecific association is the inclusion of a competing PP1-binding synthetic peptide (5 μ M), such as one containing a known R/K-I/V-X-F motif, which can compete for PP1 binding to R/K-I/V-X-F-containing regulators. These peptides not only selectively eliminate the detection of R/K-I/V-X-F-containing PP1-binding proteins, but they might also highlight PP1 regulators that utilize other domains to associate with the PP1 catalytic subunit (20,21).

13. The activity of many PP1 inhibitors is modulated by reversible protein phosphorylation. PP1 inhibitors such as inhibitor-1 and DARPP-32, which are activated following their phosphorylation by protein kinase A, are poorly detected in their basal unphosphorylated form (despite the presence of a KIQF PP1-binding motif) when overlaid with digoxigenin-PP1. These proteins are, however, more readily visualized following the stimulation of cells and tissues by hormones that elevate intracellular cAMP.
14. The commercial overlay blocking reagent (Roche) dissolves slowly. Thus, this agent should be incubated at 60°C for 10–15 min to facilitate its solubilization. This solution should, however, be cooled to room temperature prior to incubation with the protein-bound PVDF membranes.
15. Alkaline phosphatase staining of digoxigenin-PP1-overlaid PVDF membranes allows for a controlled development of the color reaction that detects the bound digoxigenin-PP1. However, other antibody visualization techniques are sometimes preferred; for example, horseradish peroxidase (HRP)-conjugated antidigoxigenin antibodies that are compatible with enhanced chemiluminescence (ECL) detection allow for multiple exposures of the developing overlays. This is particularly useful in detecting multiple proteins that might differ in their expression levels and/or PP1 affinity. Overlays using a radiolabeled PP1 catalytic subunit might not only eliminate the need for a secondary antibody but also permit the quantification of PP1 binding using a phosphorimager.
16. Recombinant PP1 catalytic subunits, widely used as probes in overlays, are expressed in *E. coli* and contain Mn²⁺ in their catalytic sites. PP1 catalytic subunits isolated from mammalian tissues contain Zn and Fe. Thus, the recombinant PP1 catalytic subunits might show differences in their association with PP1 regulators when compared with the native PP1. For example, when compared to the tissue-purified PP1, recombinant PP1 catalytic subunits show 50- to 100-fold reduced sensitivity to inhibition in vitro by PKA-phosphorylated inhibitor-1. In contrast, both phosphatases are equally inhibited by inhibitor-2.
17. Yeast two-hybrid assays and pull-downs from cell lysates using GST-fusion proteins have been widely used to analyze protein-protein interactions. The latter assays function by competing for PP1 with endogenous cellular complexes and require a significant excess of the GST-fusion proteins and might fail to detect some high-affinity PP1 regulators. In contrast, yeast two-hybrid assays, which have been pivotal in the identification of many PP1 regulators, are also flawed,

yielding numerous false positives. Finally, regulatory interactions with the PP1 catalytic subunit can be detected by testing the effects on PP activity toward the common substrate, phosphorylase-*a* (18). Although most PP1 regulators thus far analyzed have displayed the ability to inhibit the dephosphorylation of this substrate, biochemical analysis of bona fide PP1 inhibitors, such as inhibitor-1 and inhibitor-2, show that PP1 binding and inhibition are distinct events and the lack of PP1 inhibition might not by itself be evidence that a protein does not bind PP1.

18. A recommended cocktail of protease inhibitors contains PMSF (1 mM), benzamidine (1 mM), aprotinin (1 µg/mL), leupeptin (1 µg/mL), and pepstatin A (1 µg/mL), although other protease inhibitor cocktails could be equally effective.
19. It is often advantageous to utilize commercially available beads that are covalently conjugated to epitope-specific antibodies. This significantly shortens the protocol, thereby minimizing the potential proteolysis of PP1 regulators.
20. For Western immunoblot analysis of the coimmunoprecipitations, it is useful to load a small aliquot of the cell lysate to provide an assessment of the efficiency of the sedimentation.
21. Given the prediction that over 10% of proteins encoded in the human genome contain a R/K-I/V-X-F sequence, it is likely that most are not PP1 regulators. Site-directed mutagenesis that eliminates PP1-binding can confirm these regions as a source of PP1 interactions. Specifically, substitutions of other amino acids in place of I/V or F results in the abolition of PP1 association (22,23). Such mutations can also serve as critical tools when evaluating the cellular effects of over-expressing these proteins, specifically in identifying the role of PP1 association.

Acknowledgments

Work presented in this chapter was supported by National Institutes of Health research grants RO1-NS 41063 and RO1-DK 52054 awarded to SS. We also thank Douglas Weiser for critical reading.

References

1. Zhang, Z., Bai, G., Shima, M., Zhao, S., Nagao, M., and Lee, E. Y. (1993). Expression and characterization of rat protein phosphatases-1 alpha, -1 gamma 1, -1 gamma 2, and -1 delta. *Arch. Biochem. Biophys.* **303**, 402–406.
2. Ceulemans, H. and Bollen, M. (2004). Functional diversity of protein phosphatase-1, a cellular economizer and reset button. *Physiol. Rev.* **84**, 1–39.
3. Cohen, P. T. (2002). Protein phosphatase 1: targeted in many directions. *J. Cell Sci.* **115**, 241–256.
4. Gehringer, M. M. (2004). Microcystin-LR and okadaic acid-induced cellular effects: a dualistic response. *FEBS Lett.* **557**, 1–8.
5. Campos, M., Fadden, P., Alms, G., Qian, Z., and Haystead, T. A. (1996). Identification of protein phosphatase-1-binding proteins by microcystin-biotin affinity chromatography. *J. Biol. Chem.* **271**, 28,478–28,484.

6. Colbran, R. J., Bass, M. A., McNeill, R. B., et al. (1997). Association of brain protein phosphatase 1 with cytoskeletal targeting/regulatory subunits. *J. Neurochem.* **69**, 920–929.
7. Kloeker, S. and Wadzinski, B. E. (1999). Purification and identification of a novel subunit of protein serine/threonine phosphatase 4. *J. Biol. Chem.* **274**, 5339–4537.
8. Kloeker, S., Reed, R., McConnell, J. L., et al. (2003). Parallel purification of three catalytic subunits of the protein serine/threonine phosphatase 2A family (PP2A(C), PP4(C), and PP6(C)) and analysis of the interaction of PP2A(C) with alpha4 protein. *Protein Expr. Purif.* **31**, 19–33.
9. Moorhead, G., MacKintosh, R. W., Morrice, N., Gallagher, T., and MacKintosh, C. (1994). Purification of type 1 protein (serine/threonine) phosphatases by microcystin–Sephacryl affinity chromatography. *FEBS Lett.* **356**, 46–50.
10. Westphal, R. S., Anderson, K. A., Means, A. R., and Wadzinski, B. E. (1998). A signaling complex of Ca²⁺-calmodulin-dependent protein kinase IV and protein phosphatase 2A. *Science* **280**, 1258–1261.
11. Zhou, G., Golden, T., Aragon, I. V., and Honkanen, R. E. (2004). Ser/Thr protein phosphatase 5 inactivates hypoxia-induced activation of an apoptosis signal-regulating kinase 1/MKK-4/JNK signaling cascade. *J. Biol. Chem.* **279**, 46,595–46,605.
12. Tran, H. T., Ulke, A., Morrice, N., Johannes, C. J., and Moorhead, G. B. (2004). Proteomic characterization of protein phosphatase complexes of the mammalian nucleus. *Mol. Cell Proteomics* **3**, 257–265.
13. Watanabe, T., da Cruz e Silva, E. F., Huang, H. B., et al. (2003). Preparation and characterization of recombinant protein phosphatase 1. *Methods Enzymol.* **366**, 321–338.
14. Walsh, A. H., Cheng, A., and Honkanen, R. E. (1997). Fostriecin, an antitumor antibiotic with inhibitory activity against serine/threonine protein phosphatases types 1 (PP1) and 2A (PP2A), is highly selective for PP2A. *FEBS Lett.* **416**, 230–234.
15. Beullens, M., Stalmans, W., and Bollen, M. (1998). The biochemical identification and characterization of new species of protein phosphatase 1. *Methods Mol. Biol.* **93**, 145–155.
16. Van Eynde, A. and Bollen, M. (2003). Validation of interactions with protein phosphatase-1. *Methods Enzymol.* **366**, 144–156.
17. Colbran, R. J., Carmody, L. C., Bauman, P. A., Wadzinski, B. E. and Bass, M. A. (2003). Analysis of specific interactions of native protein phosphatase 1 isoforms with targeting subunits. *Methods Enzymol.* **366**, 156–175.
18. Gibbons, J. A., Weiser, D. C., and Shenolikar, S. (2005). Importance of a surface hydrophobic pocket on protein phosphatase-1 catalytic subunit in recognizing cellular regulators. *J. Biol. Chem.* **280**, 15,903–115,91.
19. Terry-Lorenzo, R. T., Carmody, L. C., Voltz, J. W., et al. (2002). The neuronal actin-binding proteins, neurabin I and neurabin II, recruit specific isoforms of protein phosphatase-1 catalytic subunits. *J. Biol. Chem.* **277**, 27,716–27,724.
20. Schillace, R. V. and Scott, J. D. (1999). Association of the type 1 protein phosphatase PP1 with the A-kinase anchoring protein AKAP220. *Curr. Biol.* **9**, 321–324.

21. Steen, R. L., Martins, S. B., Tasken, K., and Collas, P. (2000). Recruitment of protein phosphatase 1 to the nuclear envelope by A-kinase anchoring protein AKAP149 is a prerequisite for nuclear lamina assembly. *J. Cell. Biol.* **150**, 1251–1262.
22. Oliver, C. J., Terry-Lorenzo, R. T., Elliott, E., et al. (2002). Targeting protein phosphatase 1 (PP1) to the actin cytoskeleton: the neurabin I/PP1 complex regulates cell morphology. *Mol. Cell. Biol.* **22**, 4690–4701.
23. Brush, M. H., Weiser, D. C., and Shenolikar, S. (2003). Growth arrest and DNA damage-inducible protein GADD34 targets protein phosphatase 1 alpha to the endoplasmic reticulum and promotes dephosphorylation of the alpha subunit of eukaryotic translation initiation factor 2. *Mol. Cell. Biol.* **23**, 1292–1303.

Assay for Three-Way Interaction of Protein Phosphatase-1 (Glc7) With Regulatory Subunits Plus Phosphatase Inhibitor-2

Masumi Eto and David L. Brautigan

Summary

A method is described using yeast conjugation to assay the interactions of a protein phosphatase-1 (PP1) inhibitor protein with holoenzymes formed *in situ* by expression of regulatory subunit fusion proteins that recruit endogenous Glc7, the yeast ortholog of PP1. Mutations in the canonical recognition motif VxF used to bind PP1 (Glc7) allow for analysis of direct from indirect (three-way) interactions.

Key Words: Yeast two-hybrid; conjugation; Nek2; neurabin; pVP16 and pGBT

1. Introduction

Over the past half-century, the mechanisms for regulation of protein serine/threonine (Ser/Thr) phosphatase (PPP) activity have been an elusive puzzle, not yet solved. The earliest preparations of so-called PR Enzyme (*1*) dephosphorylated the enzyme phosphorylase at the single phosphorylated site Ser14. This was and still is the classic and standard substrate for assay of PPP activity, in part because the protein is abundant, it crystallizes to purity, it has a single site of phosphorylation, and the reaction with phosphorylase kinase is rapid and stoichiometric. Other groups concentrated on purification of phosphatases that activated glycogen synthase (*2–7*), converting it from a form dependent (D) on added allosteric activator glucose 6-phosphate (G6P) to a form independent (I) of added G6P. About 30 yr ago during biochemical preparations, different groups found that phosphatases were exceptionally stable to denaturing conditions such as high concentrations of urea or mercaptoethanol, precipitation with ethanol at room temperature, or digestion with trypsin, and indeed these steps produced increased yields of activity coincident with recovery of a

From: *Methods in Molecular Biology*, Volume 365: *Protein Phosphatase Protocols*
Edited by: G. Moorhead © Humana Press Inc., Totowa, NJ

35-kDa form of active phosphatase (8–13). These observations led to the hypothesis that these phosphatases were composed of a catalytic subunit and one or more regulatory subunits that at least suppressed and probably regulated activity. This concept led to the landmark discovery of the first two heat-stable protein inhibitors, inhibitor-1 (which required phosphorylation by protein kinase A [PKA] for inhibitory activity) and inhibitor-2 (which was inhibitory regardless of phosphorylation), either of which could be added back to the 35-kDa phosphatase and block its activity (14). Subsequently, a second, inhibitor-resistant phosphatase in the 35-kDa fraction was detected and separated by chromatography and the sensitive and resistant phosphatases defined as type-1 and type-2 (15,16), that are now known as PP1 and PP2A, respectively. The type 2A phosphatase was purified in multiple laboratories as a heterodimer of 60 kDa (A) and 35 kDa (C) subunits and as a heterotrimer of the AC plus different B-subunits (17–20). On the other hand, the type 1 phosphatase was more elusive. Considerable effort from multiple groups about 20 yr ago went into study of a preparation of MgATP-dependent phosphatase, an essentially inactive heterodimer of inhibitor-2 plus the 35-kDa type 1 catalytic subunit (for review, see ref. 21). Phosphorylation of Thr72 in inhibitor-2 by glycogen synthase kinase-3 (GSK3) generated conformational changes that led to facile dephosphorylation with a transient activation of the heterodimer. The story changed considerably with the purification of multisubunit forms of the PP1 phosphatase, especially those containing a glycogen-targeting subunit (called G_M) (22) or a myosin-targeting subunit (called M130, or MYPT1, or MBS) (23–25; see review, ref. 26). Interestingly, these forms of PP1 were relatively resistant to the actions of inhibitor-1 and inhibitor-2, unlike the monomeric catalytic subunit. To account for this, it was (and still is) thought that there is an either–or situation of PP1 catalytic subunit binding to a regulatory (targeting) subunit or inhibitor-2. The concept is that a common high-affinity site on PP1 is used in a mutually exclusive way to engage proteins that regulate the phosphatase, involving other secondary and weaker sites of association. These regulatory proteins contain a VxF sequence motif to dock at the common high-affinity site on PP1 (see reviews, refs. 27 and 28).

The discovery of a myosin phosphatase inhibitor phosphoprotein called CPI-17 (protein kinase C [PKC]-potentiated inhibitor of 17 kDa) demonstrated that a PP1 holoenzyme composed of catalytic and regulatory subunits bound together using the VxF motif could nonetheless be inhibited with nanomolar potency (29–31). This challenges the concept that inhibitor proteins compete with regulatory subunits for binding to PP1 and suggested that, in addition, inhibitor proteins bound to regulatory subunits (i.e., that the inhibitors were specific for distinct PP1 holoenzymes) (see Fig. 1). Shenolikar and coworkers have shown that inhibitor-1 binds to GADD34 engaged with PP1 (32). Our

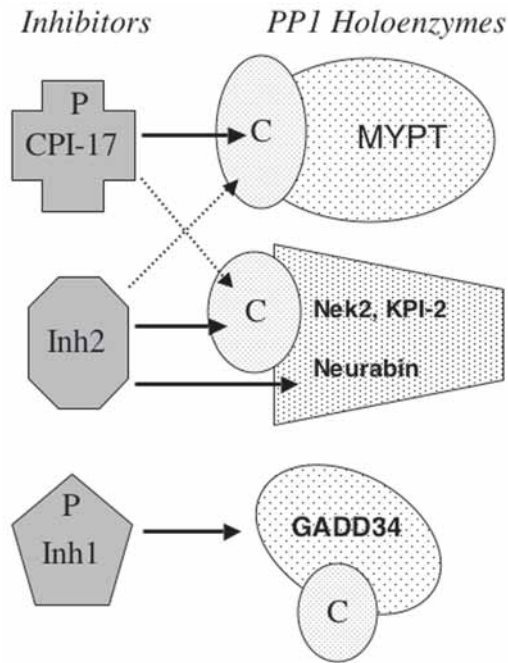


Fig. 1. Inhibitor proteins target separate PP1 holoenzymes.

group completed a yeast two-hybrid screen using inhibitor-2 as bait with a size-selected cDNA library from e9 mouse. We found 130 positives and 30 confirmed clones that identified five proteins: Nek2, neurabin, PNUTS, KIAA1079, and AB033168 (33–35). All of these proteins have VxF motifs to bind the PP1 catalytic subunit and bind inhibitor-2 as well. We have sorted them into two types: proteins that bind inhibitor-2 independent of PP1 (binding by the –AxA– mutants) and those that require PP1 for association, probably because the PP1 acts as a common partner, binding both proteins at separate sites. To confirm and test for three-way interactions of PP1 with inhibitor-2 and different regulatory subunits, we employed a yeast conjugation assay (33) described here (see Fig. 2). Fortunately, the yeast PP1 called Glc7 is similar enough in structure and function to bind subunits and inhibitors for metazoan organisms (36,37). Some of the advantages of this assay are as follows: (1) The interactions are assayed in living yeast cells under physiological conditions; (2) preparations of purified and functional recombinant proteins are unnecessary; (3) the signal/noise ratio is relatively higher, compared with a conventional GST-pull down assay; (4) it is easy to assay multiple samples (see Note 1). It is very convenient for the study of proteins that pose problems for expression

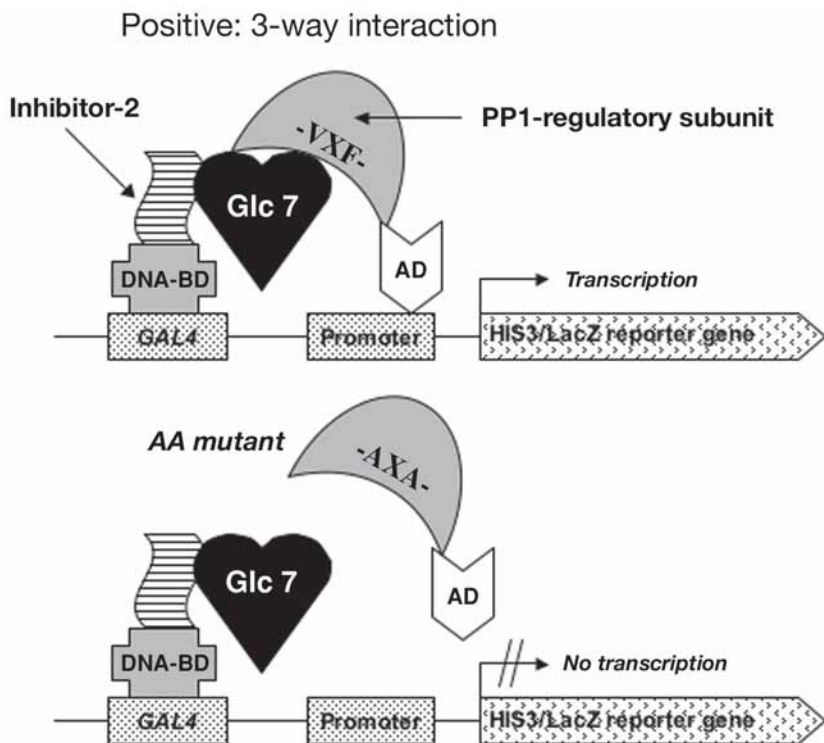


Fig. 2. Concept of the yeast three-hybrid assay for inhibitor-2.

in bacteria, such as Ser/Thr phosphatases. On the other hand, a limitation is the lack of quantification of the interactions. Regardless, we expect that the assay can prove useful to test other PP1 subunits and other PP1-inhibitor proteins.

2. Materials

1. DNA vectors pVP16 and pGBT (purchased from Clontech).
2. 30°C incubator
3. Sterilized 96-well plate with lid.
4. Sterilized loops.
5. Multi-8-channel pipet, volume variable, 10-μL and 200-μL scale.
6. Filter papers, round VMR grade no. 413, diameter: 7.5 cm and 11 cm; sterilized in a bag (dry cycle).
7. Parafilm™.
8. Solution of 20% glucose (dextrose): Dissolve 100 g of glucose with deionized water and adjust to 500 mL; autoclave to sterilize.

9. YPD plate (five each): Dissolve 2 g of Difco peptone and 1 g of yeast extract in 100 mL of deionized water in a glass 500-mL flask. Adjust pH to 6.5 with 1 M NaOH. Suspend 2 g of agar and autoclave the solution for 15 min at 120°C. Add 10 mL of 20% glucose solution; then pour approx 20 mL of the solution into 1.5 × 10-cm plastic culture dishes. Plates are placed on bench at room temperature to solidify and left over night for evaporation of excess liquid. Keep them in plastic bags at 4°C.
10. Single drop-out plates (-Leu) and (-Trp) for transformation (20 each): Mix 10.7 g of minimum SD base (Clontech cat. no. 8602-1), 0.25 g of complete supplement mix (-His/-Leu/-Trp) (Bio101 cat. no. 4530-122), and 8 g agar with 400 mL of distilled water in a 1-L flask. After autoclaving, add 40 mL 20% glucose solution and 4 mL of 100X amino acid solutions, (His plus Leu or Trp), and pour into 20 dishes. Process and store as YPD plates, as described in **item 9**.
11. Double-drop-out plate (- Leu, - Trp) (five each): Scale down the recipe of the single drop-out plates, and add 100X His.
12. Triple-drop-out plates (- His, - Leu, - Trp) (five each): Scale down the recipe of the single drop-out plate, and add no amino acids.
13. 100X His: Dissolve 0.1 g histidine with 50 mL deionized water. Filter-sterilize.
14. 100X Leu: Dissolve 0.3 g leucine with 50 mL deionized water. Filter-sterilize.
15. 100X Trp: Dissolve 0.2 g tryptophan with 50 mL deionized water. Filter-sterilize and store in the dark.
16. 1 M 3-amino-1,2,4-triazole (3-AT): Dissolve 0.84 g of 3-AT (Sigma cat. no. A-8056) with 9.8 mL of deionized water. filter-sterilize.
17. YPD liquid medium, 10 mL.
18. X-gal solution (for one 7.5-cm filter assay): Mix 87 µL of 40 mg/mL X-gal (5-bromo-4-chloro-3-indolyl-β-D-galactopyranoside in dimethyl formamide [DMF]) and 2-mercaptoethanol with 10 mL Z-buffer. Prepare fresh.
19. Z-buffer (1 L): Dissolve 16.1 g Na₂HPO₄·7H₂O, 5.50 g NaH₂PO₄·H₂O, 0.75 g KCl, 0.246 g MgSO₄·7H₂O with deionized water and adjust pH to 7.0.

3. Methods

1. Using standard procedures, prepare the plasmid vectors encoding fusion proteins with DNA-binding domain (pVP16) and transcription activation domain (pGBT). Miniprep scale of plasmid is sufficient for the assay.
2. Transform yeast W303 (MATα) and HF7c (MATa) with pGBT (Trp) and pVP16 (Leu) vectors, respectively. Harvest the colony when it becomes 3 mm in diameter (*see Note 2*).
3. Prepare master plates for transformants. Using sterilized toothpicks, colonies of pGBT and pVP16 transformants are pasted onto a quarter area of 10-cm (-)Trp and (-)Leu plates, respectively. Harvest yeast after 2–3 d, while still single colonies (*see Note 3*).
4. Dry one YPD plate for 1 h in a 30°C incubator (*see Note 4*).
5. Prepare the 96-well plate. Add 200 µL of YPD liquid medium into two lines of wells, as shown in **Fig. 3** (marked wells [1–5, A–D]).

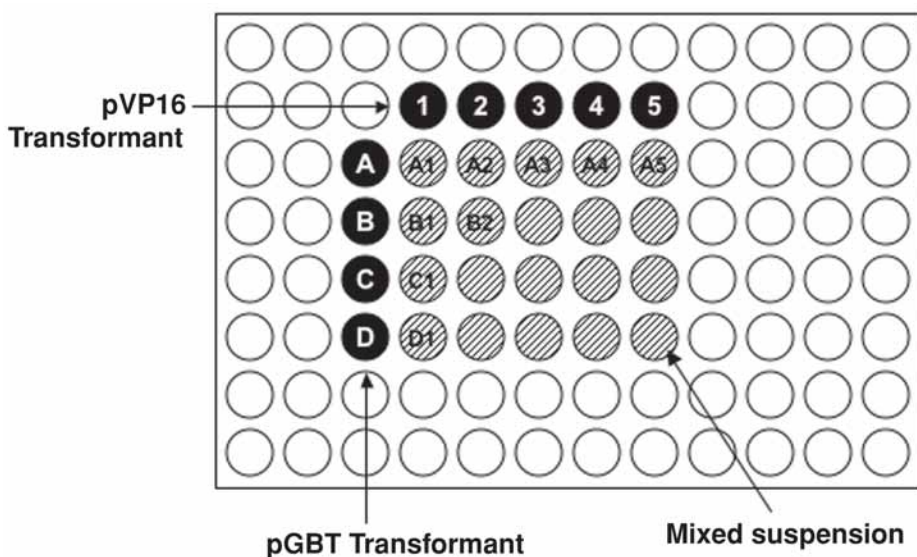


Fig. 3. A 96-well plate map for the yeast suspension mixtures.

6. Lift yeast using a loop and transfer into the YPD medium in the 96-well plate. Suspend yeast using the loop in the well. Now each transformant forms a row along the edge of a matrix (see Fig. 3).
7. Mix the yeast suspension. Dispense 20 μL of the suspension into the empty wells in the same row or column. Suspension in the top well is dispensed in wells in the column below it, and that in the side well is dispensed across the row of wells to the right. Therefore, each well in the matrix contains 40 μL of the mixed suspension (see Fig. 3 and Note 5).
8. Spot 3 μL of the suspension onto the dried YPD plate, following a grid (see Fig. 4 and Note 6).
9. Seal the plate with Parafilm, and incubate for 1–2 d (see Note 7).
10. Place a sterilized filter paper (7.5-cm diameter) onto the YPD plate and leave for 5 min (see Note 8).
11. Peel the filter paper gently (this lifts cells from the colonies) and place onto a fresh triple drop-out plate for 2 min (this transfers cells onto the plate).
12. Peel the filter paper out of the double-drop-out plate and place onto a fresh double-drop-out plate for 2 min. This produces a duplicate, or replica plate (see Note 9).
13. Seal the pair of replica plates and incubate them for 2–3 d at 30°C (see Note 10).
14. Take a photo of the plates for the record (see Fig. 5 and Note 11). (Optional: Colony lift for β -galactosidase assay for LacZ expression) (see Note 12).
15. Place a sterilized filter paper on the double-drop-out plate for 5 min.

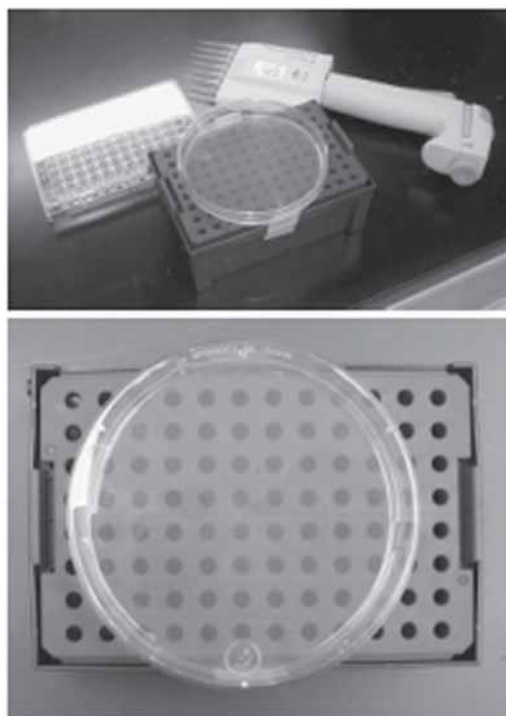


Fig. 4. Preparation of a grid for the master plate.

16. Peel the filter paper gently, flip it over (colony face up), and immerse it for 30 s in liquid N₂.
17. Thaw the filter paper face up on a piece of paper towel at room temp.
18. Blot the filter onto a larger filter paper presoaked with X-Gal solution, on a plastic pad (*see Note 13*).
19. Seal the dish and leave it in the 30°C incubator or at room temperature until blue spots appear at the spot of positive control.

4. Notes

1. This assay is based on the hypothesis that inhibitor-2 associates with select pools of PP1 holoenzymes. This can occur with or without direct interaction of I-2 with the regulatory subunits. In the assay system described here, the PP1-binding domain of a regulatory [R] subunit binds to the yeast endogenous PP1 homolog Glc7. Glc7 has biochemical properties common with the mammalian PP1 catalytic subunit. Critical residues in the PP1-docking motif, -VxF-, can be mutated into Ala, which eliminates the binding of the R-subunit segment to Glc7. Therefore, double Ala mutants -AXA- are used to determine if inhibitor-2 docks

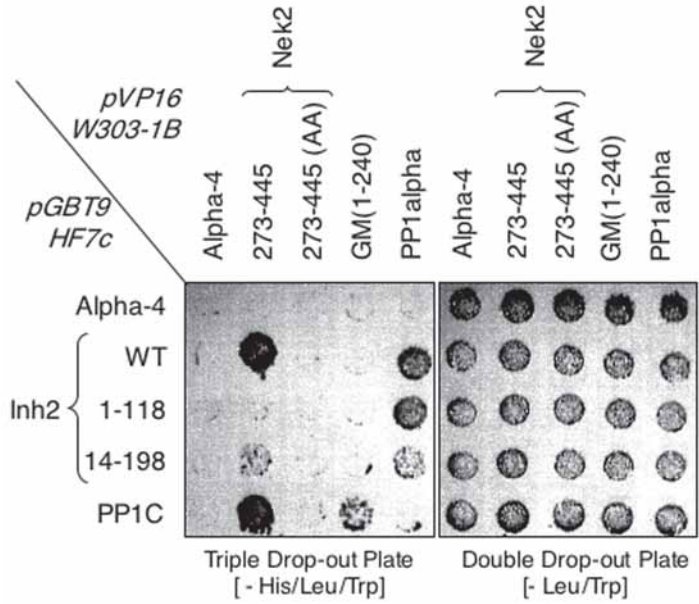


Fig. 5. Yeast colonies on triple- and double-drop-out plates.

directly or depends on binding to Glc7 that is complexed with a PP1-binding segment (see Fig. 2).

Inhibitor-2 wild type, and deletion mutants, (1–119) and (15–198), were reinserted in the pGBT vector for N-terminal fusion proteins with the GAL4 DNA-binding segment. PP1 α and PP1-binding domains of regulatory subunits, such as Nek2(273–445) and G_M(1–240) are inserted in the pVP16 vector for N-terminal-tagged fusion proteins with an activation domain. The combination between inhibitor-2 and PP1 α is used as a positive control. The cDNA fragment of the α -4 protein, a PP2A-binding protein that does not bind PP1, is inserted in both pVP16 and pGBT vectors as a negative control.

The yeast hybrid assay can detect isoform specificity on the interaction of PP1 and regulatory protein, so that the right selection of PP1 isoforms is crucial. For example, MYPT1 (1–300) associates with the δ isoform, but not with the α isoform (23–25,31).

2. All yeast handlings are done following the *Yeast Protocols Handbook* (PT3024–1, Clontech). Generally, the LiOAc/PEG method is easy for multiple transformants and yields high efficiency in transformation. Electroporation is convenient and sufficient for a few transformations. Selection of the yeast strain is critical for the sensitivity vs background. For example, the W303 (MATa) strain yields a higher sensitivity and background, compared with HF7c (MATa). We also noted variable results between single clones. The parent clone used for the transformation should be stored as a glycerol stock for the future study.

3. This process yields sufficient numbers of yeast transformants for several assays.
4. It is important to obtain clear data. See **step 10** and **Note 8**.
5. Multichannel pipette eases the process of mixing suspension on the 96-well plate.
6. Tape an empty yellow tip holder (96 holes) under the YPD plate, so as to visualize a grid via holes (see **Fig. 3**). Take a 3- μ L aliquot of the suspension and spot on the plate along holes under the plate. Try not to scratch the surface. A multichannel pipet greatly reduces the time for the spotting. This process should be done under sterilized conditions, such as on clean bench or in a hood. The suspension should be absorbed within a couple of minutes. Carefully turn over the plate and mark at the top of the matrix with a marker pen. It is not necessary to mark at each spot because colonies will appear.
7. The mating process is done on the plate, called the master plate. White yeast colonies become approx 1 mm thick. The thickness of the yeast colonies on the master plate affects on the sensitivity/background of the assay. Higher sensitivity/background is obtained from thicker yeast growth.
8. Pick up a piece of filter paper using sterilized forceps and attach the edge of the filter. When the edge becomes wet, place the filter paper down. If filter paper bubbles or bends, push the paper gently using forceps to attach it on the plate completely. If the master plate is too wet, the yeast spots will streak away (see **Note 4**).
9. Two replica plates are needed for the assay. Mark the matrix of yeast spots on the plate with a marker pen.
10. On the triple-drop-out plate, dark red yeast colonies will appear at the positive control spot. White colonies are false positives. Keep harvesting until the positive colonies are visible. Red colonies are evenly grown on the double-drop-out plate.
11. Place the plate on the white paper. Remove the lid and shoot a picture above the plate. White colonies are invisible on the white paper, so that the red positive colonies are selectively visualized. Reflection of white light increases the contrast of the photo.
12. The β -gal assay is to verify the results of His-selection assay. The blue-colored filter paper is also easy to document it using a regular scanner with personal computer. The sensitivity of this assay might be lower, compared with the His selection. Therefore, it is useful in case the background level is high in the His-selection assay.
13. Use a disposable plastic dish.

References

1. Fischer, E. H. and Brautigan, D. L. (1982) A Phosphatase by any other name: from prosthetic group removing enzyme to phosphorylase phosphatase. *Trends Biochem. Sci.* **7**, 3–4.
2. Kato, K. and Bishop, J. S. (1972) Glycogen synthetase- δ phosphatase. I. Some new properties of the partially purified enzyme from rabbit skeletal muscle. *J. Biol. Chem.* **247**, 7420–7429.

3. Larner, J. (1973) Covalent and noncovalent control of glycogen synthesis. *Ann. NY Acad. Sci.* **210**, 207–214.
4. Abe, N. and Tsuiki, S. (1974) Studies on glycogen synthase δ phosphatase of rat liver: multiple nature. *Biochim. Biophys. Acta.* **350**, 383–391
5. Stalmans, W., De Wulf, H., Hue, L., and Hers, H. G. (1974) The sequential inactivation of glycogen phosphorylase and activation of glycogen synthetase in liver after the administration of glucose to mice and rats. The mechanism of the hepatic threshold to glucose. *Eur. J. Biochem.* **41**, 117–134.
6. Nakai, C. and Thomas, J. A. (1974) Properties of a phosphoprotein phosphatase from bovine heart with activity on glycogen synthase, phosphorylase, and histone. *J. Biol. Chem.* **249**, 6459–6467.
7. Kikuchi, K., Tamura, S., Hiraga, A., and Tsuiki, S. (1977) Glycogen synthase phosphatase of rat liver. Its separation from phosphorylase phosphatase on DE-52 columns. *Biochem. Biophys. Res. Commun.* **75**, 29–37.
8. Brandt, H., Killilea, S. D., and Lee, E. Y. C. (1974) Activation of phosphorylase phosphatase by a novel procedure: evidence for a regulatory mechanism involving the release of a catalytic subunit from enzyme-inhibitor complex(es) of higher molecular weight. *Biochem. Biophys. Res. Commun.* **61**, 598–604.
9. Goris, J. and Merlevede, W. (1972) Effect of urea on the active and inactive forms of liver phosphorylase phosphatase separated by gel filtration. *Arch. Int. Physiol. Biochim.* **80**, 967–969
10. Kato, K., Kobayashi, M., and Sato, S. (1974) Multiple molecular forms of phosphoprotein phosphatase. II. Dissociation and activation of phosphorylase phosphatase from rabbit skeletal muscle. *Biochim. Biophys. Acta* **371**, 89–101.
11. Huang, F. L. and Glinsmann, W. H. (1975) Inactivation of rabbit muscle phosphorylase phosphatase by cyclic AMP-dependent kinase. *Proc. Natl. Acad. Sci. USA* **72**, 3004–3008.
12. Gratecos, D., Detwiler, T. C., Hurd, S., and Fischer, E. H. (1977) Rabbit muscle phosphorylase phosphatase. 1. Purification and chemical properties. *Biochemistry* **16**, 4812–4817.
13. Killilea, S. D., Mellgren, R. L., Aylward, J. H., Metieh, M. E., and Lee, E. Y. (1979) Liver protein phosphatases: studies of the presumptive native forms of phosphorylase phosphatase activity in liver extracts and their dissociation to a catalytic subunit of Mr 35,000. *Arch. Biochem. Biophys.* **193**, 130–139.
14. Huang, F. L. and Glinsmann, W. H. (1976) Separation and characterization of two phosphorylase phosphatase inhibitors from rabbit skeletal muscle. *Eur. J. Biochem.* **70**, 419–426.
15. Ingebritsen, T. S., Foulkes, J. G., and Cohen, P. (1980) The broad specificity protein phosphatase from mammalian liver. Separation of the Mr 35 000 catalytic subunit into two distinct enzymes. *FEBS Lett.* **119**, 9–15.
16. Ingebritsen, T. S. and Cohen, P. (1983) The protein phosphatases involved in cellular regulation. 1. Classification and substrate specificities. *Eur. J. Biochem.* **132**, 255–261.

17. Imaoka, T., Imazu, M., Usui, H., Kinohara, N., and Takeda, M. (1983). Resolution and reassociation of three distinct components from pig heart phosphoprotein phosphatase. *J. Biol. Chem.* **258**, 1526–1535.
18. Tamura, S., Kikuchi, H., Kikuchi, K., Hiraga, A., and Tsuiki, S. (1980) Purification and subunit structure of a high-molecular-weight phosphoprotein phosphatase (phosphatase II) from rat liver. *Eur. J. Biochem.* **104**, 347–355
19. Pato, M. D. and Adelstein, R. S. (1983) Purification and characterization of a multisubunit phosphatase from turkey gizzard smooth muscle. The effect of calmodulin binding to myosin light chain kinase on dephosphorylation. *J. Biol. Chem.* **258**, 7047–7054.
20. Pato, M. D., Adelstein, R. S., Crouch, D., Safer, B., Ingebritsen, T.S., and Cohen, P. (1983) The protein phosphatases involved in cellular regulation. 4. Classification of two homogeneous myosin light chain phosphatases from smooth muscle as protein phosphatase-2A1 and 2C, and a homogeneous protein phosphatase from reticulocytes active on protein synthesis initiation factor eIF-2 as protein phosphatase-2A2. *Eur. J. Biochem.* **132**, 283–287
21. Ballou, L. M. and Fischer, E. H. (1986) Phosphoprotein Phosphatases, in *The Enzymes*, (Boyer, P. D. and Krebs, E. G., eds.), Academic, London, pp. 311–361.
22. Stralfors, P., Hiraga, A., and Cohen, P. (1985) The protein phosphatases involved in cellular regulation. Purification and characterisation of the glycogen-bound form of protein phosphatase-1 from rabbit skeletal muscle. *Eur. J. Biochem.* **149**, 295–303
23. Alessi, D., MacDougall, L. K., Sola, M.M., Ikebe, M., and Cohen, P. (1992) The control of protein phosphatase-1 by targetting subunits. The major myosin phosphatase in avian smooth muscle is a novel form of protein phosphatase-1. *Eur. J. Biochem.* **210**, 1023–1035
24. Shirazi, A., Iizuka, K., Fadden, P., et al. (1994) Purification and characterization of the mammalian myosin light chain phosphatase holoenzyme. The differential effects of the holoenzyme and its subunits on smooth muscle. *J. Biol. Chem.* **269**, 31,598–31,606
25. Shimizu, H., Ito, M., Miyahara, M., et al. (1994) Characterization of the myosin-binding subunit of smooth muscle myosin phosphatase. *J. Biol. Chem.* **269**, 30,407–30,411.
26. Ito, M., Nakano, T., Erdodi, F., and Hartshorne, D. J. (2004) Myosin phosphatase: structure, regulation and function. *Mol. Cell. Biochem.* **259**, 197–209.
27. Cohen, P. T. (2002) Protein phosphatase 1-targeted in many directions. *J. Cell Sci.* **115**, 241–256.
28. Ceulemans, H. and Bollen, M. (2004) Functional diversity of protein phosphatase-1, a cellular economizer and reset button. *Physiol Rev.* **84**, 1–39
29. Eto, M., Senba, S., Morita, F., and Yazawa, M. (1997) Molecular cloning of a novel phosphorylation-dependent inhibitory protein of protein phosphatase-1 (CPI17) in smooth muscle: its specific localization in smooth muscle. *FEBS Lett.* **410**, 356–360.

30. Senba, S., Eto, M., and Yazawa, M. (1999) Identification of trimeric myosin phosphatase (PP1M) as a target for a novel PKC-potentiated protein phosphatase-1 inhibitory protein (CPI-17) in porcine aorta smooth muscle. *J. Biochem (Tokyo)* **125**, 354–362.
31. Eto, M., Kitazawa, T., and Brautigan, D. L. (2004) Phosphoprotein inhibitor CPI-17 specificity depends on allosteric regulation of protein phosphatase-1 by regulatory subunits. *Proc. Natl. Acad. Sci. USA* **101**, 8888–8893.
32. Connor, J. H., Weiser, D. C., Li, S., Hallenbeck, J. M., and Shenolikar, S. (2001) Growth arrest and DNA damage-inducible protein GADD34 assembles a novel signaling complex containing protein phosphatase 1 and inhibitor 1. *Mol. Cell. Biol.* **21**, 6841–6850.
33. Eto, M., Elliott, E., Prickett, T. D., and Brautigan, D. L. (2002) Inhibitor-2 regulates protein phosphatase-1 complexed with NimA-related kinase to induce centrosome separation. *J. Biol. Chem.* **277**, 44,013–44,020.
34. Terry-Lorenzo, R. T., Elliott, E., Weiser, D. C., Prickett, T. D., Brautigan, D. L., and Shenolikar, S. (2002) Neurabins recruit protein phosphatase-1 and inhibitor-2 to the actin cytoskeleton. *J. Biol. Chem.* **277**, 46,535–46,543.
35. Wang, H. and Brautigan, D. L. (2002) A novel transmembrane Ser/Thr kinase complexes with protein phosphatase-1 and inhibitor-2. *J. Biol. Chem.* **277**, 49,605–49,612.
36. Feng, Z.H., Wilson, S. E., Peng, Z. Y., Schlender, K. K., Reimann, E. M., and Trumbly, R. J. (1991) The yeast GLC7 gene required for glycogen accumulation encodes a type 1 protein phosphatase. *J. Biol. Chem.* **266**, 23,796–23,801.
37. Dignam, S. S., Koushik, J. S., Wang, J., Trumbly, R. J., Schlender, K. K., Lee, E. Y., and Reimann, E. M. (1998) Purification and characterization of type 1 protein phosphatase from *Saccharomyces cerevisiae*: effect of the R73C mutation. *Arch. Biochem. Biophys.* **357**, 58–66.

Phosphorylation of the Protein Phosphatase Type 1 Inhibitor Protein CPI-17 by Protein Kinase C

Michael P. Walsh, Marija Susnjar, Jingti Deng, Cindy Sutherland, Enikő Kiss, and David P. Wilson

Summary

CPI-17 is a cytosolic protein of 17 kDa that becomes a potent inhibitor of certain type 1 protein serine/threonine phosphatases, including smooth muscle myosin light-chain phosphatase (MLCP), when phosphorylated at Thr38. Several protein kinases are capable of phosphorylating CPI-17 at this site in vitro; however, in intact tissue, compelling evidence only exists for phosphorylation by protein kinase C (PKC). Agonist-induced activation of heterotrimeric G proteins of the $G_{q/11}$ family via seven-transmembrane domain-containing, G protein-coupled receptors results in phospholipase C β -mediated hydrolysis of membrane phosphatidylinositol 4,5-bisphosphate to generate inositol 1,4,5-trisphosphate (IP_3) and 1,2-diacylglycerol (DAG). IP_3 triggers Ca^{2+} release from the sarcoplasmic reticulum. DAG and Ca^{2+} together activate classical isoforms of PKC, and DAG activates novel PKC isoforms without a requirement for Ca^{2+} . Activated PKC phosphorylates CPI-17 at Thr38, enhancing its potency of inhibition of MLCP approx 1000-fold. The myosin light-chain kinase (MLCK) : MLCP activity ratio is thereby increased at the prevailing cytosolic free- Ca^{2+} concentration ($[Ca^{2+}]_i$), resulting in an increase in phosphorylation of the 20-kDa light chains of myosin II (LC_{20}) catalyzed by Ca^{2+} - and calmodulin-dependent MLCK and contraction of the smooth muscle. Physiologically, this mechanism can account for some instances of Ca^{2+} sensitization of smooth muscle contraction (i.e., an increase in force in response to agonist stimulation without a change in $[Ca^{2+}]_i$).

Key Words: CPI-17; protein kinase C; myosin light-chain phosphatase; myosin light-chain kinase; Ca^{2+} sensitization; smooth muscle contraction.

1. Introduction

Protein phosphorylation–dephosphorylation is a mechanism of posttranslational modification that is involved in the regulation of most cellular functions

From: *Methods in Molecular Biology, Volume 365: Protein Phosphatase Protocols*
Edited by: G. Moorhead © Humana Press Inc., Totowa, NJ

(1). For example, numerous enzymes are activated by phosphorylation at specific serine, threonine, or tyrosine residues and inactivated by dephosphorylation. Protein phosphorylation is catalyzed by protein kinases and dephosphorylation by protein phosphatases. Five hundred eighteen kinase genes (2) and 139 phosphatase genes (3,4) have been identified in the human genome, approx 400 of which encode serine/threonine kinases and 32 encode serine/threonine phosphatases, respectively. The complexity of signal transduction cascades involving multiple kinases and phosphatases is exemplified by the regulation of smooth muscle contraction, in which the phosphorylation and dephosphorylation of the 20-kDa light chains of myosin II (LC₂₀) plays a critical role (5). Phosphorylation of LC₂₀ is catalyzed by Ca²⁺- and calmodulin-dependent myosin light-chain kinase (MLCK) (6), which activates contraction, and dephosphorylation by myosin light-chain phosphatase (MLCP) (7), which relaxes the muscle.

Protein serine/threonine phosphatases are regulated in a variety of ways, including interaction with inhibitory proteins, many of which are, in turn, regulated by phosphorylation–dephosphorylation (8). For example, CPI-17 (protein kinase C (PKC)-potentiated inhibitory protein [for protein phosphatase type 1] of 17 kDa) is a type 1 protein phosphatase inhibitor that is expressed predominantly in smooth muscle tissues (9–11). CPI-17 becomes a potent inhibitor of the catalytic subunit of type 1 protein phosphatases when phosphorylated at Thr38 (10,12). Of particular importance, phosphorylated CPI-17 inhibits the holoenzyme of MLCP (12), a trimeric enzyme composed of a 38-kDa type 1 phosphatase catalytic subunit, δ isoform (PP1c δ), a 110-kDa regulatory subunit (MYPT1) that targets the phosphatase to myosin filaments, and a 20-kDa subunit of unknown function (7) (see Fig. 1). Orthologs of CPI-17, PHI-1 (phosphatase holoenzyme inhibitor-1) (13) and KEPI (kinase-enhanced protein phosphatase-1 inhibitor) (14) have been identified more recently and their ability to inhibit type 1 protein phosphatase activity is also activated by phosphorylation.

Several protein kinases phosphorylate CPI-17 at Thr38 in vitro: PKC (10), Rho-associated kinase (ROK) (15), protein kinase N (16), integrin-linked kinase (ILK) (17), zipper-interacting protein kinase (18), cAMP- and cGMP-dependent protein kinases (19), and p21-activated protein kinase (PAK) (20). Phosphorylation of CPI-17 at Thr38 by PKC has been demonstrated in intact vascular smooth muscle tissues in response to physiological agonists (such as histamine, phenylephrine, and endothelin-1) and pharmacological agonists (such as phorbol esters) (21–25). Evidence for phosphorylation of CPI-17 by other kinases in intact tissue is, however, lacking. The observation that the ROK inhibitor Y-27632 inhibits PKC δ with similar potency (22) (see Fig. 2) questions the conclusion, based on use of this kinase inhibitor, that ROK phosphorylates CPI-17 in intact tissue.

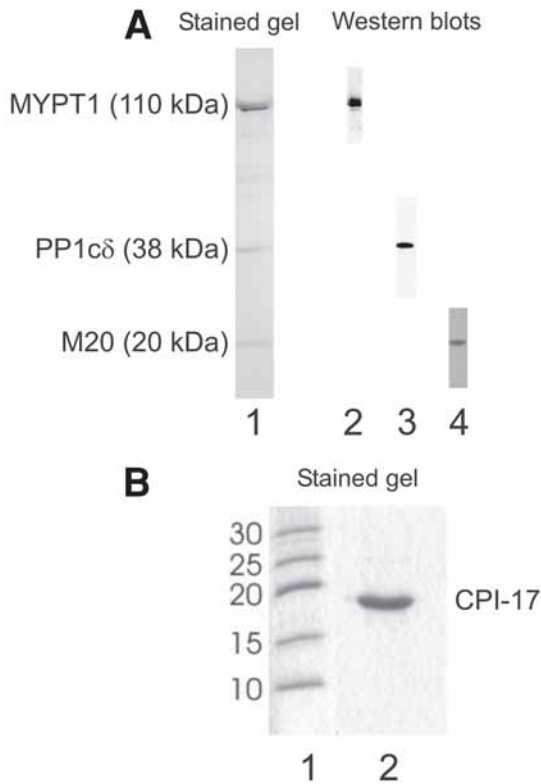


Fig. 1. Myosin light-chain phosphatase and CPI-17. **(A)** Purified myosin light-chain phosphatase was analysed by SDS-PAGE and Coomassie blue staining (lane 1) and by Western blotting with antibodies to the three subunits: MYPT1 (lane 2), PP1c (lane 3), and M20 (lane 4). **(B)** Purified recombinant CPI-17 was characterized by SDS-PAGE and Coomassie blue staining (lane 2). Molecular-weight markers are shown in lane 1 and the numbers indicate molecular weights in kDa.

Recent evidence indicates that phosphorylated CPI-17 inhibits only a subset of type 1 phosphatases (26). Specificity is achieved by the regulatory subunits associated with catalytic protein phosphatase-1 (PP1c). Thus, glycogen-bound PP1 of skeletal muscle, containing PP1c δ and G_M (the glycogen-targeting subunit), is not inhibited by phosphorylated CPI-17, whereas smooth muscle MLCP containing PP1c δ bound to the myosin-targeting MYPT1 subunit is. Glycogen-bound PP1 dephosphorylates CPI-17, whereas MLCP does not (or does so very slowly). Presumably, MYPT1, but not G_M, causes an allosteric change that greatly retards the dephosphorylation of CPI-17 at the PP1c site. A separate class of PP1 holoenzymes does not bind phosphorylated CPI-17.

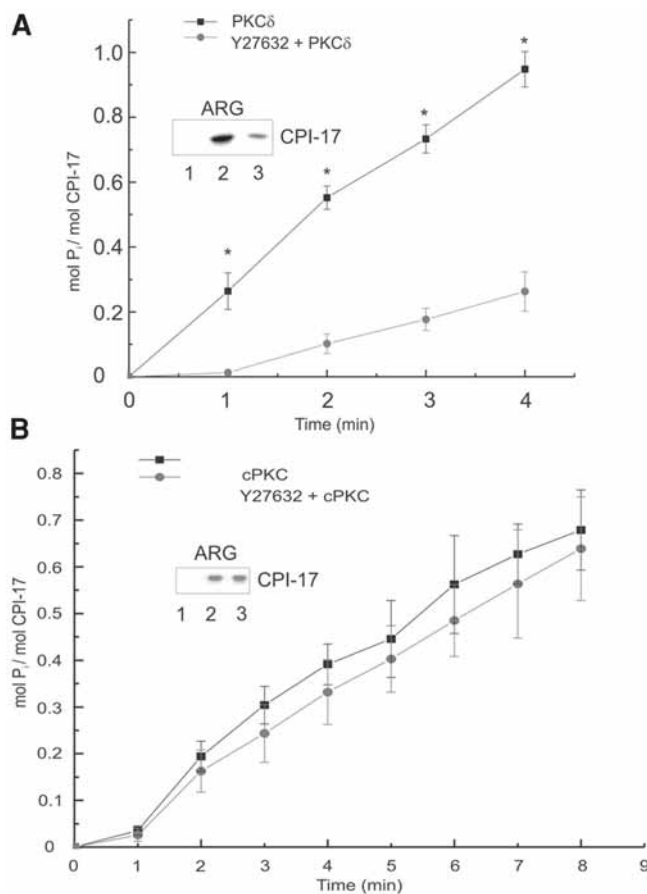


Fig. 2. Phosphorylation of CPI-17 by PKC δ and Ca²⁺-dependent PKCs and the effect of Y-27632. **(A)** Time-course of phosphorylation of purified, recombinant CPI-17 by PKC δ in the absence (closed squares) and presence (closed circles) of Y-27632 (10 μ M). **(B)** Time-course of phosphorylation of purified, recombinant CPI-17 by cPKC in the absence (closed squares) and presence (closed circles) of Y-27632 (10 μ M). Values represent mean \pm S.E. [$n = 4$ **(A)** and $n = 3$ **(B)**]. Asterisks indicate statistically significant differences. At the end of the reaction, an equal volume of SDS-gel sample buffer was added to the remainder of each reaction mixture and boiled prior to SDS-PAGE and autoradiography. The insets show the resultant autoradiographs (ARG): lanes 1, control (CPI-17 without PKC); lanes 2, CPI-17 + PKC δ **(A)** or cPKC **(B)**; lanes 3, CPI-17 + Y-27632 + PKC δ **(A)** or cPKC **(B)**. The specific activities of PKC δ and cPKC with CPI-17 as substrate were calculated to be 27.1 and 2.0 μ mol P_i/min/mg PKC, respectively. The rate of phosphorylation by cPKC was unaffected by Y-27632 but that by PKC δ was reduced to 0.7 μ mol P_i/min/mg PKC by the commonly used ROK inhibitor.

Physiologically, CPI-17 phosphorylation and MLCP inhibition have been implicated in Ca^{2+} sensitization of smooth muscle contraction ([11,21,27](#)), which refers to the process whereby stimuli can elicit a contractile response without an increase in cytosolic free- Ca^{2+} concentration ($[\text{Ca}^{2+}]_i$) ([28](#)). Most commonly, Ca^{2+} sensitization accompanies an agonist-induced increase in $[\text{Ca}^{2+}]_i$, resulting in greater force generation than is observed in response to stimuli that elicit only an increase in $[\text{Ca}^{2+}]_i$. Phosphorylated CPI-17 inhibits MLCP by direct interaction with the catalytic subunit ([29](#)), thereby shifting the equilibrium in favor of MLCK and leading to activation of cross-bridge cycling and force development or shortening of the muscle.

The purpose of this chapter is to provide practical information to allow the reader to carry out the following: (1) phosphorylation of CPI-17 in vitro by PKC, (2) analysis of the effects of CPI-17 on MLCP activity, and (3) analysis of phosphorylation of CPI-17 in intact tissue. The methods described apply equally well to other phosphatase inhibitory proteins such as PHI-1 and KEPI and to phosphorylation of these proteins by other protein serine/threonine kinases.

2. Materials

2.1. Preparation of Mixed Micelles

1. L- α -phosphatidylserine from porcine brain in chloroform (stock, 25 mg/mL) (Avanti Polar Lipids, Alabaster, AL, USA).
2. 1,2-Diolein in hexane (stock, 20 mg/mL) (Doosan Serdary Research Laboratories, London, ON, Canada).
3. Sonicator (*see* **Note 1**).

2.2. Phosphorylation Assay

1. Scintillation (β) counter.
2. Temperature-controlled water bath.
3. $[\gamma\text{-}^{32}\text{P}]\text{ATP}$ (>5000 Ci/mmol) (ICN Biomedical Inc., Aurora, OH, USA).
4. Unlabeled ATP stock solution of 40 mM in H_2O .
5. Triton X-100 and Tween-80 (Fisher Scientific, Whitby, ON, Canada).
6. Microcystin-LR (Alexis Biochemicals, San Diego, CA, USA). Stock solution of 1 mM in dimethyl sulfoxide (DMSO). Store at -20°C in 0.1-mL aliquots.
7. Buffer A: 76 mM MOPS, pH 6.2, 4 mM DTT (dithiothreitol), 4 mM β -glycerophosphate.
8. Buffer B: 200 mM Tris-HCl, pH 7.5, 100 mM MgCl_2 , 2 mM CaCl_2 , 10 μM microcystin.
9. cPKC [a mixture of Ca^{2+} -dependent PKC isoenzymes, PKCs α , β , and γ , purified from rat brain ([30](#))]. Stock solution (23 $\mu\text{g}/\text{mL}$) in 20 mM HEPES, pH 7.4, 1 mM EGTA, 1 mM EDTA, 1 mM DTT, 0.02% (w/v) NaN_3 , 0.05%

(v/v) Triton X-100, 25% (v/v) glycerol. Store at -80°C in 0.5-mL aliquots. Stable for 6 mo or longer.

10. PKC δ (N-terminal His₆-tagged, recombinant protein, of human PKC β expressed in Sf21 cells (Upstate USA Inc., Charlottesville, VA, USA). Stock solution ($0.65\text{ }\mu\text{M} = 50\text{ }\mu\text{g/mL}$) in 50 mM Tris-HCl, pH 7.5, 270 mM sucrose, 150 mM NaCl, 1 mM benzamidine, 0.2 mM phenylmethylsulfonyl fluoride, 0.1 mM EGTA, 0.1% 2-mercaptoethanol, 0.03% Brij-35. Store at -80°C . Stable for 6 mo or longer.
11. CPI-17 purified as previously described (25). Stock solution ($29.4\text{ }\mu\text{M} = 0.5\text{ mg/mL}$) in 30 mM potassium phosphate, 50 mM KCl, 1 mM DTT, 0.02% (w/v) NaN₃. Store at -80°C in 1-mL aliquots. Stable for 6 mo or longer (see Fig. 1B).
12. P81 phosphocellulose paper (Whatman, Springfield Mill, UK).

2.3. Thiophosphorylation of CPI-17

1. ATPyS (Roche Applied Science, Laval, PQ, Canada). Stock solution of 0.1 M in H₂O.
2. Unphosphorylated CPI-17 (see Subheading 2.2., item 11).
3. cPKC (see Subheading 2.2., item 9).

2.4. Back-Phosphorylation Assay

1. Thiophosphorylated CPI-17 (see Subheading 3.3.).
2. Unphosphorylated CPI-17 (see Subheading 2.2., item 11).
3. cPKC (see Subheading 2.2., item 9).

2.5. Phosphatase Assay

1. Buffer C: 250 mM Tris-HCl, pH 7.5, 600 mM KCl, 40 mM MgCl₂, 10 mM DTT, 1 mM CaCl₂, 1% (v/v) Tween-80.
2. Buffer D: 25 mM Tris-HCl, pH 7.5, 60 mM KCl, 1 mM DTT, 3.5 mM EDTA, 0.1% (v/v) Tween-80.
3. Buffer E: 25 mM Tris-HCl, pH 7.5, 0.1 mM EGTA, 1 mM benzamidine.
4. Calmodulin purified from chicken gizzard (31). Stock solution ($30\text{ }\mu\text{M} = 0.5\text{ mg/mL}$) in H₂O. Stable for 1 yr or longer.
5. MLCK purified from chicken gizzard (32). Stock solution ($0.47\text{ }\mu\text{M} = 0.05\text{ mg/mL}$) in 20 mM Tris-HCl, pH 7.5, 1 mM EGTA, 1 mM DTT. Store at -80°C in 0.5 mL-aliquots. Stable for 1 yr or longer.
6. MLCP purified from chicken gizzard (25) in 20 mM Tris-HCl, pH 7.5, 150 mM NaCl, 1 mM DTT, 0.1 mM EGTA, 5% (v/v) glycerol, 1 mM Pefabloc, 1 mM benzamidine. Store at -80°C in 0.1-mL aliquots. Stable for 6 mo or longer (see Fig. 1A).
7. LC₂₀ (20-kDa light-chain of myosin II) purified from chicken gizzard (33). Stock solution ($18\text{ }\mu\text{M} = 0.36\text{ mg/mL}$) in 20 mM MOPS, pH 7.4, 0.1 M KCl, 1 mM EGTA, 1 mM DTT. Store at -20°C in 1-mL aliquots. Stable for 1 yr or longer.
8. Phosphorylated CPI-17 (see Subheading 3.2., step 5b).
9. Unphosphorylated CPI-17 (see Subheading 2.2., item 11).

2.6. Western Blotting for Analysis of CPI-17 Phosphorylation in Tissue Samples

1. Polyclonal rabbit IgG antibody specific for CPI-17 phosphorylated at Thr38 (21).
2. Lyophilizer.
3. Transfer buffer: 10 mM CAPS, 10% (v/v) methanol, pH 11.
4. Sequi-grade™ polyvinylidene difluoride (PVDF) membrane (0.2 μ m; Bio-Rad, Mississauga, ON, Canada).
5. Tris-buffered saline with Tween (TBS-T): 20 mM Tris-HCl, pH 7.5, 0.5 M NaCl, 0.05% (v/v) Tween-20.
6. Blocking solution: 5% non-fat dry milk in TBS-T.
7. Primary antibody solution: 1 : 3000 dilution of anti-*p*[T38]CPI-17 in TBS-T containing 1% nonfat dry milk.
8. Secondary antibody: 1 : 40,000 dilution of anti-rabbit IgG-horseradish peroxidase conjugate (Chemicon, Temecula, CA, USA) in TBS-T.
9. SuperSignal® West-Femto chemiluminescence substrate (Pierce Chemical Co., Rockford, IL, USA).

3. Methods

Protein phosphorylation is most easily assayed by utilization of [γ - 32 P]ATP as substrate. The kinase catalyzes incorporation of the radiolabeled terminal phosphoryl group (γ - 32 PO $_3^{2-}$) of ATP into the serine, threonine, or tyrosine residue constituting the phosphorylation site. PKC catalyzes phosphoryl group transfer to Thr38 of CPI-17, whereas MLCK catalyzes transfer of the phosphoryl group to Ser19 of LC $_{20}$. Scintillation counting enables accurate quantification of the stoichiometry of phosphorylation. (See **Note 2**.)

3.1. Preparation of Mixed Micelles and Activated PKC

1. Mix 123.6 μ L of stock phosphatidylserine and 30.8 μ L of stock 1,2-diolein in a glass test tube (12 \times 75 mm) using a Hamilton syringe. (See **Note 3**.)
2. Dry under a stream of nitrogen.
3. Add 1 mL of 0.3% (v/v) Triton X-100 in 20 mM HEPES, pH 7.4.
4. Incubate in a water bath at 30°C for 30 min.
5. Sonicate twice for 10 s each.
6. Place on ice.

Protein kinase C is a family of related kinases that are conveniently divided into three classes (34): Classical PKC isoenzymes (PKCs α , β , and γ , collectively termed cPKC) require phospholipids, diacylglycerol, and Ca $^{2+}$ for activity; novel PKC isoenzymes (PKCs δ , ϵ , η , and θ) require phospholipids and diacylglycerol for activity but are independent of Ca $^{2+}$; and atypical PKC isoenzymes (PKCs ζ and ι/λ) are activated by protein-protein interaction rather than lipids and Ca $^{2+}$. The methods described here utilize cPKC and PKC δ and

activation is achieved by supplying the enzyme with mixed micelles made from phosphatidylserine and diolein (*see Subheading 2.1*) in the presence of Ca^{2+} (for cPKC) or EGTA (for PKC δ).

3.2. Phosphorylation Assay

1. Mix 7.5 μL of unlabeled ATP stock with 15 μL of $[\gamma\text{-}^{32}\text{P}]\text{ATP}$ stock and 127.5 μL of H_2O to give a 2 mM solution of $[\gamma\text{-}^{32}\text{P}]\text{ATP}$ with a specific activity of 200–500 cpm/pmol. (*See Note 4.*)
2. To determine the specific activity of the $[\gamma\text{-}^{32}\text{P}]\text{ATP}$ on the day of assay, withdraw triplicate aliquots (5 μL) and dilute to 100 μL with H_2O .
3. Pipet aliquots (20 μL) into a plastic scintillation vial and quantify radioactivity by Cerenkov counting in a scintillation counter using the ^3H window settings.
4. The specific radioactivity of the 2 mM $[\gamma\text{-}^{32}\text{P}]\text{ATP}$ solution is calculated from the following equation: Specific activity = cpm/2000 and the units are cpm/pmol.
 - a. For PKC δ : To a plastic 1.5-mL microfuge tube on ice, add 63 μL H_2O , 10 μL buffer A, 10 μL of freshly prepared mixed micelles (*see Subheading 3.1.*), 1 μL microcystin, 5 μL CPI-17, and 1 μL PKC δ . (*See Note 5.*)
 - b. For cPKC: To a plastic 1.5-mL microfuge tube on ice, add 57.8 μL H_2O , 10 μL buffer B, 10 μL of freshly prepared mixed micelles (*see Subheading 3.1.*), 1 μL microcystin, 7.2 μL CPI-17 (10-fold diluted stock), and 4 μL cPKC. (*See Note 5.*)
6. Mix the solution well by vortexing and equilibrate to 30°C in the water bath.
7. Start the reaction by addition of 10 μL of stock 2 mM $[\gamma\text{-}^{32}\text{P}]\text{ATP}$ to a final concentration of 0.2 mM.
8. Incubate the reaction mixture at 30°C and withdraw aliquots (20 μL) at selected times.
9. Pipet the reaction mixture aliquot onto a square (1 \times 1 cm) of P81 paper and immerse immediately in a glass 600-mL beaker containing 500 mL of 0.5% (v/v) H_3PO_4 and a stainless-steel wire mesh basket. (*See Note 6.*)
10. Wash the P81 paper squares three times for 5 min each with stirring in 500 mL of 0.5% (v/v) H_3PO_4 and once for 2 min in 500 mL of acetone.
11. Remove the wire basket from the beaker, place on a paper towel, and air-dry the P81 papers.
12. Transfer the dried P81 paper squares to plastic scintillation vials and quantify ^{32}P by Cerenkov counting (no scintillant or other liquid) in a scintillation counter using ^3H window settings.
13. Determine enzymatic activity and phosphorylation stoichiometry from the specific activity of the radiolabeled ATP. Enzymatic activity is determined from a linear plot of $\mu\text{mol P}_i$ incorporated vs time. The slope gives the rate of phosphorylation in $\mu\text{mol P}_i/\text{min}$, which is converted to specific enzymatic activity ($\mu\text{mol P}_i/\text{min}/\text{mg protein}$) by dividing by the amount of kinase (mg). Stoichiometry ($\mu\text{mol P}_i/\text{mol protein}$) = (sample cpm – blank cpm) \div (specific activity of ATP \times pmol protein), where specific activity of ATP = cpm/pmol ATP and blank cpm = cpm in an identical reaction mixture without PKC. (*See Fig. 2.*)

3.3. Thiophosphorylation of CPI-17

Thiophosphorylation is a very useful approach to use as an alternative to phosphorylation to examine the functional effects of protein phosphorylation, particularly if the experimental system is likely to contain phosphatase activity. Thiophosphorylation is achieved by replacement of ATP in the phosphorylation reaction mixture with adenosine 5'-[γ -thio]triphosphate (ATP γ S) in which S replaces one of the O atoms on the γ -phosphorus of ATP (*not* the O that links the β and γ phosphorus atoms). The advantage of this approach is that most protein serine/threonine kinases utilize ATP γ S as a substrate, but most protein serine/threonine phosphatases cannot efficiently dethiophosphorylate thiophosphorylated proteins. Thus, thiophosphorylated CPI-17 can be used, for example, in experiments with skinned (demembranated) smooth muscle tissues without running the risk of complications resulting from dephosphorylation by endogenous phosphatases.

1. To 6.7 mL of water on ice, add buffer B (1 mL), mixed micelles (1 mL) (*see Subheading 3.1.*), CPI-17 (0.7 mL), and cPKC (0.4 mL). (*See Note 7.*)
2. Incubate at 30°C in a water bath.
3. Start the reaction by addition of ATP γ S (0.2 mL of stock), giving a final concentration of 2 mM. (*See Note 8.*)
4. Incubate the reaction mixture at 30°C for 2 h to allow maximal thiophosphorylation of CPI-17.
5. Incubate for 10 min at 70°C in a water bath and cool on ice. (*See Note 9.*)
6. Centrifuge at 27,200g for 30 min to remove denatured PKC, leaving thiophosphorylated CPI-17 in the supernatant.
7. Dialyze to remove the lipids and excess ATP γ S. (*See Note 10.*)

3.4. Back-Phosphorylation Assay

The stoichiometry of thiophosphorylation of CPI-17 is calculated by “back-phosphorylation” whereby the thiophosphorylated protein is treated with radio-labeled ATP in the presence of activated PKC and ^{32}P incorporation is quantified. If the CPI-17 had been stoichiometrically thiophosphorylated, there will be no incorporation of ^{32}P into the protein. Unphosphorylated CPI-17 is included in a parallel assay as a positive control.

1. Incubate thiophosphorylated or unphosphorylated CPI-17 (2 μM) with PKC (10 nM) at 30°C in 20 mM Tris-HCl, pH 7.5, 10 mM MgCl_2 , 0.2 mM CaCl_2 , 80 $\mu\text{g/mL}$ L- α -phosphatidylserine, 8 $\mu\text{g/mL}$ of 1,2-diolein.
2. Start the reaction (total volume, 0.2 mL) by addition of [γ - ^{32}P]ATP to a final concentration of 0.2 mM.
3. Withdraw aliquots (20 μL) at selected times and spot on P81 paper for quantification of ^{32}P incorporation into CPI-17 or thiophosphorylated CPI-17 (*see Subheading 3.2.*).

3.5. Phosphatase Assay

First it is necessary to prepare the substrate for MLCP by phosphorylating Ser19 of LC₂₀ stoichiometrically (1 mol Pi/mol LC₂₀) with [γ -³²P]ATP in a reaction catalyzed by Ca²⁺- and calmodulin-dependent MLCK.

1. To 121.9 μ L of water on ice, add buffer C (26 μ L), LC₂₀ (72.2 μ L), calmodulin (8.7 μ L), and MLCK (5.2 μ L).
2. Incubate in a water bath at 30°C for 2 min.
3. Start the reaction (total volume, 260 μ L) by the addition of [γ -³²P]ATP (26 μ L). (See **Note 11**.)
4. Incubate at 30°C for 10 min to achieve stoichiometric phosphorylation of LC₂₀. (See **Fig. 3**.)
5. Stop the reaction by the addition of 1.04 mL of buffer D. (See **Note 12**.)
6. Spot aliquots (3 \times 10 μ L) of the reaction mixture onto P81 paper for quantification of LC₂₀ phosphorylation stoichiometry (see **Subheading 3.2**).

[³²P]LC₂₀ is now ready for use as a substrate to assay MLCP activity as follows:

7. Prepare the following mixtures: (1) 100 μ L buffer E; (2) 95 μ L buffer E + 5 μ L MLCP; (3) 35 μ L buffer E + 60 μ L CPI-17 + 5 μ L MLCP; (4) 35 μ L buffer E + 60 μ L phosphorylated CPI-17 + 5 μ L MLCP.
8. Incubate at 30°C for 2 min.
9. Add [³²P]LC₂₀ (100 μ L) from **step 5** to start the reaction.
10. Incubate the reaction mixtures at 30°C in a water bath.
11. Withdraw aliquots (20 μ L) at selected times and spot on P81 paper for quantification of the amount of ³²P remaining associated with LC₂₀. The decline in protein-bound ³²P with time is a measure of the MLCP activity. (See **Fig. 3**.)

3.6. Western Blotting for Analysis of CPI-17 Phosphorylation in Tissue Samples

1. Rapidly freeze tissue samples [in this case, de-endothelialized rat caudal arterial smooth muscle helical strips (33)] by immersion in dry ice-cooled 10% (w/v) trichloroacetic acid (TCA), 10 mM DTT/acetone.
2. Wash out residual TCA with 3X 1 mL of 10 mM DTT, acetone.
3. Lyophilize the tissue samples overnight, homogenize in 100 μ L of sodium dodecyl sulfate–polyacrylamide gel electrophoresis (SDS-PAGE) sample buffer, and boil.
4. Separate tissue proteins by SDS-PAGE using a 15-cm \times 0.75-mm-thick, 7.5–20% acrylamide gradient gel at 25 mA for 3.5 h (35).
5. Transfer proteins to PVDF membrane at 30 mA for 5 h in transfer buffer.
6. Wash the membrane in TBS and immerse in blocking solution for 1 h and then in primary antibody solution for 1 h.
7. Rinse the membrane 3 \times 10 min in TBS-T.
8. Incubate the membrane in secondary antibody solution for 1 h.

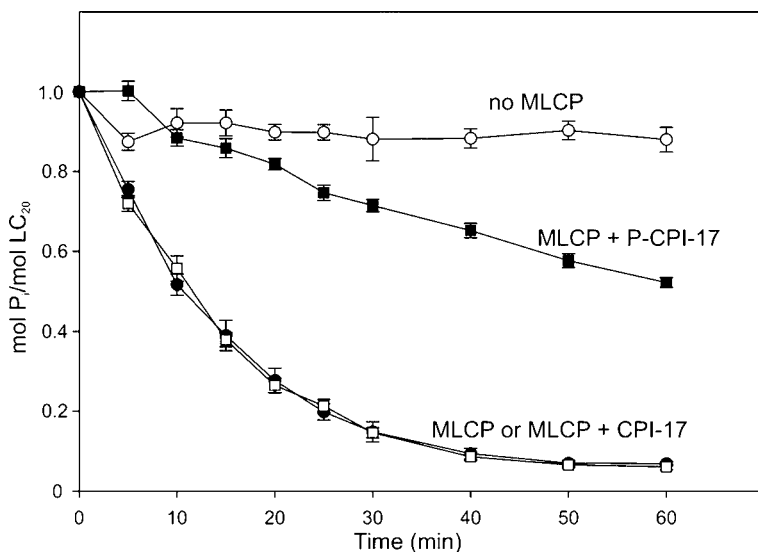


Fig. 3. Dephosphorylation of phosphorylated myosin light chain by myosin light-chain phosphatase and the effects of CPI-17 and phosphorylated CPI-17 (P-CPI-17). Time-course of dephosphorylation of $[^{32}\text{P}]\text{LC}_{20}$ by MLCP in the absence (●) and presence of CPI-17 (□) or phosphorylated CPI-17 (■). The control (○) shows no dephosphorylation of the light chain in the absence of MLCP. Phosphorylated, but not unphosphorylated, CPI-17 inhibited MLCP activity.

9. Rinse the membrane three times (10 min each) in TBS-T and once in TBS.
10. Add chemiluminescence substrate. (See Fig. 4.)

4. Notes

1. The mixed micelles for activation of PKC should be prepared fresh.
2. For any enzyme assay, it is essential to determine the time over which the reaction is linear. For noncontinuous assays, such as the phosphorylation assays described here, linearity must be determined by stopping the reaction at various points in time and quantifying product formation (e.g., phosphorylated CPI-17) or substrate loss (e.g., myosin dephosphorylation). The time over which the reaction is linear depends on the concentration of enzyme and substrate used and must be verified before selecting a suitable time (on the linear portion of the curve relating product formation, or substrate loss, and time).
3. A Hamilton syringe rather than a Pipetman is used to ensure accuracy of transfer of the lipid solutions in organic solvents.
4. The choice of specific activity of $[\gamma\text{-}^{32}\text{P}]\text{ATP}$ is dictated largely by the availability (and cost) of the proteins to be used in the assay. When these are limited, $[\gamma\text{-}^{32}\text{P}]\text{ATP}$ of higher specific activity is used.

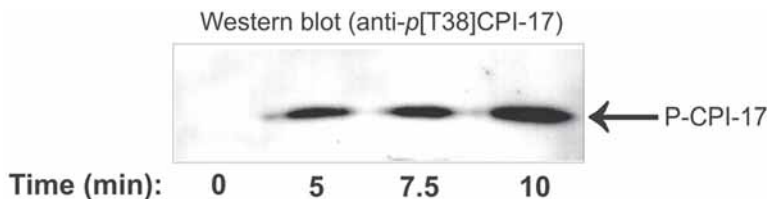


Fig. 4. Phorbol ester-induced phosphorylation of CPI-17 in rat caudal arterial smooth muscle. Helical strips of de-endothelialized rat caudal artery were treated with phorbol 12,13-dibutyrate (PdBu) ($1 \mu\text{M}$), which induced a slow, sustained contraction. Tissues were quick-frozen at the indicated times after the addition of PdBu, the proteins were separated by SDS-PAGE, and CPI-17 phosphorylation at Thr38 was analyzed by Western blotting with anti-p[T38]CPI-17. Comparable loading levels were confirmed by Western blotting with anti-CPI-17 (which recognizes both phosphorylated and unphosphorylated CPI-17) or anticalmodulin, and by staining of the nitrocellulose membrane with naphthol blue black. Data are representative of four independent experiments.

5. Stock PKC solution should be diluted just prior to addition to the assay mixture. Loss of activity is observed if the kinase is stored in dilute solution.
6. This stops the reaction.
7. Final concentrations: $2 \mu\text{M}$ CPI-17 and 11.5 nM cPKC.
8. Because ATP γ S is not as efficient a substrate for PKC as is ATP, it is necessary to carry out the thiophosphorylation at higher ATP γ S and PKC concentrations than are used for the phosphorylation of CPI-17 with ATP.
9. This inactivates the PKC, but CPI-17 is heat stable.
10. The lipids can interfere with subsequent steps if not removed and ATP γ S can inhibit cross-bridge cycling if added to permeabilized muscle preparations.
11. Reaction conditions: $5 \mu\text{M}$ LC $_{20}$, $1 \mu\text{M}$ calmodulin, 10 nM MLCK, 25 mM Tris-HCl, pH 7.5, 60 mM KCl, 4 mM MgCl $_2$, 0.1 mM CaCl $_2$, 1 mM DTT, 0.1% (v/v) Tween-80, 0.2 mM ATP.
12. EDTA chelates all the free Mg $^{2+}$, which is required for the kinase substrate (MgATP) and therefore terminates the kinase reaction.

Acknowledgments

This work was supported by grants from the Canadian Institutes of Health Research (CIHR) and the Heart & Stroke Foundation of Alberta, Nunavut & NWT. MPW is an Alberta Heritage Foundation for Medical Research (AHFMR) Medical Scientist, recipient of a Canada Research Chair (Tier I) in Biochemistry, and Director of the CIHR Group in Regulation of Vascular Contractility. EK is recipient of Fellowships from AHFMR and the Heart & Stroke Founda-

tion of Canada. DPW was recipient of fellowships from AHFMR and the Heart & Stroke Foundation of Canada.

References

1. Cohen, P. (2002) The origins of protein phosphorylation. *Nature Cell Biol.* **4**, E127–E130.
2. Manning, G., Whyte, D. B., Martinez, R., Hunter, T., and Sudarsanam, S. (2002) The protein kinase complement of the human genome. *Science* **298**, 1912–1934.
3. Alonso, A., Sasin, J., Bottini, N., et al. (2004) Protein tyrosine phosphatases in the human genome. *Cell* **117**, 699–711.
4. Honkanen, R. E. (2005) Serine/threonine protein phosphatase inhibitors with anti-tumor activity, in *Handbook of Experimental Pharmacology: Inhibitors of Protein Kinases and Protein Phosphatases* (Pinna, L. A., ed.), Springer-Verlag, Berlin, Vol. 167, pp. 295–317.
5. Allen, B. G. and Walsh, M. P. (1994) The biochemical basis of the regulation of smooth-muscle contraction. *Trends Biochem. Sci.* **19**, 362–368.
6. Kamm, K. E. and Stull, J. T. (2001) Dedicated myosin light-chain kinases with diverse cellular functions. *J. Biol. Chem.* **276**, 4527–4530.
7. Hartshorne, D. J., Ito, M., and Erdödi, F. (2004) Role of protein phosphatase type 1 in contractile functions: myosin phosphatase. *J. Biol. Chem.* **279**, 37,211–37,214.
8. Oliver, C. J. and Shenolikar, S. (1998) Physiological importance of protein phosphatase inhibitors. *Front. Biosci.* **3**, D961–D972.
9. Eto, M., Ohmori, T., Suzuki, M., Furuya, K., and Morita, F. (1995) A novel protein phosphatase-1 inhibitory protein potentiated by protein kinase C. Isolation from porcine aorta media and characterization. *J. Biochem. (Tokyo)* **118**, 1104–1107.
10. Eto, M., Senba, S., Morita, F., and Yazawa, M. (1997) Molecular cloning of a novel phosphorylation-dependent inhibitory protein of protein phosphatase-1 (CPI-17) in smooth muscle: its specific localization in smooth muscle. *FEBS Lett.* **410**, 356–360.
11. Woodsome, T. P., Eto, M., Everett, A., Brautigan, D. L., and Kitazawa, T. (2001) Expression of CPI-17 and myosin phosphatase correlates with Ca^{2+} sensitivity of protein kinase C-induced contraction in rabbit smooth muscle. *J. Physiol.* **535**, 553–564.
12. Senba, S., Eto, M., and Yazawa, M. (1999) Identification of trimeric myosin phosphatase (PP1M) as a target for a novel PKC-potentiated protein phosphatase-1 inhibitory protein (CPI17) in porcine aorta smooth muscle. *J. Biochem. (Tokyo)* **125**, 354–362.
13. Eto, M., Karginov, A., and Brautigan, D. L. (1999) A novel phosphoprotein inhibitor of protein type-1 phosphatase holoenzymes. *Biochemistry* **38**, 16,952–16,957.
14. Liu, Q. R., Zhang, P. W., Zhen, Q., Walther, D., Wang, X. B., and Uhl, G. R. (2002) KEPI, a PKC-dependent protein phosphatase 1 inhibitor regulated by morphine. *J. Biol. Chem.* **277**, 13,312–13,320.

15. Koyama, M., Ito, M., Feng, J., et al. (2000) Phosphorylation of CPI-17, an inhibitory phosphoprotein of smooth muscle myosin phosphatase, by Rho-kinase. *FEBS Lett.* **475**, 197–200.
16. Hamaguchi, T., Ito, M., Feng, J., et al. (2000) Phosphorylation of CPI-17, an inhibitor of myosin phosphatase, by protein kinase N. *Biochem. Biophys. Res. Commun.* **274**, 825–830.
17. Deng, J. T., Sutherland, C., Brautigan, D. L., Eto, M., and Walsh, M. P. (2002) Phosphorylation of the myosin phosphatase inhibitors, CPI-17 and PHI-1, by integrin-linked kinase. *Biochem. J.* **367**, 517–524.
18. MacDonald, J. A., Eto, M., Borman, M. A., Brautigan, D. L., and Haystead, T. A. J. (2001) Dual Ser and Thr phosphorylation of CPI-17, an inhibitor of myosin phosphatase, by MYPT-associated kinase. *FEBS Lett.* **493**, 91–94.
19. Erdődi, F., Kiss, E., Walsh, M. P., et al. (2003) Phosphorylation of protein phosphatase type-1 inhibitory proteins by integrin-linked kinase and cyclic nucleotide-dependent protein kinases. *Biochem. Biophys. Res. Commun.* **306**, 382–387.
20. Takizawa, N., Koga, Y., and Ikebe, M. (2002) Phosphorylation of CPI17 and myosin binding subunit of type 1 protein phosphatase by p21-activated kinase. *Biochem. Biophys. Res. Commun.* **297**, 773–778.
21. Kitazawa, T., Eto, M., Woodsome, T. P., and Brautigan, D. L. (2000) Agonists trigger G protein-mediated activation of the CPI-17 inhibitor phosphoprotein of myosin light-chain phosphatase to enhance vascular smooth muscle contractility. *J. Biol. Chem.* **275**, 9897–9900.
22. Eto, M., Kitazawa, T., Yazawa, M., Mukai, H., Ono, Y., and Brautigan, D. L. (2001) Histamine-induced vasoconstriction involves phosphorylation of a specific inhibitor protein for myosin phosphatase by protein kinase C α and δ isoforms. *J. Biol. Chem.* **276**, 29,072–29,078.
23. Niirō, N., Koga, Y., and Ikebe, M. (2003) Agonist-induced changes in the phosphorylation of the myosin-binding subunit of myosin light-chain phosphatase and CPI17, two regulatory factors of myosin light-chain phosphatase, in smooth muscle. *Biochem. J.* **369**, 117–128.
24. Kitazawa, T., Eto, M., Woodsome, T. P., and Khalequzzamana, M. D. (2003) Phosphorylation of the myosin phosphatase targeting subunit and CPI-17 during Ca^{2+} sensitization in rabbit smooth muscle. *J. Physiol.* **546**, 879–889.
25. Wilson, D. P., Susnjar, M., Kiss, E., Sutherland, C., and Walsh, M. P. (2005) Thromboxane A_2 -induced contraction of rat caudal arterial smooth muscle involves activation of Ca^{2+} entry and Ca^{2+} sensitization: Rho-associated kinase-mediated phosphorylation of MYPT1 at Thr-855 but not Thr-697. *Biochem. J.* **389**, 763–774.
26. Eto, M., Kitazawa, T., and Brautigan, D. L. (2004) Phosphoprotein inhibitor CPI-17 specificity depends on allosteric regulation of protein phosphatase-1 by regulatory subunits. *Proc. Natl. Acad. Sci. USA* **101**, 8888–8893.
27. Li, L., Eto, M., Lee, M. R., Morita, F., Yazawa, M., and Kitazawa, T. (1998) Possible involvement of the novel CPI-17 protein in protein kinase C signal transduction of rabbit arterial smooth muscle. *J. Physiol.* **508**, 871–881.

28. Somlyo, A. P. and Somlyo, A. V. (2003) Ca^{2+} sensitivity of smooth muscle and nonmuscle myosin II: modulated by G proteins, kinases, and myosin phosphatase. *Physiol. Rev.* **83**, 1325–1358.
29. Ohki, S., Eto, M., Kariya, E., et al. (2001) Solution NMR structure of the myosin phosphatase inhibitor protein CPI-17 shows phosphorylation-induced conformational changes responsible for activation. *J. Mol. Biol.* **314**, 839–849.
30. Allen, B. G., Andrea, J. E., and Walsh, M. P. (1994) Identification and characterization of protein kinase $\text{C}\zeta$ -immunoreactive proteins. *J. Biol. Chem.* **269**, 29,288–29,298.
31. Walsh, M. P., Valentine, K. A., Ngai, P. K., Carruthers, C. A., and Hollenberg, M. D. (1984) Ca^{2+} -dependent hydrophobic interaction chromatography. Isolation of a novel Ca^{2+} -binding protein and protein kinase C from bovine brain. *Biochem. J.* **224**, 117–127.
32. Ngai, P. K., Carruthers, C. A., and Walsh, M. P. (1984) Isolation of the native form of chicken gizzard myosin light-chain kinase. *Biochem. J.* **218**, 863–870.
33. Weber, L. P., Van Lierop, J. E., and Walsh, M. P. (1999) Ca^{2+} -independent phosphorylation of myosin in rat caudal artery and chicken gizzard myofilaments. *J. Physiol.* **516**, 805–824.
34. Andrea, J. E. and Walsh, M. P. (1992) Protein kinase C of smooth muscle. *Hypertension* **20**, 585–595.
35. Winder, S.J. and Walsh, M.P. (1990) Smooth muscle calponin. Inhibition of actomyosin MgATPase and regulation by phosphorylation. *J. Biol. Chem.* **265**, 10,148–10,155.

Purification of Smooth Muscle Myosin Phosphatase Using a Thiophosphorylated Myosin Light-Chain-Affinity Resin

Meredith Borman and Justin MacDonald

Summary

Many protein kinases are able to catalyze the thiophosphorylation of protein substrates via a phospho-transfer reaction using adenosine-5'-*o*(3-thiotriphosphate) (ATP γ S) (*1*), but, in general, thiophosphorylated proteins are very poor substrates for protein phosphatases (*2,3*). As a result, the protein substrate is essentially trapped in the phosphorylated state. This thiophosphorylation can be exploited in order to generate a strategy for the selective purification of protein phosphatases. Indeed, a number of thiophosphorylated protein substrates have been successfully used for the affinity purification of protein phosphatases (*4-7*). Here we describe the use of thiophosphorylated smooth muscle myosin regulatory light chains for the selective purification of the smooth muscle myosin phosphatase holoenzyme.

Key Words: Myosin phosphatase; thiophosphorylation; affinity chromatography; smooth muscle; myosin regulatory light chain

1. Introduction

Phosphorylation of myosin II plays an important role in many cellular processes, including cell motility, cytokinesis, and smooth muscle contraction (*8*). The level of myosin phosphorylation is regulated by the activities of two enzymes: myosin light-chain kinase (MLCK) (*9*) and myosin phosphatase (MP) (*10*). MP is composed of three subunits: a catalytic subunit of type 1 phosphatase, PP1c; a targeting subunit, termed myosin phosphatase target subunit (MYPT1); and a smaller subunit, M20, of unknown function (*11*). This heterotrimeric phosphatase is the target of a number of regulatory pathways that can both increase (*12,13*) and decrease (*14,15*) the activity of this enzyme.

Myosin phosphatase is believed to be specific for a single substrate *in vivo*: phosphorylated myosin. This chapter will discuss the procedures used to purify smooth muscle myosin, along with the biotinylation, thiophosphorylation, and immobilization steps required to generate an affinity resin for the purification of myosin phosphatase. Although the specific methods outlined here focus on the use of thiophosphorylated myosin as a substrate for capturing myosin phosphatase from smooth muscle tissue, the same principles can be applied to the purification of any number of protein phosphatases. The methodology described provides a powerful approach for the selective purification of protein phosphatases.

2. Materials

2.1. Purification of Myosin Regulatory Light Chain

1. Buffer A: 10 mM Tris-HCl, pH 7.5, 50 mM KCl, 2 mM EGTA, 15 mM MgCl₂, 0.2 mM dithiothreitol (DTT), 3% Triton X-100. All buffers are stored at 4°C unless otherwise noted.
2. Buffer B: 10 mM Tris-HCl, pH 7.5, 100 mM KCl, 2 mM EGTA, 0.2 mM DTT.
3. Buffer C: 40 mM imidazole, pH 7, 4 mM EDTA, 2 mM EGTA, 0.5 mM DTT, 5 mM ATP.
4. Buffer D: 50 mM Tris-HCl, pH 7.5, 1 mM DTT, 7 M urea. Store at room temperature.
5. Peristaltic pump.
6. 1 M MgCl₂.
7. 100 mM ATP, pH 7.0. Store at -20°C.
8. 200 mM EGTA, pH 7.0.
9. 200 mM NaH₂PO₄, 200 mM Na₂HPO₄.
10. Glass wool.
11. 30 mL Potter-Elvehjem homogenizer.
12. Absolute ethanol. Store at room temperature.
13. Phenyl Sepharose 6 Fast Flow (high sub) (GE Healthcare).
14. Econo column, 2.5 × 10.0 cm (Bio-Rad).
15. Dialysis buffer: 20 mM MOPS, pH 7.5, 100 mM KCl, 1 mM EDTA, 1 mM DTT.
16. Elution buffer: 10 mM MOPS, pH 7.5, 1 mM DTT.
17. Fraction collector.
18. SDS-PAGE (sodium dodecyl sulfate–polyacrylamide gel electrophoresis) equipment (such as the Bio-Rad Mini-PROTEAN 3).
19. Polyethylene glycol 8000 (PEG 8000).
20. Dialysis membrane [Spectra/Por 3, 3500 molecular weight cut off (MWCO)].

2.2. Biotinylation of Myosin Regulatory Light Chain

1. Biotinylation buffer: 50 mM Tris-HCl, pH 8.3, 5 mM EDTA, 0.1 mM DTT.
2. Buffer E: 100 mM sodium phosphate, pH 7.0, 1 mM EDTA, 1 mM DTT.
3. *N*-Iodoacetyl-*N*-biotinyloxyhexylenediamine (Pierce).

2.3. Thiophosphorylation of Myosin Regulatory Light Chain

1. MLCK (Upstate).
2. Thiophosphorylation buffer: Sodium phosphate, pH 7.0, 5 μ M calmodulin, 1 mM CaCl_2 , 25 mM MgCl_2 , 1 mM DTT, and 1 mM $\text{ATP}\gamma\text{S}$ (Sigma).
3. PBS (phosphate=buffered saline): 100 mM sodium phosphate, pH 7.2, 150 mM NaCl.
4. ^{32}P - γ -ATP (Specific activity 4500 Ci/mmol; MP Biomedicals).

2.4. Coupling of thiophosphorylated-biotinylated Regulatory Light Chain to immobilized avidin

1. Immobilized avidin (Pierce).
2. Econo column, 1.0 \times 10.0 cm (Bio-Rad).

2.5. Purification of Myosin Phosphatase

1. Buffer F: 25 mM Tris-HCl, pH 7.5, 1 mM EDTA, 1 mM DTT, 1 mM benzamidine, 0.1 mM phenylmethylsulfonyl fluoride (PMSF), 4 μ g/mL leupeptin, 1 μ g/mL pepstatin, 1 μ g/mL aprotinin.
2. Buffer G: 25 mM Tris-HCl, pH 7.5, 0.6 M NaCl, 0.5% Triton X-100 (v/v), 0.1% 2-mercaptoethanol, 2 mM EGTA, 1 mM benzamidine, 0.1 mM PMSF, 4 μ g/mL leupeptin, 1 μ g/mL pepstatin, 1 μ g/mL aprotinin.
3. Buffer H: 25 mM Tris-HCl, pH 7.5, 0.1 mM EGTA, 0.02% (w/v) Brij-35, 10% glycerol, 0.1% (v/v) 2-mercaptoethanol, 0.1 M NaCl, 1 mM benzamidine, 0.1 mM PMSF, 4 μ g/mL leupeptin, 1 μ g/mL pepstatin, 1 μ g/mL aprotinin.
4. Assay buffer: 25 mM HEPES, pH 7.4, 1 mM DTT, 1 mM EDTA.
5. ^{32}P -labeled regulatory light chain (RLC).
6. BSA (bovine serum albumin).
7. 25% (w/v) Trichloroacetic acid (TCA)
8. 96-well V-bottom microtiter plate.

3. Methods

The methods described in this section outline (1) the myosin RLC protein purification procedure, (2) the biotinylation of RLC, (3) the thiophosphorylation of RLC, (4) the generation of thiophosphorylated, biotinylated RLC-affinity capture media, and (5) the purification of a myosin phosphatase. The same principles can be applied to a multitude of substrates for the purification of a variety of protein phosphatases.

3.1. Purification of Myosin RLC from Chicken Gizzard

The purification of the myosin RLC is commonly undertaken using chicken gizzard as an excellent source for this protein. The isolation procedure for RLC is a modification of the protocol first published by Persechini and Hartshorne (16).

1. Mince 100 g of frozen chicken gizzard in a meat grinder.
2. Homogenize the gizzards in 6 vol (600 mL) of buffer A in a Waring blender (2 L capacity) on high speed for 1 min (*see Note 1*). Centrifuge the homogenate for 5 min at 3800g.
3. Discard the supernatant and repeat **step 2** four times.
4. Discard the supernatant and repeat **step 2** three times in buffer B.
5. Discard the supernatant and extract the myosin by suspending the pellet in 200 mL of buffer C in a Waring blender on high speed for 1 min. Centrifuge the homogenate for 20 min at 22,100g. Discard the pellet.
6. To the supernatant add MgCl_2 and ATP, by peristaltic pump at a rate of 1 mL/min, to a final concentration of 150 mM and 2.5 mM, respectively. Let solution stand for 10 min.
7. Centrifuge solution for 10 min at 22,100g. Filter supernatant through glass wool and discard pellet. Centrifuge filtered supernatant at 50,000g overnight.
8. Measure the volume of the supernatant and discard the pellet. Slowly add 10 vol of cold water to the supernatant while stirring.
9. Centrifuge the sample at 17,600g for 15 min. Discard the supernatant and resolubilize the pellet in 200 mL of water using a Potter–Elvehjem homogenizer.
10. With the aid of a peristaltic pump (1 mL/min, while stirring) add the following in order: 1.5 mL of 200 mM EGTA; 1.378 mL NaH_2PO_4 /9.2 mL Na_2HPO_4 ; 53 mL of 1 M MgCl_2 ; and 13.9 mL of 100 mM ATP, pH 7. Let mixture stand for 10 min at 4°C.
11. Centrifuge the sample at 186,000g for 3 h. Measure the volume of the supernatant and discard the pellet. Slowly add 10 vol of cold water while stirring.
12. Centrifuge the sample at 17,600g for 15 min. Discard the supernatant and store the pellets at 4°C overnight.
13. Resolubilize the pellets in 100 mL of buffer D at room temperature using a Potter–Elvehjem homogenizer. Stir the homogenate for 3 h at room temperature on a magnetic stir plate before subjecting to centrifugation at 31,000g for 15 min.
14. Set the supernatant aside and add an additional 50 mL of buffer D to the pellets and homogenize gently using a Potter–Elvehjem homogenizer. Centrifuge the homogenate at 31,000g for 15 min and combine the supernatant with that from **step 13**.
15. Slowly add 1 vol (150 mL) of absolute ethanol with stirring. Centrifuge the solution in a single centrifuge bottle at 17,600g for 15 min.
17. Filter the supernatant through glass wool and add an additional 1.5 vol (450 mL) of absolute ethanol with stirring. Centrifuge the solution in a single centrifuge bottle at 17,600g for 15 min.
18. Discard the supernatant and resolubilize the pellet in 30 mL of dialysis buffer. The pellet now contains a combination of the myosin regulatory and essential light chains. Dialyze the light chains against 4 by 1 L changes of dialysis buffer over 48–72 h.
19. Pour and equilibrate a 30-mL Phenyl Sepharose column with dialysis buffer (*see Note 2*). Load the dialyzed light chains on the equilibrated column at a flow rate of 1 mL/min and then wash the column with 150 mL of dialysis buffer.

20. Develop the column with a linear NaCl concentration gradient (600–0 mM) at a flow rate of 1 mL/min collecting 40 fractions (4 mL). Elute the column with an additional 150 mL of elution buffer collecting 4-mL fractions.
21. Identify all fractions containing RLC by SDS-PAGE (15% acrylamide) on Bio-Rad mini gels. Pool all fractions containing RLC and concentrate down using 3500 MWCO dialysis tubing and PEG 8000. Aliquot the concentrated RLC and store at -80°C .

3.2. Biotinylation of Myosin RLC

Iodoacetyl-LC-Biotin offers a convenient and rapid method of labeling proteins that possess a freely available sulfhydryl group ($-\text{SH}$). Biotinylated proteins can be subsequently purified using avidin–Sepharose chromatography. The protocol for biotinylating myosin RLC has been adapted from the procedure originally published by Shirazi et al. (7).

1. Incubate 10 mg of myosin RLC with 10 mM DTT for 90 min at 4°C (see **Note 3**).
2. Dialyze the reduced RLC against 100 vol of biotinylation buffer with three buffer changes.
3. Incubate the dialyzed RLC with 0.2 mM *N*-iodoacetyl-*N*-biotinylhexylene-diamine for 90 min in the dark at room temperature.
4. Remove excess *N*-iodoacetyl-*N*-biotinylhexylenediamine from the biotinylated RLC by dialysis with several changes against buffer E.

3.3. Thiophosphorylation of RLC

1. Incubate myosin RLC (5 mg/mL) with MLCK (0.1 mg) in thiophosphorylation buffer. The incubation should be carried out at 25°C for 30 min (see **Note 4**).
2. Dialyze the reaction mixture extensively against PBS, to remove the excess ATP γ S.
3. Incubate an aliquot of the thiophosphorylated RLC with MLCK (as in step 1, replacing 1 mM ATP γ S with 1 mM ATP and including a trace amount of ^{32}P - γ -ATP) to determine the extent of thiophosphorylation (see **Note 5**). Terminate the reaction by addition of 5 vol of 25% TCA. Centrifuge the reaction mixture for 5 min at 14,000g. Discard the supernatant and wash the pellet three more times with 5 vol of 25% TCA, discarding the supernatant after each centrifugation step. After the final wash, determine the amount of ^{32}P incorporation by Cerenkov counting.

3.4. Coupling of Thiophosphorylated-Biotinylated RLC to Immobilized Avidin

1. Wash immobilized avidin with 50 vol of PBS.
2. Incubate thiophosphorylated, biotinylated myosin RLC with immobilized avidin (10 mg/mL gel) rocking end over end for 1 h at 4°C (see **Note 6**).
3. Centrifuge the mixture for 1 min at 3000g and remove the supernatant.

4. Wash the bound complex with 10 vol of PBS. Spin the mixture at 3000g for 1 min. Discard the supernatant and repeat this wash step four times.
5. Transfer the thiophosphorylated, biotinylated RLC avidin resin to a glass chromatography column (1.0 × 10.0 cm) (*see Note 7*).

3.5. Purification of Myosin Phosphatase

1. Thaw 200 g of frozen pig bladders at 4°C in the presence of 5 vol buffer F. Homogenize the bladders in a Waring blender (2-L capacity) for 1 min on high speed. Centrifuge the homogenate at 15,000g for 10 min and discard the supernatant.
2. Rehomonize the pellet in 5 vol of buffer F. Centrifuge the homogenate at 15,000g for 10 min and discard the supernatant.
3. Resuspend the pellet in 2.5 vol of buffer G and homogenize in a Waring blender for 1 min on high speed. Allow the homogenate to stand for 30 min at 4°C and then centrifuge at 15,000g for 10 min.
4. Pour off the supernatant (the myofibrillar extract) and discard the pellet. To the supernatant, add 50% polyethylene glycol solution (w/v) to 12%. Let the mixture stand for 1 h at 4°C and then centrifuge at 15,000g for 10 min.
5. Discard the supernatant and resolubilize the pellet, by Dounce homogenization, in 100 mL of buffer H. Centrifuge the homogenate at 100,000g for 30 min (*see Note 8*).
6. Collect the supernatant and discard the pellet. Load the supernatant onto the thiophosphorylated, biotinylated myosin RLC avidin–Sephacrose column that has been equilibrated with 50 vol of buffer H and then wash the column with an additional 50 vol of buffer H.
7. Develop the column with a linear NaCl concentration gradient (0–1 M) at a flow rate of 1 mL/min, collecting 80 fractions (2 mL).
8. Assay column fractions by diluting 10 µL in 30 µL assay buffer in a 96-well V-bottom microtiter plate. Start reactions by the addition of ³²P-labeled myosin RLC (2 µM final concentration). Terminate reactions after 10 min at 25°C by the addition of 100 µL of 25% TCA. Add 10 µL of 10 mg/mL BSA to each reaction, hold on ice for 10 min, and centrifuge at 1250g for 10 min. Transfer 100 µL of supernatant of each reaction to a scintillation tube and determine the amount of ³²P released by Cerenkov counting.
9. Verify the purity of the fractions containing myosin phosphatase activity by resolving proteins by SDS-PAGE (10% acrylamide)

4. Notes

1. As an alternative, tissue homogenization can be performed using a Polytron (setting 7, 15 s, probe PT 10/35 ST).
2. It is important to use Phenyl Sepharose 6 Fast Flow (high sub) (Amersham Biosciences 17-0973-05). At 600 mM NaCl, you get very poor binding of the myosin light chains to Sigma's Phenyl Sepharose 6 Fast Flow (P-2334). Using Sigma's

- Phenyl Sepharose 6 Fast Flow, the NaCl concentration in the dialysis buffer must be increased to at least 2 M to ensure efficient binding.
3. Proteins to be biotinylated by Iodoacetyl-LC-Biotin must have a free sulfhydryl group available. Free thiols can be generated from disulfides by incubation with a reducing agent.
 4. Myosin light-chain kinase, like many protein kinases, utilizes ATP γ S much less efficiently than ATP. Therefore, higher concentrations of thio-ATP and an excess of MLCK are required to ensure stoichiometric thiophosphorylation. Other enzymes require a prolonged incubation time to ensure stoichiometric phosphorylation (17). It is necessary to determine the ideal conditions for each individual enzyme/substrate reaction.
 5. The back-phosphorylation reaction determines the efficiency of the prior thiophosphorylation of RLC. Knowing the number of moles of substrate (RLC) and the number of moles of ATP, along with the specific activity (cpm/nmol) of the ^{32}P - γ -ATP, the extent of thiophosphorylation (mol phosphate/mol substrate) can be calculated. In general, for the conditions described in **Subheading 3.2.**, the stoichiometry of RLC thiophosphorylation is greater than 0.8 mol phosphate/mol RLC.
 6. There are a number of alternative methods available for coupling thiophosphorylated substrates to immobilized resins. The method discussed in **Subheading 3.3.**, requires an available free sulfhydryl group ($-\text{SH}$) for substrate coupling. Alternatively, a number of resins are available that couple through free amine or carboxyl groups. In these cases, it is necessary to remove the free enzyme from the reaction mixture prior to substrate coupling. In the case of myosin RLC, TCA precipitation of the reaction mixture, following thiophosphorylation as described in **Subheading 3.2.**, followed by an ether wash step to remove TCA and centrifugation to remove denatured MLCK has been utilized as a method for removing free kinase from the reaction mixture (2). Thiophosphorylated myosin RLC can then be coupled to CNBr-activated Sepharose through a free amine group. Alternatively, it might be possible to separate the substrate from the enzyme following thiophosphorylation, using anion-exchange chromatography. Additionally, GST-tagged kinase can be used to thiophosphorylate substrate protein, and the kinase can subsequently be recovered from the reaction mixture using glutathione-Sepharose chromatography. The method used to separate the enzyme from the substrate following thiophosphorylation will depend on the individual enzyme and substrate properties.
 7. The method as described in **Subheading 3.3.** was performed using a Bio-Rad Econo column and a gravity flow column setup. Alternatively, the coupled resin can be packed into a glass FPLC column (1.0 \times 10.0 cm) for use with an automated chromatography system.
 8. At this stage, an additional fractionation step can be performed using anion-exchange chromatography. The complexity of the sample will determine whether any additional purification steps will be required.

Acknowledgments

MAB is a recipient of a Fellowship from the Heart & Stroke Foundation of Canada. JAM is a Heart & Stroke Foundation of Canada Scholar, recipient of the Protein Engineering Network of Centres of Excellence Chair in Protein Sciences, and a Canada Research Chair (Tier II) in Smooth Muscle Pathophysiology.

References

1. Goody, R. S., Eckstein, F., and Schrimmer, R. H. (1972) The enzymatic synthesis of thiophosphate analogs of nucleotides. *Biochim. Biophys. Acta* **276**, 155–161.
2. Gratecos, D., and Fischer, E. H. (1974) Adenosine 5'-*o*(3-thiotriphosphate) in the control of phosphorylase activity. *Biochem. Biophys. Res. Commun.* **58**, 960–967.
3. Morgan, M., Perry, S. V., and Ottaway, J. (1976) Myosin light-chain phosphatase. *Biochem. J.* **157**, 687–697.
4. McGowan, C. H. and Cohen, P. (1988) Protein phosphatase-2C from rabbit skeletal muscle and liver: An Mg^{2+} -dependent enzyme. *Methods Enzymol.* **159**, 416–426.
5. Tonks, N. K., Diltz, C. D., and Fischer, E. H., (1991) Purification of protein-tyrosine phosphatases from human placenta. *Methods Enzymol.* **201**, 427–442.
6. Senba, S., Eto, M., and Yazawa, M. (1999) Identification of trimeric myosin phosphatase (PP1M) as a target for a novel PKC-potentiated protein phosphatase-1 inhibitory protein (CPI17) in porcine aorta smooth muscle. *J. Biochem.* **125**, 354–362.
7. Shirazi, A., Iizuka, K., Fadden, P., et al. (1994) Purification and characterization of the mammalian myosin light chain phosphatase holoenzyme. *J. Biol. Chem.* **269**, 31,598–31,606.
8. Hartshorne, D. J. (1987) Biochemistry of the contractile process in smooth muscle, in *Physiology of the Gastrointestinal Tract* (Johnson, L. R., ed.), Raven, New York, pp. 432–482.
9. Gallagher, P. J., Herring, B. P., and Stull, J. T. (1997) Myosin light chain kinases. *J. Muscle Res. Cell Motil.* **18**, 1–16.
10. Hartshorne, D. J., Ito, M., and Erdodi, F. (1998) Myosin light chain phosphatase: subunit composition, interactions and regulation. *J Muscle Res. Cell Motil.* **19**, 325–341.
11. Alessi, D., MacDougall, L. K., Sola, M. M., Ikebe, M., and Cohen, P. (1992) The control of protein phosphatase-1 by targeting subunits. The major myosin phosphatase in avian smooth muscle is a novel form of protein phosphatase-1. *Eur. J. Biochem.* **210**, 1023–1035.
12. Wu, X., Somlyo, A. V., and Somlyo, A. P. (1996) Cyclic GMP-dependent stimulation reverses G-protein-coupled inhibition of smooth muscle myosin light chain phosphatase. *Biochem. Biophys. Res. Commun.* **220**, 658–663.
13. Lee, M. R., Li, L., and Kitazawa, T. (1997) Cyclic GMP causes Ca^{2+} desensitization in vascular smooth muscle by activating the myosin light chain phosphatase. *J. Biol. Chem.* **272**, 5063–5068.

14. Somlyo, A. P. and Somlyo, A. V. (1994) Signal transduction and regulation in smooth muscle. *Nature* **372**, 231–236.
15. Somlyo, A. P. and Somlyo, A. V. (2000) Signal transduction by G proteins, Rho-kinase and protein phosphatase to smooth muscle and non-muscle myosin II. *J. Physiol.* **522**, 177–185.
16. Persechini, A. and Hartshorne, D.J. (1983) Ordered phosphorylation of the two 20,000 molecular weight light chains of smooth muscle myosin. *Biochemistry* **22**, 470–476.
17. Connor, J. H., Quan, H., Oliver, C., and Shenolikar, S. (1998) Inhibitor-1, a regulator of protein phosphatase 1 function, in *Methods in Molecular Biology, Vol. 93: Protein Phosphatase Protocols* (Ludlow, J.W., ed.), Humana, Totowa, NJ, pp. 41–58

Proteins Interacting With *Saccharomyces cerevisiae* Type 1 Protein Phosphatase Catalytic Subunit Identified by Single-Step Affinity Purification and Mass Spectrometry

Edmund P. Walsh, Douglas J. Lamont, Kenneth A. Beattie,
and Michael J. R. Stark

Summary

The catalytic subunit of type 1 protein phosphatase (PP1_C) interacts with a large number of polypeptides in eukaryotic cells from yeast to man and these regulatory subunits can both modulate the activity of PP1_C and target it to different subcellular locations. Thus, PP1 is really a family of protein phosphatases that share a common catalytic subunit, and identifying and characterizing the PP1-associated proteins is therefore critical to understanding the cellular roles of PP1 and its ability to dephosphorylate specific substrates. Here we describe methods for affinity isolation of PP1_C-containing protein complexes in the yeast *Saccharomyces cerevisiae* and the identification of the associated polypeptides by mass spectrometry. The basic method we describe could be easily adapted to study PP1_C-associated proteins in other lower or higher eukaryotes and for characterizing the protein–protein interactions of other protein phosphatases in yeast.

Key Words: Protein–protein interactions; Glc7p; yeast; PP1; affinity isolation; protein-A affinity tag; mass spectrometry

1. Introduction

The activity of many protein phosphatases is regulated by association of the catalytic subunit with one or more regulatory or targeting subunits, which can guide the phosphatase to its correct substrates or proper cellular location ([1,2](#)). In the case of mammalian PP1_C, over 50 candidate regulatory or targeting subunits have been found so far ([3](#)). *Saccharomyces cerevisiae* (budding yeast) catalytic subunit of type 1 protein phosphatase (PP1_C) is encoded by the single,

essential gene *GLC7* and we have been interested in characterizing Glc7p-associated proteins in this model eukaryote as a means to understanding the roles of yeast protein phosphatase-1 (PP1) and uncovering new PP1-dependent cellular functions. Initial work in yeast identified around 20 PP1 regulatory and targeting subunits principally through genetic studies and use of the yeast two-hybrid system. Direct isolation of Glc7p-containing protein complexes and characterization of the polypeptides that they contain has therefore provided a complementary biochemical approach that has already identified novel roles for Glc7p, (e.g., as a component of the cleavage and polyadenylation factor [CPF] complex that is involved in mRNA 3'-end processing) (4,5). Characterization of Glc7p-containing protein complexes has also provided stronger evidence for the association of Glc7p with candidate interacting proteins identified solely through yeast genomewide two-hybrid screens (e.g., ref. 6).

By engineering yeast to express Glc7p fused to a suitable affinity tag, it is possible to isolate Glc7p-containing complexes in a single purification step. The method we describe involves the use of a protein-A tag that is linked to the amino-terminus of Glc7p by a cleavage site for TEV protease. Yeast cells expressing the tagged Glc7p are lysed and Glc7p-containing protein complexes are isolated by binding to immunoglobulin (IgG)-conjugated magnetic beads (see **Note 1**). After extensive washing to remove nonspecifically bound polypeptides, the Glc7p-containing protein complexes are released from the beads using TEV protease. Following gel electrophoresis, the proteins that have copurified with Glc7p are identified using mass spectrometry. We have focused here on the biochemical aspects of the method rather than on the generation of yeast strains encoding affinity-tagged protein phosphatases because the latter involves standard methods for yeast genetic manipulation that are well documented elsewhere (7). Although developed for analysis of yeast PP1-associated polypeptides, these procedures could be easily adapted for the analysis of PP1-associated proteins in other systems or applied to the study of other yeast protein phosphatases.

Although the basic approach described in this chapter identifies proteins that copurify with Glc7p, it does not necessarily reveal which proteins make direct contact with Glc7p. Thus, multiple components of the CPF complex copurify with Glc7p, but it is not certain with which of them Glc7p interacts directly. Because many proteins that interact directly with PP1_C in yeast and higher eukaryotes do so via a conserved motif of the form R/K-V/I-X-F (8,9), the presence of such a motif in an affinity-isolated polypeptide might provide at least an indication of which proteins should be tested for a direct interaction. By carrying out a chromatographic separation on the complexes released by TEV protease, different complexes could be separated prior to sodium dodecyl sulfate–polyacrylamide gel electrophoresis (SDS-PAGE) and mass spectrom-

etry and this might allow characterization of additional proteins that cannot be detected following one-dimensional SDS-PAGE analysis. Finally, confirmation that a specific protein is genuinely Glc7p associated can be obtained by performing an affinity isolation with a tagged version of that protein and looking for copurification of Glc7p.

2. Materials

2.1. Chemicals, Reagents and Media

1. YPD medium: 20 g/L peptone, 10 g/L yeast extract, 20 g/L D-glucose.
2. Complete Protease Inhibitors (Roche).
3. Glass beads, 0.4 mm diameter (Sigma).
4. Vibrating platform (e.g., VXR Basic IKA Vibrax, IKA®).
5. TEV protease (Life Technologies).
6. Vivaspin 500 ultrafiltration concentrator (Vivascience).
7. LDS sample buffer (Invitrogen).
8. SimplyBlue SafeStain colloidal Coomassie (Invitrogen).
9. Modified bovine trypsin (Roche; sequencing grade).
10. α -Cyano-4-hydroxy-*trans*-cinnamic acid matrix (Sigma) dissolved at 10 mg/mL in water/CH₃CN (50 : 50, v/v) containing 0.1% (v/v) trifluoroacetic acid final concentration.

2.2. Buffers

All solutions should be prepared using ultrapure water (>18 M Ω ·cm) such as that produced by a Milli-Q water purification system (Millipore).

1. Phosphate-buffered saline (PBS): 8 mM sodium phosphate buffer (pH 7.4) containing 150 mM NaCl.
2. PBS/Triton: PBS containing 1% (v/v) Triton X-100.
3. Buffer B: 0.1 M boric acid adjusted to pH 9.5 with 5 M NaOH (make up to 80% final volume initially before adjusting the pH).
4. Buffer C: PBS containing 0.1% (w/v) bovine serum albumin (BSA) (autoclaved).
5. Buffer D: 0.2 M Tris-HCl (pH 8.5), 0.1% (w/v) BSA (autoclaved).
6. Lysis buffer: 50 mM HEPES-KOH (pH 7.5), 1 mM MgCl₂, 100 mM KCl, 0.1 mM EDTA (pH 8.0), 0.1% (v/v) Triton X-100.
7. IPP150 buffer: 10 mM Tris-HCl (pH 8.0), 150 mM NaCl, 0.1% (v/v) Nonidet P40.
8. TEV cleavage buffer: 10 mM Tris-HCl (pH 8.0), 150 mM NaCl, 0.1% (v/v) Nonidet P40, 0.5 mM EDTA, 1 mM dithiothreitol (DTT) (added just before use).

2.3 Yeast Strains Expressing Protein A-Tagged PP1_C (Glc7p)

1. LKY150: *MATa ade2-1 his3-11, 15 leu2-3, 112 ura3-1 can1-100 glc7::LEU2 trp1-1::YIplac204-PrA-TEV-GLC7*
2. PWY3: *MATa ade2-1 his3-11, 15 leu2-3, 112 trp1-1 ura3-1 can1-100 [pNOPPATA-1L]*

To enable affinity isolation of yeast Glc7p and its associated polypeptides, the *GLC7* gene is modified by the addition of an affinity tag fused to the Glc7p coding sequence. A tag consisting of two “Z” domains derived from *Staphylococcus aureus* protein-A provides an efficient way to affinity-isolate Glc7p through the binding to immobilized immunoglobulin (see **Note 2**). It would be undesirable for the affinity tag to interfere with the formation of Glc7p-containing complexes, and this can be minimized by requiring the tagged Glc7p to be fully functional. Because Glc7p is essential for yeast growth, functionality of the tagged Glc7p can be ensured by requiring the tagged protein to support normal growth and viability of yeast cells. Standard yeast molecular genetic methods can be used to modify the carboxy-terminus of any yeast coding region by the addition of a protein-A affinity tag (**10**); this involves homologous recombination between a polymerase chain reaction (PCR) fragment, containing the tag linked to a selectable marker gene, and the genomic locus encoding the protein of interest. However, modification of Glc7p at its C-terminus by addition of a heterologous sequence results in loss of functionality in the *in vivo* test just described. For identification of Glc7p-associated proteins, Glc7p should, therefore, be tagged at its amino-terminus to yield a fully functional tagged protein.

The strain we use for isolating Glc7p-associated proteins (LKY150) (**11**) was generated from one in which the endogenous *GLC7* gene was deleted by replacement with the *LEU2* marker gene (*glc7::LEU2*), but which remained viable because of the presence of a plasmid carrying both *GLC7* and the *URA3* marker gene. A plasmid carrying *GLC7* was modified by insertion of a DNA fragment encoding the protein-A tag followed by a cleavage site for TEV protease into the extreme 5' end of the *GLC7* open reading frame. This plasmid was integrated at the *trp1* locus in the first strain and then the *URA3* plasmid encoding the untagged gene evicted by growth on 5-fluoroorotic acid to generate LKY150, in which the sole source of the PP1_C function was the tagged protein (PrA-TEV-Glc7p). More recently, methods have been described for directly inserting an N-terminal protein-A tag into the genomic locus encoding a protein of interest (**12**) and this provides a more straightforward route for generating yeast strains expressing N-terminally tagged PP1. To control for recovery of nonspecific polypeptides, a strain expressing the unfused protein-A tag should be used in parallel. Strain PWY3, which contains a plasmid that expresses the protein-A tag driven by the *NOPI* promoter (see **ref. 13**), provides such a control.

3. Methods

3.1. Preparation of IgG-Conjugated Magnetic Beads

For binding protein-A-tagged PP1_C, M-280 Tosyl-activated Dynabeads (Invitrogen; 142.04) are conjugated to rabbit γ -globulin (Jackson Immuno-

research Laboratories, cat. no. 011-000-002) using 3 μg γ -globulin per 10^7 beads as recommended by the manufacturer. The Invitrogen website (<http://www.invitrogen.com/>) can be consulted for the latest details on how to prepare conjugated Dynabeads. All steps utilize the MPC-1 magnet to collect the beads (*see Note 3*).

1. Dilute the volume of gamma globulin solution containing 3 mg protein (approx 100 μL) into 5 mL of buffer B.
2. Resuspend the Tosyl-activated Dynabeads for 1 min by pipetting or gentle mixing and then remove 5 mL into a 15-mL screw-cap plastic tube (Falcon). Collect the beads using the MPC-1 magnet.
3. Resuspend in 5 mL of buffer B and collect the beads again using the MPC-1 magnet.
4. Wash the beads by two further cycles of resuspension and collection, finally resuspending the beads in the 5 mL of gamma globulin solution from **step 1**.
5. Mix well and incubate at 37°C for 24 h. During this incubation, the sample must be mixed gently and continuously. This is best achieved by taping the tube to a gently rocking platform in a 37°C room.
6. Collect the beads using the MPC-1 magnet and then wash them in 3×5 mL of buffer C by resuspension, mixing the tube by gentle tilting for 5 min and then collecting the beads using the magnet.
7. Resuspend in 5 mL of buffer D and incubate with mixing (*see step 5*) at 37°C for 4 h to quench any free tosyl groups.
8. Collect the beads using the MPC-1 magnet and wash in 2×5 mL of buffer C (*see step 6*).
9. Collect the beads using the MPC-1 magnet and wash in 1×5 mL PBS/Triton for 10 min (*see step 6*) to remove unconjugated gamma globulin.
10. Collect the beads using the MPC-1 magnet and wash in 2×5 mL of buffer C (*see step 6*).
11. Resuspend the beads finally in 5 mL buffer C and store at 4°C. Sodium azide can be added as a preservative at 0.02% (w/v) if desired.

3.2. Expression and Purification of Tagged PP1_C-Containing Protein Complexes

1. Grow 3-L yeast cell culture at 29°C in sterile YPD medium until the cell density reaches $1\text{--}2 \times 10^7$ cells/mL. The culture should be split between four or five 2-L flasks shaken at approx 200 rpm to ensure good mixing and aeration.
2. Harvest cells by centrifugation at 5000g for 20 min, resuspend the cells in 200 mL of lysis buffer and recover the cells by centrifugation (5000g for 10 min). Discard the supernatant.
3. Resuspend the cell pellet in 30 mL of lysis buffer containing Complete Protease Inhibitors (added according to the manufacturer's instructions) and divide into two 50-mL screw-cap plastic tubes (Falcon).

4. Add 10 mL of 0.4-mm-diameter clean glass beads to each tube. Tape the tubes to a vibrating platform and shake very vigorously for 30 min at 4°C in a cold room (see **Note 4**).
5. Centrifuge at 5000g for 5 min at 4°C to pellet the beads and remove the supernatant to a fresh tube. Centrifuge at 20,000g for 30 min at 4°C to remove cell debris and leave a cell-free protein extract (see **Note 5**).
6. Prepare 1 mL (2×10^9) of IgG-conjugated Dynabeads by washing with 3×10 mL PBS, 3×10 mL PBS/Triton, and, finally, 3×10 mL PBS, each time mixing the beads gently, collecting them using the MPC-1 magnet, and discarding the supernatant.
7. Resuspend the beads in 1 mL PBS and add to the entire lysate from 3 l of yeast cell culture together with additional Complete Protease Inhibitors. Incubate at 4°C for 2 h with gentle rotation to bind the PP1 protein complexes to the beads.
8. Wash the beads with 3×10 mL of lysis buffer (see **Note 6**), then with 3×10 mL IPP150 buffer and, finally, with 10 mL TEV cleavage buffer.
9. Resuspend beads in 1 mL TEV cleavage buffer containing 10 μ L (100 Units) TEV protease and rotate for 2 h at room temperature (16–18°C) to allow cleavage of the protein-A tag from PrA-Glc7p, releasing the Glc7p protein complexes from the beads.
10. Collect the beads using an MPC magnetic block and concentrate the bead-free supernatant by centrifugation at 12,000g for approx 30 min at 4°C in a Vivaspinn 500 ultrafiltration concentrator, reducing the volume to about 40–50 μ L.

3.3. SDS-PAGE Gel Analysis of Glc7p Protein Complexes

Best results are normally obtained using commercially available ready-cast gels and running buffer, such as the 10% polyacrylamide Bis-Tris NuPAGE gels and MES running buffer available from Invitrogen (see **Note 7**).

1. Samples for gel analysis should be dried down to a volume of 10 μ L using a centrifugal vacuum concentrator (e.g., Speedvac). Add 10 μ L of 4X LDS sample buffer, mix briefly by vortexing, and then centrifuge the sample to collect all the liquid (vortex and spin).
2. Add 5 μ L of 50 mM DTT in Milli-Q water (10 mM final concentration), vortex, and spin.
3. Incubate at 70°C for 10 min, vortex, and spin and then allow to cool.
4. Add 5 μ L of 300 mM iodoacetamide in Milli-Q water (50 mM final concentration), vortex, and spin (see **Note 8**).
5. Incubate at room temperature in the dark for 30 min with shaking.
6. Add 10 μ L of Milli-Q water, vortex, spin, and incubate at 70°C for 10 min.
7. Load 10 μ L of Mark12 Unstained Standard (Invitrogen) in lane 1 of the SDS-PAGE gel followed by the samples, leaving a clear lane between each sample.
8. Run gel at 200 V (constant voltage) for 30–60 min using an XCell Mini-Cell or XCell SureLock gel apparatus or equivalent.
9. Stain the gel using 20 mL SimplyBlue SafeStain colloidal Coomassie (see **Note 9**). Gels should be stained and then destained in water according to the manufacturer's instructions.

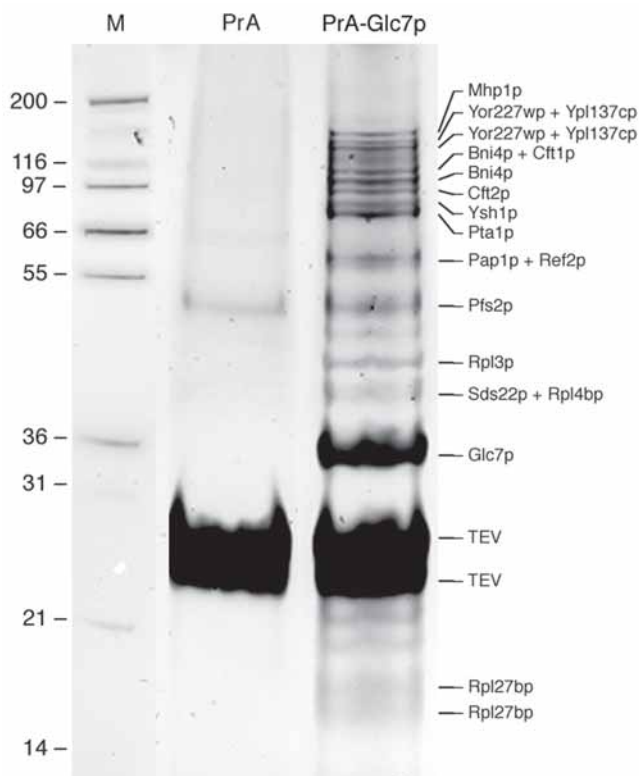


Fig. 1. Affinity isolation of Glc7p protein complexes. Protein complexes were isolated using IgG-conjugated magnetic beads from whole-cell extracts prepared from yeast cultures expressing either PrA-TEV-Glc7p (PrA-Glc7: LKY150) or PrA-TEV (PrA: PWY3) as a control. Proteins released from the beads following the addition of TEV protease were analyzed by SDS-PAGE electrophoresis and the protein bands were excised and analyzed by MALDI-TOF mass spectrometry. Proteins identified in each band by mass fingerprint analysis are indicated on the right. M, molecular mass standards (sizes in kDa). Reprinted with permission from **ref. 4**. Copyright (2002) American Chemical Society.

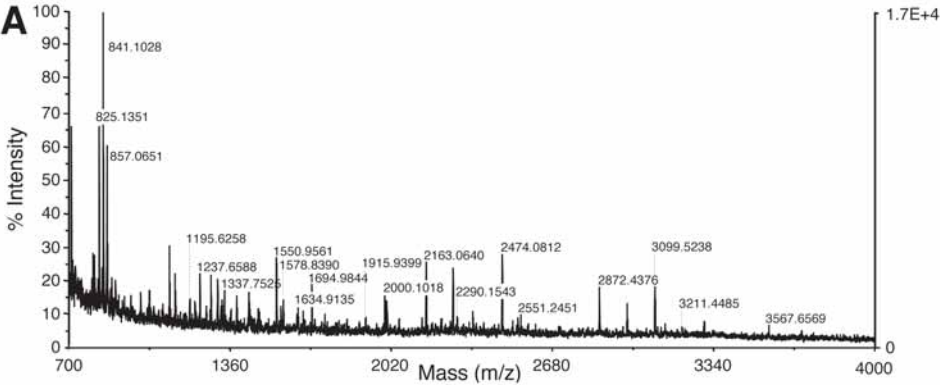
10. Comparison of the bands obtained from the strain expressing unfused protein A with those that copurify with Glc7p provides some measure of specificity, and the equivalent region of the control lane can be processed as below to demonstrate absence of a particular polypeptide from the control sample. **Figure 1** shows SDS-PAGE separation of Glc7p-associated proteins prepared as described alongside such a control sample.

3.4. In-Gel Digestion and Mass Spectrometry

Samples should be placed on a shaking platform at room temperature for all washing and incubation steps in this subsection.

1. Place the gel on a clean glass plate and excise the bands of interest from the gel in the smallest size possible (i.e., no excess around the band). Cut into 1×1 -mm pieces with a clean scalpel blade and place into a 1.5 mL microfuge tube using clean forceps.
2. Wash the band pieces with 200 μ L of Milli-Q water for 15 min.
3. Add 200 μ L of CH_3CN and wash for a further 15 min, then remove the supernatant.
4. Wash the band pieces with 200 μ L of 100 mM NH_4HCO_3 for 15 min, then remove the supernatant.
5. Wash the band pieces with 200 μ L of 100 mM $\text{NH}_4\text{HCO}_3/\text{CH}_3\text{CN}$ (50 : 50 v/v) for 15 min, then remove the supernatant (*see Note 10*).
6. Add 100 μ L of CH_3CN to dehydrate the band pieces for 10 min and remove the supernatant (*see Note 10*).
7. Dry the processed band pieces in a centrifugal vacuum concentrator for 5 min. Add a maximum of 20 μ L of 12.5 $\mu\text{g/mL}$ modified bovine trypsin in 20 mM $\text{NH}_4\text{HCO}_3/0.1\%$ (w/v) *n*-octyl-glucoside (*see Note 11*).
8. Allow the band pieces to rehydrate in digestion buffer for 30 min, adding a further 20 mM NH_4HCO_3 (minus the trypsin) to cover the gel band if needed. Incubate at 30°C overnight (> 16 h) on a shaking platform.
9. Add an equal volume of CH_3CN to the digest and incubate at 30°C for 30 min on a shaking platform.
10. For mass fingerprint analysis using matrix-assisted laser desorption ionization mass spectrometry (MALDI-MS), load one-tenth of whole digest onto a MALDI sample plate using the dried-drop method.
11. Add 1 μ L of dissolved α -cyano-4-hydroxy-*trans*-cinnamic acid matrix. Allow to dry and then carry out the mass spectrometry analysis immediately (*see Note 11*).
12. Mass spectra are searched against a suitable database using software such as ProteinProspector MS-Fit (<http://prospector.ucsf.edu/>) or Matrix Science Mascot (<http://www.matrixscience.com/>). **Figure 2A** shows a typical MALDI mass spectrum and **Fig. 2B** shows the identification of the protein from the data presented in **Fig. 2A**.

Fig. 2. Identification of Mhp1p as a Glc7p-associated protein. The band labeled Mhp1p in Fig. 1 was analyzed by MALDI-TOF-MS and by ESI-MS-MS. **(A)** Tryptic peptide mass fingerprint of Mhp1p obtained by MALDI-TOF-MS. **(B)** Results of an MS-Fit search using the spectrum shown in **(A)** that identifies Mhp1p as a significant match. **(C)** Identification of Mhp1p using capillary high-performance liquid chromatography coupled to tandem mass spectrometry. An amino acid sequence tag corresponding to the Mhp1p tryptic peptide 1057–1074 observed in **(B)** was obtained by tandem ESI-MS-MS. Note that mass spectrometry cannot discriminate between the isobaric amino acids Q/K and I/L. The peptide parent m/z value (for $[\text{M}+2\text{H}]^{2+}$) was 1026.64. **(A)** and **(C)** are reprinted with permission from **ref. 4**. Copyright (2002) American Chemical Society.

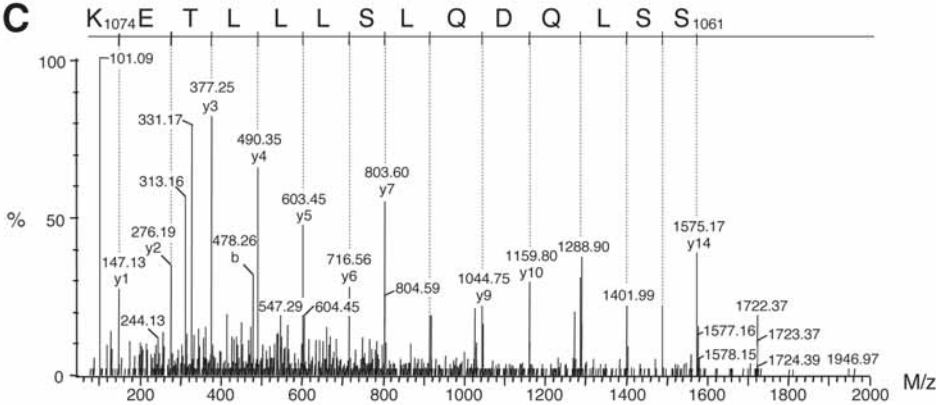


B

Rank	MOWSE Score	# (%) Masses Matched	Protein MW (Da)/pI	Species	Swissprot.111100 Accession #	Protein Name
1	1.18e+009	19/64 (29%)	155208.2 / 6.86	YEAST	P43638	MAP-HOMOLOGOUS PROTEIN 1
2	3.82e+003	7/64 (10%)	126818.6 / 6.13	MESAU	Q64398	DIACYLGLYCEROL KINASE ETA
3	2.59e+003	7/64 (10%)	147548.4 / 7.03	HSV11	Q00103	HYPOTHETICAL GENE 72 PROTEIN
4	1.57e+003	6/64 (9%)	74266.9 / 8.62	RICPR	Q9ZCB1	GLCYL-TRNA SYNTHETASE BETA CHAIN
5	1.44e+003	6/64 (9%)	73777.4 / 8.38	HUMAN	P23786	CARNITINE O-PALMITOYLTRANSFERASE II

1. 19/64 MATCHES (29%). 155208.2 DA, PI 6.86. ACC. # P43638. YEAST. MAP-HOMOLOGOUS PROTEIN 1

m/z submitted	MH ⁺ searched	Delta ppm	start	end	Peptide sequence
710.4197	710.3990	29.2116	384	389	(K)FGAFLR(K)
1085.5693	1085.5995	-27.8541	1102	1110	(K)VVHDLFDLKL(L)
1085.5693	1085.5955	-24.1487	1111	1120	(K)ILNQLNLEGGK(E)
1134.6610	1134.6271	29.8867	896	905	(K)FLSLNGTNLR(V)
1237.6588	1237.6945	-28.8393	285	295	(K)LAAFKEGNFIK(S)
1237.6588	1237.6251	27.2344	1126	1135	(R)LCFIEASLR(G)
1281.7330	1281.7068	20.4541	332	343	(K)GRPIPPHPDAPK(L)
1387.7382	1387.0004	27.2729	551	564	(R)NIVMAAAEAAAEAR(A)
1437.8727	1437.8429	20.6948	663	675	(K)KGSTDPILQLR(N)
1441.7645	1441.7222	29.3508	80	92	(R)HVSVAASLLMDNQR(A)
1550.9561	1550.9720	18.7325	434	447	(K)ITTVPLENIRPLK(H)
1578.8390	1578.8240	9.4997	93	108	(R)ANAGSTSVNTPIPPR(G)
1660.8160	1660.7462	42.0683	1159	1173	(R)KGGNQAPNSESCQR(M)
1694.9844	1694.9441	23.7580	1252	1267	(K)LVGGGDLVVDKEILNR(A)
1839.9248	1839.9111	7.4472	636	649	(K)IPHDIVYTRCCHLR(E)
2052.0551	2052.0501	2.4190	1057	1074	(K)DSQFSSLQDQLSLLTEK(A)
2354.1060	2354.0876	7.8534	448	467	(K)HVSFATNTYFNDPPQIQSK(N)
2474.0812	2474.1013	-8.1256	220	239	(R)SKTSEVYYENHPQSYHYGR(M)
2872.4376	2872.4746	-12.8826	1284	1308	(K)NDVSTILGVDELHSQGYHLHHIFK(K)
2985.2579	2985.3098	-17.3851	1212	1237	(R)EGDDSNVNHEDVPANDQQFRDEVDIK(N)
3099.5238	3099.5639	-12.9304	191	219	(R)TATISAESPPLQYNAPPSYNDTVPLTR(S)



13. More robust peptide identification can be performed by tandem mass spectrometry (e.g. MALDI-TOF-TOF [time-of-flight] analysis), or high performance liquid chromatography coupled to tandem mass spectrometry (liquid chromatography [LC]-MS-MS). An example of the methodology for this is given by Walsh et al. (4) and Fig. 2C shows a typical MS-MS spectrum obtained in this way. Note that *n*-octyl-glucoside would have to be removed by strong cation-exchange purification prior to this analysis. (See Note 12.)
14. Candidate proteins that can interact directly with Glc7p can be identified by searching their amino acid sequence using the search consensus [KR] X{0,4} [RHQKAMNST] [VI] [RHSATMK] [FW] X{0,3} [END] derived from ref. 9.

4. Notes

1. In our hands, use of IgG-conjugated magnetic beads provides an easier and cleaner approach for affinity isolation than using products such as IgG-Sepharose, which gives a higher level of nonspecific polypeptide bands in the pool of affinity-isolated material.
2. The use of protein-A tags for affinity purification of protein complexes in yeast and other systems has also recently come to prominence in the form of the tandem affinity purification (TAP) tag. In the TAP approach, the protein-A tag is joined to a calmodulin-binding peptide via the TEV cleavage site, allowing for two different sequential affinity steps. The first involves IgG-affinity isolation using the protein-A tag as described here, then after recovering complexes following TEV protease cleavage, they are reisolated on immobilized calmodulin in the presence of Ca^{2+} and recovered following Ca^{2+} chelation (14). In principle, the TAP method allows for a much cleaner isolation of protein complexes and it has been used recently to isolate large numbers of yeast protein complexes following a genomewide TAP-tagging approach (5). However, in the case of Glc7p-associated complexes, we found that the higher yield of Glc7p-associated polypeptides using the single-step protein-A tag offsets the advantages of the higher purity that can be obtained with the TAP procedure. One advantage of the TAP method is that the TEV protease used to elute the protein complexes in the first step is removed by the second step.
3. It is recommended that the tube cap is loosened before beads are collected on the MPC-1 magnet to avoid disturbing the pelleted beads when the supernatant is subsequently removed.
4. Other methods for cell breakage are perfectly acceptable (e.g., using a Bead Beater [BioSpec Products, Inc.] to apply the required force to the cell/glass bead suspension). However, it is important to ensure that the suspension does not heat up, and if using a mechanical disrupter such as a Bead Beater, the sample should be cooled on ice between repeated short bursts of disruption to prevent heating.
5. If necessary, the extract can be snap-frozen in liquid nitrogen at this stage. However, it is probably more reliable to isolate the protein complexes as quickly as possible from a freshly prepared extract.
6. Lysis buffer containing 0.5–1.0 M KCl can be used at this stage to increase the stringency of washing. Many of the most abundant yeast Glc7p-associated pro-

teins remain associated under these conditions, but although the higher salt concentrations are effective at removing proteins that are nonspecifically associated, the yield of many of the specifically associated polypeptides is reduced (4).

7. Commercial gels and running buffers such as those provided by Invitrogen are keratin free and generally perform better than home-made gels and buffers, which are much more prone to contamination by keratin. If home-made buffers and gels are used, great care must be taken when preparing these materials to exclude keratin. To minimize keratin contamination it is also recommended that all steps be undertaken in a laminar flow cabinet and that gloves be worn at all times. Two-dimensional gel separation can be used to improve the resolution of the purified proteins.
8. It is best to carry out this reductive alkylation step before running the samples on the gel.
9. SimplyBlue SafeStain colloidal Coomassie is particularly suitable because it has an end point (i.e., the gel cannot be overstained) and a detection limit of approx 10 ng per band. As an alternative, Sypro Orange (Molecular Probes) in 10% (v/v) acetic acid can be used together with detection using a Dark Reader transilluminator (Clare Chemical Research).
10. For polypeptides of 20 kDa or less, **steps 5 and 6 of Subheading 3.4.** can be omitted to minimize sample washout. For polypeptides of greater than 20 kDa, if the band pieces are still stained after **step 6**, then additional NH_4HCO_3 and $\text{NH}_4\text{HCO}_3/\text{CH}_3\text{CN}$ washes should be included.
11. For two-dimensional gel spots, reduce the trypsin solution volume to, for example 5 μL and digest in a 0.5-mL microcentrifuge tube.
12. The type of mass spectrometry that can be used will depend on the local facilities that are available. Mass fingerprints can be obtained using electrospray ionization (ESI) or MALDI mass spectrometry (MS) analysis. MALDI-MS has the advantages that it is quick, easy to carry out, requires minimal sample clean up and gives more straightforward spectra as predominantly singly-charged species are formed (e.g., **1g, 2A**). Therefore, it is ideally suited to the generation of mass fingerprint data, whereby polypeptide identification is achieved by matching the masses of multiple ions against those predicted from the database sequence of a specific protein (see, e.g., **Fig. 2B**). However, only a limited amount of sample can be loaded without concentration. Where samples are more complex (because of multiple proteins present in the gel slice), the addition of a liquid chromatography step (LC-MS) might be needed. If a tandem mass spectrometer is available (MALDI-TOF-TOF or ESI-MS-MS), more robust protein identification can be obtained by using the sequence information generated.

Acknowledgments

We acknowledge the support of the UK Medical Research Council for the development of the methods reported in this chapter and the Wellcome Trust for support of the “Fingerprints” Proteomics Facility at Dundee (JIF award 060269).

References

1. Bollen, M. (2001) Combinatorial control of protein phosphatase-1. *Trends Biochem. Sci.* **26**, 426–431.
2. Janssens, V. and Goris, J. (2001) Protein phosphatase 2A: a highly regulated family of serine/threonine phosphatases implicated in cell growth and signalling. *Biochem. J.* **353**, 417–439.
3. Cohen, P. T. (2002) Protein phosphatase 1: targeted in many directions. *J. Cell Sci.* **115**, 241–256.
4. Walsh, E. P., Lamont, D. J., Beattie, K. A., and Stark, M. J. (2002) Novel interactions of *Saccharomyces cerevisiae* type 1 protein phosphatase identified by single-step affinity purification and mass spectrometry. *Biochemistry* **41**, 2409–2420.
5. Gavin, A. C., Bosche, M., Krause, R., et al. (2002) Functional organization of the yeast proteome by systematic analysis of protein complexes. *Nature* **415**, 141–147.
6. Uetz, P., Giot, L., Cagney, G., et al. (2000) A comprehensive analysis of protein-protein interactions in *Saccharomyces cerevisiae*. *Nature* **403**, 623–627.
7. Amberg, D. C., Burke, D. J., and Strathern, J. N. (2005) *Methods in Yeast Genetics: A Cold Spring Harbor Laboratory Course Manual*, Cold Spring Harbor Laboratory, Cold Spring Harbor, NY.
8. Egloff, M. P., Johnson, D. F., Moorhead, G., Cohen, P. T., Cohen, P., and Barford, D. (1997) Structural basis for the recognition of regulatory subunits by the catalytic subunit of protein phosphatase 1. *EMBO J.* **16**, 1876–1887.
9. Zhao, S. and Lee, E. Y. (1997) A protein phosphatase-1-binding motif identified by the panning of a random peptide display library. *J. Biol. Chem.* **272**, 28,368–28,372.
10. Puig, O., Rutz, B., Luukkonen, B. G., et al. (1998) New constructs and strategies for efficient PCR-based gene manipulations in yeast. *Yeast* **14**, 1139–1146.
11. Pegg, M. W., MacKelvie, S. H., Bloecher, A., Knatko, E. V., Tatchell, K., and Stark, M. J. (2002) Essential functions of Sds22p in chromosome stability and nuclear localization of PP1. *J. Cell Sci.* **115**, 195–206.
12. Gauss, R., Trautwein, M., Sommer, T., and Spang, A. (2005) New modules for the repeated internal and N-terminal epitope tagging of genes in *Saccharomyces cerevisiae*. *Yeast* **22**, 1–12.
13. Lau, D., Kunzler, M., Braunwarth, A., et al. (2000) Purification of protein A-tagged yeast ran reveals association with a novel karyopherin beta family member, Pdr6p. *J. Biol. Chem.* **275**, 467–471.
14. Puig, O., Caspary, F., Rigaut, G., et al. (2001) The tandem affinity purification (TAP) method: a general procedure of protein complex purification. *Methods* **24**, 218–229.

Expression of Protein Histidine Phosphatase in *Escherichia coli*, Purification, and Determination of Enzyme Activity

Nicole Bäumer, Anette Mäurer, Josef Krieglstein, and Susanne Klumpp

Summary

A protein histidine phosphatase (PHP) from vertebrates was first identified in 2002. Here we describe the expression of that PHP in *Escherichia coli* and purification of the recombinant protein. In addition, a detailed protocol is provided describing determination of PHP activity in vitro. Proteins phosphorylated on histidine residues in general cannot be easily obtained. This also applies to the substrates of PHP. To circumvent that obstacle, assay conditions are introduced enabling scientists to study PHP activity using a substrate within crude homogenates of cells and tissues.

Key Words: Dephosphorylation; *E. coli*; expression; phosphorylation; protein histidine phosphatase; purification

1. Introduction

Detection of vertebrate proteins phosphorylated on histidine residues was first described in 1962 (1). As a next step, high-energy phosphohistidine was recognized as an intermediate in the course of catalysis in a number of enzymes responsible for metabolic functions (e.g., succinate thiokinase (2), nucleoside diphosphate kinases (NDPKs) (3), glucose-6-phosphatase (4) and ATP-citrate lyase (ACL) (5). Just now we are beginning to see an additional “signaling” implication for phosphohistidine in vertebrate proteins (e.g., G β , P-selectin, and annexin I). These proteins have been shown to undergo reversible phosphorylation on histidine residues (6–8). Nevertheless, histidine kinases (except for NDPKs) and histidine phosphatases remain enigmatic. This is in sharp contrast to prokaryotes in which phosphorylation of histidine residues and

subsequent transfer onto aspartate residues (“two-component-systems”) are well studied and understood (for review, *see* **ref. 9**).

1.1. Protein Histidine Phosphatase

The first protein histidine phosphatase (PHP) from vertebrates was described in 2002 (**10,11**). Two research groups independently discovered that enzyme: One used a bacterial protein autophosphorylated on histidine as a substrate and the other worked with a peptide substrate. Both approaches led to identical primary sequences of PHP (accession numbers: P83468 [rabbit] and AAN52504 [human]). PHP has a molecular mass of 13.7 kDa and is localized in the cytosol. It is ubiquitously expressed within eukaryotes and present in almost every tissue. Enzyme activity is independent of divalent cations. Phosphatase inhibitors acting on serine/threonine and tyrosine phosphatases have no effect on PHP. Searching for physiological substrates of PHP in vertebrates, we were first able to identify ACL (**12**) and, more recently, G β (**13**). These findings point to a crucial role of PHP in both metabolism and signal transduction.

1.2. Expression of PHP and Purification

Originally, we expressed PHP in Sf9 cells. This resulted an enzymatically active protein; however, the yield was poor. Although homologs of the PHP described in 2002 (**10,11**) are not present in bacteria, we were concerned about potential interference with all the histidine-phosphorylating events known to occur in prokaryotes. Fortunately, this concern was not confirmed.

In this chapter we describe the expression of PHP in *Escherichia coli*, yielding about 10 mg PHP per 1-L cell culture. Enzymatic properties of PHP expressed in bacteria were indistinguishable to the enzymatic behavior of PHP expressed in Sf9 cells. Purification of PHP from tissue has already been described (**10**). Here we introduce purification of recombinant PHP carrying a his₁₀ tag at the N-terminus. Although dealing with dephosphorylation of proteins carrying phosphohistidine, the artificial his tag of PHP does allow dephosphorylation of phosphohistidine residues.

1.3. Determination of PHP Activity

Proteins phosphorylated on histidine residues are not easily available in its pure form. Histidine kinases—except for NDPKs—are not commercially available. Furthermore, although a histidine kinase had been reported and purified from vertebrates (**14**; for review, *see* **ref. 15**), sequence information and cloning are still lacking. Despite these obstacles and in order to enable everyone to study PHP, great care was taken in this chapter to introduce the dephosphorylation of histidine-phosphorylated proteins in raw material: in soluble extracts from tis-

sues as well as in cell culture. Please note that when working with *purified* proteins (e.g., ACL), Mg^{2+} ions are recommended upon phosphorylation. In contrast, for the study of phosphorylation on histidines in proteins in the presence of contaminating serine, threonine, and tyrosine kinases, phosphatases chelators such as EDTA or EGTA are crucial ([16](#)). The assay introduced in this chapter is widely applicable to detect PHP activity in a semiquantitative manner. For the determination of the specific activity of PHP, we refer to recently published data using cheA as a substrate ([10](#)).

2. Materials

2.1. Chemicals and Enzymes

1. 70% Ethanol (p.a. grade). Store at -20°C .
2. Isopropanol. Store at -20°C .
3. Protein marker (peqGOLD Prestained Protein-Marker III; Peqlab).
4. Agarose for DNA electrophoresis (Serva).
5. Expression vector pET16b and *E. coli* BL21(DE3) (Novagen) (*see* **Note 1**).
6. Primers for polymerase chain reaction (PCR) and sequencing reactions synthesized by MWG Biotech (*see* **Notes 2** and **3**).
7. TOPO TA Cloning® Kit (plasmid pCR®2.1-TOPO®) for rapid cloning of PCR fragments (Invitrogen).
8. *Nde*I and *Bam*HI (20,000 U/mL, respectively), buffers, and bovine serum albumin (BSA) (New England Biolabs).
9. T4 DNA-ligase (10 WU/ μL) and 10X concentrated ligation buffer including 10 mM ATP, dNTPs (stock solution, 20 mM, respectively), and BioTherm™ DNA-Polymerase (5 U/ μL) and 10X concentrated buffer including 15 mM $MgCl_2$ for PCR (Genecraft).
10. $[\gamma\text{-}^{32}\text{P}]\text{ATP}$ with a specific activity of >5000 Ci/mmol (Amersham Biosciences).
11. QIAquick Gel Extraction Kit and Ni-NTA Agarose (Qiagen).

2.2. Solutions and Media

Sterilize solutions mentioned in **items 1–3** using a syringe and a $0.22\text{-}\mu\text{m}$ sterile filter (Millex™ GP; Millipore). Store aliquots at -20°C .

1. 200 mM IPTG (isopropyl- β -D-1-thiogalactopyranoside) for plates: 0.48 g in 10 mL double-distilled water (ddH_2O).
2. 500 mM Bluo-Gal (5-bromo-3-indolyl- β -D-galactopyranoside; Sigma) (*see* **Note 4**): 0.2 g in 10 mL dimethylformamide. Store in the dark at -20°C .
3. 50 mg/mL Ampicillin in ddH_2O .
4. Luria–Bertani (LB) medium: 10 g tryptone, 10 g NaCl, 5 g yeast extract in 1 L ddH_2O ; adjust to pH 7.5 and autoclave.

For pouring plates (**items 5** and **6**), use dishes (94/16) with vents. Store poured plates at 4°C .

5. LB agar with ampicillin: Add 15 g agar to 1 L of LB medium and autoclave, cool down and add 1 mL of 50 mg/mL ampicillin, and then pour plates.
6. LB agar with ampicillin, Bluo-Gal, and IPTG: Add 15 g agar to 1 L of LB medium and autoclave, cool down and add 1 mL of 50 mg/mL ampicillin, 2 mL of 500 mM Bluo-Gal, and 1 mL of 200 mM IPTG, and pour plates.
7. RNase solution (Ribonuclease I “A” [95.6 U/mg] [United States Biochemical]): 100 mg/mL in ddH₂O; incubate 10 min at 95°C to inactivate DNases. To renature ribonuclease, slowly cool down to room temperature. Store aliquots at -20°C.
8. Solution I: 50 mM Tris-HCl, pH 8.0, 10 mM EDTA; autoclave and add 100 µg/mL RNase. Store at 4°C.
9. Solution II: 200 mM NaOH, 1% (w/v) sodium dodecyl sulfate (SDS); autoclave.
10. Solution III: 3 M potassium acetate (KAc), adjust to pH 5.5 with glacial acetic acid; autoclave.
11. 3 M Sodium acetate (NaAc), pH 5.2, for precipitation of DNA.
12. 0.1 M CaCl₂; autoclave. Store at 4°C.
13. 0.1 M CaCl₂; autoclave. Add 15% of sterile glycerol. Store at 4°C.

If purification of recombinant PHP by column chromatography is carried out at 4°C (see **Note 5**), cool down buffers described in **items 14–16**.

14. Equilibration buffer: 20 mM Tris-HCl, pH 7.9, 5 mM imidazole, 250 mM NaCl.
15. Washing buffer: 20 mM Tris-HCl, pH 7.9, 50 mM imidazole, 500 mM NaCl.
16. Elution buffer: 20 mM Tris-HCl, pH 7.9, 500 mM imidazole.
17. Dialysis buffer: 25 mM Tris-HCl, pH 7.9, 2 mM of β-mercaptoethanol.
18. Sample buffer (4X concentrated): 15 mM Tris-HCl, pH 6.8, 4% (w/v) SDS, 2% β-mercaptoethanol, 8 M urea, 10% sucrose, 10 mM EDTA, and 0.01% bromophenol blue. Store at -20°C.
19. Phosphorylation buffer (10X concentrated): 250 mM Tris-HCl, pH 7.5, containing either 50 mM EDTA (for phosphorylation of cell culture lysates and tissue homogenates) or 50 mM MgCl₂ (for phosphorylation of purified substrates) (see **Note 6**).
20. 1 mM ATP, pH 7.5, dilute 1:100 to give 10 µM ATP. Store at -20°C.
21. Dephosphorylation buffer (10X concentrated): 250 mM Tris-HCl, pH 7.5.

3. Methods

1. For all reactions described in **Subheadings 3.1.–3.4.**, use sterile tips and cups.
2. Store DNA at -20°C.
3. During setup of reactions have all reagents (e.g., enzymes, buffers, DNA) on ice.

3.1. Amplification of php by PCR

Primers for amplification of the php cDNA are made with restriction sites for *Nde*I and *Bam*HI to facilitate subcloning of the PCR product into vector pET16b (see **Note 2**).

1. Set up PCR reaction in a total volume of 50 µL. Use approx 50 ng template DNA (see **Note 2**) and add 5 µL dNTPs (stock solution [see **Subheading 2.1., item 9**])

is diluted 1:10 to give 2 mM, respectively), 0.3 μL BioTherm DNA-Polymerase (5 U/ μL), 5 μL PCR reaction buffer including 15 mM MgCl_2 (10X concentrated, purchased by the supplier of the enzyme), 5 μL forward-primer and 5 μL reverse primer (2 pmol/ μL , respectively) (see **Note 2**).

2. Run PCR under the following conditions: 95°C for 5 min, 8 cycles (95°C for 1 min, 50°C for 30 s, 72°C for 1 min), 24 cycles (95°C for 1 min, 58°C for 30 s, 72°C for 1 min) and 72°C for 10 min.

3.2. Cloning of PCR Product into Expression Vector pET16b

3.2.1. TOPO Cloning

Taq polymerase-amplified PCR products can directly be introduced into a plasmid vector by TOPO TA Cloning®.

1. Clone PCR product directly into the pCR®2.1-TOPO® cloning vector as described by the manufacturer and transform the plasmid into competent *E. coli* TOP10F' cells according to **Subheading 3.3.2**. Competent *E. coli* TOP10F' (see **Note 1**) cells are provided by the manufacturer.
2. Plate cells on dishes with LB medium containing ampicillin, Bluo-Gal (see **Note 4**) and IPTG for blue/white screening. Grow overnight at 37°C.
3. Select white colonies and inoculate in 4 mL LB containing 50 $\mu\text{g}/\text{mL}$ ampicillin. Grow overnight at 37°C with shaking at 180 rpm.

3.2.2. Isolation of Plasmid DNA

All plasmids used (php-TOPO, pET16b, and php-pET16b; see **Note 1**) are isolated as follows:

1. Centrifuge 1 mL of the overnight culture at 2700g for 10 min at 4°C and discard the supernatant.
2. Resuspend cells in 100 μL of cold solution I.
3. Add 100 μL of solution II and mix gently; do not vortex.
4. Incubate for 5 min at room temperature. Add 100 μL of solution III, mix, and centrifuge at 10,600g for 15 min at 4°C.
5. Transfer supernatant in a fresh cup with 1 equal volume (approx 300 μL) of ice-cold isopropanol. For better precipitation of the plasmid DNA, incubate for at least 30 min at -20°C and then centrifuge at 10,600g for 20 min at 4°C.
6. Discard supernatant and wash pellet with ice-cold 70% ethanol. Centrifuge again and resuspend pellet in 30–50 μL ddH₂O.
7. Estimate concentration and purity of plasmid DNA by measuring the optical density at 260 and 280 nm. The ratio $\text{OD}_{260/280}$ should be 1.8–2.0.
8. Confirm clones containing the correct php DNA by sequencing (see **Note 3**).

3.2.3. Restriction and Ligation of php

1. Digest plasmids php-TOPO and pET16b (see **Note 1**) with *Nde*I and *Bam*HI: Mix 2 μg plasmid DNA in a total volume of 30 μL with 0.5 μL of each restriction

- enzyme (20,000 U/mL, respectively) and 3 μ L of the appropriate reaction buffer (10X concentrated, purchased from the supplier of the enzyme). *Bam*HI unique NEBuffer is applicable for both enzymes. For optimal activity of *Bam*HI, BSA (10 mg/mL, purchased from the supplier of the enzyme) must be added to a final concentration of 100 μ g/mL. Incubate for at least 4 h at 37°C.
2. Precipitate pET16b DNA by adding 1 equal volume of ice-cold isopropanol and 1/10 volume 3 M NaAc, pH 5.2. For better results, store DNA for at least 1 h at -20°C. Centrifuge at 20,000g for 30 min at 4°C. Discard supernatant and wash pellet with ice-cold 70% ethanol. Centrifuge again, air-dry pellet, and resuspend DNA in ddH₂O.
 3. Separate TOPO vector and php on a 0.8% agarose gel and extract the php fragment from the gel as described by the manufacturer of the gel extraction kit.
 4. Measure concentration of precipitated pET16b vector and of php fragment at 260 nm and 280 nm. The ratio OD_{260/280} should be 1.8–2.0.
 5. Ligate a threefold equimolar amount of the php fragment into digested vector pET16b: Add 21 ng php fragment and 100 ng pET16b to 2 μ L of ligation buffer including 10 mM ATP (10X concentrated, purchased from the supplier of the enzyme) and 1 μ L of T4 DNA-ligase (10 WU/ μ L) in a total volume of 20 μ L. Incubate overnight at 16°C.

3.3. Transformation of the Expression Vector php-pET16b in *E. coli*

3.3.1. Preparation of Chemically Competent *E. coli* BL21(DE3)

1. Inoculate 4 mL of LB medium supplemented with 50 μ g/mL ampicillin with *E. coli* BL21(DE3). Grow overnight at 37°C with shaking at 180 rpm.
2. Inoculate 100 mL of LB containing 50 μ g/mL ampicillin with 100 μ L of the overnight culture and cultivate at 37°C with shaking at 180 rpm until an optical density (600 nm) of 0.7–0.8 is reached.
3. Harvest cells by centrifugation at 2000g for 10 min at 4°C. Discard supernatant.
4. Wash cells with 10 mL cold 0.1 M CaCl₂.
5. Centrifuge again at 2000g for 10 min at 4°C and discard supernatant.
6. Resuspend cells in 4 mL cold 0.1 M CaCl₂ supplemented with 15% glycerol. Keep cells on ice.
7. Aliquot cells of 100 μ L.
8. Freeze aliquots directly in liquid nitrogen and store at -80°C.

3.3.2. Transformation of php-pET16b in *E. coli* BL21(DE3)

1. Thaw chemically competent cells on ice.
2. Add 10 μ L of ligation product (named php-pET16b; see **Subheading 3.2.3.**, **Fig. 1A**, and **Note 1**) and chill cells on ice for further 20–30 min.
3. Heat shock cells with the ligation product for 90 s at 42°C.
4. Cool cells for 3 min on ice and add 1 mL of LB medium.
5. Grow cells for 1 h at 37°C with shaking.
6. Harvest cells by centrifugation at 2600g for 10 min at 4°C.

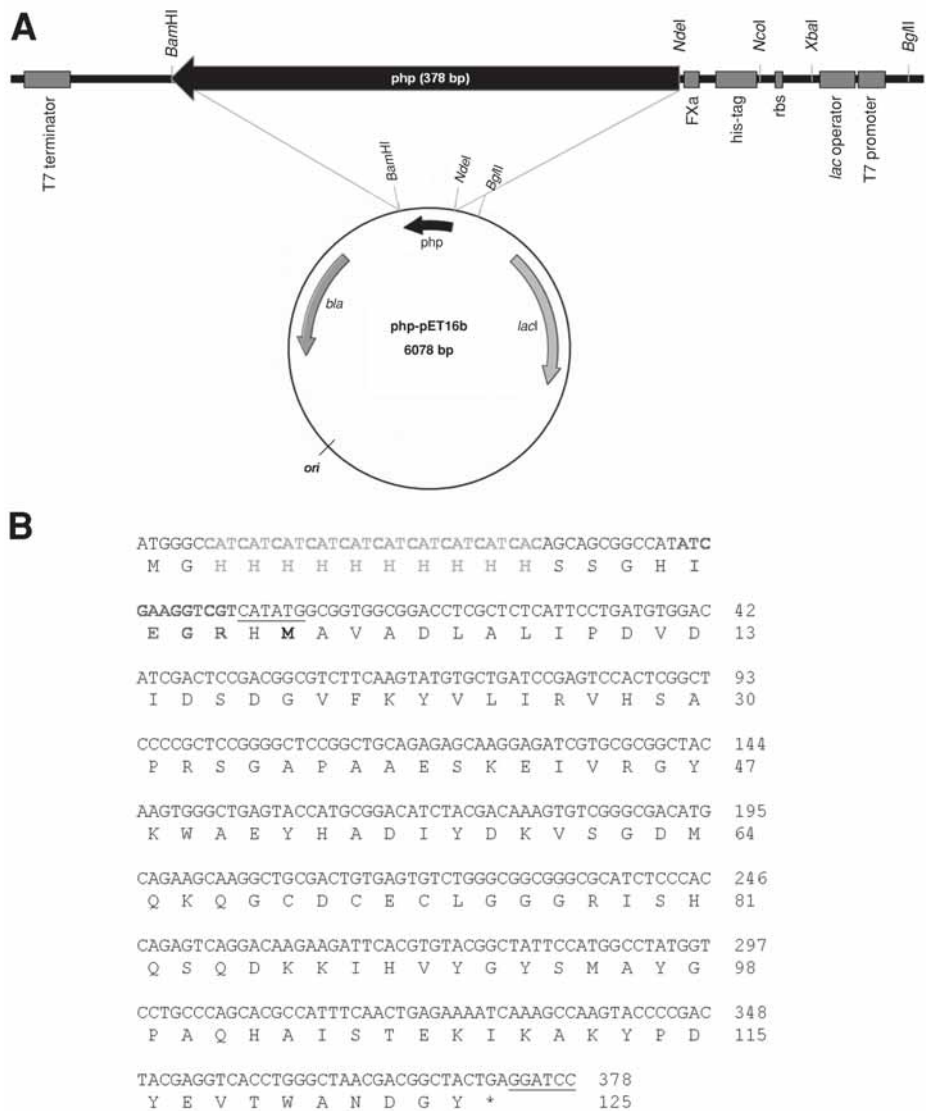


Fig. 1. (A) Schematic illustration of the expression vector php-pET16b. Restriction sites (*NdeI* and *BamHI*) for cloning of the *php* gene are indicated, as well as other restriction sites in the expression region. *php*: protein histidine phosphatase; *rbs*: ribosome-binding site; *bla*: open reading frame for β -lactamase, ampicillin resistance; *FXa*: factor Xa protease cleavage site; *lacI*: open reading frame for the lac repressor; *ori*: origin of replication, pBR322 origin. (B) Sequence of the *php* cDNA and the PHP protein including a N-terminal his-tag (light gray) and factor Xa cleavage site (dark gray). *NdeI* and *BamHI* restriction sites for cloning of the *php* cDNA are underlined. The first translated methionine (M) of PHP is indicated in bold; the asterisk indicates the end of the translation.

7. Discard approx 75% of the supernatant and resuspend cells in the remaining 200–300 μL of LB medium.
8. Plate resuspended cells on a LB dish with ampicillin.
9. Grow overnight at 37°C.
10. Isolate DNA as described in **Subheading 3.2.2.** and confirm clones containing the correct php cDNA by sequencing (*see Note 3*).

3.4. Expression of PHP in *E. coli*

1. Inoculate 3 mL of LB medium supplemented with 50 $\mu\text{g/mL}$ ampicillin with *E. coli* BL21(DE3) harboring the expression plasmid php-pET16b. Grow overnight at 37°C with shaking at 180 rpm.
2. The following day, inoculate 500 mL of LB medium (*see Note 7*) with the overnight culture. Cultivate at 37°C with shaking at 180 rpm until an optical density at 600 nm of 0.5–0.6 is reached. Induce expression with IPTG (*see Note 8*).
3. Let cells grow for an additional 5 h at 37°C with shaking at 180 rpm.
4. Harvest cells by centrifugation at 3000g for 15 min at 4°C.
5. Discard supernatant and resuspend cells in equilibration buffer (0.01 vol of the culture volume). Store at –80°C until further usage (*see Note 9*).

3.5. Purification of Recombinant PHP

1. Thaw cells on ice (*see Subheading 3.4.*).
2. Disintegrate cells by sonication (UP 200S Ultraschallprozessor, Dr. Hielscher GmbH): five to seven times for 15 s with 10-s cooling periods in between (cycle 0.5X, amplitude 100%); chill cells on ice.
3. Centrifuge sonicated material at 20,000g for 30 min at 4°C. Chill the supernatant on ice (*see Note 9*) and discard the pellet (*see Note 10*).
4. Calculate the adequate volume of 50% Ni-NTA Agarose for purification according to the amount of protein to be applied and pour the calculated volume of 50% Ni-NTA Agarose into the column (Bio-Rad; diameter 1.5 cm, tube length 15 cm) (*see Note 11*). Allow the resin to settle.

Column run can be carried out at room temperature or at 4°C (*see Note 5*).

5. Equilibrate the packed column with 10 column volumes of equilibration buffer.
6. Let run by gravity (flow rate approx 1 mL/min). Do not let beads get dry.
7. Load centrifugation supernatant (*see Notes 9 and 10*) onto the column and let continue running by gravity.
8. Wash column with 10 column volumes equilibration buffer.
9. Wash column with washing buffer until optical density of the flow-through fractions reaches zero or remains constant at 280 nm.
10. Elute PHP with elution buffer (*see Note 12*), collecting 1-mL fractions. Store eluted protein on ice. Monitor fractions at 280 nm. Pool fractions with the highest amount of protein (*see Fig. 2A*).

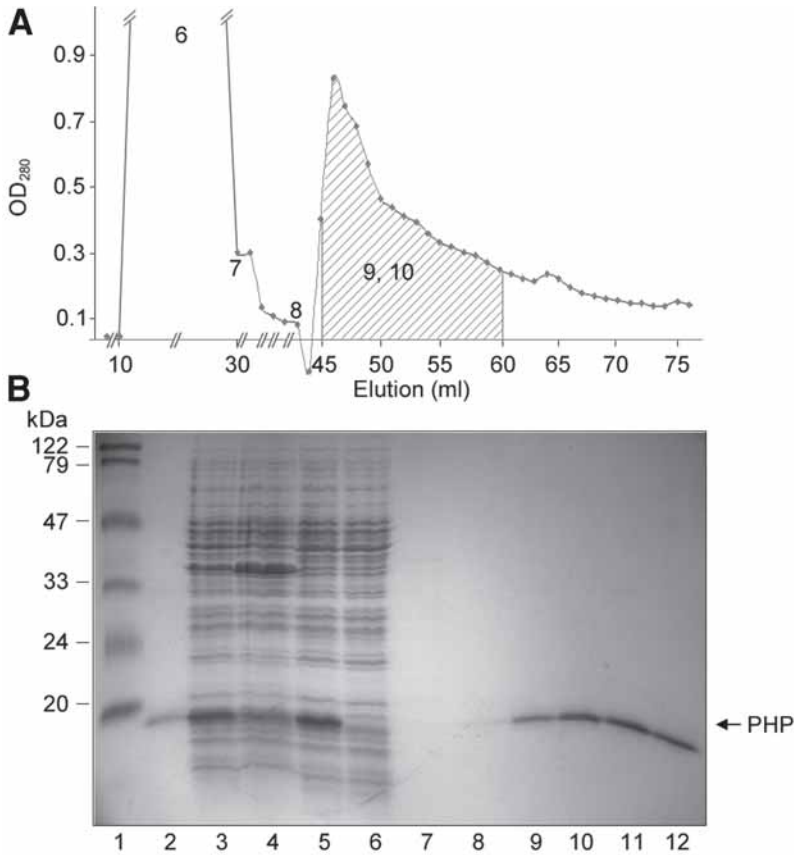


Fig. 2. Purification of recombinant PHP expressed in *E. coli*. Cells are disintegrated by sonication, centrifuged, and PHP purified by Ni-NTA-affinity chromatography. Numbering of the elution fractions in (A) refers to the fractions analyzed by SDS-PAGE in (B). (A) Representative purification of recombinant PHP at room temperature. There is no difference compared to purification performed at 4°C (see **Note 5**). The amount of protein in the different purification steps is monitored at OD₂₈₀. Shaded area: pooled fractions of purified PHP. (B) Samples of each purification step are separated by SDS-PAGE (15%) and stained with Coomassie brilliant blue G250 (lane 1: prestained Marker; lane 2: PHP (2.5 µg); lane 3: *E. coli* cells after sonication (40 µg); lane 4: centrifugation pellet of disintegrated cells resuspended in equilibration buffer (40 µg); lane 5: centrifugation supernatant of disintegrated cells (40 µg); lane 6: flow-through (40 µg); lane 7: wash with equilibration buffer (0.7 µg); lane 8: wash with washing buffer (0.7 µg); lanes 9 and 11: eluate before dialysis (2.5 µg); lanes 10 and 12: eluate after dialysis (2.5 µg); lanes 2–10: purification was carried out at room temperature; lanes 11 and 12: purification was carried out at 4°C. For details, see **Subheading 3.5**.

11. Dialyze [dialysis tubes with a molecular weight cut off (MWCO) 14,000–20,000, diameter 1.5 cm; Serva] pooled fractions against 2 L of dialysis buffer (for about 1 h) and against 5 L of dialysis buffer overnight at 4°C (see **Note 13**).
12. Store purified PHP at –80°C (see **Note 9**).
13. Check purity of PHP by SDS-PAGE (15%) (see **Fig. 2B**).

3.6. Determination of PHP Activity In Vitro

Here we describe determination of PHP activity in vitro with ACL as a substrate (ACL purified, ACL in tissue homogenates, and ACL in cell culture lysates) (see **Note 6**).

1. Determine protein concentration of purified PHP.
2. Work on ice.
3. Autophosphorylation of ACL is carried out in a 10-μL volume in the presence of 25 mM Tris-HCl, pH 7.5, including 5 mM EDTA or 5 mM MgCl₂ (1 μL of phosphorylation buffer with either EDTA or MgCl₂ [see **Note 6**]), 1 μM ATP (1 μL of 10 μM ATP, pH 7.5) including 3 μCi [γ-³²P]ATP, and either 0.1 μg of purified ACL, 100 μg of protein from soluble extract from rabbit liver or 25 μg of protein from a cell culture homogenate.
4. Incubate for 15 min at 37°C.
5. Stop phosphorylation by placing tubes on ice.
6. Dephosphorylate proteins with purified PHP in a total volume of 15 μL in the presence of 25 mM Tris-HCl, pH 7.5 (1.5 μL, 10X concentrated dephosphorylation buffer, 10 μL of the phosphorylation reaction plus PHP). For complete dephosphorylation, add 500 ng of PHP (see **Note 14**). For control, set up the same reaction without PHP.
7. Incubate for 30 min at 37°C.
8. Stop reaction with 5 μL of sample buffer.
9. Run 15% SDS-PAGE followed by autoradiography (see **Fig. 3**).

4. Notes

1. The plasmid generated by TOPO cloning is named php-TOPO; the construct of php and the expression vector pET16b is referred to as php-pET16b (see **Fig. 1A**). Plasmid php-TOPO is cultured in *E. coli* TOP10F'. This strain allows blue/white screening. Plasmid pET16b and expression plasmid php-pET16b are cultured in *E. coli* BL21(DE3). All plasmids have resistance against ampicillin.
2. Vector pVL1392-PHP (cDNA encoding the human php, constructed by Merck KGaA, Germany; see **ref. 10**) was used as template for PCR. For cloning of the php cDNA oligonucleotides with sequences 5'-**GAA TTC CAT ATG GCG GTG GCG**-3' (forward primer, F-pVL-PHP) and 5'-**GGA TCC TCA GTA GCC GTC G**-3' (reverse primer, R-pVL-PHP) were used as primers. Restriction sites *Nde*I and *Bam*HI were incorporated to facilitate subcloning of the amplification product into vector pET16b (see **Fig. 1B**). The 5' primer was based on the nucleotide residues 1–12 of php cDNA (bold) and tagged with an *Eco*RI and *Nde*I site

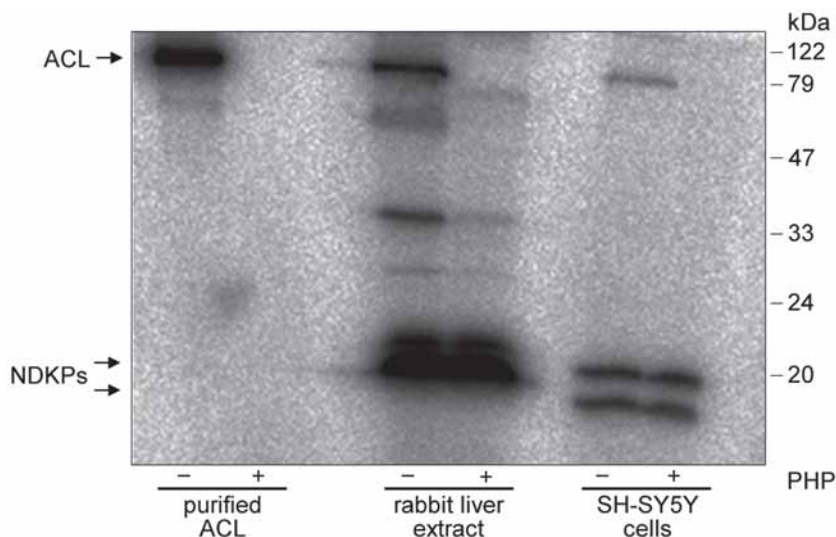


Fig. 3. Autophosphorylation of ACL and dephosphorylation of $[^{32}\text{P}]\text{ACL}$ by PHP. ACL (purified from rabbit liver, 0.1 μg ; see **Note 6**), soluble extract from rabbit liver (100 μg), and homogenate of SH-SY5Y cells (25 μg) (see **Note 6**) are phosphorylated for 15 min with 3 μCi $[\gamma\text{-}^{32}\text{P}]\text{ATP}$ in the presence of 5 mM MgCl_2 (purified ACL) or 5 mM EDTA (tissue and cells), respectively. Dephosphorylation is carried out with 500 ng PHP (+) for 30 min (see **Note 14**). For control, the same reaction is set up without PHP (-). Proteins are separated by SDS-PAGE (15%) and phosphorylation is detected by autoradiography. For details, see **Subheading 3.6**.

- (underlined); the 3'-primer that was tagged with a *Bam*HI (underlined) site was based on the nucleotide residues 366–378 of php cDNA (bold).
- For sequencing php-TOPO, M13 Reverse Primer (5'-CAGGAA ACA GCT ATG AC-3') and M13 (-20) Forward Primer (5'-GTA AAA CGA CGG CCA G-3') were used. For sequencing php-pET16b, T7 Promoter Primer (5'-TAA TAC GAC TCA CTA TAG GG-3') and T7 Terminator Primer (5'-GCT AGT TAT TGC TCA GCG G-3') were used. Sequencing reactions were carried out by SeqLab (Göttingen, Germany).
 - Bluo-Gal, applicable for identification of lac^+ colonies, is an alternative chromogenic substrate to X-Gal (5-bromo-4-chloro-3-indolyl- β -D-galactopyranoside), producing a darker color.
 - Purification of PHP can be performed at room temperature and at 4°C. We could not find any difference concerning the purification or activity of PHP. Keep in mind that purification at room temperature should be completed within 1 h.
 - For the determination of PHP activity in vitro, homogenates of any available tissue (e.g., rabbit liver soluble extract) as well as cell culture lysates (e.g.,

SH-SY5Y cells) or purified substrates of the PHP (e.g., ACL) can be used (see **Fig. 3**). Preparation of rabbit liver soluble extracts and purification of ACL from rabbit liver is described in **ref. 12**.

Autophosphorylation of purified ACL is carried out with phosphorylation buffer containing a final concentration of 5 mM MgCl₂, whereas tissue homogenates and cell culture lysates are phosphorylated with phosphorylation buffer containing a final concentration of 5 mM EDTA (see **Subheading 1.3.**).

7. You can express PHP in a larger volume of LB medium. The average amount of PHP is dependent on the culture volume used for the purification. Usually we obtain about 10 mg PHP per 1-L culture.
8. We induce expression of PHP with 10 μ M IPTG and continue cell growth for 5 h. In general, for determination of the required amount of IPTG for optimal expression, inoculate 50 mL of LB medium without ampicillin with 1 mL of an overnight culture. Cultivate at 37°C with shaking at 180 rpm until an optical density at 600 nm of 0.5–0.6 is reached. Add IPTG in different concentrations (e.g., 0, 10, 100, and 1000 μ M). Harvest cells after 1 h, 3 h, and 5 h (same cell count, verify by OD₆₀₀) by centrifugation. Check the amount of PHP by SDS-PAGE (polyacrylamide gel electrophoresis) or via Western blot analysis (see **Note 15**).
9. We have stored resuspended cell lysates (see **Subheading 3.4., step 5**) and the centrifugation supernatants (see **Subheading 3.5., step 3**) for 2 yr at –80°C without loss of activity. Similarly, storage of purified PHP at –80°C for 2 yr did not diminish PHP activity.
10. The centrifugation supernatant of disintegrated cells (input for Ni-NTA chromatography) contains 50–75% of the PHP expressed. The remaining 25–50% is recovered as insoluble aggregates in the pellet (see **Fig. 2B**). Formation of such inclusion bodies is frequently observed in *E. coli* if a high level of recombinant protein is expressed (for review see **ref. 17**).
11. The binding capacity of Ni-NTA Agarose from Qiagen is dependent on the protein to be applied and normally lies between 5 and 10 mg/mL of 6X his-tagged proteins. We usually use 2 mL of 50% Ni-NTA Agarose (column volume is 1 mL) for purification of PHP obtained from a 1-L culture (approx 10 mg).
12. For elution of PHP, a buffer containing 500 mM imidazole was found to be sufficient. Alternatively, the pH can be decreased to pH 4.5–5.3 for elution.
13. Dialysis is not absolutely necessary concerning the activity of PHP toward purified substrates, but a high concentration of imidazole in the elution buffer might interfere with components in cell culture lysates or tissue homogenates during determination of activity of PHP in vitro.
14. Normally, a minimum of 100–250 ng of PHP reduces phosphorylation of ACL by at least 50%, and addition of 500 ng of PHP results in complete dephosphorylation.
15. Protein histidine phosphatase can be detected by western blot analysis. For the generation of antibodies, rabbits had been immunized with a peptide corresponding to amino acids 8–22 of PHP (for details, see **ref. 10**).

References

1. Boyer, P. D., DeLuca, M., Ebner, K. E., Hultquist, D. E., and Peter, J. B. (1962) Identification of phosphohistidine in digests from a probable intermediate of oxidative phosphorylation. *J. Biol. Chem.* **237**, PC3306-PC3308.
2. Mitchell, R. A., Butler, L. G., and Boyer, P.D. (1964) The association of readily-soluble bound phosphohistidine from mitochondria with succinate thiokinase. *Biochem. Biophys. Res. Commun.* **16**, 545-550.
3. Walinder, O. (1968) Identification of a phosphate-incorporating protein from bovine liver as nucleoside diphosphate kinase and isolation of 1-³²P-phosphohistidine, 3-³²P-phosphohistidine, and N-ε-³²P-phospholysine from erythrocytic nucleoside diphosphate kinase, incubated with adenosine triphosphate-³²P. *J. Biol. Chem.* **243**, 3947-3952.
4. Feldman, F. and Butler, L. G. (1969) Detection and characterization of the phosphorylated form of microsomal glucose-6-phosphatase. *Biochem. Biophys. Res. Commun.* **36**, 119-125.
5. Cottam, G. L., Srere, P. A. (1969) Nature of the phosphorylated residue in citrate cleavage enzyme. *Biochem. Biophys. Res. Commun.* **35**, 895-900.
6. Wieland, T., Nürnberg, B., Ulibarri, I., Kaldenberg-Stasch, S., Schultz, G., and Jakobs, K. H. (1993) Guanine nucleotide-specific phosphate transfer by guanine nucleotide-binding regulatory protein beta-subunits. Characterization of the phosphorylated amino acid. *J. Biol. Chem.* **268**, 18,111-18,118.
7. Crovello, C. S., Furie, B. C., and Furie, B. (1995) Histidine phosphorylation of P-selectin upon stimulation of human platelets: a novel pathway for activation-dependent signal transduction. *Cell* **82**, 279-286.
8. Muimo, R., Hornickova, Z., Riemen, C. E., Gerke, V., Matthews, H., and Mehta, A. (2000) Histidine phosphorylation of annexin I in airway epithelia. *J. Biol. Chem.* **275**, 36,632-36,636.
9. Alex, L. A. and Simon, M. I. (1994) Protein histidine kinases and signal transduction in prokaryotes and eukaryotes. *Trends Genet.* **10**, 133-138.
10. Klumpp, S., Hermesmeier, J., Selke, D., et al. (2002) Protein histidine phosphatase: a novel enzyme with potency for neuronal signaling. *J. Cereb. Blood. Flow Metab.* **22**, 1420-1424.
11. Ek, P., Pettersson, G., Ek, B., Gong, F., Li, J-P., and Zetterquist, Ö. (2002) Identification and characterization of mammalian 14-kDa phosphohistidine phosphatase. *Eur. J. Biochem.* **269**, 5016-5023.
12. Klumpp, S., Bechmann, G., Mäurer, A., Selke, D., and Kriegelstein, J. (2003) ATP-citrate lyase as a substrate of protein histidine phosphatase in vertebrates. *Biochem. Biophys. Res. Commun.* **306**, 110-115.
13. Mäurer, A., Wieland, T., Meissl, F., et al. (2005) The β-subunit of G proteins is a substrate of protein histidine phosphatase. *Biochem. Biophys. Res. Commun.* **334**, 1115-1120.
14. Motojima, K. and Goto, S. (1993) A protein histidine kinase induced in rat liver by peroxisome proliferators. In vitro activation by Ras protein and guanine nucleotides. *FEBS Lett.* **319**, 75-79.

15. Besant, P. G., Tan, E., and Attwood, P. V. (2003) Mammalian protein histidine kinases. *Int. J. Biochem. Cell Biol.* **35**, 297–309.
16. Noiman, S. and Shaul, Y. (1995) Detection of histidine-phospho-proteins in animal tissues. *FEBS Lett.* **364**, 63–66.
17. Baneyx, F. and Mujacic, M. (2004) Recombinant protein folding and misfolding in *Escherichia coli*. *Nature Biotechnol.* **22**, 1399–1408.

The Use of RNA Interference to Analyze Protein Phosphatase Function in Mammalian Cells

Iain Fraser, Wei Liu, Robert Rebres, Tamara Roach, Joelle Zavzavadjian, Leah Santat, Jamie Liu, Estelle Wall, and Marc Mumby

Summary

The use of RNA interference to knock down protein phosphatases has proven to be a valuable approach to understanding the functions of these enzymes in mammalian cells. Many protein phosphatases exist as multisubunit and multigene families, which has made it difficult to assess their physiological functions using traditional approaches. The ability to selectively knock down specific subunits and individual isoforms with RNA interference has begun to make it possible to determine the contributions of individual phosphatase proteins to cellular signaling. This chapter describes methods for knocking down protein phosphatases with small interfering RNAs in easily transfectable cells and by the introduction of short-hairpin RNAs into less tractable cells using lentivirus vectors.

Key Words: Protein serine/threonine phosphatase; protein tyrosine phosphatase; protein phosphatase 2A; PP2A; SH2-containing protein tyrosine phosphatase 2; Shp2; RNA interference; small interfering RNA; short hairpin RNA; lentivirus; transfection; transduction; physiological function

1. Introduction

The introduction of methods for facile and specific depletion of individual proteins by RNA interference has ushered in a new era in cell signaling research. The ability to “knock down” individual proteins with RNA interference (RNAi) provides a generic technology for assessing the function of almost any protein ([1,2](#)). RNAi is an especially powerful tool for the analysis of protein phosphatase function. Protein phosphatases play pivotal roles in all signaling pathways that utilize reversible protein phosphorylation. Despite a wealth of biochemical information on the structure and enzymatic activities of these enzymes, many details regarding their physiological actions have remained

From: *Methods in Molecular Biology, Volume 365: Protein Phosphatase Protocols*
Edited by: G. Moorhead © Humana Press Inc., Totowa, NJ

obscure. Most protein phosphatases have broad substrate specificity when assayed in vitro. It has therefore been difficult to infer in vivo function based on in vitro activity. Highly selective inhibitors of individual phosphatases are not available. Although a variety of natural products and toxins (e.g., okadaic acid and microcystin) are potent inhibitors of protein serine/threonine phosphatase, they are generally nonselective (3). Similarly, the lack of specific inhibitors has made it difficult to assess the physiological functions of many of the protein tyrosine phosphatases. Thus, the ability to specifically ablate the activity of individual enzymes with RNAi has provided a powerful new strategy to analyze the functions of protein phosphatases.

The two examples that illustrate the methods for using RNAi to analyze phosphatase function described in this chapter are protein serine/threonine phosphatase 2A (PP2A) and SH2-containing protein tyrosine phosphatase 2 (Shp2). In the first example, small interfering RNAs (siRNA) are used to knock down individual subunits of PP2A in HeLa cells. In this case, siRNA-mediated knock down works well because HeLa cells are easy to transfect and induce a robust RNAi response. In contrast, it has been more difficult to utilize siRNAs in many other, more differentiated, cell types. Therefore, we have included a second example in a more recalcitrant cell line, the murine RAW 264.7 macrophage cell line, where siRNA has been less efficient in knocking down target proteins. In this case, we describe a procedure involving introduction of short-hairpin RNA (shRNA) via infection with lentivirus to knock down Shp2. Although considerably more complicated, the second method provides a way to utilize RNAi in a wide variety of cell types.

Protein phosphatase 2A is a multisubunit phosphatase composed of a core dimeric complex containing a catalytic subunit and a scaffold subunit. The PP2A core complex associates with a wide variety of regulatory subunits and targeting proteins that dictate its participation in a wide variety of cellular functions (4,5). The lack of specific inhibitors of PP2A, much less inhibitors specific for individual PP2A isoforms, has hampered functional analysis of this phosphatase. RNAi-mediated knock down has proven to be a highly useful tool for identifying physiological roles for individual PP2A subunits, particularly in pathways regulating cell survival. Knockdown of either the catalytic or R5/B56 regulatory subunits of PP2A causes apoptosis in *Drosophila* cells (6,7). A large scale RNAi screen in HeLa cells revealed that knock down of the α -isoform of the PP2A catalytic subunit, either isoform of the scaffold subunit (R1/A α and R1/A β), the β or γ isoforms of the R5/B56 regulatory subunits, the β isoform of the R2/B55 regulatory subunit, or the R3/PR72 regulatory subunit leads to increased apoptosis (8). Similarly, RNAi-mediated knock down of the R1/A α scaffold subunit leads to apoptosis of PC12 cells (9). Other PP2A functions identified with RNA interference include a role for the catalytic subunit

in regulating the stability of the Rb2/p130 protein (10), confirmation of a role of the R5/B56 ϵ subunit in the Wnt signaling pathway in *Xenopus* (11), roles for the R2/B55 and R5/B56 families of regulatory subunits in regulating stability of the *Drosophila* Period protein and the circadian clock (12), and roles for the R5/B56 γ subunit in regulating stability of the p300 transcriptional coactivator (13) and in pathways involved in cellular transformation (14).

The Shp2 protein tyrosine phosphatase is a positive regulator of signaling through pathways utilized by receptor tyrosine kinases and integrin receptors. Inherited mutations in *Shp2* are associated with the pathology of several human diseases, including Noonan syndrome, juvenile myelomonocytic leukemia, and the pathogenesis associated with *Helicobacter pylori* infection (15). RNA interference has not been extensively utilized to study the functions of Shp2 because of the availability of immortalized fibroblasts from Shp2-deficient mice (16), mouse cells in which Shp2 can be deleted using the Cre/LoxP system (17,18), and the effectiveness of catalytically inactive mutants of Shp2 (15). However, the lack of specific inhibitors for Shp2 makes RNAi-mediated knock down an appealing technique for studying functions of Shp2 in cell types where genetic manipulation is not possible. For example, RNAi has been used to define a function for Shp2 in the clustering of acetylcholine receptors at the neuromuscular junction of cultured muscle cells (19).

2. Materials

2.1. Cell Culture and Lysis

1. HeLa cells (ATCC, Rockville, MD); HEK 293 cells (ATCC); HEK 293T cells (ATCC); RAW 264.7 cells (ATCC).
2. Dulbecco's modified Eagle's medium (DMEM, Invitrogen).
3. HeLa growth medium: Dulbecco's modified Eagle's medium (DMEM; Invitrogen, Carlsbad, CA) plus 10% fetal bovine serum (FBS; Gemini Bio-Products, Woodland, CA).
4. HEK 293 growth medium (293 growth medium): DMEM plus 10% FBS and 2mM glutamine (Invitrogen).
5. RAW 264.7 growth medium (RAW growth medium): DMEM plus 10% FBS, 20 mM HEPES (Invitrogen), 2 mM glutamine, and 100 units penicillin G/mL (Sigma-Aldrich, St. Louis, MO).
6. Phosphate-buffered saline (PBS; Invitrogen).
7. PBS-EDTA: PBS with 2 mM EDTA, pH 7.5 (Invitrogen).
8. Trypsin solution (0.25%) with 1 mM EDTA (Invitrogen).
9. HeLa lysis buffer: 50 mM Tris-HCl, pH 7.4, 150 mM NaCl, 0.25% deoxycholate, 1 mM EDTA, 1% NP-40, 10 mM NaF, 10 mM sodium orthovanadate. One complete mini protease inhibitor cocktail tablet (Roche Applied Science, Indianapolis, IN) is added per 10 mL of lysis buffer immediately prior to use.
10. TriPure Isolation Reagent (Roche Applied Science).

11. Cell scrapers (Fisher Scientific, Hampton, NH).
12. Detergent Compatible Protein Assay Kit (Bio-Rad, Hercules, CA).
13. HSE-T buffer: 20 mM HEPES, pH7.4, 20 mM NaCl, 5 mM EDTA, 1% Triton X-100 + protease inhibitors (Roche Applied Science).

2.2. Preparation of siRNA Duplexes

1. 7 M Urea buffer: 7 M urea, 1 M Tris-HCl, pH 7.0. Solution is filtered through a 0.22- μ m filter unit and stored at room temperature.
2. RNase-free water is prepared by filtering molecular-biology-grade water through a 0.22- μ m membrane and treating with diethyl pyrocarbonate (DEPC; Sigma). The DEPC-treated water is stored at room temperature.
3. 5X Annealing buffer: 500 mM potassium acetate, 150 mM HEPES-KOH, pH 7.4, 10 mM magnesium acetate. The solution is prepared with RNase-free water, filtered through a 0.22- μ m filter, and stored at room temperature.

2.3. Transfection of Cells With siRNA, shRNA Expression Plasmids, and cDNA Expression Plasmids

1. Oligofectamine reagent (Invitrogen).
2. Lipofectamine 2000 reagent (Invitrogen).
3. Opti-MEM Plus reagent (Invitrogen).
4. Opti-MEM reduced serum medium (Invitrogen).

2.4. Isolation of Total RNA and Quantitative Real-Time Polymerase Chain Reaction

1. TriPure reagent (Invitrogen).
2. Rneasy Mini Kit (Qiagen, Valencia, CA).
3. iScript cDNA Synthesis Kit (Bio-Rad).
4. 2X iScript Supermix Buffer (Bio-Rad).
5. 10X Well Factor Stock Solution (Bio-Rad).
6. Primer DNA oligonucleotides, and Texas Red/BHQ2- and HEX/BHQ1- conjugated probe oligonucleotides for Shp2 and actin (Operon).

2.5. shRNA Cloning

1. TE buffer: 10mM Tris-HCl, pH8, 1mM EDTA.
2. 5X T4 DNA ligase buffer (Invitrogen).
3. T4 polynucleotide kinase (Roche).
4. pEN_mH1c vector (ATCC; AfCS collection).
5. *Bam*H1, *Xho*I, and *Kpn*I restriction enzymes (New England Biolabs).
6. Alkaline phosphatase (Roche).
7. QIAquick Gel Extraction Kit (Qiagen).
8. Buffer EB: 10 mM Tris-HCl, pH 8.
9. Rapid Ligation Kit (Roche).
10. Top10 *Escherichia coli* cells (Invitrogen).

11. Luria-Bertani agar plates (LB plates): 171 mM NaCl, 1.5% Bacto agar, 1% Bacto tryptone, 0.5% Bacto yeast extract, pH 7.
12. Luria-Bertani broth (LB broth): 171 mM NaCl, 1% Bacto tryptone, 0.5% Bacto yeast extract, pH 7.0.
13. Qiagen Mini Prep kit (Qiagen).
14. YFP-Shp2 cDNA expression plasmid (ATCC; AfCS collection).
15. LR Clonase enzyme (Invitrogen).
16. 5X LR Clonase buffer (Invitrogen).
17. Lentiviral pDSL_hpUCIN vector (ATCC; AfCS collection).
18. Gateway system (Invitrogen).
19. Proteinase K solution: (Invitrogen).
20. Stbl3 *E. coli* cells (Invitrogen).
21. Qiagen EndoFree Maxi kit (Qiagen).

2.6. Lentivirus Production

1. Poly-L-lysine solution (PLL solution), 20 µg poly-L-lysine/mL in PBS.
2. pCMVΔ8.91 plasmid [a gift from the Trono Lab (20)].
3. pMD.G plasmid [a gift from the Trono Lab (20)].
4. Polybrene (hexadimethrine bromide): 8 mg/mL in double-distilled water (dd H₂O).
5. Centricon Plus-80 centrifugal filter unit (Millipore).
6. Valmark Ultra-Dish Petri dishes, 100 mm × 15 mm, polystyrene (Midwest Scientific).
7. Magnetic cell sorting buffer (MACS buffer): PBS with 2 mM EDTA and 5 mg/mL bovine serum albumin (BSA).
8. Cytotfix solution (BD Biosciences).
9. Fluor-coupled anti-CD4 and isotype control antibodies (BD Pharmingen).

2.7. Sodium Dodecyl Sulfate–Polyacrylamide Gel Electrophoresis and Western Blotting

1. 4X Sodium dodecyl sulfate sample buffer: 0.2 M Tris-HCl, pH 6.8, 4% SDS, 40% glycerol, 0.4% bromphenol blue, 80 mM dithiothreitol (DTT), 0.57 M of 2-mercaptoethanol.
2. Antibody incubation buffer: 20 mM Tris-HCl, pH 7.6, 137 mM NaCl, 0.1% Tween-20, 5% nonfat dry milk, 2% BSA (Fraction V).
3. Shp2 primary antibody (Upstate Biotechnology, Waltham, MA).
4. PP2A B55α antibody M868 (21).
5. PP2A B56α antibody (Santa Cruz Biotechnology, Santa Cruz, CA).
6. PP2A B56γ antibody M880 (21).
7. PP2A B56δ antibody (Novus Biologicals, Littleton, CO).
8. ECL anti-rabbit IgG HRP-linked whole antibody from donkey (Amersham Biosciences, Piscataway, NJ).
9. SuperSignal West Pico Chemiluminescent Substrate detection reagents (Pierce Biotechnology, Rockford, IL).
10. Kodak BioMax XAR film (Kodak, Rochester, NY).

3. Methods

3.1. Knockdown of PP2A Subunits

3.1.1. Design of siRNAs to Knockdown PP2A Subunits

Various subunits of human PP2A were knocked down in HeLa cells with siRNAs. The principals used in the design of siRNAs for PP2A subunits were based on the need to use sequences that were specific for individual isoforms within each family. The coding regions of the cDNA for each of the human subunits were aligned using sequence analysis software. Nineteen nucleotide sequences that were unique to each isoform were then manually identified. The sequence of each oligonucleotide was searched against the nonredundant NCBI database to ensure that they were unique to PP2A. When possible, sequences were selected to contain a GC content of 50–60% with annealing temperatures between 60°C and 70°C. The final siRNAs for each subunit were 21 nucleotide, double-stranded RNAs (dsRNAs) containing 19 basepairs complementary to the targeted mRNA and 2 nucleotides overhanging the 3' ends (22). The subunits of PP2A that were targeted in these studies include the catalytic subunit, the R2/PR55 α subunit, and four of the R5/B56 subunit isoforms (B56 α , B56 γ , B56 δ , and B56 ϵ). Each of the R5/B56 subunit-specific siRNAs were designed to knock down all of the known splice variants of each isoform. An overhang of two T residues was incorporated at the 3' end of each oligonucleotide. For oligos targeting B56 α , B56 γ , and B56 ϵ , a mismatch pair was designed at the 19th nucleotide to enhance the efficiency of siRNA-mediated knockdown (23). The oligonucleotide sequences used to prepare siRNAs for the individual PP2A subunits are shown in Table 1.

3.1.2. Preparation of siRNA Duplexes

1. Sense and antisense 21mer RNA oligonucleotides specific for individual PP2A subunits were synthesized in the RNAi core facility at UT Southwestern Medical Center.
2. The concentrations of the synthetic RNA oligonucleotides are determined by absorbance at 260 nm. Single-stranded RNAs (ssRNAs) have a tendency to adopt secondary structures that interfere with absorbance readings. Therefore, the absorbance is determined under denaturing conditions. RNA oligonucleotides are dissolved in 1 mL of RNase-free water, and 10 μ L of dissolved oligonucleotide is diluted into 990 μ L of 7 M urea buffer. The absorbance at 260 nm is read in an ultraviolet (UV) spectrophotometer that is blanked against 7 M urea buffer and used to calculate the concentration using standard methods. Each RNA oligonucleotide is diluted to a final concentration of 50 μ M in ddH₂O, aliquoted (300 μ L/aliquot) into microcentrifuge tubes, and stored at –20°C.
3. The sense and antisense ssRNA oligonucleotides are annealed to prepare siRNA duplexes. Great care must be taken throughout these procedures to ensure RNase-

Table 1
Oligonucleotides Used for the Generation of siRNA
for Subunits of PP2A and a Control siRNA From the Luciferase Gene

Subunit	Antisense strand	Sense strand
C	GACAGAGGAUAAUUAUUCAGTT	CUGAAUAAUAUCCUCUGUCTT
B55 α	UCUCAUAGCAGAGGAGAAUTT	CUUCUCCUCUGCUAUGAGATT
B56 α	CAUGCACAGUAUUCUCAGCTT	ACUGAGAAUACUGUGCAUGTT
B56 γ	AUAUUCGAGAUGUUCCUCCTT	AGAGGAACAUCUCGAAUAUTT
B56 δ	AGGACAUCCAGCUUCUGAATT	UUCAGAAGCUGGAUGUCCUTT
B56 ϵ	GUCUUAGACGUGAUGGAAUTT	GUUCCAUCACGUCUAAGACTT
Luciferase	CGUACGCGGAAUACUUCGATT	UCGAAGUAUCCGCGUACGTT

free conditions, including the use of RNase-free pipet tips and tubes and the use of RNase-free water for the preparation of all solutions. Three hundred microlitres of corresponding sense and antisense RNA oligonucleotides are combined and 150 μ L of 5X annealing buffer is added. The mixture is heated at 90°C for 1 min and briefly centrifuged. The mixture is allowed to cool by placing the tubes in a 37°C waterbath for 1 h. The final concentration of the siRNA duplex should be 20 μ M. The siRNA duplex is aliquoted and stored at –20°C.

3.1.3. Transfection of HeLa Cells With siRNA

1. HeLa cells are normally maintained in HeLa growth medium by splitting at a 1 : 4 ratio every 3 d. One day prior to the transfection, HeLa cells are trypsinized using trypsin solution, counted, and seeded at a density of 4×10^5 cells per 60-mm culture dish. The confluency should be about 40% at the time of transfection the following day.
2. An siRNA oligonucleotide–Oligofectamine complex is prepared essentially as described by the manufacturer. Six microliters of Oligofectamine are mixed with 24 μ L of Opti-MEM and incubated for 10 min at room temperature. Twenty microliters of the siRNA duplex is diluted in 350 μ L of Opti-MEM and the diluted siRNA is gently mixed with the diluted Oligofectamine. The mixture is then incubated for 20 min at room temperature.
3. Medium is removed and the HeLa cells are rinsed once with room-temperature DMEM medium without serum. Serum-free DMEM (1.6 mL) is added to each dish, followed by the addition of 400 μ L of the siRNA–Oligofectamine complex. Cells are incubated at 37°C for 4 h. One milliliter of DMEM supplemented with 30% FBS is added and the cells are incubated for an additional 3 d, or until sufficient knock down is achieved.
4. Three days after transfection, the medium is removed and the HeLa cells are rinsed once with ice cold PBS. Four hundred microliters of HeLa lysis buffer are

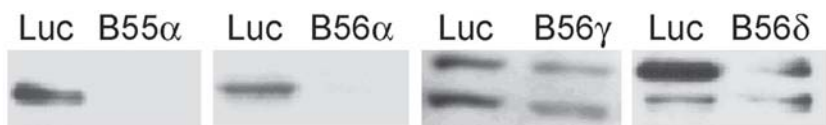


Fig. 1. Knock down of PP2A subunits in HeLa cells with siRNAs. HeLa cells were treated with siRNAs targeting the B55 α , B56 α , B56 γ , and B56 δ subunits of PP2A or a control siRNA made against luciferase as indicated. Three days after transfection, cells were lysed and 30 μ g of protein were analyzed by Western blotting with antibodies against each of the PP2A subunits as described in **Subheading 3.5**.

added and the dish is incubated on ice for 2 min. The cells are scraped off using a scraper and transferred to microcentrifuge tubes. The tubes are kept on ice for 20 min and centrifuged at 18,000g for 10 min. The supernatants are transferred to fresh tubes and either used immediately or stored at -20°C . Alternatively, RNA is isolated from the cells using the TriPure isolation reagent following the manufacturer's protocol.

5. The protein concentration is determined using the Detergent Compatible Protein Assay Kit. Thirty micrograms of lysate protein is used to determine the knock-down efficiency by Western blotting with PP2A subunit-specific antibodies (**Subheading 3.2.4**). Alternatively, knock down efficiency at the mRNA level can be determined by quantitative real-time polymerase chain reaction (PCR) (**Subheading 3.2.4**). Although knock down of the mRNA for the target does not necessarily mean that the protein has been depleted, Q-PCR can be a useful way to ensure that siRNAs are working properly. An example of results obtained using this method to knock down PP2A subunits is shown in **Fig. 1**.

3.2. Design and Construction of a shRNA to Knockdown Shp2

Direct transfection of mammalian cells with chemically synthesized siRNAs, as described above for PP2A, is the most straightforward and widely used method to knock down the expression of target genes by RNAi. However, many cell lines and primary cells cannot be transfected to a sufficiently high level to permit the efficient gene knock down required for functional studies, even with potent siRNA sequences. The model cell for the AfCS project (<http://www.signaling-gateway.org/>), the RAW264.7 murine macrophage line, falls into this category. To achieve high levels of target gene knock down in RAW264.7 cells, we developed a strategy to create and validate shRNAs, which are stably expressed throughout the cell population following infection with lentivirus. The method for achieving stable knock down of Shp2 is a multistep process. The first step involves transfection of RAW264.7 cells with four candidate siRNAs (**Subheading 3.2.1**) and selection of the most potent sequence using quantitative real-time PCR (**Subheading 3.2.2**). This siRNA

sequence is then used as the basis for design of a shRNA that is cloned into an expression plasmid vector (**Subheading 3.2.3.**). The efficacy of the siRNA sequence in the shRNA context is tested by cotransfection of HEK293 cells with a vector expressing a YFP-tagged version of Shp2 (**Subheading 3.2.4.**) and Western blotting. The validated shRNA is then subcloned to a lentiviral vector (**Subheading 3.2.5.**) to permit virus generation (**Subheading 3.3.**) and knock down of Shp2 in RAW264.7 cells (**Subheading 3.4.**).

3.2.1. Transfection of RAW264.7 Macrophages with Shp2 siRNAs

1. Four siRNAs against mouse Shp2 were designed using Dharmacon's SMARTpool algorithm ([24](#)), which can be accessed through the company website (<http://www.dharmacon.com/siRNA/>). The reference sequence used for Shp2 was Genbank accession NM_011202. The Shp2 mRNA target sequences for the four Shp2 siRNAs designed using the SMARTpool method were as follows:

Shp2-A, GGACTACTATGACCTCTAT
Shp2-B, GAACCTTCATTGTGATTGA
Shp2-C, GAAGCACAGTACCGGTTTA
Shp2-D, AGTATGCGCTCAAAGAATA

- A control siRNA targeting a region of the *lacZ* gene (CTGACCAGCGAA TACCTGT) was also synthesized. The siRNAs purchased from Dharmacon are shipped as siRNA duplexes and no annealing step is needed.
2. Plate RAW 264.7 cells in a 24-well plate at 1×10^5 cells/well in 1 mL of RAW growth medium/well and incubate at 37°C in a humidified, 5% CO₂ incubator for 24 h.
 3. Resuspend siRNAs in the resuspension buffer provided by Dharmacon to a stock concentration of 40 μ M. In an RNase-free tube, dilute 2 μ L of 40 μ M siRNA duplex with 48 μ L of Opti-MEM and mix gently. Mix Lipofectamine 2000 gently before use, and in a separate RNase-free tube, dilute 2 μ L Lipofectamine 2000 with 48 μ L Opti-MEM. Mix gently and incubate for 5 min at room temperature. Combine the diluted duplex siRNA with the diluted Lipofectamine 2000 (total volume = 100 μ L). Mix gently and incubate for 20 min at room temperature.
 4. During the 20-min incubation, aspirate medium from cells and add 100 μ L of fresh RAW growth medium. Add the Lipofectamine 2000/siRNA mixture to wells (100 μ L/well). The final siRNA concentration is 400 nM in a final volume of 200 μ L/well (*see Note 1*). Mix gently by rocking the plate, and incubate cells for 4 h at 37°C in a humidified, 5% CO₂ incubator. After 4 h, add 800 μ L of RAW growth medium to each well and continue to incubate cells at 37°C in a humidified, 5% CO₂ incubator overnight.
 5. Twenty-four hours after the first transfection, repeat the siRNA transfection process as detailed in **steps 2–4**.
 6. The cells are harvested 48 h after the second transfection for isolation of total RNA.

3.2.2. Assessment of siRNA-Mediated Shp2 Knockdown in RAW264.7 Cells by qRT-PCR

1. Total RNA is isolated from the siRNA-transfected RAW 264.7 cells using RNeasy Mini kits as described in the manufacturer's protocol. The RNA concentration is determined by UV absorbance and the total RNA samples are stored at -80°C .
2. Prepare cDNA from 1 μg of total RNA using the Bio-Rad iScript cDNA synthesis kit.
3. The Shp2 PCR primers and fluorescently labeled probe oligonucleotides for qRT-PCR were designed for use in a Bio-Rad iCycler using Beacon Designer software (Bio-Rad). Primer and probe sequences for Shp2 were as follows:

Sense amplification primer: 5'-ACGACAAAGGGGAGAGCAAC-3';

Antisense amplification primer: 5'-CCACCAACGTCGTATTTTCAGC-3';

Shp2 probe: 5'-Texas red-ACGGCAAGTCCAAAGTGACCCACG-BHQ2-3.

Primer and probe sequences for the β -actin reference were as follows:

Sense amplification primer: 5'-TCCATGAAATAAGTGGTTACAGGA-3';

Antisense amplification primer: 5'-CAGAAGCAATGCTGTACCTT-3';

b-Actin probe: 5'-HEX-TCCCTCACCTCCCAAAGCCACC-BHQ1-3'.

4. Prepare stock solutions of the amplification primers at a final concentration of 4 μM in ddH₂O and the probe oligonucleotides at a final concentration of 2 μM in ddH₂O.
5. Set up qRT-PCR reaction mix as follows. Add 1 μL each of the 4- μM stocks of Shp2 and β -actin amplification primers (200 nM final concentration), 1 μL each of the 2- μM stocks of Shp2 and β -actin probe oligonucleotides (100 nM final concentration), 10 μL of 2X iScript Supermix buffer, sufficient cDNA template to correspond to 40 ng of total RNA, and ddH₂O to bring the final volume to 20 μL . Prepare three identical qRT-PCR reactions for each sample.
6. A "well-factor plate" is required to calibrate the iCycler when utilizing different fluorescent probes on the same sample plate. Dilute the 10X Bio-Rad Well-Factor Stock solution to 1X and add 20 μL to the appropriate wells of the sample plate. Run the well-factor plate on the Bio-Rad iCycler for 7 min following the manufacturer's protocol. Once the machine stops, remove the well-factor plate and replace with the sample plate containing the qRT-PCR mixtures from **step 5**.
7. Shp2 and β -actin cDNAs are amplified using the following PCR program: 95°C for 3 min followed by 40 cycles of 95°C for 30 s, 56°C for 15 s, and 72°C for 30 s.
8. The relative level of target gene mRNA in the siRNA treated RAW cell lysates is determined by the Pfaffl method (25), using mock transfected cells as a reference. An example of the qRT-PCR quantitation in Shp2 mRNA levels following treatment with the four Shp2 siRNAs is shown in **Fig. 2**.

3.2.3. shRNA Design and Cloning

1. Once the best siRNA has been identified, it is used to generate a shRNA that can be expressed in RAW cells. Several groups have shown that siRNAs can be tran-

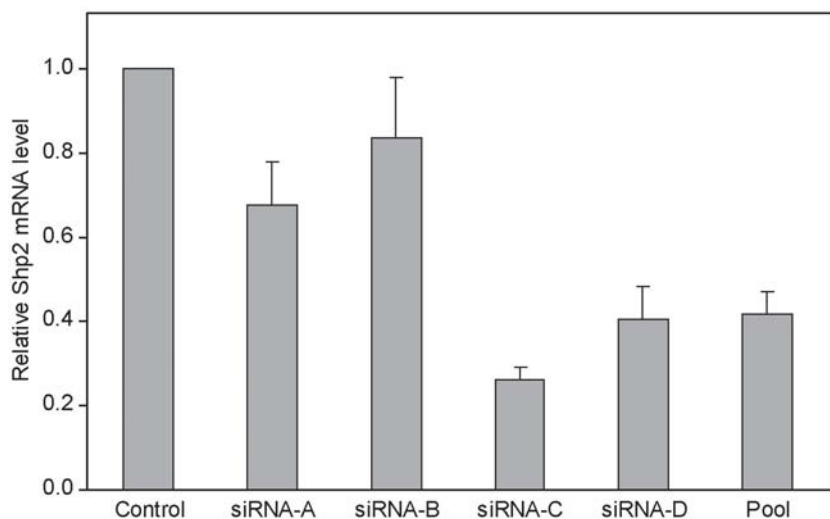


Fig. 2. Efficiency of Shp2 knock down in RAW264.7 cells with different siRNAs. RAW264.7 cells were treated with a control siRNA against *lacZ*, four individual siRNAs against Shp2 (A–D) and a “pool” of all four Shp2 siRNAs (**Subheading 3.2.1.**). At 72 h posttransfection, total RNA was harvested and the Shp2 mRNA level was assessed by quantitative RT-PCR (**Subheading 3.2.2.**).

scribed as stem-loop hairpin structures (shRNAs) under the control of RNA polymerase III promoters (26–28). The first step is to introduce the Shp2-C siRNA into an oligonucleotide linker as shown in Fig. 3 (see Note 2). Commercial vendors are used to prepare the complementary ssDNAs containing the Shp2-C siRNA (Fig. 3C).

2. The ssDNAs are annealed to generate a double-stranded oligonucleotide linker. Prepare 50- μ M stocks of the synthetic oligonucleotides in TE buffer and pipet 100 μ L of each into an RNase/DNase-free microcentrifuge tube. Incubate in a 95°C heat block for 5 min. Transfer samples quickly to a 70°C water bath for 10 min. Turn off the water bath and let the temperature drop to room temperature overnight (see Note 3). The next day, remove samples from water bath, vortex, and centrifuge briefly in a microcentrifuge.
3. Phosphorylate the 3' ends of the shRNA linker by pipetting 15 μ L of annealed oligonucleotides, 4 μ L of 5X T4 DNA ligase buffer, and 1 μ L T4 Polynucleotide Kinase into a 1.5-mL microcentrifuge tube on ice. Incubate the tube in a 37°C water bath for 1 h. Inactivate the kinase by placing sample in a 65°C water bath for 30 min. Dilute sample with 80 μ L of ddH₂O to bring the volume to 100 μ L.
4. Digest 5 μ g of pEN_mH1c vector (Fig. 3D) with *Bam*H1 and *Xho*I for 3 h at 37°C. Place the digest on ice for 2 min. Add 1 μ L alkaline phosphatase, mix, and

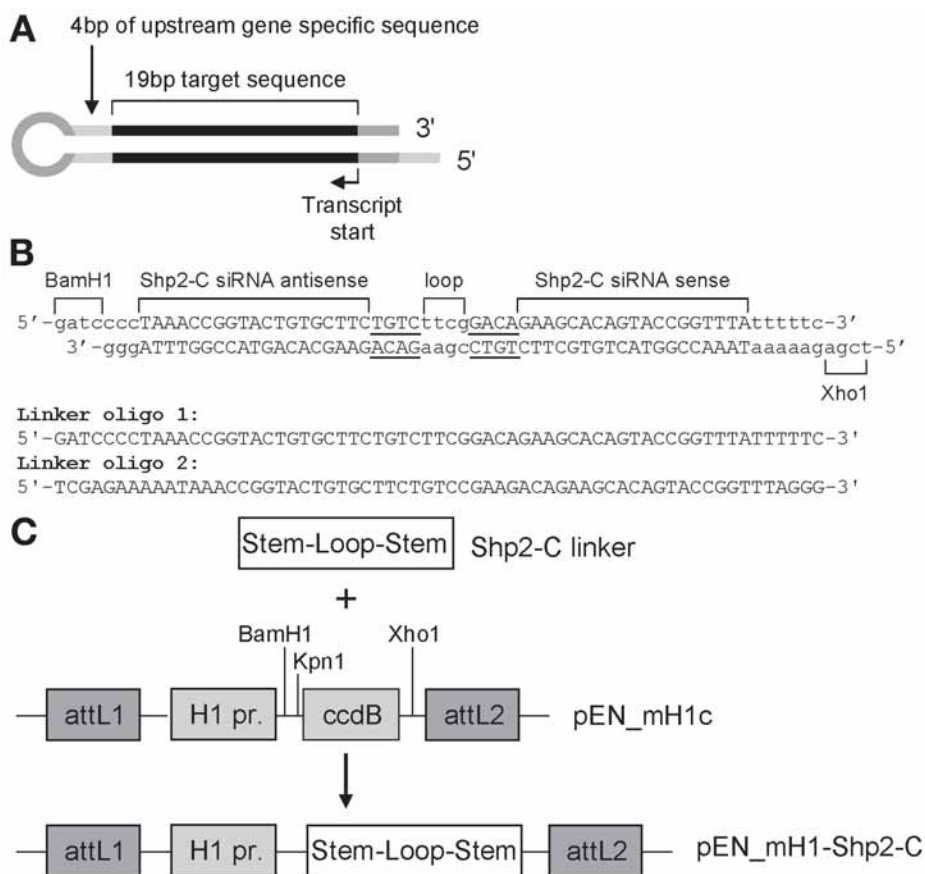


Fig. 3. Design and cloning of an shRNA linker from the SHP2-C siRNA sequence. **(A)** A schematic showing the topology of the Shp2-C shRNA transcript. The antisense strand of the siRNA sequence is transcribed first, followed by a 4bp Shp2-specific spacer, a loop, and then the complementary strand. **(B)** Design of the oligonucleotide linker for expression of the Shp2-C shRNA. Shp2 sequence is in uppercase and the 4-bp spacer sequence adjacent to the siRNA sequence is underlined. **(C)** Schematic for the insertion of the Shp2-C shRNA linker into *Bam*H1/*Xho*I digested pEN_mH1c entry vector. In the resulting pEN_mH1-Shp2-C construct, shRNA expression is driven from the mouse H1 promoter.

incubate at 37°C for 1 h. Run a portion of the digested vector on a 1% agarose gel and visualize the 4265-bp and 431-bp fragments using a UV light box (*see Note 4*). Excise the 4265-bp band and extract DNA from agarose using the QIAquick Gel Extraction Kit. Elute DNA in 60 µL of EB buffer.

5. Prepare ligation reaction on ice by pipetting 150 ng of BamH1/*Xho*I-digested pEN_mH1c into a 1.5-mL microcentrifuge tube and adding a volume of annealed

oligonucleotides sufficient to bring the final volume to 8 μ L. Ligate the digested vector and the duplex linker oligonucleotide using a Rapid Ligation Kit following manufacturer's protocol.

6. Transform 25 μ L of Top10 cells (or similar generic *E. coli* strain) with 5 μ L of the ligation reaction following the manufacturer's protocol. Plate transformed cells onto an LB agar plate containing 10 μ g/mL gentamicin using a sterile technique. Incubate the plate at 37°C overnight.
7. Pick up to six colonies and grow for 12–16 h in 5 mL LB broth containing 10 μ g/mL gentamicin. Pellet 3 mL of the bacterial culture in a 1.5-mL microcentrifuge tube by centrifuging at 13,000 rpm (approx 17,900g) in a tabletop microcentrifuge. Discard supernatant and recover plasmid DNA using the Qiagen Mini Prep kit.
8. Screen candidate clones by digesting the isolated plasmid DNA with *Kpn*I. The *Kpn*I site in the pEN_mH1c parent plasmid (**Fig. 3D**) is lost during shRNA insertion, so correct clones should give the same band pattern as an uncut control run alongside on the same gel. Candidate clones are then sequenced using the following primer, whose sequence is located in the mouse H1 promoter: ATCGCTCTTGAAGGACGACG. The resulting DNA sequence is checked to verify that all steps worked correctly and that it matches the target shRNA sequence.

3.2.4. Assessment of shRNA Efficacy

1. Although the shRNA created in the previous subsection was based on a validated siRNA sequence, it is necessary to test each shRNA to confirm that it retains activity when expressed in the context of pol III transcribed hairpin (*see Note 2*). To test the shRNA, HEK293 cells are cotransfected with the pEN_mH1-Shp2-C (**Fig. 3D**) shRNA plasmid and a plasmid encoding YFP-tagged Shp2 cDNA.
2. Plate HEK293 cells in a six-well plate at 5×10^5 cells per well in 2 mL of 293 growth medium and incubate at 37°C in a humidified 5% CO₂ incubator for 24 h.
3. In a 1.5-mL microcentrifuge tube, combine 100 μ L Opti-MEM, 1.5 μ g YFP-Shp2 expression plasmid, and 0.5 μ g pEN_mH1-Shp2-C plasmid. Lightly vortex the sample and incubate at room temperature for 15 min. Set up control samples, including YFP-Shp2 plasmid alone and YFP-Shp2 plasmid combined with a plasmid expressing a shRNA that is not targeted to Shp2, which are run in parallel with the Shp2 shRNA.
4. In a 15-mL conical centrifuge tube, mix 100 μ L Opti-MEM and 4 μ L Lipofectamine 2000. Vortex lightly to mix.
5. After the 15-min incubation (**step 3**), add 104 μ L of the Lipofectamine 2000 mixture from **step 4** to the tube containing the DNA. Vortex lightly and incubate at room temperature for 15 min.
6. Remove the media from the HEK 293 cells and add 0.8 mL Opti-MEM (prewarmed to 37°C) per well. Add 200 μ L DNA/Lipofectamine 2000 mix (**step 5**) per well of cells. Gently rock the culture plate to mix.
7. Incubate the cells at 37°C in a humidified 5% CO₂ incubator for 3 h. Add 1 mL 293 growth medium to each well. Incubate cells overnight.

8. Replace the media on the cells with 2 mL of fresh 293 growth medium. At this stage, gene knock down can be monitored by fluorescence microscopy by comparing the amount of YFP-Shp2 fluorescence in the control samples to the samples containing the Shp2-C shRNA.
9. Forty-eight hours after the transfection, protein is harvested from the cells to permit accurate assessment of YFP-Shp2 knock down by Western blot. Remove old media from RAW 264.7 cells and wash with 1 mL PBS. Aspirate wash buffer.
10. Add 200 μ L HSE-T buffer to lyse the cells and dislodge from the plate by repetitive pipetting (avoid creating excessive bubbles).
11. Place the cell lysate into a cold, sterile 1.5-mL microcentrifuge tube and centrifuge at 20,000 rpm for 20 min at 4°C in a Sorvall F-20/MICRO rotor (rcf = 51,427g).
12. Transfer the supernatant to a new, sterile microcentrifuge tube on ice and measure protein concentration using a Detergent Compatible Protein Assay Kit.
13. Protein samples for SDS-PAGE (polyacrylamide gel electrophoresis) are mixed with 4X SDS sample buffer such that the final protein concentration is 1 μ g/ μ L in 1X SDS sample buffer. Samples can be stored frozen if needed.
14. The protein lysates are resolved by SDS gel electrophoresis, transferred to nitrocellulose membranes, and probed with anti-Shp2 antibodies as described in **Subheading 3.4**.
15. **Figure 4** shows that cotransfection of HEK293 cells with the Shp2-C shRNA plasmid is very effective in knocking down co-expressed YFP-Shp2 protein.

3.2.5. Subcloning of Validated shRNA into a Lentiviral Vector by Site-Specific Recombination

1. To facilitate expression of the validated Shp2-C shRNA in RAW264.7 cells, the “cassette” containing the murine H1 promoter and the Shp2-C shRNA is subcloned from the pEN_mH1c vector into a lentiviral expression vector. This is achieved by site-specific recombination using the Gateway system (Invitrogen). A schematic of this reaction is shown in **Fig. 5**. In the presence of the required enzymes, recombination occurs between the attL sites flanking the mH1–shRNA cassette in the pEN_mH1–Shp2-C “entry” vector, and the attR sites in the lentiviral pDSL_hpUCIN “destination” vector, to create the final pLX_mH1-SHP2-C-UCIN expression construct.
2. Thaw the 5X LR Clonase buffer and enzyme mixes on ice. Vortex the LR Clonase enzyme mix briefly twice (2 s each time).
3. Mix the following components in a 1.5-mL microcentrifuge tube on ice: 2 μ L of 5X LR Clonase buffer, 150 ng pEN_mH1–Shp2-C vector, 150 ng pDSL_hpUCIN vector, 2 μ L LR Clonase Enzyme and ddH₂O to a final volume of 10 μ L. Vortex briefly to mix.
4. Incubate reactions at 25°C for 1 h.
5. Add 2 μ L of Proteinase K solution to each reaction (*see Note 5*). Incubate for 10 min at 37°C. Store reaction on ice.
6. Transform 25 μ L of Stbl3 cells (Invitrogen; *see Note 6*) with 5 μ L of LR reaction following the manufacturer’s protocol. Plate transformed cells onto LB plates

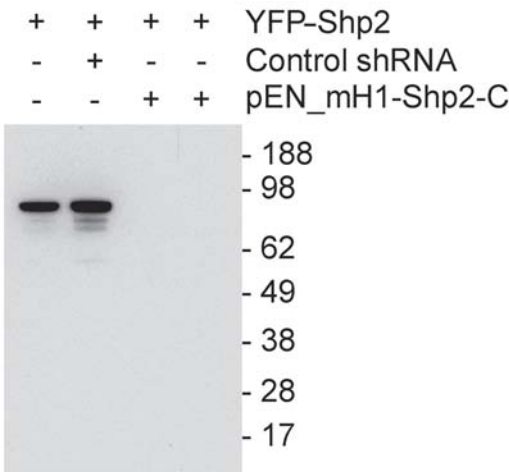


Fig. 4. Knockdown of a co-expressed YFP-Shp2 fusion protein by the Shp2-C shRNA in HEK293 cells. HEK293 cells were cotransfected with a YFP-tagged mouse Shp2 cDNA and either a control shRNA against *lacZ* or the Shp2-C shRNA. At 48 h posttransfection, cells were lysed (**Subheading 3.2.4.**) and 4 μ g of protein were analyzed by Western blotting (**Subheading 3.4.**).

containing 100 μ g/mL ampicillin antibiotic using a sterile technique. Incubate the plates at 37°C overnight.

7. Pick up to three colonies and grow 12–16 h in 5 mL LB broth containing 100 μ g/mL ampicillin. Pellet 3 mL of bacterial culture in a 1.5-mL microcentrifuge tube by centrifuging at approx 17,900g in a tabletop microcentrifuge. Discard supernatant and recover plasmid DNA using the Qiagen Mini Prep kit.
8. Screen candidate clones by digesting plasmid DNA with *Bam*H1. Correct recombinants should give two bands at approx 9.7 and 2.7 kb, as a result of cutting between the mH1 promoter and the shRNA and between the CD4 and IRES in the lentiviral vector backbone.
9. Prepare an endotoxin-free preparation of the validated pLX_mH1-SHP2-C-UCIN clone (*see Note 7*) using a Qiagen EndoFree Maxi kit.

3.3. Production of Lentivirus Expressing a Shp2 shRNA

This protocol describes the transfection of human embryonic kidney (HEK) 293 cells expressing large T-antigen (293T) for use as a packaging cell line to produce a replication-incompetent HIV-based lentivirus vector. Safe HIV-based lentiviral vector systems, including the one described below, were developed using three plasmids (vector, packaging, and envelope), which carry the viral genes required for the production of replication-incompetent lentivirus by a packaging cell line. In addition to the Shp2 shRNA expressed from the

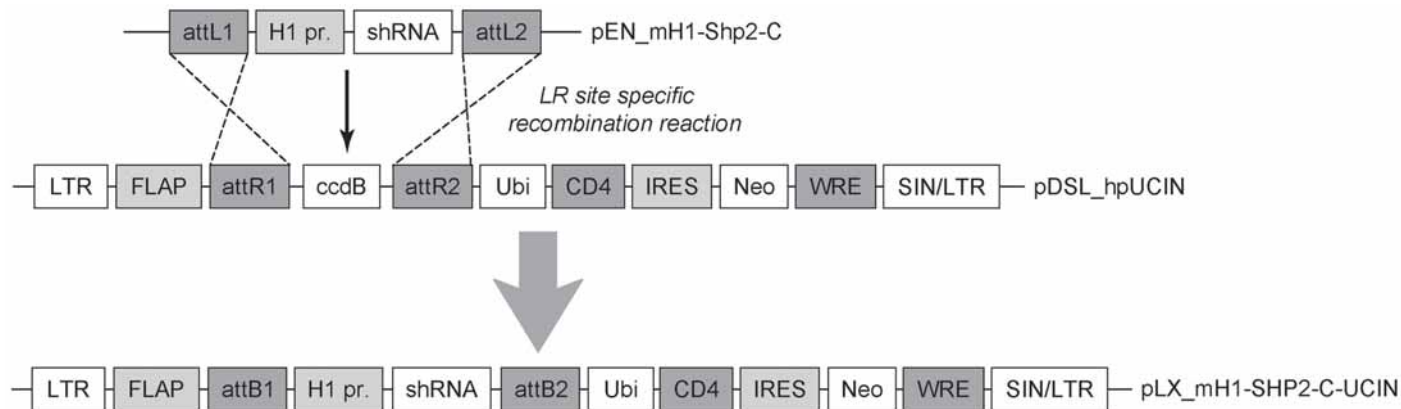


Fig. 5. Schematic of the strategy used to generate an Shp2 shRNA expressing lentiviral vector. Combining the shRNA-containing pEN_mH1c-Shp2-C plasmid with the pDSL_hpUCIN lentiviral vector in the presence of LR clonase enzyme leads to recombination between the attL and attR sites and the insertion of the mH1-Shp2-C shRNA cassette into the lentiviral backbone.

mouse H1 promoter, the pLX_mH1-SHP2-C-UCIN vector plasmid carries a viral RNA packaging signal, self-inactivating viral long-terminal repeats (SIN-LTRs), the CD4 cell surface marker expressed from the ubiquitin C promoter, and a neomycin-resistance gene translated from an IRES sequence within the CD4/neomycin bi-cistronic mRNA (see Fig. 5). The pCMVΔR8.91 packaging plasmid (20) expresses HIV gag, pol, and rev genes, but does not carry a viral RNA packaging sequence. The viral envelope plasmid, pMD.G (20) expresses vesicular stomatitis virus G envelope protein, which binds cell membrane lipids and, hence, permits entry of the “pseudotyped” lentivirus into all mammalian cells. The neomycin-resistance gene allows selection of stable populations of transduced cells, after which Shp2 knock down is assessed by both qRT-PCR (Subheading 3.2.2.) and Western blotting (Subheading 3.4.).

3.3.1. Transfection of 293T Packaging Cells

1. Prepare one to three poly-L-lysine (PLL)-coated 10 cm tissue culture dishes for plating 293T cells depending on the amount of virus needed. Disperse 4 mL of PLL solution over the bottom of each dish and incubate for 1 h at 37°C. Wash dishes with PBS (see Note 8).
2. Harvest 293T cells during log growth (50–70% confluence) using trypsin-EDTA solution at 25°C for only 1–1.5 min to limit exposure of cells to trypsin. Resuspend cells in 293 growth medium to inactivate trypsin and count the cells (see Note 9).
3. Add $(4-5) \times 10^6$ cells to each PLL-coated dish in 10 mL of 293 growth medium, ensuring even dispersal of the cells over the plate (see Note 10). Incubate for 22–26 h.
4. At least 1 h prior to transfection, change the medium on 293T cells (10 mL of 293 growth medium prewarmed at 37°C in a 5% CO₂ incubator).
5. Dilute the pLX_mH1-SHP2-C-UCIN plasmid in Opti-MEM media in a sterile polypropylene tube according to the total volume needed for replicate transfections (3 mL per transfection). We typically transfect three dishes of 293T cells in order to obtain sufficient amounts of virus. The three plasmid DNAs (Shp2 shRNA plasmid, the packaging plasmid pCMVΔ8.91R, and the envelope plasmid pMD.G) are mixed at a ratio (w/w) of 4 : 3 : 2 so that the total amount of plasmid is 30 μg/plate of cells. The plasmid DNA is then diluted with Opti-MEM to a final volume of 1.5 mL.
6. Dilute 60 μl Lipofectamine 2000 in Opti-MEM to a final volume of 1.5 mL/plate according to the manufacturer's protocol and mix gently. Incubate the solution for 5 min at room temperature.
7. Add 1.5 mL of the lipofection solution from step 6 to the diluted plasmid from step 5 and mix gently. Incubate mixture for 20 min at room temperature.
8. Add 3 mL of the plasmid/lipofectamine 2000 mixture to each dish of 293T cells in a dropwise manner to ensure distribution over the entire surface of the dish. Gently swirl contents to mix media without dislodging cells and return

transfected culture dishes to the incubator. It is important to use Biosafety Level 2 (BSL-2) procedures for handling any material that might contain lentivirus from this point forward (*see* **Note 11**).

9. Twelve to eighteen hours posttransfection, replace culture medium with 10 mL fresh, prewarmed 293 growth medium (*see* **Notes 12 and 13**).
10. Forty-eight hours posttransfection, collect the culture supernatants, which contain the lentivirus, and transfer to 50-mL conical centrifuge tubes. Chill to 4°C.
11. Centrifuge virus-containing supernatants for 5 min at 500g at 4°C.
12. Filter the supernatants through 0.45- μ m nonpyrogenic, low protein adsorption filters.
13. Reserve 0.5 mL of unconcentrated supernatant for virus titer determinations (**Subheading 3.2.3.**) and concentrate the remainder of supernatant as described in **Subheading 3.3.2.**

3.3.2. Concentration and Storage of Lentivirus

1. For routine infection of RAW 264.7, a concentrated stock of the Shp2 shRNA lentivirus is prepared from the culture supernatants derived in **Subheading 3.3.1.**
2. Sterilize a Centricon Plus-80 centrifugal filter unit and remove trace amounts of glycerin according to the manufacturer's instructions (*see* **Note 14**). Be sure to remove any residual wash solution prior to use.
3. Add 15–80 mL of unconcentrated lentivirus-containing supernatant from the transfected 293T cells into sample filter cups of the Centricon and reassemble the units.
4. Centrifuge units for 90–120 min at 3000g at 4°C until the volume has been reduced approx 100-fold. Dispose of medium in the filtrate collection cup using BSL-2 procedures.
5. Collect virus-rich retentate in the sample filter cup of the Centricon by placing the retentate cup on top of the sample filter cup. Invert the unit and centrifuge for 5 min at 1000g at 4°C.
6. Aliquot the concentrated lentivirus from the retentate cup into sterile cryovial tubes for storage (20–50 μ L/aliquot). The lentivirus concentrate is viscous because of the concentration of serum proteins and it must be pipetted slowly and carefully.
7. For long-term storage, snap-freeze the virus concentrate in cryovials by immersing in liquid nitrogen and store at –80°C. Although the lentivirus can be stored for long periods this way, there is typically a 30–50% loss of viral titer following freezing and thawing.
8. For short-term storage, the concentrated viral stocks are relatively stable at 4°C. The viral stocks have been stable at 4°C for at least 2 wk, but we have not tested beyond this period.

3.3.3. Lentivirus Titration

In order to achieve optimal infection of RAW 264.7 (or other) cells, it is important to use the correct ratio of cells to infectious viral particles. This ratio

is also known as the multiplicity of infection (MOI). The number of viable infectious viral particles in the concentrated lentivirus stock is determined from a viral titration experiment. Viral infection is scored by fluorescence flow cytometry to detect the presence of the CD4 protein on the surface of infected cells. The CD4 expression cassette was included as a marker in the pLX_mH1-SHP2-C-UCIN plasmid (*see* Fig. 5). The infectious viral titer is determined in the unconcentrated culture supernatant collected from the packaging cells, the concentrated viral stock, and in the concentrated viral stock following a freeze-thaw cycle. Comparison of the titer of these preparations aids in the identification of sources of viral loss, which can be an important problem. When performing viral titration experiments it is important to determine the titer within 1 wk of planned use for virus stored at 4°C.

1. Plate 293T cells harvested from log phase cultures in 12-well tissue culture plates at a concentration of 1.44×10^5 cells/well and incubate overnight. Visually confirm that the 293T cells are healthy, evenly distributed, and at 40–50% confluence at time of infection.
2. Thaw aliquots of frozen virus to be tested on ice.
3. Aspirate medium from 293T cells and add 0.9 mL of prewarmed 293 growth medium containing 8 µg/mL polybrene. Return plates to incubator.
4. Dilute viral solutions in 293 growth medium containing 8 µg/mL polybrene. A final volume of 100 µL is needed for each dilution and each sample will be diluted another 10-fold when added to the cells. A set of serial dilutions (usually three) over the range 10^{-1} – 10^{-3} is tested for unconcentrated virus and a range of 10^{-2} – 10^{-5} is tested for concentrated virus.
5. Add 100 µL of each virus dilution to wells of 293T cells (in 0.9 mL of media). Add 100 µL of 293 growth media/polybrene that does not contain virus to several wells to serve as matched uninfected controls. Incubate cells for 24 h.
6. After 24 h, replace the media with fresh 293 growth medium and return plates to the incubator.
7. Harvest cells for flow cytometric analysis 48–72 h after infection. Cells are harvested by repetitive pipetting in PBS-EDTA rather than with trypsin-EDTA solution to avoid loss of cell surface CD4. Pool the media supernatant, washes, and dislodged cells from each sample well into FACS tubes to ensure that all cells are included.
8. Pellet cells by centrifugation (300g, 5 min, 4°C).
9. Resuspend cells in 0.1 mL of MACS buffer for staining with fluor-coupled anti-hCD4 or isotype control antibodies (BD Pharmingen) according to the manufacturer's recommendations. Wash and collect the stained cells by centrifugation.
10. Gently resuspend cells in 100 µL Cytotfix solution and incubate on ice for 20 min. Add 2 mL of ice-cold MACS buffer, centrifuge, and resuspend cells in 0.5 mL MACS buffer.
11. Determine the percentage of CD4-positive cells by cytometric analysis by comparison of the infected samples with the noninfected samples and the antibody

isotype control (*see* **Note 15**). Identify samples in which the infection rate is 3–10% and calculate the number of cells infected on the day of infection. This is approximately equivalent to number of infectious virus particles added per well assuming a 1 : 1 infection ratio. The number of active viruses detected is used with the volume and dilution of virus stock to calculate the virus concentration in the stock solution (*see* **Note 16**).

3.4 Knockdown of *Shp2* in RAW 264.7 Cells With *shRNA* Lentivirus

The method described below is used to generate stable populations of RAW 264.7 cells in which *Shp2* has been knocked down. The steps in this process include infection of the cells, selection of virally infected cells, and assessment of the level of *Shp2* knock down.

3.4.1. Infection of RAW264.7 Cells With Lentivirus Expressing *Shp2 shRNA*

1. Plate RAW 264.7 cells in 12-well tissue culture plates at a density of 1×10^6 cells per well in RAW growth medium. Incubate the plate at 37°C in a 5% CO₂ incubator for 30 min to 3 h to allow cells to adhere.
2. Calculate the amount of viral stock required to obtain an MOI of five 293T-transducing units per RAW 264.7 cell. The viral concentration should be 1×10^7 viruses/mL to facilitate cell interaction. These infection conditions routinely result in 10–25% transduction efficiencies, suggesting that one productive viral integration occurs for every twenty-five viruses used on RAW 264.7 cells.
3. Mix the appropriate volume of the viral stock solution, 10 µL of a 200-µg/mL polybrene solution (final concentration 4 µg/mL), and RAW growth medium to bring the volume to 500 µL (*see* **Note 17**). Warm the infection mixture at 37°C for 5 min.
4. Aspirate medium from the RAW 264.7 cells and immediately add 500 µL of the warmed virus/polybrene/medium mixture into each well.
5. Incubate at 37°C, 5% CO₂ for 4 h.
6. Add an additional 1.5 mL of RAW growth medium and incubate overnight.
7. Remove the media and transfer into a centrifuge tubes. Gently harvest the cells by adding PBS-EDTA solution for 3–10 min at 4°C. Rinse wells with PBS-EDTA. Add the released cells and washes to the same centrifuge tube. Centrifuge the cells for 5 min at 300g at 4°C and resuspend them in RAW growth medium. Count the cells.
8. Plate the infected cells in 10-cm Petri dishes at a density of 1×10^6 cells per dish. Maintain the cells for 24–48 h prior to drug selection.

3.4.2. Cell Selection

1. RAW 264.7 cells infected with the *Shp2 shRNA* lentivirus are selected by growing cells in G418. Expression of the neomycin gene from the lentiviral vector confers resistance to this drug. Infected RAW 264.7 cells from **Subheading 3.4.1.**

are harvested, replated, and maintained in RAW growth medium containing 100 $\mu\text{g/mL}$ G418.

2. The cell populations are monitored every few days for the expression of CD4 using the cytometric analysis described in **Subheading 3.3.3**.
3. Once the cells in the population are >95% positive for expression of CD4 (typically 4–7 d), the efficiency of Shp2 knock down is determined (*see Note 18*).

3.4.3. Assessment of Shp2 Knockdown in Cell Lines Infected With Shp2 shRNA-Expressing Lentivirus

1. Prepare total RNA or protein lysate from the lentivirally infected stable cell lines as described in **Subheadings 3.2.2.** and **3.2.4.**, respectively.
2. Assess the target gene mRNA level by qRT-PCR as described in **Subheading 3.2.2.**
3. **Figure 6A** shows the results of qRT-PCR experiments to determine mRNA levels in a selected population of RAW 264.7 cells infected with Shp2-C shRNA lentivirus. The level of mRNA was substantially reduced by day 10 following infection and remained low throughout the 37-d-period tested.
4. When adequate antibodies are available, knock down is assessed by Western blotting.
5. The protein lysates are analyzed by SDS gel electrophoresis and Western blotting with anti-Shp2 antibodies as described in **Subheading 3.5.**
6. **Figure 6B** shows the level of Shp2 protein at various times following infection in the Shp2-C shRNA-expressing cell line. When compared to the decrease in mRNA, the decrease in Shp2 protein was considerably slower. By 19 and 26 d after infection, there was a substantial reduction in Shp2 protein.
7. Once sufficient knock down has been established, the cell populations are used for analysis of signal transduction activities and other functional assays.

3.5. SDS-PAGE and Western Blotting

1. Protein samples in 1X SDS sample buffer are prepared from HeLa cells transfected with PP2A siRNAs (**Subheading 3.1.3.**), HEK293 cells transfected with Shp2 shRNA-expression plasmids (**Subheading 3.2.4.**), or from RAW 264.7 cells infected with Shp2 shRNA-expressing lentivirus (**Subheading 3.4.3.**). Standard methods are used to resolve proteins by SDS-PAGE and transfer them to nitrocellulose membranes for Western blot analysis. Detailed protocols are available on the AfCS/Nature Signaling Gateway website (www.signaling-gateway.org) under Protocols within the Data Center.
2. Primary antibodies against PP2A and Shp2 were diluted in antibody incubation buffer and incubated with the blots as follows:
 - a. Shp2 antibody: 1 : 750, incubate for 3 h at room temperature;
 - b. PP2A B55 α antibody: 1 : 5,000, incubate overnight at 4°C;
 - c. PP2A B56 α antibody: 1 : 500, incubate overnight at 4°C;
 - d. PP2A B56 γ antibody: 1 : 1,000, incubate overnight at 4°C;
 - e. PP2A B56 δ antibody: 1 : 1,000, incubate overnight at 4°C.

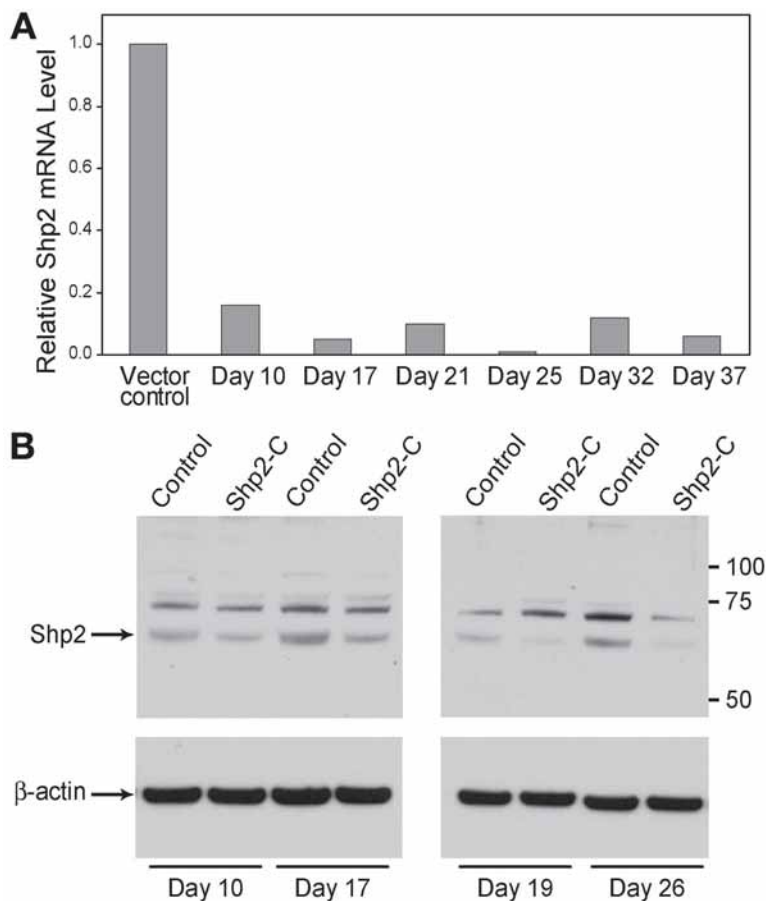


Fig. 6. Knockdown of Shp2 in RAW 264.7 following infection with an shRNA-expressing lentivirus. RAW264.7 cells were infected with the Shp2-C-expressing lentivirus, and transduced cells were selected for neomycin resistance. RNA and protein samples were harvested at various time-points postinfection, and the knock down of endogenous Shp2 was assessed at the mRNA level by qRT-PCR (A) and the protein level by Western blot (B).

3. After incubation with primary antibodies, the blots are incubated for 1 h with ECL anti-rabbit IgG HRP-linked antibody diluted 1 : 2000 in antibody incubation buffer.
4. Quickly rinse blot once with 0.1% TBST. Wash blot three times with 25 mL of 0.1% TBST for 5 min each wash. Wash blot once with 35 mL of 0.1% TBST for 1 h.
5. After rinsing, the blot is incubated with a freshly prepared solution of SuperSignal West Pico Chemiluminescent Substrate for 4 min.

6. Place blot in transparent sheet protector, being careful not to trap air bubbles. Expose blot to Kodak BioMax XAR film for appropriate time interval to produce optimal detection of target protein.

4. Notes

1. Although the siRNA concentration of 400 nM is high relative to that used successfully with other cell types, our results indicate this higher concentration is needed because of the low transfection efficiency of RAW 264.7 cells. For any given siRNA, we have found that a comparable level of knock down can be achieved with a 10-fold lower siRNA concentration in NIH3T3 cells. Therefore the siRNA concentration should be titrated to determine the lowest effective concentration needed for each cell type.
2. We have tested many different shRNA design topologies in an effort to maximize retention of siRNA potency when the sequence is expressed as a shRNA. The design shown in [Fig. 2B](#) was based on principles described by Paddison et al. (29), and although it was successful for Shp2, we have yet to identify a shRNA structure that guarantees retention of siRNA potency. It is therefore important to test each shRNA to confirm that the potency of its corresponding siRNA is retained.
3. We have found that slow annealing of the long oligonucleotides required for the shRNA linkers leads to more efficient cloning. The large thermal capacity of a water bath cooling from 70°C overnight facilitates this process.
4. The pEN_mH1c shRNA cloning vector shown in [Fig. 3C](#) has a sequence labeled “ccdB” between the shRNA cloning sites. This represents a gene that is lethal to *E. coli*, which prevents any background colonies from the parent vector in the subcloning reaction. We have found that this vector design facilitates recovery of >90% positive clones from the shRNA cloning step. The pEN_mH1c parent plasmid can be propagated in the DB3.1 strain of bacteria (Invitrogen), which has been engineered to be resistant to the toxic effect of ccdB.
5. The LR recombination reaction will continue beyond the 1-h incubation described. It is possible therefore to add only 1 µL of Proteinase K to 5 µL of the LR reaction and continue incubation of the remaining 5 µL overnight. If the efficiency of the initial transformation is suboptimal, this “backup” reaction will invariably give a higher number of recombinants.
6. Lentivector plasmids that contain direct repeats can be unstable when replicating in bacteria. We have found that the Stbl 3 cells produce a consistently higher yield of plasmid DNA for lentiviral vectors.
7. In comparative tests, we have seen improved lentiviral titers if all of the plasmids for viral production are prepared endotoxin-free.
8. The 293T cells are adherent but easily detached by media shear force. PLL coating of tissue culture-treated Petri dishes allows easier maintenance of cell monolayers during virus production. PLL-coated dishes can be prepared up to 7 d prior to use.
9. The 293T cells change over time. It is good practice to initially make a large number of frozen aliquots of early passage cells, which can subsequently be

thawed and passaged at regular intervals. In our laboratory, each thaw of 293T cells is not cultured for more than 3 mo. 293T cells used for virus production should not be allowed to reach confluence during routine passage because this affects cell cycling and, thus, virus production. The length of time that the cells are exposed to trypsin during cell harvesting is important: Overdigestion will cause cell death. The serum in culture medium provides excess protein substrate/protease inhibitors to stop digestion of cell membrane proteins by trypsin. Viability counts of harvested cell suspensions should be checked periodically to ensure viability.

10. The exact cell number/area for plating needs to be determined for each 293T line in order to give 80–90% confluence at the time of transfection (22–26 h after plating). When PLL-coated dishes are used, cells adhere firmly as soon as they contact the dish. Adding cells in a large volume and then gently rocking the dish is necessary to obtain even dispersal of adherent cells over the dish. Cells must also be in a single-cell suspension, not clumped, to ensure even plating.
11. Dispose of all potentially lentivirus-contaminated waste according to BSL-2 procedures. This includes working in a flow hood for any procedure able to produce aerosol, rinsing/soaking pipet tips, and so forth in 10% bleach, and disposing of all waste as biohazardous material. Clean all surfaces and centrifuges with 10% bleach followed by 70% ethanol.
12. If contamination problems persist during the transfection procedure, the diluted DNA transfection mixture can be sterile-filtered before mixing with the lipofection reagent.
13. If green fluorescence protein (GFP)-expressing vector plasmids were used, transfection efficiency can be assessed by observing the transfected cells with an inverted fluorescence microscope 24 h posttransfection. This provides a valuable intermediate for troubleshooting.
14. Sterilization of Centricon units. We do not routinely perform this step, but it can be done following the manufacturer's instructions. Aseptic technique and addition of antibiotics to target cells at the time of infection, and 1 wk postinfection, have resulted in negligible contamination during most infections.
15. Space considerations preclude a detailed description of the methods used for flow cytometric analysis. Standard methods for antibody staining of cell surface markers and flow cytometry can be found in manufacturers' recommendations for fluor-coupled antibodies and cytometers.
16. Sample titer calculation: 2.88×10^5 cells/well at time of infection, 5% CD4-positive using 0.1 mL of 10^3 dilution of stock yields 1.44×10^8 viruses/mL stock [$= (2.88 \times 10^5)(0.05)(10^3)(10)$]. Estimated viral titers vary with the particular vector construct used and can be related to differences in marker expression.
17. To allow accurate pipetting of infection volumes, prepare excess volume (i.e., 600 μ L) so that 500 μ L is available per well for infection.
18. Stability of knockdown by RNAi: Once transduced cells have been selected to a level acceptable for use of the population in assays (e.g., > 95%), the effectiveness of target knock down can be determined at both the mRNA and protein level

(where specific antibodies are available). For each target and specific RNAi sequence, the effectiveness and duration of knock down varies, including maintenance of knockdown following freeze/thaw of cell lines. Hence, samples should be taken at the time of assay to assess knock down. If experiments are performed over a series of weeks, samples should be taken for each assay or at the beginning and end of the assay period.

References

1. Hannon, G. J. and Rossi, J. J. (2004) Unlocking the potential of the human genome with RNA interference. *Nature* **431**, 371–378.
2. Meister, G. and Tuschl, T. (2004) Mechanisms of gene silencing by double-stranded RNA. *Nature* **431**, 343–349.
3. MacKintosh, C. and MacKintosh, R. W. (1994) Inhibitors of protein kinases and phosphatases. *Trends Biochem. Sci.* **19**, 444–448.
4. Janssens, V. and Goris, J. (2001) Protein phosphatase 2A: a highly regulated family of serine/threonine phosphatases implicated in cell growth and signalling. *Biochem. J.* **353**, 417–439.
5. Silverstein, A. M., Davis, A. J., Bielinski, V. A., Esplin, E. D., Mahmood, N. A., and Mumby, M. C. (2003) Protein phosphatase 2A, in *Handbook of Cellular Signaling. Volume 2*. (Bradshaw, R. A. and Dennis, E. A., eds.), Academic, New York.
6. Li, X., Scuderi, A., Letsou, A., and Virshup, D. M. (2002) B56-associated protein phosphatase 2A is required for survival and protects from apoptosis in *Drosophila melanogaster*. *Mol. Cell. Biol.* **22**, 3674–3684.
7. Silverstein, A. M., Barrow, C. A., Davis, A. J., and Mumby, M. C. (2002) Actions of PP2A on the MAP kinase pathway and apoptosis are mediated by distinct regulatory subunits. *Proc. Natl. Acad. Sci. USA* **99**, 4221–4226.
8. MacKeigan, J. P., Murphy, L. O., and Blenis, J. (2005) Sensitized RNAi screen of human kinases and phosphatases identifies new regulators of apoptosis and chemoresistance. *Nature Cell Biol.* **7**, 591–600.
9. Strack, S., Cribbs, J. T., and Gomez, L. (2004) Critical role for protein phosphatase 2A heterotrimers in mammalian cell survival. *J. Biol. Chem.* **279**, 47,732–47,739.
10. Vuocolo, S., Purev, E., Zhang, D., et al. (2003) Protein Phosphatase 2A Associates with Rb2/p130 and mediates retinoic acid-induced growth suppression of ovarian carcinoma cells. *J. Biol. Chem.* **278**, 41881–41889.
11. Yang, J., Wu, J., Tan, C., and Klein, P. S. (2003) PP2A:B56epsilon is required for Wnt/beta-catenin signaling during embryonic development. *Development* **130**, 5569–5578.
12. Sathyanarayanan, S., Zheng, X., Xiao, R., and Sehgal, A. (2004) Posttranslational regulation of *Drosophila* PERIOD protein by protein phosphatase 2A. *Cell* **116**, 603–615.
13. Chen, J., St-Germain, J. R., and Li, Q. (2005) B56 regulatory subunit of protein phosphatase 2A mediates valproic acid-induced p300 degradation. *Mol. Cell. Biol.* **25**, 525–532.

14. Chen, W., Possemato, R., Campbell, K. T., Plattner, C. A., Pallas, D. C., and Hahn, W. C. (2004) Identification of specific PP2A complexes involved in human cell transformation. *Cancer Cell* **5**, 127–136.
15. Neel, B. G., Gu, H., and Pao, L. (2003) The “Shp”ing news: SH2 domain-containing tyrosine phosphatases in cell signaling. *Trends Biochem. Sci.* **28**, 284–293.
16. Saxton, T. M., Henkemeyer, M., Gasca, S., et al. (1997) Abnormal mesoderm patterning in mouse embryos mutant for the SH2 tyrosine phosphatase Shp-2. *EMBO J.* **16**, 2352–2364.
17. Zhang, S. Q., Yang, W., Kontaridis, M. I., et al. (2004) Shp2 regulates SRC family kinase activity and Ras/Erk activation by controlling Csk recruitment. *Mol. Cell* **13**, 341–355.
18. Rusanescu, G., Yang, W., Bai, A., Neel, B. G., and Feig, L. A. (2005) Tyrosine phosphatase SHP-2 is a mediator of activity-dependent neuronal excitotoxicity. *EMBO J.* **24**, 305–314.
19. Madhavan, R., Zhao, X. T., Ruegg, M. A., and Peng, H. B. (2005) Tyrosine phosphatase regulation of MuSK-dependent acetylcholine receptor clustering. *Mol. Cell Neurosci.* **28**, 403–416.
20. Salmon, P., Kindler, V., Ducey, O., Chapuis, B., Zubler, R. H., and Trono, D. (2000) High-level transgene expression in human hematopoietic progenitors and differentiated blood lineages after transduction with improved lentiviral vectors. *Blood* **96**, 3392–3398.
21. Kamibayashi, C., Estes, R., Lickteig, R. L., Yang, S.-I., Craft, C., and Mumby, M. C. (1994) Comparison of heterotrimeric protein phosphatase 2A containing different B subunits. *J. Biol. Chem.* **269**, 20139–20148.
22. Elbashir, S. M., Harborth, J., Lendeckel, W., Yalcin, A., Weber, K., and Tuschl, T. (2001) Duplexes of 21-nucleotide RNAs mediate RNA interference in cultured mammalian cells. *Nature* **411**, 494–498.
23. Schwarz, D. S., Hutvagner, G., Du, T., Xu, Z., Aronin, N., and Zamore, P. D. (2003) Asymmetry in the assembly of the RNAi enzyme complex. *Cell* **115**, 199–208.
24. Boese, Q., Leake, D., Reynolds, A., et al. (2005) Mechanistic insights aid computational short interfering RNA design. *Methods Enzymol.* **392**, 73–96.
25. Pfaffl, M. W. (2001) A new mathematical model for relative quantification in real-time RT-PCR. *Nucleic Acids Res.* **29**, e45.
26. Brummelkamp, T. R., Bernards, R., and Agami, R. (2002) A system for stable expression of short interfering RNAs in mammalian cells. *Science* **296**, 550–553.
27. Paul, C. P., Good, P. D., Winer, I., and Engelke, D. R. (2002) Effective expression of small interfering RNA in human cells. *Nat. Biotechnol.* **20**, 505–508.
28. Paddison, P. J., Caudy, A. A., Bernstein, E., Hannon, G. J., and Conklin, D. S. (2002) Short hairpin RNAs (shRNAs) induce sequence-specific silencing in mammalian cells. *Genes Dev.* **16**, 948–958.
29. Paddison, P. J., Silva, J. M., Conklin, D. S., et al. (2004) A resource for large-scale RNA-interference-based screens in mammals. *Nature* **428**, 427–431.

Recognition of a PP2C Interaction Motif in Several Plant Protein Kinases

Niranjan Chakraborty, Masaru Ohta, and Jian-Kang Zhu

Summary

Protein phosphatase 2Cs (PP2Cs) constitute a major class of phosphatases in plants. PP2Cs play important roles in many signaling pathways by countering the action of specific protein kinases. In addition to their role in several environmental stress-related signal transduction pathways, they are also involved in plant metabolism. Protein phosphatases often physically associate with their protein kinase counterparts. One approach to understanding PP2C function is to identify their interacting protein kinases. We describe a yeast two-hybrid assay system used in our lab to determine the interaction between members of the PP2C family and protein kinases in the SOS2 family. This chapter and the cited articles describing related work might be of help in discovering interactions between other protein phosphatases and kinases.

Key Words: PP2C; protein kinase; SOS2; ABI2; yeast two-hybrid

1. Introduction

1.1. *Plant PP2C: A Brief Overview*

Reversible protein phosphorylation is a fundamental mechanism by which living organisms regulate cellular processes in response to developmental, hormonal, and environmental cues. The phosphorylation status of a protein is determined by the balance between the activities of protein kinases and protein phosphatases. Although the catalytic cores of all eukaryotic protein kinases share extensive similarities in both primary and three-dimensional structures, protein phosphatases display much more diversity. Protein phosphatases can be divided into two major classes: protein tyrosine phosphatases (PTPs) and protein serine/threonine phosphatases. Protein tyrosine phosphatases include PTPs and dual-specificity phosphatases (DSPTPs). The protein serine/

From: *Methods in Molecular Biology, Volume 365: Protein Phosphatase Protocols*
Edited by: G. Moorhead © Humana Press Inc., Totowa, NJ

threonine phosphatases are further classified into the PPP and PPM gene families based on their amino acid sequences. The PPP family includes so-called “signature phosphatases” (types 1 [PP1], 2A [PP2A], and 2B [PP2B]), whereas the PPM family includes type 2C (PP2C) and pyruvate dehydrogenase phosphatase (1).

1.2. Function of PP2C in Plants

The PP2Cs constitute the largest family of protein phosphatases in plants, with 76 members in *Arabidopsis* genome. With merely 15 PP2Cs found in the human genome, 8 in worm and 10 in fly (2), the multiplicity of PP2C in plants suggests broader functional diversity than in other eukaryotes. Members of the PP2C family dephosphorylate the α -subunit of phosphorylase kinase. They require magnesium or manganese for activities and are insensitive to okadaic acids, microcystin, and calyculin A, which are inhibitors of PP1 and PP2A (3,4). Unlike other families of protein phosphatases, members of the PP2C family are monomeric, lacking regulatory subunits (3,4). Most of *Arabidopsis* PP2Cs (44 out of 76) have catalytic domains at their C-terminus with different N-terminal extensions (2).

The PP2Cs are known to reverse stress-induced protein kinase cascades in eukaryotes. For example, PP2C negatively regulate the high-osmolarity glycerol (HOG) mitogen-activated protein kinase (MAPK) pathway by directly dephosphorylating Hog1 MAPK in yeast (5). In plants, alfalfa MP2C can dephosphorylate and inactivate the wound-induced SIMK (stress-induced MAPK), suggesting that MP2C is a part of a negative feedback loop for the SIMK signaling pathway (6).

1.3. PP2Cs Are Negative Regulators of ABA Signaling

The *Arabidopsis* PP2Cs fall into 10 groups (A–J), and ABI1 and ABI2 belong to the group A of PP2C (2). Genetic analysis of *abi1* and *abi2* mutants, their revertants, transient expression studies, and analysis of transgenic antisense plants have revealed that PP2Cs function as negative regulators of ABA signaling (4,7–9). Transient expression assays have demonstrated that ABA signaling could be repressed by ABI-type PP2C, but not by KAPP or other protein phosphatase such as PP1, PP2A, or PP2B, indicating that this function is specific to ABI-type PP2C phosphatases (7). There are as many as nine group-A PP2C members in *Arabidopsis*, which might have redundant functions. (10). ABI1 and ABI2 contribute nearly 50% of the ABA-induced PP2C activity, indicating that other PP2Cs are also involved in ABA signaling (8).

ABI1 and ABI2 encode homologous proteins and are transcriptionally upregulated by ABA (5). In *abi1* and *abi2* mutants, the same Gly to Asp amino acid substitution has occurred at equivalent position in ABI1 and ABI2 proteins,

which causes a significant reduction of the ABI1 and ABI2 phosphatase activity (7). The *abi1-1* and *abi2-1* mutations are dominant and lead to largely overlapping sets of phenotypic alterations, including ABA-resistant seed germination and seedling growth, reduced seed dormancy, abnormal stomatal regulation, and defects in various responses to drought stress. Owing to the dominant nature of these mutations, it is still uncertain whether ABI1 and ABI2 were involved in ABA signaling or if the dominant mutations create unspecific phenotypes that are not related to the original function of the wild-type protein.

Several studies have shown that ABI1 and ABI2 have distinct functions in ABA signaling. Guard cells of *abi1-1* and *abi2-1* plants are disrupted in ABA activation of hyperpolarization-activated Ca^{2+} (ICa) channels (11,12). However, the *abi1-1* mutant treated with ABA did not induce production of reactive oxygen species (ROS) but H_2O_2 activation of ICa channels and H_2O_2 -induced stomatal closing was not disrupted. This suggested that *abi1-1* impairs ABA signaling between ABA perception and ROS production. Conversely, *abi2-1* impaired H_2O_2 activation of ICa, H_2O_2 -induced stomatal closing, and ABA-elicited ROS production. These results suggested that both PP2Cs function at different levels of the same pathway: *abi1-1* acts upstream and *abi2-1* acts downstream of ABA-induced ROS production in guard cells (12). ABA-induction of the alcohol dehydrogenase gene was reduced in *abi2* plants, but not in *abi1* plants (13). *abi1* but not *abi2* mutation abolished induction of cold-regulated (COR) genes by ABA (14). It was found that ABI1 and ABI2 could interact with proteins that are involved in several signaling pathways. SOS2 (Salt Overly Sensitive 2) and some of the SOS2-related protein kinases, PKSs (protein kinase S), interact with ABI1 and ABI2 (15,16). ABI1 also interacts with the ABA-inducible transcription factor ATHB6. ATHB6 promoter-reporter expression was abrogated in *abi1-1* mutant plants, indicating that ABI1 acts upstream of the transcription factor (17).

1.4. Interaction of ABI2 and SOS2

The *Arabidopsis* SOS2 is a serine/threonine kinase that is necessary for sodium and potassium ion homeostasis and salt tolerance (18). SOS2 kinase is activated by the calcium-binding protein SOS3, together with calcium elicited by salt stress (19). The SOS3–SOS2 kinase complex is required for the phosphorylation and activation of the plasma membrane Na^+/H^+ antiporter encoded by the *SOS1* gene (20). *Arabidopsis* SOS2 is a member of a family of 25 protein kinases that are known as protein kinase S (PKS) (21).

We have isolated proteins that interact with SOS2 kinase by yeast two-hybrid screening. Seven of the 101 putative interacting clones encode ABI2 (16). The interaction of SOS2 with ABI2 is mediated through a novel protein domain of 37 amino acid residues, designated as the protein phosphatase interaction (PPI)

motif of the SOS2 that is necessary and sufficient for interaction with ABI2 (16). The PPI motif is conserved in *Arabidopsis* PKS proteins and in the DNA damage repair and replication block checkpoint kinase (Chk1) in various organisms including human. Mutations in the conserved amino acid residues in the PPI motif abolish the interaction of SOS2 with ABI2, indicating that these amino acid residues are important for the interaction with ABI2. Further, a protein kinase interaction (PKI) domain in ABI2 was identified and the interaction specificity between PKS and the ABI phosphatases was investigated. The interaction between SOS2 and ABI2 was disrupted by the *abi2-1* mutation, which causes increased tolerance to salt shock and ABA insensitivity in plants (16).

Some PKSs interact strongly with ABI2, whereas others interact preferentially with ABI1. For example, SOS2, PKS3, PKS11, and PKS24 preferentially interact with ABI2, whereas PKS18 strongly interact with ABI1 (16). PKS3 and its interacting calcium sensor ScaBP5 are regulators of ABA signaling (15). Transgenic plants expressing a constitutive active form of *PKS11* were more resistant to a higher concentration of glucose, suggesting a role of PKS11 in sugar signaling (22). PKS18 is also involved in ABA signaling because RNA interference (RNAi) of *PKS18* conferred ABA insensitivity and transgenic plants expressing an active form of PKS18 were hypersensitive to ABA (23). *sos2* and *sos3* mutants are specific defective in salt tolerance but not in ABA responses (18,24). PKS3 and PKS18 are involved in ABA signaling, but not in salt tolerance (15,23). These studies suggest that different combinations of PKS/SOS2 kinase–ABI1/2 phosphatase complexes might regulate specific signaling pathways.

2. Materials

2.1. Preparation of Test Bait and Interacting Prey Plasmids

We use pAS2 (25) and pACT2 (26) plasmid vectors to make bait and prey constructs, respectively. The polymerase chain reaction (PCR) is the most preferred experiment for construct preparation, as it greatly helps to make the insert fragments of genes of interest in frame with the vectors. Refer to standard protocols such as “Molecular Cloning” for PCR. However, verify the constructs by restriction digestion/sequencing before proceeding to the next step.

2.2. Yeast Transformation

Transformation of yeast cells can be carried out by the methods developed by Ito et al. (27) and modified by Schiestl and Gietz (28), Hill et al. (29), and Gietz et al. (30).

1. YPD medium (1 L): 20 g Difco peptone, 10 g Yeast extract, 18 g Bactoagar (for plates only). Dissolve in 950 mL of H₂O and adjust pH to 5.8, autoclave, and cool to approx 55°C. Add glucose to 2% (50 mL of sterile 40% stock solution).

2. SD medium (1 L): 717 mg dropout, 20 g glucose, 1 mL of 1 N NaOH, 10 mL each of 100X amino acid, Bactoagar 20 g (if necessary). Fill up to 900 mL.

Synthetic dropout (SD) is a minimal medium that includes a yeast nitrogen base, a carbon source (generally 2% dextrose), and “dropout” solution that contains essential nutrients (such as amino acids and nucleotides). After autoclaving, wait until the solution is cooled down to 55°C and add 100 mL of 10X YNB (yeast nitrogen base without amino acids; Difco cat. no. 0919-15-3). It is convenient to put a magnetic stirrer bar into the bottle when you autoclave the medium. This helps to mix the medium well after autoclaving.

3. 10X YNB (1 L): dissolve 67 g of the powder in distilled water and sterilize by filtration (0.45- μ m filter) and store at 4°C (*see Note 1*). We usually make the dropout containing the following amino acids and nucleotides. Take 0.15 g Ile, 0.1 g Ura, 0.75 g Val, 0.1 g Ade, 0.1 g Arg, 0.15 g Lys, 0.1 g Met, 0.25 g Phe, 1 g Thr, and 0.15 g Tyr. Mix and grind these nutrients well with mortar and pestle. You can stock the dropout at room temperature. In order to select transformants, you should supplement the following amino acids to the SD medium:

Vector	Amino acid
pAS2	Leu, His
pACT2	Trp, His
pAS2 + pACT2	His

4. 100X amino acid solution: 0.2 g His, 0.2 g Trp, 1 g Leu and dissolve each of them in 100 mL of distilled water and autoclave. 100X amino acids should be kept at 4°C in the dark (Trp is susceptible to photodegradation).
5. 1X TE/LiAc buffer (LATE buffer): 100 mM lithium acetate, 10 mM Tris-HCl, pH 7.5, and 1 mM EDTA. Sterilize by autoclaving.
6. 10 mg/mL salmon sperm carrier DNA. Sonicated. (Salmon sperm carrier DNA in solution can be purchased from commercial sources or can be prepared using a standard method.)
7. PLATE buffer: 40% PEG 4000 in LATE buffer. Dissolve 40 g of PEG 4000 in 100 mL of the LATE buffer. Sterilize by autoclaving; avoid repeated autoclaving.

2.3. Colony-Lift β -Galactosidase Filter Assays

1. Z buffer (1 L): 16.1 g $\text{Na}_2\text{HPO}_4 \cdot 7\text{H}_2\text{O}$, 5.50 g $\text{NaH}_2\text{PO}_4 \cdot \text{H}_2\text{O}$, 0.75 g KCl, $\text{MgSO}_4 \cdot 7\text{H}_2\text{O}$ 0.246 g. Adjust to pH 7.0 and autoclave.
2. X-gal stock solution: Dissolve 5-bromo-4-chloro-3-indolyl- β -D-galactopyranoside (X-gal) in *N,N*-dimethylformamide (DMF) at a concentration of 20 mg/mL. Store in the dark at -20°C.
3. Z buffer/X-gal solution: 100 mL Z buffer, 0.27 mL β -mercaptoethanol (β -ME), 1.67 mL X-gal stock solution. Mix these reagents and use immediately.

4. Whatman #5 or VWR grade 410 paper filters: 75-mm filters (e.g., VWR #28321-055) for use with 100-mm plates or 125-mm filters (e.g., VWR #28321-113) for use with 150-mm plates.

2.4. *In vitro* Protein-Binding Assay

1. Lysis buffer: 20 mM Tris-HCl, pH 8.0, 200 mM NaCl, 1 mM EDTA, pH 8.0, 0.5% Nonidet P40 (just before use, add protease inhibitors to the following final concentrations: 2 $\mu\text{g}/\mu\text{L}$ aprotinin, 1 $\mu\text{g}/\mu\text{L}$ leupeptin, 0.7 $\mu\text{g}/\text{mL}$ pepstatin, and 25 $\mu\text{g}/\text{mL}$ phenylmethylsulfonyl fluoride).
2. Binding buffer: 20 mM Tris-HCl, pH 7.5, 150 mM NaCl, 1 mM CaCl_2 , 0.1% Nonidet P-40.

3. Methods

3.1. Yeast Transformation

1. For inoculation, take a single colony 2–3 mm in diameter and scrape the entire colony into 10 mL of YPD. Grow the preculture at 30°C for overnight with shaking at 200 rpm.
2. Add the preculture to produce optical density (OD_{600}) of 0.2–0.3 into 50 mL of main culture and grow further at 30°C until it reaches mid log phase.
3. Pellet the cells by centrifuging at 1000g at 25°C for 5 min. Resuspend the pellet in 35 mL of distilled water and collect the cells again as same as above. Resuspend the cells in 1.5 mL of LATE buffer.
4. Combine the following components in a 1.5-mL tube:

Competent cells	100 μL (<i>see</i> Note 2)
PLATE buffer	600 μL
10 mg/mL Salmon sperm DNA	5 μL
Plasmid DNA	0.1 μg

5. Incubate the transformation mixtures at 30°C for 30 min with gentle shaking.
6. Add 70 μL of dimethyl sulfoxide (DMSO) and incubate at 42°C for 15 min. Pellet the cells by the centrifugation and resuspend in 100 μL of TE.
7. Plate the cells onto an appropriate SD agar plate (*see* above).
8. Incubate the plates at 30°C for 1 or 2 d until colonies become 2–3 mm in diameter.
9. Streak several colonies to new plates and grow them at 30°C for 1 or 2 d.

3.2. Colony-Lift β -galactosidase Filter Assays

1. In the case that a few colonies are to be assayed, streak them directly onto SD agar plates. Incubate the plates at 30°C for 1–2 days (*see* **Note 3**) and then proceed with the β -galactosidase assay as described in the following steps.
2. For each plate, presoak a sterile Whatman #5 or VWR grade 410 filter by placing it in 2.5–5 mL of Z buffer/X-gal solution in a clean 100- or 150-mm plate.
3. Place a clean, dry filter over the surface of the plate of colonies to be assayed (*see* **Note 4**).

4. Carefully lift the filter off the agar plate with forceps and transfer it (colonies facing up) to a pool of liquid nitrogen (*see Note 5*) and submerge the filters for 10 s.
5. Remove the filter from the liquid nitrogen and allow it to thaw at room temperature (this treatment permeabilizes the cells).
6. Carefully place the filter, colony side up, on the presoaked filter (from **step 2**). Avoid trapping air bubbles under or between the filters.
7. Incubate the filters at 30°C and check them periodically for the appearance of a blue color on the colonies (*see Note 6*).
8. If you are conducting a screening, identify the β -galactosidase-producing colonies by aligning the filter to the agar plate and pick the corresponding positive colonies from the original plates to fresh medium.

3.3. Yeast Two-Hybrid Screen and Interaction Assay

Colony-lift β -galactosidase filter assays can be used for both screening of interacting proteins and confirmation of the interaction between proteins of interest. When you carry out the two-hybrid experiments for the confirmation of the interactions, you do not have to handle plates and filters aseptically. To do the colony-lift β -galactosidase filter assays semiquantitatively, you must be careful to keep equal amount of colonies among samples. We usually prepare the plates for the colony-lift β -galactosidase filter assays as follows. Inoculate colonies into SD liquid medium and grow them for overnight at 30°C. Check their OD₆₀₀. Harvest the cells by centrifugation and resuspend them in D.W. so as to adjust their OD₆₀₀ values to 0.1. Drop 20 μ L of the cell suspensions (4×10^4 cells) onto SD agar plates and incubate at 30°C for 2 d. In the author's laboratory, the gene for the test protein, SOS2, is fused to the GAL4 DNA-BD in the pAS2 vector and the gene for the target protein ABI2 is fused to the GAL4 AD in the pACT2 vector. To evaluate a positive interaction between test and target proteins, you must make combinations of bait and prey for control experiments. If a combination of your bait construct with pACT2 empty vector or a combination of pAS2 empty vector with your prey construct does not give any background level of positive signal, then the positive signal observed on the colonies harboring your test and target constructs can be considered as a positive interaction.

Using a yeast two-hybrid approach, we screened for proteins that interact with the protein kinase SOS2 from a λ -ACT cDNA library prepared from mRNA isolated from young *Arabidopsis* seedlings (31). This library can be converted to a pACT plasmid library by infecting *Escherichia coli* BNN132 cells. You can construct a GAL4 AD fusion expression library in pACT2 using either intronless genomic DNA or cDNA such that at least 10^6 different hybrid proteins will be expressed (*see Note 7*). (Commercial cDNA libraries from a variety of species and tissues are also available.)

3.4. Identification of Interaction Motif in Test Proteins

Once an interaction between the test and target proteins is confirmed, it might be possible to identify the motif of the test protein that mediates the interaction with the target protein. Usually, deletion clones are made in prey, when a minimal interacting domain is identified. In the authors' laboratory, serial deletions of SOS2 in the bait vector pAS2 were made in order to identify a minimal region of SOS2 that is sufficient and/or necessary for interaction with ABI2. However, *ABI2* could not be used as bait, because pAS-ABI2 activates the *lacZ* reporter gene in yeast. It is important that every deletion construct in bait should be checked for their background transcriptional activation in yeast cells by setting a negative control with an empty prey vector (pACT2) for every bait construct. Some proteins acquire transcriptional activation by removing a portion of the protein, even though the full length does not show transcriptional activation at all. We made two bait constructs, each containing the C-terminal regulatory or N-terminal catalytic domain of SOS2. Because the ABI2 prey interacted with the C-terminal regulatory but not with the N-terminal catalytic domain in bait, we further determined that the minimal C-terminal regulatory sequence of SOS2 interacts with ABI2 using the yeast two-hybrid assay and then made serial deletions in the C-terminal regulatory region. The deletion constructs can be made by PCR with pairs of forward and reverse primers containing suitable restriction sites for cloning. The resulting PCR products can then be digested and inserted between the corresponding sites of pAS2. We found that the SOS2 sequence between amino acid 333 and 369, designated as PPI motif, is necessary and sufficient for interaction with ABI2.

In the next step, we tested the highly conserved amino acid residues in the PPI motif of SOS2. The experiment was to further elucidate the amino acids important for protein interaction. This was done by mutating the conserved amino acid residues of the test protein and then studying the impact of the mutations on the protein interaction. Mutations can be easily introduced by an inverse PCR-based site-directed mutagenesis with double-stranded plasmid DNA as templates. First, you have to phosphorylate one of the PCR primers at the 5' end, followed by PCR with high-fidelity *Taq* DNA polymerase. The resulting PCR products should be digested with *DpnI* to remove the template plasmid DNA and select for the synthesized DNA-containing mutations. Because DNA isolated from most *E. coli* strains is dam methylated, it is susceptible to *DpnI* digestion, which is specific for methylated DNA. After digestion, the PCR products are purified by gel electrophoresis, followed by self-ligation. Finally, the circular PCR products are transformed into *E. coli*. All plasmid constructs are completely sequenced to ensure that there is no PCR or cloning errors.

3.5. In Vitro Protein-Binding Assay

It is necessary that the interaction of a test protein with a target protein in yeast two-hybrid assay be confirmed by in vitro protein-binding assays such as a pull-down assay. For the pull-down assay, you have to make two kinds of plasmid construct to express a GST-fusion protein and an in vitro translated protein. We used pGEX-2TK (Pharmacia) and pET146 (Novagen) for the GST fusion and the in vitro translated proteins, respectively (16).

3.5.1. Preparation of GST-Fusion Proteins

1. Make the plasmid construct in an appropriate vector for the GST-fusion protein (e.g., pGEX-2TK) and transform it into the BL21 DE3 *E. coli* strain (Novagen).
2. Inoculate a single colony into 1 L of Luria-Bertani medium containing 100 µg/mL ampicillin and incubate the medium at 30°C until the OD₆₀₀ reaches 0.5–0.7 (freshly transformed colonies give better results of protein expression). You can reduce the size of the culture medium if your protein is well produced in *E. coli* cells.
3. Induce the recombinant protein expression with 0.5 mM isopropyl-thio-β-galactoside (IPTG) and incubate 30°C for another 6 h.
4. Harvest the cells by centrifugation at 5000g for 15 min at 4°C and resuspend the cells in 20 mL of the lysis buffer.
5. Purify the recombinant fusion proteins from bacterial lysates with glutathione–Sephadex (Pharmacia) described in the manufacturer's protocol.

3.5.2. In Vitro Pull-Down Assay

1. Insert the coding region of the test or interacting protein in a vector for the in vitro translation system such as pET146 (Novagen). Level the expressed proteins by in vitro translation using ³⁵S methionine.
2. Incubate aliquots of the ³⁵S-labeled protein with 20 µg of GST-fusion proteins on Sepharose beads in 150 µL of the binding buffer under constant rocking for 1 h at 4°C. For negative controls, incubate the ³⁵S-labeled protein with 20 µg of GST-Rb and GST beads as same as above.
3. Centrifuge the mixture at 1000 rpm for 2 min at 4°C.
4. Wash the beads extensively with the ice-cold binding buffer. Repeat the washes three times.
5. Elute the bound proteins with sodium dodecyl sulfate–polyacrylamide gel electrophoresis (SDS-PAGE) loading buffer (see Note 8).
6. Resolve the bound protein on 7.5% SDS-PAGE and detect the bound protein by fluorography.

4. Notes

1. Warm up the 10X YNB before you mix it with the autoclaved agar medium. Otherwise, the agar starts to solidify immediately after you add the chilled 10X YNB.

2. When screening a library, competent cells should be used immediately. However, for small-scale (routine) transformations, the competent cells can be stored at room temperature for several hours without a significant reduction in competency.
3. For best results, use fresh colonies (i.e., grown at 30°C for 2–4 d), 1–3 mm in diameter. If the entire colony was lifted onto the filter, pick it from the filter or incubate the original plate for 1–2 d to regrow the colony.
4. Nitrocellulose filters also can be used, but they are prone to crack when frozen.
5. Liquid nitrogen should be handled with care. Always wear thick gloves and goggles when handling liquid nitrogen.
6. The time that it takes colonies producing β -galactosidase to turn blue varies, typically from 30 min to 8 h in a library screening. Prolonged incubation (>8 h) tends to give false positives.
7. If you construct your own library, you will obtain enough material to perform a library-scale transformation without an extra amplification step. However, be sure to reserve a 1.0-mL aliquot of your library, frozen in 25% glycerol, so that you can go back and amplify it at a later time if necessary.
8. If you get only a low signal, you should change the ion concentration in the binding buffer or incubate target proteins with GST-fusion proteins longer than previously.

References

1. Cohen, P. T. (1997) Novel protein serine/threonine phosphatases: variety is the spice of life. *Trends Biochem. Sci.* **22**, 245–251.
2. Schweighofer, A., Hirt, H., and Meskiene, I. (2004) Plant PP2C phosphatases: emerging functions in stress signaling. *Trends Plant Sci.* **9**, 236–242.
3. Smith, R. D. and Walker, J. C. (1996) Plant protein phosphatases. *Ann. Rev. Plant Physiol. Plant Mol. Biol.* **47**, 101–125.
4. Rodriguez, P. L. (1998) Protein phosphatase 2C (PP2C) function in higher plants. *Plant Mol. Biol.* **38**, 919–927.
5. Warmka, J., Hanneman, J., Lee, J., Amin, D., and Ota, I. (2001) Ptc1, a type 2C Ser/Thr phosphatase, inactivates the HOG pathway by dephosphorylating the mitogen-activated protein kinase Hog1. *Mol. Cell. Biol.* **21**, 51–60.
6. Meskiene, I., Baudouin, E., Schweighofer, A., et al. (2003) The stress-induced protein phosphatase 2C is a negative regulator of a mitogen-activated protein kinase. *J. Biol. Chem.* **278**, 18,945–18,952.
7. Sheen, J. (1998) Mutational analysis of protein phosphatase 2C involved in abscisic acid signal transduction in higher plants. *Proc. Natl. Acad. Sci. USA* **95**, 975–980.
8. Merlot, S., Gosti, F., Guenier, D., Vavasseur, A., and Giraudat, J. (2001) The ABI1 and ABI2 protein phosphatases 2C act in a negative feedback regulatory loop of the abscisic acid signalling pathway. *Plant J.* **25**, 295–303.
9. Gosti, F., Beaudoin, N., Serizet, C., Web, A. A. R., Vartanian, N., and Giraudat, J. (1999), ABI1 protein phosphatase 2C is a negative regulator of abscisic acid signaling. *Plant Cell* **11**, 1897–1909.

10. Wu, Y., Sanchez, J. P., Molina, L. L., Himmel, A., Grill, E., and Chua, N.-H. (2003) The *abi1-1* mutation blocks ABA signaling downstream of cADPR action. *Plant J.* **34**, 307–315.
11. Allen, G. J., Kuchitsu, K., Chu, S. P., Murata, Y., and Schroeder, J. I. (1999) *Arabidopsis abi1-1* and *abi2-1* phosphatase mutations reduce abscisic acid-induced cytoplasmic calcium rises in guard cells. *Plant Cell* **11**, 1785–1798.
12. Murata, Y., Pie, Z.-M., Mori, I. C., and Schroeder, J. (2001) Absciscic acid activation of plasma membrane Ca^{2+} channels in guard cells requires cytosolic NAD(P)H and is differentially disrupted upstream and downstream of reactive oxygen species production in *abi1-1* and *abi2-1* protein phosphatase 2C mutants. *Plant Cell* **13**, 2513–2523.
13. de Bruxelles, G. L., Peacock, W. J., Dennis, E. S., and Dolferus, R. (1996) Absciscic acid induces the alcohol dehydrogenase gene in *Arabidopsis*. *Plant Physiol.* **111**, 381–391.
14. Gilmour, S. J. and Thomashow, M. F. (1991). Cold acclimation and cold-regulated gene expression in ABA mutants of *Arabidopsis thaliana*. *Plant Mol. Biol.* **17**, 1233–1240.
15. Guo, Y., Xiong L., Song, C. P., Halfter, U., and Jhu, J.K. (2002) A calcium sensor and its interacting protein kinase are global regulators of abscisic acid signaling in *Arabidopsis*. *Dev. Cell* **3**, 233–244.
16. Ohta, M., Guo, Y., Halfter, U., and Zhu, J.-K. (2003) A novel domain in the protein kinase SOS2 mediates interaction with the protein phosphatase 2C ABI2. *Proc. Natl. Acad. Sci USA* **100**, 11,771–11,776.
17. Himmelbach, A., Leube, M., Hohener, B., and Grill, E. (2002) Homeodomain protein ATHB6 is a target of the protein phosphatase ABI1 and regulates hormone responses in *Arabidopsis*. *EMBO J.* **21**, 3029–3038.
18. Zhu, J. K., Liu, J., and Xiong, L. (1998) Genetic analysis of salt tolerance in *Arabidopsis*. Evidence for a critical role of potassium nutrition. *Plant Cell* **10**, 1181–1191.
19. Halfter, U., Ishitani, M., and Zhu, J. K. (2000) The *Arabidopsis* SOS2 protein kinase physically interacts with and is activated by the calcium-binding protein SOS3. *Proc. Natl. Acad. Sci. USA* **97**, 3735–3740.
20. Shi, H., Ishitani, M., Kim, C., and Zhu, J. K. (2000) The *Arabidopsis thaliana* salt tolerance gene *SOS1* encodes a putative Na^+/H^+ antiporter. *Proc. Natl. Acad. Sci. USA* **97**, 6896–6901.
21. Guo, Y., Halfter, U., Ishitani, M., and Zhu, J. K. (2001) Molecular characterization of functional domains in the protein kinase SOS2 that is required for plant salt tolerance. *Plant Cell* **13**, 1383–1400.
22. Gong, D., Gong, Z., Guo, Y., Chen, X., and Zhu, J.-K. (2002) Biochemical and functional characterization of PKS11, a novel *Arabidopsis* protein kinase. *J. Biol. Chem.* **277**, 28,340–28,350.
23. Gong, D., Zhang, C., Chen, X., Gong, Z., and Zhu, J.-K. (2002) Constitutive activation and transgenic evaluation of the function of an *Arabidopsis* PKS protein kinase. *J. Biol. Chem.* **277**, 42,088–42,096.

24. Liu, J. and Zhu, J.-K. (1998) A calcium sensor homolog required for plant salt tolerance. *Science* **280**, 1943–1945
25. Harper, J. W., Adami, G. R., Wei, N., Keyomarsi, K., and Elledge, S. J. (1993) The p21 Cdk-interacting protein Cip 1 is a potent inhibitor of G1 cyclin-dependent kinases. *Cel* **75**, 805–816.
26. Durfee, T., Becherer, K., Chen, P. L., et al. (1993) The retinoblastoma protein associates with the protein phosphatase type 1 catalytic subunit. *Genes Dev.* **7**, 555–569.
27. Ito, H., Fukada, Y., Murata, K., and Kimura, A (1983) Transformation of intact yeast cells treated with alkali cations. *J. Bacteriol.* **153**, 163–168.
28. Schiestl, R. H. and Gietz, R. D. (1989) High efficiency transformation of intact cells using single stranded nucleic acids as a carrier. *Curr. Genet.* **16**, 339–346.
29. Hill, J., Donald, K. A., and Griffiths, D. E. (1991) DMSO-enhanced whole cell yeast transformation. *Nucleic Acids Res.* **19**, 5791.
30. Gietz, D., St. Jean, A. Woods, R. A., and Schiestl, R. H. (1992) Improved method for high efficiency transformation of intact yeast cells. *Nucleic Acids Res.* **20**, 1425.
31. Kim, J., Harter, K., and Theologis, A. (1997) Protein–protein interactions among the Aux/IAA proteins. *Proc. Natl. Acad. Sci. USA.* **94**, 11,786–11,791.

Use of Yeast Genetic Tools to Define Biological Roles of Novel Protein Phosphatases

Joaquín Ariño, Antonio Casamayor, Amparo Ruiz, Ivan Muñoz, and Maribel Marquina

Summary

Regulatable gene expression is a powerful genetic tool for analyzing the function of a given gene product. The use of tetracycline-regulatable promoters in yeast represents a substantial improvement over previously described methods for gene regulation. Here we show how this approach can be used to analyze the biological role of serine/threonine phosphatase catalytic or putative regulatory subunits by constructing chromosomal or plasmid-borne conditional mutants. This is particularly useful given the large variety of important biological processes performed by these of enzymes, often necessities for cell survival, which makes in some cases infeasible the generation of null mutants.

Key Words: Gene expression; tetracycline-regulatable promoter; doxycycline; protein phosphatase; regulatory subunit; yeast

1. Introduction

The high level of evolutionary conservation for many Ser/Thr protein phosphatases combined with the remarkable accessibility to genetic and genomic experimental approaches of the budding yeast *Saccharomyces cerevisiae* makes this organism a very useful tool for phosphatase research. However, some of these enzymes perform essential functions, as it happens for the budding yeast type 1 protein phosphatase, encoded by a single gene (*GLC7*). In this case, the classical approach of constructing a deletion mutant to analyze gene function is not valid. In other cases, an excess of phosphatase function is detrimental for the cell. Therefore, uncontrolled overexpression based in the use of high-copy plasmids results in poor growth or other defects, making the assessment of cellular functions difficult. In addition to the use of classical

genetic approaches (i.e., isolation of temperature-sensitive mutants), these problems can be circumvented by means of regulatable gene expression systems. Expression vectors based on promoters such as those of *GAL1*, *MET3*, or *CUP1* have been traditionally used for these purposes (1). However, the use of these promoters involves changes in culture conditions (i.e., carbon source in the case of *GAL1*) that could result in undesired effects. On the contrary, the use of tetracycline derivatives for regulated gene expression offers a number of advantages, such as not being metabolized by the yeast cells and having none or little influence on cell growth, among others. Initially developed for use in mammalian cells, this system has been adapted to other organisms, including *S. cerevisiae*. Here we will focus on specific uses of this methodology, but the interested reader will find additional information in refs. 2–4.

In this work we will present two alternatives for doxycycline-regulatable expression: (1) insertion of the doxycycline-regulatable promoter at the chromosomal region of the native gene promoter and (2) expression of the gene from a plasmid bearing the doxycycline-regulatable promoter elements (see a schematic depiction of both strategies in Fig. 1). Ideally, the first alternative should be the choice, as it is straightforward enough and provides a very convenient experimental system. However, it has been described (and we have experienced) a number of cases in which successful integration could not be achieved using the replacement cassette described here, perhaps because of its relatively large size related to the usually short promoter sequences to be replaced. To solve this problem, an improved *tetO* replacement system was recently proposed, in which integration of the transactivator (tTA) element into the yeast genome allows the design of a shorter cassette (5). However, although in some cases this improved method has solved the problem, we have had examples in which effective regulation has not been achieved. Furthermore, its use is bound to the utilization of a specific strain, which might not be convenient for a given experiment. Therefore, expression from a plasmid should be considered as a suitable alternative. We present examples of the use of these techniques to generate tools to analyze the functions of essential genes encoding known or putative protein phosphatases regulatory subunits, such as *HAL3*, *VHS3*, *YKL088w*, and *YPII*. Hal3 is an inhibitory subunit of the serine/threonine (Ser/Thr) Ppz1 protein phosphatase (6), and deletion of *HAL3* is synthetically lethal with mutation of *SIT4*, a gene encoding a Ser/Thr protein phosphatase (7–9). Vhs3 is structurally related to Hal3 and also behaves as an inhibitory subunit of Ppz1. The *hal3 vhs3* double mutation is lethal, but this effect is not mediated by Ppz1 (10). *YKL088w* is an essential gene encoding a protein that is also related to Hal3 and Vhs3. Finally, *YPII* is an essential gene that acts as inhibitory subunit of

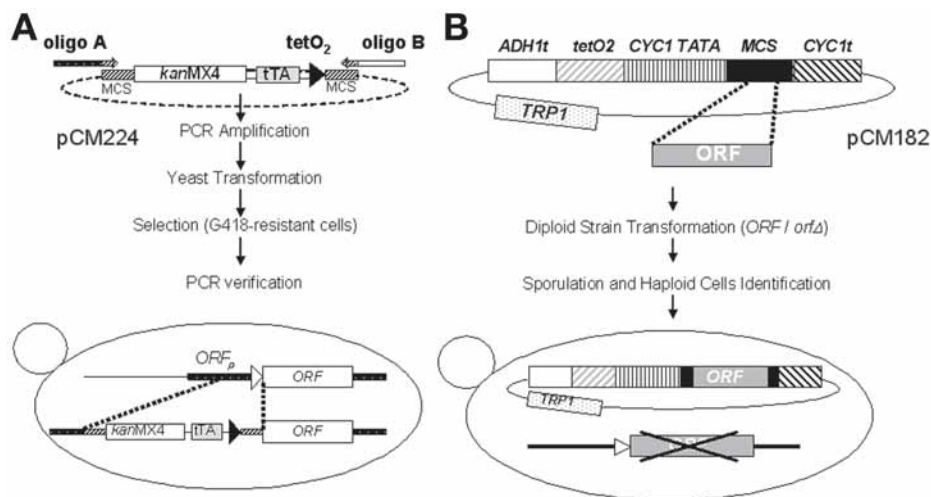


Fig 1. Different strategies for promoter substitution. **(A)** Native promoter replacement. Oligonucleotides A and B are used as primers for polymerase chain reaction (PCR) amplification of the substitution cassette, containing the multicloning site (MCS), the *KanMX4* selectable marker, the tetracycline-responsive tTA activator gene, and the *tetO* promoter. The 5' ends of each oligonucleotide (about 40 bp) are homologous to genomic sequences. The 5' end of oligonucleotide A corresponds to a region within the open reading frame (ORF) promoter. In oligonucleotide B, the 5' end usually corresponds to the beginning of the coding sequence. Plasmid pCM224 (14) containing two copies of the *tetO* box is used as the template. The PCR-amplified cassette (about 3.9 kbp) is gel-purified and used to transform yeast cells in order to replace a given region of the ORF native promoter by homologous recombination. Selection for G418-resistant cells and verification by PCR allow one to identify cells with the proper genomic integration. **(B)** Expression controlled from a plasmid. The ORF coding sequence is cloned into the MCS present in the pCM182 centromeric plasmid under the control of two copies of the *tetO* promoter and downstream of the *CYC1* TATA box (16). The resultant construct is used to transform diploid cells, heterozygous for the *ORF* disruption. After selection for the *TRP1* marker, cells are induced to sporulate. Haploid cells carrying the genomic *orfΔ* mutation and the plasmid are then selected. Genetic elements are not drawn to scale.

the yeast type 1 protein phosphatase Glc7 and regulates still unknown functions of this phosphatase (11).

2. Materials

Materials required for standard yeast manipulation techniques, growth media, and so forth can be found in refs. 12 and 13.

2.1. Obtaining a Doxycycline Regulatable Conditional Mutant by Chromosomal Promoter Replacement

1. Polymerase chain reaction (PCR) reagents: high-fidelity DNA polymerase, buffer, and oligonucleotides.
2. 0.5-mL PCR sterile tubes.
3. Microwave oven (optional).
4. G-418 (Calbiochem; #345810): Prepare 100X stock solution at 20 mg/mL in water, store at -20°C in small aliquots.
5. Freshly prepared G-418 (0.2 mg/mL) YPD agar plates.
6. Doxycycline (Sigma; D-9891): Prepare stock solution at 5 mg/mL in 50% ethanol (see **Note 1**).

2.2. Obtaining a Doxycycline-Regulatable Conditional Mutant Using the tetO-Promoter Present in Plasmid pCM182

1. Desired heterozygous diploid yeast strain.
2. Capped 10-mL sterile plastic tubes.
3. Capped 15-mL conical polystyrene sterile plastic tubes.
4. Reagents and materials for random spore analysis:
 - a. Zymoliasse solution (1 mg/mL). We use zymoliasse-20T (20,000 units/g) from *Arthrobacter luteus* supplied by MP Biomedicals (Aurora, Ohio). It should be freshly prepared prior use.
 - b. β -Mercaptoethanol.
 - c. 0.5-mm acid-washed glass beads (Sigma).
 - d. Hemocytometer counting chamber (Neubauer).
5. Appropriate yeast media plates.
6. Yeast mating tester strains.

Other materials are listed in **Subheading 2.1**.

3. Methods

3.1. Obtaining a Doxycycline-Regulatable Conditional Mutant by Chromosomal Promoter Replacement

1. Generate a insertion/substitution cassette using a PCR strategy with oligonucleotide A, oligonucleotide B, and plasmid pCM224 (**14**). These oligonucleotides should overlap at least 40 nt with the regions to which the cassette must recombine (**Fig. 1A**).
2. Gel-purify the PCR product and use it to transform a haploid yeast strain. Use at least 1 μg of DNA. After transformation, resuspend cells in fresh liquid YPD media (0.5 mL) and incubate cells for 3 h at 28°C . This step dramatically enhances transformation efficiency because it allows cells to become resistant to G-418 prior to plating.
3. Plate transformation on freshly prepared G-418 YPD agar plates (see **Note 2**).

4. Incubate at 28°C for 2–3 d.
5. Pick colonies and streak them onto freshly prepared G-418 YPD plates. Incubate plates for 48 h at 28°C. Good candidates should grow after this second round of selection.
6. Check proper integration by PCR using appropriate oligonucleotides (i.e., one hybridizing in the chromosome outside of the replacement cassette and the other inside the *kanMX4* region; see [Fig. 1A](#) and [ref. 15](#)). We normally analyze different clones using colony PCR. This procedure is easier and faster than obtaining genomic DNA from each clone, although not as reliable. For this purpose, pick a small amount of a single colony with a sterile tip and put it in the wall of a PCR Eppendorf tube (avoid contamination by agar medium). Heat it using a microwave oven (90 s at maximum power; keep the tube uncapped) and immediately store the tube at –20°C for at least 5 min. Add the reagents for the PCR reaction to this tube directly. Evaluate positives by running the PCR product on an agarose gel.
7. Check the phenotype of the conditional mutants by using different concentrations of doxycycline (see [Note 3](#)). Assay the growth rate (or any other suitable phenotype) of different clones using plates or liquid media. (See [Fig. 2](#) for examples.)

3.2. Obtaining a Doxycycline Regulatable Conditional Mutant Using the tetO-Promoter Present in Plasmid pCM182

1. Clone desired open reading frame (ORF) in plasmid pCM182 multicloning site (MCS) with appropriate restriction enzymes (see [Fig. 1B](#)). Other plasmids from the same family ([16](#)) can be used following the same procedure. The use of an epitope-tagged (Myc, FLAG, HA, etc.) ORF is extremely helpful to easily monitor the amount of gene product after doxycycline treatment.
2. Use the resulting construct to transform a diploid yeast strain heterozygous for the mutation of the gene to be studied and select transformants by plating in the appropriate synthetic medium (i.e., lacking Trp in the case of pCM182).
3. Inoculate colonies and grow to saturation in 5 mL of the appropriate synthetic medium for plasmid selection.
4. Collect the cells by centrifugation and wash them twice with water and at least once with sporulation medium. Resuspend the cells in 5 mL of the sporulation medium described in [ref. 12](#).
5. Incubate the culture at 28°C for 4–7 d in order to obtain a significant percentage (> 50%) of sporulating cells. The efficiency of sporulation (percentage of sporulated cells at a given time after incubation) depends substantially on the genetic background and on the specific media used to induce sporulation.
6. Isolate colonies arising from individual spores following the procedure used for random spore analysis (see [Note 4](#)). At the end of the procedure, cells are dispersed on synthetic medium plates, allowing selection for both the chromosomal mutation in the gene of interest and the presence of the plasmid (see [Note 5](#)).

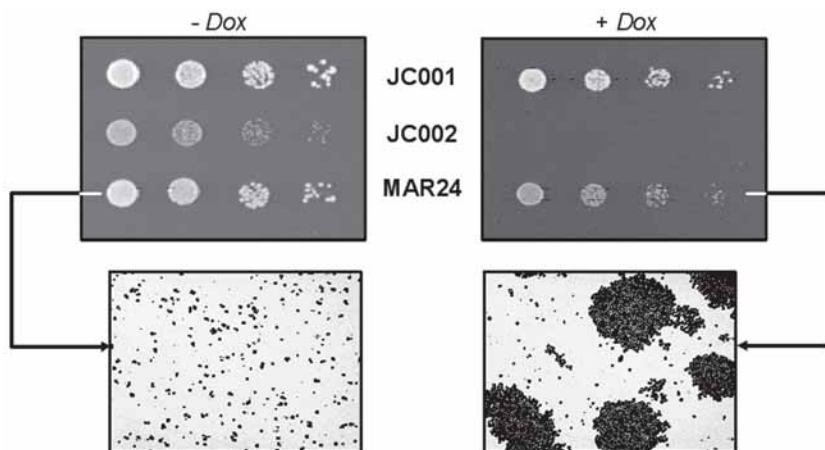


Fig 2. Example of use of a *tetO* promoter to study the effects of the lack of *HAL3* gene product in different mutant backgrounds. Blocking *tetO*-controlled *HAL3* expression by doxycycline (strain JC001) in an otherwise wild-type background does not reduce growth, but in liquid culture, it induces flocculation slightly (not shown). Repression of *HAL3* transcription by doxycycline in *tetO:HAL3 sit4Δ* cells (strain JC002) fully mimics the synthetic lethality of the *hal3Δ sit4Δ* double mutant (9). *tetO:HAL3 vhs3Δ* cells (strain MAR24) in the presence of doxycycline only show a weak growth defect in solid medium. However, they present a strong flocculation phenotype in liquid cultures. + Dox denotes the addition of 50 µg/mL doxycycline to the complete synthetic medium. Serial dilutions of the cultures are presented.

7. Identify and select haploid cells by mating-type determination, crossing them with the mating tester haploid strains (*MATa* or *MATα*) following protocols described in **ref. 17**. Use exponentially growing tester cells preferentially. Diploid cells are unable to mate.
8. Characterize in selected haploid cells the phenotypes attributable to repression of the gene under the control of the doxycycline-regulatable promoter. It is advisable to test different colonies for phenotypes and to evaluate a range of doxycycline concentrations (*see Note 3*).
9. If the ORF has been epitope tagged (or specific antibodies are available), it is desirable to monitor the amount of the protein expressed from the plasmid by immunoblot or related techniques (*see Fig. 3*).

4. Notes

1. Doxycycline stock solution must be stored at -20°C in a dark tube to protect it from light. Do not use a stock solution older than 2 mo.
2. G-418 plates should be freshly prepared, ideally the day before yeast transformation and always stored at 4°C . Discard plates stored for more than 1 wk.

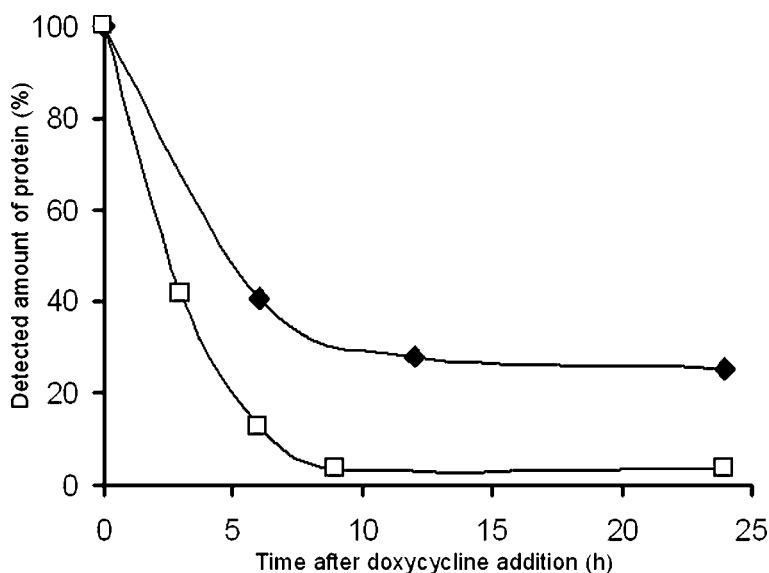


Fig 3. Regulating expression of two essential phosphatase-related genes by use of a plasmid-borne doxycycline-regulatable system. Haploid yeast cells deleted for the *YKL088w* (diamonds) or *YPII* (squares) ORFs were transformed with epitope-tagged versions of each gene expressed under the control of the *tetO* promoter in the pCM182 plasmid (see Fig. 1B). Cultures were treated with 50 $\mu\text{g}/\text{mL}$ doxycycline in synthetic medium lacking Trp and whole-cell extracts were prepared from culture samples taken at different time points. Forty micrograms of total protein were electrophoresed and the tagged proteins were detected by immunoblot using commercial antibodies. Note that the lowest level for each protein is achieved after 8–10 h of exposure to doxycycline.

3. Doxycycline plates should be freshly prepared and stored at 4°C. Discard plates older than 1 mo. We have successfully used doxycycline in the 20- to 100- $\mu\text{g}/\text{mL}$ range. Concentrations of 200 $\mu\text{g}/\text{mL}$ already affect growth of most wild-type cells.
4. We use the protocol described in ref. 12 with some modifications: Briefly, we spin down 1 mL of the sporulating culture and resuspend cells in 5 mL of sterile water. Ten units of Zymolias and 10 μL of β -mercaptoethanol are added and cells are incubated overnight (instead of 1 h with 500 units of β -glucuronidase). The suspension is centrifuged and the cells are resuspended in 0.2 mL of sterile water. From this point, the protocol described in ref. 17 is resumed.
5. In the case that mutation of the chromosomal copy of the gene has been made with the *KanMX4* module, first plate cells in G-418-containing YPD plates (G-418 selection works poorly on synthetic medium). Grow cells for 2–3 d and

replica plate them in appropriate dropout synthetic medium for plasmid-bearing marker selection. Using the described random spore analysis does not preclude obtaining some colonies arising from diploid cells. Because haploid cell colonies, after 2 d of growth, are usually slightly smaller than diploids, it is advisable to avoid the larger ones.

References

1. Stark, M. J. (1998) Yeast gene analysis, in *Methods in Microbiology* (Brown, A. J. P. and Tuite, M., eds.), Academic, San Diego. pp. 83–99.
2. Arino, J. and Herrero, E. (2003) Use of tetracycline-regulatable promoters for functional analysis of protein phosphatases in yeast. *Methods Enzymol.* **366**, 347–358.
3. Gossen, M., Bonin, A. L., and Bujard, H. (1993) Control of gene activity in higher eukaryotic cells by prokaryotic regulatory elements. *Trends Biochem.Sci.* **18**, 471–475.
4. Gossen, M., Freundlieb, S., Bender, G., Muller, G., Hillen, W., and Bujard, H. (1995) Transcriptional activation by tetracyclines in mammalian cells. *Science* **268**, 1766–1769.
5. Yen, K., Gitsham, P., Wishart, J., Oliver, S. G., and Zhang, N. (2003) An improved tetO promoter replacement system for regulating the expression of yeast genes. *Yeast* **20**, 1255–1262.
6. de Nadal, E., Clotet, J., Posas, F., Serrano, R., Gomez, N., and Arino, J. (1998) The yeast halotolerance determinant Hal3p is an inhibitory subunit of the Ppz1p Ser/Thr protein phosphatase. *Proc. Natl. Acad. Sci. USA* **95**, 7357–7362.
7. Ferrando, A., Kron, S. J., Rios, G., Fink, G. R., and Serrano, R. (1995) Regulation of cation transport in *Saccharomyces cerevisiae* by the salt tolerance gene HAL3. *Mol. Cell. Biol.* **15**, 5470–5481.
8. Di Como, C. J., Bose, R., and Arndt, K. T. (1995) Overexpression of SIS2, which contains an extremely acidic region, increases the expression of SWI4, CLN1 and CLN2 in sit4 mutants. *Genetics* **139**, 95–107.
9. Simon, E., Clotet, J., Calero, F., Ramos, J., and Arino, J. (2001) A screening for high copy suppressors of the sit4 hal3 synthetically lethal phenotype reveals a role for the yeast Nha1 antiporter in cell cycle regulation. *J. Biol. Chem.* **276**, 29,740–29,747.
10. Ruiz, A., Munoz, I., Serrano, R., Gonzalez, A., Simon, E., and Arino, J. (2004) Functional characterization of the *Saccharomyces cerevisiae* VHS3 gene: a regulatory subunit of the Ppz1 protein phosphatase with novel, phosphatase-unrelated functions. *J. Biol. Chem.* **279**, 34421–34430.
11. Garcia-Gimeno, M. A., Munoz, I., Arino, J., and Sanz, P. (2003) Molecular characterization of Ypi1, a novel *Saccharomyces cerevisiae* type 1 protein phosphatase inhibitor. *J. Biol. Chem.* **278**, 47,744–47,752.
12. Adams, A., Gottschling, D. E., Kaiser, C. A., and Stearns, T. (eds.) (1997) *Methods in Yeast Genetics*, Cold Spring Harbor Laboratory Press, Cold Spring Harbor, NY.

13. Sherman, F. (1991) Guide to yeast genetics and molecular biology. *Methods Enzymol.* **194**, 3–21.
14. Belli, G., Gari, E., Aldea, M., and Herrero, E. (1998) Functional analysis of yeast essential genes using a promoter-substitution cassette and the tetracycline-regulatable dual expression system. *Yeast* **14**, 1127–1138.
15. Wach, A., Brachat, A., Pohlmann, R., and Philippsen, P. (1994) New heterologous modules for classical or PCR-based gene disruptions in *Saccharomyces cerevisiae*. *Yeast* **10**, 1793–1808.
16. Gari, E., Piedrafita, L., Aldea, M., and Herrero, E. (1997) A set of vectors with a tetracycline-regulatable promoter system for modulated gene expression in *Saccharomyces cerevisiae*. *Yeast* **13**, 837–848.
17. Treco, D. A. and Winston, F. (1998) In *Current Protocols in Molecular Biology* (Ausubel, F. M., Brent, R., Kingston, R. E., et al., eds.), Wiley, New York, pp. 13.2.10–13.2.12.

Targeting of PP2C in Budding Yeast

Irene M. Ota and James Mapes

Summary

Type 2C Ser/Thr phosphatases or PP2Cs are monomeric metal-requiring protein phosphatases that are present in prokaryotes and eukaryotes. In the yeast *Saccharomyces cerevisiae*, there are seven PP2Cs called PTCs (phosphatase 2C). Molecular genetic studies have implicated PTCs in many different functions, including RNA splicing, the unfolded protein response, mitogen-activated protein kinase (MAPK) pathway, and cell-cycle regulation. We have shown that three PTCs (Ptc1, Ptc2, and Ptc3), regulate the stress-activated high-osmolarity glycerol (HOG) mitogen-activated protein kinase (MAPK) pathway. Proteomics studies have provided additional possible functions for these phosphatases by identifying interacting proteins. These studies have also provided the possible means by which these phosphatases are targeted to their substrates. For example, Nbp2–Ptc1 was identified as an interacting pair in yeast two-hybrid studies, and Nbp2 was found together with Ptc1 and HOG pathway kinases. We have shown that Nbp2 is an adapter in this pathway, mediating interaction between Ptc1 and the Pbs2 MAP/ERK kinase in the HOG pathway.

Key Words: PP2C; Ptc1; Nbp2; adapter; MAPK; MEK; budding yeast

1. Introduction

Phosphatase 2C (PTC) regulation of the high-osmolarity glycerol mitogen-activated protein kinase (HOG MAPK) pathway has been established using genetic and biochemical approaches in yeast (*1–3*). Three PTCs inactivate the HOG pathway by dephosphorylating the phospho-Thr (threonine) residue in the activation loop of the Hog1 MAPK (*see Fig. 1A*). How PP2Cs are targeted to MAPK pathways is not well understood. Proteomics provided a clue that Nbp2 might be a Ptc1-targeting protein. Two global yeast two-hybrid studies identified Nbp2–Ptc1 as an interacting pair (*4,5*), and a global protein complex isolation study identified Nbp2 with components of the HOG pathway

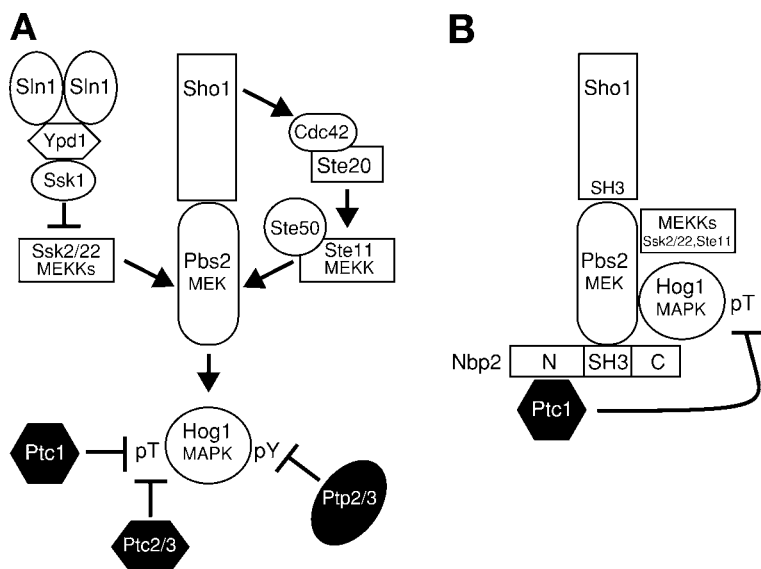


Fig. 1. Activation of the HOG MAPK pathway and its negative regulation by protein phosphatases. **(A)** The yeast stress-activated HOG MAPK pathway contains a three-kinase cascade that comprises the Ssk2, Ssk22, and Ste11 MEKKs, the Pbs2 MEK, and the Hog1 MAPK. The Sln1-Ypd1-Ssk1 branch negatively regulates the Ssk2/22 MEKKs, and Sho1 positively regulates the Ste11 MEKK. Two classes of phosphatases regulate Hog1, which requires phosphorylation of Thr and Tyr (tyrosine) in the sequence, TGY, for activation. Ptc1, Ptc2 and Ptc3, dephosphorylate phospho-Thr, and the protein tyrosine phosphatases (PTPs) Ptp2 and Ptp3 dephosphorylate phospho-Tyr. **(B)** Nbp2 negatively regulates the HOG pathway by recruiting Ptc1 to the Pbs2 scaffold, facilitating Hog1 inactivation.

including the Pbs2 MEK, the Ssk2 MEKK, and Ptc1 (6). We showed that Nbp2 is a Ptc1-targeting protein and functioned as an adapter between Ptc1 and Pbs2 (see Fig. 1B) (7). Because Pbs2 is also a scaffold protein that binds the MEKKs and Hog1 MAPK in this pathway (8), Ptc1 might inactivate multiple kinases in this pathway. Methods similar to those we have used in this study can be applied to identify other PTC adapters.

Phenotypic assays can be used to test whether a novel gene might regulate the HOG pathway. Such assays are particularly useful for identifying phosphatase adapters because they would not be expected to show sequence similarities to protein phosphatases. The basic premise is that if the PTC is a negative regulator of the pathway, its adapter will likely behave as such. The phenotypic assay used here relies on the observation that hyperactivation of the HOG pathway is lethal. The mutations most useful for testing potential

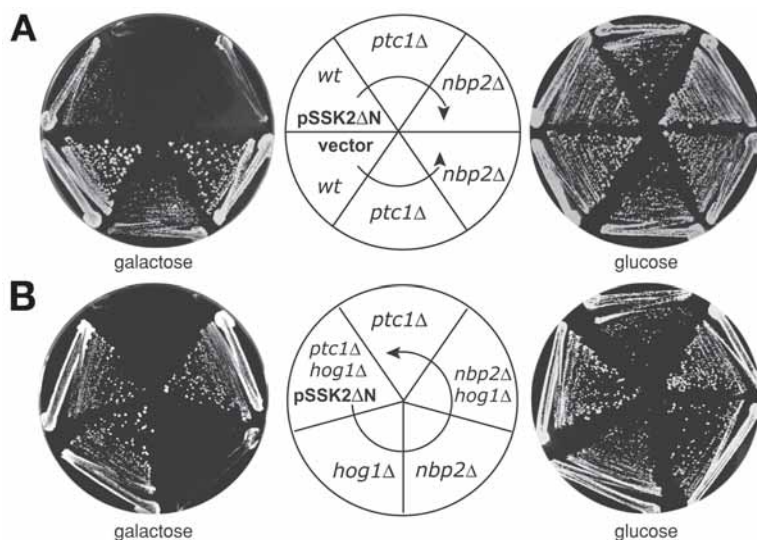


Fig. 2. Strains lacking *NBP2* exhibit growth defects due to *HOG1*. **(A)** Deletion of *NBP2* or *PTC1* is lethal when the hyperactive MEKK allele *SSK2ΔN* is expressed. Wild-type, *ptc1Δ*, and *nbp2Δ* strains in the JD52 background were transformed with pSSK2ΔN, a multicopy plasmid expressing *SSK2ΔN* under regulation of the *GAL1* promoter, or the empty vector pYES2. Strains were grown on selective medium containing galactose or glucose at 30°C for 3 d. **(B)** Lethality resulting from *SSK2ΔN* overexpression in the *nbp2Δ* and *ptc1Δ* strains is due to *HOG1*. The *ptc1Δ*, *nbp2Δ*, and *hog1Δ* single mutants and the *ptc1Δ hog1Δ* and *nbp2Δ hog1Δ* double mutants in the JD52 background were transformed with pSSK2ΔN and grown on selective medium containing galactose or glucose at 30°C for 3 d.

negative regulators are those that moderately activate the HOG pathway, such as the hyperactive MEKK allele *SSK2ΔN*. In combination with deletion of negative regulators such as *PTC1* and protein tyrosine phosphatases (PTPs) (see Fig. 1A) (2,7), overexpression of *SSK2ΔN* leads to greater activation of the HOG pathway and is lethal (see Fig. 2). Indeed, deletion of *NBP2* is lethal in this background.

If phenotypic assays support a role for a novel gene as a negative regulator, it is important to verify that it does so by having a biochemical effect on the pathway. Because we previously showed that Ptc1 affects the activity of the Hog1 MAPK (2), we examined Hog1 kinase activity isolated from osmotic-stressed yeast in the presence and absence of *NBP2*. Strains lacking *NBP2* behaved similarly to those lacking *PTC1* in that there is slightly increased basal Hog1 activity and a pronounced inability to inactivate Hog1 during adaptation (see Fig. 3) (2,7).

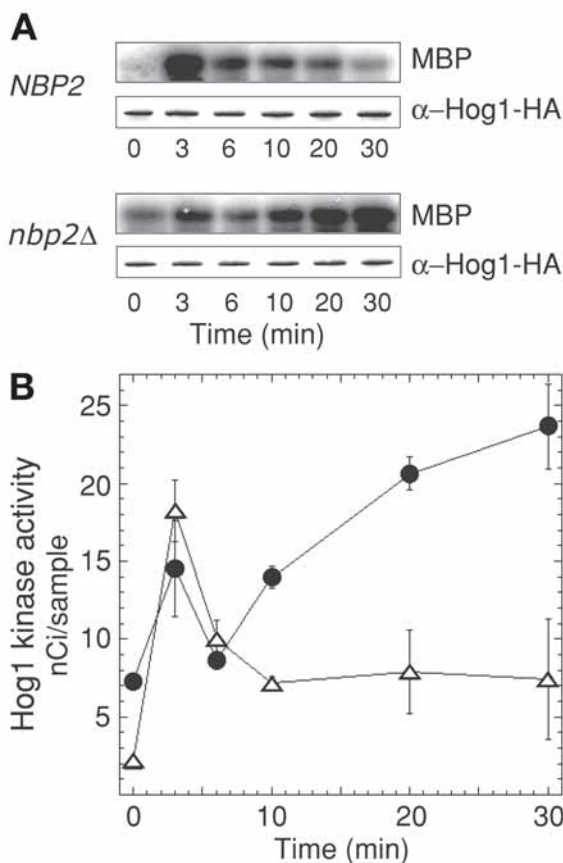


Fig. 3. Hog1 kinase activity is elevated in yeast lacking *NBP2*. Hog1 kinase activity was examined prior to and following stress in wild type and *nbp2 Δ* . **(A)** Hog1 kinase activity was examined in the *hog1 Δ* strain IMY100 and in the *nbp2 Δ hog1 Δ* strain JMY29, each carrying the Hog1-HA expression plasmid pHOG1-ha2. Before (time 0) and after exposure to osmotic stress (0.4 M NaCl) for various times, Hog1-HA was immunoprecipitated and incubated with MBP and [γ - 32 P]ATP. Radiolabel incorporated into MBP was examined by sodium dodecyl sulfate–polyacrylamide gel electrophoresis (SDS-PAGE) and visualized using the PhosphorImager. The amount of Hog1-HA expressed was the same in the two strains as indicated by the anti-HA blots. **(B)** Graph of Hog1 kinase assays performed as in **(A)**, for wild type (triangles) and *nbp2 Δ* (circles) from three independent experiments. The plot shows the mean \pm the standard deviation.

That Nbp2 might function as an adapter was suggested by its presence in a complex with Ptc1 and HOG pathway kinases (6). Pbs2 seemed a likely candidate for an Nbp2 interactor, as Nbp2 contains an SH3 domain, and Pbs2 binds Sho1, another SH3 domain-containing protein (see Fig. 1) (9). Ptc1 was also a

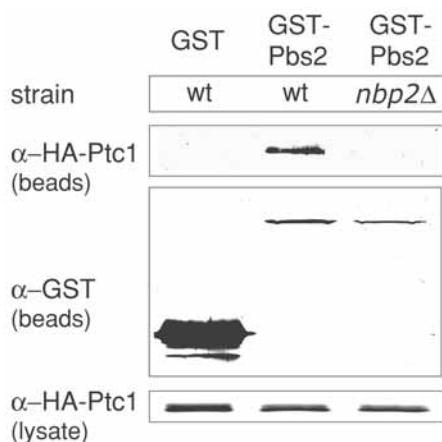


Fig. 4. Nbp2 mediates Pbs2–Ptc1 interaction. Binding of GST-Pbs2 or GST to HA-Ptc1 was examined in the wild type (JD52) and *nbp2Δ* (JHM17) strains. The strains carried pGST-PBS2, or the empty vector p(EG)KT expressing GST alone, and pHA-PTC1. GST-Pbs2 was isolated from yeast extracts using glutathione–Sepharose, and the coprecipitated material was examined by SDS-PAGE and immunoblotting with anti-GST and anti-HA antibodies.

possible candidate for an Nbp2 interactor because it bound specifically to Nbp2 (7); that is, Ptc2 and Ptc3 were unable to bind Nbp2. To demonstrate that Nbp2 is an adapter, mediating interaction between Ptc1 and Pbs2, coprecipitation assays were performed in yeast lysates and using purified proteins. As predicted for an adapter, Ptc1 bound Pbs2 only when Nbp2 was present in yeast lysates (see Fig. 4). The architecture of the phosphatase–adapter–kinase complex was revealed by identifying interacting domains. Using recombinant proteins, we showed that the Nbp2 N-terminal domain bound Ptc1 and the Nbp2 SH3 domain bound Pbs2 (see Fig. 5) (7).

2. Materials

2.1. Yeast Strains and Media

1. Yeast strains for the phenotypic and coprecipitation assays were produced in the galactose-inducible strain JD52 (*MATa trp1–Δ63 ura3–52 his3Δ200 leu2–3,112 lys2–801 GAL+*) because it allows overexpression of genes from the strong *GAL1/10* promoters when grown on galactose-containing media (7).
2. Yeast strains lacking the *NBP2*, *PTC1*, and *HOG1* genes in the JD52 background are JHM17 (*nbp2Δ*), IMY107 (*ptc1Δ*), and JHM34 (*nbp2Δ hog1Δ*) (7).
3. Hog1 kinase assays were performed in strains IMY100 (*hog1Δ*), JHM29 (*nbp2Δ hog1Δ*) and IMY103 (*ptc1Δ hog1Δ*), in the BBY45 background (7).

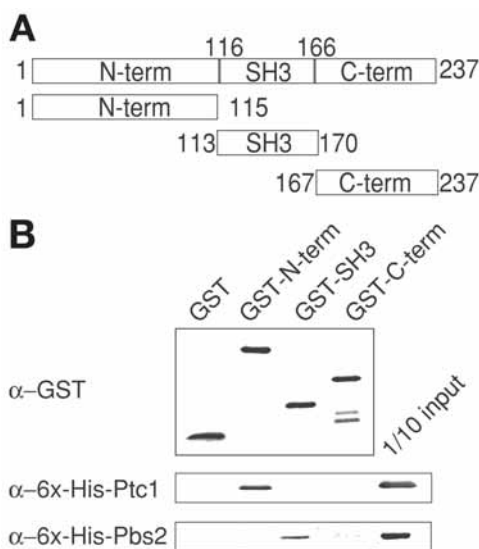


Fig. 5. Identification of Nbp2 domains required for association with Ptc1 and Pbs2. **(A)** Schematic representation of Nbp2 and its fragments used in the Pbs2- and Ptc1-binding experiments. Nbp2 is a 237-residue protein with a central SH3 domain corresponding to residues 113–170. The N-terminal and C-terminal domains are novel. **(B)** Recombinant Nbp2 N-terminal domain and Nbp2 SH3 domain bind Ptc1 and Pbs2, respectively. The ability of GST-Nbp2 N-terminal, GST-Nbp2-SH3, and GST-Nbp2 C-terminal domains, or GST alone to bind 6xHis-Ptc1 and 6xHis-Pbs2 was assessed. The bound material was examined using anti-GST and anti-6xHis antibodies. The rightmost lane shows one-tenth the amount of 6xHis-Ptc1 and 6xHis-Pbs2 that was incubated with the GST-Nbp2-fusion proteins.

4. Wild-type and mutant strains are cultured on rich media containing 2% glucose (YPD) or on synthetic media containing 2% glucose (SD) (10). Synthetic media lacking amino acids or uracil allows for the selection of cells bearing plasmids that carry nutritional markers. Galactose (2%) is used instead of glucose in synthetic media to induce overexpression from the *GAL1/10* promoters (SM+Gal).

2.2. Plasmids

1. pSSK2ΔN expresses the hyperactive MEKK allele *SSK2ΔN* from the *GAL1* promoter in the multicopy vector pYES2 bearing the selectable marker *URA3* (2).
2. pHOG1-ha2 expresses the Hog1 MAPK tagged with the hemagglutinin (ha) epitope from its endogenous promoter in the multicopy vector pRS423 (2μ *HIS3*) (2).
3. pGST-Pbs2 expresses GST-Pbs2 from the *GAL* promoter from the vector p(EG)KT (2μ *URA3*) (7).

4. pHA-Ptc1 expresses ha-tagged Ptc1 in yeast from the multicopy vector pRS423 (2 μ HIS3) (2).
5. GST-Nbp2 and its fragments are expressed in *Escherichia coli* from pGEX6P-1 (Amersham Biosciences) (7).
6. pRSETa-Ptc1 and pRSETa-Pbs2 express 6xHis-Ptc1 and 6xHis-Pbs2, respectively, in *E. coli* from pRSETa (Invitrogen) (2,7).

2.3. Yeast Transformation

1. Yeast is transformed by the method of Dohmen (11). Buffer A: 10 mM bicine, pH 8.35, 1 M sorbitol, 3% ethylene glycol.
2. Buffer B: 200 mM bicine, pH 8.35, 40% PEG 1000.
3. Buffer C: 10 mM bicine, pH 8.35, 150 mM NaCl.
4. Calf thymus DNA (Sigma).

2.4. Hog1 Kinase Assay

1. Lysis buffer: 50 mM Tris-HCl, pH 7.5, 50 mM NaCl, 5 mM EGTA, 5 mM MgCl₂, 0.1% Triton X-100, 1 mM dithiothreitol (DTT) containing protein phosphatase inhibitors (50 mM β -glycerophosphate and 1 mM sodium orthovanadate; Sigma), and protease inhibitor cocktail, which includes leupeptin, pepstatin A, antipain, aprotinin, and chymostatin, each at 20 μ g/mL (Sigma) and 1 mM phenyl methylsulfonyl fluoride (PMSF).
2. Glass beads (0.5 mm; Sigma).
3. Anti-HA antibody (HA.11; Covance).
4. Protein A-Sepharose (Repligen).
5. Wash buffer is the same as lysis buffer except that it contains 150 mM NaCl and no protease inhibitors.
6. Kinase assay buffer: 50 mM Tris-HCl, pH 7.5, 50 mM NaCl, 2 mM EGTA, 10 mM MgCl₂, 50 mM β -glycerophosphate, 0.1 mM sodium orthovanadate, 1 mM DTT.
7. Hog1 kinase substrates are myelin basic protein (Sigma) and [γ -³²P]ATP (10 mCi/mL; Amersham Biosciences).
8. 10X Laemmli sample buffer: 150 mM Tris-HCl, pH 6.8, 5% sodium dodecyl sulfate (SDS), 3% of 2-mercaptoethanol, 25% glycerol, 0.5% bromphenol blue.

2.5. Coprecipitation Assays in Yeast Extracts

1. Lysis buffer: 50 mM Tris-HCl, pH 7.5, 50 mM NaCl, 0.1% Triton X-100, 5 mM MgCl₂, 5 mM MnCl₂, 0.1% mercaptoethanol, and protease inhibitor cocktail as above.
2. Glutathione-Sepharose (Amersham Biosciences).

2.6. Purification of Yeast Proteins Expressed in *E. coli*

1. GST-fusion proteins and 6xHis-fusion proteins are expressed in the *E. coli* strain BL21(DE3)pLysS (Novagen).
2. 2X YT medium (Qbiogene).
3. Isopropyl- β -D-thiogalactoside (IPTG; Gold Biotechnology).

4. GST-protein lysis buffer: 20 mM Tris-HCl, pH 8.0, 100 mM NaCl, 0.05% Triton X-100, and 1 mM PMSF.
5. Nutator shaker (Clay Adams).
6. Glutathione elution buffer: *E. coli* lysis buffer, 20 mM glutathione (Sigma).
7. 6xHis-protein lysis buffer: 20 mM Tris-HCl, pH 8.0, and 100 mM NaCl.
8. Cobalt affinity resin (Talon, Clontech).
9. Cobalt affinity wash buffer: 20 mM Tris-HCl, pH 8.0, 100 mM NaCl, and 10 mM imidazole.
10. Binding buffer: 50 mM Tris-HCl, pH 7.5, 50 mM NaCl, and 0.05% Triton X-100.

2.7. Immunoblotting

1. Proteins are transferred from SDS-PAGE (polyacrylamide gel electrophoresis) to PVDF using the Genie Blotter (Idea Scientific).
2. Transfer buffer: 25 mM Tris base, 192 mM glycine, 20% methanol, 0.01% SDS.
3. Blocking buffer: 1% bovine serum albumin (BSA) (fraction V; Sigma) or 1% milk in TNST (15 mM Tris-HCl, pH 7.4, 0.84% NaCl, 0.1% Tween-20).
4. Primary antibodies are anti-HA (HA.11; Covance), anti-GST (Amersham Biosciences), and anti-His₆ (Covance).
5. Secondary antibodies are conjugated to alkaline phosphatase and include anti-mouse (Promega) and anti-goat (Sigma) antibodies.
6. BCIP/NBT (Promega).

3. Methods

In the phenotypic assay to test whether *NBP2* is a negative regulator, the hyperactive MEKK allele *SSK2ΔN* is used. Overexpression of *SSK2ΔN* from the *GAL1* promoter causes a growth defect when grown on media containing galactose and is lethal in the absence of negative regulators such as *PTC1* or *NBP2* (see Fig. 2). The severity of the growth defects as a result of this mutant allele might differ between yeast strain backgrounds, so it is important to compare the deletion of the candidate negative regulator gene in the same background as the controls.

Hog1 kinase assays were performed to test whether Nbp2 mediates Ptc1 inactivation of Hog1. Like other MAPKs, full Hog1 kinase activity requires phosphorylation of a Thr and a Tyr residue in the activation loop (2,12). Phosphorylation of the Thr residue alone confers partial activity, whereas phosphorylation of the Tyr residue alone has no activity (13). We could not identify an antibody that specifically detects Hog1-phospho-Thr, so Hog1 kinase assays were performed.

Coprecipitation assays among Nbp2, Ptc1, and Pbs2 were performed in yeast lysates and in vitro using recombinant proteins. One critical test was a coprecipitation assay performed in yeast, which showed that Nbp2 is necessary for Ptc1 to bind Pbs2 (see Fig. 4). Further studies in yeast and those using

purified recombinant proteins showed that different Nbp2 domains bind Ptc1 and Pbs2 (see Fig. 5). The use of recombinant proteins was necessary to establish that Nbp2 binds Ptc1 and the Pbs2 MEK in the absence of other yeast proteins.

3.1. Phenotypic Assay to Test Whether a Novel Gene Is a Negative Regulator of the HOG MAPK Pathway

1. Test whether overexpression of *SSK2ΔN*, a hyperactive MEKK allele in the HOG pathway, is lethal when a candidate negative regulator such as *NBP2* is deleted. Compare *nbp2Δ* (JHM17) to *ptc1Δ* (IMY107), which is known to be lethal when *SSK2ΔN* is overexpressed. Include the wild type (JD52), which shows a modest growth defect when *SSK2ΔN* is overexpressed. See Fig. 2 for an example.
2. Transform each deletion strain and the wild type with the pSSK2ΔN plasmid and select the desired strains on synthetic media lacking uracil and containing glucose (SD-Ura). The parent vector, pYES2, which does not contain *SSK2ΔN*, can be used as a negative control.
3. To transform cells, prepare competent cells by growing cultures to exponential phase, optical density (OD₆₀₀) from 0.6 to 1.2, and harvesting 10 mL by centrifugation.
4. Wash the cells by resuspending in 5 mL of buffer A and centrifuging. Resuspend cells in 200 μL of buffer A containing 11 μL of dimethyl sulfoxide (DMSO) and freeze at -80°C (see Note 1).
5. Add 1–5 μL (0.1 μg or less) of plasmid DNA to the frozen cells and thaw. If highly purified DNA is used, it is necessary to add carrier DNA, such as 5 μL of calf thymus DNA. Add approx 1 mL of buffer B, mix by inverting, and incubate for 1 h at 30°C.
6. Isolate the cells by centrifuging at low speed, 1050g in an Eppendorf centrifuge, and wash the cell pellet in buffer C.
7. Resuspend the cells in approx 100–200 μL of buffer C, plate onto selective media, and incubate at 30°C for 3–4 d. Streak colonies onto a fresh plate of SD-Ura to purify the strains.
8. Compare the growth of the *nbp2Δ*, *ptc1Δ*, and wild type strains, each bearing pSSK2ΔN when *SSK2ΔN* is overexpressed. To overexpress *SSK2ΔN*, grow the strains on solid synthetic media containing 2% galactose and lacking uracil (SM + Gal-Ura). Streak single colonies onto SM + Gal-Ura and grow at 30°C. Prepare a parallel SD-Ura plate, which contains 2% glucose but no galactose as a control, where all strains should grow well because *SSK2ΔN* is not overexpressed. Strains bearing the negative control empty vector pYES2 can be compared on the same plates. (See Fig. 2.)
9. The extent of growth on solid media will show whether the novel gene is a potential regulator of the HOG pathway. For example, the *nbp2Δ* and *ptc1Δ* strains expressing pSSK2ΔN cannot form single colonies on SM + Gal-Ura, whereas the wild type produces colonies (see Fig. 2). Alternative methods to examine growth differences are described in Note 2.

10. If deletion of the candidate negative regulator is lethal when *SSK2ΔN* is overexpressed, further evidence for regulation of the HOG pathway can be gained by asking whether deletion of genes encoding HOG pathway kinases restores growth. For example, we compared *nbp2Δ hog1Δ* (JHM29) overexpressing *SSK2ΔN* to the strains above. The *nbp2Δ hog1Δ* strain grew significantly better than the *nbp2Δ* strain, suggesting that the growth defect in the *nbp2Δ* strain overexpressing *SSK2ΔN* is the result of Hog1 hyperactivation (see Fig. 2).

3.2. Biochemical Assay to Test Whether a Novel Gene Is a Regulator of the HOG Pathway

1. Perform Hog1 kinase assays to test candidate regulators of the HOG pathway. Compare Hog1 kinase activity in an *nbp2Δ hog1Δ* (JHM29), *ptc1Δ hog1Δ* (IMY103), and *hog1Δ* (IMY100) strain, each carrying the pHOG-ha2 plasmid expressing hemagglutinin epitope-tagged Hog1.
2. Transform the yeast strains with pHOG1-ha2 and select on SD-His.
3. Grow each yeast strain in liquid SD-His media to exponential phase at 30°C (OD₆₀₀ approx 0.6–1.0). Harvest cells from 10 mL of culture for the 0 min time-point.
4. Induce Hog1 kinase activity by exposing the cultures to 0.4 M NaCl by adding the appropriate volume of 5 M NaCl. Continue growing at 30°C.
5. Harvest the cells at various times, generally 2.5, 5, 10, 20, and 30 min following osmotic stress by centrifuging 10.9 mL of culture, taking into account the increased volume as a result of the added 5 M NaCl.
6. Break open the cells in lysis buffer using glass beads. Typically, the cells are lysed in 200 μL of lysis buffer with approx 80 μL of glass beads. Vortex cells approx 15 s and then cool on ice for 15 s. Repeat four to six times.
7. Centrifuge the mixture at 14,550g in an Eppendorf microfuge at 4°C and collect the supernatant.
8. Immunoprecipitate Hog1-ha from lysates using 2.5 μL of anti-HA antibody and 12.5 μL of protein A–Sepharose and incubate at 4°C for 1 h.
9. Wash immunoprecipitated Hog1-ha by resuspending in 600 μL of cold wash buffer and centrifuging. Repeat two more times.
10. Assay Hog1-ha kinase activity by resuspending the resin in 10 μL of 2X kinase assay buffer and incubating with 5 μL of 2 mg/mL myelin basic protein (MBP) and 5 μL of 0.8 mM [γ -³²P]ATP (8000 cpm/pmol) for 30 min at 30°C. Terminate the reactions by adding 3 μL of 10X Laemmli sample buffer and boiling for 3 min.
11. Examine ³²P incorporation into MBP by SDS-PAGE and quantify by Phosphor-Imager analysis (Molecular Dynamics).

3.3. Test for Adapter Function by Performing Coprecipitation Assays in Yeast Lysates

1. Produce yeast strains expressing the two proteins whose interaction is predicted to be mediated by an adapter protein. One yeast strain is the wild type and the second is the mutant lacking the adapter. In this case, glutathione-S-transferase

fused to Pbs2 (GST-Pbs2) and the hemagglutinin epitope fused to Ptc1 (HA-Ptc1) were coexpressed in JD52 (wild type) and JHM17 (*nbp2Δ*). The empty vector, pEG(KT), can also be transformed as a negative control. Transform the two plasmids into each yeast strain simultaneously and select the cotransformants on SD-Ura-His solid media.

2. Grow cultures to exponential phase in SD-Ura-His liquid media. Harvest the cells from 150 mL of culture at approx 1 OD at 600 nm by centrifuging at full speed in a clinical centrifuge for 10 min at room temperature.
3. Disrupt the cells using glass beads and 600 μ L of cold lysis buffer and centrifuge at 14,550g in an Eppendorf centrifuge at 4°C to obtain the supernatant.
4. Prepare the glutathione–Sepharose resin for incubation with lysates. Wash 100 μ L of resin with 1 mL of cold phosphate-buffered saline (PBS) by mixing gently and centrifuging at low speed (1055g in an Eppendorf centrifuge). Remove the supernatant and add 100 μ L of lysis buffer to produce a 1 : 1 slurry.
5. Incubate the lysates with 60 μ L of slurry (30 μ L of glutathione–Sepharose resin) for 1 h at 4°C.
6. Wash the resin by resuspending in 800 μ L of cold lysis buffer and collecting the resin by centrifuging at low speed at 4°C. Repeat two to three times using buffers of increasing stringency; the concentration of NaCl can be raised twofold to sevenfold.
7. Boil the resin in 30 μ L of 4X Laemmli sample buffer and examine the coprecipitated proteins by SDS-PAGE and immunoblotting.
8. Transfer proteins from the gel to PVDF using the Genie blotting system. Prepare the PVDF membrane by wetting in methanol approx 10 s and rinsing in water for 3 min. Equilibrate the membrane in transfer buffer for 3 min.
9. Place the PVDF membrane on the gel, being careful to exclude bubbles, and sandwich between two pieces of filter paper wetted in transfer buffer.
10. In the blotting cassette, place the electrode (cathode), plastic mesh, and two layers of sponges and cover with cold transfer buffer. Place the gel–PVDF wrapped in filter paper on top of the sponges, being careful to avoid bubbles. The PVDF membrane should be on top of the gel so that proteins transfer to the membrane. Cover with additional sponges prewetted in transfer buffer, fill with transfer buffer, and then place the second plastic mesh, second electrode (anode), and plastic cover into the cassette. The cassette is then placed in the holder and the assembly is submerged in ice. Connect the electrodes to the power supply and blot for 30 min at 24 V.
11. Remove the blot and incubate in blocking buffer for 30 min at room temperature on a rocking platform.
12. The blot is then cut to separate the GST-Pbs2 band from the HA-Ptc1 band.
13. Dilute the anti-GST and anti-HA antibodies 1 : 1000 in TNST and incubate the blots in the appropriate antibodies for 30 min at room temperature on the rocker.
14. Wash the blots for 5 min with TNST at least three times.
15. Incubate the anti-GST blot with anti-goat secondary antibody at a 1 : 5000 dilution in TNST and the anti-HA blot in anti-mouse secondary antibody at a 1 : 7500 dilution in TNST for 30 min at room temperature on the rocker.

16. Wash the blots three times with TNST.
17. Visualize the blots with BCIP/NBT. See [Fig. 4](#) for an example: GST-Pbs2 coprecipitates with 6xHisPtc1 in the wild-type strain but not in the *nbp2Δ* strain.

3.4 Coprecipitation Assay Using Purified Recombinant Nbp2, Pbs2, and Ptc1

1. Produce GST and 6xHis-fusion proteins in *E. coli*. GST-Nbp2 and -Nbp2 fragments are expressed from pGEX-6P-1 plasmids, and 6xHisPtc1 and 6xHisPbs2 are expressed from pRSETa in *E. coli* BL21(DE3) pLysS.
2. Grow the strains in 500 mL of 2X YT medium at 37°C to log phase ($OD_{600} \approx 0.6\text{--}1.0$), cool to 23°C, and induce with 0.3–0.5 mM IPTG at 23°C for 2 h.
3. The cells expressing GST-Nbp2-fusion proteins are lysed by sonication in 10 mL of cold GST-protein lysis buffer. Cells are sonicated for 30 s at the 7.75 setting on the Misonix sonicator and then cooled on ice for 3 min. Repeat two to three times.
4. Centrifuge the lysates at 10,000g for 15 min at 4°C and remove the supernatant.
5. The supernatants are incubated with 0.75 mL of packed glutathione–Sephadex resin for 1 h at 4°C on a Nutator shaker. Centrifuge the mixture at low speed (setting 3 on a clinical centrifuge) for 2 min and remove the supernatant.
6. Wash the resin by adding 20 mL of cold lysis buffer, mixing on the Nutator for 10 min, and centrifuging at low speed.
7. Remove the supernatant and pack the resin into a 5-mL column and elute the GST-fusion proteins with the same buffer containing 20 mM glutathione and collect 0.5 mL fractions (see **Note 3**). Fractions containing GST-fusion proteins are identified by SDS-PAGE, pooled, and dialyzed against PBS, and the protein is quantified using the Bradford assay.
8. To purify 6xHis-Ptc1 and 6xHis-Pbs2, cells are lysed by sonicating in 25 mL of 6xHis-protein lysis buffer.
9. The clarified lysate is mixed with 1.25 mL of Co^{2+} -immobilized metal-affinity resin for 1 h at 4°C on the Nutator.
10. The mixture is centrifuged at low speed and the supernatant is removed.
11. The resin is washed with 15 mL of cold cobalt-affinity wash buffer. The resin is packed into a 5-mL column and 6xHis-Ptc1 and 6xHis-Pbs2 are eluted at room temperature with the same buffer containing 75 mM imidazole. Collect 0.5-mL fractions and identify those fractions containing the 6xHis proteins by SDS-PAGE (see **Note 4**).
12. Binding between GST-tagged Nbp2 fragments or GST and 6xHis-Ptc1 or 6xHis-Pbs2 is examined as follows. One microliter of 100 μ M GST-tagged protein is mixed with 5 μ L of 10 μ M of 6xHis-Ptc1 or 5 μ L of 10 μ M 6xHis-Pbs2 for 1 h at 4°C with 50 μ L of glutathione–Sephadex resin in 100 μ L of binding buffer.
13. Wash the resin two to three times with 5 bed volumes of binding buffer and then two to three times with 5 bed volumes of buffer containing 150 mM NaCl.
14. The bound material is examined by SDS-PAGE and immunoblotting with anti-GST and anti-His₆ antibodies as described above.

4. Notes

1. Freezing the yeast competent cells by placing them in a -80°C freezer is preferred to freezing them in dry ice/acetone, which reduces competency in our hands.
2. Two additional methods to examine growth differences might be more sensitive. In one method, serial dilutions of each strain are made and the diluted cultures are spotted onto SD-Ura and SM+Gal-Ura media. Spots from the most dilute cultures of HOG hyperactivated mutant strains will show no growth, whereas the wild type grows. In another method, the doubling time of strains can be compared when they are grown in liquid media. Growth can be monitored by recording optical density at 600 nm. A more rigorous method is to determine the number of live cells by plating them onto YPD and counting the number of colonies that form.
3. It might be necessary to adjust the pH if 20 mM glutathione is added to the elution buffer instead of the typically recommended concentration of 10 mM glutathione. It is critical that the elution buffer be near pH 8 to be effective.
4. Expression of GST- and 6xHis-tagged proteins from pGEX6P-1 and pRSETa has been sufficiently strong that we have been able to identify the prominent bands as the desired proteins by SDS-PAGE and Coomassie staining. To confirm that the bands are the tagged proteins, or if expression of the tagged protein is low, immunoblotting should be performed.

Acknowledgment

This work was funded by a grant from the American Cancer Society.

References

1. Maeda, T., Tsai, A.Y., and Saito, H. (1993) Mutations in a protein tyrosine phosphatase gene (*PTP2*) and a protein serine/threonine phosphatase gene (*PTC1*) cause a synthetic growth defect in *Saccharomyces cerevisiae*. *Mol. Cell. Biol.* **13**, 5408–5417.
2. Warmka, J., Hanneman, J., Lee, J., Amin, D., and Ota, I. (2001) Ptc1, a type 2C Ser/Thr phosphatase, inactivates the HOG pathway by dephosphorylating the mitogen-activated protein kinase Hog1. *Mol. Cell. Biol.* **21**, 51–60.
3. Young, C., Mapes, J., Hanneman, J., Al-Zarban, S., and Ota, I. (2002) Role of Ptc2 type 2C Ser/Thr phosphatase in yeast high-osmolarity glycerol pathway inactivation. *Euk. Cell* **1**, 1032–1040.
4. Ito, T., Tashiro, K., Muta, S., et al. (2000) Toward a protein-protein interaction map of the budding yeast: A comprehensive system to examine two-hybrid interactions in all possible combinations between yeast proteins. *Proc. Natl. Acad. Sci. USA* **97**, 1143–1147.
5. Uetz, P., Giot, L., Cagney, G., et al. (2000) A comprehensive analysis of protein-protein interactions in *Saccharomyces cerevisiae*. *Nature* **403**, 623–627.
6. Ho, Y., Gruhler, A., Hellbut, A., et al. (2002) Systematic identification of protein complexes in *Saccharomyces cerevisiae* by mass spectrometry. *Nature* **415**, 180–183.

7. Mapes, J. and Ota, I. (2004) Nbp2 targets the Ptc1 type 2C Ser/Thr phosphatase to the HOG MAPK pathway. *EMBO J.* **23**, 302–311.
8. Posas, F. and Saito, H. (1997) Osmotic activation of the HOG MAPK pathway via Ste11p MAPKKK: scaffold role of Pbs2p MAPKK. *Science* **276**, 1702–1705.
9. Maeda, T., Takekawa, M., and Saito, H. (1995) Activation of yeast PBS2 MAPKK by MAPKKKs or by binding of an SH3-containing osmosensor. *Science* **269**, 554–558.
10. Sherman, F., Fink, G. R., and Hicks, J. B. (1986) *Methods in Yeast Genetics*. Cold Spring Harbor Laboratory, Cold Spring Harbor, NY, pp. 177–186.
11. Dohmen, R. J. (1991) An efficient transformation procedure enabling long-term storage of competent cells of various yeast genera. *Yeast* **7**, 691–692.
12. Schuller, C., Brewster, J. L., Alexander, M. R., Gustin, M. C., and Ruis, H. (1994) The HOG pathway controls osmotic regulation of transcription via the stress response element (STRE) of the *Saccharomyces cerevisiae* *CTT1* gene. *EMBO J.* **13**, 4382–4389.
13. Bell, M. and Engelberg, D. (2003) Phosphorylation of Tyr-176 of the yeast MAPK Hog1/p38 is not vital for Hog1 biological activity. *J. Biol. Chem.* **278**, 14,603–14,606.

Phosphatase Targets in TOR Signaling

Estela Jacinto

Summary

Cells undergo growth or increase in mass in the presence of nutrients. A key signaling molecule that responds to the presence of nutrients is the target of rapamycin (TOR). TOR is a highly conserved protein kinase and is the target of the growth inhibitor rapamycin. In response to nutrients, TOR promotes the phosphorylation of its downstream targets, leading to increased protein synthesis and decreased protein turnover. In yeast, a major mechanism for the downstream regulation of TOR effectors is by inhibition of the type 2A-related phosphatase SIT4. TOR negatively regulates SIT4 by promoting the association of SIT4 with TAP42. When TOR is inactivated by rapamycin treatment or nitrogen starvation, downstream effectors of TOR such as the serine/threonine protein kinase NPR1 and the TAP42 interacting protein TIP41 are dephosphorylated in a SIT4-dependent manner. The phosphorylation state of NPR1 and TIP41 provides a convenient readout in yeast to assay for TOR and SIT4 activities under growth-promoting or growth-inhibitory conditions.

Key Words: Growth; TOR; rapamycin; SIT4; NPR1; TIP41; dephosphorylation; nitrogen starvation; SDS-PAGE; isoelectric focusing; two-dimensional gel electrophoresis

1. Introduction

In yeast and mammals, the target of rapamycin (TOR) controls cell growth in response to the presence of nutrients ([1](#)). In the budding yeast *Saccharomyces cerevisiae*, TOR is active in the presence of a good nitrogen source such as ammonium or glutamine. Under this condition, TOR negatively regulates the phosphatase SIT4 by promoting the binding of TAP42 to SIT4 ([2](#)). TOR promotes the TAP42/SIT4 association by regulation of the TAP42-interacting protein TIP41 ([3](#)). Upon nitrogen starvation or treatment with the growth-inhibitory drug rapamycin, TOR becomes inactive while TIP41

becomes dephosphorylated, binds, and inhibits TAP42. Consequently, SIT4 dephosphorylates and activates a number of target proteins involved in scavenging secondary nitrogen sources, such as the serine/threonine (Ser/Thr) kinase NPR1 and the transcription factor GLN3 (3,4). TIP41 binding to TAP42 and the dephosphorylation of TIP41 are also SIT4 dependent, suggesting that SIT4 targets TIP41 as part of a feedback loop (3). Such a feedback loop enhances the association of TAP42 with TIP41, to subsequently amplify SIT4 activity that could account for the rapid dephosphorylation of NPR1 under TOR-inactivating conditions.

Whether TOR directly phosphorylates NPR1, GLN3, and TIP41 remains to be demonstrated. It has been shown in mammals, however, that mammalian TOR (mTOR) can directly phosphorylate the translation regulators 4EBP and S6K (5–7). Like NPR1 and GLN3, 4EBP and S6K are phosphorylated at multiple sites and become rapidly dephosphorylated when mTOR is inactivated by rapamycin treatment or nutrient starvation (8–11). Hence, similar to yeast TOR regulation of NPR1 and GLN3, mTOR can also regulate 4EBP and S6K by inhibition of phosphatases (12).

2. Materials

2.1. Yeast Culture and Lysis

1. YPD (rich medium) (QBiogene, Irvine, CA).
2. SD (synthetic minimal media) (QBiogene, Irvine, CA).
3. Amino acid mixture (QBiogene, Irvine, CA).
4. Yeast nitrogen base (YNB; without ammonium sulfate and without amino acids): 10 mM ammonium sulfate, 1 mg/mL proline, together with 2% glucose, 40 µg/mL tryptophan, 20 µg/mL histidine, and 20 µg/mL uracil. These three amino acids are required to satisfy the auxotrophies of our strains and cannot be used as a nitrogen source.
5. Rapamycin (1 mg/mL stock) dissolved in drug vehicle (90% ethanol and 10% Tween-20).
6. Phosphate-buffered saline (PBS) 10X stock: 1.37 M NaCl, 27 mM KCl, 100 mM Na₂HPO₄, 18 mM KH₂PO₄ (adjust to pH 7.4 with HCl if necessary). To prepare 1X PBS, mix nine parts water with one part 10X PBS.
7. Lysis buffer 1 : 1X PBS + 1% NP-40 supplemented with protease inhibitors (2 µg/mL each of aprotinin, leupeptin, pepstatin A, 1 mM phenylmethylsulfonyl fluoride [PMSF]) and phosphatase inhibitors (10 mM each of NaF, NaN₃, pNPP, NaPPi, and β-glycerophosphate).
8. Lysis buffer 2 or TNE lysis buffer: 0.1M Tris-HCl, pH 8, 1% NP-40, 1mM EDTA supplemented with protease and phosphatase inhibitors, 0.1 µg/mL RNase A.
9. Glass beads (Biospec Products, Bartlesville, OK), bead beater (FastPrep; Savant Instruments, Qbiogene, Irvine, CA).
10. Protein Assay Kit (Bio-Rad, Hercules, CA).

2.2. One-Dimensional SDS-PAGE

1. 4X sodium dodecyl sulfate (SDS) loading dye: 200 mM Tris-HCl, pH 6.8, 400 mM dithiothreitol (DTT), 8% SDS, 0.4% bromophenol blue, 40% glycerol. Store at 4°C.
2. Precision Plus Protein Standards (Bio-Rad, Hercules, CA).
3. Mini-PROTEAN3 Electrophoresis Module (10-well casting module) (Bio-Rad, Hercules, CA).
4. Separating buffer (4X): 1.5 M Tris-HCl, pH 8.7, 0.4% SDS. Store at room temperature.
5. Stacking buffer (4X): 0.5 M Tris-HCl, pH 6.8, 0.4% SDS. Store at room temperature.
6. 30% Acrylamide/0.8% bisacrylamide solution (Amresco, Solon, OH).
7. N,N,N,N'-Tetramethylethylenediamine (TEMED; Bio-Rad, Hercules, CA).
7. Ammonium persulfate: Prepare 10% solution in water. Store at 4°C and use within 2 wk.
8. 7.5% Separating gel: 3.75 mL of 30% acrylamide/0.8% bisacrylamide solution, 3.75 mL 4X separating buffer, 7.5 mL water, 50 µL of 10% ammonium persulfate, 10 µL TEMED.
9. 20% Propanol.
10. Stacking gel: 650 µL 30% acrylamide/0.8% bisacrylamide, 1.25 mL 4X stacking buffer, 3.05 mL water, 100 µL 10% ammonium persulfate, 5 µL TEMED.
11. Running buffer (5X): 125 mM Tris-HCl, 960 mM glycine, 0.5% (w/v) SDS. Store at room temperature. Prepare 1X by mixing four parts water and one part 5X running buffer.

2.3. Immunoprecipitation and Dephosphorylation

1. Anti-HA antibody (Berkeley Antibody Co., Richmond, CA).
2. Protein G–Sepharose (Amersham Biosciences, Uppsala, Sweden).
3. Alkaline phosphatase (New England Biolabs, Beverly, MA).
4. CIP buffer: 50 mM Tris-HCl, pH 8.5, 5 mM MgCl₂.

2.4. Isoelectric Focusing

1. Buffer B: 21.4% CHAPS, 107 mM DTT, and 21.4 mL IEF buffer NL3–10 (Amersham Biosciences, Uppsala, Sweden).
2. Bromophenol blue.
3. IPG chamber (Amersham Biosciences, Uppsala, Sweden).
4. Immobiline DryStrip pH 3–10 NL 18 cm (Amersham Biosciences, Uppsala, Sweden).
5. Immobiline DryStrip Cover Fluid (Amersham Biosciences, Uppsala, Sweden).
6. IPGPhor apparatus (Amersham Biosciences, Uppsala, Sweden).

2.5. Second-Dimension SDS-PAGE

1. Hoefer vertical electrophoresis unit, 18 × 16-cm plates (Hoefer Inc., San Francisco, CA)

2. 10% Separating gel: 5 mL of 30% acrylamide/0.8% bisacrylamide (*see Subheading 2.2.*), 3.75 mL of 4X separating buffer (*see Subheading 2.2.*), 6.25 mL water, 50 μ L ammonium persulfate, 10 μ L TEMED.
3. SDS equilibration buffer: 50 mM Tris-HCl, pH 6.8, 6 M urea, 30% glycerol, 2% SDS, pinch of Coomassie blue.
4. Equilibration tray for 18-cm strips (Bio-Rad, Hercules, CA)
5. Running buffer: 25 mM Tris, 192 mM glycine, 0.1% SDS.
6. Agarose sealing solution: 0.5g agarose, 100 mL running buffer, pinch of Coomassie blue.

2.6. Western Blotting

1. Mini Trans-blot and Trans-blot cells (Bio-Rad, Hercules, CA).
2. Transfer buffer: 39 mM glycine, 48 mM Tris base, 0.037% (w/v) SDS, 20% methanol.
3. 3 MM paper (Whatman, Florham Park, NJ).
4. Immobilon-P (Millipore, Bedford, MA).
5. Methanol.
6. Wash buffer or PBS-T: PBS, 0.2% Tween-20.
7. Blocking buffer: wash buffer + 5% dried milk.
8. Primary antibody: anti-HA antibody diluted in blocking buffer.
9. Secondary antibody: anti-mouse IgG conjugated to horseradish peroxidase (Amersham Pharmacia Biotech, Uppsala, Sweden).
10. Enhanced chemiluminescent (ECL) reagents (Amersham Biosciences, Buckinghamshire, England)
11. Bio-Max film (Kodak, Rochester, NY).

3. Methods

Activation of TOR in yeast can be assayed by evaluating the phosphorylation state of NPR1 or GLN3 ([3,4,13,14](#)). When TOR is active, NPR1 and GLN3 are hyperphosphorylated and appear as multiple bands when fractionated on 7.5% SDS-PAGE (polyacrylamide gel electrophoresis). Inactivation of TOR by nitrogen starvation or rapamycin treatment dephosphorylates NPR1 and GLN3, resulting in a faster migrating and a more discrete single band on SDS-PAGE. The dephosphorylation of NPR1 and GLN3 is SIT4 dependent, and although evidence is lacking that these proteins are directly dephosphorylated by SIT4, the dephosphorylation of NPR1 and GLN3 provides an easy and straightforward method to assay both the decrease in TOR activity and the increase in SIT4 activity. The dephosphorylation of other SIT4 targets such as TIP41 can also be used as a readout for SIT4 and TOR activity. Although TIP41 is not hyperphosphorylated compared to NPR1 or GLN3 and thus does not display an obvious mobility change on one-dimensional SDS-PAGE, the phosphorylation state of TIP41 can be assayed using two-dimensional gel electrophoresis.

Table 1
Yeast Strains and Plasmids used in This Study

Strain	Genotype
TB50a	<i>MATa leu2-3,112 ura3-52 trp1 his3 rme1 HMLa</i>
JK9-3da	<i>MATa leu2-3,112 ura3-52 trp1 his4 rme1 HMLa</i>
TS64-1a	<i>JK9-3da sit4::kanMX4</i>
Plasmid	Description
pEJ23	YEplac181 (2 μ , LEU2) expressing N-terminally tagged HA-NPR1 under its own promoter
pEJ120	pHAC181 (2 μ , LEU2) expressing C-terminally 3XHA-tagged TIP41 under its own promoter

3.1. Yeast Culture and Lysis

1. Wild-type (JK9 or TB50) and *sit4* (TS64) strains (see **Table 1**) containing pHA-NPR1 (pEJ23) are grown in synthetic minimal media (SD) complemented with amino acid mixture minus leucine, at 30°C. Cells are typically grown to OD = 0.4 (see **Note 1**). Strains containing pTIP41-HA (pEJ120) are grown similarly.
2. For the nitrogen-starved condition, cells are grown overnight in yeast nitrogen base (YNB) without ammonium sulfate and without amino acids, supplemented with 10 mM ammonium sulfate, 2% glucose, plus tryptophan, uracil, and histidine. The following day, cells are resuspended for 1 h in fresh YNB media supplemented with 2% glucose, tryptophan, histidine, and uracil containing either ammonium, proline, or water.
3. For rapamycin-treated cells, rapamycin (at a final concentration of 100 ng/mL) or drug vehicle is added 30 min prior to harvest.
4. Cell cultures expressing HA-NPR1 (40 OD total) or TIP41-HA (50 OD total) are poured into 50-mL Falcon tubes and centrifuged (700g) at 4°C for 5 min. The supernatant is discarded.
5. For cultures expressing HA-NPR1, cells are resuspended in 1 mL of cold lysis buffer 1 (containing protease and phosphatase inhibitors), whereas cultures expressing TIP41-HA are lysed in 1 mL cold lysis buffer 2-(containing protease and phosphatase inhibitors, RNase A), then transferred to a 2 mL screw-cap tube containing glass beads (glass beads occupy about one-third of the volume of the tube). Cells are lysed by mechanical disruption in a bead beater for 6 \times 30-s pulses at 4°C (cold room) (see **Note 2**).
6. To recover lysates, a hole is punctured at the bottom of the screw-cap tube. The tube is then snapped on top of a 1.5-mL Eppendorf microtube. Lysates are recovered by centrifugation at 80g, 4°C for 2 min. The screw-cap tube (containing beads) are discarded. Lysates are then further cleared by centrifugation of the

sample (now on the Eppendorf tube) for 13,000 rpm 10 min, 4°C for 5 min. The cleared lysates are recovered and the pellet is discarded. Protein concentration of the lysates are determined using the Bio-Rad Protein Assay Kit (Bio-Rad, Hercules, CA) and a spectrophotometer. Total lysates containing HA-NPR1 are subjected to one-dimensional SDS-PAGE, whereas lysates containing TIP41-HA undergo immunoprecipitation before two-dimensional gel analysis.

3.2. One Dimensional SDS-PAGE for HA-NPR1

1. A 0.75-mm-thick, 7.5% minigel is prepared using the Mini-PROTEAN3 electrophoresis module from Bio-Rad. The separating gel is poured between the assembled glass plates/spacers, leaving space (about 30 mm) to accommodate the stacking gel. The poured gel is overlaid with about 500 μ L propanol. The gel should polymerize in about 30 min.
2. The propanol is poured off and the top of the gel is rinsed with water.
3. The stacking gel is prepared and poured on top of the separating gel. The comb is inserted into the separating gel immediately. The stacking gel should polymerize within 15 min. The comb can be removed once the stacking gel has polymerized.
4. The gel unit is assembled into the electrophoresis tank and filled up with running buffer.
5. Samples are prepared by adding 4X SDS gel loading buffer into lysates containing HA-NPR1 (50 μ g total protein) and then boiled for 3 min on a heat block (*see Note 3*). The samples are loaded into the wells (volume loaded is typically 10–20 μ L per well). The first or last lane is loaded with 10 μ L prestained molecular weight-markers.
6. After the running dye has run off the gel, the power supply is turned off and Western blotting is performed (proceed to **Subheading 3.6.**).

3.3. Immunoprecipitation and Dephosphorylation of TIP41-HA

1. Eight milligrams of cell extract containing TIP41-HA is incubated with anti-HA antibody (typically 1 μ L) and 40 μ L of protein-G bead slurry and rocked for 3 h at 4°C.
2. The mixture is centrifuged briefly for 1 min at 4°C. The supernatant is discarded.
3. The immunoprecipitates are washed with 800 μ L of TSNE (TNE + 0.15 M NaCl) and centrifuged briefly at 4°C. The supernatant is discarded. The washings are performed three times.
4. Immunoprecipitates are resuspended in 150 μ L of CIP buffer with or without 100 units of alkaline phosphatase (*see Note 4*). The reaction is incubated for 1 h at 37°C and then briefly centrifuged. The supernatant is discarded.
5. The immunoprecipitates are washed twice with 1 mL TNE.

3.4. Isoelectric Focusing of TIP41-HA

1. The washed immunoprecipitates are resuspended in 440 μ L TNE, with the addition of 322 mg urea, 117 mg thiourea, and 6.6 μ L β -mercaptoethanol for each sample. The reaction is incubated for 30 min at 37°C.

2. The samples are centrifuged and the supernatant is recovered.
3. Buffer B (242 μ L) and a few crystals of bromophenol blue are added to the supernatant.
4. Then 300 μ L of the sample is loaded into the IPG chamber (strip holder) (*see Note 5*) by pipetting along the length of the chamber, making sure that the sample forms a continuous line from one end of the chamber to the other and contacts the electrodes.
5. Using forceps, the protective cover from the IPG strip is first peeled off and discarded. While holding the strip with forceps on the square end, the strip is positioned on the top of the sample, with the gel side of the strip in contact with the sample (face down) and the pointed (anodic) end of the strip directed toward the pointed end of the chamber. The strip is slowly lowered into the sample, pointed end first, being careful not to trap bubbles under the strip. Finally, the cathodic (square) end of the strip is lowered into the chamber, making sure that the IPG gel contacts the chamber electrodes at each end.
6. The chamber is then filled with DryStrip cover fluid (*see Note 6*) and covered with the chamber lid.
7. Chambers are loaded onto an IPGPhor apparatus. The chamber is positioned such that the pointed end is over the anode (pointing to the back of the unit) and the square end is over the cathode. Make sure that the two external electrodes under the chamber make metal-to-metal contact with the apparatus.
8. Strips are rehydrated for 12 h at 22°C, followed by isoelectric focusing. The following protocol for isoelectric focusing using the IPGPhor apparatus is applied: 500 V for 1 h, 1000 V for 1 h, 8000 V for 48 h, and 500 V for 99 h, 50 μ A per strip.
9. Typically, a total of 185,000 V h is reached before proceeding to the second-dimension analysis (*see Note 7*).

3.5. Second-Dimension SDS-PAGE of TIP41-HA

1. A 1.5-mm-thick, 10% separating gel is prepared using the Hoefer vertical electrophoresis unit (18 \times 16-cm plates). (No stacking gel is needed.) The poured gel is overlaid with 20% propanol (about 1 mL). While the gel is polymerizing, the strips are washed as follows.
2. The strip is recovered from the chamber by using forceps to pick up the strip from either end. Using an equilibration tray, each strip is washed and equilibrated separately for 3 min in 5 mL SDS equilibration buffer. This washing procedure is repeated five times.
3. After the gel has polymerized, the propanol is poured off and the gel is rinsed with water. The gel is assembled onto the Hoefer apparatus and gel is covered with running buffer.
4. Using forceps to hold the strip on one end, the strip is loaded in between the gel plates, on top of the separating gel (*see Note 8*). The strip can be cut on one or both ends to accommodate its length into the gel. Once the strip is loaded, the running buffer is removed by gently pouring it off from the gel.

5. Liquefied agarose sealing solution (*see Note 9*) is poured into the gel, just enough to cover the strip. After a couple of minutes, running buffer is added and the SDS-PAGE is performed to separate proteins according to size. Electrophoresis is terminated when the blue dye runs off. Western blotting is then performed to detect the protein.

3.6. Western Blotting of HA-NPR1 and TIP41-HA

1. A transfer tank (Mini-Trans blot cell for HA-NPR1 and Trans-blot cell for TIP41-HA) is partly filled with transfer buffer.
2. A tray that is large enough to accommodate the transfer cassette is partially filled with transfer buffer. One side of the transfer cassette is laid out into the tray containing the transfer buffer. A piece of foam is laid on top of the cassette and a sheet of 3 MM paper (the size of or slightly larger than the separating gel) is then assembled on top of the foam. Make sure that the transfer buffer is enough to wet the foam and paper.
3. The gel unit is disconnected from the power supply and disassembled. The stacking gel, where present, is cut out and discarded. One corner of the separating gel is cut out to allow its orientation to be tracked. The separating gel is then laid on top of the 3 MM paper.
4. A sheet of PVDF (Immobilon-P) membrane is cut out to roughly the exact size of the separating gel with one corner cut out for orientation. The membrane is wet with methanol completely, followed by running buffer. It is then laid out on top of and oriented into the separating gel, making sure that no bubbles are trapped between the membrane and gel.
5. A second piece of 3 MM paper (same size as the first one) is dipped into the transfer buffer and then laid out on top of the membrane, followed by a second wet piece of foam. The transfer cassette is then closed and loaded into the transfer tank (*see Note 10*). More transfer buffer is added to the tank if necessary. (The membrane has to be fully immersed in transfer buffer.)
5. The transfer is carried out at 4°C (either in the cold room or the tank is submerged in an ice bath) and a magnetic stir bar in the tank is activated. The tank is covered with the lid and the electrodes connected to the power supply. Transfers can be accomplished at either 30 V overnight or 70 V for 2 h.
6. Once the transfer is complete, the power supply is switched off, and the cassette is taken out of the tank. The membrane is recovered while the paper, gel, and buffer are discarded.
7. The membrane is incubated in blocking buffer for 1 h at room temperature (*see Note 11*).
8. The blocking buffer is removed and the membrane is incubated with the primary antibody (anti-HA antibody diluted in blocking buffer 1 : 1000) (*see Note 12*). The incubation is performed at 4°C overnight on a rocking platform.
9. The primary antibody is discarded and the membrane is washed with 10–20 mL PBS-T three times for 15 min each on a rocking platform.

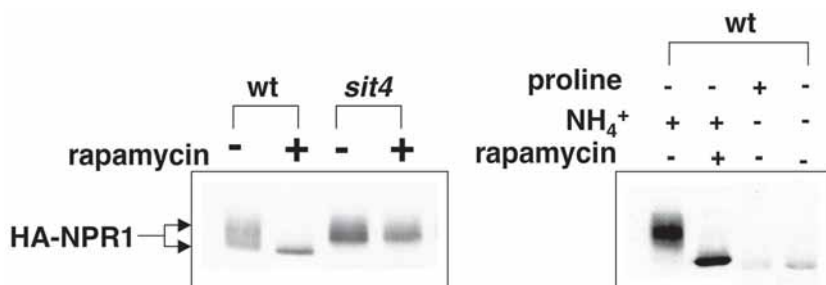


Fig. 1. NPR1 is hyperphosphorylated in *sit4* cells. Wild-type (wt) (JK9=3da) or *sit4* (TS64=1a) cells carrying the plasmid pHA-NPR1 (pEJ23) were grown to log phase at 30°C and then treated for 30 min with either 100 ng/mL rapamycin or drug vehicle alone, or nitrogen starved for 1 h. Cells were harvested and lysed. Total cellular extracts were fractionated on 7.5% SDS-PAGE. Western blotting was performed and HA-NPR1 was detected using HA-antibody. (Reproduced in part from **ref. 3** with permission from Elsevier.)

10. The secondary antibody (diluted in blocking buffer 1 : 10000) is added and the membrane is incubated for 1 h at room temperature on a rocking platform.
11. The secondary antibody solution is discarded and the membrane is washed with 10–20 mL PBS-T three times for 15 min each on a rocking platform.
13. Once the final wash is removed from the blot, the membrane is drained well (but not dried). Two-milliliter aliquots of the ECL reagents are added into the membrane and mixed by swirling to ensure even coverage.
14. The blot is removed from the ECL reagents and drained to remove excess fluid. The blot is then wrapped in plastic wrap and placed in an X-ray film cassette. In the dark room, the film is laid out on top of the wrapped membrane. Exposure time will depend on the strength of the signal. Typically, 1- to 10-minute exposure time is sufficient. HA-NPR1 migrates close to 100 kDa (see **Fig. 1**). TIP41-HA migrates as five major distinct spots in an estimated *pI* range of 5.0–6.0, at the expected molecular weight of 41 kDa (see **Fig. 2**).

4. Notes

1. The *sit4* strain grows more slowly than the wild-type strain. It is recommended to grow a preculture of *sit4* ahead of the wild type to achieve the same total OD as wild-type cells upon harvest.
2. After each 30-s pulse, the tubes are removed from the cell disruptor and kept on ice for 3 min before the next round of mechanical disruption begins to avoid protein degradation.
3. It is important that the total number of proteins for each sample be similar for comparison of phosphorylation. It is also important not to overload (i.e., use too

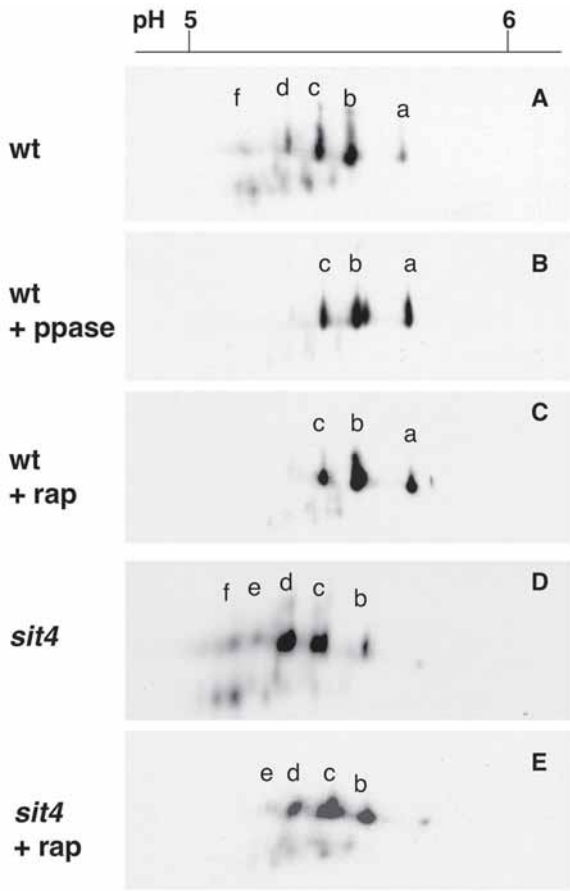


Fig. 2. Dephosphorylation of TIP41 is SIT4 dependent. (A–E) Wild-type (wt) (TB50a) or *sit4* mutant (TS64-1a) cells were grown to log phase at 30°C and then treated for 30 min with 100 ng/mL rapamycin (rap) or drug vehicle alone. TIP41-HA immunoprecipitates were incubated either with or without alkaline phosphatase (ppase) at 37°C for 1 h. First-dimension analysis was performed by isoelectric focusing on a pH 3–10 NL gradient strip followed by a second-dimension analysis on 10% SDS-PAGE. TIP41-HA was detected by immunoblotting using anti-HA antibody. Figure panels encompass pH 5–6 from left to right. (Reproduced from **ref. 3** with permission from Elsevier.)

much total protein) a lane. Some strains (such as *tip41*) might have increased NPR1 expression compared to wild type. Therefore, it might be necessary to use less total protein for such a strain to be able to compare the phosphorylation state with the wild type.

4. Excess alkaline phosphatase is added to the immunoprecipitates as a control for dephosphorylation of TIP41-HA.
5. The chamber or strip holder is made of a thermally conductive aluminum oxide ceramic. Rinse well with water and mild liquid detergent to clean (do not use abrasive cleansers or solvents).
6. Mineral oil can be used alternatively. The fluid is applied to minimize evaporation and urea crystallization.
7. As isoelectric focusing proceeds, the bromophenol blue tracking dye migrates toward the anode and leaves the strip well before focusing is complete. Therefore, a colorless strip is no indication that focusing is complete. If tracking dye does not move, check if current is applied across the strip. Make sure that the chamber electrodes are in contact with the electrode areas of the apparatus.
8. The presence of running buffer allows the strip to be easily loaded on top of the separating gel. It is important that the orientation be noted and it is recommended that consistency is observed when loading several gel strips (e.g., keep the anode end on the left side and the strip's gel face toward the front). Running six strips on six gel assemblies is manageable by one person (more than this, the likelihood of mistakes and negligence increases). Strips can also be frozen at -20°C to be processed on the second dimension at a later time.
9. Agarose sealing solution is microwaved until liquefied. Use a hot-plate stirrer to keep the solution warm to prevent congealing while strips and gels are being assembled.
10. Make sure that the cassette is placed such that the membrane is between the gel and the anode (This is crucial to allow the protein to be transferred from the gel to membrane. If orientation is wrong, the proteins are lost from the gel into the buffer!)
11. For a minigel (gel containing HA-NPR1), 10 mL of blocking buffer is used. For the large gel (containing TIP41-HA), 20 mL of blocking buffer is sufficient.
12. The minimum amount of buffer is used, just enough to cover the membrane, to limit the amount of the antibody to be used.

Acknowledgments

The author would like to thank Professor Mike Hall for his mentorship. This work was supported by the Cancer Research Institute and the American Heart Association.

References

1. Jacinto, E. and Hall, M. N. (2003) TOR signalling in bugs, brain and brawn. *Nature Rev. Mol. Cell. Biol.* **4**, 117–126.
2. Di Como, C. J. and Arndt, K. T. (1996) Nutrients, via the TOR proteins, stimulate the association of TAP42 with type 2A phosphatases. *Genes Dev.* **10**, 1904–1916.
3. Jacinto, E., Guo, B., Arndt, K. T., Schmelzle, T., and Hall, M. N. (2001) TIP41 interacts with TAP42 and negatively regulates the TOR signaling pathway. *Mol. Cell* **8**, 1017–26.

4. Beck, T. and Hall, M. N. (1999) The TOR signalling pathway controls nuclear localization of nutrient-regulated transcription factors. *Nature* **402**, 689–692.
5. Brunn, G. J., Hudson, C. C., Sekulic, A., et al. (1997) Phosphorylation of the translational repressor PHAS-I by the mammalian target of rapamycin. *Science* **277**, 99–101.
6. Burnett, P. E., Barrow, R. K., Cohen, N. A., Snyder, S. H. and Sabatini, D. M. (1998) RAFT1 phosphorylation of the translational regulators p70 S6 kinase and 4E-BP1. *Proc. Natl. Acad. Sci. USA* **95**, 1432–1437.
7. Kim, D. H., Sarbassov dos, D., Ali, S. M., et al. (2002) mTOR interacts with raptor to form a nutrient-sensitive complex that signals to the cell growth machinery. *Cell* **110**, 163–175.
8. Chung, J., Kuo, C. J., Crabtree, G. R., and Blenis, J. (1992) Rapamycin-FKBP specifically blocks growth-dependent activation of and signaling by the 70 kd S6 protein kinases. *Cell* **69**, 1227–1236.
9. Price, D. J., Grove, J. R., Calvo, V., Avruch, J., and Bierer, B. E. (1992) Rapamycin-induced inhibition of the 70-kilodalton S6 protein kinases. *Science* **257**, 973–977.
10. Graves, L. M., Bornfeldt, K. E., Argast, G. M., et al. (1995) cAMP- and rapamycin-sensitive regulation of the association of eukaryotic initiation factor 4E and the translational regulator PHAS-I in aortic smooth muscle cells. *Proc. Natl. Acad. Sci. USA* **92**, 7222–7226.
11. Beretta, L., Gingras, A. C., Svitkin, Y. V., Hall, M. N., and Sonenberg, N. (1996) Rapamycin blocks the phosphorylation of 4E-BP1 and inhibits cap-dependent initiation of translation. *EMBO J.* **15**, 658–664.
12. Peterson, R. T., Desai, B. N., Hardwick, J. S., and Schreiber, S. L. (1999) Protein phosphatase 2A interacts with the 70-kDa S6 kinase and is activated by inhibition of FKBP12-rapamycin association protein. *Proc. Natl. Acad. Sci. USA* **96**, 4438–4442.
13. Schmidt, A., Beck, T., Koller, A., Kunz, J., and Hall, M. N. (1998) The TOR nutrient signalling pathway phosphorylates NPR1 and inhibits turnover of the tryptophan permease. *EMBO J.* **17**, 6924–6931.
14. Bertram, P. G., Choi, J. H., Carvalho, J., et al. (2000) Tripartite regulation of Gln3p by TOR, Ure2p, and phosphatases. *J Biol. Chem.* **275**, 35,727–35,733.

Functional Characterization of Small CTD Phosphatases

Michele Yeo and Patrick S. Lin

Summary

The carboxyl-terminal domain (CTD) of the largest subunit of RNA polymerase (RNAP) II undergoes reversible phosphorylation with each round of transcription essential for the regulation of gene expression. A family of small CTD phosphatases (SCPs) was identified based on a homology search to TFIIIF-associating CTD phosphatase 1 (FCP1). Unlike FCP1, SCP preferentially catalyze the dephosphorylation of Ser⁵ within the CTD and is especially active toward RNAP II phosphorylated by TFIIH (1). Recently, SCP1 was demonstrated as a transcriptional regulator that acts to silence neuronal genes (2). This chapter describes the procedures for various assays involved in the discovery and functional characterization of SCFs.

Key Words: RNA polymerase II; carboxyl-terminal domain; CTD phosphatase; SCP; REST/NRSF; neuronal gene silencing

1. Introduction

The carboxyl-terminal domain (CTD) of the largest subunit of RNA polymerase (RNAP) II consists of tandem repeats of the consensus sequence Tyr₁Ser₂Pro₃Thr₄Ser₅Pro₆Ser₇ with as few as 17 copies in the human malaria parasite *Plasmodium falciparum* to as many as 52 copies in complex eukaryotes such as mouse and human. The hypophosphorylated form of the enzyme, RNAP IIA, is involved in transcript initiation, whereas the hyperphosphorylated form, RNAP IIO, is involved in transcript elongation. During each round of transcription, the CTD undergoes reversible phosphorylation, predominantly at Ser₂ and Ser₅ within the heptapeptide repeat. Changes in the pattern of CTD phosphorylation (3) influence the recruitment of protein factors involved in the production of a mature transcript (4). Accordingly, CTD kinases and CTD phosphatases serve as important regulators that facilitate the progression of RNAP II in initiation, elongation, and RNA processing. TFIIIF-associating CTD

phosphatase 1 (FCP1) catalyzes the dephosphorylation of RNAP II (for a review, see **ref. 5**) and is thought to play a major role in polymerase recycling concomitant with or shortly after termination (**6**). FCP1 is the founding member of a family of phosphatases whose members share the signature motif DXDX(T/V) similar to those found in phosphotransferases and phosphohydrolases (**7**). Although FCP1 efficiently removes phosphates from Ser₂ and Ser₅ in vitro (**8**), it is primarily responsible for the turnover of Ser₂ phosphates in vivo, as suggested by the observation in *fcp1* yeast mutants that Ser₂ phosphorylation increases in promoter distal regions while Ser₅ phosphorylation levels remain unchanged (**9**). Accordingly, a search ensued thereafter to find the CTD phosphatase(s) responsible for the removal of Ser₅ phosphates in early elongation.

Examination of the database revealed additional genes that consist of a domain with homology to the FCP1 catalytic site. Three closely related human genes encoding small proteins with the FCP1 catalytic domain, but lacking the BRCT domain, have been identified and named small CTD phosphatases (SCPs) (see **Fig. 1**).

The X-ray crystallographic structure of SCP1 has revealed a core fold and an active center similar to those of phosphohydrolases that contain the DXDX(T/V) amino acid signature motif (**10**). The first aspartate in the signature motif undergoes metal-assisted phosphorylation during catalysis, resulting in a phospho-aspartate intermediate. A unique β -sheeted insert adjacent to the active site of SCPs and FCP1 is proposed to bind the CTD of RNAP II and thereby confer specificity (**10**).

SCP1 preferentially dephosphorylates Ser₅ within the CTD of RNAP II and the activity is stimulated by RNAP II-associated protein 74 (RAP74) (**1**). The enzymatic specificity of SCP1 was confirmed using a four-heptad repeat peptide substrate. Furthermore, in reporter gene assays, expression of SCP1 inhibited activated transcription from a variety of promoters, whereas the phosphatase-inactive mutant of SCP1-enhanced transcription (**1**). Accordingly, it was postulated that the phosphatase activity of SCP1 might play a role in the negative regulation of gene expression. Indeed, the possible role of SCP1 in gene silencing has recently been described (**2**).

Repressor element 1 (RE-1) silencing factor/neuron-restrictive silencer factor (REST/NRSF) is a Zn²⁺-finger containing protein that binds a 23-bp RE-1 DNA element found in many neuronal genes (**11,12**). The binding of REST/NRSF to DNA initiates the formation of a protein complex that represses gene expression by deacetylating histones and demethylating both DNA and histone H3 (**13,14**). These covalent chromatin modifications effectively reduce transcription, leading to the silencing of neuronal gene expression.

Northern Blot and *in situ* analyses reveal that the pattern of SCP1 expression parallels that of REST/NRSF (**2**) and suggest that SCP1 and REST might

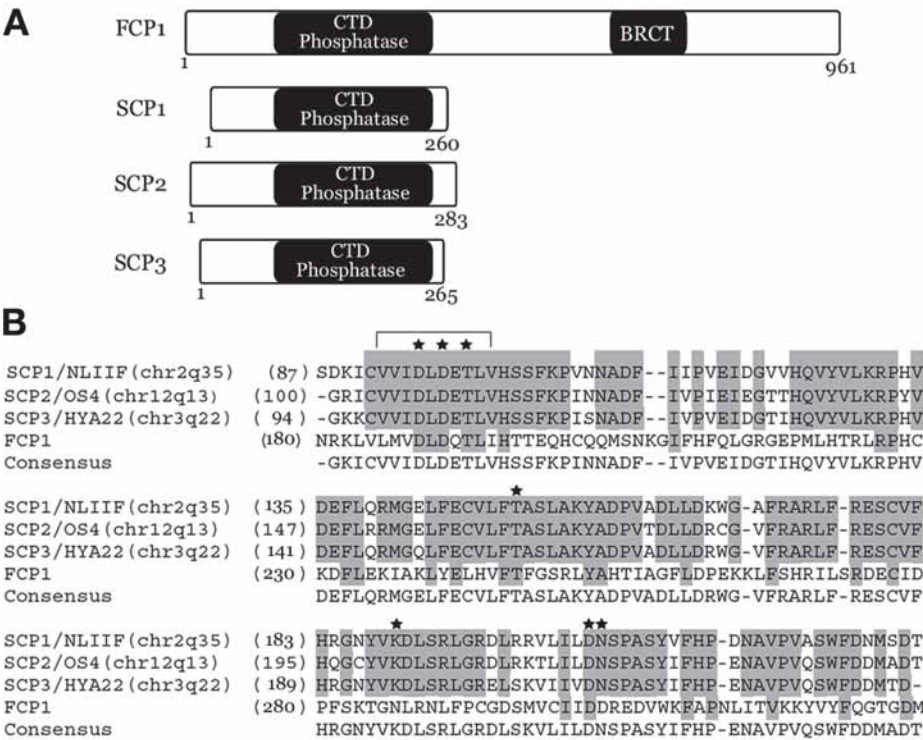


Fig. 1. Alignment of amino acid sequences surrounding the catalytic domain and relation of SCP to FCP1. **(A)** Domain structures of FCP1 and SCP proteins. **(B)** Sequence alignment and relationship of SCPs with FCP1. The bracket indicates the conserved signature motif and active site residues are marked by asterisks (*I*). Shaded gray areas show regions of identity. Alternative descriptive names and chromosome locations are indicated. Multiple alignments were carried out using the ClustalW algorithm with vector NTI Suite (Informax) (*see Note 1*).

function together to silence neuronal genes. Indeed, SCP1 coimmunoprecipitates with REST, whereas a dominant negative form of REST was unable to bind SCP1, suggesting that SCP1 and REST form a physical complex (2). Furthermore, chromatin immunoprecipitation (ChIP) analysis using primers specific for RE-1 elements of several neuronal genes reveals that SCP1 is recruited to REST/NRSF complexes. Finally, the knockdown of the single copy of SCP1 in cultured *Drosophila* SL2 cells by RNAi unmasks neuronal gene expression. Taken together, SCP activity appears to be an evolutionary conserved transcriptional regulator that acts to silence neuronal genes. Although the negative influence of SCPs on neuronal gene expression might be mediated by dephosphorylation of

RNAP II CTD, it remains possible that other phosphatase substrates might also mediate these effects (**15**).

2. Materials

2.1. Expression of GST-SCP1 and GST-SCP1dn

1. hSCP1/hSCP1dn cDNA cloned in pGEX4T-1 vector (Pharmacia).
2. *Escherichia coli* BL21(DE3) cells (Stratagene) for transformation.
3. Bacterial culture medium: Luria–Bertani (LB) + 50 µg/mL ampicillin (LB-Amp).
4. GST-Bind Resin (Novagen).
5. PBST buffer: PBS with 0.05% (v/v) Tween-20.
6. Resuspension buffer: PBST, 2 mM EDTA, 0.1% (v/v) β-mercaptoethanol.
7. IPTG: 0.1 M stock solution in water.
8. Protease inhibitor cocktail (Novagen).
9. Glutathione-S-transferase GST elution buffer: 10 mM reduced glutathione in water (Sigma) (see **Note 2**).

2.2. CTD Phosphatase Assay

2.2.1. para-Nitrophenylphosphate as Substrate

1. para-nitrophenylphosphate (pNPP, Upstate Biotechnology).
2. 10X pNPP reaction buffer: 50 mM Tris-acetate, pH 5.5, 10 mM MgCl₂, 10% (v/v). glycerol, 0.5 mM dithiothreitol (DTT), 20 mM pNPP.
3. 0.25 N Sodium hydroxide for quenching reactions.

2.2.2. Biotinylated CTD Phosphopeptide as Substrate

1. N-Terminal biotinylated CTD phosphopeptides, composed of four tandem repeats of either YpSPTSPS or YSPTpSPS (pS indicates phosphoserine), were synthesized (Alpha Diagnostics, TX).
2. 10X Phosphopeptide reaction buffer: 50 mM Tris-acetate, pH 5.5, 10 mM MgCl₂, 10% (v/v) glycerol, 0.5 mM DTT, 25 mM phosphopeptide (see **Note 3**).
3. Malachite green reagent and phosphate standard (Biomol).

2.2.3. GST-CTDo and RNAP IIO as Substrates

1. Mouse recombinant GST-CTDa (unphosphorylated CTD) [expressed and purified by Kang and Dahmus (**16**)].
2. Calf thymus RNAP IIA [purified by the method of Hodo and Blatti (**17**) with modifications as described by Kang and Dahmus (**18**)].
3. Human recombinant casein kinase II (CKII) (Upstate Biotechnology).
4. Mouse recombinant mitogen-activated protein kinase 2/extracellular signal-regulated kinase 2 (MAPK2/ERK2) (Upstate Biotechnology).
5. RAP74 [expressed and purified by Wang et al. (**19**)].
6. CKII/CTD kinase buffer: 25 mM Tris-HCl, pH 7.9, 8 mM MgCl₂, 5% (v/v) glycerol, 0.007% (v/v) Triton X-100, 1 mM DTT.

7. CTD phosphatase buffer: 50 mM Tris-HCl, pH 7.9, 10 mM MgCl₂, 20% (v/v) glycerol, 0.025% (v/v) Tween-80, 0.1 mM EDTA, 5 mM DTT.
8. [γ -³²P]ATP (6000 Ci/mmol; PerkinElmer Life Sciences).
9. 5X Sample buffer: 300 mM Tris-HCl, pH 6.8, 10% (w/v) sodium dodecyl sulfate (SDS), 25% (v/v) β -mercaptoethanol, 0.04% (w/v) bromophenol blue.
10. Phosphor imager (Molecular Dynamics Storm 860).

2.3. RNAi in *SL2 Insect Cell Line*

2.3.1. Growth of *Drosophila SL2 Cells*

1. Schneider's *Drosophila* medium (Invitrogen).
2. Fetal bovine serum (FBS), penicillin–streptomycin (Invitrogen).
3. SL2 cells (ATCC cat. no. CRL-1963).
4. DES serum-free medium (Invitrogen).

2.3.2. Purification of Double-Stranded RNA

1. MEGASCRIP[®] kit (Ambion).
2. MicroSpin S-400 columns (Pharmacia).

3. Methods

3.1. Expression of *GST-SCP1* and *GST-SCP1dn*

3.1.1. Growth and Harvesting of Bacteria Lysate

1. BL21(DE3) cells transformed with either pGEX4T1-hSCP1 or pGEX4T1-hSCP1dn are inoculated in LB-Amp media and grown at 37°C on a 250-rpm shaker overnight.
2. The next morning, the culture is added to 900 mL prewarmed LB-Amp. The culture is grown until A_{600 nm} reaches 0.5.
3. IPTG (final 0.1 mM) is added to the 1-L culture. The culture is allowed to grow until A_{600 nm} is 1.2 (see **Note 4**).
4. The culture is poured into two 500-mL centrifuge bottles and pelleted at 3080g for 10 min at 4°C.
5. The pellet is resuspended in 10 mL of resuspension buffer with added protease inhibitor (see **Note 5**).
6. The bacteria is lysed by passing through the French Press two times at 12,000 psi.
7. The pressed lysate is transferred to a 15-mL centrifuge tube and cellular debris is pelleted at 8200g for 10 min at 4°C. The supernatant is aliquoted and stored at -70°C.

3.1.2. Protein Purification

1. Prior to use, the GST resin is washed several times with resuspension buffer. Final resuspension is in 1 mL of buffer (this gives a 50% slurry).
2. Protein lysate (1 mL) is incubated with 0.25 mL of 50% GST beads in a 1.5-mL Eppendorf tube at 4°C with mixing for 1 h.

3. The beads are centrifuged at 2300g for 2 min and washed four times with resuspension buffer.
4. The GST elution buffer (0.25 mL) is added to the beads and incubated with agitation at room temperature. The tubes are spun and the supernatant is collected. The elution is repeated one more time and the eluate is consolidated (*see* **Note 6**).

3.2. CTD phosphatase Assays

3.2.1. Using pNPP as Substrate

1. The reaction is started when 50 pmol GST-SCP1 is added to 1X reaction buffer in a total volume of 0.2 mL per tube.
2. The tubes are incubated at 37°C for 1 h, after which the reaction is quenched by adding 0.8 mL of 0.25 N NaOH.
3. Release of *para*-nitrophenyl (yellow) is determined by using a spectrophotometer and measuring absorbance at $A_{600\text{ nm}}$.

3.2.2. Using CTD Phosphopeptide as Substrate

1. The reaction is started when 20–100 pmol GST-SCP1 is added to 1X phosphopeptide reaction buffer in a total volume of 0.05 mL per tube.
2. The tubes are incubated at 37°C for 1 h, after which the reaction is stopped by adding 0.5 mL of malachite green reagent.
3. Phosphate release is determined using a spectrophotometer to measure absorbance at $A_{620\text{ nm}}$ and quantified relative to a phosphate standard curve.

3.2.3. Using GST-CTDo as Substrate

1. GST-CTDa is radiolabeled as follows: 15 pmol recombinant GST-CTDa, 10 units CKII, and 2 μM of [γ - ^{32}P]ATP are added to CKII/CTD kinase buffer in a total volume of 100 μL (*see* **Note 7**).
2. The CKII-labeling reaction is incubated at 37°C for 10 min.
3. 0.5 M EDTA (4.2 μL) is added to the reaction (for a final 20 mM EDTA).
4. GST-CTDa is converted to GST-CTDo (phosphorylated CTD) in the same reaction mixture with the addition of 300 mU of MAPK2/ERK2 in the presence of 2 mM cold ATP (*see* **Note 8**).
5. The kinase reaction is incubated at 30°C for 30 min (*see* **Fig. 2A**).
6. 4 M KCl (2.75 μL) is added to the reaction (for a final 10 mM KCl).
7. The resultant GST-CTDo is passed through a glutathione–agarose column with a step elution of 15 mM glutathione. Two-drop fractions are collected (approx 35 μL volume per fraction) (*see* **Note 9**).
8. The CTD phosphatase assay is initiated by the addition of 4 pmol GST-SCP1 in 20 μL CTD phosphatase buffer containing 75 fmol ^{32}P -labeled GST-CTDo and 7 pmol RAP74.
9. The phosphatase reaction is incubated at 30°C for 30 min.
10. The reaction is terminated by the addition of 5 μL of 5X sample buffer.
11. GST-CTDa and GST-CTDo proteins are resolved on 8% SDS-PAGE.

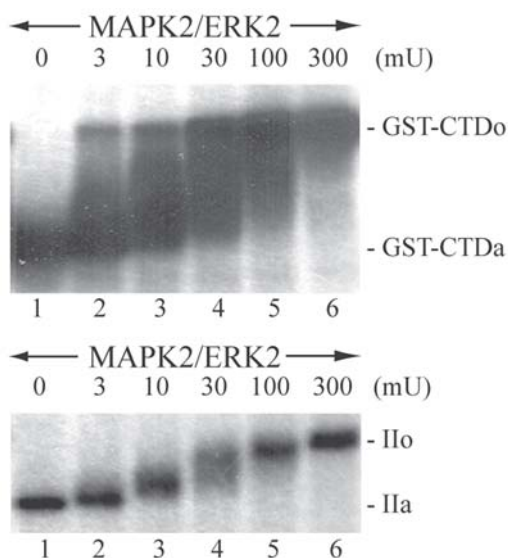


Fig. 2. Preparation of GST-CTDo and RNAP IIO. Recombinant GST-CTD and purified calf thymus RNAP IIA were labeled with ^{32}P by phosphorylation with CKII and subsequently incubated with 2 mM unlabeled ATP in the presence of increasing amounts of MAPK2/ERK2. Reactions contain equimolar amounts of GST-CTD (A) and RNAP II (B). The difference in band intensity is a result of differences in the efficiency of CKII labeling. Reaction products were resolved on 6% SDS-PAGE. The positions of GST-CTDa and GST-CTDo and subunits IIA and IIO are indicated.

12. The percent conversion of GST-CTDo to GST-CTDa is quantitated and analyzed using a phosphor imager.

3.2.4. Using RNAP IIO as substrate

1. RNAP IIA is radiolabeled as follows: 15 pmol calf thymus RNAP IIA, 10 units CKII, and 2 μM of $[\gamma\text{-}^{32}\text{P}]\text{ATP}$ are added to CKII/CTD kinase buffer in a total volume of 100 μL (see **Note 7**).
2. The CKII-labeling reaction is incubated at 37°C for 10 min.
3. 0.5 M EDTA (4.2 μL) is added to the reaction (for a final 20 mM EDTA).
4. RNAP IIA is converted to RNAP IIO in the same reaction mixture with the addition of 300 mU of MAPK2/ERK2 in the presence of 2 mM cold ATP (see **Note 8**).
5. The kinase reaction is incubated at 30°C for 30 min (see **Fig. 2B**).
6. 4 M KCl (2.75 μL) is added to the reaction (for a final 10 mM KCl).
7. The resultant RNAP IIO is passed through a DE53 column with a step elution of 0.5 M KCl. Two-drop fractions are collected (approx 35 μL volume per fraction) (see **Note 10**).CPI-7

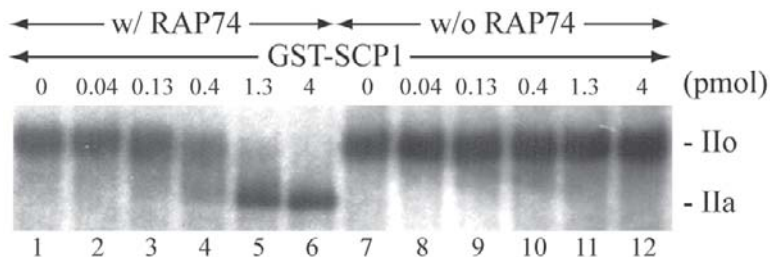


Fig. 3. Dephosphorylation of RNAP IIO by SCP1 in the presence and absence of RAP74. RNAP IIO substrate (prepared by in vitro phosphorylation with TFIIF) was incubated with increasing amounts of SCP1 in the presence (lanes 1–6) and absence (lanes 7–12) of RAP74, and subsequently analyzed on 5% SDS-PAGE. The positions of subunits Ila and Ilo are indicated.

8. The CTD phosphatase assay is initiated by the addition of 4 pmol GST-SCP1 in 20 μ L CTD phosphatase buffer containing 18 fmol 32 P-labeled RNAP IIO and 7 pmol RAP74.
9. The phosphatase reaction is incubated at 30°C for 30 min.
10. The reaction is terminated by the addition of 5 μ L of 5X sample buffer.
11. RNAP IIA and IIO largest subunits (IIa and Ilo, respectively) are resolved on 5% sodium dodecyl sulfate–polyacrylamide gel electrophoresis (SDS-PAGE) (*see Note 11*).
12. The percentage conversion of RNAP IIO to RNAP IIA is quantitated and analyzed using a phosphor imager (*see Fig. 3*).

3.3. RNAi in Cultured *Drosophila* SL2 Cells

3.3.1. Growth of SL2 Cells

SL2 cells are maintained in Schneider's *Drosophila* medium supplemented with 10% FBS and 50 U/mL penicillin, 50 μ g/mL streptomycin. The cells were grown at room temperature without carbon dioxide at a cell concentration of 10^5 cells/cm².

3.3.2. Purification of Double-Stranded RNA

1. Starting with SCP1 cDNA subcloned in a suitable vector, a 700-bp DNA fragment spanning 121–653 nt was generated using PCR. Each primer used in the polymerase chain reaction (PCR) contained a 5' T7 RNA polymerase binding site. (GAATTAATACGACTCACTATAGGGAGA) followed by sequences specific for the targeted gene.
2. The PCR products are purified by passing through the Microspin S-400 columns.
3. Using the MEGASCRIPt kit, the purified PCR products are used as templates for transcription to produce double-stranded RNA (dsRNA).

4. The dsRNA products are ethanol-precipitated and resuspended in water. The dsRNAs are annealed by incubation at 65°C for 30 min followed by slow cooling to room temperature. Six micrograms of dsRNA are analyzed by 1% agarose gel electrophoresis to ensure that the majority of the dsRNA exists as a single band of approx 700 bp. The dsRNA is stored at -20°C.

3.3.3. Induction of RNAi in SL2 Cells

1. SL2 cells are diluted to 10⁶ cells/mL in DES serum-free medium. One mL of cells are plated per well of a six-well cell culture dish.
2. 20 µg of dsRNA is added directly to the cells per well, followed by vigorous agitation. The cells are incubated with dsRNA for 30 min at room temperature.
3. Schneider's *Drosophila* medium (2 mL) containing FBS is added. The cells are incubated for an additional 3 d to allow for turnover of the target transcript and protein, which are assayed by reverse-transcriptase PCR and Western blotting, respectively (2).

4. Notes

1. The GenBank accession numbers for the human CTD phosphatases are as follows: SCP1, AAP34397; SCP2, AAP34399; SCP3, AAP34400; FCP1, AAD42088.
2. The GST elution buffer must be prepared fresh immediately before use to prevent oxidation of glutathione.
3. It is worth noting that the conditions required to observe SCP1 activity with synthetic peptide substrates, especially pH, differ significantly from reactions in which native RNAP IIO serves as a substrate. The pH optimum for SCP1 toward synthetic CTD phosphopeptide is 5.5, whereas the pH optimum for SCP1 toward native RNAP II is 7.9, with no apparent activity at 5.5.
4. Prior to induction, remove 0.1 mL of cells and add 0.1 mL of SDS sample buffer. The samples are boiled for 10 min and 10 µL is used for SDS-PAGE. Hourly samples can be collected to determine optimal induction time. Sharper bands can be obtained if the culture is passed through a syringe several times to fragment the DNA.
5. Keep culture on ice as long as possible from this step forward to minimize proteolysis.
6. About 25% of GST-SCP1 and its mutant expressed in BL21 cells is expected to be in the soluble fraction. The eluted protein is dialyzed against the buffer for its intended use.
7. The mammalian RNAP II CTD contains at its very C-terminus a consensus CKII phosphorylation site that lies outside of the last CTD repeat. The in vitro phosphorylation of RNAP II with CKII in the presence of [γ -³²P]ATP has been used by investigators to label RNAP II for a variety of studies (18,20,21). The subsequent incubation of RNAP II with CTD kinase in the presence of excess unlabeled ATP has been used for the preparation of RNAP IIO substrates to examine CTD phosphatase activity (1,8,21,22). Because only the most carboxyl-terminal serine (CKII site) is labeled with ³²P and lies outside the consensus repeat, complete dephosphorylation by a protein phosphatase specific for the CTD results in

an electrophoretic mobility shift of subunit Ilo back to the position of subunit Ila without the loss of label (23).

8. Although MAPK2/ERK2 can easily convert GST-CTDa to GST-CTDo using the described protocol, conditions have not been defined that result in the efficient conversion of GST-CTDa to GST-CTDo with mammalian TFIIH, P-TEFb, and other CTD kinases (8).
9. It is recommended that one verifies and confirms the complete conversion of GST-CTDa to GST-CTDo or RNAP IIA to RNAP IIO via SDS-PAGE. The 0.5 μ L aliquots of (1) the starting GST-CTDa or RNAP IIA substrate, (2) GST-CTDo or RNAP IIO product prior to purification over the glutathione-agarose column or DE53 column, respectively, and (3) individual eluted fractions can be assayed to ensure completion of the phosphorylation reaction.
10. In addition to MAPK2/ERK2, different CTD kinases can be used to generate distinct isozymes of RNAP IIO (8). TFIIH, positive transcription elongation factor-b (P-TEFb), and cdc2 kinase can all be used to prepare different RNAP IIO. Given that different CTD kinases exhibit different specificity toward RNAP IIA by phosphorylating either Ser², Ser⁵, or Ser² and Ser⁵ within the CTD repeat, a panel of RNAP IIO substrates can be generated as excellent tools to evaluate the specificity of CTD phosphatases (1,8,23).
11. An equimolar mixture of RNAP IIO and GST-CTDo can be used in the same reaction to examine the dependence of CTD phosphatase(s) activity on native RNAP II (8,23). For assays involving both substrates in the same reaction, a 6% SDS-PAGE gel permits the best resolution of the phosphorylated and unphosphorylated species.

Acknowledgments

We gratefully acknowledge our mentors Gordon N. Gill and Michael E. Dahmus for their years of guidance and support. This work was supported by National Institutes of Health grants DK13149 (to GNG) and GM33300 (to MED).

References

1. Yeo, M., Lin, P. S., Dahmus, M. E., and Gill, G. N. (2003) A novel RNA polymerase II C-terminal domain phosphatase that preferentially dephosphorylates serine 5. *J. Biol. Chem.* **278**, 26,078–26,085.
2. Yeo, M., Lee, S. K., Lee, B., Ruiz, E. C., Pfaff, S. L., and Gill, G. N. (2005) Small CTD phosphatases function in silencing neuronal gene expression. *Science* **307**, 596–600.
3. Komarnitsky, P., Cho, E. J., and Buratowski, S. (2000) Different phosphorylated forms of RNA polymerase II and associated mRNA processing factors during transcription. *Genes Dev.* **14**, 2452–2460.
4. Orphanides, G. and Reinberg, D. (2002) A unified theory of gene expression. *Cell* **108**, 439–451.

5. Lin, P. S., Marshall, N. F., and Dahmus, M. E. (2002) CTD phosphatase: role in RNA polymerase II cycling and the regulation of transcript elongation. *Prog. Nucleic Acid Res. Mol. Biol.* **72**, 333–365.
6. Cho, H., Kim, T. K., Mancebo, H., Lane, W. S., Flores, O., and Reinberg, D. (1999) A protein phosphatase functions to recycle RNA polymerase II. *Genes Dev.* **13**, 1540–1552.
7. Collet, J. F., Stroobant, V., Pirard, M., Delpierre, G., and Van Schaftingen, E. (1998) A new class of phosphotransferases phosphorylated on an aspartate residue in an amino-terminal DXDX(T/V) motif. *J. Biol. Chem.* **273**, 14,107–14,112.
8. Lin, P. S., Dubois, M. F., and Dahmus, M. E. (2002) TFIIF-associating carboxyl-terminal domain phosphatase dephosphorylates phosphoserines 2 and 5 of RNA polymerase II. *J. Biol. Chem.* **277**, 45,949–45,956.
9. Cho, E. J., Kobor, M. S., Kim, M., Greenblatt, J., and Buratowski S. (2001) Opposing effects of Ctk1 kinase and Fcp1 phosphatase at Ser 2 of the RNA polymerase II C-terminal domain. *Genes Dev.* **15**, 3319–3329.
10. Kamenski, T., Heilmeier, S., Meinhart, A., and Cramer, P. (2004) Structure and mechanism of RNA polymerase II CTD phosphatases. *Mol. Cell* **5**, 399–407.
11. Chong, J. A., Tapia-Ramirez, J., Kim, S., et al. (1995) REST: a mammalian silencer protein that restricts sodium channel gene expression to neurons. *Cell* **80**, 949–957.
12. Schoenherr, C. J. and Anderson, D. J. (1995) The neuron-restrictive silencer factor (NRSF): a coordinate repressor of multiple neuron-specific genes. *Science* **267**, 1360–1363.
13. Hakimi, M. A., Bochar, D. A., Chenoweth, J., Lane, W. S., Mandel, G., and Shiekhhattar, R. (2002) A core-BRAF35 complex containing histone deacetylase mediates repression of neuronal-specific genes. *Proc. Natl. Acad. Sci. USA* **99**, 7420–7425.
14. Kokura, K., Kaul, S. C., Wadhwa, R., et al. (2001) The Ski protein family is required for MeCP2-mediated transcriptional repression. *J. Biol. Chem.* **276**, 34,115–34,121.
15. Maile, T., Kwoczynski, S., Katzenberger, R. J., Wassarman, D. A., and Sauer, F. (2004) TAF1 activates transcription by phosphorylation of serine 33 in histone H2B. *Science* **304**, 1010–1014.
16. Kang, M. E. and Dahmus, M. E. (1995) The photoactivated cross-linking of recombinant C-terminal domain to proteins in a HeLa cell transcription extract that comigrate with transcription factors IIE and IIF. *J. Biol. Chem.* **270**, 23,390–23,397.
17. Hodo, H. G. and Blatti, S. P. (1977) Purification using polyethylenimine precipitation and low molecular weight subunit analyses of calf thymus and wheat germ DNA-dependent RNA polymerase II. *Biochemistry* **16**, 2334–2343.
18. Kang, M. E. and Dahmus, M. E. (1993) RNA polymerases IIA and IIO have distinct roles during transcription from the TATA-less murine dihydrofolate reductase promoter. *J. Biol. Chem.* **268**, 25,033–25,040.

19. Wang, B. Q., Lei, L., and Burton, Z. F. (1994) Importance of codon preference for production of human RAP74 and reconstitution of the RAP30/74 complex. *Protein Express. Purif.* **5**, 476–485.
20. Payne, J. M. and Dahmus, M. E. (1993) Partial purification and characterization of two distinct protein kinases that differentially phosphorylate the carboxyl-terminal domain of RNA polymerase subunit IIa. *J. Biol. Chem.* **268**, 80–87.
21. Chambers, R. S. and Dahmus, M. E. (1994) Purification and characterization of a phosphatase from HeLa cells which dephosphorylates the C-terminal domain of RNA polymerase II. *J. Biol. Chem.* **269**, 26,243–26,248.
22. Chambers, R. S., Wang, B. Q., Burton, Z. F., and Dahmus, M. E. (1995) The activity of COOH-terminal domain phosphatase is regulated by a docking site on RNA polymerase II and by the general transcription factors IIF and IIB. *J. Biol. Chem.* **270**, 14,962–14,969.
23. Lin, P. S. and Dahmus, M. E. (2003) Dephosphorylation of the carboxyl-terminal domain of RNA polymerase II. *Methods Enz.* **370**, 155–165.

Genome-Scale Discovery and Characterization of Class-Specific Protein Sequences

An Example Using the Protein Phosphatases of Arabidopsis thaliana

David Kerk

Summary

The increasing pace of acquisition of fully sequenced genomes makes desirable a program of discovery and characterization of protein sequences of biologically significant structural classes. An example is protein phosphatases, involved in modulating reversible protein phosphorylation events underlying the whole gamut of cellular biology. The ready availability of software that can be downloaded to run on a personal computer, or accessed on a server via the Web, allows appropriate sequences to be collected and analyzed. A process is outlined here that has been successfully employed in the description of the genomic complement of protein phosphatase catalytic subunits from the model plant *Arabidopsis thaliana*. However, the methods are general and readily adapted to deal with any desired class of protein, from any organism of interest.

Key Words: Protein phosphatases; *Arabidopsis thaliana*; functional genomics

1. Introduction

Reversible protein phosphorylation, mediated by protein kinases and protein phosphatases, represents one of the most widely employed regulatory mechanisms in cellular physiology. It is especially desirable to obtain more data about protein phosphatases, as knowledge in this area has traditionally lagged somewhat behind the more heavily investigated protein kinases. Yet several recent reports have stressed the emerging significance of protein phosphatases for the understanding and potential treatment of human disease (1–3). Several years ago our laboratory published a survey of the catalytic subunits of protein phosphatases encoded by the genome of the model plant *Arabidopsis*

From: *Methods in Molecular Biology*, Volume 365: *Protein Phosphatase Protocols*
Edited by: G. Moorhead © Humana Press Inc., Totowa, NJ

thaliana (4). At that time, knowledge of the physiological significance of protein phosphatases was confined to a few well-studied examples. Since that time, newer studies have begun to reveal the more widespread significance of protein phosphatases in plant physiology (5–7). This chapter is an updated report on the latest set of protein phosphatase catalytic subunits detectable in the revised genome sequence of *A. thaliana*. The bioinformatic techniques underlying this analysis are universal in scope, however, and readily modified to study the genome-scale distribution of protein sequences of any class of interest to an investigator.

The sequence alignment tool BLAST (8) is routinely used on a genomic scale now to pick out newly inferred coding sequences with a high degree of similarity to previously characterized proteins. This annotated information, in many instances, has provided valuable initial leads into the possible functions of a putative protein. However, in many instances, similarity between two proteins at the primary sequence level is insufficient to provide confidence in a hypothesis of homology. A variety of techniques have been developed that utilize the information inherent in a set of similar sequences to produce a sequence “probe,” which captures the collective structural variation of the whole set. These are in fact mathematical models that specify a probability that a given amino acid will occupy a given position within the sequence. The input to such mathematical models is typically a multiple-sequence alignment, which generates a series of columns where characters from the various component sequences are optimally aligned (for the principles underlying multiple-sequence alignment, the reader is referred to **ref. 9**). From this starting material, sequence probe models can be produced, which have been described as “position-specific scoring matrices” (PSSMs), “profiles,” “generalized profiles,” or “Hidden Markov Models,” depending on details of the technique and model formulation. It has been demonstrated on many occasions that multiple-sequence-based models have superior power to find distantly related sequences (“sensitivity”) while rejecting sequences whose structural resemblance is the result of chance alone (“specificity”) (e.g., see **ref. 10**). The collection of sequences of interest is an iterative process. An initial sequence model is generated (typically from a curated set of related protein sequences) and used to search the database, where it detects and retrieves similar sequences. These are then added to the previous multiple-sequence alignment. A revised model is then generated, and the search-and-retrieval process is repeated until no further sequences of interest are obtained. This chapter will feature the use of Hidden Markov Models as the multisequence probe, as implemented in the program package HMMER (11).

An additional very powerful use of multiple-sequence alignments is the analysis of critical conserved residues, with functional inferences often being

possible, and the reconstruction of patterns of sequence evolution through the inference of phylogenetic trees. Such a tree represents a graphical hypothesis of the evolutionary relationship between sequences. Although there are several tree inference methods, whose theoretical justifications vary, the intuitive principle is maintained that sequences closer together in the tree are in some sense more highly related (share a more recent common ancestor) than those more distant in the tree. A well-constructed phylogenetic tree, in addition to describing an evolutionary scenario for the sequences at hand, also has very practical applications. Sequences that are closely adjoining in the tree share substantial structural similarity and might have functional similarities as well. Thus, a rational strategy can be adopted for sampling the function of a large number of unknown sequences by examination of a well-chosen set that spans a number of regions of a tree.

Three methods are the most widely employed for phylogenetic tree inference. The Neighbor Joining procedure ([12,13](#)) is an algorithmic process that determines a single best tree, starting with an estimate of evolutionary distance between sequences. The Maximum Parsimony method ([13,14](#)) determines the tree that contains the fewest sequence changes from a postulated ancestral sequence. This involves two distinct processes: generation of candidate tree topologies and evaluation of each by an optimality criterion. Maximum Likelihood determines the tree that has the highest probability of arising from the given sequence dataset. This also involves a topology generation procedure and an optimality criterion ([13](#)).

A measure of reliability of the branch points (“nodes”) of phylogenetic trees that is commonly employed is the “bootstrap.” The procedure consists of producing replicate multiple-sequence alignments (“bootstrap replicates”) where the size of the dataset remains constant, but columns of data from the original alignment are used randomly. The tree inference procedure is then used to generate a tree from each bootstrap replicate alignment, and a “consensus” tree is then derived from this set. Each node in the tree is assigned a “bootstrap number” corresponding to the percent of the replicate trees in which that node appears. A node is considered to be stable when this percentage is high (50% is common as a minimum for consideration) and when it is confirmed by multiple tree inference procedures. For a more detailed discussion of phylogenetic tree inference approaches and evaluation by the bootstrap procedure, the reader is referred to **ref. 13**.

This chapter will present a detailed procedure for utilizing the above techniques to identify protein phosphatase catalytic subunits. The dataset will cover three principle sequence types: the serine/threonine phosphatases (STs) of the protein phosphatase P (PPP) family, STs of the protein phosphatase *M* (PPM) family (protein phosphatase 2C [PP2C] subfamily), and dual-specificity

(tyrosine and serine/threonine) phosphatases (DSPs). For more details about protein phosphatases, the reader is referred to **refs. 4** and **15**. The reader is referred to **Fig. 1**, which contains a flowchart of the procedures to be presented.

2. Materials

2.1. Starting Motif Models and Multiple-Sequence Alignments

1. To work with a motif or domain of interest, use the Pfam database (**16**): <http://pfam.wustl.edu/>.
2. To work with *A. thaliana* protein phosphatase classes, alignments can be obtained from the author's website: http://www.ptloma.edu/biology/faculty/Kerk/ppa_data.htm.

2.2. Organismal Protein Database

1. General sites to research genome projects: GOLD (Genomes On Line Database) (**17**) <http://www.genomesonline.org/>; NCBI (National Center for Biotechnology Information) Genomic Biology page: <http://www.ncbi.nlm.nih.gov/Genomes/>; DOE (Department of Energy) JGI (Joint Genomes Institute): <http://www.jgi.doe.gov/>.
2. *A. thaliana* genome information: TAIR (The Arabidopsis Information Resource) (**18**) <http://www.arabidopsis.org/>; TIGR (The Institute for Genomic Research) <http://www.tigr.org/tdb/e2k1/ath1/>.

2.3. Database Search Software

1. HMMER (**11**) : <http://hmmer.wustl.edu/>.
2. Cygwin (a Linux-like environment that allows a version of HMMER to run on a personal computer with Windows): <http://www.cygwin.com/>.

2.4. Multiple-Sequence Alignment Software

1. ClustalX (**19**): <http://bips.u-strasbg.fr/fr/Documentation/ClustalX/>.
2. MUSCLE (**20**): <http://www.drive5.com/muscle/>.

2.5. Alignment Evaluation

TCoffee (**21**): http://igs-server.cnrs-mrs.fr/Tcoffee/tcoffee_cgi/index.cgi.

2.6. Sequence Display and Editing Software

GeneDoc (**22**): <http://www.psc.edu/biomed/genedoc/>.

2.7. Phylogenetic Tree Inference Software

1. PHYLIP : <http://evolution.genetics.washington.edu/phylip.html>.
2. TREE-PUZZLE (**23**): <http://www.tree-puzzle.de/>.

2.8. Phylogenetic Tree Viewing Software

TreeView (**24**): <http://taxonomy.zoology.gla.ac.uk/rod/treeview.html>.

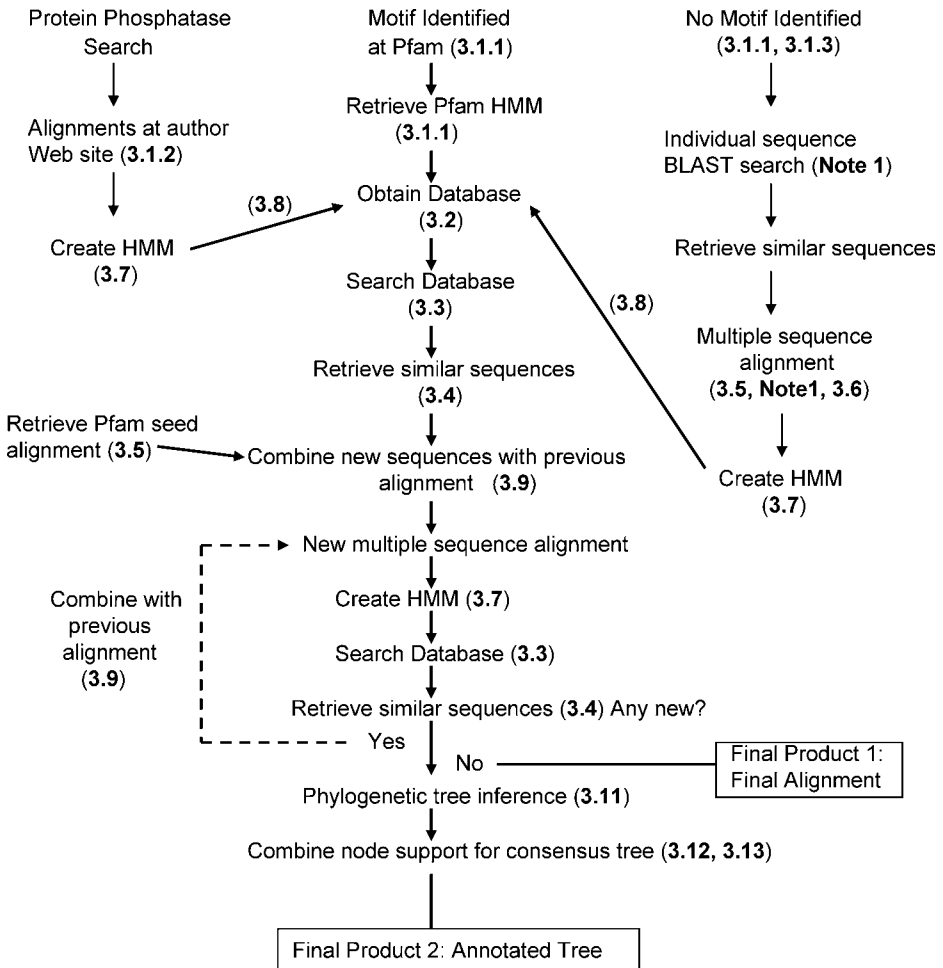


Fig. 1. Schematic chart of bioinformatic workflow. The sequential procedures to be followed by an investigator in the discovery and characterization of a protein class of interest are diagrammed. Three possible initial approaches are presented in the three columns, with the most generally applicable one being in the center. The relevant sections of the chapter are given in parentheses. The two final products of the analysis are boxed.

3. Methods

3.1. Obtaining an Appropriate Sequence Model

3.1.1. A General Approach

An investigator might wish to search for sequences containing a type of domain or motif that has previously been characterized. This interest might

arise from reading the literature or through initial analysis of a particular sequence under study. In either instance, a useful starting point is the Pfam (“Protein families”) database. This resource contains a large collection of motif models, which are in the form of Hidden Markov Models (HMMs) constructed from multiple-sequence alignments, using the HMMER software package. To facilitate the retrieval of these models, the database has both text-based and sequence-based search capabilities.

1. Retrieval of a motif model based on text information. At the Pfam homepage, the links “BROWSE PFAM” or “KEYWORD SEARCH” can be used to find entries for motifs discussed in the literature. If a link is activated for a motif, the result is the display of an “entry” page, where a summary description of the motif, literature references, and a link to the HMM itself are stored. At the bottom of this page is a section entitled “HMMER Build Information”. There is a link “Pfam_ls”, which leads to a model designed to find complete motifs in a target sequence. This model can then be downloaded and used to search any desired database. (Note: In this and all subsequent sections discussing HMMER program features, basic options are presented. For a full discussion of the background to this package and its many advanced options, the reader is referred to the HMMER user manual, available at the HMMER website).
2. Retrieval of a motif model based on sequence information. At the Pfam homepage, the feature “PROTEIN SEARCH” can be used by pasting in a desired query sequence. The results page that comes up will include a graphic summary of any motif hits which the sequence contains and links to those motifs, that when activated will bring up the corresponding motif “entry” page. The motif model can then be retrieved as described above.

3.1.2. A Specific Approach Directed Toward Protein Phosphatase Classes

If the reader is specifically interested in classes of protein phosphatases, then multiple-sequence alignments are available at the author’s website: http://www.ptloma.edu/biology/faculty/Kerk/ppa_data.htm.

An initial model can then be made, as described in **Subheading 3.7**.

3.1.3. Beginning a Search Without a Motif Model

Analysis of a sequence of interest at Pfam might reveal that it contains no previously characterized motifs. Provided that there are at least some sequences present in public databases with a reasonable degree of similarity, it is still possible to develop a multiple-sequence alignment and sequence model (*see Note 1*).

3.2. Identification and Download of a Sequence Database

Once a suitable starting model is in hand, it can be used to search an appropriate sequence database. This can be located using the sites given in **Subheading 2**.

3.3. Search of the Sequence Database with the Sequence Model

To search a sequence database with HMMER:

1. Place the new HMM and the database to be searched in the same directory on your computer
2. Invoke the search with the following command syntax:
`hmmsearch -E 1 modelname databasename > outputfilename`
HMMER is a fast program; this search will only take a few minutes.

3.4. Harvest of New Sequence Hits Obtained by Use of the Sequence Model

HMMER returns a text file from the search, which contains several sections. The top section lists the sequences (“hits”) found by the search motif model, with information about each derived from the annotation line in the database entry. The sequences are presented in rank order with the best first. The ranking is by alignment score and by “*E* value.” The latter is a useful statistical measure of the number of times a random sequence with that numerical score would be returned from the database search by chance alone. *E*-Values can range from 0 (the very best possible) to 10, which is the default program setting. In practice, it is up to the investigator to determine an acceptable cutoff *E* value. A value closer to 0 (e.g., e^{-10}) would achieve greater specificity, whereas the suggested value of 1 achieves greater sensitivity. Given that candidate sequences will be evaluated for structural similarity by the exacting method of construction of multiple-sequence alignments (see below), any false positives obtained at this step should become apparent later. The next section tabulates the hit sequence names, starting and stopping point in the sequence with similarity to the model, the start and stop position of the model region that was aligned to the new sequence, and the score and *E* value for the hit. The final section consists of the alignments between the HMM and each sequence hit. For each hit, the HMM sequence is on top, the hit sequence is on the bottom, and between them are symbols or letters indicating the degree of similarity at each position.

1. Copy the second section of the HMMER output (the list of motif hits) and place it into a new text file.
2. Import this file into a spreadsheet program.

3.5. Creation of a Multiple-Sequence Alignment From Database Sequence Hits

There are now several alternative programs available to perform multiple-sequence alignments. ClustalX (19) is the oldest and still has many useful features (see later). TCooffee (21) also has some excellent features, but for

genome-scale work, it has the restricting limitation that it cannot generate an alignment of more than 50 sequences. MUSCLE (20) and ProbCons (25) are relative newcomers. ProbCons has the highest objective alignment accuracy of any method reported to date; however, MUSCLE is by far the fastest. Because genome-scale applications often involve large alignments, this chapter will present the use of MUSCLE (see below).

High-quality multiple-sequence alignments of a large number of protein phosphatase sequences from various classes were constructed for the study of Kerk et al (4). Nevertheless, for this chapter, new alignments were made from scratch. This was done for two reasons: (1) The genome had undergone several revisions since the referenced 2002 publication and sequences might have been revised based on newer mRNA data; (2) new multiple-sequence alignment methods had been published since that date (MUSCLE and ProbCons), that warranted evaluation on these datasets. For this study, then, an HMM was constructed which corresponds to each of the previous alignments (procedure to be described below). This model was used to search a recent *A. thaliana* protein sequence database. A set of sequence hits was collected (including the sequences present in the old alignments, plus other new hits), and new alignments were built. Of the available multiple-sequence alignment construction methods introduced earlier, MUSCLE and ProbCons performed best with the present datasets, yielding alignments of roughly equivalent quality (evaluation procedure to be presented below). The procedure for using MUSCLE is presented in **Note 1**.

If the investigator found a motif of interest at Pfam, it is now necessary to retrieve a multiple-sequence alignment containing sequences possessing this motif. If one goes back to the Pfam “entry” page for the motif described earlier (**Subheading 3.1.1**), there is a section labeled “Alignment.” The default setting is “Seed,” which indicates a manually curated alignment. Use the “retrieve alignment” feature to obtain this alignment in either “GCG MSF format” or “Aligned FASTA format.” Proceed to **Subheading 3.9**.

3.6. Editing the Multiple-Sequence Alignment

The output from any multiple-sequence alignment program will typically require manual examination and hand-editing. This requires a flexible, easy-to-use editing program. Although the program SeqLab in the Wisconsin Sequence Analysis package (Accelrys) has long been a favorite, it requires a license, which might be beyond the means of some investigators. The program GeneDoc is free and runs on a personal computer with a convenient graphical user interface. The program is highly flexible and contains numerous features, which must be explored to discover what the user desires as optimal settings. A group of recommended configuration settings is given below.

3.6.1. Rearranging Sequences to Optimize the Alignment

1. Open the sequence file to be edited. If this is a revised file done with ClustalX using the Profile Alignment Mode and saved in the “.msf” format, it can be opened directly. If it was generated with MUSCLE and is an aligned FASTA file (in the “.afa” format), then a “blank” page must be created and the Import function used [“File” → “Import” → “FASTA (Pearson)”]
2. On the top toolbar, second row, are two buttons that control alternative screen displays, which can be very helpful. The “C” (“Conserved”) button allows the sequences to be displayed in black and white, but with conserved columns highlighted. The “P” (“Properties”) button shows sequences in color, arranged by user-defined chemical criteria (*see* **Note 2**).
3. Other useful editor functions are (1) “Arrange” → “Slide Sequences”, (2) “Arrange → Insert Gaps in Other Sequences”, and (3) “Arrange → Delete Gaps from Other Sequences”.
4. Using the editor functions, rearrange the sequences to obtain the optimal alignment by eye (i.e., the alignment that seems to conserve the greatest number of characters in columns across the alignment).

3.6.2. Evaluating the Quality of the Alignment

It is often helpful, particularly with a divergent (and therefore difficult) sequence set, to obtain an objective evaluation of the quality of the multiple-sequence alignment. If the alignment has less than 50 sequences total, this can be performed by the TCoffee server (*see* **Note 3**). Select “Evaluate a multiple alignment” → “Advanced”; upload the sequence file (it must be in “.aln” format); select “Pairwise methods” → “Mslow_pair” (unselect the other options); select “Multiple Methods” → “Mclustalw_aln”. When the run is completed, open the link “score_html” in a new browser window.

A graphical output is produced that shows a numerical score for the whole alignment, a score for each sequence, and a color-coded display showing areas with more and less trustworthy alignment. If warranted by this output, the editing step can be repeated to revise the appearance of the alignment.

3.6.3. Deleting Data From the Alignment

At this point, it is usually desirable to delete either entire sequences, or delete columns of poorly aligned sequence, as appropriate to the needs of the project (*see* **Notes 4** and **5**). To delete taxa (entire sequences) in GeneDoc: “Project” → “Edit Sequence List” → Highlight sequence → “Delete” → “OK” → “Done”. To select and delete columns of data in GeneDoc: “Edit” → “Select Columns”; “Edit” → “Delete All Data”. It is desirable at this point to repeat the evaluation of the revised alignment (**Subheading 3.6.2.**) to assess the effects of deleting columns. As a rule of thumb, a good alignment with a “well-behaved” set of sequences (not too divergent) might give a total score in the

sixties or seventies (e.g., see **Fig. 2A,B**). A good alignment with a divergent set of sequences might give a total score in the forties (e.g., see **Fig. 4**). If at this point the alignment appears poor, a different strategy might be necessary (see **Note 6**). Once the alignment has been optimized, GeneDoc can print it out or it can produce a Rich Text Format (“.rtf”) file as follows: “Edit” → “Select Blocks for Copy” → click on the alignment → “Edit” → “Copy Selected Blocks to” → “RTF File”. This file can then be opened by Microsoft Word and labeled as desired. It can then be converted into a Portable Document Format (“.pdf”) file if the program Adobe Acrobat is available.

3.7. Creation of an HMM

The completed multiple-sequence alignment is used to create a model to be used for subsequent database searches.

1. Create a Hidden Markov Model with the HMMER software. The HMMER package is command-line-driven software. It will run on a personal computer with Windows if the Cygwin environment has been installed. The command syntax is `hmmbuild yourhmmfilename youralignmentfilename`. *Note:* HMMER requires the alignment to be in ClustalW (“.aln”) format.

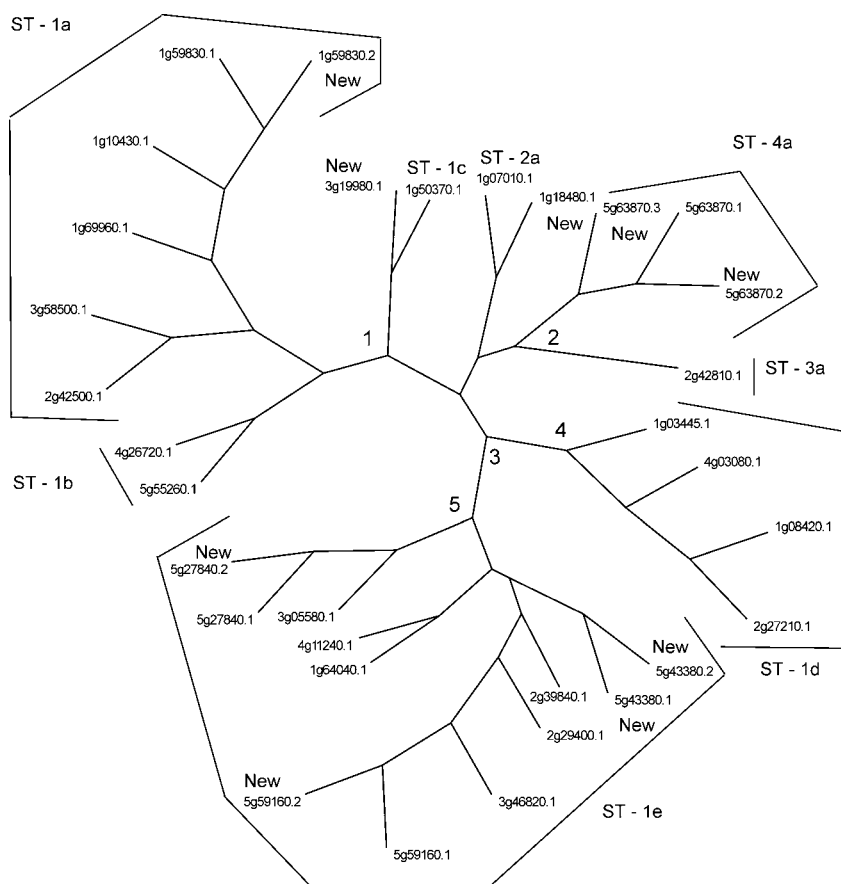
It is worth taking note of the screen information that comes up at the end of this run. It displays the Average Score, Min Score, and Max Score obtained by the input alignment with the newly created model: The higher the scores, the better. With some experience working with HMMER, it becomes easier to recognize a good multiple-sequence alignment by the way that these scores behave. Better alignments tend to produce higher scores.

2. Calibrate the new HMM. For the new HMM to be maximally effective, it needs to be calibrated. This entails producing many randomized sequences, testing the model against these, and summarizing the model’s performance statistics. The model file is modified so that these results “tag along” with it, which enhances the specificity of its performance later. The command syntax is `hmmcalibrate yourhmmfilename`.

Fig. 2A,B. Multiple-sequence alignment of ST protein phosphatase sequences. Sequences were collected and aligned through the repetitive process of database searching, alignment building, evaluation, and editing, model building, and database re-searching described in **Subheading 2**. The initial HMM was derived from the ST protein phosphatase sequence alignment of Kerk et al. (4). This represents a “well-behaved” alignment where sequences (with the exception of 1g18480.1) were not very difficult to align. The overall TCoffee evaluation score for this alignment was 68, with individual sequence scores ranging from 26 to 76. The following sequences were rejected during the alignment process: At1g48120.1, At2g42500.2, At5g10900.1. Multiple-sequence alignment of ST protein phosphatase sequences.

B

[illegible]



_100

Fig. 3. Radial phylogenetic tree from ST protein phosphatase sequence comparisons. Multiple-sequence alignments were subjected to phylogenetic tree inference by Neighbor Joining (NJ) using the ClustalX program, Maximum Parsimony (Pars) using PHYLIP, and Maximum Likelihood (ML) using Tree-Puzzle, as detailed in **Subheading 3**. The topology of the Maximum Parsimony tree is shown. Clusters are labeled as in Figs. 2 and 3 of Kerk et al. (4). Newly identified sequences are labeled "New." The correspondence between the cluster designations and conventional protein phosphatase terminology is as follows: ST-1e = PP1; ST-1a = PP2A; ST-1b = PP4; ST-1c = PP6; ST-3a = PP5; ST-4a = PP7; ST-1d = Kelch domain PPP. The percent bootstrap support for the indicated nodes is as follows (NJ, Pars, ML): 1 (100, 98.6, 68.2); 2 (51.9, 99.1, 51.6); 3 (100, 59.8, 57.2); 4 (100, 97.8, 66.8); 5 (89.1, 99.1, 68.9). Note that most of the deep nodes of the tree can be resolved; this reflects agreement among the tree inference methods, with adequate bootstrap support. This is a consequence of the relatively high degree of conservation of the sequences (as revealed by an inspection of the multiple-sequence alignment and the relatively high alignment evaluation scores).

The screen information displayed at the end of this run is also worth noting. “Mu” (the mode of the distribution of random scores) and “max” (the best random score) are displayed. Now, smaller is better. These scores will be negative. One wants to see the largest spread possible between the max of the random scores and the min of the scores from the alignment used to make the model. This indicates that the model will be more specific (will have a higher discriminating ability between random sequences and true positives).

3.8. Repeat the Database Search and Harvest of Hits

Repeat the work in **Subheadings 3.2–3.4**.

3.9. Creation of a Modified Multiple-Sequence Alignment

The next task is to combine the newly found database hit sequences to the previously constructed multiple-sequence alignment. A program that has features convenient for this purpose is ClustalX (an implementation of the ClustalW package with a convenient graphical user interface for a personal computer). Change the control window from “Multiple Alignment Mode” (the default) to “Profile Alignment Mode”. Then load the old alignment as follows: “File” → “Load Profile 1”; then direct the program to the alignment file. Load the new sequence(s) as follows: “File” → “Load Profile 2”; then direct the program to a text file of the sequences. When this setup is completed, the alignment works as follows: “Alignment” → “Align Sequences to Profile 1”.

3.10. Repetition of Processes

Repeat processes **Subheadings 3.6**. (multiple-sequence alignment editing), **3.7**. (HMM creation), **3.3**. (database search), and **3.4**. (harvest of hits) until no new sequence hits at the cutoff *E* value are obtained.

3.11. Inferring a Phylogenetic Tree From Multiple-Sequence Alignment Data

3.11.1. The Neighbor Joining Method

Open ClustalX and load the multiple-sequence alignment file. Set the tree output format so that the bootstrap numbers are at the nodes, rather than the default (at the branches): “Trees” → “Output format options” → “Bootstrap labels on NODE” → “CLOSE”. Set up the bootstrapped Neighbor Joining run: “Trees” → “Bootstrap NJ Tree” → “Random number generator seed” → enter a numerical value (to make sure the runs are randomized, do not use the default value all the time); “Number of bootstrap trials” → set a numerical value (usually 1000). For moderate-sized alignments (<100 sequences), this is very fast. For very large alignments (hundreds of sequences), it might take a few hours, or run it overnight. “SAVE PHYLIP TREE AS” → enter output file name.

Note that the format of the output file is “.phb”; this will be readable by the tree output viewing program (see **Subheading 3.12.**).

3.11.2. The Maximum Parsimony Method

A widely used implementation of Maximum Parsimony is a component of the PHYLIP package. This is a command-line-driven program. A run involves several steps: (1) produce a set of bootstrap replicate alignments; (2) apply maximum parsimony; and (3) generate a consensus phylogenetic tree. All PHYLIP programs want to work with an input file called “infile” and produce an output file called “outfile” (or, sometimes, “outtree”). As these are not very informative, UNIX commands can be used to rename files at each step (see below).

1. Use GeneDoc to create an output file in PHYLIP format. It is important to observe name-length restrictions for PHYLIP (see **Note 7**). “File” → “Export” → “Phylip” → “Export” → create a file name → “Save” → “Done.”
2. Place the PHYLIP alignment file in the directory where the tree output is desired.
3. Execute the PHYLIP program “Seqboot” to create the bootstrap replicate alignments. To start the program, use the command seqboot (hit Enter). The program will now prompt you for the full name of the input file; *yourfilename* (hit Enter); in response to the screen prompt, type *r* (for replicates) (hit Enter); “number of replicates” → enter a number (usually 1000); in response to the screen prompt, type *y* (for yes) (hit Enter); “Random number seed (must be odd)” → enter a number (use a different number for different runs) (hit Enter). The program will create an output file called “outfile”. Rename this file as follows: `mv outfile yournewfilename` (hit Enter). The program seqboot is very fast; this will be done in a few seconds.
4. Execute the PHYLIP program “Protpars” (for protein maximum parsimony). To start the program, use the command protpars (hit Enter). The program will now prompt for the full name of the input file *yourfilename* (hit Enter); in response to the screen prompt, type *j* (hit Enter) (this toggles the switch to randomize the sequence input order); “Random number seed (must be odd)” → enter a number (use a different number for different runs) (hit Enter); “Number of times to jumble” → enter a number (e.g., 1) (hit Enter); in response to the screen prompt, type *m* (hit Enter) (this toggles the switch to analyze multiple data sets); “Multiple datasets or multiple weights (type D or W)” → type *d* (hit Enter); “How many data sets?” → Type number processed by seqboot above (hit Enter); in response to the screen prompt, type *y* (for yes) (hit Enter).

Protpars is very slow compared to ClustalX’s Neighbor Joining. A small alignment (approx 30 sequences) will take a couple of hours. A larger alignment (approx 100 sequences) will require an overnight run. An alignment with hundreds of sequences might take several days, depending on how many bootstrap replicates that you have specified and the number of processes running on your system.

Protpars can be very demanding of system resources for large datasets (alignments over about 150 sequences). It might be necessary to break the run up into smaller portions to obtain all of the desired bootstrap replicates (*see Note 8*).

The program will return two output files: “outfile” is a text file showing a rough graphical representation of the parsimony tree(s) for each replicate bootstrap alignment; “outtree” is the file containing the text (Newick) representation of each of the parsimony trees for the bootstrap replicate alignments. The “outfile” might be very large (several megabytes) for a large alignment run with many bootstrap replicates. The “outtree” file will be fairly small. Rename the protpars output files: `mv outfile yournewfilename` (hit Enter); `mv outtree yournewfilename` (hit Enter).

5. Execute the PHYLIP program “consense” to create a consensus phylogenetic tree. To start the program, use the command `consense` (hit Enter). The program will now prompt for the full name of the input file; *yourfilename* (hit Enter). Run this program on default settings by hitting *y* (for yes) at the screen prompt after the input file is loaded. This program produces two output files: “outfile” and “outtree.” These files have the same contents described above, except for the consensus tree. The latter is the desired file for further analysis. Rename the consense output files: `mv outfile yournewfilename` (hit Enter); `mv outtree yournewfilename` (hit Enter).

3.11.3. The Maximum Likelihood Method

The Maximum Likelihood approach is intrinsically the most computationally intensive of the phylogenetic tree inference methods, as there are several levels at which complex probability calculations must be performed. The TREE-PUZZLE program (23) implements an approximation of this approach, where the probability calculations are applied to successive sets of sequences: four at a time. This conceptual approximation is called “quartet puzzling.” The quartet trees are then combined in different orders into a large number of intermediate trees, which are then summarized in a final consensus tree. This approximation makes the Maximum Likelihood approach practical for routine use. Even so, the program can be time-consuming. The analysis of a small alignment (approx 30 sequences) takes about 5 min, whereas that of a large dataset (approx 100 sequences) takes about 2 h. TREE-PUZZLE can run on a personal computer, but it uses a command-line-type interface.

1. Use GeneDoc to create a multiple-sequence alignment in PHYLIP format (“.phy”): “File” → “Export” → “Type of File” → “Phylip”.
2. Starting the program produces the screen prompt “Please enter file name.” This will be *yourfilename* if the file is in the same directory as the program executable. If the data file is in a different directory, then it is necessary to enter here a full path to the file, plus the file name. At the screen prompt, type *j* and hit Enter. This toggles the “List puzzling step trees?” option from “No” to “unique topologies.” This is necessary to produce detailed output from which a consensus tree can be

reconstructed later. At the screen prompt, type *m* and hit Enter. This toggles the “Model of substitution” option. Repeat this process until “BLOSUM62” appears. To begin the program, type *y* (for yes) and hit Enter.

3. The program produces four output files: “yourfilename.dist,” “yourfilename.puzzle” (a summary of the run information and a text representation of the consensus tree), “yourfilename.tree” (a Newick formatted consensus tree file), and “yourfilename.ptorder” (a file with each of the intermediate trees in Newick format) (this last will be a large file—several megabytes).

The trees that the program produces by default displays nodes resolved at the 50% support level or better. For some purposes, this might be adequate. However, it is often desirable to compare the support for all nodes in the output trees. To do this, set the flag to list all the puzzling tree steps, as explained above. This allows the consense program of PHYLIP to produce a consensus tree with support for all nodes labeled.

4. Export the “.ptorder” file to a directory accessible to the PHYLIP program package
5. Use the PHYLIP program consense to produce a consensus tree from this TREE-PUZZLE “.ptorder” file, as in **Subheading 3.11.2., step 5.**

3.12 Viewing the Phylogenetic Trees

The output of the phylogenetic tree inference programs is a text file with tree information in the Newick format. This must be read by appropriate software to display the familiar graphic representations. A convenient program is TreeView, which can open trees formatted either as “tree” files (“.ph” or “.phb”) or text files. There are several display options controlled by a top row of toolbar buttons. Two useful representations are “Radial tree” or “Rectangular cladogram”. Bootstrap values can be displayed by “Tree” → “show internal edge labels”. Various font styles and sizes are available (sometimes it is necessary to reduce the font size to optimize display of crowded trees). Results can be printed out (larger alignments on multiple pages): “File” → “Print setup” → “Pages” (1–3). Graphic images can be saved: “File” → “Save as graphic”. This will be a “.emf” file (a vector graphic file), which can be imported into other graphics programs.

3.13 Annotating the Phylogenetic Tree

The investigator will want to compare the support for the various nodes of the phylogenetic trees produced by the different inference methods. Hallmarks of high-quality dataset are trees whose topologies are concordant (i.e., identical or similar branching patterns) and where nodes enjoy strong bootstrap support (at least 50%) (e.g., **Figs. 3** and **5**, and **Table 1**).

4. Notes

1. If the investigator begins with a single sequence without known motifs, the first step is to perform a BLASTP search. A convenient site is at the National Center



Fig. 4. Multiple-sequence alignment of DSP protein phosphatase sequences. Sequences were collected and aligned through the repetitive process of database searching, alignment building, evaluation and editing, model building, and database re-searching described in **Subheading 3**. The initial HMM was derived from the DSP protein phosphatase sequence alignment of Kerk et al. (4). This represents a more difficult alignment. The critical conserved Asp (D) at position 56 in the alignment lies in a variable loop with little sequence conservation. Three sequences have a Glu (E) at this position, and their catalytic activity would be verified experimentally (At1g05000.1, At2g32960.1, At4g03960.1). The overall TCoffee evaluation score for this alignment was 41, with individual sequence scores ranging from 26 to 50. The following sequences were rejected during the alignment process: At1g71860.1, At1g71860.2.

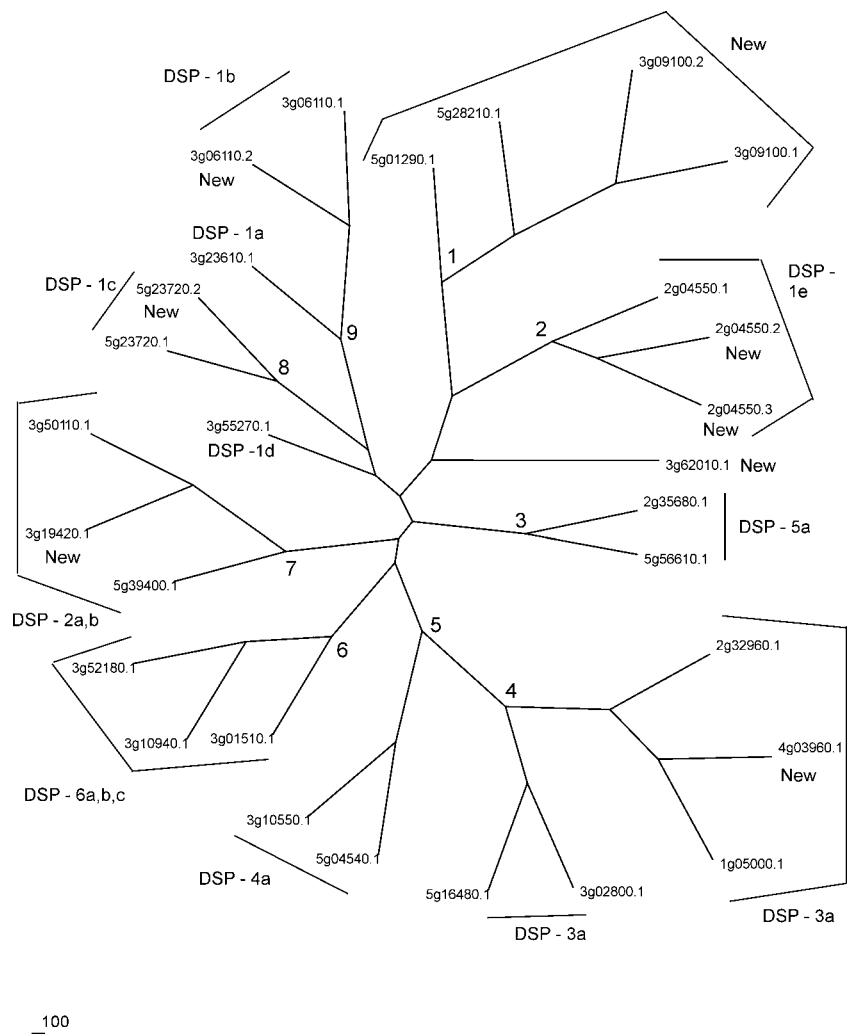


Fig. 5. Radial phylogenetic tree from DSP sequence comparisons. Multiple-sequence alignments were subjected to phylogenetic tree inference by Neighbor Joining (NJ) using the ClustalX program, Maximum Parsimony (Pars) using PHYLIP, and Maximum Likelihood (ML) using Tree-Puzzle, as detailed in **Subheading 3**. The topology of the Maximum Parsimony tree is shown. Clusters are labeled as in Figs. 5 and 6 of Kerk et al. (4). Newly identified sequences are labeled "New." The correspondence between the cluster designations and previously established structural relationships is as follows: DSP-2a,b = PTEN-related; DSP-6a,b,c = Laforin-related; New = putative mRNA capping proteins. The percent bootstrap support for the indicated nodes is as follows (NJ, Pars, ML): 1 (100, 98.9, 93); 2 (100, 98.9, 97.1); 3 (100, 98.9, 95.8); 4 (100, 97.8, 78.3); 5 (59.8, 64.2, 31.4); 6 (99.7, 84.3, 69.3); 7 (100, 98.5, 53.9);

for Biotechnology Information (NCBI): <http://www.ncbi.nlm.nih.gov/BLAST/>. One can then harvest the sequences with strong to moderate E values ($E < e^{-10}$ or lower) and align with MUSCLE. Once an initial multiple-sequence alignment is obtained, proceed as discussed in **Subheading 3.6**. The use of MUSCLE to obtain that initial alignment will be detailed here. MUSCLE is a command-line-driven program that runs under a command screen in Windows. “Start” → “Run” → “cmd” brings up the command screen. To navigate to the appropriate directory, use the commands “cd” to changes directories; “dir” lists the contents of directories. Remember that spaces in folder names are not recognized (e.g., the command cd Program Files must be entered as cd “Program Files”). The easiest thing to do is to place the input files in the same directory as the program. The command syntax is as follows: muscle -in *yourinputfile* -out *youroutputfile*. The default output file type is “.afa”, which is an aligned FASTA format. This is fine to input into GeneDoc. For this project, MUSCLE with default settings produced high-quality starting alignments, with an input sequence set containing a size range of about 100 to about 400 residues. Like any global alignment program, however, MUSCLE will probably not perform well if there are extreme variations in sequence length. If this is the case, it is advisable to try to isolate those sequence regions that contain features that require examination in more detail.

2. Configuration of GeneDoc. Shading of conserved residues: Toolbar, top “C” button (“Configuration Dialog”) → “Shade” tab → Leave default shading scheme; “Conserved Percent”: Primary 80, Secondary 65, Tertiary 50; → “Property” tab → “Level 3” → Highlight Level 1 in the text window, then “Edit” → when the “Edit/Add Property Group” dialog box appears, enter the character(s) you desire, then “OK.” “Text color” → select from the color palette (black or white characters work well here), then “OK.” “Back Color” → select from the color palette (suggested color choices are listed below), then “OK.” This is done in turn for the seven levels, to produce the following color scheme (this reproduces the default color scheme of the ClustalX application, facilitating use of both programs easily): Level 1: G (Black on Orange); Level 2: P (Black on Yellow); Level 3: TSNQ (Black on Green); Level 4: WLVMAFC (White on Blue); Level 5: HY (Black on Cyan); Level 6: ED (Black on Magenta); Level 7: KR (Black on Red). When this is completed, go to the top text toolbar, and use “Project” → “Save User Defaults.” When an alignment file is first loaded after this, it is necessary to use “Project” → “Load User Defaults.” After this first use, in subsequent uses of that alignment, the program will automatically load these settings. The “C” (“Conserved”) and “P” (“Properties”) buttons on the toolbar can now be used to

8 (100, 98.9, 95.3); 9(100, 98.7, 99.8). Note that the deep nodes of the tree cannot be resolved; there is either disagreement among the topologies of the tree inference methods or the bootstrap support is weak (below 50%). This is a consequence of the divergence of the sequences (as revealed by an inspection of the multiple-sequence alignment and the relatively low alignment evaluation scores).

Table 1
Summary of PP2C Phylogenetic Tree Data

Cluster	Neighbor Joining	Maximum Parsimony	Maximum Likelihood	Newly identified sequences in cluster
<i>A. thaliana</i> #1a	100	93.7	95.2	At2g46920.2
<i>A. thaliana</i> #2b	100	98.2	33.8	At3g05640.2, At3g16800.2, At4g03415.1, At5g27930.2
Plant #1	100	92.2	67.2	None
Plant #2	99.5	42	94.8	None
Plant #3	76.9	39.3	59.1	At1g78200.2, At2g20630.2, At3g15260.2
Plant #4c	64.6	78.1	61.7	None
Plant #5	100	98.2	61.4	At3g62260.2
Plant #6	100	98.2	84.2	At3g55050.2, At4g38520.2
Plant #7	100	98.2	63.4	At1g09160.2
Plant #8	100	98.2	72.9	None
Newd	100	98.2	33.8	At2g30170.1, At4g16580.1, At4g33500.1, At5g66720.1 At5g66720.2

Note: Multiple-sequence alignments were subjected to phylogenetic tree inference by Neighbor Joining using the ClustalX program, Maximum Parsimony using PHYLIP, and Maximum Likelihood using TREE-PUZZLE, as detailed in **Subheading 3**. Cluster names are from Kerk et al. (4). (However, only *A. thaliana* sequences were run in this analysis.) Percentage bootstrap support for each cluster node is given for each of the tree inference methods. The correspondence between the cluster designations of Kerk et al. (4) and Schweighofer et al. (7) is as follows: Plant # 1 = Group A; Plant #2 = Group B; *A. thaliana* #1 = Group C; Plant #6 = Group D; *A. thaliana* #2 = Group E; Plant #3 = Group F; Plant #5 = Group G; Plant #7 = Group H; Plant #8 = Group I.

a Sequence At2g46920.1 was first placed in this cluster by Schweighofer et al. (7). The gene product was characterized by Yu et al. (27).

b Sequences At4g32950.1 and At5g26010.1 were first placed in this cluster by Schweighofer et al. (7).

c This cluster now contains the previously identified but unallied sequence At1g18030.1.

d Each of these sequences lacks motif 6, 1 of the 11 classic structural motifs of the PP2C class (28). They should be considered “PP2C-like” until their enzymatic activity has been tested experimentally.

The following sequences were rejected during the alignment process: At1g17545.1, At1g22280.2, At1g79630.2, At2g35350.1, At3g23360.1, At3g27140.1, At3g51370.2, At4g08260.1, At4g27800.2, At4g27800.3, and At4g31860.2. The sequence At4g11040.1 was newly identified in this study but could not be resolved into a cluster in the trees. The sequence At1g75010.1, which was classified as a PP2C by Kerk et al. (4), was determined in this analysis to be a false positive.

alternate between black-and-white conservation and color amino acid properties views of the alignment. Other useful GeneDoc settings are as follows: Top “C” (“Configuration”) button → “Project” tab → “Seq block sizing” → “Fixed” 7500 (this eliminates the default sequence block screen wrap-around); Top “C” (“Configuration”) button → “Project” tab → “Font Settings” → Points 14 (for middle-aged eyes!); Top “C” (“Configuration”) button → “Project” tab → “Max Name Len” → 15.

3. Unfortunately, the TCoffee server limits evaluation to alignments of 50 sequences or less. One might very well have a larger alignment. It is still possible to get an idea about the quality of an alignment by splitting it into portions, each within the above size restriction. GeneDoc allows editing of the sequence list: “Project” → “Edit sequences list”. When this dialog box appears, one can highlight sequences and either change their order within the list or delete them. It is possible to create a “top” and “bottom” alignment, for example, each containing half of the sequences and to evaluate these. However, by default, most alignment programs put the best sequences in the alignment on top and the worst on the bottom, so this strategy would produce a “bottom” alignment that has a systematic bias to get a lower evaluation score. GeneDoc can shuffle the order of the input sequences to put them in alphabetical order by using the “Sort Name” function. Now if the alignment is split up and the pieces evaluated, there will be much less systematic error in each.
4. The general topic of what to leave in and what to remove from a multiple-sequence alignment (i.e., how conservatively or how radically to edit it) is one on which there is no general consensus within the bioinformatic community. Leaving everything in will, in principle, maximize the available phylogenetic signal, and removing material will reduce it. However, that assumes that all characters are optimally aligned, which is rarely the case. Another view would be that to remove apparently poorly aligned sequence regions actually improves the phylogenetic signal by removing material that can be misleading to the analysis. That is the approach used in this study. It is the author’s experience that models that are constructed from “gappy” alignments where regions are poorly aligned perform less well (i.e., are less sensitive and specific in detection of distant homologues in database searches) than models from more tightly edited alignments. As a suggested rule of thumb, once the best revised sequence alignment has been obtained by rearranging sequence characters, remove any column from the alignment where the number of gaps exceeds half of the total number of sequences.
5. The goal of the project will guide the editing strategy for the multiple-sequence alignment. In our lab’s work with protein phosphatases, our goal has been to classify sequences that would be most useful for biochemical/molecular study by the community of experimentalists. Because the conserved sequence characteristics of the various protein phosphatase classes are well known (a useful summary compilation is presented in **ref. 26**), we have chosen to be very conservative and to reject from the final alignment any sequences missing critical conserved residues. The rationale is to leave in sequences that are the most likely to be

- enzymatically active. On the other hand, were one interested in examining the evolutionary relationships of all protein phosphatase like sequences, even those that might not be enzymatically active, then one would choose to leave those sequences in the final alignment. A compromise employed in Kerk et al. (4) and also in this study is to note those sequences that were rejected at the final alignment stage.
6. A poor quality alignment might result if the alignment program were presented with a very divergent sequence set. This could be remedied by adopting a more conservative strategy. The *E*-value cutoff for sequence hits using the HMM (**Sub-heading 3.4.**) or using a BLAST search (*see Note 1*) can be lowered to something like *e*-20 or *e*-30. This will insure that the initial set of sequences used to construct the first-level alignment share a greater level of similarity. The *E*-value cutoff during subsequent rounds could then be relaxed (e.g., *e*-10, *e*-05).
 7. The PHYLIP package has an unfortunate restriction on the length of the names of sequences in a multiple-sequence alignment: 10 characters maximum. This often requires creation of an alignment version with edited sequence names conforming to this limit. GeneDoc allows this by the following procedure: "Project" → "Edit sequences list" → highlight a sequence → "Details" → shorten the sequence name in the new dialog box → "OK."
 8. In the case of a very large alignment (approx 150 sequences or more), there might be trouble with the PHYLIP program protpars not being able to finish a run properly when large numbers of bootstrap replicates are desired (e.g., 200 or more). This is apparently the result of the high demand for system resources by this program. An approach to get around this problem is to run protpars with sets of 50 or 100 bootstrap replicate alignments at once. Then, when all the output files have been obtained, prior to construction of the consensus tree, it is possible to concatenate the several parsimony outtree files, using the UNIX "cat" command: `cat file1 file2 file3 > file4` (this will concatenate as many files as desired). The program consense seems to have no problem running jobs for large numbers of bootstrap replicates once this file is obtained.

Acknowledgments

The author gratefully acknowledges the support of the National Science Foundation (NSF ROA DBI-9975808; MCB-0209686).

References

1. Zhang, Z.-Y. (2001) Protein tyrosine phosphatases: prospects for therapeutics. *Curr. Opin. Chem. Biol.* **5**, 416–423.
2. Alonso, A., Sasin, J., Bottini, N., et al. (2004) Protein tyrosine phosphatases in the human genome. *Cell* **117**, 699–711.
3. MacKeigan, J.P., Murphy, L.O., and Blenis, J. (2005) Sensitized RNAi screen of human kinases and phosphatases identifies new regulators of apoptosis and chemoresistance. *Nat. Cell Biol.* **7**, 591–600.

4. Kerk, D., Bulgrien, J., Smith, D.W., Barsam, B., Veretnik, S., and Gribskov M. (2002) The complement of protein phosphatase catalytic subunits encoded in the genome of *Arabidopsis*. *Plant Physiol.* **129**,908–925.
5. Monroe-Augustus, M., Zolman, B.K., and Bartel, B. (2003) IBR5, a dual-specificity phosphatase-like protein modulating auxin and abscisic acid responsiveness in *Arabidopsis*. *Plant Cell* **15**, 2979–2991.
6. Mora-Garcia, S., Vert, G., Yin, Y., Cano-Delgado, A., Cheong, H., and Chory, J. (2004) Nuclear protein phosphatases with Kelch-repeat domains modulate the response to brassinosteroids in *Arabidopsis*. *Genes Dev.* **18**, 448–460.
7. Schweighofer, A., Hirt, H., and Meskiene I. (2004) Plant PP2C phosphatases: emerging functions in stress signaling. *Trends Plant Sci.* **9**, 236–243.
8. Altschul, S.F., Gish, W., Miller, W., Myers, E.W., and Lipman, D.J. (1990) Basic local alignment search tool. *J. Mol. Biol.* **215**, 403–410.
9. Mount, D.W. (2004) *Bioinformatics: Sequence and Genome Analysis*, 2nd ed., Cold Spring Harbor Laboratory Press, Cold Spring Harbor, NY, pp. 163–226.
10. Gribskov, M. and Veretnik, S. (1996) Identification of sequence patterns with profile analysis. *Methods Enzymol.* **266**, 198–211.
11. Eddy, S.R. (1998) Profile hidden Markov models. *Bioinformatics* **14**, 755–763.
12. Saitou, N. and Nei, M. (1987) The neighbor-joining method: a new method for reconstructing phylogenetic trees. *Mol. Biol. Evol.* **4**, 406–425.
13. D. L. Swofford, G. J. Olsen, P. J. Waddell, and D. M. Hillis (1996) Phylogenetic inference, in *Molecular Systematics*, 2nd ed. (Hillis, D. M., Moritz, C., and Mable, B. K., eds.), Sinauer Associates, Sunderland, MA, pp. 407–514.
14. Felsenstein, J. (1996) Inferring phylogenies from protein sequences by parsimony, distance, and likelihood methods. *Methods Enzymol.* **266**, 418–426.
15. Luan, S. (2003) Protein phosphatases in plants. *Annu. Rev. Plant Biol.* **54**, 63–92.
16. Bateman, A., Coin, L., Durbin, R., et al. (2004) The Pfam protein families database. *Nucleic Acids Res.* **32**, D138–D141.
17. Bernal, A., Ear, U., and Kyrpides, N. (2001) Genomes OnLine Database (GOLD): a monitor of genome projects world-wide. *Nuc. Acids Res.* **29**, 126–127.
18. Rhee, S. Y., Beavis, W., Berardini, T. Z., et al. (2003) The Arabidopsis Information Resource (TAIR): a model organism database providing a centralized, curated gateway to *Arabidopsis* biology, research materials and community. *Nucleic Acids Res.* **31**, 224–228.
19. Thompson, J. D., Gibson, T. J., Plewniak, F., Jeanmougin, F., and Higgins, D. G. (1997) The ClustalX windows interface: flexible strategies for multiple-sequence alignment aided by quality analysis tools. *Nucleic Acids Res.* **24**, 4876–4882.
20. Edgar, R. C. (2004) MUSCLE: multiple-sequence alignment with high accuracy and high throughput. *Nucleic Acids Res.* **32**, 1792–1797.
21. Poirot, O., Suhre, K., Abergel, C., O'Toole, E., and Notredame, C. (2004) 3DCoffee: a web server for mixing Sequences and Structures into multiple-sequence alignments. *Nuc. Acids Res.* **32**, W37–W40.
22. Nicholas, K.B., Nicholas, H.B. Jr., and Deerfield, D.W. II. (1997) GeneDoc: analysis and visualization of genetic variation. *EMBNEW.NEWS* **4**, 14.

23. Schmidt, H.A., Strimmer, K., Vingron, M., and von Haeseler, A. (2002) TREE-PUZZLE: maximum likelihood phylogenetic analysis using quartets and parallel computing. *Bioinformatics* **18**, 502–504.
24. Page, R.D.M. (1996) TreeView: An application to display phylogenetic trees on personal computers. *Computer Applic. Biol. Sci.* **12**, 357–358.
25. Do, C.B., Mahabhashyam, M.S., Brudno, M., and Batzoglou, S. (2005) ProbCons: probabilistic consistency-based multiple-sequence alignment. *Genome Res.* **15**, 330–340.
26. Shi, L., Potts, M., and Kennelly, P.J. (1998) The serine, threonine, and/or tyrosine-specific protein kinases and protein phosphatases of prokaryotic organisms: a family portrait. *FEMS Microbiol. Rev.* **22**, 229–253.
27. Yu, L.P., Miller, A.K., and Clark, S.E. (2003) POLTERGEIST encodes a protein phosphatase 2C that regulates CLAVATA pathways controlling stem cell identity at *Arabidopsis* shoot and flower meristems. *Curr. Biol.* **13**, 179–188.
28. Bork, P., Brown, N.P., Hegri, H., and Schultz, J. (1996) The protein phosphatase 2C (PP2C) superfamily: detection of bacterial homologues. *Prot. Sci.* **5**, 1421–1425.

Yeast Substrate-Trapping System for Isolating Substrates of Protein Tyrosine Phosphatases

Masahide Fukada and Masaharu Noda

Summary

Protein tyrosine phosphorylation, controlled by the activities of both protein tyrosine kinases (PTKs) and protein tyrosine phosphatases (PTPs), plays critical roles in a wide variety of cellular events. However, in contrast to the PTKs, our understanding of the biological functions of PTPs has been limited to date. This is mainly the result of the difficulty in identifying the substrate molecules of individual PTPs. We described a genetic method to screen for PTP substrates, which we have named the “yeast substrate-trapping system.” This method is based on the yeast two-hybrid system with two essential modifications: the conditional expression of a PTK to tyrosine-phosphorylate the prey protein, and screening using a substrate-trap PTP mutant as bait. This system is conceptually applicable to all the PTPs, because it is based on PTP–substrate interaction *in vivo*, namely the substrate recognition of individual PTPs. The identification of physiological substrates will shed light on the physiological functions of individual PTPs.

Key Words: Protein tyrosine phosphatase; protein tyrosine kinase; substrate screening; substrate-trapping mutant; tyrosine phosphorylation; yeast two-hybrid system; protein–protein interactions; Ptp^{prz}

1. Introduction

Protein tyrosine phosphorylation, controlled by the activities of both protein tyrosine kinases (PTKs) and protein tyrosine phosphatases (PTPs), plays critical roles in a wide variety of cellular events, including cell proliferation, differentiation, migration, metabolism, and death. (1,2). However, in contrast to the PTKs, our understanding of the biological functions of PTPs has been limited because of a lack of information concerning the physiological substrates of the respective PTPs. Several years ago, two types of substrate-trap PTP mutant were developed based on a mechanistic feature of substrate recognition

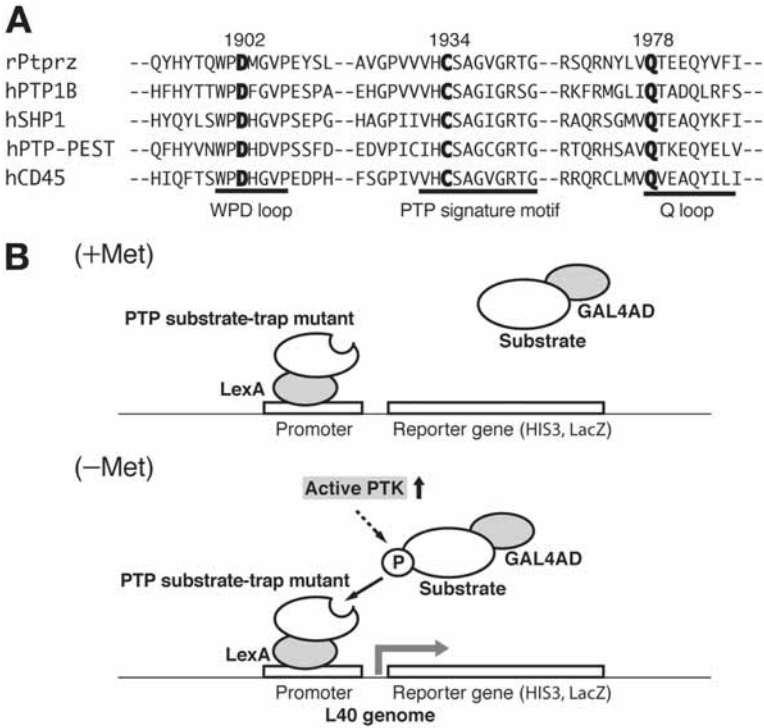


Fig. 1. PTP sequence alignment and schematic representation of the yeast substrate-trapping system. (A) Amino-acid-sequence alignment of the catalytic domain of representative PTPs. The mutated amino acids in the substrate-trap mutants are shown in bold. The residue position for rat Ptp_{prz} is shown. The relevant conserved motifs are indicated with underlines. (B) Top: In the presence of methionine (+Met), active PTK is not induced and, therefore, recognition of the substrate by the substrate-trap PTP mutant never occurs. Bottom: In the absence of methionine (-Met), substrates are tyrosine-phosphorylated by the active PTK and trapped by the substrate-trap PTP mutant, and as a result, expression of the reporter gene occurs from the host genome. (Reproduced from **ref. 9**.)

revealed for some PTPs (3,4). These mutants harbor a substitution in invariant amino acid residues in the PTP catalytic domain (see Fig. 1A). In one mutant, an active-site cysteine (Cys) residue is replaced with a serine (Ser) (3); in the other, an aspartic acid (Asp) residue is replaced with an alanine (Ala) (4). Both mutants form a stable complex with their substrates as a result of the impaired catalytic activity (3,4). However, only a limited number of PTP substrates have been identified using these mutants by a typical biochemical technique in vitro (3-7). The application of this strategy to all the PTPs seems difficult because most of the substrates identified to date were restricted to relatively abundant

and highly tyrosine-phosphorylated cellular proteins. Therefore, the development of a standard method applicable to all PTPs has long been awaited.

In this chapter, we describe a genetic method to screen for PTP substrates that we have named the “yeast substrate-trapping system.” This method was originally developed to isolate substrates for protein tyrosine phosphatase receptor type Z (Ptrz) (8), and we and others have already succeeded in the isolation of substrate molecules for PTPs by using this method (8–10). This method is based on the yeast two-hybrid system, which has been used extensively in studies on protein–protein interactions: Bait and prey proteins are fused to the DNA-binding domain or transcription-activating domain of a transcription factor, respectively, and therefore, the physical interaction between the two proteins in the yeast nucleus was converted to reporter-gene expression (11). To apply this powerful method to the detection of the PTP–substrate interaction, two improvements were required. First, the conditional expression of a PTK was necessary to tyrosine-phosphorylate the prey protein because little tyrosine phosphorylation occurs in the native yeast (12). Second, a substrate-trap PTP mutant was adopted as bait because of the transient nature of the binding between the wild-type PTP and its substrates. A schematic representation of the yeast substrate-trapping system is shown in Fig. 1B. In this system, the bait vector continuously expresses the substrate-trap PTP mutant fused to LexA and conditionally expresses an active PTK. When yeast cells are cultured in medium containing methionine (Met), expression of the active PTK is suppressed. Under these conditions, tyrosine-phosphorylation-dependent interaction between the bait molecule (the substrate-trap PTP mutant) and the prey molecule (the substrate) does not occur (see Fig. 1B, top). When yeast cells are cultured in the absence of Met, however, the active PTK is expressed, tyrosine-phosphorylation of the substrate occurs, and subsequently interaction between the substrate-trap PTP mutant and substrate begins to yield the reporter-gene expression (see Fig. 1B, bottom).

This method has the advantage that continuously interacting molecules for a PTP are also identified at the same time. The identification of physiological substrates, together with continuously interacting molecules, will lead to a full understanding of the physiological roles of individual PTPs.

2. Materials

1. pBridgeLexA/v-src vector (9; see Note 1).
2. cDNA of the substrate-trap PTP mutant (see Note 2).
3. cDNA of an appropriate active PTK (In case v-src is not appropriate; see Note 3).
4. Prey (library) vector.
5. *Saccharomyces cerevisiae* strain, L40 (13).
6. YPDA medium: 10 g/L yeast extract, 20 g/L Difco peptone, 20 g/L D-glucose, and 0.4 g/L L-adenine hemisulfate salt.

7. 10X Basic amino acid solution: 300 mg/L L-isoleucine, 1500 mg/L L-valine, 200 mg/L L-adenine hemisulfate salt, 200 mg/L L-arginine HCl, 200 mg/L *L-histidine HCl monohydrate, 1000 mg/L *L-leucine, 300 mg/L L-lysine HCl, 500 mg/L L-phenylalanine, 2000 mg/L L-threonine, 200 mg/L *L-tryptophan, 300 mg/L L-tyrosine, and 200 mg/L L-uracil. The asterisk indicates the dropout amino acid. L-Methionine is not included.
8. 10X Dropout solution (the basic amino acid in which only the dropout amino acid[s] is omitted).
9. A series of synthetic dropout media [SDM; 6.7 g/L yeast nitrogen base without amino acids, 20 g/L D-glucose, 1X Respective dropout solution, 20 g/L agar (only for plates), and 149.2 mg/L L-methionine (1 mM; only for +Met medium)].
10. 1X TE: 10 mM Tris-HCl, pH 7.5, and 1 mM EDTA.
11. 1X LiAc/TE: 0.1 M lithium acetate in TE.
12. PEG/LiAc: 40% PEG 3350 and 0.1 M lithium acetate in TE.
13. Salmon sperm DNA: 2 mg/mL in TE.
14. Dimethyl sulfoxide (DMSO).
15. Liquid nitrogen.
16. Z buffer: 0.1 M phosphate buffer, pH 7.0, 10 mM KCl, and 1 mM MgSO₄.
17. X-gal solution: 20 mg/mL of 5-bromo-4-chloro-3-indolyl- β -D-galactopyranoside in *N,N*-dimethylformamide.
18. Z buffer/X-gal: 100 mL of Z buffer, 0.27 mL of 2-mercaptoethanol, and 1.67 mL of X-gal solution.
19. Nitrocellulose filter (OPTITRAN BA-S85; Schleicher & Schuell, Keene, NH).

3. Methods

The screening of the substrates is performed in two steps. In the first step, library transformation and colony selection under the condition that the active PTK is expressed are conducted. As the second step, discrimination of the clones obtained in the first step between the substrate candidates and continuously interacting molecules is performed.

The methods described outline (1) the construction of the vectors used in the yeast substrate-trapping system, (2) the preparation of the competent cells for the library screening, (3) the library transformation and the first step of the screening, and (4) the identification of substrate molecules. The general procedures for the library screening described are essentially in accord with the manufacturer's directions (e.g., MATCHMAKER library user manual; Clontech, Palo Alto, CA).

3.1. Vector Construction

3.1.1. Bait Vector

The pBridgeLexA/v-src vector has a multiple-cloning site (MCS), which is located downstream of the LexA-coding sequence, for insertion of a substrate-

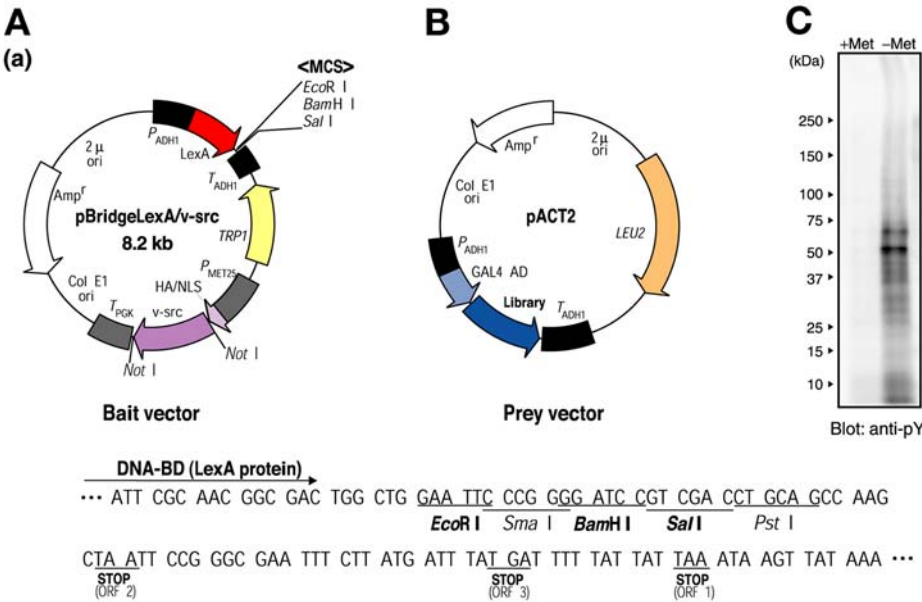


Fig. 2. Bait and prey vectors and tyrosine phosphorylation by the PTK expressed in the yeast. (A,a) Structure of the pBridgeLexA/v-src vector. The PTP substrate-trap mutant is inserted into the MCS in-frame with LexA. (A,b) DNA sequence of the MCS region in the bait vector. Unique restriction sites are shown in bold. The *SmaI* and *PstI* sites are not shown in bold because both sites exist in the v-src sequence. (B) Structure of the pACT2 vector (Clontech). (C) Cellular proteins in the yeast are highly tyrosine-phosphorylated when v-src is induced in the absence of methionine (–Met), whereas almost no tyrosine-phosphorylation is observed in the presence of methionine (+Met). L40 cells transformed with pBridgeLexA/v-src were cultured in the medium both with and without 1 mM methionine for 24 h, and the tyrosine-phosphorylation of cellular proteins was analyzed by Western blotting with antiphosphotyrosine 4G10 antibody. (Reproduced from ref. 9.)

trap PTP mutant (see Fig. 2A). As an active PTK, v-src cDNA is inserted into the *NotI* site in this vector (see Note 4). To prepare the bait vector, a substrate-trap PTP mutant needs to be inserted in-frame with LexA (see Note 5). The vector thus prepared continuously expresses the substrate-trap PTP mutant fused to LexA under the control of the *ADH1* promoter and conditionally expresses v-src (as an active PTK) under the control of the *MET25* promoter, which drives the gene expression in the absence of Met and completely represses it in the presence of 1 mM Met (see Fig. 2A, part a and C). This vector has a nutritional-marker gene, *TRP1*, which allows yeast cells to grow in a medium lacking tryptophan (Trp).

3.1.2. Prey (Library) Vector

The prey vector expresses the library cDNAs as fusion proteins with the GAL4 transcription activating domain and harbors a nutritional marker gene, *LEU2*, that allows yeast cells to grow in a medium lacking leucine (Leu). Such prey vectors are commercially available, for instance, from Clontech, pACT2 (see [Fig. 2B](#)) and pGAD10.

3.2. Preparation of the Competent Cells

The *Saccharomyces cerevisiae* strain used for screening is L40, which harbors the reporter genes *LacZ* and *HIS3* under the control of minimal *GAL1* and *HIS3* promoters, respectively, both fused to multimerized LexA-binding sites ([13](#)). L40 cells are first transformed with the bait vector alone, and the transformant is next used for the library transformation as the reporter strain.

3.2.1. Transformation of the Bait Vector

L40 cells are transformed with the bait vector and transformants are selected based on growth on plates of SDM lacking Trp but containing 1 mM Met (–Trp, +Met/SDM). The colonies appearing on the selective plates are to be freshly maintained in culture by restreaking every 2–4 d on plates (–Trp, +Met/SDM). The method for the DNA transformation of yeast cells is the same as described below.

3.2.2. Check of the Reporter Strain

We recommend testing the transformant in advance as to whether *HIS3* or *LacZ* expression is not induced by the bait vector alone. The background expression of *HIS3* should be tested by the growth of the transformants on the selective plate (–Trp, –His, –Met/SDM), at least for 1 wk (see [Note 6](#)). The background expression of *LacZ* should be tested by filter-lift β -galactosidase assay on the selective plates (–Trp, \pm Met/SDM) (see [Subheading 3.4.](#)).

We also recommend confirming that the LexA-PTP-fusion protein and active PTK are expressed in the yeast cells. Transformants are cultured for 24 h at 30°C in 3 mL of liquid medium (–Trp, \pm Met/SDM) with shaking at 250 rpm, and then cells are collected by centrifugation. Then the yeast cell lysate is prepared and subjected to Western blot analysis with appropriate antibodies. An example of the Western blot analysis of the yeast cell lysates with antiphosphotyrosine antibody is shown in [Fig. 2C](#) to check the inductive expression of *v-src* in the yeast cell transformed with pBridgeLexA/*v-src*.

3.2.3. Preparation of the Competent Cells

1. Inoculate 50 mL of liquid medium (–Trp, +Met/SDM) with several fresh colonies (2–3 mm in diameter) of L40 reporter strain transformed with the bait vector.

2. Incubate for 24–48 h at 30°C with shaking at 250 rpm to the stationary phase ($OD_{600} > 1.5$).
3. Transfer the culture into a flask containing 200 mL of prewarmed YPDA medium (30°C), and further incubate for 4 h at 30°C with shaking at 250 rpm (OD_{600} = approx 0.5).
4. The cells are collected by centrifugation at 1000g for 5 min and resuspended in 50 mL of sterile H₂O for washing.
5. Again, cells are collected by centrifugation, and the cell pellet is resuspended in 1.5 mL of 1X LiAc/TE at room temperature. Competent cells thus prepared are used within 1 h for the next library transformation.

3.3. Transformation and Screening of the Library

In the first step of the screening, the cDNA library is screened under the condition that the active PTK is expressed and positive colonies are selected based on cell growth on a medium lacking histidine (His), namely by the expression of the reporter gene *HIS3* (Fig. 1B, bottom). It should be noted that the clones isolated at this stage include candidates for both the substrates and continuously interacting molecules (see Note 7).

1. Library DNA (10–50 µg), salmon sperm DNA (1 mg), yeast competent cells (1 mL), and PEG/LiAc (6 mL) are well mixed in a 15-mL polypropylene tube by vortex.
2. Incubate for 30 min at 30°C with shaking at 200 rpm.
3. Add 700 µL of DMSO and mix gently.
4. The cells are heat-shocked for 15 min in a 42°C water bath and chilled on ice for 3 min.
5. The cells are collected by centrifugation at 1000g for 5 min, resuspended in 5 mL of 1X TE, and spread on the plates (–Leu, –Trp, –His, –Met/SDM).
6. The plates are incubated at 30°C until colonies appear; this will take 1–2 wk.
7. The colonies appearing on the selective plates are to be freshly maintained in culture by restreaking every 2–4 d on plates (–Leu, –Trp, +Met/SDM) for further analysis.

3.4. Identification of Substrate Molecules by Filter-Lift β -Galactosidase Assays

To identify candidates for the substrate among the clones isolated in the first step of the screening, the discrimination step is requisite. For this purpose, the filter-lift β -galactosidase assay using the expression of another reporter gene, *LacZ*, is performed in pairs in the presence and absence of PTK expression: The clones that show interactions (*LacZ* expression) only when PTK is expressed are candidates for the PTP substrate.

1. Sterile nitrocellulose filters are first placed on plates of –Leu, –Trp, –Met/SDM and –Leu, –Trp, +Met/SDM.

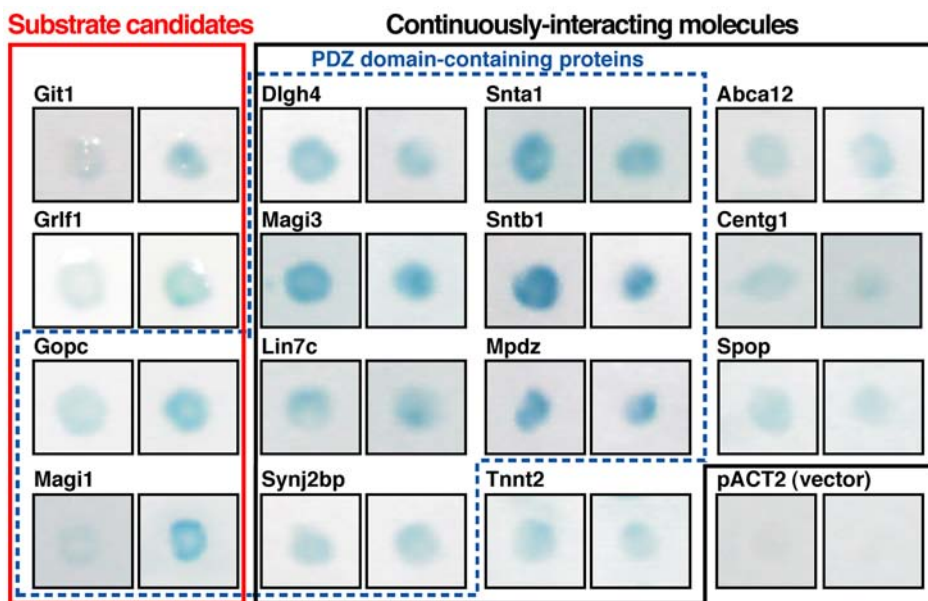


Fig. 3. Filter-lift β -galactosidase assay. All the clones isolated from the first-step screening for substrates of Ptp^{trz} were subjected to a filter-lift β -galactosidase assay in both the presence (left) and absence (right) of 1 mM methionine. Yeast colonies were cultured for 2 d and developed for 3 h at 30°C for color detection. Clones are classified into two groups that show different or equal color intensities under the two conditions. Substrates are identified as clones that show more intensive signals when the PTK is expressed. (Reproduced from **ref. 9**.)

2. Fresh colonies of respective clones are directly streaked on each filter, and cultured for 48 h at 30°C (*see Note 8*).
3. The filters are lifted off the plates and sunk into a pool of liquid nitrogen for 10 s to completely freeze the cells.
4. The frozen filters are allowed to thaw for 5 min at room temperature (colony-side up).
5. The filters are each placed, colony-side up, on another filter presoaked in 700 μ L of X-gal-containing coloring solution (X-gal/Z buffer).
6. The filters are incubated at 30°C and checked periodically for the appearance of blue colonies. The colonies that show an increase in blue color development (this will take several minutes to 24 h) on induction of the active PTK (cultured on –Met plates) are selected as substrate candidates. The results when the substrate-trap Ptp^{trz} mutant was used as bait are shown in **Fig. 3**.

To conclude that the candidate molecules thus isolated are indeed substrates for respective PTPs, further analyses would be required (*see Note 9*).

4. Notes

1. For construction of the pBridgeLexA/v-src vector (see [Fig. 2A](#)), the DNA-binding region of the GAL4 sequence of the pBridge vector (Clontech) was replaced with the full-length LexA-coding sequence of pBTM116 and then the v-src-coding sequence of pBaBePurov-src ([14](#)) was inserted into the *NotI* site ([9](#)). The pBridgeLexA/v-src vector is available to researchers on request from the author (M.N.).
2. We recommend the Asp-to-Ala mutant as a substrate-trap mutant because this type of PTP mutant has been found to have better substrate-trapping ability than the Cys-to-Ser mutant ([4,15](#)). In fact, we could not isolate any positive clones when using the Cys (1934) Ser mutant of Ptpz as bait ([9](#)). Recently, an improved PTP1B substrate-trap double mutant, Asp-to-Ala; Gln-to-Ala, was designed and characterized ([1111](#)). This type of substrate-trap mutant might improve the efficiency of isolating substrates also with the yeast substrate-trapping system. An amino-acid-sequence alignment including the mutated amino acids in these substrate-trap mutants is shown in [Fig. 1A](#).
3. The selection of an appropriate PTK for substrates would be an important factor. We utilized v-src as the active PTK to tyrosine-phosphorylate the prey proteins because src-family kinases have important regulatory functions in growth cones of neurons, where Ptpz is known to be abundant ([17](#)). If the appropriate PTK is not known, we recommend the use of v-src because it has a broad substrate specificity ([18](#)) and is highly active in yeast and also mammalian cells ([19,20](#)). In addition, although it was reported that the expression of v-src in yeast *S. cerevisiae* has a considerable effect on cell growth ([19,21](#)), the expression of v-src in our system had no inhibitory effect on cell growth, where numerous yeast proteins are also tyrosine-phosphorylated (see [Fig. 2C](#)). If any candidate molecules cannot be isolated using v-src, one should change from v-src to other PTKs.
4. Insertion of a PTK cDNA into a *NotI* site of the pBridge vector (Clontech) yields a PTK derivative in which an HA epitope and a nuclear localization sequence (NLS) are fused to the N-terminus. This might facilitate the tyrosine phosphorylation of the prey protein in the yeast nucleus, where the interaction between the substrate and substrate-trap PTP mutant must occur.
5. In the model case using Ptpz, the whole intracellular region of rat Ptpz1 (amino acid residues 1748–2316; GenBank accession no. U09357) with a replacement of Asp (1902) with Ala was used as a substrate-trap mutant ([8,9](#)) (see [Fig. 1A](#)).
6. If the transformants can grow on the selective plate, the addition of 3-aminotriazole (an inhibitor of His3 protein) at the optimized concentration is required to block the background cell growth in the first step of the screening. In the case of screening for Ptpz substrates, 3-aminotriazole was not required because no background cell growth was observed ([8,9](#)).
7. In the yeast substrate-trapping system, the standard two-hybrid system also appears to work, even when the active PTK is expressed. If PTP contains some domains responsible for protein–protein interactions, a mutation or deletion of

such domains might be effective in reducing the numbers of positive clones that are not substrates in the first step of screening. For example, Ptpz has a PDZ-binding motif at its C-terminus, therefore 9 of 15 clones isolated from first-step screening for Ptpz substrates were PDZ domain-containing proteins (see Fig. 3). These PDZ-mediated interactions were abolished when the PDZ-binding motif in the substrate-trap Ptpz mutant was deleted, even though the substrate candidates still showed interaction with this mutant (9).

8. This is enough time for the cells to grow on filters and express PTK on the Met-minus plate.
9. For example, we concluded that G-protein-coupled receptor kinase-interactor 1 (Git1) is one of the substrates for Ptpz based on the following findings (8): (1) Ptpz dephosphorylates tyrosine phosphorylated Git1 *in vitro*; (2) the interaction between Git1 and the Ptpz substrate-trap mutant is dependent on the tyrosine phosphorylation of Git1 in mammalian cells; (3) Git1 and Ptpz are colocalized *in vivo* and in cultured cells; (4) tyrosine phosphorylation of Git1 is upregulated in response to treatment with pleiotrophin, a natural ligand for Ptpz. As the first step in the verification of candidate molecules, we usually perform an “*in vitro* PTP assay” to test whether candidate molecules are indeed dephosphorylated by the PTP (9).

Acknowledgments

We thank Dr. Hiroyuki Kawachi and Dr. Akihiro Fujikawa for their significant contribution to the development of this method, Dr. Hisataka Sabe for the pBaBePurov-src vectors, and Dr. Paul Bartel and Dr. Stan Fields for the pBTM116 vector. We also thank Ms. Akiko Kodama for secretarial assistance. This work was supported by grants from the Ministry of Education, Science, Sports and Culture of Japan, Japan Science and Technology Agency (CREST), Yamada Science Foundation, and Novartis Foundation (Japan) for the Promotion of Science.

References

1. Tonks, N. K. and Neel, B. G. (1996) From form to function: signaling by protein tyrosine phosphatases. *Cell* **87**, 365–368.
2. Neel, B. G. and Tonks, N. K. (1997) Protein tyrosine phosphatase in signal transduction. *Curr. Opin. Cell Biol.* **9**, 193–204.
3. Milarski, K. L., Zhu, G., Pearl, C. G., et al. (1993) Sequence specificity in recognition of the epidermal growth factor receptor by protein tyrosine phosphatase 1B. *J. Biol. Chem.* **268**, 23,634–23,639.
4. Flint, A. J., Tiganis, T., Barford, D., and Tonks, N. K. (1997) Development of “substrate-trapping” mutants to identify physiological substrates of protein tyrosine phosphatases. *Proc. Natl. Acad. Sci. USA* **94**, 1680–1685.
5. Furukawa, T., Itoh, M., Krueger, N. X., Streuli, M., and Saito, H. (1994) Specific interaction of the CD45 protein-tyrosine phosphatase with tyrosine-phosphorylated CD3 ζ chain. *Proc. Natl. Acad. Sci. USA* **91**, 10,928–10,932.

6. Garton, A. J., Flint, A. J., and Tonks, N. K. (1996) Identification of p130^{cas} as a substrate for the cytosolic protein tyrosine phosphatase PTP-PEST. *Mol. Cell. Biol.* **16**, 6408–6418.
7. Meng, K., Rodriguez-Pena, A., Dimitrov, T., et al. (2000) Pleiotrophin signals increased tyrosine phosphorylation of β -catenin through inactivation of the intrinsic catalytic activity of the receptor-type protein tyrosine phosphatase β/ζ . *Proc. Natl. Acad. Sci. USA* **97**, 2603–2608.
8. Kawachi, H., Fujikawa, A., Maeda, N., and Noda, M. (2001) Identification of GIT1/Cat-1 as a substrate molecule of protein tyrosine phosphatase ζ/β by the yeast substrate-trapping system. *Proc. Natl. Acad. Sci. USA* **98**, 6593–6598.
9. Fukada, M., Kawachi, H., Fujikawa, A., and Noda, M. (2005) Yeast substrate-trapping system for isolating substrates of protein tyrosine phosphatases: Isolation of substrates for protein tyrosine phosphatase receptor type α . *Methods* **35**, 54–63.
10. Tsuboi, N., Utsunomiya, T., Roberts, R. L., et al. (2002) *Mol. Biol. Cell* **13** (Suppl.), 429a.
11. Fields, S. and Song, O. (1989) A novel genetic system to detect protein–protein interactions. *Nature* **340**, 245–246.
12. Castellanos, R. M. and Mazon, M. J. (1985) Identification of phosphotyrosine in yeast proteins and of a protein tyrosine kinase associated with the plasma membrane. *J. Biol. Chem.* **260**, 8240–8242.
13. Vojtek, A. B., Hollenberg, S. M., and Cooper, J. A. (1993) Mammalian Ras interacts directly with the serine/threonine kinase Raf. *Cell* **74**, 205–214.
14. Sabe, H., Okada, M., Nakagawa, H., and Hanafusa, H. (1992) Activation of c-Src in cells bearing v-Crk and its suppression by Csk. *Mol. Cell. Biol.* **12**, 4706–4713.
15. Zhang, Y.-L., Yao, Z.-J., Sarmiento, M., Wu, L., Burke, T. R., Jr., and Zhang, Z.-Y. (2000) Thermodynamic study of ligand binding to protein-tyrosine phosphatase 1B and its substrate-trapping mutants. *J. Biol. Chem.* **275**, 34,205–34,212.
16. Xie, L., Zhang, Y.-L., and Zhang, Z.-Y. (2002) Design and characterization of an improved protein tyrosine phosphatase substrate-trapping mutant. *Biochemistry* **41**, 4032–4039.
17. Maeda, N. and Noda, M. (1998) Involvement of receptor-like protein tyrosine phosphatase ζ /RPTP β and its ligand pleiotrophin/heparin-binding growth-associated molecule (HB-GAM) in neuronal migration. *J. Cell Biol.* **142**, 203–216.
18. Songyang, Z., Carraway, K. L. 3rd., Eck, M. J., et al. (1995) Catalytic specificity of protein-tyrosine kinases is critical for selective signalling. *Nature* **373**, 536–539.
19. Brugge, J. S., Jarosik, G., Andersen, J., Queral-Lustig, A., Fedor-Chaiken, M., and Broach, J. R. (1987) Expression of Rous sarcoma virus transforming protein pp60v-src in *Saccharomyces cerevisiae* cells. *Mol. Cell. Biol.* **7**, 2180–2187.
20. Kamps, M. P. and Sefton, B. M. (1988) Most of the substrates of oncogenic viral tyrosine protein kinases can be phosphorylated by cellular tyrosine protein kinases in normal cells. *Oncogene Res.* **3**, 105–115.
21. Kornbluth, S., Jove, R., and Hanafusa, H. (1987) Characterization of avian and viral p60src proteins expressed in yeast. *Proc. Natl. Acad. Sci. USA* **84**, 4455–4459.

Index

A

Acetylcholine receptor, 263
ACL, 248, 249, 256–258
Acute myeloblastic leukemia, 15
Adapter, 310–311, 313, 317–318
Affinity chromatography, 183, 187, 190
Affinity isolation, 235–238, 241, 244
Affinity matrix, 39–43, 63, 64
Alignment software, 353–354
Alkaline phosphatase, 332, 333
Anti-FLAG immunoprecipitation, 104
Anti-FLAG M2 agarose, 106
Anti-peptide antibodies, 113
Ataxia-Telangiectasia Mutated (ATM), 47–58
ATM autophosphorylation, 47–57
Autoimmune diabetes, 15
Autophosphorylation, 248, 256–258

B

Beta-galactosidase, 159, 160, 162, 163, 166, 167, 168, 171, 175
Bioinformatics software, 350
Biotin, 39–43
Biotinylation, 226, 227, 229
Blast, 171, 348
Bovine heart, 127, 128, 129, 130
Budding yeast, 322

C

Cdk, 157, 170
Cell cycle, 133, 142, 156
Cell imaging, 134, 136, 137, 138, 140, 145, 147, 150
Cell labeling [³⁵S]methionine, 118
Chromosomal promoter replacement, 302

ClustalX, 359

Competent BL21 (DE3) cells, 251

Co-precipitation 313, 315–316, 318, 320

CPI17, 198, 210–213

Cre/LoxP, 263

Calyculin A, 23, 24, 25, 26, 30, 31, 36

Cantharidin, 23, 24, 25, 27, 31, 37

D

6,8-Difluoro-4-methylumbelliferyl phosphate (DiMFUP), 61–68

DAPI, 136, 137, 139, 142, 144, 152

Dioxygenin, 187

DNA transfection, 190

Doxycycline, 300, 302–304

Drosophila, 155, 156, 157, 158, 159, 161, 162, 164, 165, 169, 170, 171, 173, 174

Dual-specificity phosphatases, 10

E

Epitope tagging 116

Escherichia coli, 167, 247, 251, 252, 254–256

Eya, 3, 11

F

FCP1 336

Fe-binding protein 131

Filter-lift β -galactosidase assay, 377–378

FK506, 6

Flag-tagged, 63, 65, 102

Fluorescence lifetime imaging microscopy (FLIM), 134, 135, 138, 148, 149, 150, 153

Fluorescence microscopy, 134, 137, 140, 144, 147, 150
 Fluorescence recovery after photobleaching (FRAP), 133, 134, 137, 138, 142, 144, 148, 150, 152
 Fluorescence resonance energy transfer (FRET), 133, 134, 135, 137, 138, 144, 145, 146, 147, 148, 149, 150, 152, 153
 Fluorescent protein fusions, 133
 Fluorophore, 135, 137, 148, 149
 Four E binding protein (4EBP), 324
 Fourteen three three (14-3-3), 127
 Fostriecin, 23, 24, 25, 26, 27, 30, 31, 32, 34, 35–37, 50

G

GADD34, 186, 198
 Gel electrophoresis 2D, 325–326, 329
 Gene expression, 300, 307
 GeneDoc, 354–356, 365, 367
 GFP immunofluorescence, 77
 Glc7, 199, 203, 204, 299, 301
 Glc7p, 236–238, 240–242, 244
 GLN3, 324, 326
 Glycogen phosphorylase- α 50, 54, 128
 Glycogen synthase kinase 3 (GSK3), 198
 GM 204, 211
 Green fluorescent protein (GFP), 134, 135, 138, 143, 144, 150
 G-beta, 248

H

HAD domain, 3
 HAL3, 300, 304
 HEK 293 cells, 101, 263, 273, 275, 293
 HEK 293T cell, 263, 275, 277–280, 283, 284
 HeLa cell, 139, 146, 262, 263, 266, 267, 268, 281
 His Tag, 248, 253, 256–258
 Histidine phosphatase (PHP), 247–258

Histidine phosphatase (PHP) activity, 248, 249, 256, 257, 258
 Histidine phosphatase (PHP) purification, 247, 248, 250, 254, 255, 257, 258
 Histidine phosphatase (PHP) substrate, 248–250, 256, 258
 Histone H1, 121
 HMMER, 353, 356
 HOG pathway, 309–310, 312, 317–318, 321
 Hog1, 310–312, 315–316, 318
 Hyperphosphorylation, 323, 331

I

IgG-conjugated magnetic beads, 236–239, 240, 241, 244
 Immunoblotting, 316, 319, 321
 Immunocytochemistry, 191
 Immunodeficiencies, 15
 Immunoprecipitation, 186, 189, 191, 194, 312, 318, 325–328
 Immunostaining, 138, 140, 141
 Inhibitor-1, 192–194, 198, 210
 Inhibitor-2, 193, 194, 198–200, 204
 Integrin receptors, 263
 Ionizing radiation, 47, 51
 Isoelectric focusing, 325, 328, 333

J, K

Juvenile myelomonocytic leukemia, 263
 KEPI, 210, 213

L

Lentivirus, 261, 262, 268, 275, 277–285
 LKY150, 237, 238, 241
 Luciferase, 267, 268
 Lafora's epilepsy, 15

M

M130/MYPT1/MBS, 158, 169, 198, 204, 210, 211, 225
 M20, 211, 225

- MAPK, 309, 311, 314, 316
Mass spectrometry, 235, 236, 241–245
Mathematical models of sequence analysis, 348
MEK, 310, 317
MEKK, 310–311, 314, 316–317
Micelle preparation, 213, 219
Microcystin, 39, 40, 41, 43, 50
Microcystin-biotin-Sepharose, 39–43
Microcystin-LR, 183, 186, 191, 213, 216
Microcystin-Sepharose, 39–43
Mitosis, 142, 153, 156
mRNA splicing, 149, 156
Muscle, 354, 362, 365
Muscle dystrophies, 15
Myelin basic protein, 121, 318
Myelodysplastic syndrome, 15
Myosin light chain kinase (MLCK), 210, 213–215, 218, 225, 231
Myosin light chain phosphatase (MLCP), 210, 211, 213, 218, 219
Myosin phosphatase (MP), 225
- N**
Nbp2, 309–318, 320
Ni-NTA agarose, 254, 255, 258
Nitrogen starvation, 323, 326–327, 331
Nodularia spumigena, 26
Nodularin, 23, 24, 26, 31
Noonan syndrome, 15, 263
NPR1, 324, 326–328, 330–333
Nuclear speckle, 139, 147, 149, 150, 151
- O**
Okadaic acid, 23, 24, 25, 26, 30, 31, 32, 34, 35–37, 39, 47, 48, 50, 56, 64, 65, 67
Opitz BBB/G syndrome, 15
- P**
P300 Transcription Coactivator 263, 285
Pathogenesis associated with *Helicobacter pylori*, 263
Pbs2 310, 312–313, 316–317, 319–320
PC12 cell line, 262
pCR[®] 2.1-TOPO[®] vector, 249, 251
pET16b vector, 251–253, 256, 257
Pfam, 352
PHI-1, 210, 213
Phosphatase assay, 50, 54, 56, 58, 61–69, 107, 115, 122, 340–342
Phosphatase targets, 329
Para nitrophenyl phosphate (pNPP), 33, 127
Phosphorylase kinase, 128
Phosphorylase phosphatase, 131
Phosphorylase-*b*, 128
Phosphorylation assay, 213, 216, 219
Phylogenetic trees, 349, 359–362, 365, 367–368
PKC, 198, 209, 210, 212, 213, 215, 216, 219, 220
Polymerase chain reaction (PCR), 249–251, 256, 301–302
PP1, 4, 5, 11, 23–26, 30–32, 34, 35, 27, 127, 130, 133, 134, 138, 139, 140, 142, 143, 144, 145, 146, 147, 148, 150, 152, 155–160, 163, 165, 166, 168, 169, 171, 173–175, 181–182, 184–194, 198–200, 203, 204, 210, 211
PP1 alpha, 139, 156, 158
PP1 beta/delta, 139, 156
PP1 catalytic subunit (PP1c), 235–239
PP1 gamma, 139, 142, 143, 145, 147, 148, 150, 156
PP1 measuring activity, 54, 55, 56
PP1 overlays, 182, 184–187, 189–193
PP1 regulatory subunit, 235, 236
PP1 targeting subunits, 39, 43
PP1 conserved binding motif, 236, 246
PP2A, 4, 5, 11, 15, 23–26, 30–32, 34, 35–36, 183, 198, 204
PP2A catalytic subunit, 262, 266
PP2A catalytic subunit *a*-isoform, 262
PP2A R1/ α scaffold subunit, 262
PP2A R1/ β scaffold subunit, 262

PP2A R2/B55 β regulatory subunit, 262, 263
 PP2A R2/PR55 α , 266
 PP2A R3/PR72 regulatory subunit, 262
 PP2A R5/B56 α , γ , δ , ϵ regulatory subunit, 262, 263, 265, 266
 PP2A, B-subunits, 71, 86
 PP2A, CDC55, 72
 PP2A, immune complex, 61–68
 PP2A, methylation, 72
 PP2A, PPH21, 72
 PP2A, PPH22, 72
 PP2A, PR65 α , 85
 PP2A, PR65 β , 85
 PP2A, purification, 43
 PP2A, regulation of ATM, 47–58
 PP2A, Rts1p, 73
 PP2A, Tpd3p, 72, 73
 PP2A, activity assay, 54, 55, 56, 61–68
 PP2Ac, 127, 129, 130, 131
 PP2B, 4, 6, 11, 23–26, 30–31, 33, 37, 43
 PP2C, 4, 11, 25, 26, 33, 37, 309
 PP4, 24–26, 30–32, 34, 35–36, 39, 43, 44, 54, 56, 57, 183
 PP5, 11, 24–26, 30–35, 39, 43, 45, 54, 56, 57, 183
 PP6, 183
 PP7, 24, 25, 30, 31, 43
 Preparation of competent yeast, 376–377
 Protein A tag, 236, 237, 238, 240, 244
 Protein expression, 339–340
 Protein phosphatase, 128, 131, 133, 155, 156, 159, 171, 299–301, 306
 Protein phosphatase assay, 188, 189, 214, 218
 Protein phosphatase inhibitors, 262
 Protein phosphatase type 1 (PP1), 235–240
 Protein serine/threonine phosphatase 2A (PP2A), 262, 265, 266, 267, 268, 281, 285, 286
 Protein tyrosine phosphatases, 248, 262, 310–311, 371–373
 PWY3, 237, 238, 241

Q

qRT-PCR, 270, 271, 281, 282, 286

R

R5/B56 γ subunit, 263
 Rabbit skeletal muscle, 128
 Rapamycin, 323–324, 326–327, 331–332
 RAW 264.7 cells, 262, 263, 269, 270, 274, 278, 280–283
 Rb2/p130 protein, 263, 285
 Receptor tyrosine kinases, 263
 REST/NRSF, 336–337
 Reticulocyte lysate, 90
 RNA interference (RNAi), 261–263, 266, 268, 284, 285, 342
 RNA polymerase II, 335

S

S6K, 324
Saccharomyces cerevisiae, 72, 163, 165, 235
 SCP1, 336–337
 SDS PAGE, 312–313, 316, 318–321, 325–326, 328, 331–332
 Sf9 cells, 248
 SH2-containing protein tyrosine phosphatase 2 (Shp2), 262–266, 268–283
 SH3 domains, 312, 314
 Sho1, 312
 Short-hairpin RNA (shRNA), 262, 264, 268, 269–278, 280–283, 286
 Signal transduction, 278
 Silver stain, 105
 SIT4, 300, 304, 323–324, 326–327, 331–332
 Site-directed mutagenesis, 87
 Small interfering RNAs (siRNA), 262, 264, 266–273, 281, 283

T

TAP42, 323, 324
 Targeting subunits, 127, 129, 133, 134, 138, 155, 158, 159

- Tautomycin, 23, 24, 25, 27, 30, 31
Tetracycline regulatable promoter, 299, 307
TEV protease, 236–238, 240, 241, 244, 246
Thiophosphorylation, 214, 217, 220, 226, 227
Time-lapse fluorescence microscopy, 133
Time-lapse imaging, 142
TIP41, 323–324, 326–330, 332–333
TOPO TA Cloning[®], 250–252, 256, 257
TOR, 323–324, 326–327
Transfection, 135, 136, 138, 140, 145, 147, 261, 264, 267–269, 271, 273–275, 277, 278, 283, 284
Transformation, 251, 252
Translation regulators, 324
Tyrosine phosphatase, 2, 3, 4, 10, 11, 62
Tyrosine kinase, 2, 10
Tyrosine phosphorylation, 371
- W**
Western blotting, 211, 215, 218, 220, 326, 330–332
Wnt signaling pathway, 263
- Y**
Yeast, 299–307
Yeast conjugation assay, 198
Yeast substrate-trapping system, 373
Yeast transformation, 377
Yeast two-hybrid, 155, 159, 172, 199, 236

